PROCEEDINGS OF THE FIRST ANNUAL W. O. Recora MEMORIAL SYMPOSIUM, OCTOBER 1975, SIOUX FALLS, SOUTH DAKOTA

GEOLOGICAL SURVEY
PROFESSIONAL PAPER 1015

PROCEEDINGS OF THE
FIRST ANNUAL
WILLIAM T. PECORA
MEMORIAL SYMPOSIUM,
OCTOBER 1975,
SIOUX FALLS, SOUTH DAKOTA

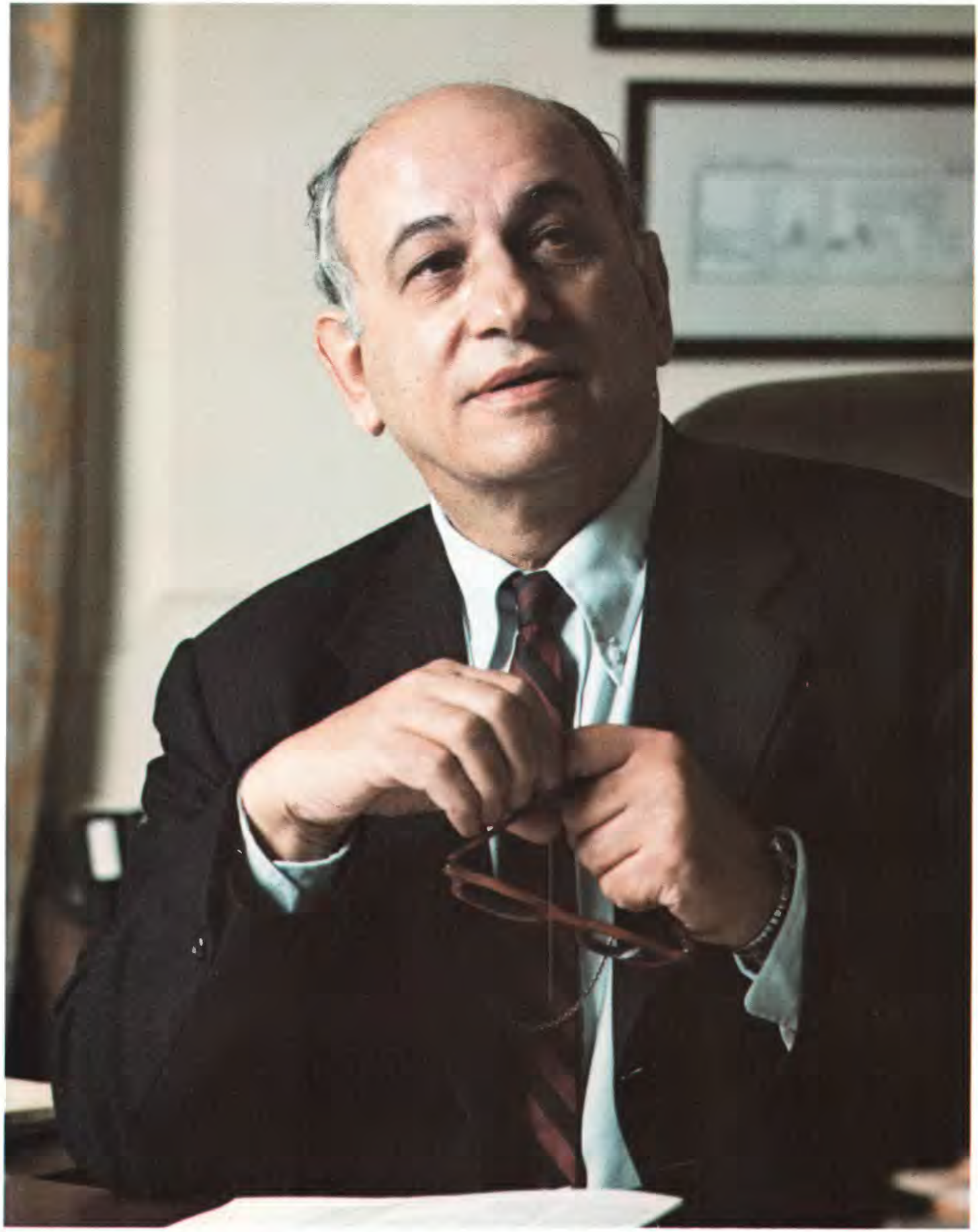

WILLIAM T. PECORA

PROCEEDINGS OF THE FIRST ANNUAL WILLIAM T. PECORA MEMORIAL SYMPOSIUM, OCTOBER 1975, SIOUX FALLS, SOUTH DAKOTA

P.W. WOLL and W. A. FISCHER, Editors

GEOLOGICAL SURVEY PROFESSIONAL PAPER 1015

Sponsored by
American Mining Congress

in concert with
U.S. Geological Survey
American Association of Petroleum Geologists
American Society of Photogrammetry
The Association of American Geographers
The Geological Society of America
Society of Economic Geologists

UNITED STATES GOVERNMENT PRINTING OFFICE : 1977

UNITED STATES DEPARTMENT OF THE INTERIOR

Cecil D. Andrus, Secretary

GEOLOGICAL SURVEY

V. E. McKelvey, Director

The U.S. Geological Survey agreed to publish the proceeding of the first annual William T. Pecora Memorial Symposium in its Professional Paper series because the subject material is related to the mission of the Survey. The usual standards for this series have been modified to accommodate the variety of styles used by the participants in this symposium. All color illustrations are placed at the front of the book for economy in printing. They are identified by the names of the authors of the papers from which they are extracted.

Library of Congress Cataloging in Publication Data

William T. Pecora Memorial Symposium, 1st, Sioux Falls, S. D., 1975.
Proceedings of the First Annual William T. Pecora Memorial Symposium, October 1975, Sioux Falls, South Dakota.

(U. S. Geological Survey professional paper; 1015)
Supt. of Docs. no.: I 19.16:1015
1. Prospecting—Remote sensing—Congresses.
I. Woll, Priscilla W. II. Fischer, William A., 1919– III. American Mining Congress.
IV. Series: United States. Geological Survey. Professional paper; 1015.
TN270.A1W54 1975 622'.15 76-608272

COLOR ILLUSTRATIONS

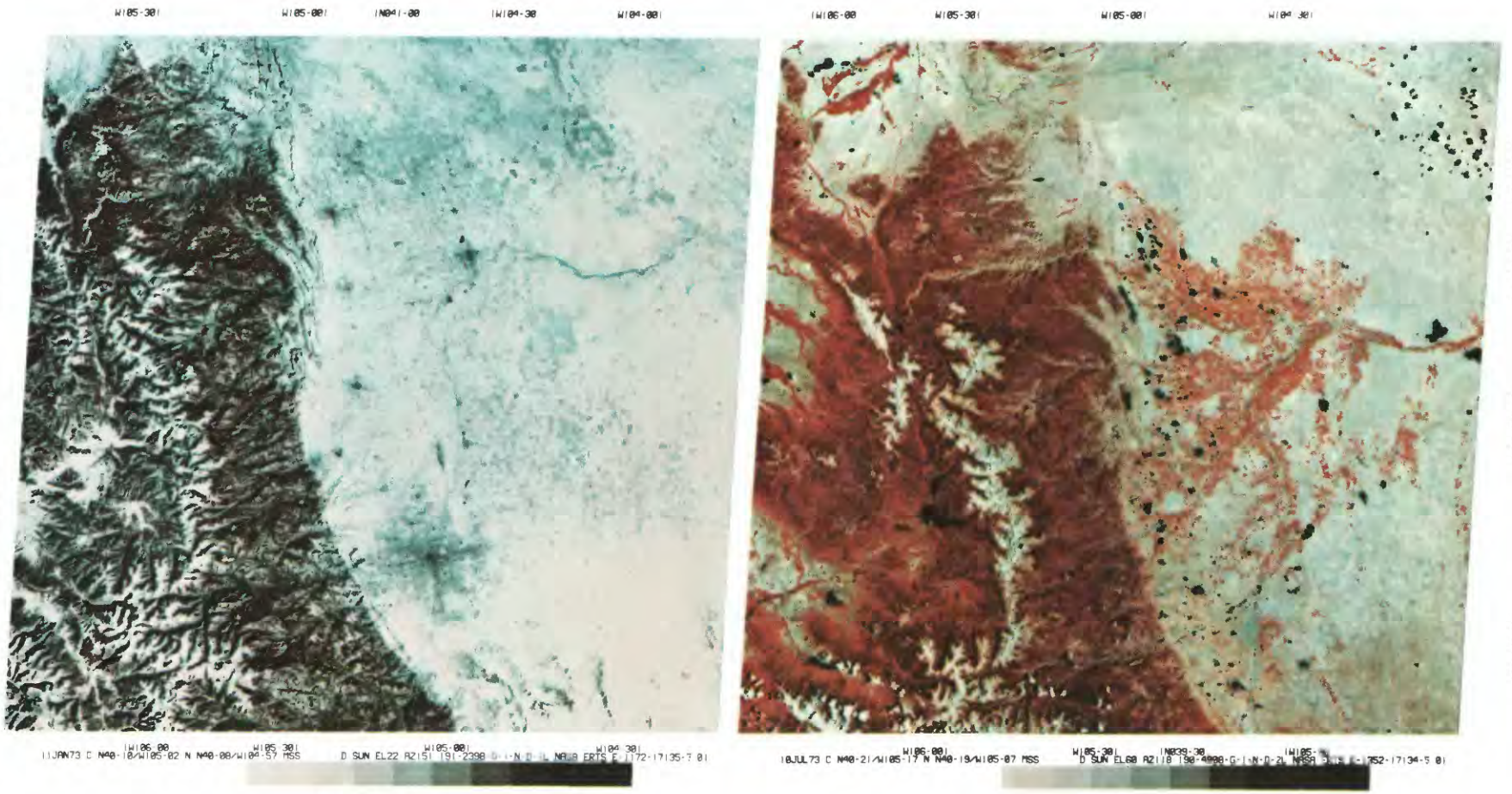

Jan. 73

- Road net
- Urbanization
- Enhanced topography

July 73

- Surface water
- Vegetation
- Land use

FIGURE 7.—Seasonal mapping with ERTS, Denver area.

COLVOCORESSES

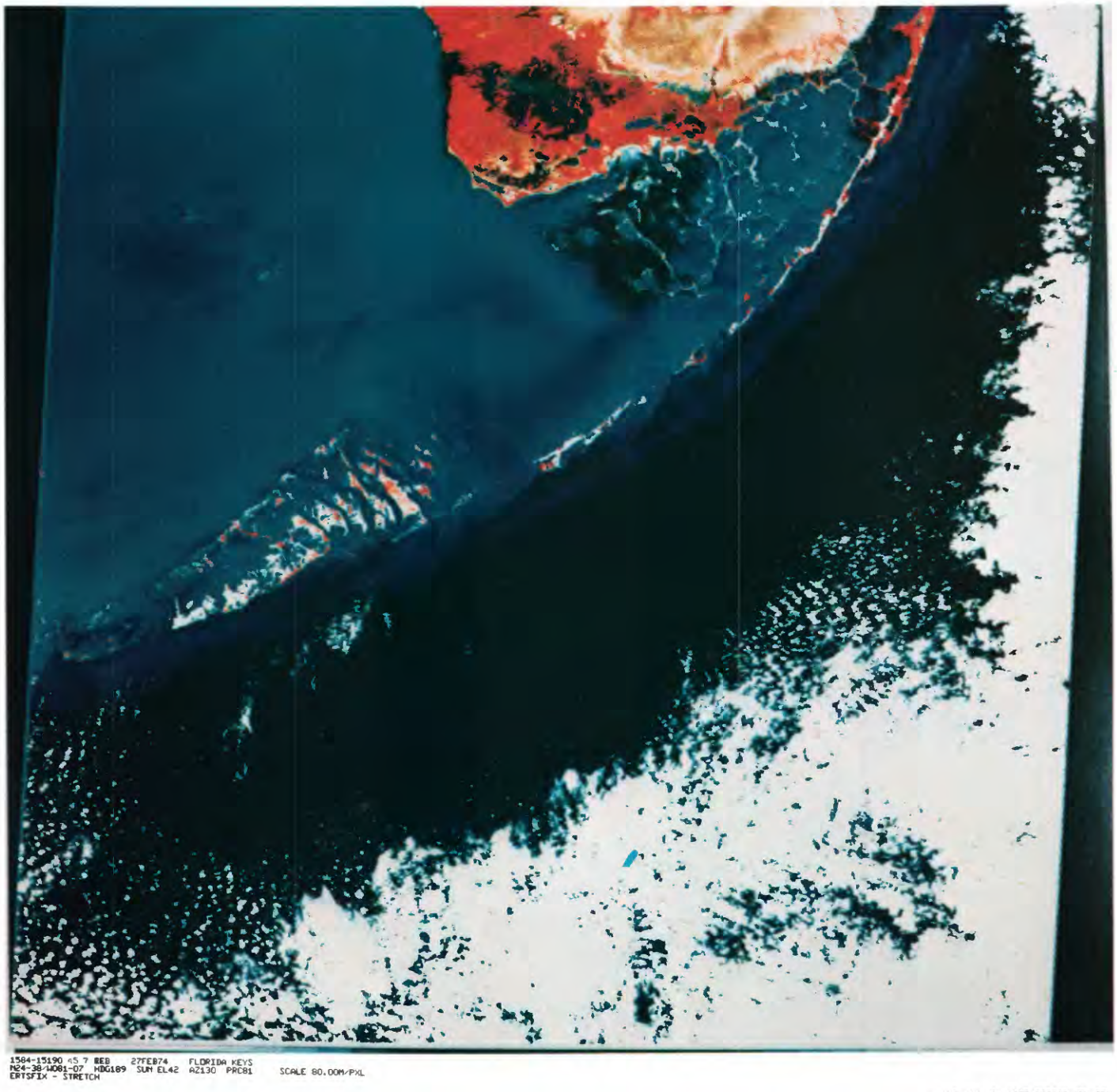

FIGURE 11.—Florida Keys (Landsat).

COLVOCORESSES

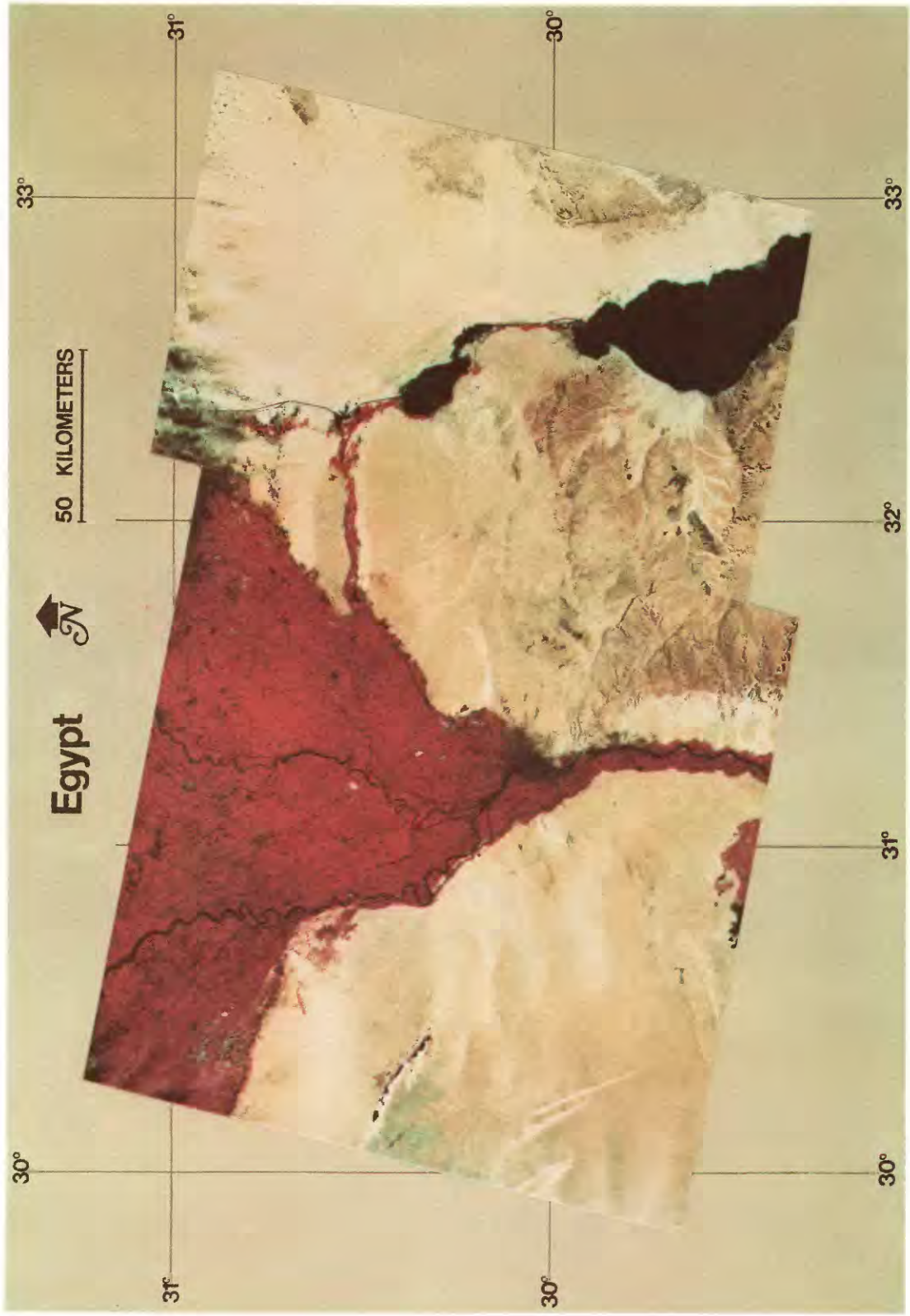

FIGURE 3.—Landsat-1 false-color mosaic of Egypt. Images 1236–07552, March 16, 1973, and 1165–08002, January 4, 1973.

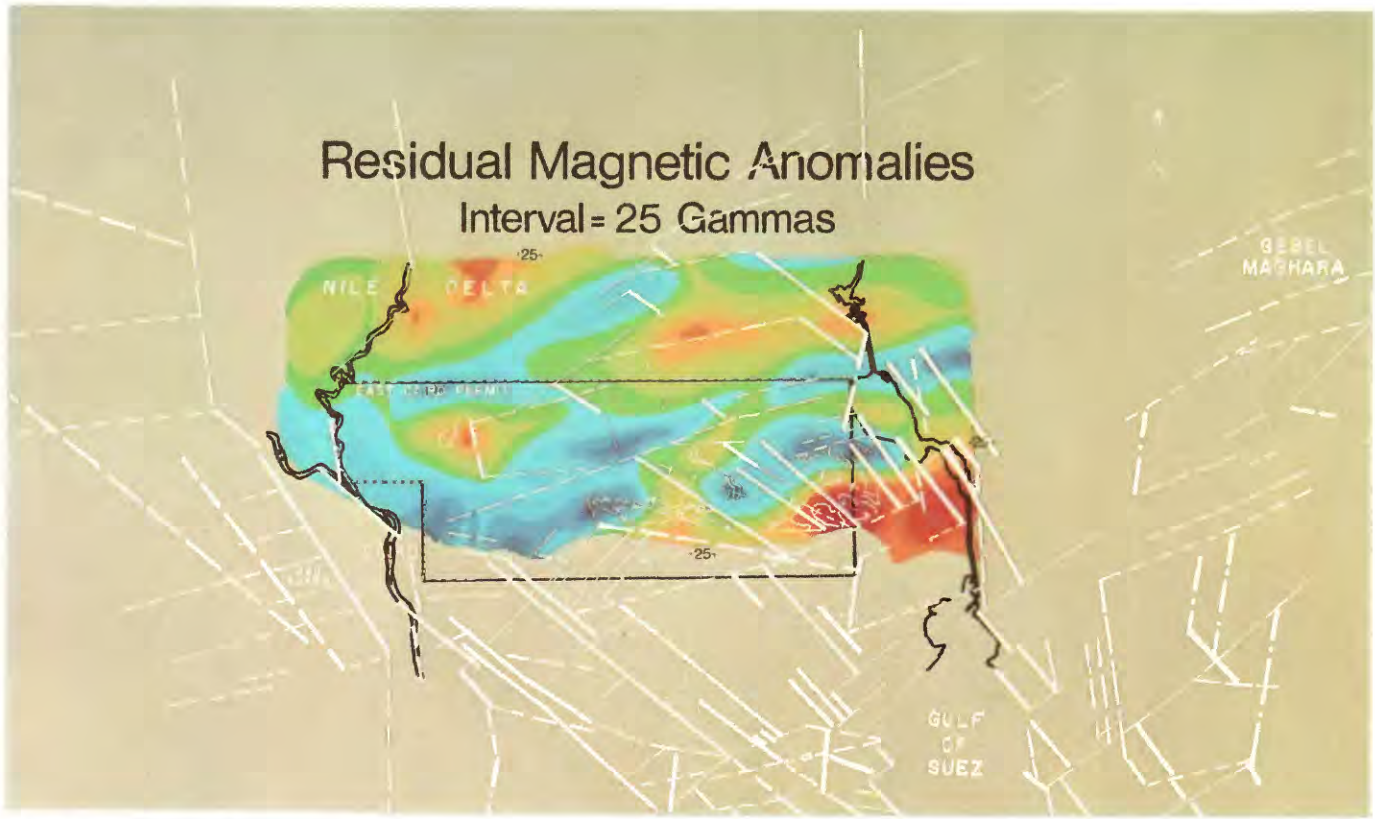

FIGURE 8.—Residual total magnetic intensity map with Landsat interpretation superimposed. The +25 gamma contour is at the division between yellow and green; values increase toward the warmer colors and decrease toward the cooler colors in 25-gamma increments.

BENTZ AND GUTMAN

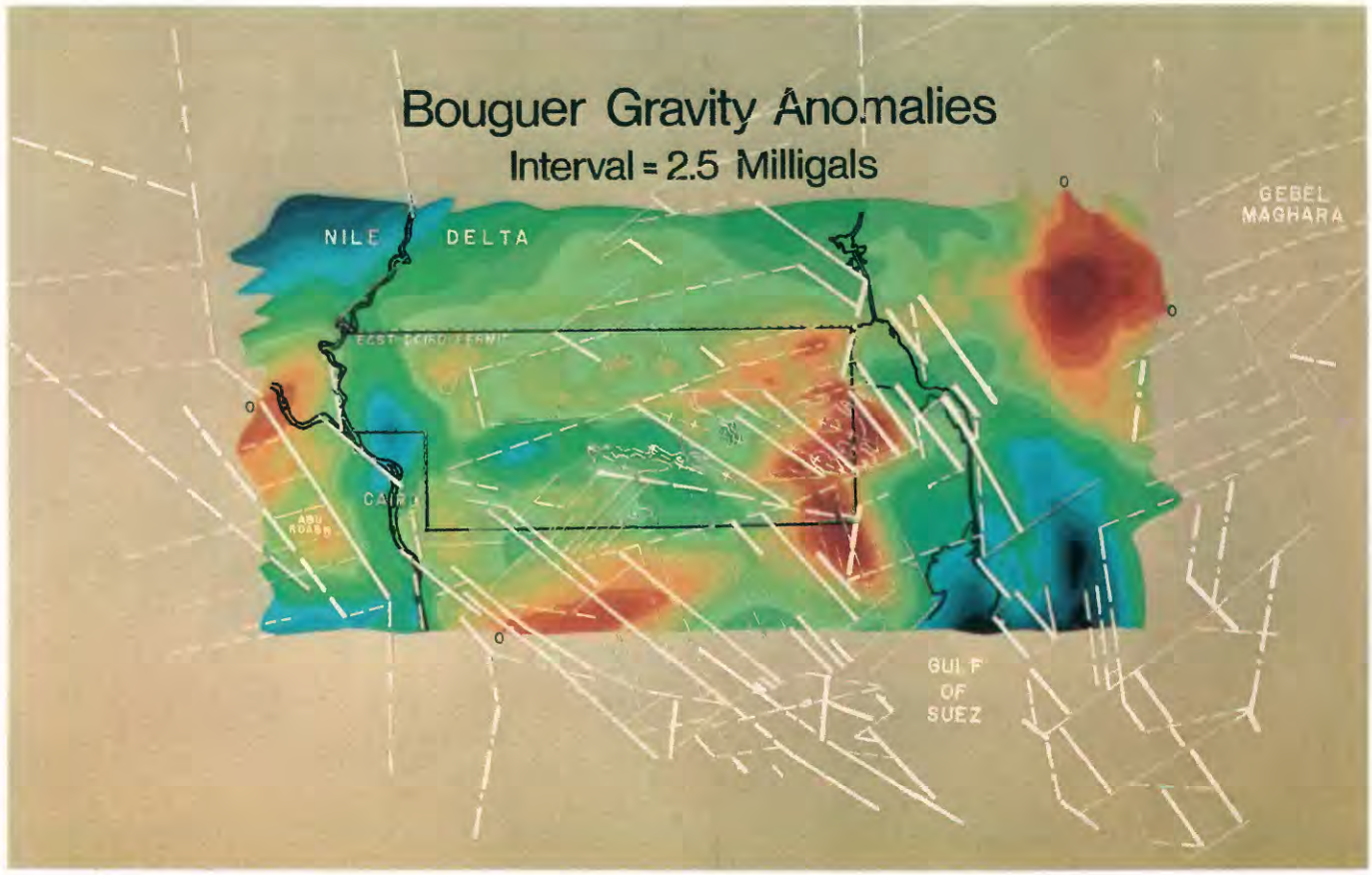

FIGURE 9.—Bouguer anomaly map with Landsat interpretation superimposed. The zero milligal contour is at the division between yellow and yellow-ochre; values increase toward the warmer colors and decrease toward the cooler colors in 2.5-milligal increments.

BENTZ AND GUTMAN

FIGURE 11.—Landsat–1 false-color mosaic of Yemen. Images 1082–07011, October 13, 1972; 1082–07013, October 13, 1972; 1117–06562, November 17, 1972; and 1117–06565, November 17, 1972.

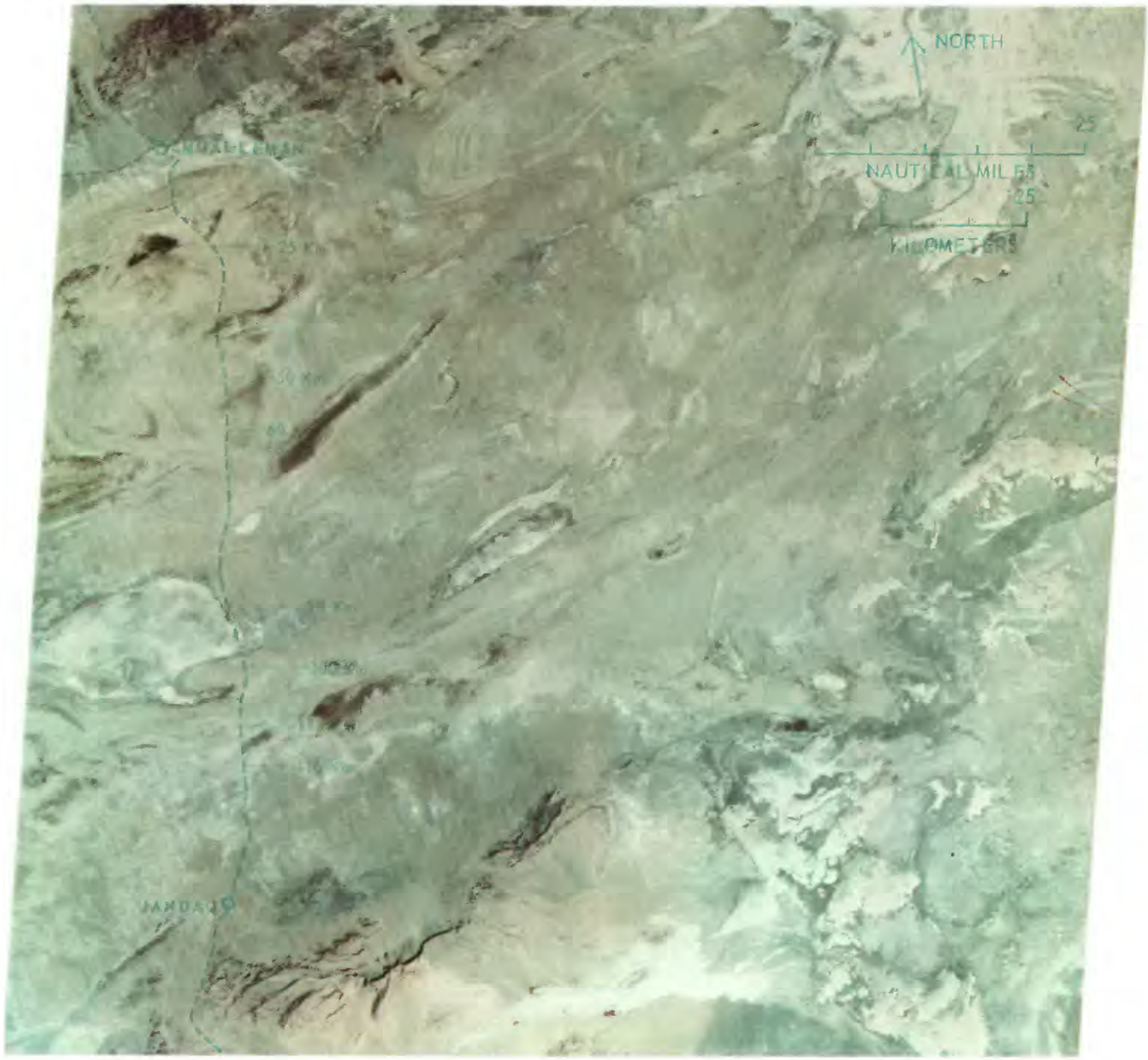

FIGURE 6.—Great Kavir, September 20, 1972; false-color composite of ERTS–1 image EDC–010015.

FIGURE 7.—Great Kavir, May 12, 1973; false-color composite of ERTS–1 image EDC–010019.

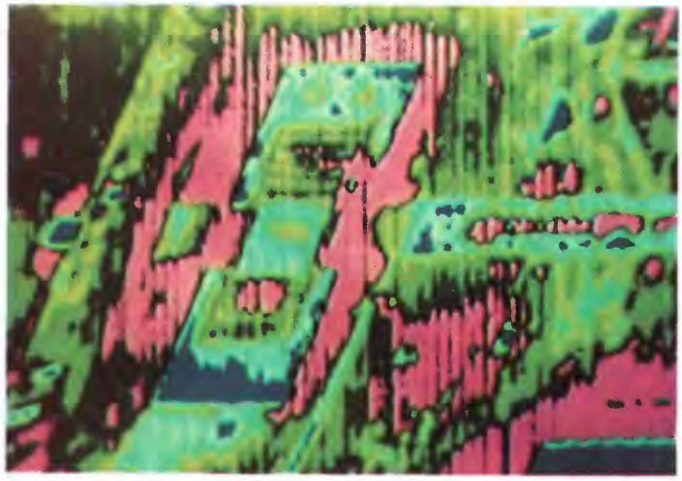

FIGURE 9.—Machine-aided enhancement of thermal-infrared imagery. (Daedalus Enterprises, Inc.)

EICHEN AND PASCUCCI

FIGURE 10.—Mineral occurrence overlay—synthesized overlay of analyses from Landsat aeromagnetic and gravimetric data.

EICHEN AND PASCUCCI

EXPLANATION

Black.—Swaths are known faults or coincidents of ERTS lineaments with aeromagnetic and gravity lineaments.
Circular areas denote intersections.

Blue.—Swaths are coincidents of ERTS lineaments with aeromagnetic or gravity lineaments.
Circular areas denote intersections.

Major through-going lineament system.

Light dots.—Areas of known mines.

FIGURE 12.—Composite map showing lineaments interpreted from Landsat (yellow), SLAR (red), and *U–2* (black) photography.

EICHEN AND PASCUCCI

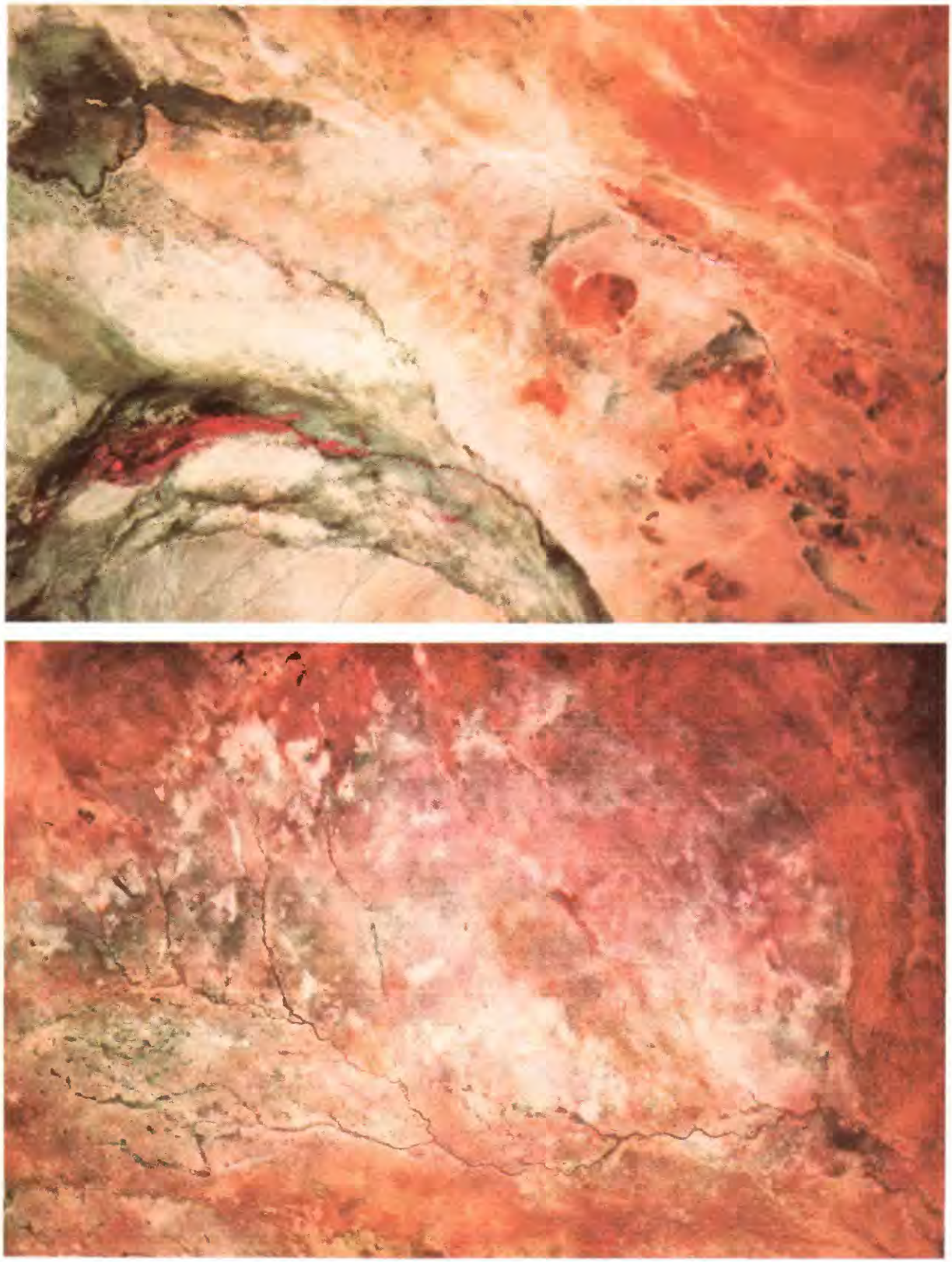

FIGURE 6*A* (above) and *B* (below).—The upper scene includes the area of the Ewaso N'Giro depression, the southern half of Landsat image 1190–07054. The Yamicha lava plateau lies at the extreme northwest corner. The lower scene is the area east of Wajir, including Anomaly A, the southern half of image 1189–07000. These color composites were made by combining a blue image of band 4, a green image of band 5, and red images of bands 6 and 7 on an additive-color viewer and copying the scenes on Ektachrome film. Location and true orientation shown on figure 8 (p. 150). Scale about 1:1,000,000.

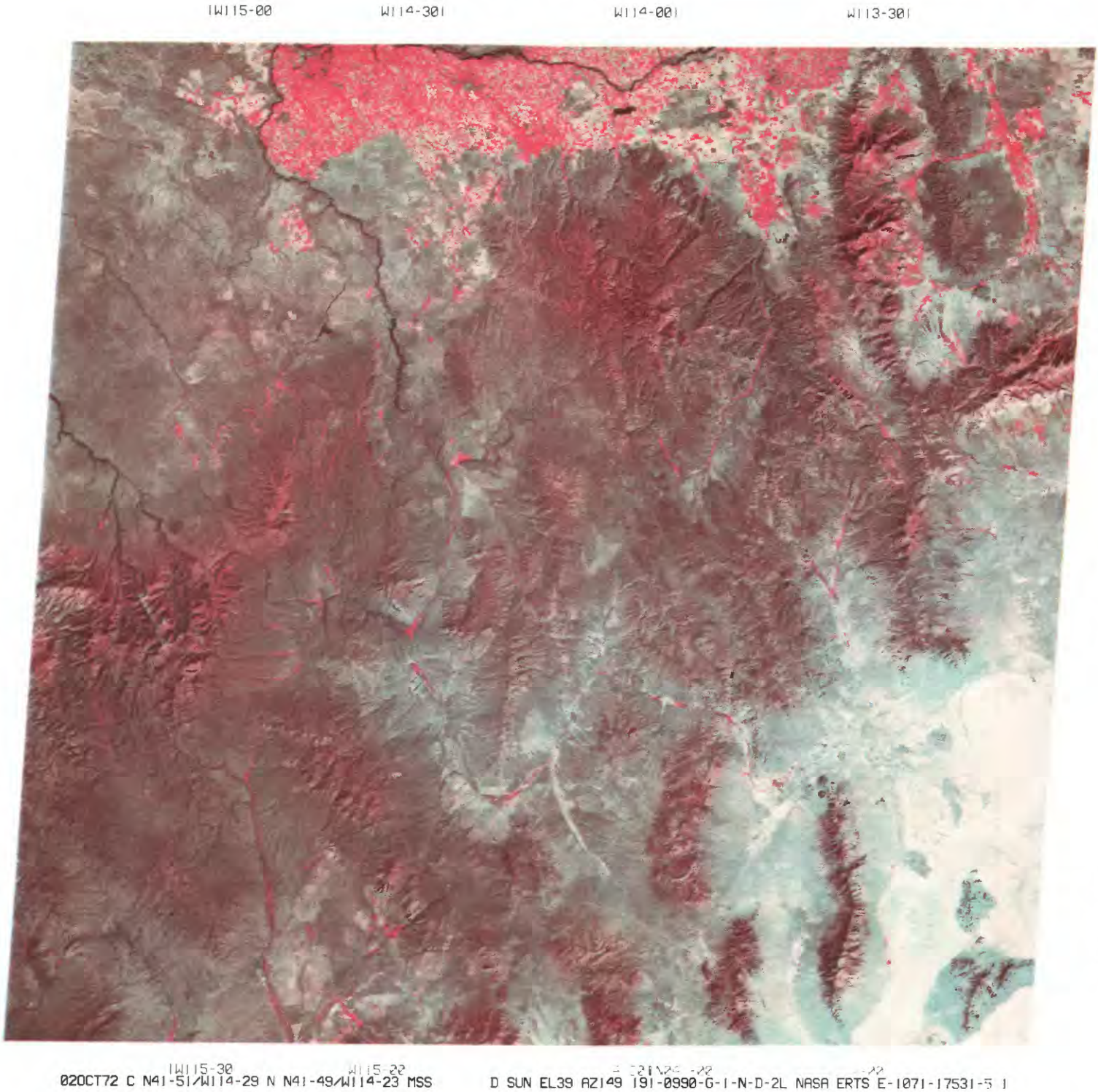

FIGURE 12.—False-color composite image of a Landsat scene of the region of the Great Basin south of Twin Falls, Idaho. Image 1071–17531, October 2, 1972.

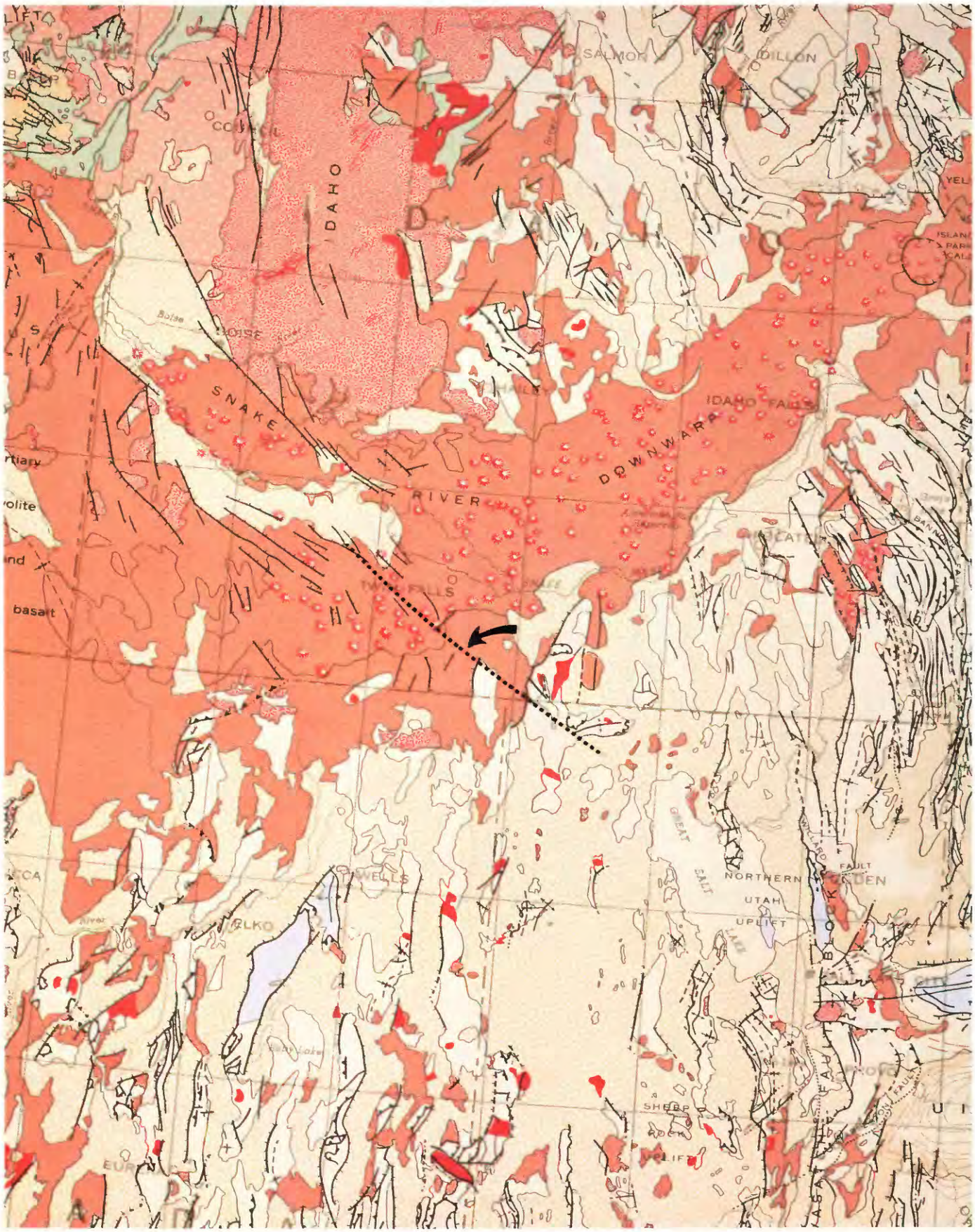

FIGURE 13.—Landsat lineament mapped to scale on "The Tectonic Map of the United States." (Modified from USGS and AAPG, 1961.)

FIGURE 6.—Simulated natural color Landsat image of the Nabesna quadrangle. Image made from mosaic of scenes 1692–20150 and 1692–20152 taken June 15, 1974.

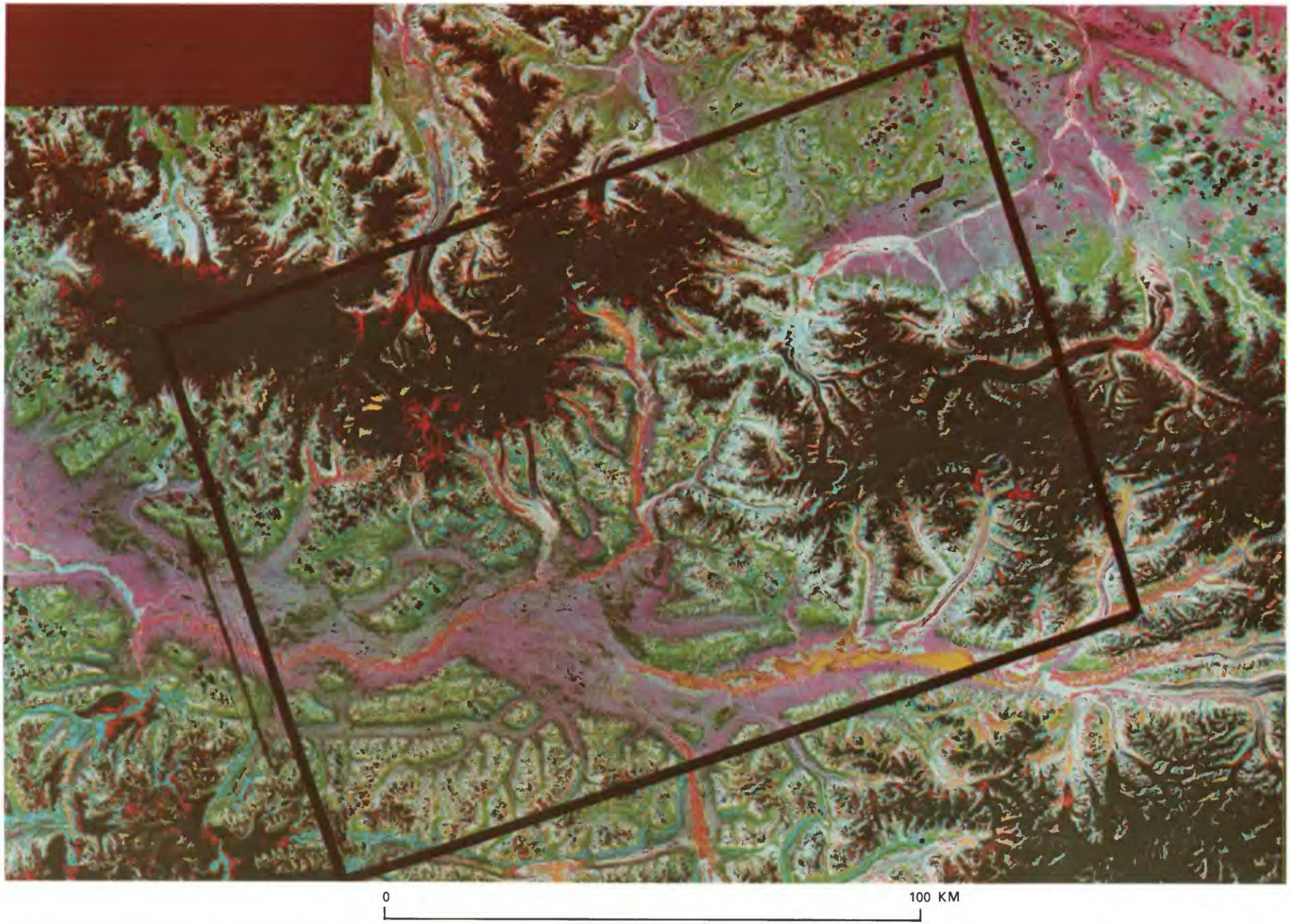

FIGURE 7.—False-color image with sinusoidal stretch of the McCarthy quadrangle. Images made from mosaic of scenes 1350–20223 taken July 8, 1973, and 1709–20090 taken July 2, 1974.

ALBERT AND CHAVEZ

FIGURE 8.—Color combination of HH (green) and HV (yellow) imagery near Freeport, Texas. Marshy areas which produce high HV returns appear yellow.

DELLWIG AND MOORE

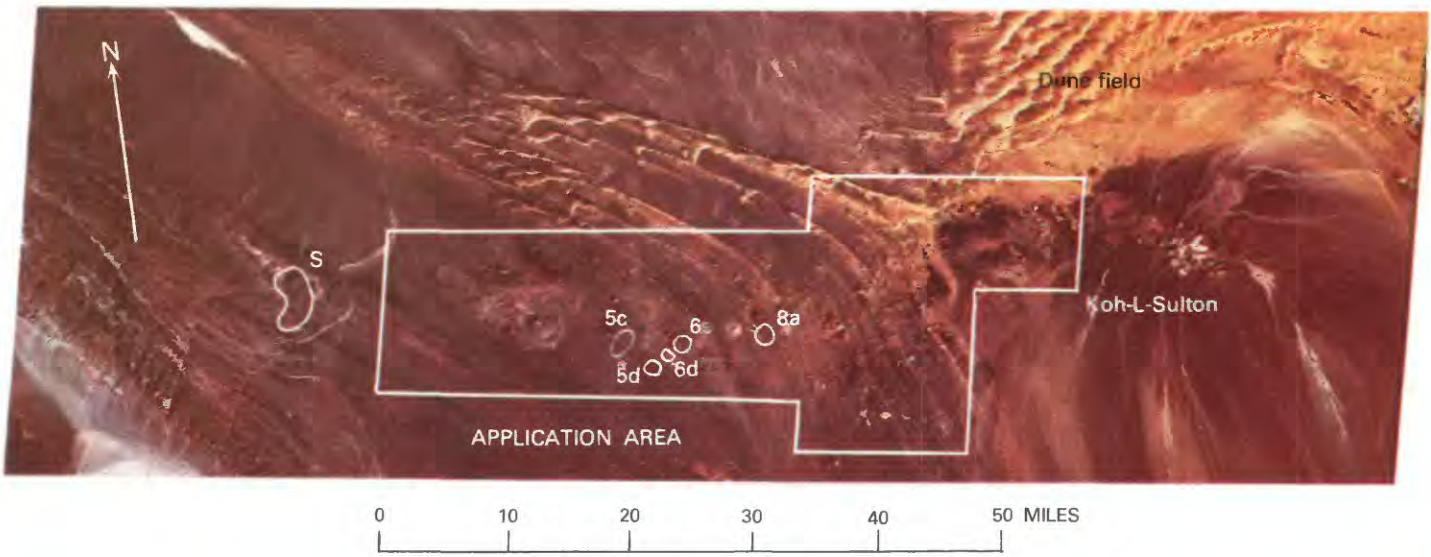

FIGURE 2.—Enhanced false-color composite of part of Landsat image 1125–05545. Location of the Saindak porphyry copper deposit is indicated by "S", new prospects located as a result of the digital processing experiment are shown at 5–c, 5–d, 6–d, 6–e, and 8–a. The light-toned patches at the crest of the volcano Koh-i-Sultan are altered rock resulting from fumarolic action.

SCHMIDT AND BERNSTEIN

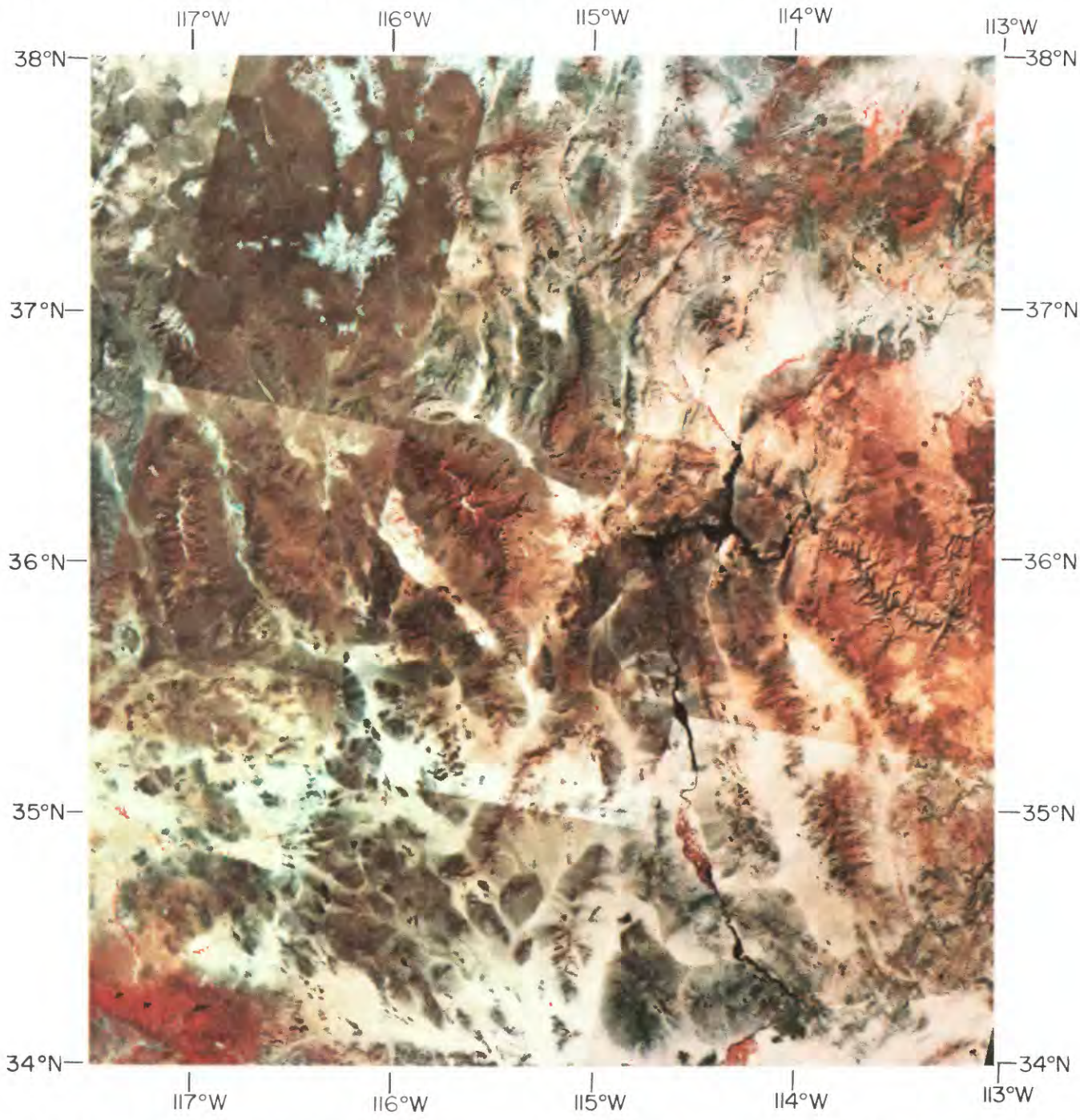

FIGURE 2.—False-color mosaic of 11 Landsat–1 MSS composites covering the area of study outlined in figure 1. Identification numbers for the frames used in this mosaic are shown in figure 3 (p. 255). See text for discussion of the MSS bands and printing filters used in producing the composites.

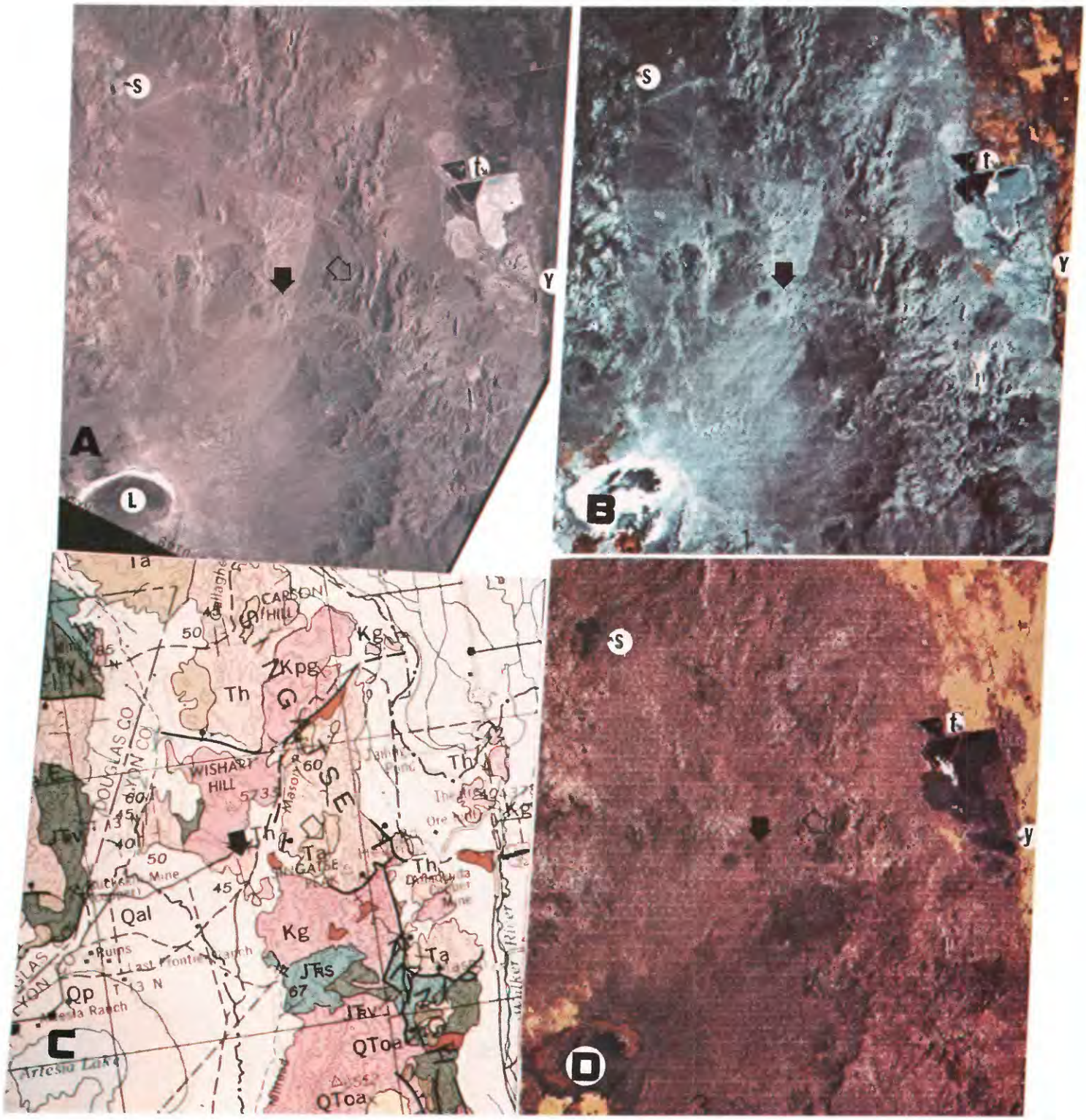

FIGURE 7.—Comparison of aerial photography (*A*), Landsat color image (*B*), Landsat color ratio image (*D*), and geological map (C), for Yerington, Nevada. The satellite materials are prepared directly from the CCT's. 7*A*, Ektachrome color print, taken from 20 km (RB 57, MX 248, August 11, 1973). 7*B*, Color infrared image made from CCT, 1397–18051, August 24, 1973, 13 days later than the aerial photograph; Dicomed print using digital data in an enhanced mode (note increased contrast). 7*C*, Published geological map (Moore, 1969). 7*D*; Color ratio image made from the same CCT data as for 7*B*, Dicomed print, using ratios R74, R64, and R54.

Note the similarity between the color patches on 7*D* and the geological patterns on the map, 7*C*, especially the areas of Ta (Alta volcanics)—open arrow, and Th (Hartford Hill volcanics)—solid arrow. Also Kg (granodiorite) and the porphyritic granodiorite (Kpg).

LYON

Geological studies by space means in the U.S.S.R.—Continued

PROCEEDINGS OF
THE FIRST ANNUAL WILLIAM T. PECORA MEMORIAL SYMPOSIUM
OCTOBER 1975, SIOUX FALLS, SOUTH DAKOTA

Opening Remarks to the First William T. Pecora Memorial Symposium

By Vincent E. McKelvey,
Director, U.S. Geological Survey

Governor Kneip, Dr. Overton, Ladies, and Gentlemen:

It is a great privilege for me to be able to open this First William T. Pecora Memorial Symposium. Bill Pecora was a remarkable man—a great scientist, a philosopher in the broadest sense of that term, and an inspiring leader. He considered himself to be a "field-boot" geologist and so characterized himself, as a matter of fact, in those terms in a speech here in 1970 when the EROS Data Center was still on the drawing board.

But while he was, indeed, an outstanding "field-boot" geologist, by taking the lead in forming the EROS Program and pressing hard for its development, he showed himself to be a visionary, both in his recognition of the possible applications of space technology to the study of the Earth, and of the need for it to help satisfy the requirement of a world pressing hard in the means of assessment.

Bill saw the rapidly accelerating needs for resources and for the preservation of environmental quality as well, and he saw the great potential in satellite observations for helping to provide the worldwide information needed to achieve both of those objectives. Much of Bill Pecora's vision has already been realized. NASA has provided the technology to acquire valuable satellite data, and the people of Sioux Falls, the Congress, and the Federal Administration have made it possible for the full community of scientists, technologists, and environmentalists to obtain and interpret and use the data through the Sioux Falls EROS Data Center. As papers here to be presented will show, new uses and applications of satellite imagery are being developed and formatted. Indeed, we have already had a glimpse of some of those applications in the description which Governor Kneip gave us of the activities already in progress here in the State of South Dakota.

Many people and organizations have contributed to these achievements, but naturally I am proud of the part which the Geological Survey and the Department of the Interior have played in bringing about a program that has fostered international relations and improved interorganizational and interdisciplinary exchange and communication and is adding to our understanding of the Earth and its resources. These contributions flowed from Bill Pecora's imaginative leadership, and it is fitting, indeed, that this Symposium be named in his honor.

A word, now, about the William T. Pecora Symposium. This is, of course, the first of what we hope will be a long series devoted to the exchange of experience and knowledge in the application of remotely sensed data. Because of Bill Pecora's great interest in mineral resources and because of the exciting progress being made in the applications of Landsat data to mineral exploration, it seemed appropiate to focus this First Symposium on mineral and mineral fuel exploration—and we are glad that the American Mining Congress was able to take the lead in sponsoring it.

The next Symposium will be primarily sponsored by the American Society of Photogrammetry and will be held here in Sioux Falls next August 23–27. The theme will be "Mapping with Remote Sensing," a topic fundamental to all resource and environmental efforts. We anticipate that subsequent symposia will address other themes, such as wildlife preservation, forestry, water resources, and others. The Survey has no desire to direct the content of these symposia, but we do pledge continued support to the interested scientific societies to make this a forum for the development and exchange of knowledge in keeping with the vision of a truly great man, William T. Pecora.

PROCEEDINGS OF
THE FIRST ANNUAL WILLIAM T. PECORA MEMORIAL SYMPOSIUM
OCTOBER 1975, SIOUX FALLS, SOUTH DAKOTA

International Implications of Landsat Data From a Geological Viewpoint

By John A. Reinemund,
U.S. Geological Survey, Reston, Virginia 22092

INTRODUCTION

It is indeed a privilege and an honor for me to have a part in this William T. Pecora Memorial Symposium on the applications of remote sensing to mineral and mineral fuel exploration. Although I am certainly no expert on remote sensing, I have been continuously involved in the international program of the U.S. Geological Survey for about 20 years and have been a fascinated observer of the impact remote-sensing technology has had, both in our own program and in overall cooperation between the nations of the world.

It seems especially fitting that we should discuss the international implications of Landsat data at a symposium honoring Dr. Pecora. Not only was he primarily responsible for the Survey's strong effort to develop an earth resources satellite system, in cooperation with the National Aeronautics and Space Administration (NASA), but he was also vitally interested in the potential applications of that system to international resources problems. His interest in the international applications was a logical outgrowth of his participation in the Survey's international program more than 30 years ago, when he assisted in surveys for strategic minerals in Latin America (Pecora, 1944; Pecora and Fahey, 1949, 1950; Pecora, Klepper, and others, 1950; Pecora, Switzer, and others, 1950). His enthusiasm for international cooperation, and his recognition of the mutual benefits to be gained from joint studies of geological phenomena, in cooperation with scientists abroad, were to a considerable extent responsible for the steady growth in the Survey's program in international geology and the strong emphasis on international applications of Landsat data which has characterized the Survey's efforts in remote sensing.

SIGNIFICANCE AND SCOPE OF THIS DISCUSSION

It is interesting to note that the problems with which Dr. Pecora and other Survey geologists (Dorr, 1944; Johnston, 1947) were primarily involved in their Latin American work 30 years ago—the international supply of critically needed mineral raw materials—is once again a subject of intense international concern. This concern has been partly responsible for the worldwide interest in Landsat applications. Geologists in the industrialized countries recognize the need to greatly accelerate the exploration and assessment of world resources to help meet their nations' future import requirements, and they look to Landsat data as an aid in this process. Their interest was reflected at the meeting of the European Geological Societies in Reading, England, last month when 10 percent of the 130 presentations dealt with Landsat applications to mineral investigations on five continents.

We here in the United States are also increasingly concerned, as discussed recently in a Conference on Requirements for Fulfilling a National Materials Policy (Promisel, 1974), for in the last 3 years our annual imports of energy and mineral raw materials have risen from about $4 billion or 11 percent of total needs to about $20 billion or 27 percent of total needs, and last year we imported more than half our requirements of 23 mineral commodities (Secretary of the Interior, 1975). But most developing countries are even more concerned with the need to increase

TABLE 1.—*Other countries for which Landsat data have been provided by the EROS Data Center*

Afghanistan	Denmark	Israel	Nepal	Spain
Algeria	Dominican Republic	Italy	Netherlands	Sudan
Argentina	Ecuador	Jamaica	New Zealand	Surinam
Australia	El Savador	Japan	Nicaragua	Swaziland
Austria	Ethiopia	Jordan	Niger	Sweden
Bangladesh	Finland	Kenya	Nigeria	Switzerland
Barbados	France	Khmer Republic	Norway	Taiwan
Belgium	Gabon	Korea	Pakistan	Tanzania
Bolivia	Gambia	Kuwait	Panama	Thailand
Brazil	Germany, East	Lebanon	Paraguay	Trinidad
Brunei	Germany, West	Lesotho	Peru	Tunisia
Bulgaria	Ghana	Liberia	Philippines	Turkey
Burma	Greece	Libya	Poland	United Arab Republic
Canada	Guatemala	Luxembourg	Portgual	United Kingdom
Central African	Guinea	Madagascar	Rhodesia	Upper Volta
Republic	Guyana	Malawi	Romania	Uruguay
Chile	Honduras	Malaysia	Saudi Arabia	U.S.S.R.
China	Hungary	Mali	Senegal	Venezuela
Colombia	Iceland	Mauritania	Sierra Leone	Yemen
Costa Rica	India	Mauritius	Singapore	Yugoslavia
Cyprus	Indonesia	Mexico	South Africa	Zaïre
Czechoslovakia	Iran	Morocco	South Vietnam	Zambia
Dahomey	Ireland			

worldwide resources exploration and assessment, because they not only compete for access to raw materials for their own internal needs but are faced with the necessity of increasing raw-material exports to pay for imports of food, manufactured goods, and technology. And it is in the developing countries, where mineral surveys are generally not well advanced, that the use of Landsat data can be especially helpful to accelerate mapping, improve existing maps, and identify geologic conditions favorable for mineralization.

So it is that at this critical time, when industrial and and developing countries alike are faced with the urgent need for intensified resources studies, that the Landsat system, along with other satellite and aircraft systems, offers a new, powerful, and challenging tool, the full dimensions of which have not yet been realized. The worldwide interest in this tool is evident from the number of articles, meetings, and projects that deal with it. In our Geological Survey program last year, for example, 58 scientists from 35 countries attended the two international courses given here at the EROS Data Center, and 127 scientists from 24 countries participated in seminars or workshops we conducted abroad. About 55 governments are currently sponsoring experimental applications of Landsat imagery, and most of these involve cooperation with one or more organizations in the United States. The EROS Data Center has supplied Landsat materials to 111 countries (see table 1), and already this year data for more than 50,000 Landsat frames have been purchased by private and governmental users for areas outside the United States.

In this discussion I do not propose to describe or illustrate in detail the specific applications of Landsat data that are, or may become, internationally important. Many excellent presentations to follow in this symposium will do this far better than I could. However, I would like to comment briefly on some significant applications of Landsat data in other countries, on the basis of the rapid growth in the international use of Landsat data, on the more significant benefits of participation in the Landsat program, and on constraints that could prevent the most effective use of this new technology.

SIGNIFICANT INTERNATIONAL APPLICATIONS OF LANDSAT DATA

Geologists around the world are focusing most of their attention, in one way or another, on three major problems: Accelerating and intensifying the exploration and assessment of resources, as mentioned previously; protecting and efficiently utilizing the environment; and minimizing the effects of natural disasters. Landsat data have important applications in each of these problem areas, and the papers that follow illustrate these applications. Many of the recent applications were reviewed in the Tenth International Symposium on Remote Sensing of Environment held in Ann Arbor, Michigan (Environmental Research In-

stitute of Michigan, 1975), earlier this month. An initial evaluation of economic value of these applications was made last year by Lietzke (1974).

With regard to resources exploration and assessment, the principal applications of Landsat data have been in accelerating the mapping of unexplored territory and in improving existing maps. The cooperative mapping of high-relief mountain provinces such as the Himalaya Mountains, the Alps (Bodechtel and Lammerer, 1973) and the Andean Cordillera (Carter, 1975), which will no doubt be illustrated later this morning by Dr. Carlos Brockmann, is especially significant because we have not previously been able to obtain synoptic and essentially distortion-free images of these provinces, which are so important for an understanding of mineral genesis. Equally significant is the application of Landsat data to study of the Precambrian shield areas, as has been described recently by Weecksteen (1974) for West Africa, Corrêa (1975) for Brazil, and Blodget, Brown, and Moik (1975) for Arabia. The use of Landsat multispectral techniques permits the identification and definition of contacts that are not readily located without the use of this new tool. And in studies currently underway, it has been possible to correlate the geology in the shield areas on the opposite sides of the Red Sea (Abdul-Gawad and Tubbesing, 1975) and to demonstrate the value of Landsat data characteristics in long-distance correlation of geologic units.

Extensive and highly significant revisions of structural maps are underway in many countries using Landsat imagery, and these are especially significant in prospecting for minerals and hydrocarbons. For example, a new map of Thailand is nearing completion as a joint effort by Prayong Angsuwathana of the Thai Department of Mineral Resources and S. J. Gawarecki of the U.S. Geological Survey, and a new map of Pakistan has been prepared by Kazmi [1] in which it has been possible to classify faults on age of movement.

A closely related and highly significant use of Landsat data in East Asia by Maurice Terman of the Geological Survey, as a contribution to a 35-nation cooperative Circum-Pacific Map Project (International Union of Geological Sciences, 1975), is in the evaluation of the relative accuracy of existing geologic maps. This demonstrates the value of Landsat data for checking geologic map accuracy as well as for improving and augmenting map detail.

[1] Kazmi, A. H., 1975, Application of ERTS–1 imagery to recent tectonic studies in Pakistan: Unpub. rept. prepared for the Geological Survey of Pakistan.

Perhaps no use of Landsat data has created more interest recently than the identification of major structural lineaments, many of which seem to be related to the distribution of minerals and hydrocarbons (Lathram and others, 1973; Saunders and Thomas, 1973). Several papers to be presented at this Symposium deal with this subject, and important work has been done in Australia and in several countries in Asia, South America, and North America. Some important known ore bodies, such as Broken Hill in New South Wales, seem clearly related to major lineaments, at least some of which reflect through-going structures of major dimensions in the continental crust. Agah (1975) has reported on lineaments across the Zagros Mountains in Iran that seem related both to facies changes in the sedimentary sequence and to hydrocarbon distribution. This line of research is of such widespread interest and importance that an international research project on correlation of structural data derived from satellite and other sources with distribution of known mineral deposits is now being considered under the International Geological Correlation Program jointly sponsored by the International Union of Geological Sciences and UNESCO.

An equally challenging use of Landsat data in the detection of ore deposits through digital-processing techniques is discussed in six presentations to follow, here in this Symposium. The work carried out by Schmidt in Pakistan is especially indicative of the impact and potential of Landsat data, when applied to a well-studied terrain, in which the extent and significance of the mineralization were much more apparent after digital processing of Landsat data. The technique of digital analysis to detect alteration in rocks and soil, and also changes in vegetation related to mineralization, may prove to be one of the most important applications for accelerating mineral exploration.

Geologists concerned with environmental studies and surficial phenomena are having spectacular success with Landsat data. The work of McKee and others (McKee and others, 1973; McKee, 1975), for example, in worldwide studies of sand seas, provides a basis for classification and evaluation of environmental changes in the principal desert areas that could not readily be made without Landsat data. In a recent study of Landsat applications in the Sahelian zone in Africa, Cooley and Turner (1975) demonstrated the usefulness in identifying and mapping laterite duricrust, locating areas favorable for ground water, classifying land for agricultural potential, and many other highly significant uses. A series of environmental studies using Landsat data is being

carried out cooperatively by Egyptian and United States scientists (Galal, 1975), and similar programs are underway or planned in several other African countries. Mapping effects of tin mining in shallow-water offshore areas has proved feasible using Landsat data along the coast of Malaysia; the United Nations is now studying the environmental effects of strip mining of tin on land in that country by use of Landsat data, comparable to studies of mining areas in the United States (Wier and others, 1973; Chase and Pettyjohn, 1973; Alexander and others, 1973). George Taylor of the Geological Survey, using Landsat data in western Brazil, identified an alluvial fan of such huge dimensions—half as big as the State of Iowa—that it has never before been recognized. The work in Iran to be described by D. B. Krinsley later in this Symposium, is an outstanding example of the application of the data in the interpretation of dry lake deposits, monitoring of desert environments, and engineering planning in areas typical of vast arid regions in the developing countries.

A most promising and significant application of the Landsat system is for the monitoring of natural disasters and the development of early warning systems, especially of flood and volcanoes. A recent study by Robinove (1975) on behalf of the Agency for International Development (AID) has demonstrated the excellent possibilities for using Landsat imagery in damage assessment for floods, drought, fire, and glacier movement, and the possible uses of the Landsat Data Collection System in warning of the danger of floods, earthquakes, volcanic eruptions, glacier movements, and water pollution. Monitoring of seismicity associated with volcanism (Ward and others, 1973) which is now underway in Central America, the United States, Alaska, Hawaii, and Iceland, using a total of 18 data collection platforms relaying through Landsat, may be prototype of a worldwide satellite volcanic monitoring system. The applicability to assessment of flood damages has already been demonstrated through studies of flooding in the Mississippi Valley and in Pakistan, and it is likely that programs of flood warning, monitoring, and damage assessment, using the Data Collection System and satellite imagery, will eventually be established in the world's major river systems, assuming an operational satellite system is established. Such a flood warning and assessment system may, in fact, be an adequate justification for an operational earth-resources satellite system.

BASIS FOR GROWTH IN INTERNATIONAL USE OF LANDSAT DATA

It seems pertinent to examine the basis for the remarkable growth in the use of Landsat data around the world. As I noted previously, this growth reflects the recognized value of the Landsat applications in the attack on major problem areas in geology and in other earth-science disciplines. But what are the special conditions under which international participation in the Landsat program has flourished, and what can we learn about the possibilities of future participation from a study of these conditions?

In my opinion the widespread use of Landsat data is mainly a result of three actions: The decision to develop Landsat as an international system with open participation in its use; the establishment of facilities and procedures here at the EROS Data Center for worldwide distribution of the data; and the efforts that have been made to transfer knowledge of Landsat technology to other countries.

The fundamental basis for the development of Landsat as an operational system has, of course, been the United States' insistence on unrestricted availability of the data and on international cooperation in its use. The United States position was reaffirmed by Dr. Kissinger on August 11 in Montreal when he stated:

> Earth-sensing satellites . . . can dramatically help nations to assess their resources and to develop their potential. In the Sahel region of Africa we have seen the tremendous potential of this technology in dealing with natural disasters. The United States has urged in the United Nations that the new knowledge be made freely and widely available. . . . While we believe that knowledge of the earth and its environment gained from outer space should be broadly shared, we recognize that this must be accompanied by efforts to insure that all countries will fully understand the significance of this new knowledge.

The United States position was also defined more specifically with regard to the Landsat system earlier this month at Ann Arbor by Dr. Leonard Jaffe of NASA (Jaffe, 1975).

From the geological viewpoint, the NASA program of sponsoring cooperative research projects with scientists in other countries, to experiment with applications of Landsat data, has been of tremendous importance. Many of the presentations to follow contain results of those projects. Thirty-six countries participated in 95 cooperative research projects with Landsat–1 data, of which 54 projects involved geoscience applications, and 35 countries are participating in 39 projects with Landsat–2 data, of which 30 involve the geological sciences.

This NASA-sponsored program has not only demonstrated uses of the data and encouraged the participation of foreign scientists, but it has also given other countries a feeling of mutual involvement in the development of a new technology—a feeling that they are genuine participants and not mere bystanders. And it is interesting to note that, in most of the countries participating actively in the Landsat program, geological agencies have been very active. In fact, in about 40 percent of the 55 or so countries sponsoring Landsat applications, geological or mapping agencies are the lead agencies in Landsat cooperation.

Most important to continuing and practical use, in my opinion, is the availability of the data at modest cost through the EROS Data Center here in Sioux Falls. This has revolutionized the planning of geologic programs around the world; for, except in areas of persistent cloud cover, it has given national and international agencies, private industry, and research institutions alike an assured source of data in a variety of formats and a facility to which they could turn with their problems. This availability of data, and guidance, will be vastly expanded, of course, as regional receiving stations and distributing facilities are established to augment those now operating in four countries and as national information centers are developed such as those already established in 17 Latin American countries through the joint efforts of the Inter-American Geodetic Survey (IAGS), the U.S. Geological Survey, and local country agencies (table 2).

TABLE 2.—*Other countries having existing or planned facilities using the Landsat system.*

Data receiving and distribution stations			
Existing			Planned
Canada			Chile [1]
Brazil			Iran
Italy			Zaïre
Data information centers			
Latin America			Other
Argentina	Dominican Republic	Panama	Thailand
Brazil	Ecuador	Paraguay	Indonesia
Bolivia	El Salvador	Peru	Iran
Chile	Guatemala	Venezuela	Italy (Food and Agriculture Organization)
Colombia	Honduras	Uruguay	Pakistan
Costa Rica	Nicaragua		Turkey

Data collection platforms			
Canada	33		Hydrometeorology studies.
Iceland	2		Volcano and earthquake studies.
Guatemala	7		do.
Nicaragua	4		do.
El Salvador	1		do.

[1] Agreement formalized after this Symposium was held.

And the use of Landsat data has also been intensively fostered, of course, by the efforts to transfer remote-sensing technology to other countries through various means. AID has played an important role in sponsoring seminars abroad and participant training here at the EROS Data Center. The U.S. Geological Survey, mainly on behalf of AID, has helped conduct six seminars or workshops in Asia and the Far East, attended by more than 350 participants from 25 countries, and four seminars in Africa attended by 200 participants from 16 countries (table 3). In addition, the Survey, in cooperation with IAGS, has helped conduct seven seminars or workshops in Latin America involving several hundred participants from virtually all Latin American countries, including, earlier this year, an initial workshop in the use of the Landsat Data Collection System. The Survey has now conducted five international training courses here at Sioux Falls involving about 135 participants from 40 countries. These activities have been augmented by the ten Symposiums on Remote Sensing of the Environment sponsored by the Environmental Research Institute of Michigan and by the meetings of Landsat investigators sponsored by NASA.

TABLE 3.—*Landsat regional seminars and workshops in which the U.S. Geological Survey has been involved*

	Asia and Far East
1971____	Seminar/workshop on remote sensing in Southwest Asia, at Ankara, Turkey.
1972____	Seminar/workshop on remote sensing in Southwest Asia, at Tehran, Iran.
1973____	Seminar on remote sensing in East Asia, at Bangkok, Thailand.
1973____	Seminar/workshop on remote sensing in East Asia, at Manila, Philippines
1974____	Seminar/workshop on remote sensing in East Asia, at Bangkok, Thailand.
1975____	Seminar/worksohp on remote sensing in East Asia, Lahore, Pakistan.
	Africa
1973____	Seminar/workshop on remote sensing in the Sahelian zone, at Bamako, Mali.
1974____	Seminar/workshop on remote sensing in East Africa, at Nairobi, Kenya.
1975____	Seminar/workshop on remote sensing in West Africa, at Bamako, Mali.
1975____	Seminar on remote sensing in West Africa, at Accra, Ghana.
	Latin America (cooperative with Inter-American Geodetic Survey in Panama).
1971____	First training course in remote sensing.
1972____	Second training course in remote sensing.
1972____	Remote sensing course for Latin America.
1973____	Third training course in remote sensing.
1973____	First Pan-American Symposium on Remote Sensing.
1974____	Workshop on multiband image manipulation and resource interpretation.
1975____	Workshop on Data Collection System.

The United Nations has also contributed to the transfer of Landsat technology by sponsoring worldwide meetings, such as one held earlier this year in Canada, and regional meetings to review the progress on the use of the data (Chipman, 1975). It is especially gratifying to note the beginnings of technology transfer in Brazil, where the Brazilian Space Agency (INPE), in cooperation with the Committee on Space Research, conducted a meeting last year on space applications of direct interest to developing countries. It was attended by 28 scientists from 17 nations.

INSTITUTIONAL BENEFITS OF PARTICIPATION IN THE LANDSAT PROGRAM

I have already mentioned the advantages of using Landsat data in accelerating the exploration and assessment of resources, protecting and utilizing the environment, and minimizing the effects of natural disasters, which are in themselves an adequate justification for encouraging the widespread use of the Landsat system. But I believe there are additional benefits also for institutions and programs that participate in the use of Landsat data, especially in the developing countries. These may be summarized as follows:

1. *More systematic observation and interpretation of resources data:* As the Landsat data are systematic and multispectral, their use encourages standardization in handling, processing, and interpretation procedures, as well as for more penetrating study than has commonly been applied to aerial photography. Proper use of the data imposes a discipline on the geologist that will probably (and hopefully) carry over into all aspects of his work.
2. *Increased knowledge and use of data-processing techniques:* Because the Landsat data are computerized, their use provides an opportunity to demonstrate the techniques and advantages of data processing and perhaps to hasten the use of data processing in handling other types of geologic data.
3. *Development of photoreproduction and distribution capacity:* In order to provide data for multiple uses and to permit the visual analysis of multispectral imagery, photoreproduction and distribution capability must ultimately be developed in user countries or in regional data centers. For example, Thailand has now developed such capability and is serving the needs of its own agencies and of the Mekong countries. This capability provides a basis also for issuing multicolor photo maps, such as the gridded image map of the Thailand Central Plain issued last month by the National Research Council of Thailand.
4. *Better planning and monitoring of programs:* It is now routine practice in many countries to utilize Landsat images for planning projects and plotting the progress of surveys or installations.

5. *Promotion of interdisciplinary coordination and interagency contacts:* Because Landsat data are applicable to nearly all earth-science disciplines, most user countries have found it expedient to develop interagency coordinating mechanisms. In Thailand, for example, a National Committee, operating under the National Research Council, has been established to coordinate the Landsat program involving participants from 24 agencies and universities. A similar body functions vigorously in Turkey. This type of mechanism results in much closer coordination between agencies than existed previously.
6. *Promotion of international cooperation:* The many symposiums, seminars, workshops, and data-exchange mechanisms that are based on Landsat applications have provided a vast acceleration in earth-science cooperation and a new community of international remote-sensing specialists. As regional data centers and receiving stations are established, the process of cooperation will be advanced further and regularized.

It should not be inferred that these institutional and program benefits inevitably follow whenever a country uses Landsat data, but I think it is fair to say that developing countries participating extensively in the Landsat program have generally realized most or all of these peripheral benefits.

POTENTIAL CONSTRAINTS ON FUTURE USE OF LANDSAT DATA

In closing my remarks, I call your attention to possible constraints on the widespread and effective use of Landsat data in international geology, which we must seek to avoid. It would indeed be a tragedy if for various reasons we do not fully develop and utilize this magnificent technology to help with the major worldwide problems of geology and other earth sciences, and I feel that we should keep these possible constraints in mind.

Within the developing countries, the effective use of Landsat data in the future will depend on sustaining the initial interest that has been aroused because the technology is new and promising and avoiding bureaucratic controls that restrict and stifle the use of the data. The experience with the introduction of aerial photography in developing countries several decades ago shows that once the initial enthusiasm was dissipated, the use of photography by local geologists and agencies became very desultory, undisciplined, and nondefinitive. Moreover, in many countries, use of photography was restricted by bureaucratic red tape and lack of interagency cooperation. Unfortunately, these same tendencies are already appearing in some countries and could prevent the full use of Landsat data.

Another potential constraint is the failure to complete the transfer of remote-sensing technology to the developing countries. Few developing countries are using the Landsat data adequately even in simple photographic mode; even fewer countries make effective use of the multispectral characteristics of the Landsat data, and scarcely any have the capacity for digital analysis that we now realize has such high potential. Yet already there are signs of weakening in the programs for training and transfer of technology, and too little emphasis is being given to assistance in the fundamental problems of establishing national institutions and programs that can take full advantage of remote-sensing technology. It is at least as important that international cooperation complete the process of technology transfer as that it fully explore the potential scientific applications of the Landsat system.

And finally, and perhaps of greatest concern, is the possible failure to continue moving forward toward a fully operational earth resources satellite system, either because of political and security restrictions on the operation of the system or because of failure to provide adequate funds for building the system. Having demonstrated the great value of satellite data in geology and other earth sciences, it would indeed be a tragedy if we could not develop a fully operational satellite system, with a full complement of ground receiving stations, multipurpose satellites, adequately distributed data collection platforms, and data distribution centers. Such a failure would be ironic in view of the newly evident need for greatly intensified exploration and assessment of world resources that was, I think, a major factor in the original concept of Landsat as visualized by Dr. Pecora.

It may be appropriate here to recall the words of the Honorable Harlan Cleveland, Director of International Affairs for the Aspen Institute, at a recent Conference on the Role of Professional Associations in an Interdependent World, in Washington. He said:

> We are gathered here because in one way or another we want to be leaders in coping with interdependence. If each of us merely says what he or she came to say and departs, we will miss a great opportunity. To match the macroproblems we face together, we need to build an international consortium of the concerned, a community of continouus consultation about the human purpose our miraculous techniques and our professional practices are going to serve. . . . If we miss this chance, here or soon, we who presume to leadership will deserve that devastatingly snide comment of Giraudoux: 'The privilege of the great is to watch catastrophe from a terrace'.

I submit that promoting effective development and utilization of the Landsat and other satellite systems for use in attacking major problem areas in geology may be one way to help avoid watching catastrophe from a terrace.

REFERENCES

Abdul-Gawad, M., and Tubbesing, L., 1975, Identification and interpretation of tectonic features from ERTS–1 imagery of southwestern North America and the Red Sea area: Natl. Tech. Inf. Service Rept. No. E75–10291, NASA–CR–142835, 190 p.

Agah, S., 1975, Geological application of ERTS–1 imagery in the National Iranian Oil Company for geological mapping and prospect evaluation: Central Treaty Organ., Workshop on the Application of Remote Sensing Data and Methods, Lahore, Pakistan, Preprint, Mar. 1–8, 1975, 3 p.

Alexander, S. S., Dein, J., and Gold, D. P., 1973, The use of ERTS–1 MSS data for mapping strip mines and acid mine drainage in Pennsylvania: Goddard Space Flight Center Symposium on Significant Results Obtained from Earth Resources Technology Satellite–1, New Carrollton, Md., March 5–9, 1973, v. 1, Tech. Presentations, Sec. A, p. 569–576.

Blodget, H. W., Brown, G. F., and Moik, J. G., 1975, Geological mapping in northwestern Saudi Arabia using LANDSAT multispectral techniques: Natl. Aeronautics and Space Admin., Goddard Space Flight Center Rept. X–923–75–206, August 1975, 21 p.

Bodechtel, J., and Lammerer, B., 1973, New aspects of the tectonics of the Alps and the Apennines revealed by ERTS–1 data: Goddard Space Flight Center Symposium on Significant Results Obtained from Earth Resources Satellite–1, New Carrollton, Md., March 5–9, 1973, v. 1, Tech. Presentations, Sec. A., p. 493–500.

Carter, W. D., 1975, Mineral resource investigations in South America using Landsat data: Michigan Environmental Research Inst., Internat. Symposium on Remote Sensing of Environment, 10th, Ann Arbor, October 6–10, 1975, Summaries, p. 146.

Chase, P. E., and Pettyjohn, W., 1973, ERTS–1 investigation of ecological effects of strip mining in eastern Ohio: Goddard Space Flight Center Symposium on Significant Results Obtained from Earth Resources Technology Satellite–1, New Carrollton, Md., March 5–9, 1973, v. 1, Tech. Presentations, Sec. A, p. 561–568.

Chipman, Ralph, 1975, International and regional approaches to remote sensing for development: Michigan Environmental Research Inst., Internat. Symposium on Remote Sensing of Environment, 10th, Ann Arbor, Oct. 6–10, 1975, Summaries, p. 209.

Cook, J. J., and Istvan, L. B., 1975, A cursory survey of the status of remote sensing activity for earth resources surveys and environmental monitoring in developing countries: Michigan Environmental Research Inst., paper commissioned for Nat. Acad. Sci. Committee on Remote Sensing Development, 10 p.

Cooley, M. E., and Turner, R. M., 1975, Applications of ERTS products in range and water management problems, Sahelian Zone, Mali, Upper Volta, and Niger: U.S. Geol. Survey Open-File Report 75–46, 68 p.

Corrêa, A. C., 1975, A regional mapping program and mineral resources survey based on remote sensing data: Michigan Environmental Research Inst., Internat. Symposium on Remote Sensing of Environment, 10th, Ann Arbor, Oct. 6–10, 1975, Summaries, p. 151.

Dorr, J. V. N. 2nd., 1944, Foreign work by the Geological Survey, U.S. Dept. of Interior [abs.]: Econ. Geology, v. 39, no. 1, p. 90.

Environmental Research Institute of Michigan, 1975, Tenth International Symposium on Remote Sensing of the Environment, Oct. 6–10, 1975: Ann Arbor, Michigan Environmental Research Inst.—Univ. Michigan Extension Service, Summaries, 209 p.

Farhoudi, G., 1975, ERTS photograph interpretation of Kazerun area (Iran): Central Treaty Organization Seminar on the Application of Remote Sensing Technology to Natural Resources Development, Lahore, Pakistan, Preprint, Mar. 2–9, 1975, 11 p.

Galal, Salah, 1975, Remote sensing in Egypt: Nature, v. 256, no. 5515, July 24, p. 252.

International Union of Geological Sciences, 1975, Geological Newsletter: Internat. Union Geol. Sci. Quart. Jour., v. 1975, no. 2, June 30, p. 169–171.

Jaffe, Leonard, 1975, International interests in Landsat data: Michigan Environmental Research Inst., Internat. Symposium on Remote Sensing of Environment, 10th, Ann Arbor, Oct. 6–10, 1975, Summaries, p. 31.

Johnston, W. D., Jr., 1947, The U.S. Geological Survey in other American republics: U.S. Dept. State Record, v. 3, no. 2, p. 8–14; Washington Acad. Sci. Jour., v. 37, no. 10, p. 376.

Lathram, E. H., Tailleur, I. L., Patton, W. W., Jr., 1973, Preliminary geologic applications of ERTS–1 imagery in Alaska: Goddard Space Flight Center Symposium on Significant Results Obtained from Earth Resources Technology Satellite–1, New Carrollton, Md., March 5–9, 1973, v. 1, Tech. Presentations, Sec. A., p. 257–264.

Lietzke, K. R., 1974, The economic value of remote sensing of earth resources from space: an ERTS overview and the value of continuity of service: v. 7, Nonreplenishable Natural Resources: Minerals, Fossil Fuels, and Geothermal Energy Sources: Natl. Tech. Inf. Service Rept. No. N75–14212 5WN, NASA–CR–141264 Rept. 74–2002–10, v. 7, 85 p.

McKee, E. D., 1975, The study of sand seas on a global scale: Mich. Environmental Research Inst., Internat. Symposium on Remote Sensing of Environment, 10th, Ann Arbor, Oct. 6–10, 1975, Summaries, p. 134.

McKee, E. D., Breed, C. S., and Harris, L. F., 1973, A study of morphology, provenance, and movement of desert sand seas in Africa, Asia, and Australia: Goddard Space Flight Center Symposium on Significant Results Obtained from Earth Resources Satellite–1, New Carrollton, Md., March 5–9, 1973, v. 1, Tech. Presentations, Sec. A, p. 291–304.

National Aeronautics and Space Administration, 1975, Aeronautics and space report of the President: 1974 activities: Washington, U.S. Govt. Printing Office, p. 76–77.

Pecora, W. T., 1944, Nickel-silicate and associated nickel-cobalt-manganese oxide deposits near Sao José do Tocantins, Goiáz, Brazil: U.S. Geol. Survey Bull. 935–E, p. 247–305, pls. 44–50, figs. 12–14, [in Portuguese] in collaboration with A. L. M. Barbosa, Brazil Div. Fomento Produçao Mineral Bol. 64, 69 p., 1944.

Pecora, W. T., and Fahey, J. J., 1949, The Corrego Frio pegmatite, Minas Gerais—scorzalite and souzalite, two new phosphate minerals: Am. Mineralogist, v. 34, no. 1–2, p. 83–93.

Pecora, W. T., and Fahey, J. J., 1950, The lazulite-scorzalite isomorphous series: Am. Mineralogist, v. 35, no. 1–2, p. 1–18.

Pecora, W. T., Klepper, M. R., Larrabee, D. M., Barbosa, A. L. M., and Frayha, Resk, 1950, Mica deposits in Minas Gerais, Brazil: U.S. Geol. Survey Bull. 964–C, p. 205–305, pls. 14–17, figs. 6–38.

Pecora, W. T., Switzer, George, Barbosa, A. L. M., and Myers, A. T., 1950, Structure and mineralogy of the Golconda pegmatite, Minas Gerais, Brazil: Am. Mineralogist, v. 35, no. 9–10, p. 889–901.

Promisel, N. E., 1974, International problems and opportunities: a role for the technical societies and many others, *in* Huddle, F. P., ed., Requirements for fulfilling a national materials policy: U.S. Congress Office of Technology Assessment, Engineering Found. Conf., Henniker, New Hampshire, Aug. 11–16, 1974, Proc., p. 79–84.

Robinove, C. J., 1975, Disaster assessment and warning with Landsats: Michigan Environmental Research Inst., Internat. Symposium on Remote Sensing of Environment, 10th, Ann Arbor, Oct. 6–10, 1975, Summaries, p. 116.

Saunders, D. F., and Thomas, G. E., 1973, Evaluation of commercial utility of ERTS–A imagery in structural reconnaissance for minerals and petroleum: Goddard Space Flight Center Symposium on Significant Results Obtained from Earth Resources Satellite–1, New Carrollton, Md., March 5–9, 1973, v. 1, Tech. Presentations, Sec. A, p. 523–530.

Secretary of the Interior, 1975, Mining and minerals policy: Annual Report under the Mining and Minerals Policy Act of 1970: Washington, U.S. Govt. Printing Office, 63 p.

Ward, P. L., Eaton, J. P., Endo, E., Harlow, D., Marquez, D., and Allen, R., 1973, Establishment, test, and evaluation of a prototype volcano-surveillance system: Goddard Space Flight Center Symposium on Significant Results Obtained from Earth Resources Satellite–1, New Carrollton, Md., March 5–9, 1973, v. 1, Tech. Presentations, Sec. A, p. 305–316.

Weecksteen, Guy, 1974, Structural geology investigation in the Republics of Dahomey and Togoland, Africa, using ERTS–1 multispectral images: Natl. Tech. Inf. Service Rept. No. E75–10237, NASA–CR–142425, 22 p.

Wier, C. W., Wobber, F. J., Russell, O. R., and Amato, R. V., 1973, Fracture mapping and strip mine inventory in the Midwest by using ERTS–1 imagery: Goddard Space Flight Center Symposium on Significant Results Obtained from Earth Resources Technology Satellite–1, New Carrollton, Md., March 5–9, 1973, v. 1, Tech. Presentations, Sec. A, p. 553–560.

PROCEEDINGS OF
THE FIRST ANNUAL WILLIAM T. PECORA MEMORIAL SYMPOSIUM,
OCTOBER 1975, SIOUX FALLS, SOUTH DAKOTA

NASA Plans for Future Earth Resources Missions

By William Nordberg,
NASA Goddard Space Flight Center, Greenbelt, Maryland 20771

ABSTRACT

Landsats have proven that Earth observations from space are capable of providing information which is useful in a number of applications that are of vital concern to society. These applications include the management of food, water, and fiber resources; exploration and management of energy and mineral resources; and protection of our life-sustaining environment.

However, in order to fully satisfy the needs for such applications, it will be necessary to: improve the present satellites and sensors, extract useful information from these observations more quickly and reliably, and improve the mechanism by which this information is transferred to end users.

A number of developments are now underway to improve sensors and observing systems. They include the third Landsat, to be launched in 1977, which will make high resolution images of surface temperatures to improve crop, other vegetation, and soil classifications. A Heat Capacity Mapping Mission (HCMM) is also planned for 1977 to map surface temperatures at hours of maximum and minimum heating. It is expected that soil moisture patterns, and soil or rock compositions, can be distinguished better with such a satellite than with Landsats which do not scan the Earth at times that are optimum for this purpose. A Thematic Mapper is now under development to make Earth surface images with a radiometric accuracy of about 0.5 percent in six spectral bands and with a spatial resolution of about 30–40 m. This instrument could be used for Earth observations by 1980; however, a satellite mission to fly this Thematic Mapper has not yet been approved.

Automatic identification and classification methods are being developed to extract information such as crop and forage acreages, amounts of runoff, and types of land use directly from the satellite observations. A number of Applications Systems Verification Tests are being conducted particularly in the areas of crop and land-use inventory and runoff prediction to demonstrate the direct transfer of space-acquired information to end users.

When speaking about plans for the future, it is not only desirable, but, I believe, also necessary to look back at one's accomplishments in order to establish the basis on which future developments can be, and should be, based. In the area of surveying the Earth's resources and environment from space, we can look back upon a very solid basis, indeed, which provides us with a clear understanding of the objectives and needs for future developments.

For more than a decade, weather satellites have made global observations of atmospheric and Earth surface conditions which could be applied to a better understanding of geophysical processes involving Earth resources and the environment. Recently, Landsats have proven that Earth observations from space are capable of providing information that is of vital concern to society; namely, for the management of food, water, and fiber resources, for the exploration and management of energy and mineral resources, and for the protection of our life-sustaining environment.

From this experience, we have learned that in the future it will be necessary to concentrate on three general activities:

1. To improve our spaceborne observing and measuring techniques, in order to make them more specific to the applications which they will be designed to achieve.
2. To provide for ground-based facilities and to organize ground operations such that specific useful information can be extracted more rapidly and more reliably than is now possible with the highly experimental Landsats.
3. To improve the mechanism by which the information that results from satellite observations filters down to the end-users and is integrated, not only in their day to day operations, but also in their planning and budget considerations.

This last aspect of our planning depends not only on past technical achievements and on the soundness of our technological approach to the future, but it also depends very strongly on economic and political considerations. I am very much concerned that our most diligent and competent technical plans for future Earth-observing systems will be fruitless and doomed to fail if users are not willing to make the necessary investments and commitments to reap the benefits of this new technology.

Let us now take a brief look at the present state of Earth resources and environmental surveys from space. Table 1 summarizes the types and purposes of both satellites that are now operating and satellites that are being built to firm launch schedules. Thematic maps can now be obtained, at least theoretically, every 9 days, of anywhere in the world (outside a circle of 10 degrees around each pole) with the two Landsats that are in orbit. These maps can be obtained from the images acquired by Landsats–1 and –2 in four spectral bands of reflected solar radiation along swaths 185 km wide. But, Landsat–1, which was 3 years old in July 1975, can transmit data only directly to receiving stations; it cannot store pictures on its tape recorders anymore. Therefore, observations every 9 days are possible only where such receiving stations exist. This is the case for North America, via three stations in the U.S. and one in Canada; over South America, via a Brazilian station; and over Europe and North Africa, via a station in Italy. Direct transmissions of observations over Southwest Asia, Southeast Europe, and Northeast Africa will soon be possible via a station that is being procured by Iran. A station to be located in Zaïre will cover most of the remainder of Africa. Interest in such receiving stations has also been expressed by a variety of additional countries, so that thematic mapping every 9 days using two Landsats is expected to cover increasingly large areas of the world. Other areas, which are not within range of such receiving stations, must depend on the data stored on the tape recorders that still function on Landsat–2. Such coverage occurs, of course, much less frequently; namely, one to several times per year, depending on interest expressed by people in these areas.

In addition, observations relating to earth resources management and environmental protection are available from the operational weather satellite system that is maintained by the National Oceanic and Atmospheric Administration (NOAA). Aside from continuous observations of cloud formations and atmospheric temperature soundings for the purpose of weather

TABLE 1.—*Earth resources and environmental survey satellites, operating and in preparation*

Operating as of October 1975:	
Landsat–1, 1972	4–band thematic.
Landsat–2, 1975	Mapping (80–m resolution).
NOAA–3, 1973	Sea surface temperature.
NOAA–4, 1974	Ice and snow (optical, 1–km resolution).
Nimbus–5 and -6, 1972 and 1975	Sea ice (microwave, 30–km resolution).
SATELLITE TRACKING	Continuous gravity field.
In preparation:	
Landsat–C, 1977	4–band thematic mapping (80–m resolution).
	Thermal mapping (200–m resolution).
	Panchromatic imaging (40–m resolution).
APPLICATIONS EXPLORER–A, 1977	"Heat capacity" mapping (500–m resolution).
Nimbus–G, 1978	Ocean color and temperature (500–m resolution).
	Sea ice and sea state.
	Air pollution.
Seasat–A, 1978	Sea ice and sea state.
TIROS–N, 1978	Global atmosphere and sea surface observations.

forecasting, these satellites also provide global maps of surface temperatures and images of snow and ice cover in the visible and infrared spectrum with about 1-km resolution. NOAA–3 and –4 are operating now, and, as soon as one of these satellites fails, it will be replaced by a new one, to keep two in operation at all times.

Microwave sensors on Nimbus–5 have mapped the extent and, to a cetrain degree, the structure of polar sea ice and of the Greenland and Antarctic ice sheets, since December 1972.

Another significant geophysical result was obtained through tracking more than 30 satellites during the last 10 years. Analyses of perturbations of the orbits of these satellites have made it possible to determine the Earth's gravity field on a global scale with a spatial resolution that would be economically prohibitive by any other means.

Now, I should like to turn to our plans for the immediate future. These involve satellites and missions which are being readied for launch during the next few years. Our highest priority is to supplement the thematic mapping, which has been so eminently successful with the first two Landsats, with images of surface temperatures. The multispectral scanner, which will be flown on the third Landsat in 1977, will include a fifth band to measure and image radiation emitted by the Earth's surface in the 10.5- to 11.5-μm wavelength range. It is expected that surface temperature maps with a spatial resolution of about 200 m can be obtained from these measurements. Adding this temperature mapping capability to the Landsat system is expected to improve significantly our capability of classifying crops, vegetation, and soils.

Experiments conducted with Skylab and with aircraft flights have shown that for some applications, higher spatial resolutions than those of Landsat–1 and –2 are desired, especially for urban land-use mapping and for the detection of transient phenomena. The Return Beam Vidicon (RBV) cameras which have seen very little use with Landsats–1 and –2 will be reconfigured for this purpose on Landsat–C. Instead of three cameras in three spectral bands, two panchromatic cameras will be used to cover the same 185-km-wide swath that the multispectral scanner (MSS) covers, but the cameras will provide twice the spatial resolution of the MSS, namely about 40 m.

The potential of deriving soil moisture and surface composition information for both agricultural and hydogeological purposes, is being further pursued with the socalled "Heat Capacity Mapping Mission" (HCMM), which is expected to fly on the first applications explorer satellite in 1977. In contrast to the observatory class spacecraft of the Nimbus or Landsat type, which carry many or very complex instruments, each applications explorer will carry only one relatively simple instrument. The HCMM, for example, will only carry a 10.5- to 11.5-μm temperature mapping radiometer, with a spatial resolution of about 500 m. For reference purposes, a visible radiation channel of the same spatial resolution will also be included. The advantage of such a mission is that the orbital characteristics can be chosen to suit one and only one objective. In this particular case, the objective is to map surface temperatures at hours of maximum and minimum heating; that is, during early afternoon and early morning hours.

The surface temperature extremes, measured at those times, will provide a better indication of the heat capacity of the ground than the Landsat–C temperature maps which must be obtained at mid-morning and late evening in order to accommodate the other four spectral bands. It is expected that soil moisture patterns and soil or rock compositions can be distinguished better with the HCMM mission than with Landsat. Coverage with the HCMM will be such that each area of the Earth will be observed at least once every week during consecutive morning and afternoon passes from which heat capacity determinations will be attempted. Data can be read out only via direct transmission to ground stations and the format of the transmissions will be compatible with Landsat data acquisition stations.

Probably the last of the big, complex Earth-viewing observatories before the advent of Spacelab will be Nimbus–7 (called Nimbus–G before launch). Aside from making such measurements as the global radiative energy budget, solar ultraviolet radiation, and global ozone distributions for the purpose of continuously monitoring these important environmental parameters, Nimbus–G will demonstrate the feasibility of monitoring air and water pollution from space. Inferences concerning water quailty, including nutrient content will be attempted from measurements of water color with a coastal zone color scanner (CZCS). The scanner will map water surfaces in six spectral bands ranging from shortwave blue to the near-infrared with a spatial resolution of about 500 m. In contrast to Landsat images, these measurements will be conducted in spectral bands which are particularly sensitive to the signatures of various water characteristics, such as sedimentation, chlorophyll, various types of pollutants, and bottom features. It is expected that observations in all major coastal zones of the world will be made twice every week with the CZCS on Nimbus–G. Test flights of the Nimbus CZCS on a

U–2 aircraft over the N.Y. bight, have shown clearly the dumping of acid wastes by barges and the drift patterns of the resulting pollution. Similar aircraft tests were conducted with *U–2*'s off the west coast of Florida to determine the feasibility of detecting and mapping the occurrence of red tides with Nimbus–G.

Both Nimbus–G and Seasat will continue the monitoring of sea ice with microwave sensors. But, in contrast to Nimbus–5 and –6, the passive microwave sensor on Nimbus–G and on Seasat will provide simultaneous images at five different wavelengths with spatial resolutions ranging from 25 km at the short wavelengths to 200 km at the longest wavelength. In addition to ice mapping, these observations will also permit the measurement of sea state and sea surface temperature, regardless of cloud cover. Seasat–1 will also carry an imaging radar for the purpose of sea state and sea ice observations; however, because of data handling limitations on this satellite, it appears very unlikely that substantial amounts of radar observations will be made by Seasat over land surfaces.

The TIROS–N system to be placed in operation in 1978, is intended to improve the operational observations now made with the NOAA satellites and will include perhaps even such environmental monitoring as sea ice, solar radiation, and atmospheric composition.

Now, I should like to turn to the missions which are not yet in preparation but which we think will be absolutely necessary to provide the information that is needed for efficient earth resources management and environmental planning (table 2). We believe that the key to Landsat follow-on missions will be the development of a new thematic mapper. This instrument would perform measurements with greater radiometric accuracy than the MSS on Landsat. Six spectral bands will be more appropriately placed and afford greater spatial resolutions than the MSS. The spatial resolution will be 30–40 m in all but the surface temperature measuring bands, and a radiometric accuracy of about 0.5 percent is expected to be achieved. A spectral band in the near-infrared range around 1.6 μm would be included. This band is particularly important for agricultural and vegetation surveys. We are planning to initiate the full development of this instrument during the next fiscal year. However, a satellite mission to fly this Thematic Mapper has not yet been approved.

Another significant part of the planning for Landsat follow-on missions must be the redesign and reorganization of the data acquisition, information extraction, and data utilization scheme. Landsat–1 and –2 observations had been analyzed for a great variety of purposes by many hundreds of individual investigators in more than 40 countries. Many governmental organizations, especially in the U.S., Canada, and Brazil, have applied these observations as aids to their operations, such as sea and lake ice surveys, preparations of environmental impact statements, runoff predictions, flood potential assessments, updating or improvement of navigational charts and geological and general purpose maps, especially in sparsely populated or rapidly changing areas. In addition, several tens of thousands of individuals and organizations from all over the world have ordered Landsat data for their private purposes from the EROS Data Center in Sioux Falls. However, all of this happened many months or even years after the observations had been taken. The present Landsat data processing and information extraction scheme is not suited for efficient operational applications. For follow-on systems we cannot use the mail to ship raw data tapes from outlying data acquisition stations such as Alaska and California to a central processing station. In fact, we must decentralize the conversion process from raw data tapes to image tapes or hard copies, to the greatest extent possible. This will be facilitated by an all digital processing system. Worldwide data will be transmitted from the satellite to the U.S. via a tracking and data relay satellite and local data should be acquired by direct transmission to acquisition stations which should be placed to cover all major land masses of the Earth.

TABLE 2.—*Earth resources and environmental survey satellites, planned and in prospect*

Planned:	
Landsat–D, 1980	Thematic mapper.
Applications Explorer–C (Magsat), 1980	Magnetic survey.
Prospected—mid–1980's:	
Seasat follow-on	Sea state, icebergs, and ocean currents.
Climate Monitoring	Land use, radiation budget, and stratosphere.
Shuttle/Spacelab Experiment	Radar surveys.
Gravsat	Gravity field surveys.
SEOS	Geosynchronous environmental surveys.

In the U.S., data should be distributed via efficient communications links to decentralized processing stations which would generate those images, and apply those information extraction algorithms, that are suited to their patricular applications. Those who must acquire and process data in real time for operational purposes must now work with NASA and help plan the data acquisition, processing, and information extraction schemes for Landsat follow-on systems.

We are also planning another applications explorer mission for Earth survey purposes. The third such mission, to be launched in 1980, is planned to carry sensors to map the magnetic field of the Earth. Measurements with the Orbiting Geophysical Observatory (OGO), almost 10 years ago, have proven the feasibility of extracting latitudinal and longitudinal variations of the solid Earth magnetic field from orbital magnetometer measurements. Similar measurements from a Magsat, which would be designed specifically to map the field of the solid Earth, would be much more accurate and provide higher resolution than the OGO measurements. The results would serve to improve our understanding of the crustal structure of the planet, if not provide supplementary information for geophysical exploration.

Beyond Landsat follow-on and the Magsat missions, all our plans are highly speculative and not even in the firm proposal stage. In table 2, they are summarized as prospective missions. They include the possible survey of ocean conditions, such as sea ice, sea state, hazards to navigation, oil spills, and marine resources on an operational basis. Undoubtedly, satellites will have to be flown to make observations that are necessary to monitor and detect climate trends. Such observations include the survey of land use and concomitant albedo changes. The Spacelab on the "Shuttle" space transportation system will provide an inexhaustable facility for testing new observing techniques, particularly Earth survey radars. A set of sattelites whose orbital motions will be critically monitored, may be used to make an accurate survey of the Earth's gravitational field. Finally, the ultimate Earth survey test might be a Synchronous Earth Observing Satellite (SEOS) which would provide essentially continuous observations of Landsat quality, over almost an entire hemisphere.

In conclusion, I should like to note that our technical base for planning future Earth-observing missions is well established. Our objectives for future missions are highly focussed and the technical feasibility of the missions we are planning, and those that we are dreaming about is clearly demonstrated. The hard facts of life are, however, that in today's environment, neither the best and most competent technical planning nor the most dedicated enthusiasm will suffice.

What is needed is an unequivocal concensus that the new systems which we are planning and which we wish to implement are not only feasible, but are also beneficial. This consensus must particularly include those who are considered the utlimate beneficiaries, namely, the end-users of this new technology. The broader this consensus is and the stronger commitments are made on the part of the users, the sooner we can expect that our plans and hopes for such new systems will be fulfilled.

PROCEEDINGS OF
THE FIRST ANNUAL WILLIAM T. PECORA MEMORIAL SYMPOSIUM,
OCTOBER 1975, SIOUX FALLS, SOUTH DAKOTA

Application of Remote Sensing (Landsat Data) to Petroleum Exploration

By Michael T. Halbouty,
Consulting Geologist and Petroleum Engineer, Houston, Texas 77056

ABSTRACT

The Landsat project is the most significant mission ever flown by NASA. The program has afforded the opportunity for the mineral and energy industries in the United States to improve the Nation's domestic resource base in a shorter time and at a more reasonable cost than would have been possible without the Landsat data.

Properly interpreted information from these images could save corporations millions of dollars in unnecessary exploration and development efforts and at the same time provide possible geologic clues which could lead to the discovery of tremendous reserves. The more the Landsat data are used, the more innovations for their use will be established.

Landsat data have broad use in the minerals/fuel field, including the following general applications:

1. Detection of large-scale geologic structures that were previously unknown and which may be significant with respect to the localization of hydrocarbons. Such features are commonly not recognizable on traditional aerial photographs.
2. The possible detection of very subtle tonal anomalies that may represent alteration of the soils resulting from mini-seeps of gas from hydrocarbon reservoirs.
3. The potential for detecting natural marine oil seeps with consequent improvement in efficiency of offshore exploration.
4. Detection of outcrops of important minerals and metals, especially in hostile environments.
5. The monitoring of ice distribution and movement in Arctic areas, such as may affect transport of materials in and out of the Arctic, the cost of seismic exploration in arctic sea ice areas, and the safety of exploration and production operations.
6. The monitoring of oilfield development and transport facilities, such as the Alaskan pipeline and an assessment of this development upon the environment.
7. The potential for improved communication and decisionmaking within petroleum companies.

The proper use of Landsat imagery affords the explorationist a most rapid and inexpensive tool which could add immeasurably to his existing geological knowledge.

PROCEEDINGS OF
THE FIRST ANNUAL WILLIAM T. PECORA MEMORIAL SYMPOSIUM,
OCTOBER 1975, SIOUX FALLS, SOUTH DAKOTA

Landsat Application to Resource Exploration and Gas Planning

By Dr. Carlos E. Brockmann,
Director, Landsat/Bolivia
Servicio Geologico de Bolivia, La Paz, Bolivia

ABSTRACT

The Bolivian Landsat Program is a multidisciplinary research project aimed at developing the applications and use of Landsat, Skylab, and other remote-sensing imagery for the inventory and development of the natural resources of Bolivia. Under our Petroleum Exploration Subprogram, preliminary studies are being undertaken for the general delineation of the potential petroleum areas on the Chaco-Beni Plain at the margin of the Brazilian Shield. By interpretation of the morphology and drainage of the region, we were able to define the presence of anticlines that will be subject to verification by seismic exploration.

Under the Mining Exploration Subprogram, a direct relation was found to exist in the morphostructural zones of the Cordillera and the Altiplano (Highlands) between the faulting and settling of the igneous bodies from which mineralization has originated. Tonal anomalies, geomorphology, and structural features have defined potential areas for mineral prospecting.

Interpretations of Landsat imagery, Skylab photos and photoindexes enabled the selection of several alternatives in the design of the route of the proposed Santa Cruz-Puerto Suárez gasline. The proposed alternative routes are not as long as the existing railroad length. At the present time standard elevation, distance and bearing surveys of the proposed routes have not been made.

INTRODUCTION

The Bolivian Government is interested in obtaining basic and necessary information on the natural resources of the country, and for this reason Landsat and Skylab remote-sensing data are being actively evaluated and used.

The Bolivia Landsat Program was created in order to make proposed multidisciplinary studies with the participation of the Geological Service of Bolivia, Yacimientos Petrolíferos Fiscales Bolivianos (National Oil Company) and Bolivia Mining Corporation (COMIBOL), the principal institutions that conduct research in geology, soils, forestry, and land use; studies are also being undertaken in agronomy in coordination with the Ministry of Agriculture. Hydrologic work is accomplished jointly with the Meteorologic and Hydrologic Service, and the Military Geographical Institute is in charge of the cartographic research.

Due to the success obtained from the developed research activities, the Bolivia Landsat Program is now systematically conducting operational work in different zones of the country.

GEOLOGIC PROVINCES IN BOLIVIA

There are six geologic provinces in Bolivia from east to west as follows (fig. 1):

I. Brazilian Shield.
II. Chaco-Beni Plain.
III. Subandes Belt.
IV. Eastern and Central Cordillera.
V. Altiplano (Highlands).
VI. Western Cordillera.

I. Brazilian Shield

The Brazilian Shield is located in the eastern section of the country; it is considered to be a gently sloping erosion surface that has an average altitude

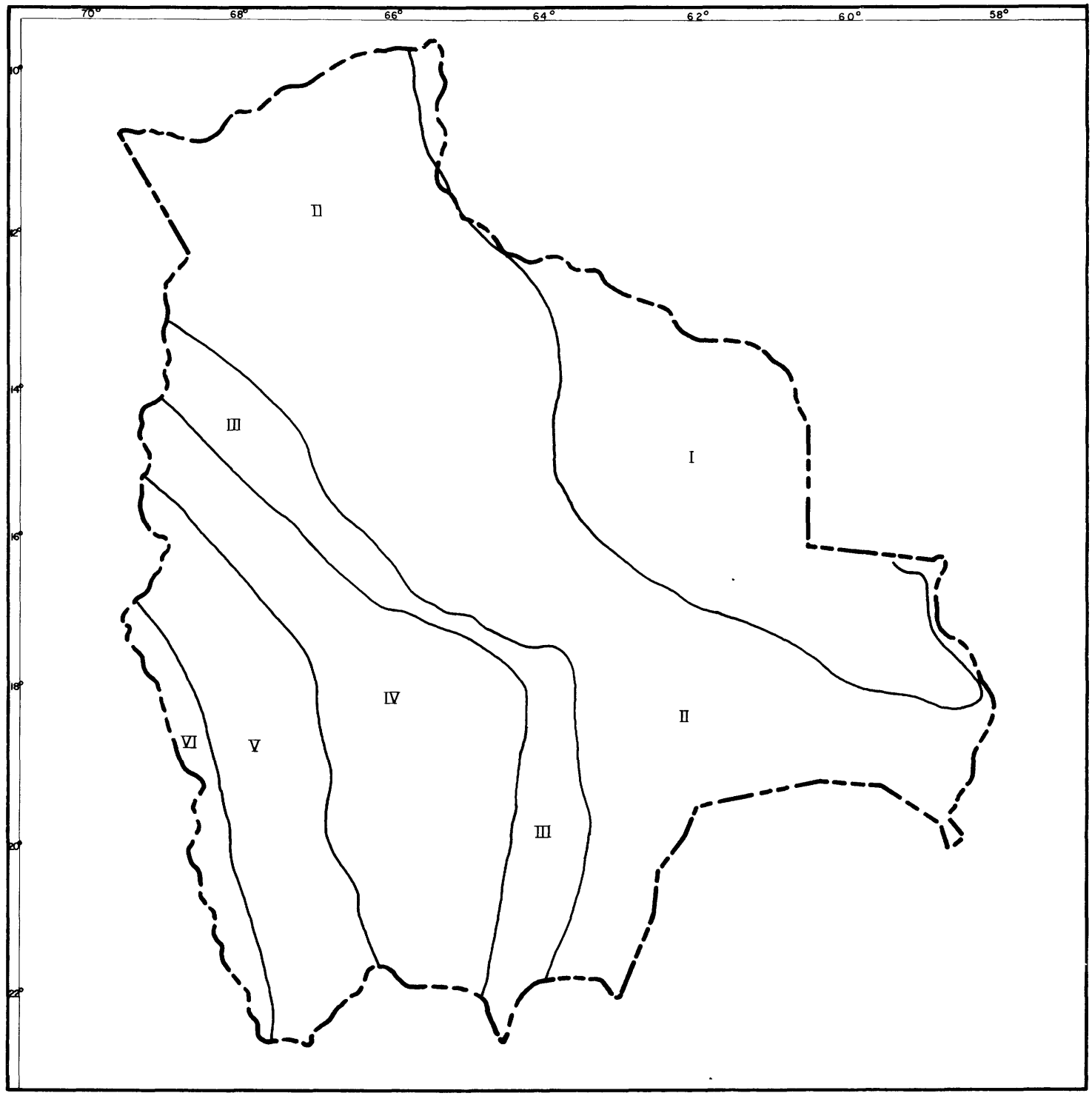

FIGURE 1.—Geological provinces of Bolivia. Scale 1:8,000,000. I, Brazilian Shield, II, Chaco-Beni Plain; III, Subandes Belt; IV, Central and Eastern Cordillera; V, Altiplano; and VI, Western Cordillera.

of 300 m above sea level. It is formed by Precambrian and Cambrian granitic and metamorphic rocks with erosional remnants.

It is known that metallic and nonmetallic ore deposits exist in this zone but, as yet, they have not been extensively explored or developed.

II. Chaco-Beni Plain

The Chaco-Beni Plain lies between the Brazilian Shield and the Subandes Belt on the east and west, respectively. It is a major geotectonic unit where thick beds of sedimentary rocks have accumulated and lie unconformably on the crystalline basement. In general, it has a slight regional slope at the north with a slight fold in the western section. The plain is considered to be an important area for the accumulation of oil.

III. Subandes Belt

The Subandes Belt is located between the Chaco-Beni Plain and the Eastern and Central Cordillera. It is formed by a series of parallel ridges which coincide with narrow longitudinal anticlines, generally cut by thrust faults along which rocks of different ages outcrop along their strike. The depressions or valleys correspond to synclines. This area is one of the best known petroleum provinces in Bolivia.

IV. Eastern and Central Cordillera

The Eastern and Central Cordillera, also known as a Paleozoic block, is characterized by major uplift with altitudes that can approach 6,400 m. A main characteristic of this province is the noticeable relief inversion where the high topography coincides with synclinal structures and depressions coincide with anticlines.

The central and western sections of this geologic province are intruded by granitic rocks and are highly mineralized.

V. Altiplano

The Altiplano forms a well-defined geologic province which is considered to be a "Rift" block basin that formed in conjunction with the "Uplift" type movements of adjacent blocks that occurred during the Tertiary. Later, denudation of the high parts occurred forming an extensive pediment plain.

There are mineral deposits along the boundaries of this geologic province.

VI. Western Cordillera

The Western Cordillera is the result of vertical movements associated with intense volcanic activity in the late Tertiary; an alined volcanic chain exists forming mountains with elevations that are generally more than 5,000 m in height.

RESULTS OF THE GEOLOGIC-GEOMORPHOLOGIC INTERPRETATIONS IN THE CHACO-BENI PLAIN

PETROLEUM EXPLORATION

Yacimientos Petrolíferos Fiscales Bolivianos is in charge of the Petroleum Exploration Subprogram, which is aimed at delimiting, in an adequate manner, petroleum potential areas in the Chaco-Beni Plain and Subandes Belt. These areas have proven to be petroleum provinces in the middle and southern part of the country. The project also attempts to provide new structural information on faults and lineaments that can be correlated with existing geologic data of the fields in actual production.

With these objectives, an evaluation of the Chaco-Beni Plain section was done on the Rogaguado Lake-San Borja images within the coordinates 65°00′–67°00′ W. longitude and 12°30′–15°30′ S. latitude, at a scale of 1:1,000,000, covering an approximate area of 62,900 km^2. Work was done on Landsat images 1045–13563 and 1045–13570, bands 5 and 7, corresponding to 0.6–0.7- and 0.8–1.1- μm wavelengths of the electromagnetic spectrum.

Among the most important features that were mapped are lakes which were not represented in any existing map of the region. Some of the lakes have rectangular and square shapes, the edges of which are alined on N. 43° E. and N. 21–45° W. strikes (fig. 2).

On the basis of previous observations and by correlating existing geologic data of the zones with studies of satellite images, it was possible to deduce that there is a great influence of the Brazilian Shield on the Quaternary sediments of this zone, which have a varied thickness ranging from 441 to 812 m. The boundary between the Brazilian Shield and the adjacent Quaternary basin is clearly displayed and defined by drainage patterns and subdued topography. Some surface patterns could be related to the potential accumulation of oil.

Similarly, the drainage interpretation of the zone of Cobija-Puerto Heath was obtained from the 1191–14082 and 1191–14084 images, within the coordinates 67°30′–69°30′ W. longitude and 10°00′–13°30′ S. latitude, using band 7 only in order to observe and delineate adequately the drainage system and areas of flooding (fig. 3).

Drainage anomalies, such as the deflection of streams, alinement of river valleys, lakes, and topography, made it possible to locate apparent anticlinal structures, the axes of which strike west-northwest, roughly parallel to the Subandes Belt in this region.

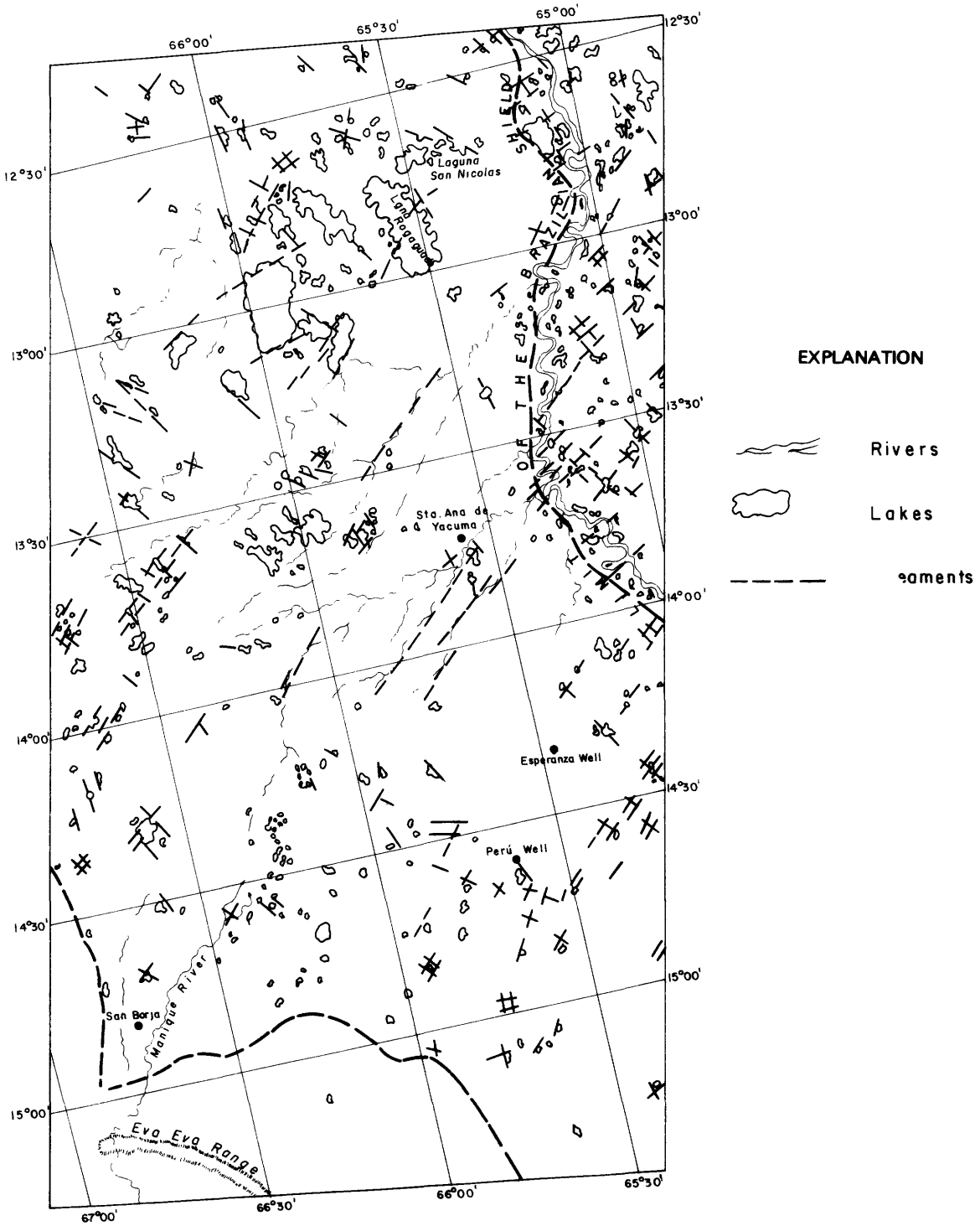

FIGURE 2.—Geologic and geomorphological map of the San Borja-Mamore River and Rogaguado Lake region of Bolivia made from ERTS images. Scale 1:1,900,000.

Straight river courses trending northeast-southwest and south-southwest appear to strike along lineaments which are apparently related to faults. Recently obtained seismic reflection data have confirmed the presence of two faults which coincide with the lineaments previously mapped on Landsat–1 imagery.

Similar geologic photointerpretation was conducted on Skylab photos on the Santa Cruz area where the most important petroleum and gas fields are presently being exploited (fig. 4).

The Santa Cruz area is located in the transition zone of the piedmont toward the subandean ridges,

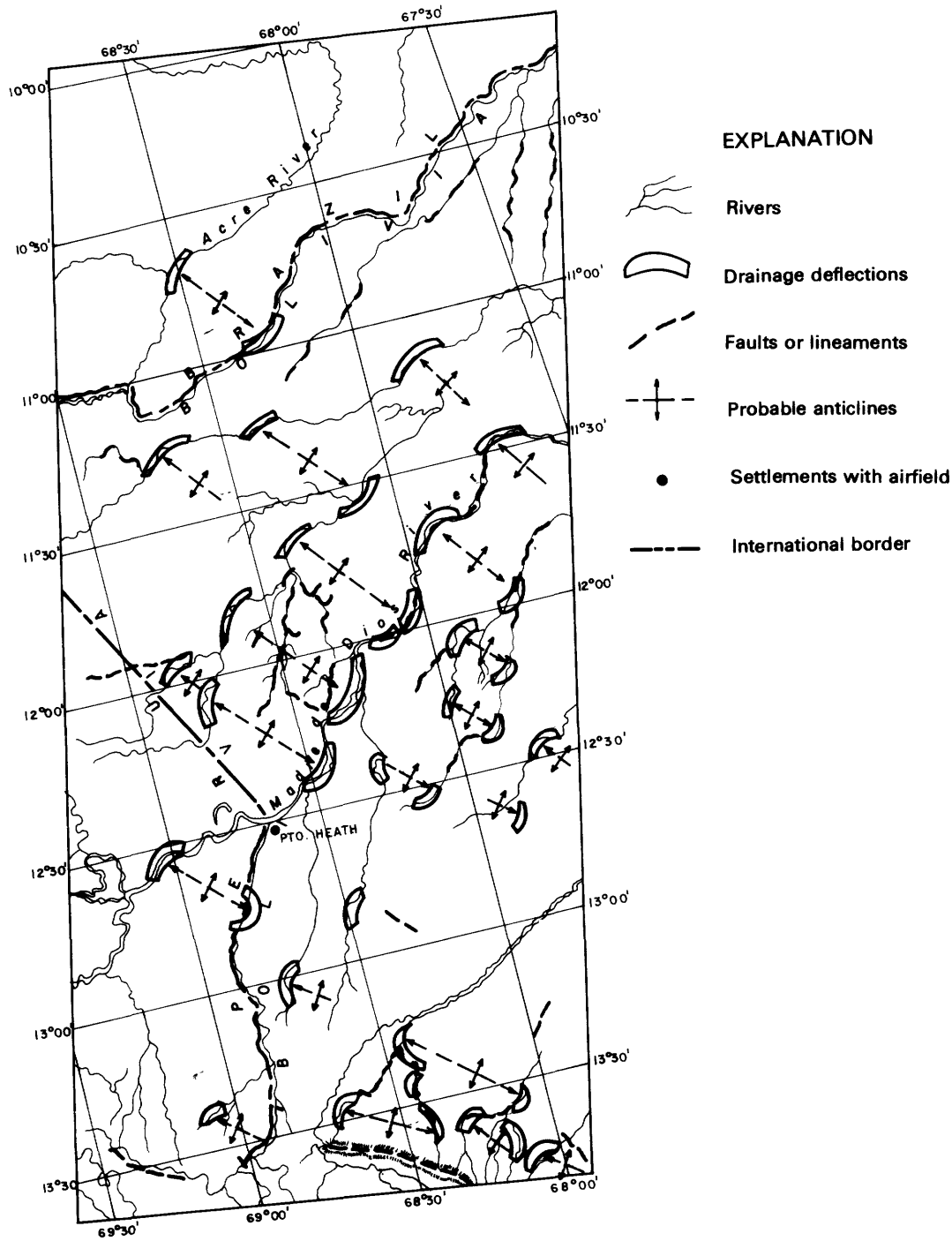

FIGURE 3.—Drainage interpretation from ERTS images of the Cobija-Puerto Heath and Rio Madre de Dios-Ixiamas River area. Scale 1:2,400,000.

where subdued topography, uniform lithology, and low dips make it difficult to obtain adequate photogeologic information using conventional aerial photographs.

Using photograph, SL–2–A–339, bands 1–5, with its large area synoptic view, it was possible to correlate major structural features, with diverse geological data, and has permitted us to define new potential petroleum areas. Eleven anomalies were found to be correlated with subsurface anticlinal structures as corroborated by the wells drilled in the Cedro and Moreno anticlines.

In summary, we can conclude with the fact that hyperaltitude images for studies of vast areas, let us obtain a panoramic view of the area and make it

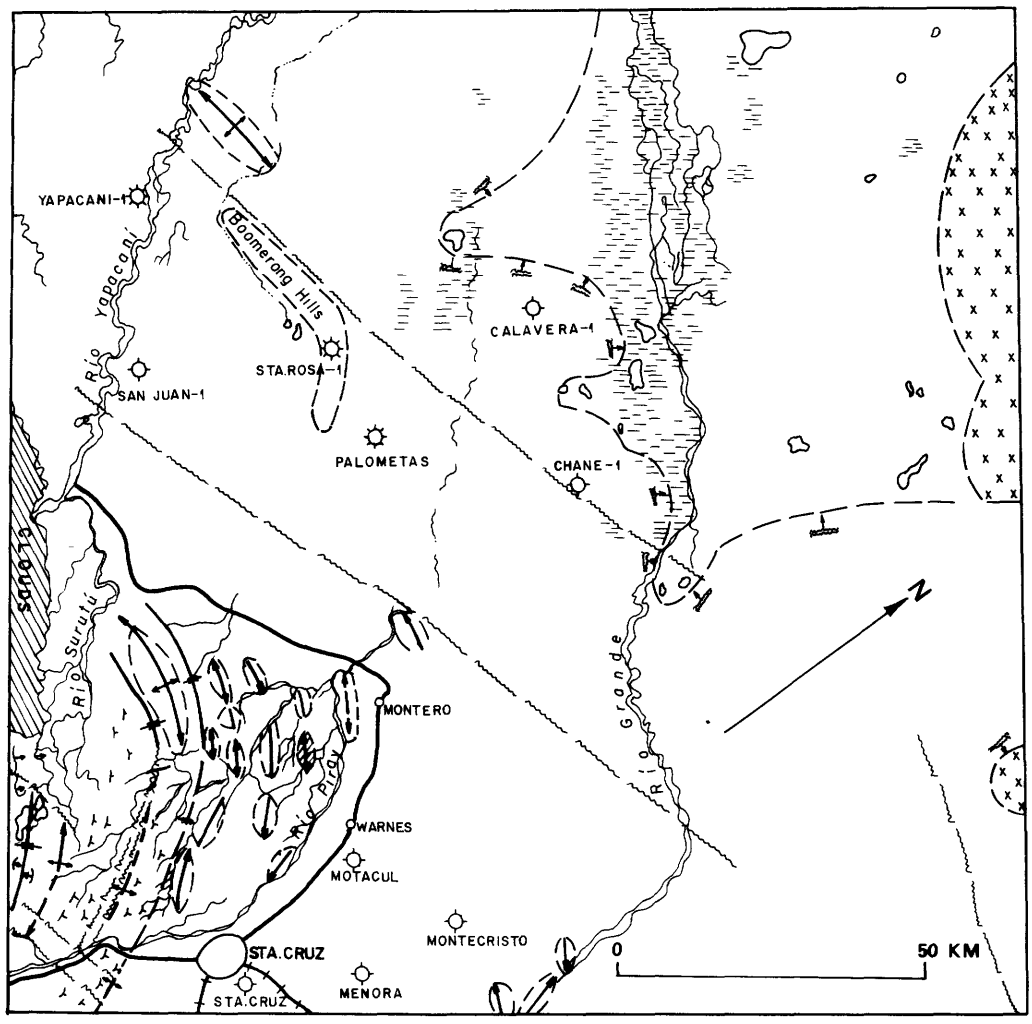

FIGURE 4.—Geological interpretations from Skylab image SL-2-A-339 of the Santa Cruz-Montero-Buena Vista area of Bolivia. Approximate scale 1:800,000.

possible to correlate structural and geologic data which are basic to petroleum exploration.

MINING EXPLORATION

The Mining Exploration Subprogram is conducted by the Mining Corporation of Bolivia using Landsat imagery interpretation aimed at locating new favorable areas for exploration and exploitation of mining resources.

Because of the scale limitations of Landsat imagery for visual interpretation, the conventional mineral resource evaluation methods were modified. Generally,

mining exploration methods are conducted at large scales ranging from 1:1,000 to 1:5,000, and generally close to known exploration and mining sites. However, new maps at 1:250,000 scale are being prepared for the purpose of establishing regional genetic relations of the mineralized bodies, their host rocks, structures and, where present, alteration zones.

Results of the Landsat imagery interpretation are important because it was possible to identify lineaments related to faults, tonal anomalies, and geomorphic anomalies which, when correlated to the existing information, let us delimit new potential mining areas.

To establish a methodology which could let us evaluate the mineralized zones from different points of view, the geomorphic characteristics, tonal differences, and drainage patterns were studied and considered to be fundamental criteria.

Tonal anomalies are defined as being the delimitation of zones with tonal characteristics that are different from the surrounding area and which may be related to intense zones of weathering, contact aureoles, vegetation concentration, facies variations of certain formations, and hydrothermal alteration.

Geomorphic anomalies are shapes that vary from the general tendency of the landscape and which are generally related to endogenic processes, such as magmatism and diapirism.

Tectonic-Structural anomalies are zones affected by the intersection of faults and lineaments, generally of regional character, and related to the emplacement of igneous bodies. They are generally represented by straight courses of streams and valleys.

FIELD RESULTS

With the purpose of proving the relationship of existing mineralization with anomalies defined by Landsat interpretation, fieldwork was performed in the area covered by Landsat image 1010–14033, selecting the best defined zones. The field results can be summarized as follows (fig. 5):

1. The Structural Anomaly of Patacamaya is located 15 km to the northeast of the town of the same name on the Tapacari lineament at its intersection with the Achuta lineament. There are several mineralized subvolcanic bodies along the Tapacari lineament.

   Field verification tests were negative at the lineaments intersection, due possibly to thick cover of Quaternary sediments that exist in the zone.

2. Structural Anomaly of Huayllamarca is located on the ridge of the same name. It corresponds to a fault zone where a direct relation between the anomalies, longitudinal faults, and diapirous rocks were determined. There we found copper minerals in the form of sulfates and carbonates.

3. Geomorphic Anomaly of Laurani is located close to the town of Sica Sica. It coincides geologically with a subvolcanic body, where dacites and andesites are known; this igneous body appears to be related to the Colquencha-Laurani and Achiri-Umala lineament intersection which strike northwest and southeast, respectively.

   Fieldwork showed a direct relation between the anomaly and igneous activity with strong hydrothermal alteration and mineralization consisting of copper, silver, and lead minerals that are actually being exploited.

4. Tonal Anomalies of Sica Sica are located 10 km from the town, where fieldwork has determined the presence of sedimentary rocks with discordant red tones in contact with Paleozoic rocks with gray tones. The objective of this reconnaissance was to identify a possible alteration zone as the zone is located along the intersection of two regional faults. No evidence of mineralization was found.

5. Geomorphic Anomalies of Antaquira are located southwest of the town of Caquiaviri, where the direct relation between a longitudinal fault, a synclinal structure and subvolcanic intrusive rocks was found. Copper mineralization was found for the first time in the fault and joints that comprise the zone.

CONCLUSIONS

It was proven that mineralization can be found associated with longitudinal faults in the structural anomalies (Huayllamarca and others) identified on Landsat images.

The geomorphic anomalies are important as they always coincide with intrusive bodies and/or subvolcanic bodies, which are generally mineralized.

When systematic and sufficient detailed fieldwork were accomplished on major lineaments, these areas became interesting for mineral and petroleum exploration.

Even though the present example of tonal anomaly did not provide the expected positive result, there is evidence in other studied zones that tone has a relation with mineralization processes.

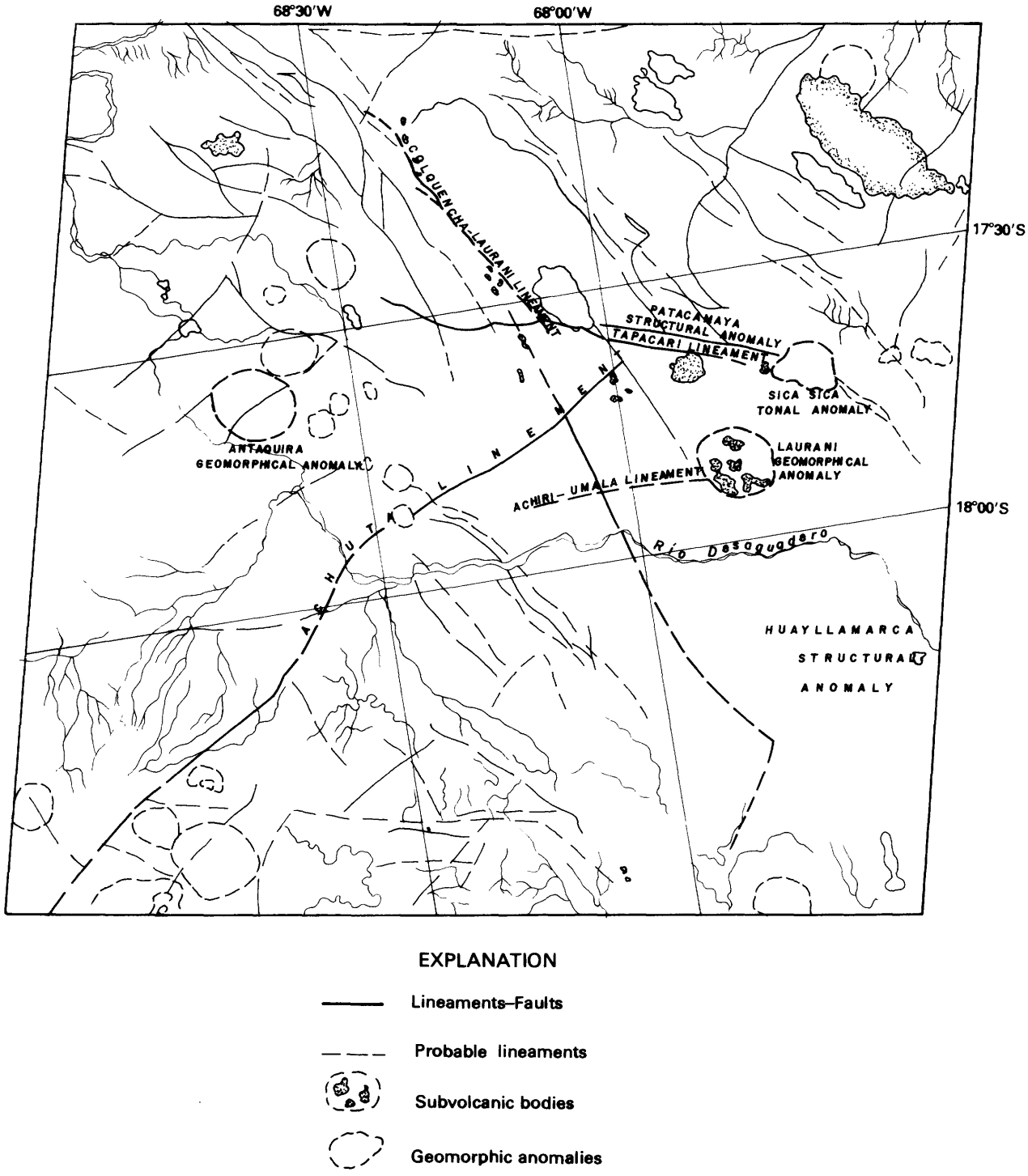

FIGURE 5.—Mineralogical map. Approximate scale 1:1,250,000.

PRELIMINARY SELECTION OF THE SANTA CRUZ-PUERTO SUAREZ GASLINE ROUTE

OBJECTIVES

The principal objective of the present work was to study the applicability of the Landsat imagery for the location of the most direct route of the Santa Cruz-Puerto Suarez gasline in relation to the actual existing railroad and to design several alternative routes.

Methodology and materials used.

In order to comply with the proposed objectives and due to the scanty cartographic information of the

area, the Landsat–1 imagery that covers the zone with a maximum of 30-percent cloud cover was selected and supported by a Skylab space photograph. We also used a photoindex of available aerial photographs that cover the study area.

Images 1240–13415, 1240–13421, 1005–13344, 1005–13350, 1111–13243, bands 5 and 7, photograph SL–2–190A–339, bands 2 and 6, and the photoindex of the South Roboré area, were used due to the lack of satellite images of this section at the time the work was begun. The study was undertaken at a 1:250,000 scale, using the Santa Cruz-Corumba railroad as a reference to prepare the corresponding map.

As the study area contains peculiar geomorphologic features, the first general physiographic map of the zone was prepared. In it we attempted to delimit the boundary of the Brazilian Shield in relation to the Chaco-Beni Plain, the Chiquitos Ridges, and other important geomorphologic features that could affect the selection of the preliminary route. Lagoons, rivers, creeks, hills, sand dunes, and especially the "Izozog Bañados (swamps)" and the "Otuquis Bañados (headwaters)", lowland areas that are subject to temporary flooding, were all decisive in the selection of the route that the gasline should have.

STUDY AREA DESCRIPTION

Generally, the Brazilian Shield in this zone is expressed as a peneplane where isolated granitic rocks and metamorphic rock outcrops exist and are separated from the San José, Roboré, and Quimone Ridges by a poorly drained depression filled with Quaternary sediments (fig. 6).

The Chaco-Beni Plain corresponds to a poorly drained alluvial plain covered by low vegetation in the area of the Izozog Bañados and Otuquis Bañados. In these areas there are a great number of small braided rivers and scattered temporary lagoons, which are characterized by being located in topographic depressions with poor drainage.

The interpretation work was performed with images obtained during the period of the lowest stage of the rivers. The use of images, taken mainly at the end of the rainy season, is considered necessary for the accurate mapping of the flooding areas.

PRELIMINARY ALTERNATIVES OF THE ROUTE

Considering the locations of Santa Cruz city and the gasfields in exploitation as a starting point for the gasline to the town of Puerto Suarez and taking as basic parameters the longitude route and physiographic conditions of the area for the construction and maintenance of the route, the following alternatives were designed:

1. *Colpa Field-Puerto Suarez alternative*

Two routes [subalternatives] were considered for the portion of this alternative from the Colpa Field to Pozo del Tigre station. The alternative continues then as a single route to Puerto Suarez.

North Alternative

Approximate distance: 604.4 km.
Average altitude: Colpa Field 345 m above mean sea level.

Striking directly south-southeast from the Colpa Field for a distance of 138 km we can arrive at the Pozo del Tigre station. Field conditions along this route are good and characterized by gentle topography with adequate drainage where soils are generally limy-clayey sand. However, it is necessary to indicate that in the first stage of it, the Piray and Grande Rivers would have to be crossed. Their meandering courses must be studied in detail from existing supplementary information.

South Alternative

Approximate distance: 607.1 km.
Average altitude: Pozo del Tigre 272 m above mean sea level.
Colpa Field 345 m above mean sea level.

This alternative was designed with a southeast strike and an approximate distance of 140.7 km between the Colpa Field and Pozo del Tigre station, where the gasline crossing the Grande River would parallel the actual railroad bridge.

This subalternative has the advantages of being located farther away from the town of Warnes and of crossing the Grande River in an area where geologic information obtained for the bridge construction is available. Another positive characteristic for this section would be the fact that the route would parallel the railroad, facilitating by this way tube material transportation and would avoid new path construction. However, problems can be foreseen on the route right-of-way, as there is intense agricultural activity in the area.

Common Point

From Pozo del Tigre station, the route is common for both subalternatives and parallels the railroad with an east-southeast strike displaced from it an approximate distance of 2 km to the south. The purpose for this was to reduce the distance to the surroundings of the Musuruquí station (74.8 km distance, 358 m altitude) where the north edge of the Izozog Bañados is flooded and marshy during the rainy season. Total lengths of these proposed sections of gas-

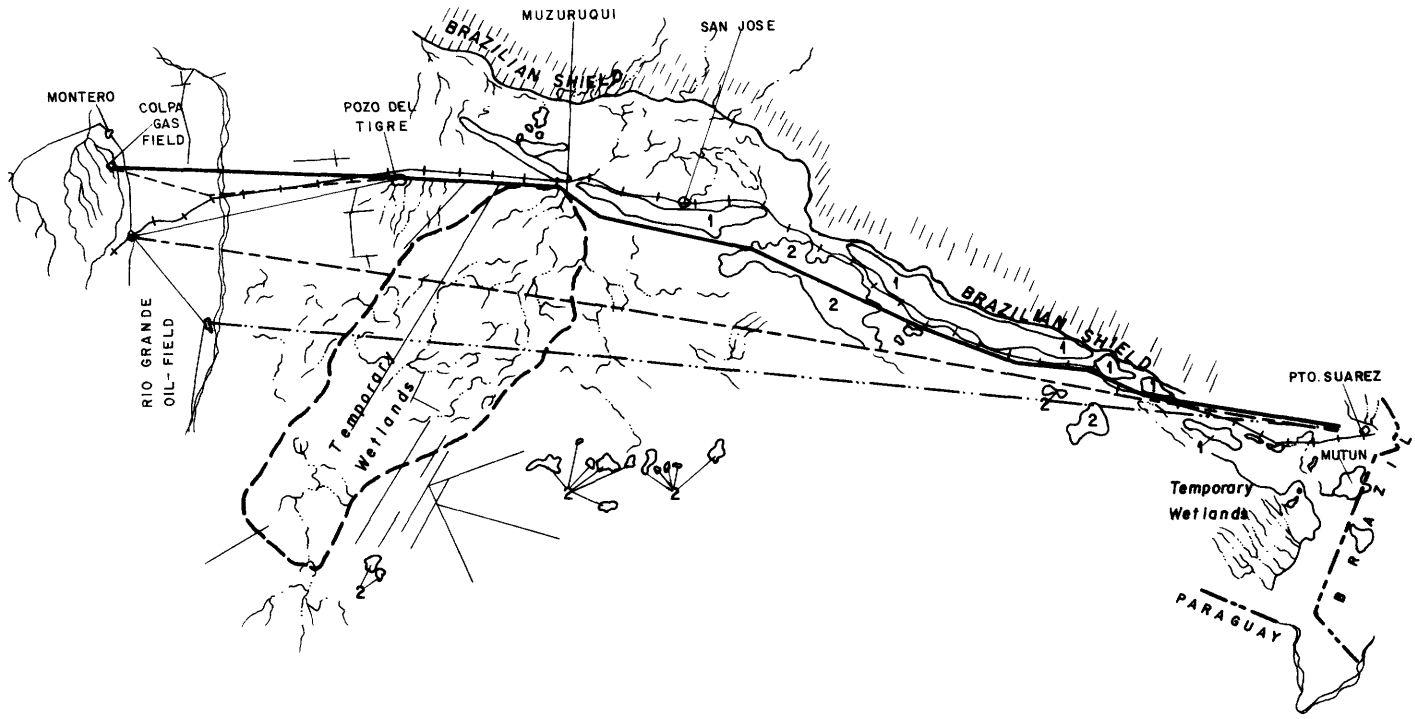

FIGURE 6.—Gasline selective routes. Approximate scale 1:3,500,000.

line are 215.8 and 218.8 km for the north and south subalternatives, respectively.

As it can be noticed, the proposed designs to the Musuruquí station do not present much variation in relation to the railroad. It is from this point that we propose the route to go south of the San José Ridge in a direct line to near the town of Roboré.

The chosen route in this section is supported by the fact that the area is well drained; there are few, if any, rock outcrops and the soils are generally sandy having formed by the erosion of the San José Ridge. The route will go through a smooth plateau with a uniform altitude in the east section where it is presumed that sufficient soil thickness would be found for the excavation of the gasline trench.

Making a comparison of this route with the actual railroad in the same section that lies between Musuruquí and Roboré, there appear to be several negative factors: (1) the construction of the bridge over the Quimome River indicated that there is insufficient soil thickness for the excavation of the trench, a factor that would increase the construction cost; (2) this zone is characterized by bad drainage in which temporary lagoons appear during the rainy season; and (3) the most important factor, if this route paralleling the railroad is selected, is related to the distance as it is 13 km more than the distance proposed south of the bridge.

2. *Santa Cruz city-Puerto Suarez route*

This route was designed to collect the gas from the different production fields surrounding Santa Cruz city.

North Alternative

Santa Cruz city-Pozo del Tigre station-Puerto Suarez.
Distance: 591.9 km.
Altitude: Santa Cruz 465 m above mean sea level.
Puerto Suarez 220 m above mean sea level.

There is a distance of 125.5 km from Santa Cruz city to the common point of the Pozo del Tigre station where an alluvial plain is the main landscape. It consists mainly of limy sand that extends along the main route already designed from Puerto Suarez.

As a restriction for the selection of this alternative, it must be indicated that a suitable crossing of the Grande River must be chosen where its course is only slightly meandering. Also, to be considered is the construction of the feeder gaslines from the producing areas to the common point in the vicinity of Santa Cruz city.

Direct Alternative

Santa Cruz city-Puerto Suarez
Distance: 574.1 km.

Generally, it must be indicated that this alternative would go first through the similar terrain described previously but with a significant problem. The Izozog Bañados is considered to be a potential problem area, both for the construction and maintenance of the line, especially during the rainy season.

3. *Grande River Field-Puerto Suarez alternative*

Distance: 539.5 km.
Altitude: Rio Grande Field 338 m above mean sea level.
Puerto Suarez 220 m above mean sea level.

This possible route was delineated because the Rio Grande Field is the biggest deposit of gas reserves in the country, and the route would be the most direct to the town of Puerto Suarez. The design route, however, would cross the Izozog Bañados, a total distance of 92 km. This potentially difficult terrain constitutes the most serious restriction that must be considered.

CONCLUSIONS

The area maps prepared for this study are the most up-to-date information available for the study of the selection of the route for the gasline. Landsat imagery, due to its regional coverage and geometric accuracy along with the multispectral factors, has enabled us to obtain the information of extensive areas both quickly and economically in comparison with the more conventional aerial methods.

RECOMMENDATIONS

- To make an aerial reconnaissance at a low altitude, combining the existing aerial photographs with Landsat imagery.
- To make a new study with Landsat–2 imagery to obtain more information with the multitemporal coverage in order to delineate more accurately the area influenced by temporary flooding.
- To study in detail the course of all the rivers that would have to be crossed in order to select the most suitable points for the construction of the bridges.
- To make an economic study on each one of the alternatives detailed before, relating distance to construction and maintenance. These factors will help the ultimate selection of the route.

TABLE 1.—Comparison of alternative gasline routes

Alternatives	Distance (km)	Comparative sheet				
		Railroad km difference	Distance evaluation	Physiographic evaluation	Construction and maintenance	Total
Colpa Field-Puerto Suarez:						
North Alternative	604.400	−25.600	x x x	x x x x x	x x x x	12
South Alternative	607.100	−22.900	x x	x x x x x	x x x x	11
Santa Cruz city-Puerto Suarez:						
North [Route] Alternative	591.900	−38.100	x x x	x x x x	x x x x	11
Direct [Route] Alternative	574.100	−55.900	x x x x	x	x	6
Rio Grande [River] Field—Puerto Suarez	539.500	−90.500	x x x x x	x	x	7
Railroad Route:						
Santa Cruz-Puerto Suarez	630	------	x	x x	x x x	6

x x x x x Excellent
x x x x Good
x x x Regular
x x Bad
x Very Bad

SELECTED REFERENCES

Anonymous, 1975, Technical report of the Thematic Cartographic Project of the Department of La Paz: La Paz, ERTS Program/Bolivia, Servicio Geologico de Bolivia, Office rept., July.

Brockmann, Q. Carlos, 1974, Preliminary alternatives of the Santa Cruz-Puerto Suarez gasline route: La Paz, ERTS Program/Bolivia, Servicio Geologico de Bolivia, Office rept., October.

Claure, H., 1974, ERTS imagery research for mining exploration: La Paz, Mining Corporation of Bolivia for ERTS Program, Servicio Geologico de Bolivia, Office rept., June.

Luizaga, S., 1975, Information on the revised Anomalous Zones detected through the technological satellite ERTS–1: La Paz, Servicio Geologico de Bolivia, Office rept., March.

Oblitas G., Jaime, Salinas E., Carlos, Davila E., Juan, Cabrera V., Arturo, and Hidalgo F., Manuel, 1973, Summary of the petroleum geology of Bolivia: La Paz, Yacimientos Petroliferos Fiscales Bolivianos, 92 p.

Vargas, Carlos, 1973a, Drainage interpretation of the ERTS images of the Cobija- Puerto Heath-Madre de Dios River-Ixiamas area: Yacimientos Petroliferos Fiscales Bolivianos: La Paz, ERTS Program Bolivia, Servicio Geologico de Bolivia, Office rept., September.

———1973b, Results of the geologic-geomorphical study of two ERTS images of the San Borja Zone-Mamore River-Rogaguado Lake-West of Bolivia: La Paz, Yacimientos Petroliferos Fiscales Bolivianos, Office rept., August.

———1975, Geologic-physiographical interpretation of the Skylab photograph corresponding to the Santa Cruz-Montero-Buena Vista area: Yacimientos Petroliferos Fiscales Bolivianos: La Paz, ERTS Program Bolivia, Servicio Geologico de Bolivia, Office rept., February.

PROCEEDINGS OF
THE FIRST ANNUAL WILLIAM T. PECORA MEMORIAL SYMPOSIUM,
OCTOBER 1975, SIOUX FALLS, SOUTH DAKOTA

An Overview of Canadian Progress in the Use of Landsat Data in Geology

By A. F. Gregory, President
Gregory Geoscience Ltd., Ottawa, Canada,
and L. W. Morley, Director
Canada Centre for Remote Sensing, Ottawa, Canada

ABSTRACT

During the past 3 years, Canadian geologists have been assessing the geological use of Landsat data in the context of a vast but relatively well known hinterland. Although few in number, these geologists comprise the largest single class of users of Canadian Landsat data. In particular, a few oil and mineral exploration companies and consultants appear to use as many images as the other 90 percent of the geological users, excluding reference collections.

Most Canadian geological users have a relatively long and broad experience with Landsat data. Visual interpretation of black and white prints is the principal method of analysis. There has been little research into automated processing; however, a major advance in digital classification of arctic terrain is imminent.

Practical applications are related primarily to reconnaissance for geological structure and disposition of surficial materials. Half of the users claim a modest to large benefit from use of Landsat data but cannot identify specific dollar benefits.

The level of development of practical geologic applications in Canada is greater than predicted in a pre-ERTS forecast. Visual interpretation of Landsat images will soon become a prime tool, in conjunction with others, for geological reconnaissance. The technique will be especially valuable in poorly explored arid areas where vegetational cover is sparse. Automated processing will remain in the research stage until specific low-cost methodologies are developed.

LANDSAT IN A CANADIAN CONTEXT

Canada, with a territory covering nearly 3.9 million square miles, is the largest country in the Western Hemisphere and the second largest in the world. Canadian terrain is extremely diverse, comprising almost semitropical areas in southern Ontario and southern British Columbia, great mountain arcs, wide fertile prairies, a vast lake-strewn interior, and seemingly endless stretches of northern wilderness and tundra. Eighty-nine percent of this area is not settled; indeed 95 percent of all Canadians live in 10 percent of the area comprising an irregular fringe along the border with the United States of America.

From a geologist's viewpoint, Canada is composed of 17 geological provinces in four main categories: continental shelf, platform, orogen, and shield. Geologically, the youngest provinces are the Atlantic, Pacific, and Arctic Continental Shelves. They comprise slightly deformed sediments and volcanics, mainly of Mesozoic and Cenozoic age. The St. Lawrence, Interior, Arctic, and Hudson Platforms comprise thick, flat-lying Phanerozoic strata over crystalline basement. The Appalachian, Cordilleran, and Innuitian Orogens are mountain belts of deformed and metamorphosed sedimentary and volcanic rocks, mainly of Phanerozoic and Proterozoic age, and granitic intrusions. The remaining seven geological provinces comprise the Canadian Shield which is composed of Precambrian rocks. The Grenville, Churchill, Southern, and Bear provinces embrace Proterozoic orogenic belts. The Superior, Slave, and Nain provinces comprise metasedimentary and metavolcanic rocks of older Archean age, including the oldest continental crust known in Canada.

The mineral industry is one of the most important sectors of the Canadian economy. The value of mineral production in 1974 was $11.6 billion, of which fossil fuels represented 44 percent, metals 42 percent,

nonmetallics 8 percent, and structural materials 6 percent. Much was exported, mainly to the United States, Britain, and Japan. Principal mineral products were oil, natural gas, nickel, copper, iron ore, zinc, asbestos, cement, and sand and gravel. Of the major geological provinces, the Interior Platform yields in value about 40 percent of all mineral production, mainly fossil fuels, and the Canadian Shield about 35 percent, mainly metals.

Recorded Canadian history began with the quest for these and other riches in the New World. The search for economic gain was a particular stimulus, and indeed is a continuing theme, throughout Canadian history although the nation became a reality just over 100 years ago. Despite its vast area and relatively young age as a nation, Canada has been well explored and mapped at reconnaissance scales. For example, an updated coverage of black and white aerial photographs is maintained for all of Canada at scales between 1:63,360 and 1:15,000. The whole country has been surveyed and mapped with high standards at a scale of 1:250,000, thus presenting a relatively detailed depiction of relief, river systems, transportation facilities, forest cover, and centres of population. Bedrock geology has now been mapped over 95 percent of the nation at reconnaissance scales of 1:250,000 and smaller, although only about 20 percent of the overlying Quaternary sediments have been mapped at similar scales.

A vast but relatively well-known hinterland, thus, is the context in which Canadian geologists have assessed the geological use of Landsat data. The experiences reported here reflect involvement in the ERTS-Landsat program from early planning in the United States through direct readout of data at our own receiving station to current research and applications (Morley, 1971). The information comes from sources too numerous to acknowledge here, including industrial, academic, and government members of the Working Group on Geoscience of the Canadian Advisory Committee on Remote Sensing, staff and files of the Canada Centre for Remote Sensing, and contributions from private companies.

DEVELOPMENT OF CANADIAN GEOLOGICAL INTEREST IN THE LANDSAT CONCEPT

HISTORY

Over the past 60 years, but especially since 1945, photogeology has made significant contributions to the science and practice of geological mapping. In the early 1960's, the term "remote sensing" was adopted when other parts of the electromagnetic spectrum were used. Of course, geophysics had been developed earlier for other wave bands but, in this paper, such techniques are not considered as remote sensing (Gregory, 1972). During the past few years, space platforms have added new dimensions to the remote sensing of geology (Gregory and Moore, 1976).

The late Professor H. L. Cameron was probably the first Canadian geologist to demonstrate the possibilities of synoptic, small-scale photography and other novel methods of remote sensing. By the early 1960's, he was using stereoscopic, time-lapse methods to study early space photography for the National Aeronautics and Space Administration (NASA). In 1963, he briefly reviewed his work in a paper to the First Seminar on Air Photo Interpretation in the Development of Canada (Cameron, 1964). At the same seminar, W. A. Fischer of the USGS reviewed his pioneer work in geological remote sensing and emphasized the broadening spectral capabilities (Fischer, 1964).

The enthusiastic but practical presentations of these two specialists were responsible for awakening the interest of Canadian geoscientists to the potential of remote sensing in all its aspects. The combination of that seminar with personal experiences in geophysics and photogeology lead the authors of this paper to initiate remote-sensing projects in 1964 and eventually to establish a remote-sensing section within the Geophysics Division of the Geological Survey of Canada.

By early 1967, serious consideration was being given to possible Canadian involvement with the resource satellites that were being planned in the United States by the Department of the Interior and NASA. In 1968, one of us (LWM) initiated planning for Canadian participation in remote sensing while the other (AFG) reviewed contemporary planning in the United States. It is interesting to note that at that time, geological applications of satellite data were expected to be significant, especially for structure and geomorphology, although of lesser importance than applications related to land use, forestry, surface water, agriculture, etc. Training, research, and development of applications were considered to be prime needs (Gregory and Morley, 1969).

Following a national review and recommendations presented in 1971, the Canada Centre for Remote Sensing was established with Dr. Morley as founding director. In 1972, he also became chairman of the Canadian Advisory Committee on Remote Sensing while Dr. Gregory was appointed chairman of that committee's Working Group on Geoscience.

CANADIAN EXPECTATIONS FOR REMOTE SENSING OF GEOLOGY BY SATELLITES

Timely acquisition and interpretation of data from Landsat–1 was recommended by the previous Working Group on Geology (1971, p. 10). However, that working group reported the main geological need to be for airborne sensing, particularly aerial photography. It was concluded that for use in Canada, satellite data "will provide valuable new information about the surficial geology of Canada, which is incompletely mapped at any scale. However, these data will add only supplementary information on gross structure and bedrock geology, most of which has been mapped at scales smaller than 1:250,000 and much at larger scales" (ibid, p. 11). It was further concluded that "there are few geologic requirements for continuous repetitive surveys" (ibid, p. 11), atlhough their use was foreseen for seasonal and temporal analyses, e.g., studies of terrain, erosion, and sedimentation.

Because of the limited availability of Landsat data during the year following launch of the satellite on July 23, 1972, expectations of Canadian geoscientists changed little. Most geoscientists continued to view Landsat as very experimental. However, a few geologists used standard photogeologic techniques on Landsat images and reported potential, low-cost applications for mapping structural geology, particularly linears, and for planning exploration projects. Seasonal enhancements of geological features suggested that the original expectation of little requirement for repetitive data was incorrect (Working Group on Geoscience, 1972 and 1973).

The advent of Landsat fired unrealistic geological expectations, especially among nongeoscientists, both in Canada and abroad (Gregory, 1973, p. 88). However, practicality grew over the following year as relevant results of Landsat analyses became available.

USERS OF CANADIAN LANDSAT DATA

BASIS OF ANALYSIS

The following analyses of Canadian users of Landsat data are based on three sets of data: (1) The current Canada Centre for Remote Sensing 'National Air Photo Library (CCRS 'NAPL) computer listing of sales of standard Landsat products for the 3 years ending September 15, 1975; (2) returns from a questionnaire on the geological use of Landsat data which was mailed in early August 1975; and (3) the current CCRS computer listing of scientists and engineers with an interest in remote sensing, as of August 22, 1975.

NUMBER OF USERS

As of August 1975, 3307 separate persons and organizations had registered an interest in Canadian remote sensing by returning a report to the Canada Centre for Remote Sensing. While there is, undoubtedly, some overlap in representation between individuals and organizations, this number reflects a solid base of participation in remote sensing in Canada.

Among the 3307 listings, there was much greater interest in remote sensing applied to the geosciences (1078) than to any other single scientific discipline or practice. A breakdown of user interest (table 1) shows that range of interests as well as the overlap in them. Contacts (i.e., letters, visits, and telephoned enquiries) at the User Services Section of the Canada Centre for Remote Sensing confirm a continuing major interest in remote sensing applied to the geosciences (30–40 percent of all contacts each month).

Major and more-or-less equal interest was expressed by representatives of companies, federal and provincial governments, and educational institutions (table 2).

SALES OF CANADIAN LANDSAT DATA

Interest is not a very satisfactory way of defining users of Landsat data. Another current indication of use, which is hardly more precise, is a cumulative list of customers who purchased Landsat data through the National Air Photo Library (NAPL). On this list of 536 customers, 205 (38 percent) could be identified as having a major geological base, i.e., a geological

TABLE 1.—*Relative interest in remote sensing by user discipline, August 1975*

Category	Number	Percent
Total Interest	3307	100
Agriculture (including Soils)	694	20
Atmospheric Sciences	348	10
Cartography/Photogrammetry	643	19
Fisheries	373	11
Forestry	697	21
Geography	674	20
Geology	1078	32
Glaciology/Ice Reconnaissance	389	11
Hydrology	616	18
Oceanography/Marine Science	414	12
Wildlife/Livestock	461	13

NOTE: Sums exceed listed totals because of multiple interests expressed by a single individual or organization.

TABLE 2.—*Relative interest in remote sensing by economic sector, August 1975*

Category	Number	Percent
Companies	752	26
Educational Institutions	692	24
Federal Government Agencies	664	23
Provincial Government Agencies	539	18
Foreign Government Agencies	124	4
Private Individuals	110	3
Municipal Government Agencies	29	1
Regional Government Agencies	20	1
International Organizations	7	0
Total	2937	100

TABLE 3.—*Net sales of standard Landsat products for 3 years ending September 15, 1975*

Product	Total net sales	Net geological sales	Percent geol.
B & W prints	60,016	32,506	54.2
Colour prints	7,209	1,925	26.7
B & W transparencies	18,354	1,471	8.0
Colour transparencies	3,185	531	16.7
Total	88,764	36,433	41.0

NOTE: These figures represent net sales external to the National Air Photo Library and the Canada Centre for Remote Sensing. They do not include images of Canadian terrain sold by EROS (U.S. Geological Survey) in Sioux Falls, S.Dak. or by ISIS (a private company) in Prince Albert, Saskatchewan. It is possible that these latter sales are equal to or greater than sales reported here.

survey, an oil or mining company, or a consultant. The next largest identifiable groups of users were foresters (45), library and information services (41), and geographers (39), each with 7 to 8 percent of the number of customers. However, there is a large group of individuals and otherwise unidentifiable purchasers (155 or 29 percent), which was not amenable to classification.

A semiquantitative estimate of the number of geological users was made from a computer printout of net sales (i.e., excluding images generated for internal use at the CCRS and NAPL) of standard Landsat products* in Canada up to September 15, 1975 (table 3). This analysis indicates that 41 percent of net sales were made to identified geological users. However, there were uncertainties in classifying customers as nongeological; hence the statistics are minimal although the trends are real.

* Standard Landsat products are 9 × 9 inch prints and transparencies, both colour and black and white.

CLASSES OF GEOLOGICAL USERS

A precise breakdown of purchasers by subdiscipline within the geosciences is difficult to achieve. However, the results of a questionnaire prepared in support of this paper permit a semiquantitative analysis. Of the 173 questionnaires sent to selected purchasers with an identifiable geoscience interest, 70 (41 percent) were returned by December 31, 1975. These returns (table 4) show that mineral exploration companies (45 or 64 percent) are the largest users of Landsat data among Canadian geological users, excluding the major collection in the Geological Survey of Canada.

The industrial sector was represented by returns from 52 companies and consultants. Of these, 4 companies concerned with oil and gas exploration, 1 company concerned with mining exploration, and 3 consulting companies reported that they each analyze over 100 Landsat scenes per year. One company in each class reported using over 500 scenes per year. Indeed, these 8 major users, by their own reports, appear to use more images annually than all other 62 users combined.

The computer listing of sales by NAPL (table 3) provides another means of assessing the classes of purchasers within the geoscience community. Of the 36,433 standard products sold to recognized geological users (table 5), about half (18,022) comprise black and white prints in a national collection at the Geological Survey of Canada. The balance (18,411 standard products) was sold to the various users noted previously. The figures in table 5 confirm the conclusion that in terms of number of users, number of images purchased, and number of scenes analyzed, the mineral exploration companies are by far the largest users of Canadian Landsat data for geological applications. Similar companies also appear to be major users of Landsat data in the United States (Sabins, 1974) and Australia (U.K. Remote Sensing Society Newsletter No. 7, p. 14, Nov. 1975).

RANGE OF EXPERIENCE

Of the 70 users returning questionnaires, 31 percent (22) started using satellite data in 1972, immediately after the launch of Landsat–1; 40 percent (28) began their use in 1973; 23 percent (16) in 1974; and only 6 percent (4) started in 1975. Of these same users with experience in Canada, 24 percent (17) have experience with Landsat data for other parts of North America, and 21 percent (15) have similar experience for other parts of the world.

TABLE 4.—*Geological users of Landsat data, 1975*

Class	Annual use (scenes per year)						
	10	10–50	50–100	100–500	500	Unknown	Total
Geological survey and research:							
(a) Gov'ts	1	3	3	--	--	--	7
(b) Universities	4	4	1	--	--	--	9
Mineral exploration:							
(a) Oil and gas	3	3	3	3	1	1	14
(b) Ore	7	12	7	--	1	1	28
(c) Combined	--	2	1	--	--	--	3
Consultants and contractors	1	3	--	2	1	--	7
Not specified	--	1	1	--	--	--	2
Total	16	28	16	5	3	2	70

TABLE 5.—*Net sales of standard Landsat products to recognized geological users*
[Excluding a national collection at G.S.C.]

Class	BWPRT*	CPRT*	BWTRA*	CTRA*	Total	Percent of total net products
Oil and gas exploration companies	3448	164	414	200	4226	22.9
Mining exploration companies	4020	486	229	85	4820	26.2
Consulting and contracting companies	2192	154	187	95	2628	14.3
Federal agencies	2463	755	244	72	3534	19.2
Provincial agencies	1373	323	309	65	2070	11.2
Academic institutions	941	37	88	12	1078	5.9
Other	47	6	----	2	55	0.3
Net Products	14,484	1925	1471	531	18,411	100
National collection, G.S.C.					18,022	
Total products sold to recognized geological users:					36,433	

* BWPRT = black and white prints.
CPRT = colour prints.
BWTRA = black and white transparencies.
CTRA = colour transparencies.

LEVEL OF CANADIAN TECHNOLOGY FOR GEOLOGICAL INTERPRETATION

Most users (93 percent of the 70 respondents) commonly use visual interpretation based on standard photogeologic techniques. The remainder reported rare or nil use of such techniques. Enlargements and projections are commonly used for interpretation at scales as great as 1:250,000. Two major users and seven smaller users reported working at scales as large as 1:50,000. Thirty-six percent (25) of the users reported that they had tried seasonal enhancements, but only 13 percent (9) noted that they did so commonly. Ten users (14 percent) reported using machine assistance, 6 did so commonly. Comparable figures for digital processing are 6 and 1. Of the seven users reporting common use of machine and digital assistance, only one purchases more than 100 scenes per year.

Most users (62 or 88 percent) use black and white prints while about half have used colour prints (37), enlarged prints (38), or black and white transparencies (32). The strong preference by geological users for black and white prints extends to all classes of such users (table 5). Few users (<1 percent) have worked with computer compatible tapes (CCT's) or enlarged transparencies, although 70 mm transparencies have been more widely used (21 percent). All four MSS bands and colour composites are the preferred materials for 40 percent (28) of the users while the remainder prefer band 6 either alone or in conjunction with band 5 and/or band 7. Band 4 receives less use although it is ordered frequently.

In summary, the analytical technique in common use among geologists at this time appears to be visual interpretation of black and white prints. Very little research seems to be directed to machine and computer assistance for geological applications, although there are a few notable exceptions.

CURRENT GEOLOGICAL USES OF LANDSAT DATA

GENERAL

Interpretation, or the extraction of information about the surface of the Earth, is the prime use of Landsat data. Such use may be in support of research to increase scientific knowledge or in support of practical applications to meet economic and social goals (Gregory and Moore, 1976). Practical applications are commonly assumed to have a high probability for imminent return on investment. The distinction is judgmental and lacks clarity. Other uses, such as reference collections, illustrations, educational displays, and works of art have not been assessed, although the first, in particular, requires large numbers of images.

During the past 3 years, much of the use of Landsat data fell into the category of research as Canadian geologists strove to define potential applications, particularly for use in geological mapping. However, only 13 percent of the respondents to the 1975 questionnaire considered that they were conducting research currently. Hence there has been a steady growth in the practical application of Landsat data. Accordingly, we have attempted to sort and outline the various Canadian uses of Landsat data under the two categories of research and practical application.

RESEARCH

Currently available results of research show a primary concern with the development of techniques to identify and map geological structures and the disposition of major classes of rock. Standard photogeologic techniques were extended to the specific geometry and data for Landsat, with emphasis on texture and pattern. Thus, early visual studies established that many Canadian geological provinces have characteristic bulk textures and that geological lineaments and structures may be well expressed in Landsat data (Gregory and Moore, 1975 and 1976; Palabekliroglu, 1974a and b; Moore and Gregory, 1974; and Slaney, 1974). Similar analyses suggested practical applications in hydrogeology (Ozoray, 1974). The utility of temporal (or seasonal) analyses was demonstrated by Moore and Gregory (1974). Optical Fourier spectra were used by Arsenault and others (1974) to select and enhance linear features. In addition, they showed that holographic filtering could be used to detect simple characteristic shapes.

Spectral discrimination for geological purposes does not appear to have received adequate research in Canada, at least outside the bounds of commercial proprietary knowledge. Spectral discrimination of vegetational anomalies and possible applications in mineral exploration have been considered (see, for example, Working Group on Geoscience, 1974), but to date no success or systematic use has been confirmed. However, a most significant development has been reported in the spectral discrimination of terrain classes in the Canadian Arctic (Boydell, 1974, and subsequent personal communication). This evaluation shows that multispectral analysis of Landsat data, using CCT's and the Bendix MAD unit, could comprise a potentially more rapid and relatively accurate alternative to the conventional methods of preparing preliminary terrain maps by airphoto analysis. At the present stage of development, the validity of terrain classes is dependent upon detailed knowledge of the terrain and is not absolute, thus hindering general extrapolation and regional mapping. This research, however, is being continued by the Terrain Sciences Division of the Geological Survey of Canada.

A strong interest in ice reconnaissance was indicated by major users of Landsat data in the oil and gas industry. Attendant research has focussed on breakup and freezeup patterns in the Beaufort Sea and on the measurement of floe size and rates of movement during those periods.

PRACTICAL APPLICATIONS

No practical applications of Canadian Landsat data are currently documented in the literature. This reflects, in part, the newness of such applications in that case histories are still subject to field investigation

and, in part, the common commercial requirement for protection of proprietary rights with respect to methodology and results. The questionnaire previously mentioned, however, shows that Landsat images are being widely, intensively, and systematically used by mineral exploration companies and consultants. The practical objectives of such applications are relatively simple, as revealed by respondents to that questionnaire. A regional overview of geology is the prime requisite of 86 percent of the users, 67 percent are particularly interested in analyzing linears, and 41 percent in the selection of targets for more detailed investigation (c.f., Sabins, 1974; Collins and others, 1975, for U.S.). Secondary objectives included spectral discrimination of rock types and alterations (27 percent), which surely was mainly experimental, and the use of images as base maps for planning and managing exploration projects (26 percent). About 13 percent of the respondents reported using Landsat images for each of the following: recording environment in the vicinity of producing sites, regional overview of logistical factors, and classification of materials. The principal information derived from the Landsat data comprises: geological structures (66 percent), disposition and classification of rock units (46 percent), and surficial geology (34 percent). Other types of information, each reported by less than 10 percent of the respondents, include information related to soil type, erosion and sedimentation, terrain classes, surface water, land use, construction aggregate, ground water, natural disasters, and waste disposal. Other interesting uses, each reported by one respondent, were: spectral discrimination of zones of subsidence and correlation with aeromagnetic data.

While published case histories are lacking at present, there are several Canadian projects to which Landsat data are known to have made major or prime contributions. For example, they have been used to assess the structural framework of metallogenic provinces (linear analyses), to define structural and lithologic targets for diamond exploration in Africa and Canada (linear and spectral analyses), to plan alternate routes for a pipeline (mapping of well-drained ridges formed by glacial fluting), to classify mine wastes at a scale of 1:50,000 (spectral analyses), and for geological mapping to locate rock types, folds, and faults of importance in oil and gas exploration. In addition, as noted previously, there are active projects for mapping ice conditions related to oil and gas exploration in the Beaufort Sea and for forecasting snow and ice cover to assist in planning mineral exploration in northern Canada.

BENEFITS FROM USE OF LANDSAT DATA

Respondents to the questionnaire reported that the major benefits which they recognized from their use of Landsat data were:

1. Acquisition of geological information that is not readily available otherwise (64 percent);
2. Acquisition of supporting information to be integrated with other data (53 percent); and
3. Saving in time in assessing the regional geology (48 percent).

About 20 percent of the respondents reported that their use of Landsat data had resulted in a lower cost for assessing regional geology, had assisted in reduction of area for detailed study, and had assisted in mineral prospecting. Unfortunately, from a scientific viewpoint, a successful application of Landsat data in mineral exploration is least likely to be disclosed publicly. About 14 percent of the respondents reported receiving additional nongeologic information that was not readily available otherwise.

Ninety-three percent of the respondents reported that their use of Landsat data had contributed to their geoscience programs; 43 percent (30) considered the contribution to have been modest; 8 percent (5) considered it large, while 43 percent (30) considered it minimal; and 7 percent did not answer. Specific cost savings could not be identified by 41 percent (29), while 13 percent (9) consider there was no measureable saving, and 46 percent (32) did not answer the question.

These responses about benefits confirm the view that Landsat data, in conjunction with other types of data, are employed extensively in the regional reconnaissance which precedes more expensive, detailed methods of exploration. As is well known, many different geological, geophysical, and geochemical techniques are employed in compiling the information that eventually leads to a mineral discovery. Thus, it is simplistic and unrealistic to credit a discovery to a single methodology. It is equally unrealistic to expect an identifiable cost benefit to be assigned to a specific use of Landsat data. However, it is significant that 50 percent of the respondents, including 6 of the 8 major users, claim a modest to large benefit from their use of Landsat data.

FORECAST OF TRENDS

The utilization of Landsat data will continue to follow the typical use curve that describes the temporal development of new technology. With respect to visual photogeologic interpretation, the use of Landsat data has rapidly risen to "Panacea Peak," fallen into

"Sanity Slump," and is now beginning to climb "Reality Rise" toward the "Plateau of Practicality." However, the geological goals of practical spectral discrimination and automated processing have yet to be defined, and regular low-cost production has not been achieved.

Further research in these latter fields will be hindered by the fundamental limitations of surficial obscuration (lichens, vegetation, and overburden) and the lack of the third dimension, depth. Such limitations suggest that major support for this research must be obtained from organizations concerned with surficial mapping (e.g., governments and universities) rather than from mineral exploration companies which have equal or greater concerns with depth. Nevertheless, there are compositional contrasts of geoscience interest (e.g., gossans, alteration zones, and vegetational anomalies) that can serve to focus further research by means of spectral and automated analyses. The subsequent development of practical applications will be guided by the fact that these techniques, like all other methods of exploration, will not be specific but, rather, will undoubtedly present a multiplicity of anomalies for field checking.

Visual interpretation of Landsat images will continue to receive increasing acceptance as a tool, in conjunction with others, for developing concepts to guide mineral exploration and geological mapping, both in Canada and abroad. Landsat images will soon become a prime tool for regional geological reconnaissance, especially for poorly explored, arid and semiarid areas. This will probably become true even if Landsat were to fail in the near future. However, much additional experience must be accumulated before geologists can confidently associate mineral deposits with features on Landsat images. In particular, the ubiquitous linears will require classification and analysis before their geological significance can be fully understood. In this growth of practical applications, transparencies will be substituted for prints in laboratory analyses because of the inherently greater resolution; however, prints will be preferred for annotation and field studies. Improved instrumentation will be developed to assist such analyses.

Spectral discrimination and automated processing will evolve very slowly until substantial funding and dedicated programs are developed in support of geological applications. A major and practical advance in terrain classification by automated methods appears imminent. However, because of complex interrelationships between bedrock, soil, water, and vegetation, automated pattern recognition will remain unattainable for all but the simplest geological goals (Gregory, 1973, p. 89; Sabins, 1974) and even there may be too expensive for practical application. While Landsat data have the advantage of uniform raked illumination, minimum geometric distortion, synoptic view, and worldwide coverage, it is primarily the related low cost of purchase and analysis that has led to their widespread adoption for regional reconnaissance. Spectral discrimination and automated processing will not be adopted for regular use until their current high costs are reduced. Indeed, as Kite (1975) has noted, it remains to be shown that such methods will be significant for mineral exploration and geological mapping. Perhaps the most useful future development for geoscientists will simply be an increase in resolution to 2 or 3 times that currently attained with Landsat.

CONCLUSIONS

Canadian interest in Landsat data is widely spread and more-or-less equally divided among companies, educational institutions, and government agencies.

Geoscientists have had a long, continuing, and major involvement with the Canadian Landsat program. However, at present only about 10 percent of the geoscientists have a strong commitment to the activity.

Current data defining sales and use of Landsat data show that identified geoscience organizations are major, if not the principal, users of Landsat data. Excluding reference collections, mineral exploration companies and consultants are the principal users.

Most (71 percent) geological users of Landsat data have been using such data since 1973 at least; the remainder started more recently but primarily in 1974. Nearly a quarter of the Canadian users have experience with Landsat data for other parts of the world.

Visual photogeologic interpretation of black and white prints comprises the principal Canadian method of analysis. Digital processing and machine assistance have not really been assessed for geological applications, and little relevant research has been reported.

Most Canadian research has been directed to the development of visual techniques to meet specific requirements for the analysis of texture and patterns in Landsat images. However, there has been a major advance in the digital classification of Arctic terrain.

Practical applications are not yet documented in the literature. However, known examples are related primarily to reconnaissance for geological structure and disposition of surficial materials. Half of the geological users of Landsat data claim a modest to large benefit from such use but cannot identify a specific dollar benefit.

In view of the major geoscience involvement, increased support is warranted for research into digital and automated methods of processing Landsat data to meet geological objectives. In particular, this should include temporal change detection, spectral discrimination and ratioing, and directional filtering, if warranted by developments in linear analysis.

The level of development of practical geologic applications in Canada is greater than predicted in a pre-Landsat forecast. Visual interpretation of Landsat images will soon become a prime tool, in conjunction with others for regional exploration, particularly in arid regions. Automated processing will remain in the research stage until low-cost methodologies are developed to meet specific geological objectives.

Because the specific Canadian context comprises a large, well-mapped terrain, the conclusions reached here should be extrapolated with caution to other different and less-explored terrains.

REFERENCES

Arsenault, H. H., Sequin, M. K., Brousseau, N., and April, G., 1974, Le traitment optique des Images ERTS: Canadian Symposium on Remote Sensing, 2d, Guelph 1975, Proc., v. 2, pp. 488–493.

Boydell, A. N., 1974, Evaluation of the potential uses of Earth Resources Technology Satellite (ERTS–1) data for small scale terrain mapping in Canada's North: Internat. Soc. Photogramm. Comm. VII, Symposium on Remote Sensing of Environment, Alberta 1974, Proc., pp. 329–340.

Cameron, H. L., 1964, Photo interpretation in geotechnical investigations: Canada Interdept. Comm. on Aerial Surveys, Seminar on Airphoto Interpretation in the Development of Canada, Proc., pt. 4, pp. 10–20.

Collins, R. J., Petzel, G. J., and Everett, J. R., 1975, An evaluation of ERTS data for petroleum exploration (abs.): University of Kansas Space Technology Centre, Case History Research Conference on Remote Sensing, Lawrence, Kansas, pp. 8–10.

Fischer, W. A., 1964, Geological interpretation from airphotos: Canada Interdept. Comm. on Aerial Surveys, Seminar on Airphoto Interpretation in the Development of Canada, Proc., pt. 4, pp. 21–31.

Gregory, A. F., 1972, What do we mean by remote sensing?: Canadian Symposium on Remote Sensing, 1st, Ottawa 1972, Proc., pp. 33–37.

———1973, A possible Canadian role in future global remote sensing: Can. Aeronautics and Space Jour., v. 19, no. 3, pp. 85–92.

Gregory, A. F., and Moore, H. D., 1975, The role of remote sensing in mineral exploration with special reference to ERTS–1: Canadian Inst. of Mining and Metallurgy Bull., v. 68, no. 757, pp. 67–72.

———1976, Recent advances in geologic applications of remote sensing from space: Internat. Astronautical Fed. Astronautical Congress, 24th, Baku 1973, Astronautical Research: 1973, pp. 1–18.

Gregory, A. F., and Morley, L. W., 1969, Remote sensing and the solid-earth science, *in* Background papers on the Earth Sciences in Canada: Geol. Survey of Canada Paper 69–56, pp. 170–179.

Kite, R. L., 1975, Research on techniques for photographic enhancement of ERTS imagery for geologic applications (abs.): University of Kansas Space Technology Centre, Case History Conference on Remote Sensing, Lawrence, Kansas, pp. 28–30.

Moore, H. D., and Gregory, A. F., 1974, Temporal analyses of ERTS–1 images for forest and tundra and their significance in visual interpretation of geology: Canadian Symposium on Remote Sensing, 2d, Guelph 1975, Proc., v. 1, pp. 47–58.

Morley, L. W., 1971, Canada's approach to remote sensing: Internat. Symposium on Remote Sensing of the Environment, 7th, Ann Arbor, Mich. 1971, Proc., v. 1, pp. 3–18.

Ozoray, G., 1974, Lineament analysis using ERTS–1 images of Alberta: Internat. Water Resources Assoc. Internat. Seminar and Exposition on Water Resources Instrumentation, Chicago 1974, Water Resources Instrumentation, pp. 456–466.

Palabekiroglu, S., 1974a, The value of ERTS–1 imagery for mineral exploration: Canadian Symposium on Remote Sensing, 2d, Guelph 1975, Proc., v. 2, pp. 464–470.

———1974b, ERTS–1 imagery: The valuable tool of geoscientists: Internat. Soc. Photogramm. Comm. IV Symposium on Remote Sensing and Photo Interpretation, Proc., pp. 597–609.

Sabins, F. F., Jr., 1974, Oil exploration needs for digital processing of imagery: Photogramm. Engineering, v. 40, no. 10, pp. 1197–1200.

Slaney, V. R., 1974, Satellite imagery applied to earth science in Canada: Internat. Soc. Photogramm. Comm. IV Symposium on Remote Sensing and Photo Interpretation, Proc., pp. 555–572.

Woolnough, D. F., 1975, Theoretical accuracies of space mapping for Canada: The Canadian Surveyor, v. 29, no. 3, pp. 267–276.

Working Group on Cartographic and Photogrammetry, 1974, Report of the Working Group on Cartography and Photogrammetry, *in* Canadian Advisory Committee on Remote Sensing, 1974 Report: pp. 48–49.

Working Group on Geology, 1971, Resource satellites and remote airborne sensing for Canada: Report No. 6, Geology: Ottawa, Dept. of Energy, Mines and Resources.

Working Group on Geoscience, 1972, Report of the Working Group on Geoscience, *in* Canadian Advisory Committee on Remote Sensing, 1972 Report: Ottawa, Dept. of Energy, Mines and Resources, pp. 77–80.

———1973, Report of the Working Group on Geoscience, *in* Canadian Advisory Committee on Remote Sensing, 1973 Report: Ottawa, Dept. of Energy, Mines and Resources, pp. 72–83.

———1974, Report of the Working Group on Geoscience, *in* Canadian Advisory Committee on Remote Sensing, 1974 Report: p. 85.

PROCEEDINGS OF
THE FIRST ANNUAL WILLIAM T. PECORA MEMORIAL SYMPOSIUM,
OCTOBER 1975, SIOUX FALLS, SOUTH DAKOTA

Mapping and Charting from Landsat

By Alden P. Colvocoresses,
U.S. Geological Survey, Reston, Virginia 22092

INTRODUCTION

Although I once was a mining engineer, I have been a mapmaker for the past 25 years, and my work is no more related to the oil and mining industry than it is to any other map-using group.

Mapmakers, as well as others, now have a satellite in orbit known as Landsat—previously known as ERTS (Earth Resources Technology Satellite)—by which we can map the Earth at the smaller scales in image form. Since there is a wealth of written data available, I have no intention of trying to cover Landsat mapping in any detail. Those of you who want more information are invited to drop me a note, or see me personally, and I will be happy to respond. A few of the more pertinent references are appended to this paper.

To me, mapping is fundamental to man's efforts to understand and live on this planet, and as persons concerned with exploration for petroleum and other mineral resources, I am sure you will agree. But what and how well can we map with Landsat? By the use of photographs I will illustrate some of the things that can be done and leave it to you to decide to what extent Landsat mapping can be applied to your specific problems.

LIMITATIONS

First, let me cover what we cannot do with Landsat. Objects too small to be recorded by the 79-m (260-ft) Landsat picture element cannot be seen on the imagery. Although the capture of specific detail is affected by contrast and shape, most features smaller than 8 or 10 acres, unless they are very high contrast or linear features such as roads and canals, will be lost. Second, we cannot use Landsat for topographic mapping because the system is basically orthographic, precluding the determination of elevations. Where suitable topographic data exist, a stereopair portraying topography can be processed from Landsat, and such a pair is, in fact, available to you as a handout. However, remember that the elevation data used to form the model did not come from Landsat.

UNIQUE CHARACTERISTICS

Most of you are familiar with aerial photography, so let's look at the unique advantages of Landsat imagery as compared with aerial photographs.

Continuity.—Can you imagine covering the Earth every 18 days with photography? I can't, but—subject to cloud cover, priorities, and transmission capabilities—Landsat does this, and moreover Landsat-1 has done it for more than 3 years. Just look at the published index maps showing only 2 years of Landsat coverage. Even so, we have a long way to go to adequately image the Earth for mapping and related purposes.

Near real time.—Most of the things you are looking for are fixed, but sooner or later you are going to want to see the results of a significant event. If it is local, an air photo is the way to go, but if it is widespread or in an isolated area, Landsat can help as figure 1 illustrates. This huge, seasonally dry area is shown here inundated, and the effects of this inundation will remain for several months. I would hate to have to map this changing condition with aerial photographs.

Geometric fidelity.—Landsat produces near-orthographic imagery of high geometric fidelity, and image maps with accuracy compatible with the 1:250,000 scale can be produced. Relief displacement is minimal, and the mapping is relatively cheap and simple as compared with mapping from aerial photographs. Figure 2 shows where we have actually corrected the standard 1:250,000-scale line map in the Phoenix area.

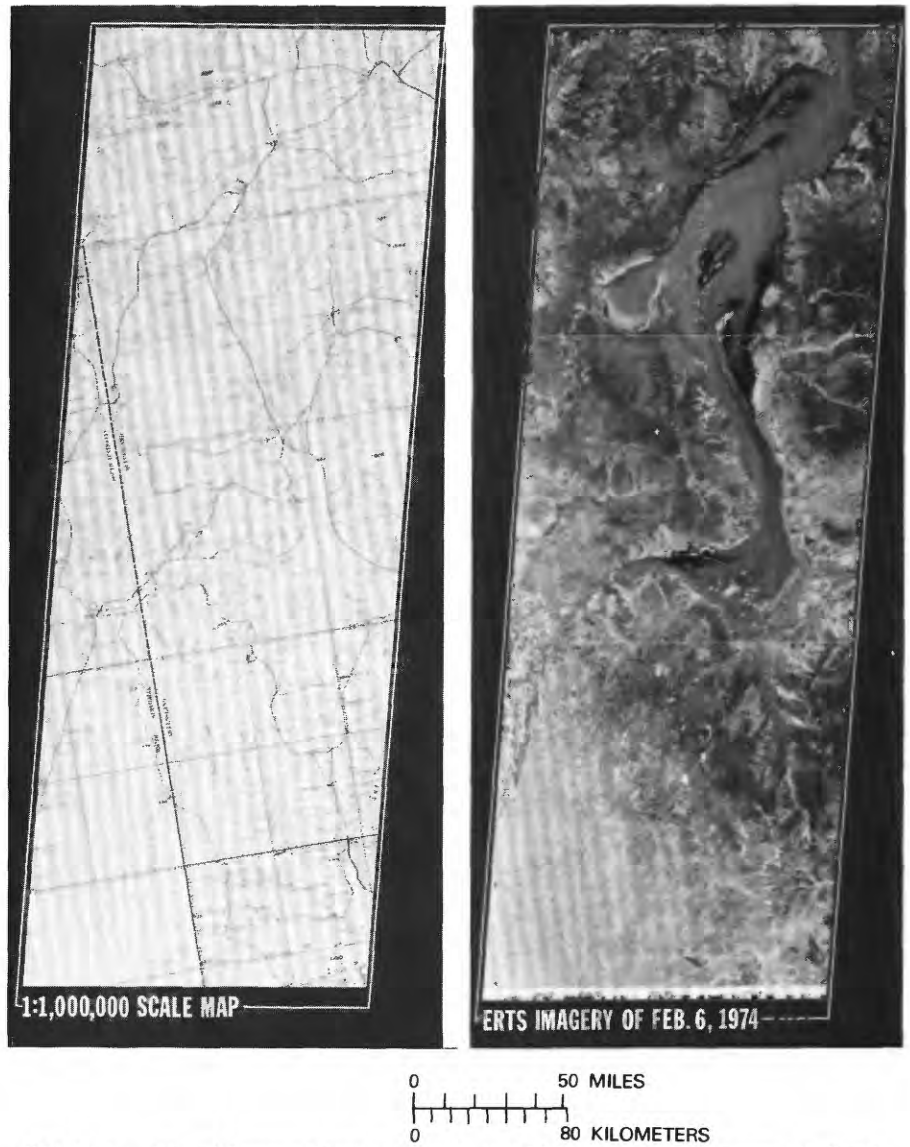

FIGURE 1.—Map of Cooper Creek, Australia, and ERTS imagery of the creek in flood.

Landsat is revealing many small- and medium-scale map errors and omissions in various parts of the world, and corrections and revisions based on Landsat are being applied by several mapping agencies. The Canadians, in particular, utilize Landsat for map revision—even up to the scale of 1:50,000 in provisional form. The World Bank is finding Landsat imagery to be far more accurate than available maps in many areas of the world where they have projects.

Multispectral compatibility.—On aerial film we record a broad waveband in black and white or at the most three narrower discrete wavebands in color. Landsat now records four discrete wavebands as digital radiometric values, including a band beyond the range of film cameras. Band 7 of the multispectral scanner (MSS) records 0.8 to 1.1 μm whereas aerial film cuts off at 0.8 μm. Look at the advantages of this near-infrared waveband (figs. 3 and 4). Landsat–C will also have a thermal band, which again is beyond the range of aerial films. The combining of waveband responses either by digital or photographic methods is, of course, spectacular, and Larry Rowan (USGS) will show how combinations can be applied to bring out or emphasize features of specific geologic interest.

Suitability for automation.—Landsat output is digital as well as continuous. Coupled with its geometric fidelity it has the potential of becoming an automated mapping system. The imagery is now cast on a defined map projection which we call the Space Oblique Mercator (fig. 5). As mentioned, Landsat also covers the same basic area every 18 days and thus forms a map series based on the nominal scenes covered (fig.

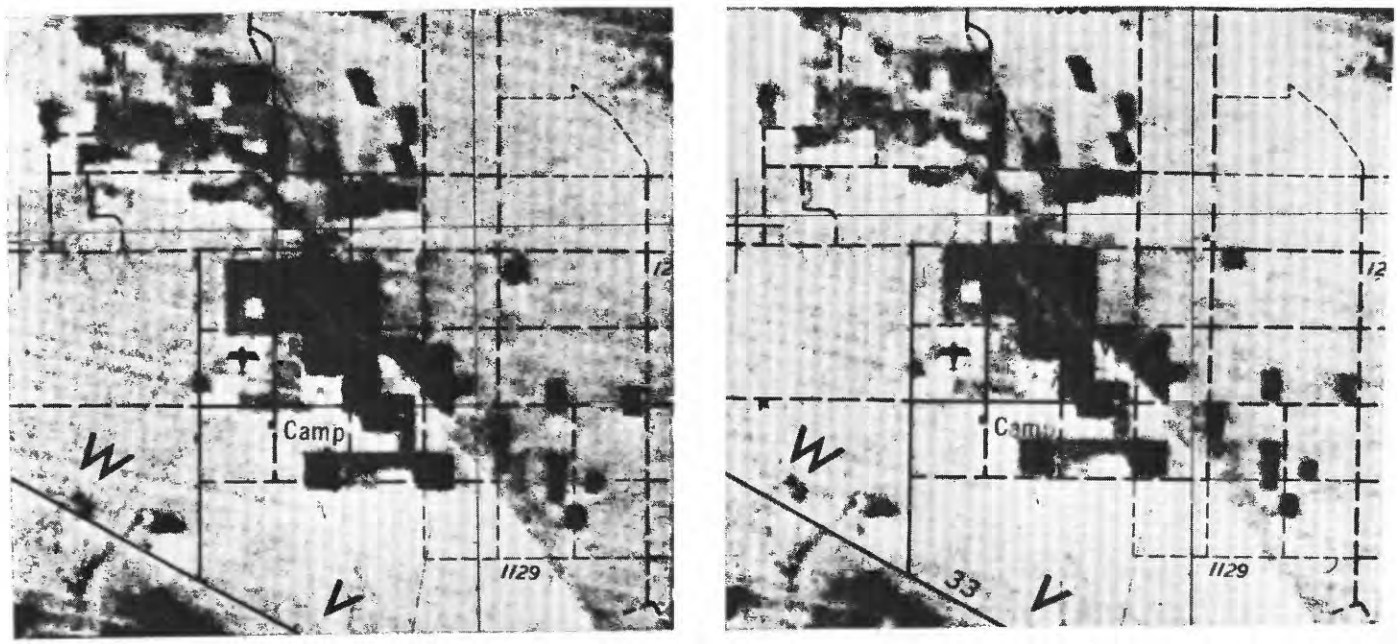

FIGURE 2.—Map accuracy improved by Landsat imagery. Map detail (planimetry) was moved about 1 mm (0.04 in.) on this 1:250,000-scale map of Phoenix to conform with the detail on the Landsat image. The image was found to be correct.

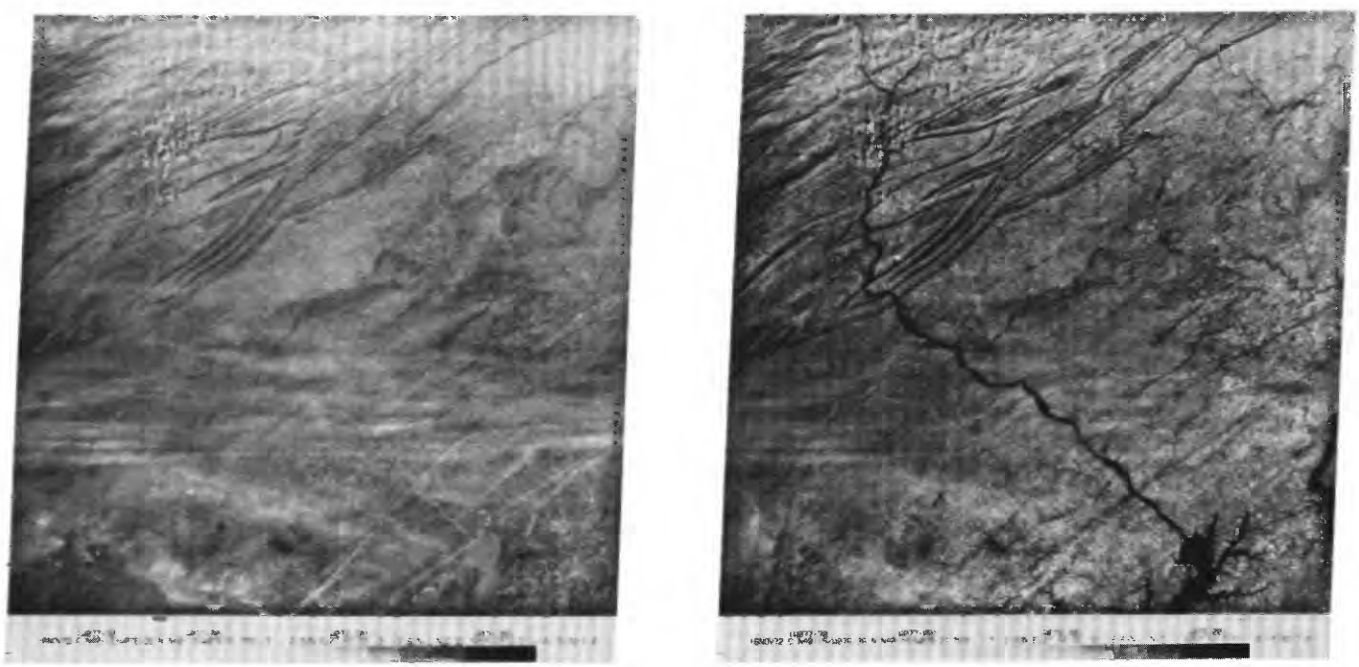

FIGURE 3.—Thin cloud penetration capability of ERTS IR sensor, southeast Pennsylvania, November 16, 1972.

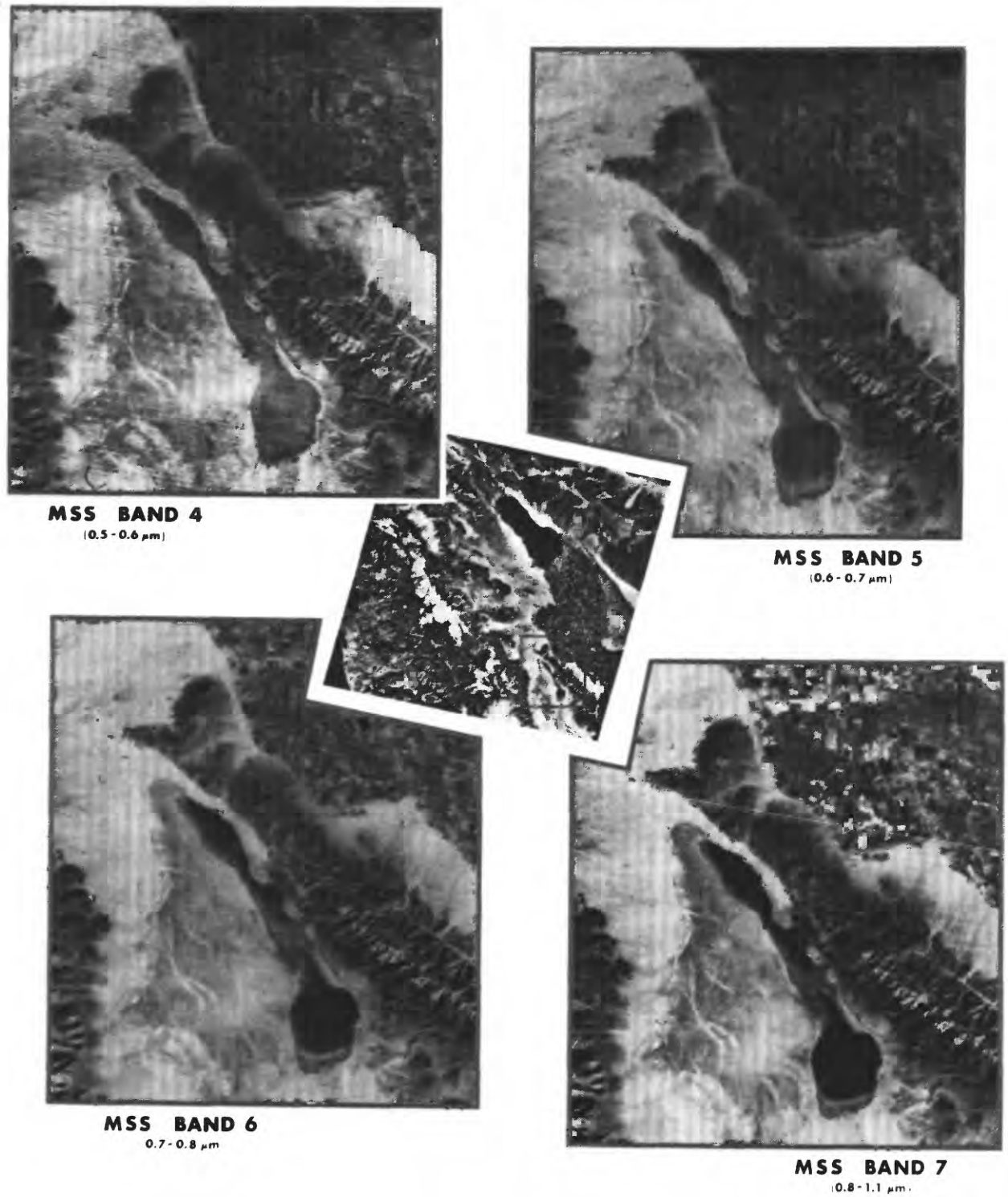

FIGURE 4.—Water boundary delineation from ERTS, Laguna Salada, northern Mexico.

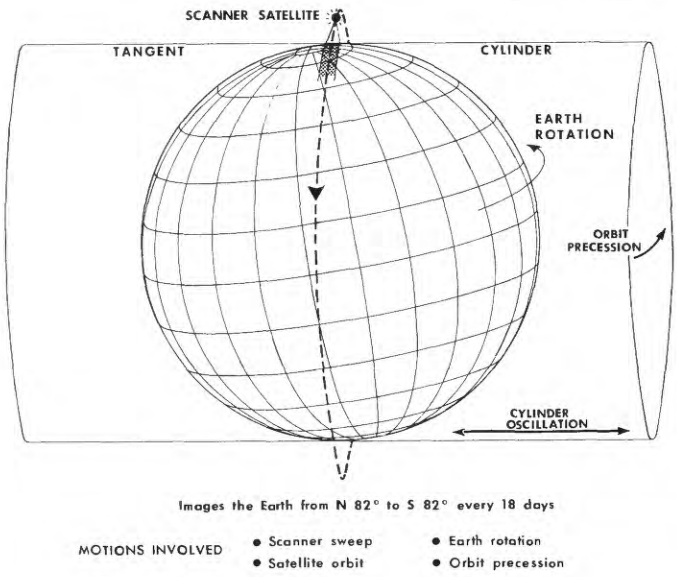

FIGURE 5.—Space Oblique Mercator projection.

6). These characteristics mean that Landsat image maps can be made in a few days time when needed. Making maps from aerial photographs, as you know, is a matter of months or even years. Currently, total time involved is about 5 years per standard map in the Geological Survey.

CARTOGRAPHIC APPLICATIONS

Now let's look at what Landsat can do cartographically. Obviously, it can portray topography even though it can't define the contours. Moreover, it portrays topography under different conditions of seasons. Let's look at the Denver area (fig. 7, p. VI). Note how differently the topography, as well as other features, are recorded. Or let's look at Lac Manicouagan, Canada (fig. 8). Note how the lower Sun angle enhances the topography and how different the same features appear.

Seasonal differences are obvious, but even in the same season and with the same lighting we should look at any given area at least two or three times so that fixed features can be separated from temporal phenomena and anomalies in image processing. Under the existing Landsat program a minimum of 10 years is needed to obtain suitable coverage for the definitive mapping of even the Earth's *fixed* features. Of course, if long-term temporal and seasonal changes are to be mapped, a remote-sensing system such as Landsat must be extended indefinitely—and I trust that it will.

The word Landsat implies land coverage, and the satellite was not designed to tell us much about the oceans. But how about coastal areas and particularly the shallow seas? I know two things about these shallow seas—they are extensive and they are very poorly mapped. From what I hear, they are also of ever increasing economic importance. Landsat's water-penetration capability is 10 to 20 m (33 to 66 ft) even under ideal conditions, but we have asked the National Aeronautics and Space Administration to adjust one MSS channel on Landsat–C which should increase this capability. I realize that most of the continental shelves are covered by water deeper than 20 m, but providing data even down to this depth would, I believe, be highly significant. Let's look at what can now be done with Landsat in the shallow seas (fig 9).

The published hydrographic chart obviously needs revision. In the Caribbean, figure 10 shows Landsat response related to depth over a well-charted bank, and nearer to home (fig. 11, p. VII).

For a variety of reasons this application is pretty well limited to the mid and lower latitudes. In the high latitudes, I suspect that the monitoring and mapping of sea ice may be the most important application (other than land area analysis) of concern to the oil industry. In Canada, a quick-look facility which transmits Landsat data directly to users in a matter of a day or so after reception has been developed and put to use. On Landsat–C, the thermal channel could double the frequency of observations as compared to Landsat–1 and –2 because useful observations can also be obtained at night. Also note that the meteorological satellites of National Oceanic and Atmospheric Administration (NOAA) and the Department of Defense (DOD) Defense Meteorological Satellite Program provides some excellent data on sea ice. Once we coordinate data from the three satellite systems of NASA, NOAA, and DOD, effective surveillance of sea ice can become a reality.

Landsat is not designed for atmospheric studies, but it will certainly record sizable smoke plumes from gas flares. The DOD weather satellite I previously mentioned can clearly record nighttime illumination, which includes the gas flares themselves (figs. 12 and 13). Note what appear to be flares in Northwest Canada. If they are not gas flares, I hope one of you may be able to offer some other explanation. The bright spots certainly correlate with the oil and gas fields of Alberta and British Columbia. A recent Canadian report indicates over 2.5 billion cubic feet of gas per month are being flared in Alberta alone.

According to one authority (Library of Congress) more petroleum products are being burned up in

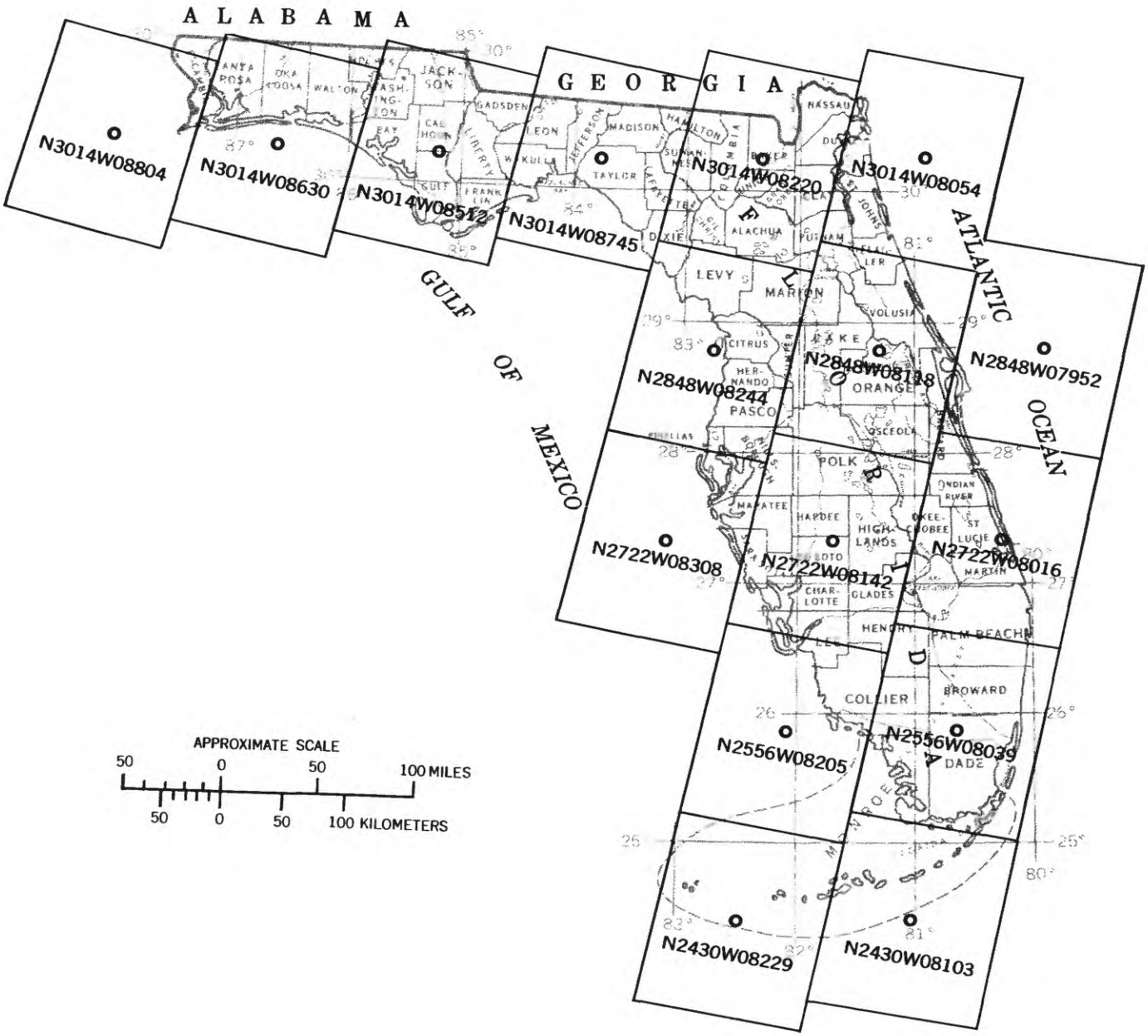

FIGURE 6.—Nominal ERTS scenes—Florida.

flares on a worldwide basis, than are being used productively. Landsat–1 and –2 cannot record flare illumination, but the thermal channel of Landsat–C should provide some meaningful signatures. Again, by combining the data from Landsat and the meteorological satellites, gas flaring can be monitored in both quantitative and positional terms on a worldwide basis.

Another application of Landsat that I wish to mention is the recording of artificially induced signals. The easiest signal to use is nothing more than a solar beam reflected to the satellite by a mirror. The mirror may be as small as half a metre (20 inches) on a side, but it can saturate a Landsat picture element (pixel).

Figure 14 shows how three mirrors located in the vicinity of our Reston building were recorded by Landsat. Similar mirrors can be set up at various remote stations, including offshore drilling platforms, and we plan to set up such mirrors in Antarctica during the next few months. The technique provides a visible position mark for an otherwise nondefined point. Incidentally, using this technique requires considerable expertise and close coordination with NASA,

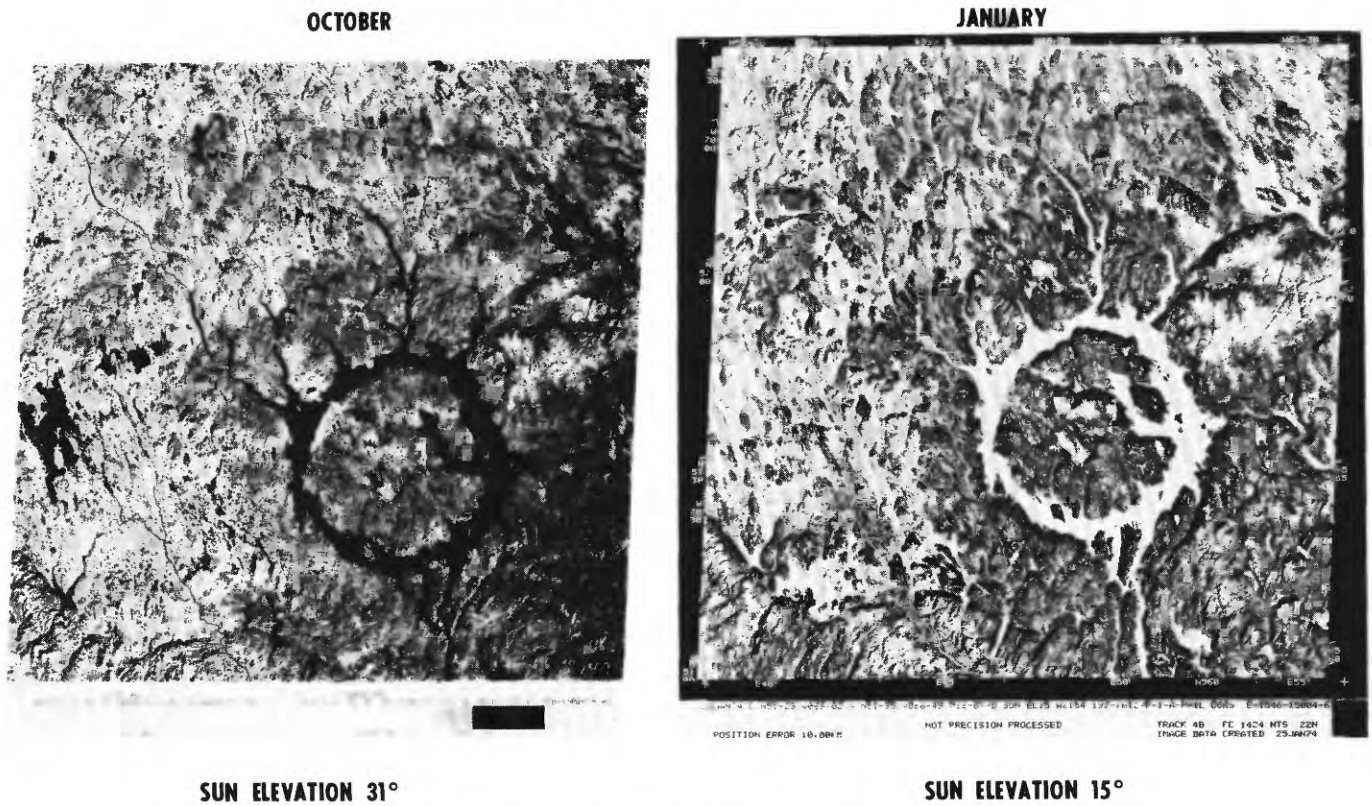

FIGURE 8.—Lac Manicouagan, Canada. Landsat imagery of a huge flooded impact (meteoritic) crater.

but its practical application should be further tested. You may want to contact Mr. Evans (1974) of Stanford Research Institute for further information. He is the one who originated this novel technique.

The last application is the actual image mapping. Landsat maps are being made for various parts of the world in ever increasing numbers, and in a wide variety of forms as figures 15, 16, 17, and 18 indicate.

Florida and Arizona are on public sale by the USGS. The entire conterminous United States has been printed (USGS) in small-scale mosaic form (also on public sale) and anyone who has the need and the money, can now make such a map of practically any land area in the world. Once we justify it, this coverage can also include the shallow seas. Technical data relative to such map compilation are contained in Chapman (1974), Colvocoresses (1975), McEwen and Asbeck (1975), and McEwen and Schoonmaker (1974).

SUMMARY AND CONCLUSION

I've covered technical aspects of Landsat as it applies to cartography. I feel sure that such a satellite system can in fact map the land and shallow seas of the Earth at scales as large as 1:250,000. However, I ask that you do not take the system for granted. It is a program that has lots of competition for the available space dollars. If you, individually or collectively, feel that the program is worthwhile and should continue, you must say so. My immediate concern is that Landsat may be converted into a specialized satellite to meet some particular problem of immediate concern. To me, that would be a mistake. We need basic information about this Earth in a continuous, uniform, and readily usable form. That is what Landsat is providing, and I strongly recommend that it be continued in the same basic form for the foreseeable future. Before we concentrate on a successor to Landsat, we should define the satellite that will immediately follow Landsat–C which may expire by 1979 or 1980. I suggest we now work on Landsat–D and perhaps –E, and if they fly in the form established by Landsat–1, –2, and –C, I for one will not be disappointed. We have got a winner, so let's stay with it until we are sure we have something better.

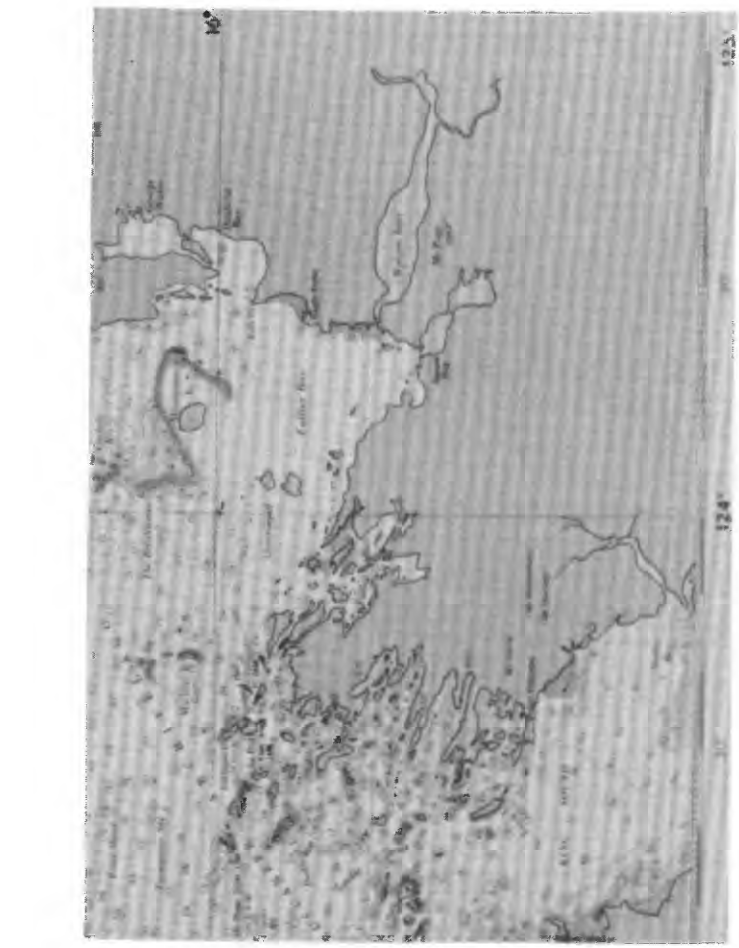

NAUTICAL CHART
(MERCATOR PROJECTION)

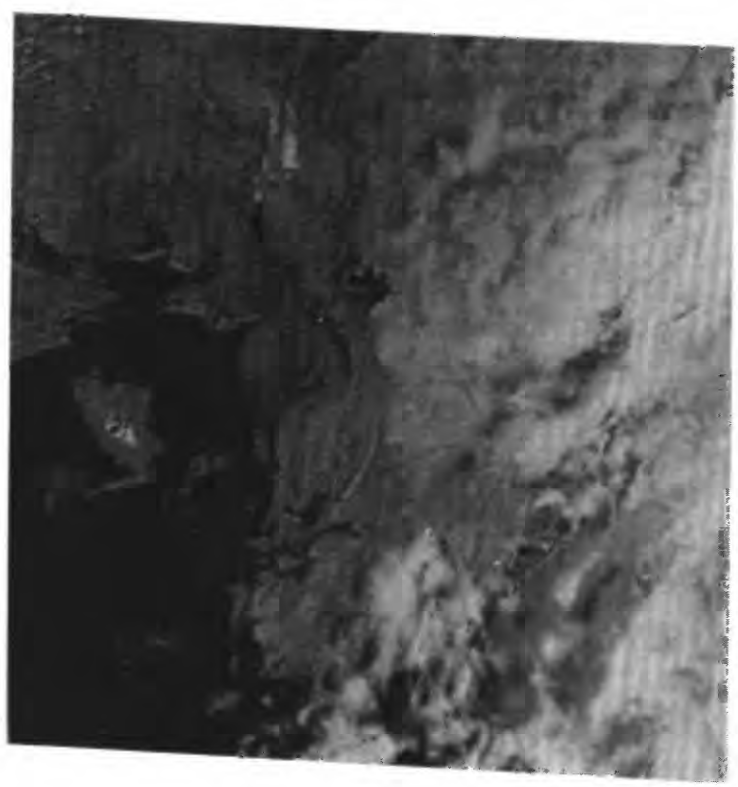

ERTS IMAGE

FIGURE 9.—Comparison of nautical chart and ERTS image, Collier Bay, Australia. Scales of the originals are approximately 1:1,000,000.

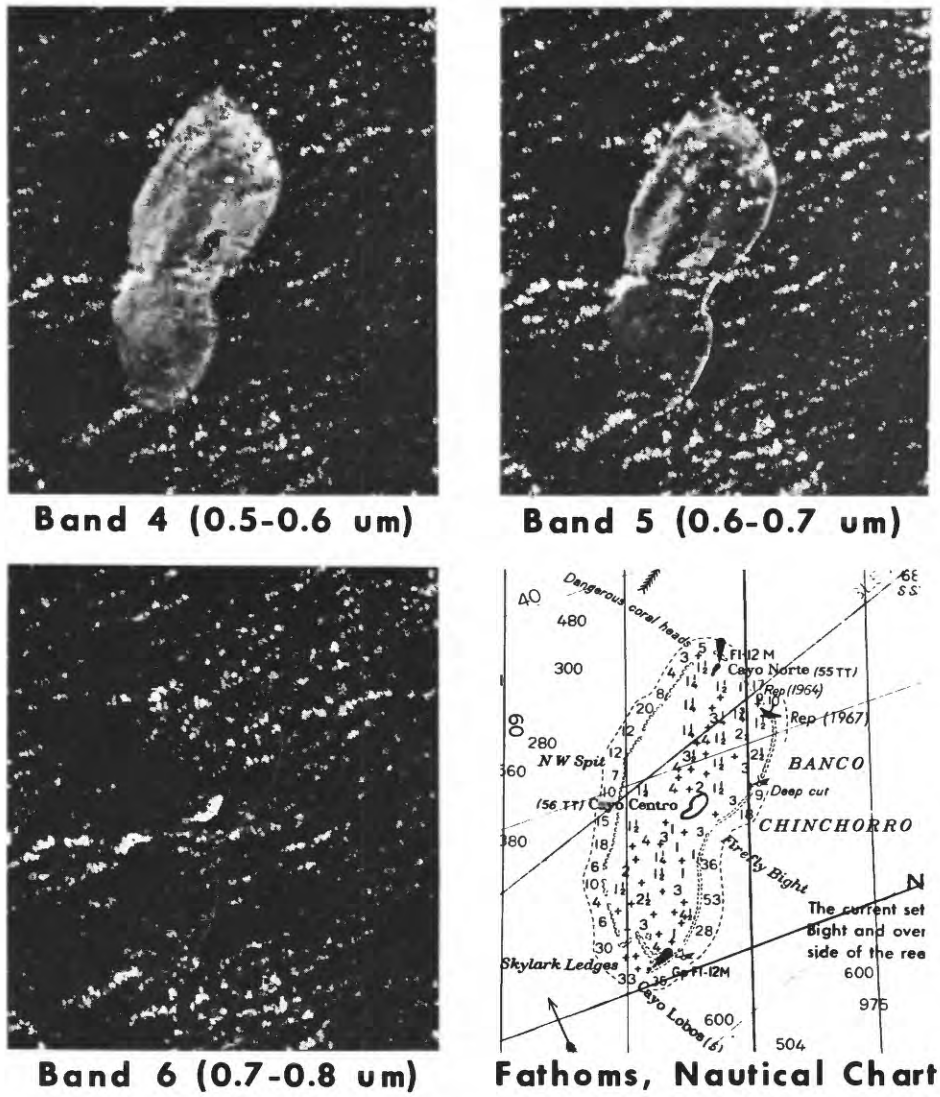

FIGURE 10.—ERTS correlation to nautical chart, Banco Chinchorro, Yucatan, Mexico.

FIGURE 12.—Gas flares in Saudi Arabia (Landsat).

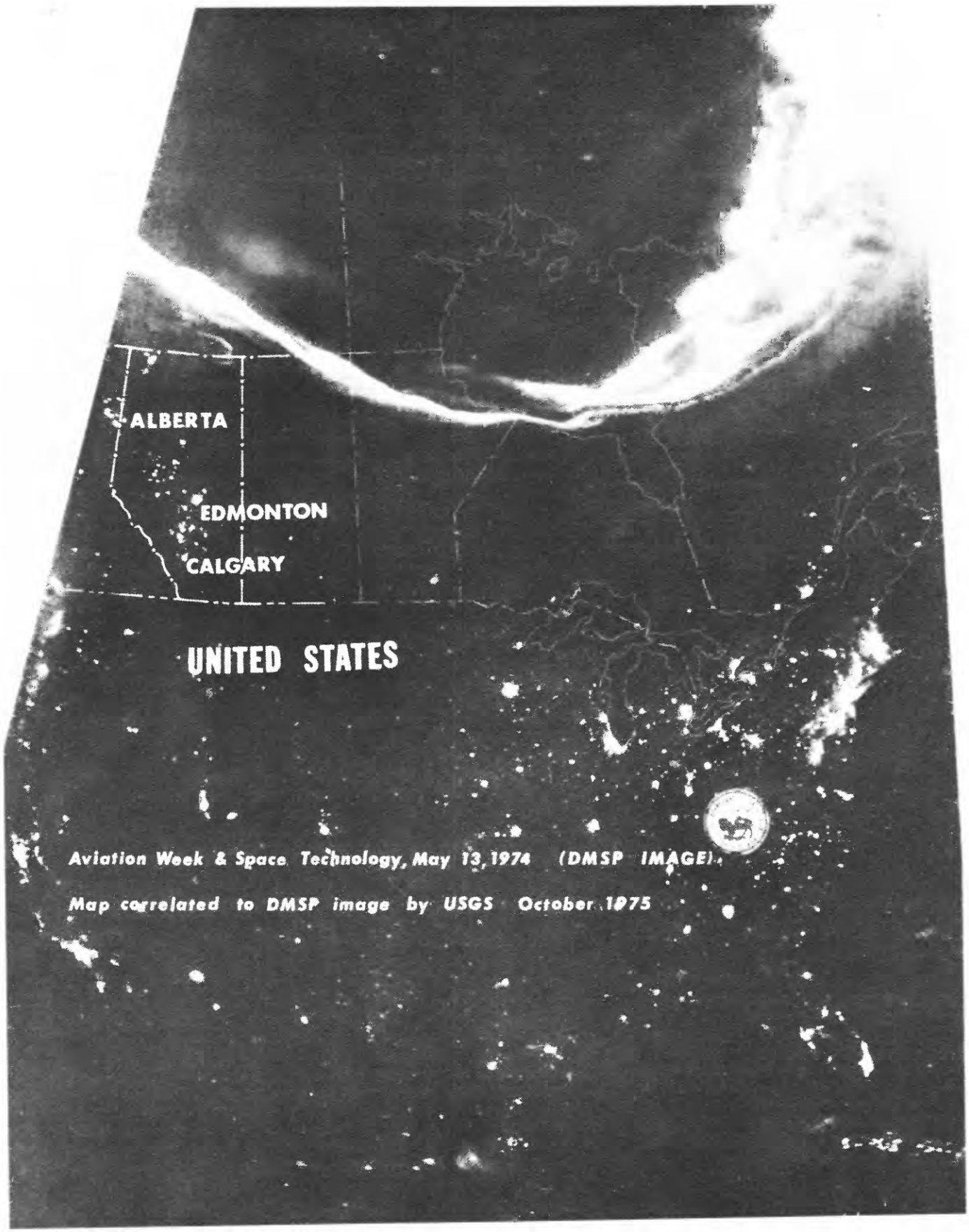

FIGURE 13.—DMSP image.

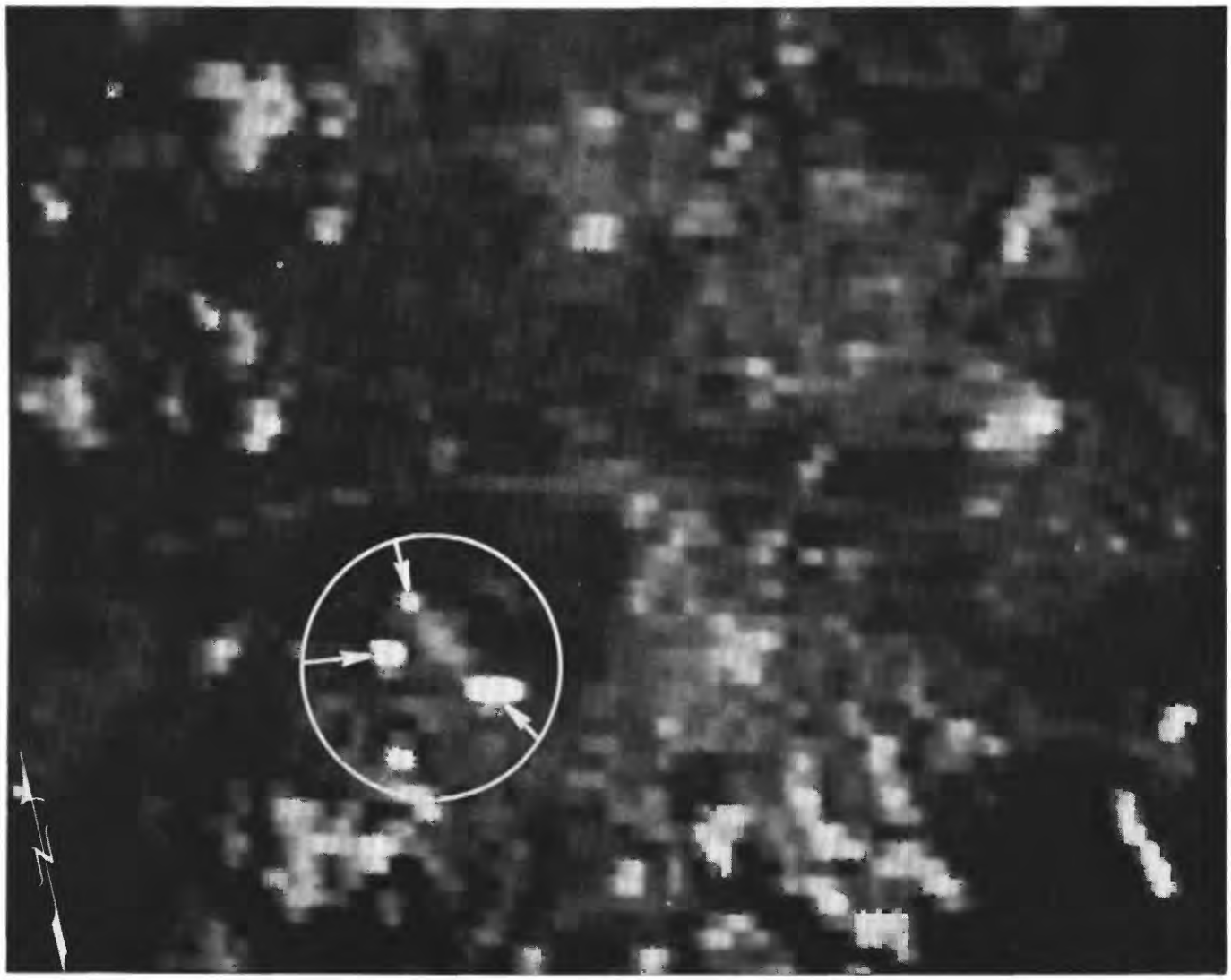

FIGURE 14.—Enlargement of a portion of ERTS image showing mirror response. Arrows point to pixels illuminated by small mirrors on the ground.

CANADA

THE NATIONAL CAPITAL REGION

LA RÉGION DE LA CAPITALE NATIONALE

REMOTE SENSING FROM SPACE

This experimental space photomap was produced from a portion of an image acquired by the Multi-Spectral Scanner (MSS) aboard the NASA Earth Resources Technology Satellite (ERTS 1) on June 3, 1973 from an altitude of 900 km (560 miles). The false colour image was made by combining images from 3 of the 4 spectral bands recorded by the scanner system.

Spectral band	Wavelength in nanometers	Colour in photomap
4	500- 600 (green)	blue
5	600- 700 (red)	green
7	800-1100 (infra-red)	red

This representation is termed false colour since the colours in the photomap do not correspond to the wavelengths sensed by the scanner. It is similar to the representation provided by false colour infra-red film used in aerial photography of natural resources.

In the photomap, clear, deep water shows as dark blue or black. Shallow or turbid water as lighter blue, and urban areas (built-up land) and soil exposures as blue-grey. Vegetation, having a high reflectance in the near infra-red, appears as shades of red, with cultivated fields appearing in bright red, coniferous forest a deeper red, and marshes a greyish-red or maroon colour.

ERTS-1 has provided images of every part of Canada and these images are being studied by scientists for applications in resource mapping and environmental monitoring.

LEGEND

Town
Highway
Airport
Quarry

TÉLÉDÉTECTION PAR SATELLITE

bande spectrale	longueur d'onde en nanomètres	couleur sur la carte
4	500- 600 (vert)	bleu
5	600- 700 (rouge)	vert
7	800-1100 (infrarouge)	rouge

FIGURE 15.—The National Capital Region, Ontario–Quebec, Canada.

FIGURE 16.—Phoenix.

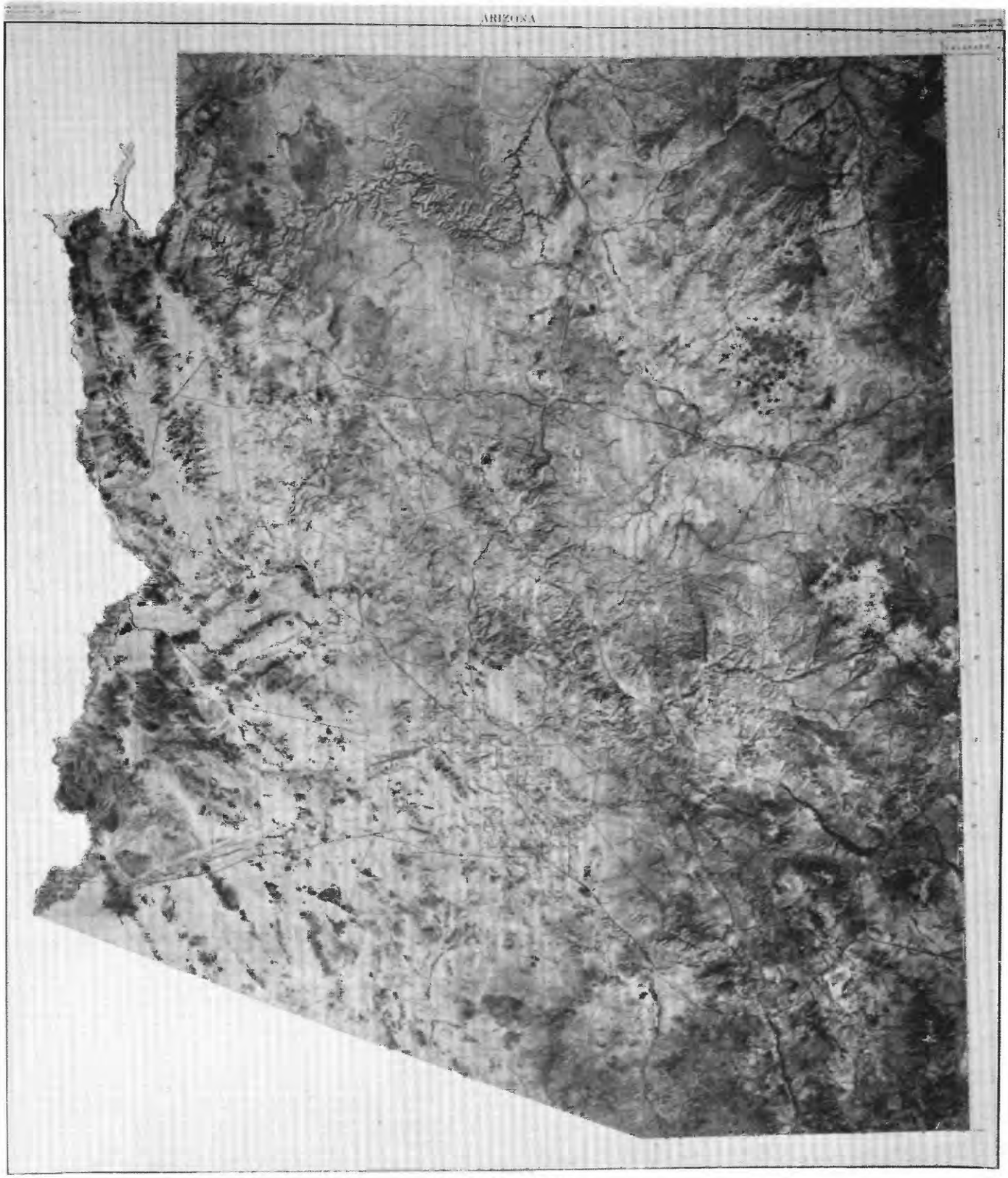

FIGURE 17.—Arizona.

FIGURE 18.—Florida.

SELECTED REFERENCES

Chapman, W. H., 1974, Gridding of ERTS images: Am. Cong. Surveying and Mapping Fall Convention, Wash., D.C. 1974, Proc., p. 15–19.

Colvocoresses, A. P., 1974–1975, Marking ERTS images with reflecting mirrors: Memorandum EC–24–ERTS with addendum. (Unpub.)

——— 1975, Evaluation of the cartographic application of ERTS–1 imagery: The American Cartographer, v. 2, no. 1.

Evans, W. E., 1974, Marking ERTS images with a small mirror reflector: Photogrammetric Engineering, p. 665–672.

McEwen, R. B., and Asbeck, T. A., 1975, Analytical triangulation with ERTS: Am. Soc. Photogramm. Am. Cong. Surveying and Mapping Convention, Wash., D.C. 1975, Proc., p. 490–503.

McEwen, R. B., and Schoonmaker, J. W., Jr., 1974, ERTS color image maps (abs.): Am. Soc. Photogramm. Fall Convention, Wash., D.C. 1974, Proc., p. 240.

PROCEEDINGS OF
THE FIRST ANNUAL WILLIAM T. PECORA MEMORIAL SYMPOSIUM,
OCTOBER 1975, SIOUX FALLS, SOUTH DAKOTA

Relationship of Mineral Resources to Linear Features in Mexico as Determined from Landsat Data

By Ing. Guillermo P. Salas,
Director General, Consejo de Recursos Naturales no Renovables, Mexico, D. F.

ABSTRACT

The author presents an exercise carried out in the "Mexican Neovolcanic Axis Metallogenetic Province" to relate traces of large diastrophic movements on the Earth's surface to mineral deposits.

The geologic history of the Neovolcanic Axis is presented and related to the lineaments that may be observed from Landsat imagery. A number of large lineaments 100 km long oriented east-west are believed to be great faults. There is also evidence of NE-SW fracturing and north-south faulting. A predominating NW-SE lineament trend parallels the structural expression of the early Eocene orogeny (Laramide). The latter is better observed in the eastern part of the Neovolcanic Axis Metallogenetic Province.

Comments are made regarding the masking of extensive diastrophic evidence by recent bolson or valley-fill accumulation, as well as by extrusive igneous rock flows which have not been subjected to diatrophic adjustment since their empacement at the surface.

It was found that mineralization does have a good coincidence with particularly large lineaments shown in Landsat imagery. An incidence of mineralization is particularly noticeable where the structural features are multidirectional, perhaps caused by the emplacement of deep-seated plutons which also give rise to metallogenetic processes.

It is concluded that lineaments observable in Landsat imagery will enhance target area selection considerably.

INTRODUCTION

This study has attempted to relate surficial evidence of diastrophic movement visible on Landsat–1 imagery along the Mexican Neovolcanic Axis (fig. 1) to metallogenetic processes.

To accomplish this objective the trends of orientation of long lineaments, generally several tens of kilometres in length, were observed to relate tectonics to the geology of the area.

An overlay map was made of the known mineral occurrences in the area (fig. 2). It was noticed that certain metallogenetic processes show incidence along more intensively disturbed areas.

The quality of the Landsat–1 imagery was not the best; this notwithstanding, most of the band 7 images used showed good contrast and clarity, and the features under study were clearly observed although cloud cover restricts interpretation in some areas.

The author was able to identify lineaments and faults of lengths varying from 10 to more than 100 km, which are difficult or impossible to detect through the use of normal scale aerial photographs. It is expected that the results of this preliminary study may help to stimulate similar exercises in Mexico and elsewhere in Latin America.

It was impossible for the author to correlate observed evidence with real ground-truth evidence everywhere. The only correlation possible regarding the type of rock involved in diastrophic movements was taken from geologic maps along the Neovolcanic Axis and from previous visits of the author to the mining districts of El Oro and Tlalpujahua, Taxco, and others.

The results obtained confirm the author's contention that diastrophic movements of large dimensions involved a segment of the lithosphere at great depths, proportional to the length of the surface fracture. These phenomena in turn enhance the possibilities of mineralizing solutions reaching areas at the surface

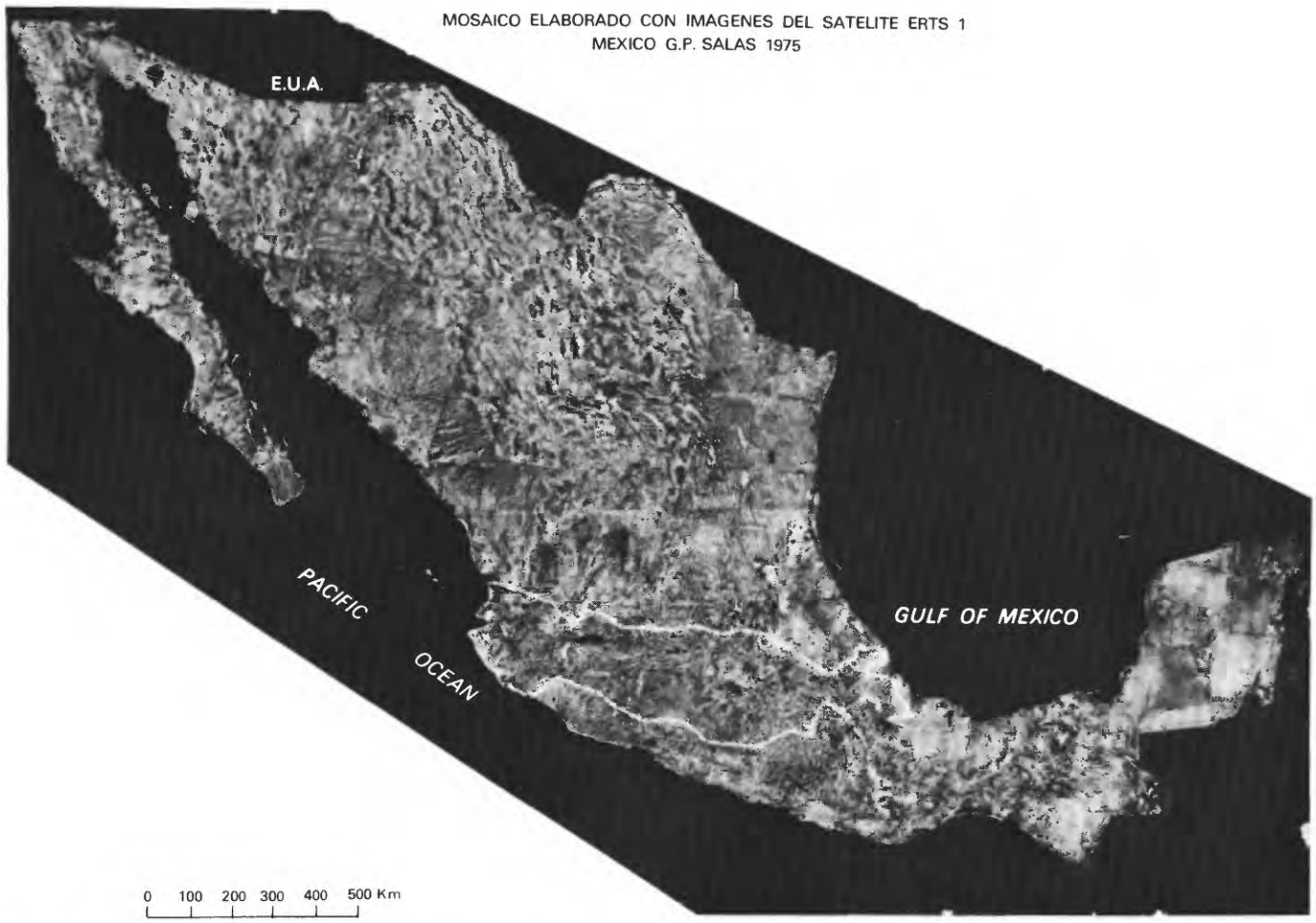

FIGURE 1.—Composite of Mexico from Landsat–1 imagery showing in white line the Neovolcanic Axis Metallogenetic Province.

or near the surface and, through metallogenetic processes, becoming ore bodies.

GENERAL GEOLOGY OF THE NEOVOLCANIC AXIS

Unfortunately, no real effort has been made to study the geology of the strip of many volcanoes that has been called the Mexican Neovolcanic Axis (Mooser, 1972). Mooser, who has done much of the work in the region, thought that the Mexican volcanic strip "could be the surface evidence of a very large transverse fault of Continental dimensions." He claims that the irregular trend of zigzag fractures with large volcanoes at fracture intersection prove their origin within recent geological ages. This large transversal fracture represented mainly by extensive surface flows of andesitic lavas suffered large displacements in late Tertiary time and could have been originated by the fusion of the Cocos Plate after subduction into the Acapulco Trench.

This notwithstanding, oceanographic maps of the Pacific Ocean west of the continental part of Mexico do not show any structural or physiographic sea floor features trending into the Neovolcanic Axis as a reflection of a structural transversal fault. Rather, it looks as though the Clarion Fault might have been diverted southeast towards and into the Acapulco Trench (fig. 3).

Gastil (1973), agreeing with some of Mooser's proposals, considers that the structural lineaments marking the western limit of the Sierra Madre Occidental and the eastern end of the Basin and Range province of northern Mexico and southwestern United States, have been displaced eastwards along the same so-called transverse fault of Mooser for approximately 160 km. He seems to have noticed a displacement of the axis of a regional gravity Bouguer anomaly on the western part of continental Mexico (fig. 4), which he interprets to have been displaced a similar distance eastward. The silver deposits map of Mexico (Salas

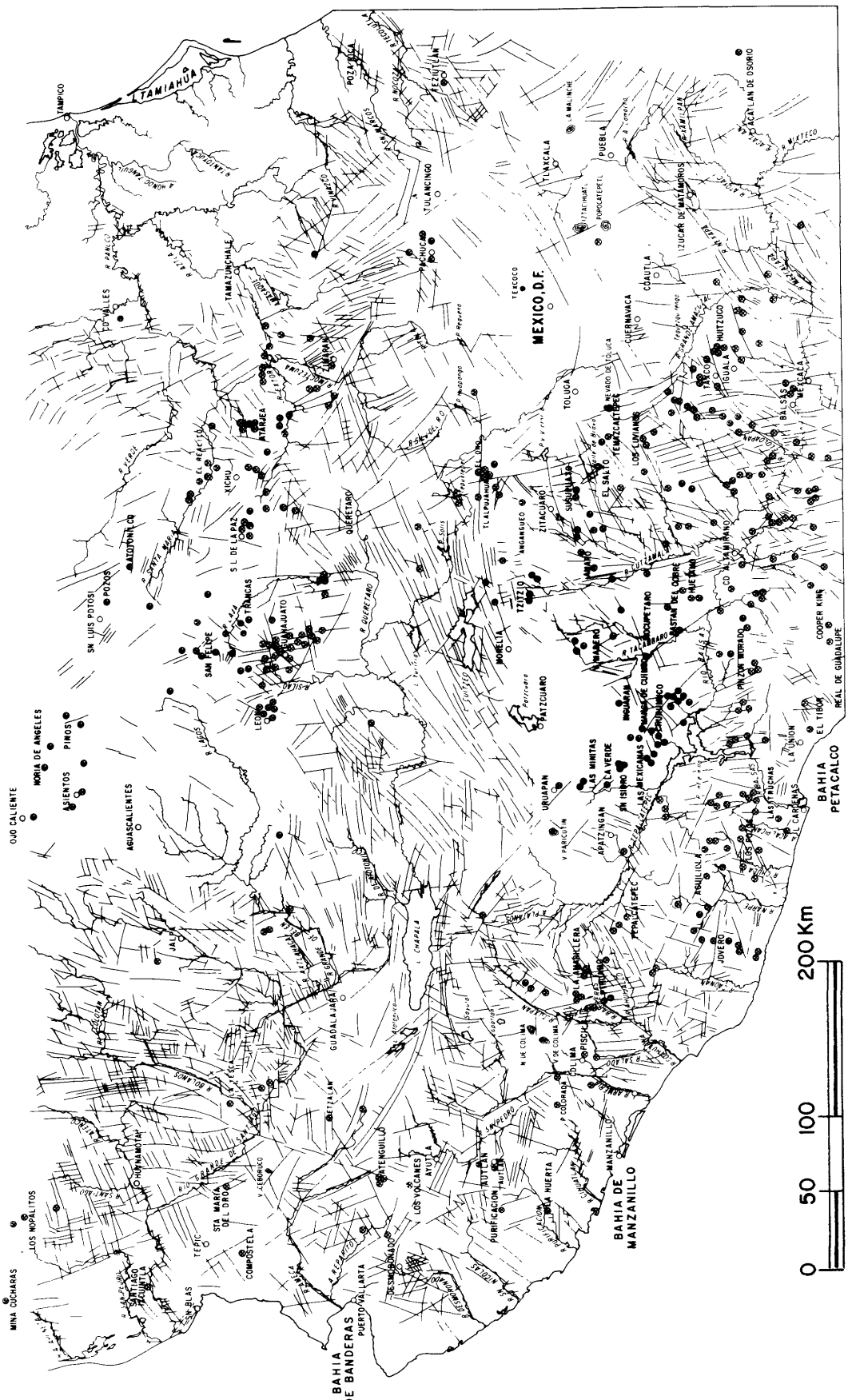

FIGURE 2.—Structural interpretation of Landsat-1 imagery showing incidence of faults, fractures, mines, and adits.

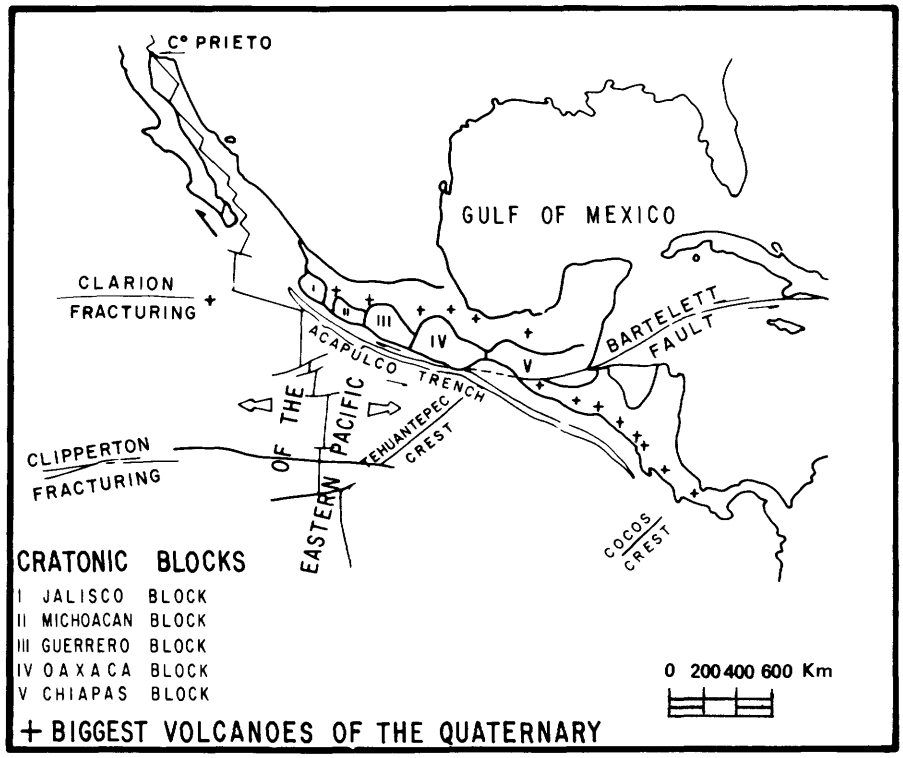

FIGURE 3.—East Pacific Rise and Neovolcanic Axis structure. (After Mooser, 1972.)

and Gonzalez, 1967) provides further evidence of a major right lateral transverse displacement along the Neovolcanic Axis. Displacement of the silver provinces of the Sierra Madre Occidental, eastward to match silver provinces along the Guanajuato-Pachuca province agree with Mooser's 160-km right lateral displacement (fig. 5). The author's study of fracture trends and evidence from the Landsat imagery, however, does not show continuity of large fractures which could sustain Gastil's proposal.

Undoubtedly, Mooser's and Gastil's research are the best efforts to get first-hand information about the Mexican Neovolcanic Axis' modern geology. Unfortunately, the observations were apparently based on isolated visits to different Neovolcanic Axis localities with lack of continuity in time or space, so that they may yet require a thorough revision.

There are discrepancies in the above-mentioned authors' results. For instance, within the Neovolcanic Axis Metallogenetic Province, andesite surface flows predominate on its western end, and andesites and rhyolites predominantly appear on the eastern part of the province. This is not explained by Mooser or Gastil. There is a large metamorphic basement complex of pre-Cretaceous age between Cabo Corrientes and Barra de Navidad, which extends inland almost to Talpa, Jalisco. The origin of this intrusive massif has not been explained by either of the authors nor is its importance noted within the Neovolcanic Axis Metallogenetic Province. Apparently, this metamorphic basement complex underlies the volcanic sequence of andesites and outcrops between Talpa, Jalisco, and Bahía de Banderas, Jalisco, eastward to Ameca and southward to the town of Autlán, Jalisco. Thus it has large bearing on tectonic surface evidence.

On the other hand, the metamorphic basement complex is itself intruded by a granodiorite pluton, probably of Cretaceous age, but certainly pre-Tertiary. These phenomena can be observed south of Puerto Vallarta and west of Talpa, Jalisco. Another wide area of intrusive acid igneous rocks is at Purificación and Armeriá Rivers west of the city of Colima (fig. 6).

In studying the tectonic lineaments of the western part of the Neovolcanic Axis, consideration must be given to extensive outcrops of sedimentary rocks of Cretaceous age in the eastern part of the State of Colima and the southern part of the Neovolcanic Axis in the States of Jalisco and Michoacán. In this case, most of the Cretaceous section is made up of a thick limestone sequence interbedded with sandstone and shale formations.

From the meridian of the city of Morelia eastward (fig. 6), the Neovolcanic Axis is bordered on the south by another large area of metamorphic rocks which is

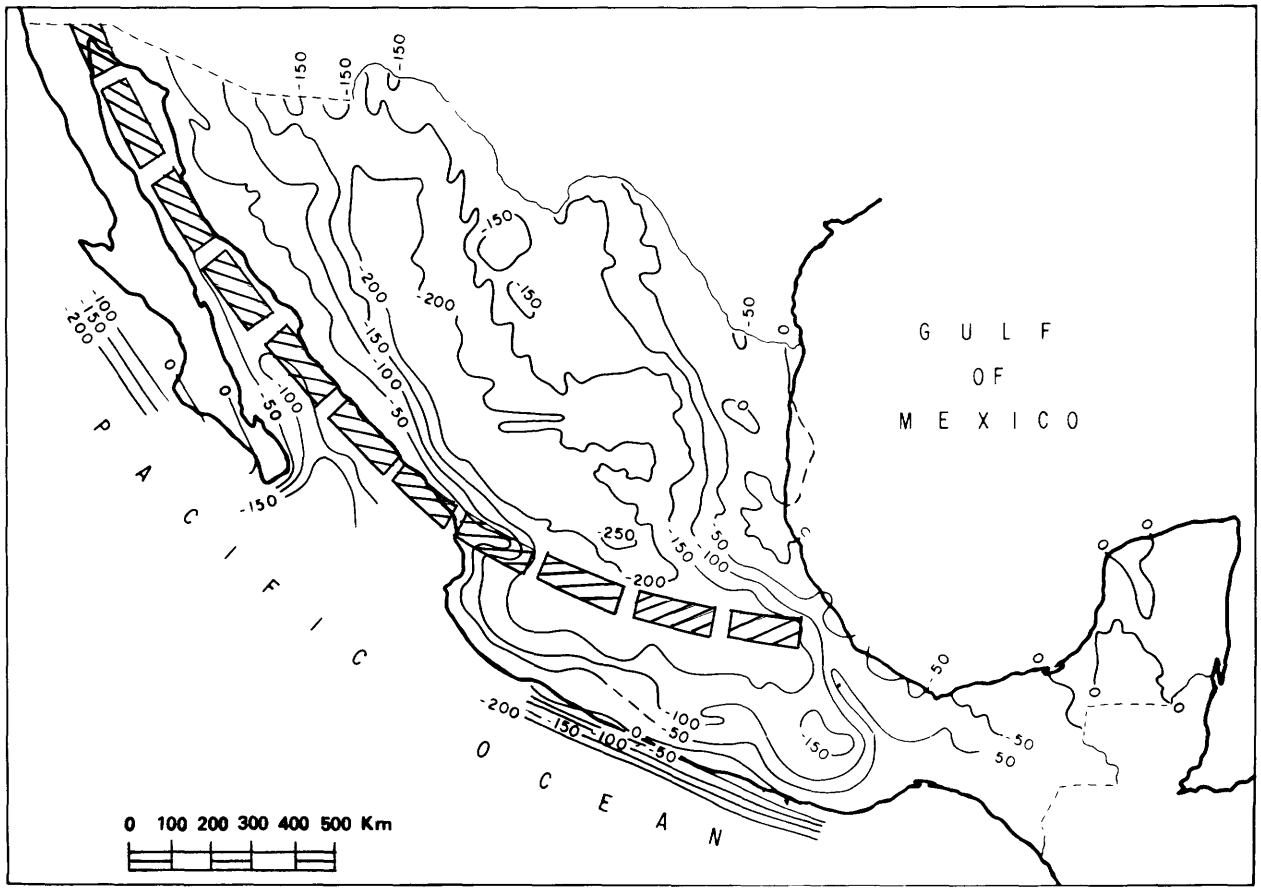

FIGURE 4.—Bouguer anomalies showing coincidence of strong gradient with Sierra Madre Occidental (Gastil, 1973).

clearly visible immediately west of Valle de Bravo in the State of Mexico, as well as by a thick sedimentary section in the States of Michoacán and Guerrero west of Taxco. At this latter place the basement metamorphic complex underlying a thick sedimentary section outcrops extensively north of the city of Taxco. Eastward from the Valley of Mexico to the Gulf of Mexico, a sequence of volcanic rocks of late and middle Cenozoic age outcrop extensively. This volcanic sequence overlies the thick geosynclinal facies of the Sierra Madre Oriental section of thick limestone sequences and thinner shale and sandstone formations. This can be noticed around the town of Oriente to the east of the city of Puebla eastward to the city of Orizaba, Veracruz. The northern border of the Neovolcanic Axis is made up of the same volcanic sequence previously mentioned, to the town of Mizantla, Veracruz, just south of Poza Rica. This massif, the Teziutlán Massif, made up of the volcanic sequence and some intrusives, extends southward almost to the city and port of Veracruz on the Gulf of Mexico.

Because of the heterogeneity of the section that has been affected by diastrophic distortions, it is well to keep in mind in the interpretation of lineaments from Landsat imagery, that the different type of rock and their different ages of emplacement will of course behave differently to tectonic stresses. Also, lineaments that appear in older sections, like the basement complex, will not necessarily show in surrounding country which may be capped by a more recent volcanic sequence.

It is also well to keep in mind the way lineaments and evidence of distortion will appear in the imagery studied, if one considers that there are important intrusives such as those at Tamasula, Jalisco, at Mascota on the Río Ameca south of Zapotlán, Jalisco, and along mountains of igneous rocks which lie to the west of Ameca and Etsatlán in the State of Jalisco. There are a large number of stocks at Rosales and Tacámbaro in the State of Michoacán, that can readily be seen in the Geologic Map of Mexico (Mejorada, 1968). There are intrusives which may not outcrop, as is the case of those that underlie a volcanic andesitic and rhyolitic sequence at the mining district of El Oro and Tlalpujahua. In this case, mining activity has revealed that these intrusive stocks and dikes are post-

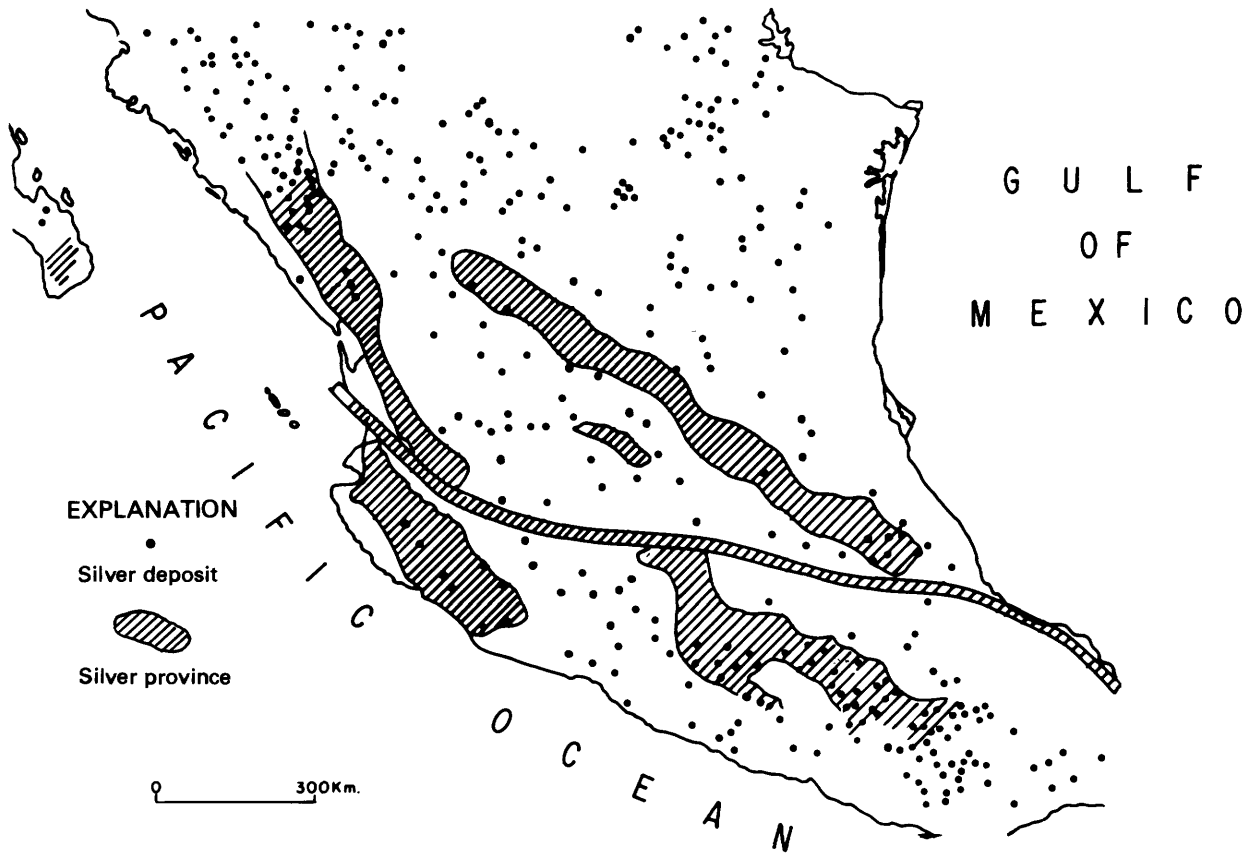

FIGURE 5.—Trend of orientation of silver deposits in Mexico showing apparent displacement of subprovinces (Gastil, 1973).

volcanic sequence in age and may have caused the mineralization (fig. 6).

If the lithologic heterogeneity of the stratigraphic column and the age of the volcanic sequence which covers most of the Neovolcanic Axis is studied, perhaps an explanation will be found for the variety of orientation of fracture and faulting which may be observed in the Landsat–1 imagery.

Gastil (1973) suggested that a zone of cortical weakness which extended northwestward and formed the Gulf of California, existed in the area that is now occupied by the Neovolcanic Axis. He advocates the thesis that the zone of weakness might have existed during the Mesozoic and that at that time the lateral and longitudinal displacement started to separate the peninsula of Baja California from the continent. He concludes also that the rupture movement was intensified during Oligocene and that later, during Miocene time, coincided with the eruption of ignimbrites and igneous extrusives which eventually formed the Basin and Range province to the north in the areas of Arizona, New Mexico, Sonora, and Chihuahua.

According to Gastil (1973), the real dislodging of the peninsula may have started approximately 14 million years ago. This may have originated the Neovolcanic Axis displacement of the andesite-rhyolite sequence which constitutes the volcanic sequence outcropping there.

Finally, the larger features, alineaments of fractures and faults, observed from Landsat–1 imagery do not result from one or two diastrophic movements but are the result of any number of diastrophic movements that are coincident with the emplacement of the volcanic sequence and the intrusive rocks.

IMAGERY INTERPRETATION

Except for a few major fractures, such as those mentioned at the mining district of El Oro and Tlalpujahua, State of Mexico, the rest of the features in figure 7 have not been checked extensively in the field. Consequently, it is obvious that a large part of these structural features are inferred. They are highly interpretational, and they should be so considered when studying the interpreted figures.

In spite of the quality of the photos, which were not the best, and the possibility of obtaining better band mixes with more contrast, the lineaments of

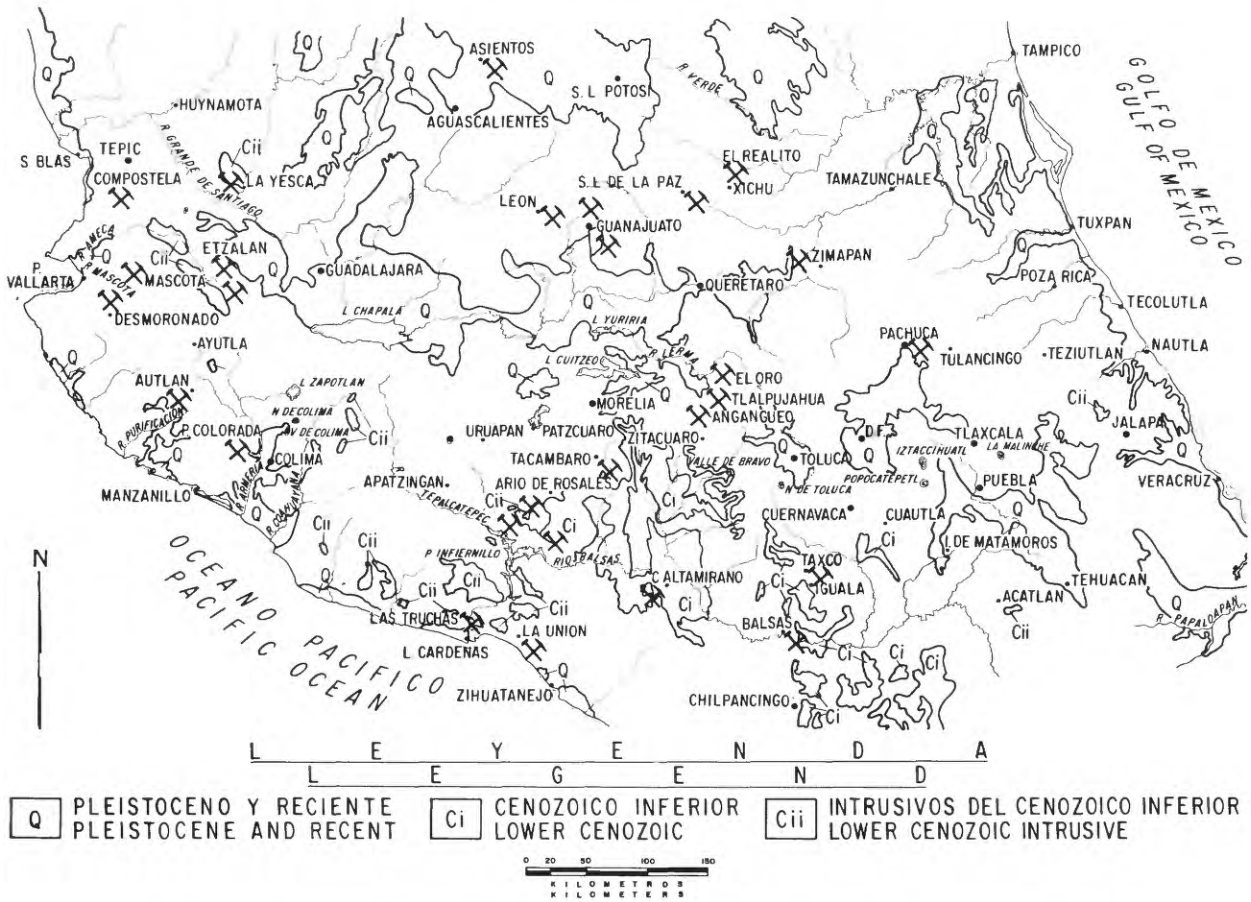

FIGURE 6.—Schematic geologic map of the Neovolcanic Axis Metallogenetic Province of Mexico.

mountains, valleys, visible fracture lines, and intrusives, are easy to detect as lineaments of diastrophic origin. There are mountainous areas with extensive valleys and other features such as straight line oriented vegetation in arid valleys which would indicate moisture from fractures under the alluvium. Also the tectonic or structural control of river courses is observed in drainage patterns in the northwestern part of the Neovolcanic Axis, north of Bahía de Banderas and in the Río Acaponeta, Río San Pedro, Río Santiago, and other rivers in the State of Jalisco. The Laguna de Chapala seems to be the result of a graben. This is evidence of Mooser's proposed anticline along these features.

The imagery studied shows a number of east-west trending lakes in the States of Michoacán and Querétaro. These, however, are due to dammed rivers that may not necessarily be controlled by structural features. The east-west orientation of the river basins may be coincidental. For instance, the Lago Cuitzeo may be caused by a water table suspended by lava flows damming a river basin.

On the other hand, in the northeast part of the Neovolcanic Axis, lineaments are controlled by the Sierra Madre Oriental folds which run definitely NW-SE. In some areas a NE-SW displacement of these folds and faults may be observed on transverse faults.

It is well to emphasize that fractures and faults that have been observed and marked by the author definitely tend to show that there is no continuity of east-west orientation to substantiate the thesis advocated by other authors, that the origin of the Mexican Neovolcanic Axis could have been an old east-west cortical line of weakness.

It is well to emphasize also that there are fault lines longer than 100 km, such as the parallel faults immediately south of Lake Atotonilco, which run north and south. Notice also the north-south 100-km-long fault which occurs between the town of Yesca, Nayarit, and the Ceboruco volcano (northwestern area, fig. 2). The latter may be connected with the faulting and structural control shown by the emplacement of the igneous massif which crops out close to the town of Yesca. There are in connection with this

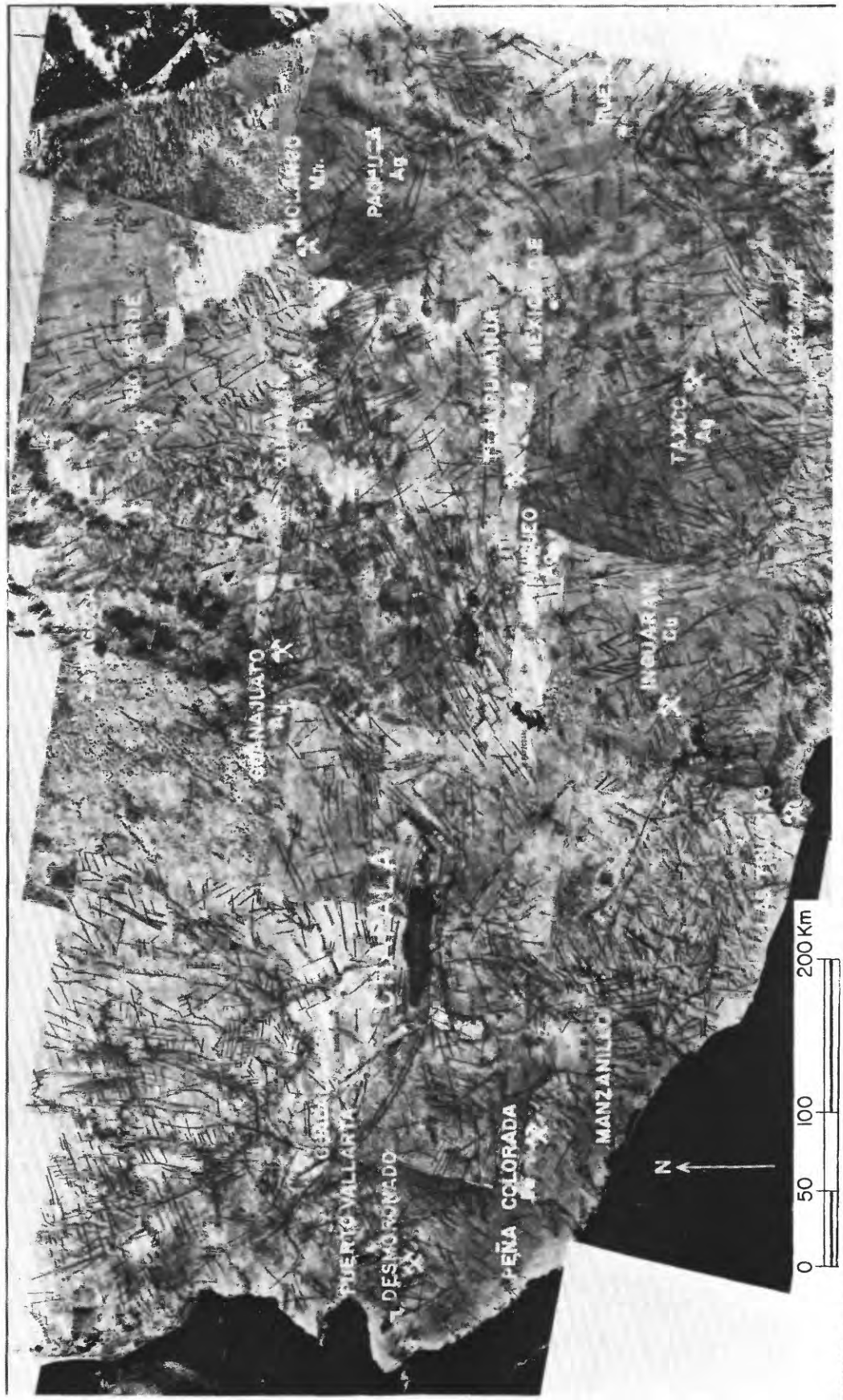

FIGURE 7.—Landsat-1 imagery of the Neovolcanic Axis of Mexico showing predominance of northwest-southeast and northeast-southwest trending faults and shorter fractures.

igneous massif a cluster of quite noticeable faults, some 20 to 30 km long, that cross the north-south faults. This cluster of smaller faults shows a marked tendency of orientation NE-SW. This phenomenon can be observed to the north and east of Río Coahuayana, southeast and east of the city of Colima, 70 km east of the city (southwestern area, fig. 2). A similar phenomenon can be observed as NE-SW faults cross NW-SE faults 35 km to the north and southeast of the city of Zimapan, State of Hidalgo (east-central area, fig. 2). In this case, these crossed faults are usually short, less than 40 km long.

In the central part of the area, in the State of Guerrero, and southwest of the city of Iguala, a cluster of faults trends NE-SW. The same NE-SW orientation predominates in practically all the small faults (30–40 km long). Again, within 100 km radius of Ciudad Altamirano, Guerrero (south-central area, fig. 2), there are any number of areas in which clusters of faults several tens of kilometres long appear, all of them oriented NE-SW. Examples are the area north and south of Lago Cuitzeo, and between this lake and Laguna Yuriria, in the State of Michoacán (central area, fig. 2), and also east of Lake Chapala and along Río Huizcata northeast of the city of Guanajuato. Tectonics related to intrusions are shown by a number of faults which appear in an area called Cerro Desmoronado, some 30 km east of Puerto Vallarta on the Pacific side of the Neovolcanic Axis. Here faults are multidirectional, and the author believes that these are caused by the later intrusives to the west of the town of Talpa. It looks like the stock pierced and dislocated the volcanic sequence, also giving origin to the mineralization. In this Cerro Desmoronado area, which shows extensive mineralization, are the famous Amaltea and Cuale mines of the Compañía Minera Fresnillo, S. A.

A long east-west fault which appears extensively in the literature of the Neovolcanic Axis, is the so-called Falla de Acambay. The town of Acambay lies some 20 km north of the mining district of El Oro and Tlalpujahua. East-west faulting appears at the mining district and not necessarily at the town of Acambay. This fault is some 100 km long, but does not connect with those of Chapala, and, as formerly mentioned, it is more likely that this faulting occurred due to the emplacement of intrusives which underlie the El Oro and Tlalpujahua mining district.

Emphasis must be made on the lack of continuity of many of these tectonic features as observed in Landsat–1 imagery. There are extensive lava flows of recent age, which may not reflect structural distortions of large magnitude and of previous geological ages. That is, Quaternary extrusives and pyroclastics may disguise evidence of diastrophic or tectonic movements.

This may be the case of the mining district of Pachuca. Serious efforts have been made to decipher structural control therein. Both to the north and south of Pachuca City, Quaternary volcanics and pyroclastics of great thicknesses completely disguise any structural features that might have been observed otherwise. Forty or 50 km north of the Pachuca mining district, evidence of the Sierra Madre Oriental folding may be observed in high mountains where thick limestone sequences outcrop. These show a perfect lineament oriented NW-SE, but Quaternary volcanics and pyroclastics cover older rocks which might otherwise have shown tectonic features.

TECTONIC FEATURES AS RELATED TO METALLOGENETIC PROCESSES

A general study of the principal structural features in Mexico revealed an intimate relationship of tectonics of continental scale with metallogenetic processes which have given rise to the principal mining districts in the country.

The author has subdivided the country into six metallogenetic provinces. The Neovolcanic Axis Metallogenetic Province, which is the main object of this exercise, is one of them. It is bound on the north, from west to east, by the southern end of Sierra Madre Occidental, the Central Plateau Province, and the Sierra Madre Oriental. The southern boundary is made up, from west to east, by the Sierra Madre del Sur and the Sierra Madre Oriental's southern continuation.

As previously stated, it is the author's contention that metallogenetic processes are controlled by orogenic movements along lines of diastrophic weakness. There has been some previous work done along this line by Russian economic geologists and metallogenecists. In 1940, a group of Russian geologists, under the direction of Y. A. Bilikin, studied the factors that rule the distribution of minerals that constitute ore on the Earth's surface. Shatalov reported on this work in 1972, and the Canadian geologists, McCarthy and Potter (1962), studied the Soviet's results with regard to the origin of mineral deposits.

Bilikin's group prepared a thorough statistical compilation of the Soviet Union's different geologic districts, mineral deposits, their geologic environment, the country rock types, absolute age of mineralization of the country rock itself, and the age of tectonisms that gave rise to the accumulation. Bilikin (1955) reports to have found an intimate relation in time and

a recurrent relationship regarding composition of ore deposits between the complex specific minerals and the specific intrusive rocks. These in turn were all related to a tectonic cycle in a zone of mobile belts. The Canadian geologists thought this interesting enough to attempt such a study of the eastern part of Canada and the Rocky Mountains province of British Columbia.

There are a number of results of research on metallogenetic processes which relates ore deposits to intrusive and/or extrusive igneous rocks. Krauskopf's (1967) study, for example, is a very well documented study of orogenies with regard to the metallogenesis of ore deposits and the relation that these have to different igneous rock emplacements. Thus, it is reasonable to assume that ore deposit genetics are intimately related to the emplacement of those igneous rocks mentioned, and they in turn are related to orogenic epochs.

The origin of ore deposits is not within the scope of this exercise. Rather, their occurrence with respect to movements along mobile belts is under study. It is important to demonstrate that the magma which is originated in the upper part of the mantle, possibly just below the Mohorovicic Discontinuity or immediately above it, finds its way upward through the lithosphere by using large fractures and faults to rise toward the surface. Consequently, the author's Landsat–1 imagery study to relate large faulted areas to metallogenetic processes has used that concept as a basis for his contention.

To substantiate this thesis, the author points out the occurrence of large mineral deposits along the large fractured lines in the Neovolcanic Axis Metallogenetic Province such as the area in the east-central part of it, including the Pachuca silver deposits, the Zimapan lead-zinc-silver deposits, the Taxco lead-zinc-silver and fluorite deposits, the El Oro and Tlalpujahua gold and silver deposits and the Angangueo silver and gold deposits. Other somewhat smaller deposits lie along the extreme western part of the Neovolcanic Axis Metallogenetic Province, such as the lead-zinc-copper-silver deposits of Cuale and Amaltea in the Cerro Desmoronado area, immediately southeast of Puerto Vallarta on the Pacific seaboard (fig. 7).

All of these mineralized areas occur along very extensively faulted areas. Faulting may occur oriented east-west, as at El Oro and Tlalpujahua; or NE-SW, as at Zimapan; or as at Taxco where faulting occurs oriented mainly WNW-ESE; or multidirectional faulting and fracturing as at Cuale and Amaltea in Cerro Desmoronado, south of Puerto Vallarta.

From all these observations, the author surmises that if the tectonic feature is large enough, that is, if faulting occurs along more than 50 to 100 km, this by necessity must have also affected a large thickness of the lithosphere reaching into the asthenosphere, or the upper part of the mantle, where magmatic material exists. This magma, along with its constituent fluids, finds its way through the large faulted area towards the surface. The longer it has to migrate through the lithosphere the better opportunity it has to dissolve additional chemicals which eventually will form ore deposits useful to man at the nearest surface part of the lithosphere and/or outcropping.

Figure 2 shows incidence of mineral occurrences along and in, or about, intensively disturbed areas.

DESCRIPTION OF SOME MINERAL DEPOSITS ALONG THE MEXICAN NEOVOLCANIC AXIS AS RELATED TO TECTONIC FEATURES

Specialized literature described adequately the geology of ore deposits of importance along the Neovolcanic Axis Metallogenetic Province. Consequently, and congruently with the thesis herein sustained, the author described only in general those tectonic features that have controlled mineralization in certain important mining districts.

PACHUCA Y REAL DEL MONTE MINING DISTRICT, STATE OF HIDALGO

This is the most important mining district in this province (fig. 8). Geyne and others (1963), in their monumental work have an excellent description of this district, which is located 100 km north-northeast of Mexico City, at the eastern edge of the Central Plateau Metallogenetic Province or the northeastern edge of the Neovolcanic Axis Metallogenetic Province. This mining district occurs precisely in the area where the folded belt of the Sierra Madre Oriental Metallogenetic Province plunges under an andesitic volcanic sequence. East-west faults, 20-30 km long, are vaguely shown in the Landsat–1 imagery, but may be mapped on the ground. The volcanic sequence is of Pliocene-Pleistocene age and has not been eroded intensely enough to reveal more clearly structural features beneath the strata. Some NW-SE, N-S, and NE-SW faulting may be observed in the satellite photos but not as clearly as on the ground. Valley fill and Quaternary rhyolitic lava flows mask the largest structures.

The rock in this district consists of volcanoclastic material interstratified with low dipping andesite and rhyolite flows. The lowermost beds, at 1,000-m depth,

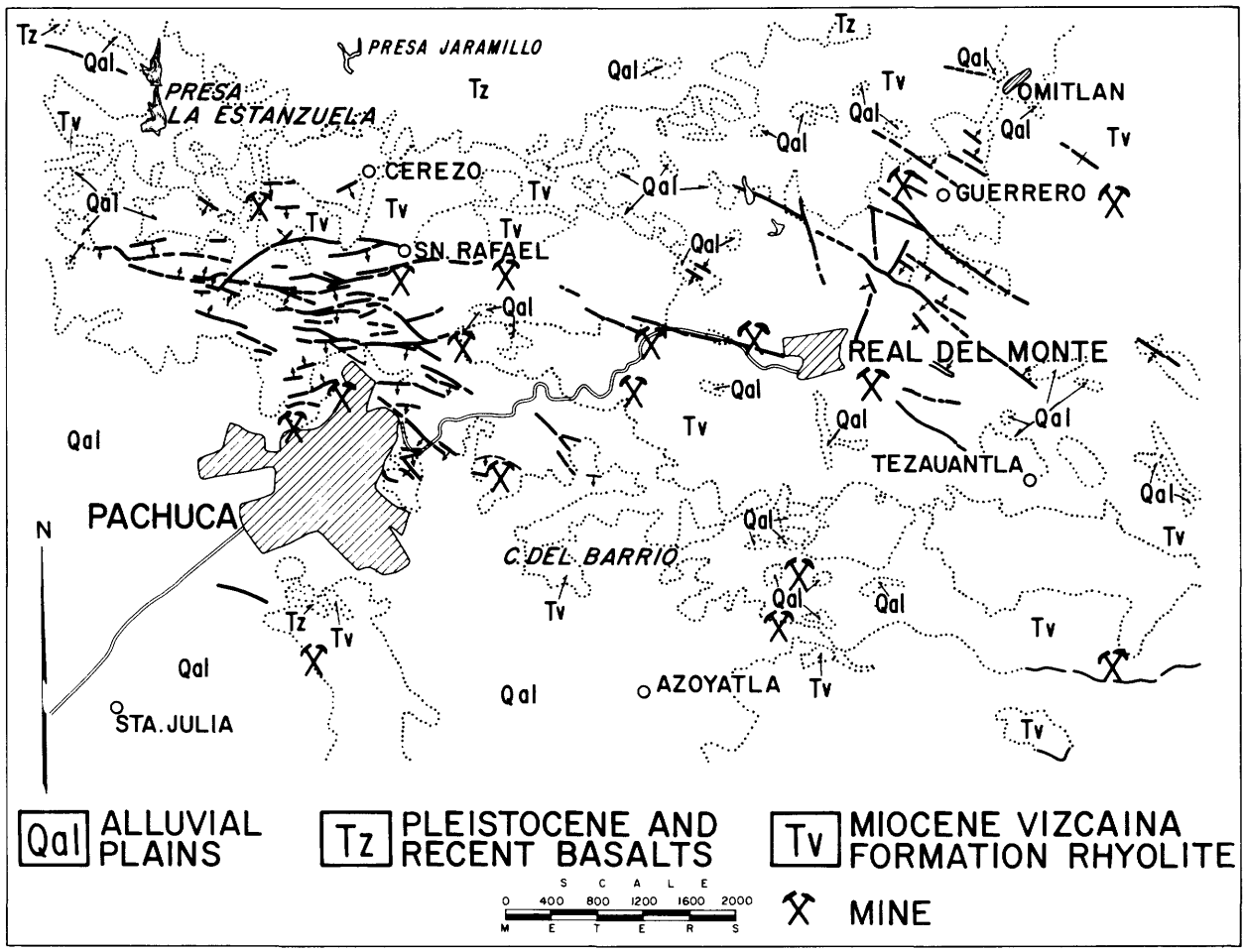

FIGURE 8.—Structural map of Pachuca (Geyne and others, 1963) showing east-west and northwest-southeast faults and veins. Notice Quaternary rhyolite flows mask surface fault traces.

are probably of early Oligocene age and the uppermost are probably of late Pliocene and/or Pleistocene (Geyne and others, 1963). The whole volcanic sequence lies unconformably over the eroded, downfaulted, and intensively folded marine limestone sequence of the upper Mesozoic which forms the Sierra Madre Oriental. Immediately to the north of the city of Pachuca, this folded sequence of the Sierra Madre Oriental shows a perfect NW-SE lineament.

The Tertiary rocks have been deformed by several oscillating movements of varied intensities. These structural features have developed numerous faults with steep dips. The faults are usually of the normal tension type. However, this faulting shows well marked east-west strikes, but also some north-south and WNW-ESE orientations. It seems that the structural movement occurred at the end of the Oligocene and during the Miocene and was followed by the emplacement of dacitic-porphyry dikes and quartziferous dikes and sills. These dikes show a definite east-west orientation and undoubtedly were emplaced through faults which have the same orientation. Their age is post-Laramide.

Unfortunately, most of this information has been obtained underground and surface evidence though relatively abundant is certainly not clearly observable from Landsat–1 imagery in this particular case.

TAXCO MINING DISTRICT, STATE OF GUERRERO

This mining district (fig. 9) lies approximately 120 km southwest of Mexico City.

The region suffered tectonic distortion apparently in two different geologic epochs. The Cretaceous rocks outcropping show large folding in the shape of anticlines with axes locally oriented NE-SW. North-south folding is also occasionally observable. Mineralization occurs both in sedimentary and metamorphic rocks of the basement complex. On the other hand, the area suffered distortion caused by the early

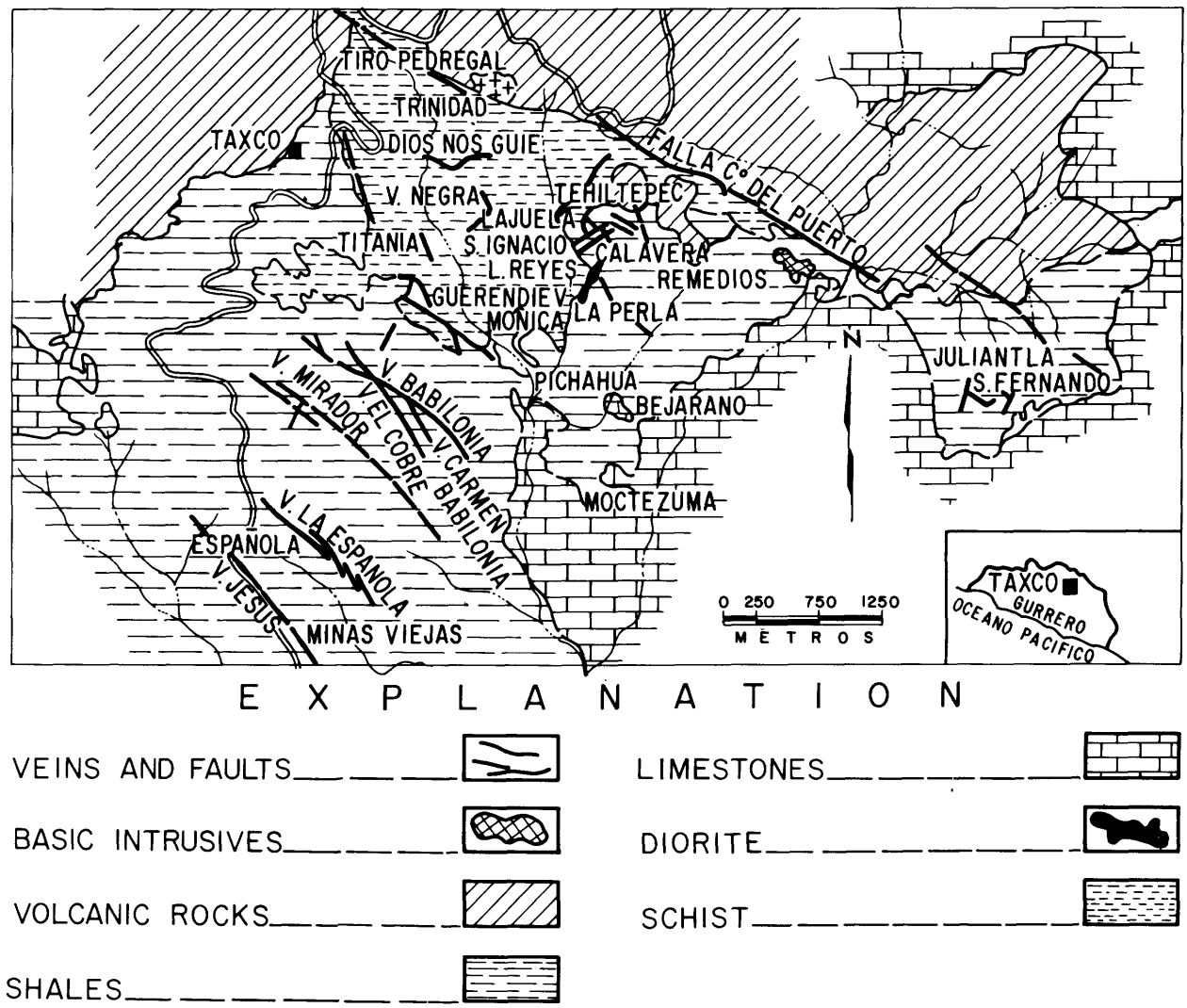

FIGURE 9.—Taxco mining district, State of Guerrero, showing vein control by faults and fractures. (After Fowler and others, 1948.)

Eocene orogeny (Laramide), and NW-SE trending large faulting predominates and may be observed in Landsat–1 imagery.

There was another very clear tectonic orogenic movement which occurred at the end of the Pliocene. Fries (1960), has also found evidence of intense deformation at the beginning of the Pleistocene. This seems to correlate well with orogenic movements in the mining district of Pachuca.

The Taxco mining district's main ore production is lead, zinc, silver, and gold. The ore occurs as vein filling of fractures and faults of the Taxco schists at Mina El Pedregal. Ore bodies also occur in fractured limestones of Cretaceous age at Mina El Pedregal, La Concha, and San Antonio. Again mineralization occurs in clastic beds of the Mezcala Formation at the Mina Jesús. Finally, a very weak mineralization process reached the lowermost part of the overlying Tertiary volcanic sequence. All of this indicates that the mineralization was contemporary with the fracturing systems of the late Pliocene and early Pleistocene much as it happens in Pachuca. However, the main metallogenetic processes seem to have taken place in the late Oligocene or early Miocene and probably renewed in more recent geologic epochs.

HUAHUAXTLA MINING DISTRICT, STATE OF GUERRERO

This ore body is located approximately 15 km northwest of the city of Iguala, Guerrero. The ore bodies occur in faulted Morelos Formation as well as the Cuautla and Mezcala section of the Middle and Upper Cretaceous. The Huitzuco mercury district, 20

km east to Iguala, also contains mercury and antimony which occur principally in faulted limestone of the Morelos Formation of Cretaceous age as well as in dolomite and anhydrite. Here again, there is indirect evidence of post-Cretaceous mineralization. It is thus possible to correlate mineralization metallogenetic processes to the same orogenic movements that gave origin to the Pachuca and Taxco ore deposits.

EL ORO AND TLALPUJAHUA MINING DISTRICT, STATE OF MEXICO

This is a district which has been developed since 1521 and shut down partially until recently. It produces epithermal cavity and vein-filling gold and silver deposits. Stockworks are also common. The ground rock is made up of black slate (fig. 10).

The veins fill cavities in great and small faults which run nearly east and west. They are covered by andesitic rocks of the volcanic sequence of post-mineralization age. Again, in this district, it is estimated that metallogenesis took place during early Miocene time, as shown in the principal veins called San Rafael, La Verde, and San José de la Borda.

The El Oro and Tlalpujahua mining district is controlled by large, parallel faults over 100 km long. Here NE-SW trending faults of less extension, and NW-SE short faulting also occur, some of which is rather recent much as it happens in Taxco and Pachuca. In the author's opinion this faulting may be the reason for the enrichment of the pre-Miocene and Miocene mineralization. The author believes that volcanic action of Pliocene-Pleistocene age caused the reworking of the original ore and gave rise to enrichment.

OTHER LESS IMPORTANT MINING DISTRICTS

There are any number of smaller mining districts which occur where clusters of large and small fractures show in the Landsat–1 imagery. For instance, the intrusive that gave rise to the Tetela gold mine in the northern part of the State of Puebla, approximate-

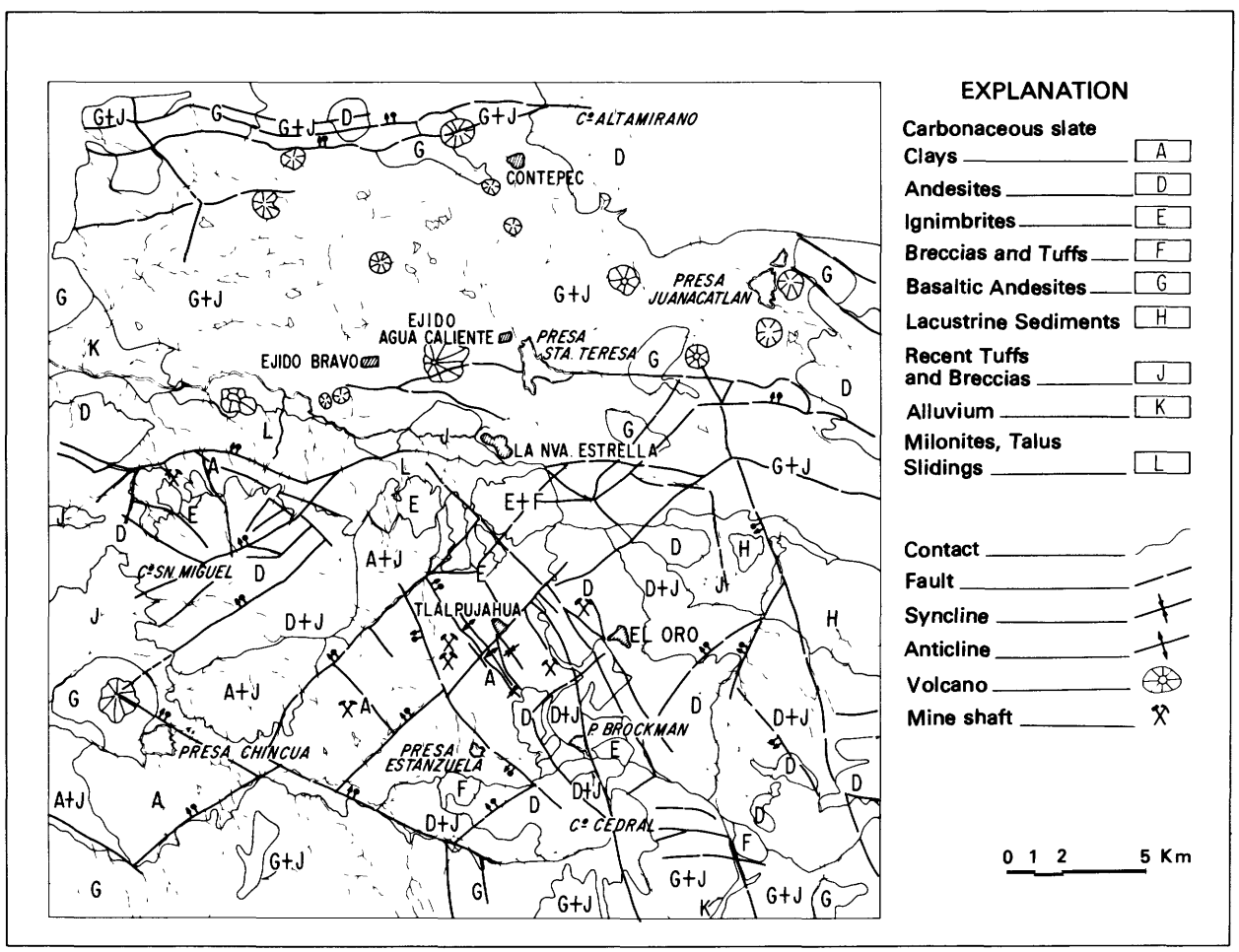

FIGURE 10.—El Oro–Tlalpujahua mining district.

ly 80 km northeast of the city of Tlaxcala, is one such result of the tectonic distortion.

Again, in the immediate vicinity of the town of Teziutlán in the northeastern part of the State of Puebla and at the edge of the Gulf of Mexico watershed, there are copper mines which originated at the contact of the intrusive rocks and limestones of post-Cretaceous age. In the immediate vicinity and farther north, the abandoned iron mines of Tatatila and the copper and gold deposit called Las Minas, 30 km northwest of the capital city of Jalapa, occur in intensely folded and faulted areas which show both the typical volcanic sequence structures of the Neovolcanic Axis Metallogenetic Province and the NW-SE trending controlling axis of folds and faults of the Sierra Madre Oriental orogeny (Laramide).

Along the western part of the area, smaller faults show a marked tendency of orientation NE-SW. This phenomenon can be observed to the north and east of Río Cohaguayana 27 km southeast and east of the city of Colima. In the State of Hidalgo, a similar phenomenon can be observed as NE-SW faults cross NW-SE faults, immediately to the north and southeast of the city of Zimapan, Hidalgo. In this case, these cross faults are usually short, less than 40 km long.

In the central part of the area, in the State of Guerrero, immediately to the east and northeast of Ciudad Altamirano, a cluster of NE-SW short faults, less than 30 km long, intersect long NW-SE trending faults which show up predominantly along the Río Cutzamala from the area of Ciudad Altamirano northward to the town of Tzitzio.

It seems that mineralization follows the NW-SE preting Landsat imagery for mineral or hydrocarbon NE-SW trending short faults intersect the longer ones. These are controlled by the early Eocene orogeny (Laramide).

The author wishes to stress the fact that in interpreting Landsat imagery for mineral or hydrocarbon exploration purposes in areas such as the Neovolcanic Axis of Mexico where very recent volcanic sequences mask older tectonic features, one must extrapolate into the area structural lineament from more eroded or uplifted areas where they can be observed clearly.

It certainly enhances the possibilities of selecting prospective areas by helping to pinpoint targets.

REFERENCES

Bilikin, Y. A., 1955, Metallogenetic province and epochs: Moscow, Gosgcoldekhizdat.

Fowler, G. M., Hernon, R. M., and Stone, E. A., 1948, The Taxco mining district, Guerrero, Mexico: International Geological Congress, 18th, London 1948, Report of the Eighteenth Session, pt. 7, p. 2–12.

Fries, Carl, 1960, Geología del Estado de Morelos y de partes adyacentes de Mexico y Guerrero, región central meridional de Mexico: Mexico Instituto de Geología, Bull. 60.

Gastil, G. R., 1973, Evidence for strike-slip displacement beneath the Trans-Mexican Volcanic Belt: Stanford University School of Earth Sciences, Conference in Tectonic Problems of the San Andreas Fault System, Proc.

Geyne, A. R., Fries, Carl, Segerstrom, Kenneth, Black, R. F., and Wilson, E. I. F., 1963, Geology and mineral deposits of the Pachuca-Real del Monte district, State of Hidalgo: Mexico, Consejo de Recursos Naturales no Renovables Extra-series publication 5E, p. 203–222, illust., 7 tables.

Krauskopf, K. B., 1967, Source rocks for metal-bearing fluids, *in* Barnes, H. L., ed., Geochemistry of hydrothermal ore deposits: New York, Holt, Rinehart and Winston, p. 1–33.

McCarthy, W. D. A. I., and Potter, R. R., 1962, Mineralization as related to structural deformation igneous activity and sedimentation in folded geosynclines: Canadian Mining Journal, v. 83 no. 4, p. 83–87.

Mejorada, S. H. S., ed., 1968, Carta Geologica de la Republica Mexicana: Comite de la Carta Geologica de Mexico, 1 sh., 1:2,000,000.

Mooser, Federico, 1972, The Mexican Volcanic Belt, structure and tectonics: Geofísica Internacional, v. 12, no. 2.

Salas, G. P., and Gonzalez, R. G., 1967, Yacimientos de Plata en México: Instituto de Geología, U.N.A.M., Mexico.

Shatalov, Ye. T., ed., 1972, Metallogenic analysis of ore-controlling factors in ore regions: Moscow, Izd. Nedra, 295 p., illust.

PROCEEDINGS OF
THE FIRST ANNUAL WILLIAM T. PECORA MEMORIAL SYMPOSIUM,
OCTOBER 1975, SIOUX FALLS, SOUTH DAKOTA

Landsat Contributions to Studies of Plate Tectonics

By Jan Kutina,
Laboratory of Global Tectonics and Metallogeny,
Washington Technical Institute, Washington, D.C. 20008
and William D. Carter,
U.S. Geological Survey, Reston, Virginia 22090

ABSTRACT

Tectolinear interpretation of satellite image mosaics has proven to be a powerful method for tracing the course of basement fracture zones which have been propagated upward through a platform cover and even through orogenic belts. The method has also been applied to locate fracture zones, the orientations of which have been changed by rotation of lithospheric plates.

A tectolinear interpretation map of the United States by W. D. Carter, set in context with structural geological knowledge of the Canadian Shield, suggests that the Hudson Bay paleolineament (HBP) of J. Kutina may extend into the Precambrian basement of the Eastern United States. Spatial correlation of significant ore districts with the HBP and associated structures in Canada (both in the Archean greenstone belt and outside) suggests that important ore concentrations may also exist along the probable extension of the HBP beneath the sedimentary cover of the Eastern United States, where it may intersect with an east-west trending fracture zone, distinguished by A. V. Heyl (1972), between 38° and 40°N. in the Central and Eastern United States. A number of Mississippi Valley-type ore deposits are spatially associated with this east-west fracture zone.

Three major northwest-trending lineaments have also been delineated in South America, and their extension into the Andean Region has been traced by statistical treatment of linears in the Landsat mosaics. These northwest-trending lineaments may very well have been E–W fracture zones in the paleogeographic orientation of South America before it was separated from Africa.

INTRODUCTION

The investigations carried out in the last decades by Ewing, Heezen, Hess, their coworkers, students, and followers have brought new insight in the knowledge of the structure of the upper parts of the Earth. One of the outcomes of this scientific trend was the concept of the "new global tectonics" as introduced by Isacks, Oliver, and Sykes (1968), Morgan (1968), Le Pichon (1968) and others. This concept, referred to also as "plate tectonics," has revived the old continental drift hypothesis of Alfred Wegener, giving it a new geophysical interpretation.

Since the time of the above papers, an enormous literature on plate tectonics has accumulated, with some papers accepting it as a proven model, and others expressing different degrees of agreement or disagreement with the new concept. The controversy which exists in the world literature is reflected well in the volume of papers "Plate Tectonics—Assessments and Reassessments," edited by Kahle (1974). There are a number of other critical papers that should be mentioned, especially that by Sheinmann (1973).

The basic postulate of the new theory shows that the upper parts of the Earth's body are composed of a number of rigid plates that are not in a fixed position but which move and the boundaries of which have changed in the course of geological time. These changes involved processes of different orders of magnitude which are mutually interrelated and are of basic importance for certain geochemical processes.

Metallogenic studies have shown that there exists a relationship between mineralization of various types and ages and the different types of plate boundaries

(Guild, 1974). One of the most important discoveries was recognition of the role of subduction or Benioff zones on metallogenic processes connected with partial melting of the subducted oceanic crust and generation of a special type of magma. The origin of porphyry copper deposits especially of the Andean orogenic belt has been explained in these terms (Sillitoe, 1972a, b).

Many deposits, however, are located in the interior of the present plates, far from their boundaries. Some of them may be related, as Guild (1973) and others have shown, to former plate boundaries, but many ore deposits apparently do not exhibit such a relationship.

Several authors, who studied metallogeny of broad regions such as the Western United States or Transbaikalia have recognized that the distribution of major endogenic ore deposits is controlled, beside other factors, by major fracture zones, and often by their intersections (Kutina, 1969; Favorskaya and others, 1974).

As a follow up of these investigations, Kutina (1974) carried out a systematic study of structural control of ore deposition in selected regions of four continents. Correlating his results he concluded that large endogenic ore deposits and ore districts are usually located in the vicinity of, or above the intersection of, deep-seated fractures, fracture zones or zones of weakness that belong to four sets, N–S, E–W, NW, and NE, or to some of these four sets, propagating upward from deeper levels. The upward propagation of these fractures proceeds differently in different regions depending on their geological evolution. As a consequence, not all of these fracture sets are developed or clearly expressed in the surface or subsurface portion of each region and the detection of some of them requires detailed studies by different methods. Reactivation of movements proceeded along these fracture zones at different geological times.

There exists a relationship between the intraplate tectonics and the course of the plate boundaries. For instance, one of the ore-controlling fracture sets of continental Central America (the NW–SE one) is parallel to the Middle America Arc, the boundary between the Cocos Plate and the Caribbean Plate. Ore deposits of a post-Laramide age lie closer to the plate boundary than the majority of the older ore deposits (Kutina, 1974).

The reconstruction of the pre-Cretaceous ("pre-drift") configuration of the present plates has mostly been done by analyzing magnetic anomalies of the sea floor, by applying paleomagnetic data, and by geometric fitting of the continental margins. Therefore, King (1970) correctly notes, when referring to Bullard's reconstruction of the continents on opposite sides of the Atlantic, that the reconstruction has been done without regard for the inner constitution of the blocks or plates.

Correlation of the geology of the matching sides of continents, which are supposed to have been separated from each other, has been done in several instances. Also, the extension of metallogenic provinces across such boundaries has similarly been tested by several authors with reasonable success.

These correlations, though of principal importance, are usually not sufficient to estimate the angle of rotation of the plates and are not sufficient geological evidence to provide an independent check of the amount of rotation deduced by geophysical methods. Also the question of possible disappearance of a part of a continental mass by disintegration and subsidence often remains unanswered.

Detection and plotting of major, deep-seated fracture zones, especially those which are ore-controlling, provide a new, additional tool in fitting crustal plates back together. This kind of study is in initial stages because our knowledge of the pattern of deep-seated fractures within the individual plates is insufficient.

The results of Kutina's (1974) study in different parts of four continents and of an independent investigation by Favorskaya and others (1974) show a real possibility of comparing the positions and orientations of ore-controlling fracture zones of the individual plates.

The use of the above metallogenic data in testing the validity of plates' rotation as derived by geophysical methods presents, however, a number of problems. One of them is distinguishing whether or not some of the ore-controlling fracture zones represent new tectonic elements, superimposed on the old fracture pattern. Another question is whether zones of tectonic weakness may or may not exist in the substratum over which the lithospheric plates are supposed to be moving. And, if they exist, how far they can influence the tectonics and metallogenic processes in marginal parts and in the interior of the plates. Some of these questions are discussed separately (Kutina, 1976).

The introduction of Landsat (ERTS) imagery and the construction of image mosaics provides a new, common base for systematic study of linear features in broad territories. Swarms of lineaments extending sometimes for several hundreds of miles and crossing boundaries of different geological units are likely to reflect the course of major fracture zones in deeper

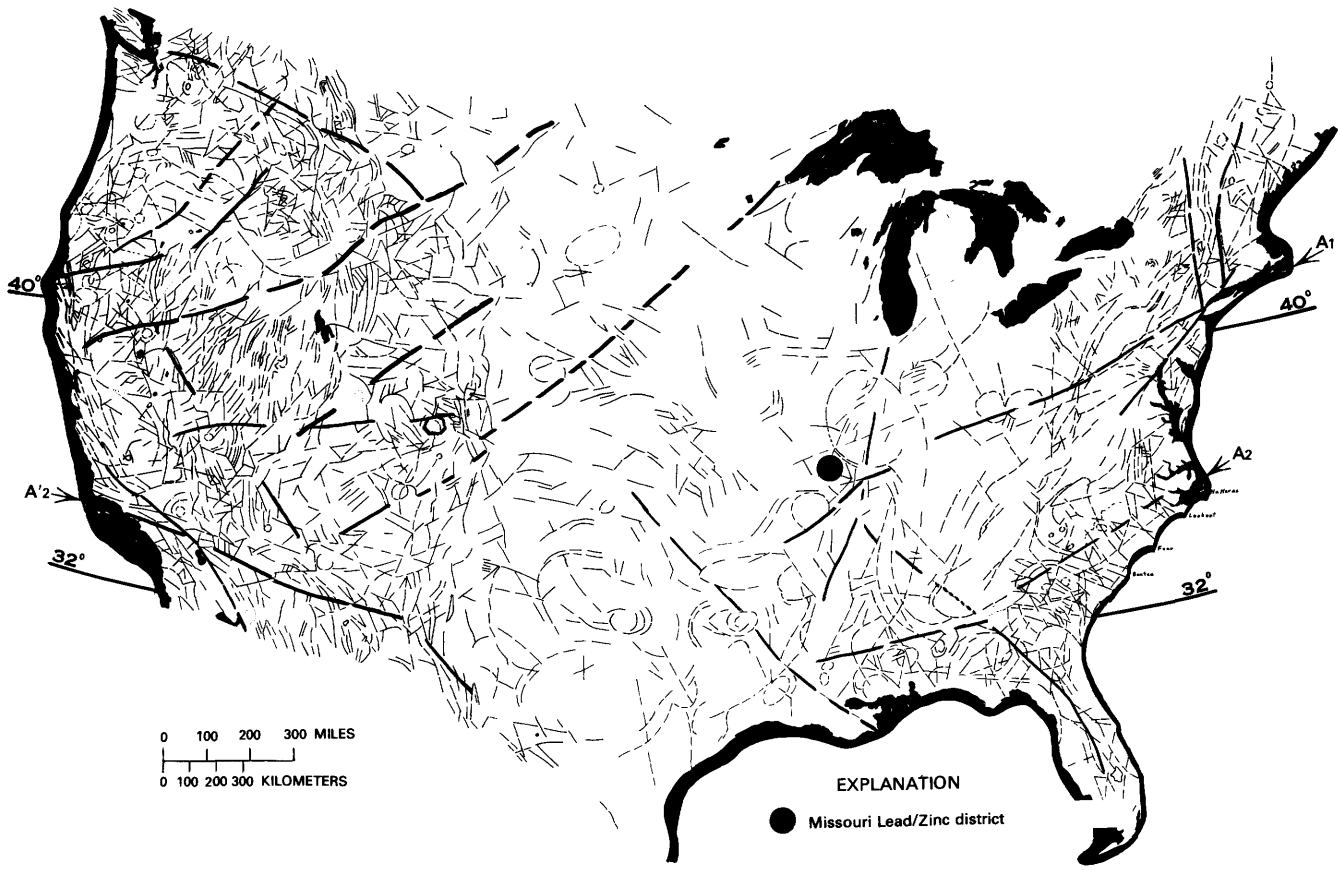

FIGURE 1.—Tectolinear interpretation of a 1:5,000,000-scale ERTS–1 mosaic of the United States by W. D. Carter, 1974.

Lineament A_1 essentially corresponds to the 38th Parallel Lineament of Heyl (1968, 1972) and represents its independent discovery by satellite imagery.

In view of the metallogenic importance which the A_1 lineament plays, the lineaments A_2–A'_2, revealed by the same ERTS–1 mosaic, deserve special attention.

levels of the Earth's crust which have been propagated upward due to movement of crustal blocks.

The detection of such lineaments and their correlation with the distribution of ore deposits may very effectively help to solve long-standing controversial questions and will help to map the pattern of major deep-seated fractures which is needed for correlation of the intraplate tectonics and between individual plates. The relationships between the location of ore deposits and the course and intersection of the lineaments coming from these studies may be of great assistance in mineral exploration.

In the present paper, two examples are presented. They come from a joint study of the authors, using some of Carter's tectolinear interpretations of Landsat mosaics.

The paper, originally presented at the Pecora Symposium at Sioux Falls, October 1975, has been updated by references to papers by Regan and others (1975), Stewart (1976), and Callahan (1976).

CONTRIBUTION TO THE INTRAPLATE TECTONICS OF THE EASTERN UNITED STATES

Figure 1 is the first tectolinear interpretation of a mosaic of satellite images of the United States as compiled by Carter in 1974. The illustration is based on the analysis of a mosaic of the conterminous United States consisting of 595 Landsat–1 images published at the scale of 1:5,000,000 (U.S. Geological Survey, 1974).

The illustration is presented here in its original form without any additional changes in order to serve as a base not influenced by genetic concepts.

Some of the longer lineaments have been marked by heavy lines by Carter, but several others can similarly be distinguished. For instance, two broad north-south trending swarms of linears can be recognized in the Western United States, one at the longitudes enclosing the Great Salt Lake and the other extending

through Colorado and southward. The first one essentially extends along the north-south fracture trajectory +6 and the other along +9 of the model by Kutina (1969).

Two of the most prominent features of figure 1 are the major east-northeast-trending lineaments in the Eastern United States. One of them is located between latitudes 38° and 40°N. and is marked A_1 in figure 1, and the other extends between 32° and 36°N., and is marked A_2. A_2 has a prominent counterpart in the Western United States, marked A'_2.

Lineament A_1 of figure 1 intersects the Appalachian orogen in the easternmost part of the country and apparently displaces the Precambrian of eastern Pennsylvania and New Jersey in a right-lateral sense and in places, as a pronounced curvature of the Appalachians. This apparent displacement has been recognized by Drake and Woodward (1963) who interpreted it as a right-lateral wrench fault extending seaward (Cornwall-Kelvin displacement). The continental part of this displacement has been doubted later by Root (1970).

The course of the lineament A_1 (fig. 1) as recognized on the 1:5,000,000-scale mosaic should be understood as its first approximation. It is therefore not surprising that the east-northeast trend of this lineament as it appears in the easternmost part of the United States differs from the east-west strike of the Cornwall-Kelvin displacement of Drake and Woodward (1963) who applied geological and geophysical criteria on a more detailed scale. The main power and contribution of the ERTS–1 mosaic lies in its synoptic view covering a broad territory in which the respective lineament, though less accurate in detail, could have been traced for a long distance.

Overlaying the pattern of linear features of figure 1 with the distribution of the main ore deposits of endogenic and controversial origin shows (fig. 2) that most of the major Mississippi Valley-type deposits of lead, zinc, fluorite, and barite are spatially associated with the east-northeast-trending lineament or fracture zone A_1. This regularity with further structural and lithological control was recognized as early as 1968 and 1972 by Heyl, who described the respective lineament as the 38th Parallel Lineament.

The 38th Parallel Lineament is probably plotted more accurately by Heyl than in figure 2 as the geological and metallogenic interpretation by Heyl is based on more detailed maps. Nevertheless, the 1:5,000,000-scale mosaic of Landsat–1 images proved useful in detecting the same regularity. Moreover, it is probable that more detailed information available from Landsat images at larger scales and the applica-

FIGURE 2.—Tectolinear interpretation of the eastern part of the United States, set in context with some structural and metallogenic features of the Canadian Shield.

Note especially the distribution of the Mississippi Valley-type deposits of lead, zinc, fluorite, and barite, many of which concentrate—in accordance with Heyl (1968, 1972)—in a belt following the 38th Parallel Lineament.

The east-northeast-trending 38th Parallel Lineament traverses the Appalachian orogen at a latitude close to 40°N., with an apparent right-lateral displacement of the Precambrian, thus giving support to the Cornwall-Kelvin wrench fault of Drake and Woodward (1963).

EXPLANATION

I. Precambrian of the Canadian Shield and the outcropping Precambrian of the eastern part of the United States (simplified from King and Beikman, 1974).

II. Younger rocks, mostly covering Precambrian basement.

III. Canada: major ore fields in the Precambrian south of Hudson Bay, both in the Archean greenstone belts (1–4) and outside (5, 6).

United States: two ore deposits in the Precambrian of the northeastern United States (20, 21) and the Ducktown deposit in Tennessee (14).

IV. Ore districts and major deposits of the Mississippi Valley-type and a few smaller lead-zinc deposits of the Eastern United States.

V. Deposits of other types (17, 18).

ORE DEPOSITS AND DISTRICTS

Canada:

1. Val d'Or district.
2. Noranda district.
3. Timmins district.
4. Chibougamau district.
5. Cobalt district and other deposits.
6. Sudbury district.

United States:

7. Upper Mississippi Valley district.
8. Illinois-Kentucky district.
9. Tri-State district of Missouri, Kansas, and Oklahoma.
10. Central Missouri district.
11. } Southeast Missouri lead district.
12. }
13. }
14. Ducktown district, Tennessee.
15. The Mascot-Jefferson City zinc district, Tennessee.
16. Austinville-Ivanhoe district, Virginia.
17. Hamme district, North Carolina.
18. Cornwall deposit, Pennsylvania.
19. Friedensville deposit, Pennsylvania.
20. Franklin Furnace and Sterling Hill, New Jersey.
21. Balmat-Edwards, New York.
22. Central Kentucky district.
23. Cumberland River deposit.
24. Shenandoah Valley (Timberville), Virginia.
25. Northern Arkansas district.
26. Northeast Arkansas district.
27. Central Tennessee district.


HUDSON BAY
HUDSON BAY PALEOLINEAMENT
UNGAVA BAY
JAMES BAY
SUPERIOR PROVINCE
GRENVILLE PROVINCE
St Lawrence River
40°
40°
0 400 MILES
0 600 KILOMETERS
I
II
III (Nos.14,20,21)
IV
V

tion of enhancement techniques would provide a more complete geological plot of the lineament, especially at places where its course was interpolated due to lack of structural information.

Thus, the 38th Parallel Lineament (A_1 in fig. 1) is (1) spatially associated with the distribution of major deposits of the Mississippi Valley—type and (2) may displace the Precambrian at the intersection with the Appalachian orogen. Therefore, the above lineament appears to be a significant structural element of the Central and Eastern United States or its basement.

The experience from global metallogeny shows that the chances for economic concentration of metals increase along intersection of orogens by transversal deep-seated fracture zones, especially if ore deposits have been detected along them at other places. Accordingly, the area of the intersection of the Appalachians by the 38th Parallel Lineament may be postulated as a target area for mineral exploration. A number of ore deposits and occurrences have already been found in this area, among them the magnetite deposits of Cornwall and Grace connected with the diabase magmatism in the Triassic basin (Lapham, 1970; Sims, 1970) and the sphalerite deposit of Friedensville located in the Cambrian and Ordovician carbonate sediments (Callahan, 1970), both in Pennsylvania (18 and 19 in fig. 2). The unique character of these deposits (including the deposits of Franklin Furnace and Ogdensburg in rocks of Precambrian age) within the metallogeny of the Appalachians has been stressed already by Guild (written comm., 1968), who assumed their possible relation to deep basement offsets along an intersecting lineament.

In view of the above significance which the 38th Parallel Lineament plays, special attention should also be given to the other east-northeast-trending lineament (A_2 and A'_2, fig. 1) running parallel to the former and located between the latitudes 32° and 36°N. in the Eastern United States and close to 34°N. in the Western United States.

The courses of lineaments A_2 and A'_2 essentially parallel the outline of the North American craton (with the basement rocks as old as 1,700 to 850 m.y.) against the encircling marginal miogeosynclines, as these two units have recently been distinguished by Stewart (1976). According to Stewart, the miogeosynclines started to form at approximately 850 m.y. indicating the initial stages of rifting. If the above relation is true, these lineaments may contribute to the definition of the southern boundary of the North American craton.

Another very interesting correlation may exist between lineaments A_1 and A_2, A'_2 of figure 1, and the northern and southern boundaries; respectively, of a newly detected belt of magnetic highs in the global magnetic anomaly map (Regan and others, 1975). The belt extends in an essentially east-west direction with some tendencies to turn east-northeasterly to northeasterly between latitudes 30° and 40°N. through nearly the whole United States. Lineaments A_2 and A'_2 of figure 1 follow very closely the southern boundary of the belt of magnetic highs. Since lineaments A_2 and A'_2 also parallel, to some degree, the southern boundary of the North American craton, it is possible that the three features are interrelated.

Figure 2 sets the tectolinear interpretation of the ERTS–1 mosaic of the Eastern United States in context with some structural features of the Canadian Shield. The illustration shows the course of the Hudson Bay paleolineament (HBP) as postulated by Kutina (1971) as well as the main ore fields south of Hudson Bay. The Val d'Or-Noranda-Timmins ore field (1–3 in fig. 2), located in an Archean greenstone belt, contains about 1,500 occurrences of gold and about half that number of copper (Kutina and Fabbri, 1972).

The aim of the plot of the Canadian ore fields is to initiate discussion of possible presence of important mineral concentrations in the Precambrian basement of the Eastern United States. If the HBP and its parallel structures with which some of the ore concentrations both within the greenstone belts and outside are spatially associated, extends southward into the basement of the United States, it may play a role in structural control of ore deposition. From this viewpoint there may be special interest in the swarm of north-south lineaments south of Lake Ontario and farther south, which may possibly reflect upward propagation of southern extension of the HBP from the Precambrian basement. The respective swarm of north-south lineaments intersects the east-northeast-trending "38th Parallel Lineament" in the area north of location No. 16 in figure 2. In the area of this intersection, a coal basin has developed in western Virginia. The shape of the basin as expressed in the "Geological Map of the United States" (King and Beikman, 1974) is symmetrical along the directions of the two intersecting sets of lineaments.

Several areas with numerous gold occurrences and old small-scale mining operations for gold are known in the Eastern United States (Callahan, 1976). Though the primary source of this gold is in outcropping rocks which are considerably younger than the greenstone belts in Canada, the presence and distribution of gold in the Eastern United States is of special interest as it may represent remobilization of this metal from older rocks of the basement.

POSSIBLE EXTENSION OF MAJOR FRACTURE ZONES FROM THE INTERIOR OF THE SOUTH AMERICAN PLATE INTO THE ANDES OROGENIC BELT

A discussion of this question, preliminarily presented at the Sioux Falls symposium, has been further extended and included in another paper, "The Metallogenic Role of East-West Fracture Zones in South America with Regard to the Motion of Lithospheric Plates (with an Example from Brazil)," to be published in Djalma Guimaraes Volume, Boletim, Universidade de Brasilia.

ACKNOWLEDGMENTS

The senior author thanks Bethlehem Steel Corporation for the agreement to use some of his results from a consultant assignment.

Thanks are given Dr. Stephen J. Gawarecki and Mr. W. S. Kowalik for references to some papers.

SELECTED REFERENCES

Callahan, J. E., 1976, Are there Witwatersrand types of gold deposits in the Triassic basins of the Southeast ?: Geol. Soc. America, Abs., v. 8, no. 2, p. 144–145.

Callahan, W. H., 1970, Geology of the Friedensville mine, Lehigh County, Pennsylvania, *in* Ridge, J. D., ed., Ore deposits in the United States 1933–1967: Am. Inst. Mining Engineers, v. I, p. 95–107.

Carter, W. D., 1974, Tectolinear interpretation of an ERTS–1 mosaic, La Paz area, southwest Bolivia, southeast Peru and northern Chile: Committee of Space Research Plenary Mtg., 17th, Sao Jose dos Campos, Brazil, preprint.

Drake, C. L., and Woodward, H. P., 1963, Appalachian curvature, wrench faulting, and offshore structure: New York Acad. Science, Trans., v. 26, p. 48–63.

Favorskaya, M. A., Tomson, I. N., Baskina, V. A., Volchanskaya, I. K., and Polyakova, O. P., 1974, Global regularities in the distribution of big ore deposits (in Russian): Moscow, Nedra, 193 p.

Guild, P. W., 1973, Massive sulfide deposits as indicators of former plate boundaries: U.S. Geol. Survey, Open file rept., 11 p.

——— 1974, Application of global tectonics theory to metallogenic studies: Internat. Assoc. on the Genesis of Ore Deposits Symposium on Ore Deposits of the Tethys Region in the Context of Global Tectonics, Varna, Bulgaria, preprint.

Heyl, A. V., 1968, The 38th Parallel Lineament and its relationship to ore deposits (abs.): Econ. Geology, v. 63, p. 88.

——— 1972, The 38th Parallel Lineament and its relationship to ore deposits: Econ. Geology, v. 67, p. 879–894.

Isacks, B., Oliver, J., and Sykes, L. R., 1968, Seismology and the new global tectonics: Jour. Geophys. Research, v. 73, p. 5855–5898.

Kahle, C. F., ed., 1974, Plate tectonics—assessments and reassessments: Am. Assoc. Petroleum Geologists, Memoir 23, 514 p.

King, P. B., 1970, Tectonics and geophysics of eastern North America, *in* Johnson, H., and Smith, B. L., The megatectonics of continents and oceans: New Brunswick, N.J., Rutgers Univ. Press, p. 74–112.

King, P. B., and Beikman, H. M., 1974, Geologic map of the United States: U.S. Geol. Survey, 1:2,500,-000.

Kutina, Jan, 1969, Hydrothermal ore deposits in the western United States: a new concept of structural control of distribution: Science, v. 165, p. 1113–1119.

——— 1971, The Hudson Bay Paleolineament and anomalous concentration of metals along it: Econ. Geology, v. 66, p. 314–325.

——— 1973, Structural control of volcanic ore deposits in the context of global tectonics: Internat. Symposium on Volcanism and Associated Metallogenesis, Bucharest, Romania, Sept. 1973, preprint.

——— 1976, Relationship between the distribution of big endogenic ore deposits and the basement fracture pattern—Examples from four continents, *in* Internat. Conf. on the New Basement Tectonics, 1st, Salt Lake City, June 1974: Utah Geol. Assoc. Pub. 5, p. 565–593.

——— 1976, Lithospheric plate motions—one of the factors controlling distribution of ore deposits in some mineral belts: Mineralium Deposita, in press.

Kutina, Jan, and Fabbri, A., 1972, Relationship of structural lineaments and mineral occurrences in the Abitibi area of the Canadian Shield: Geol. Survey Canada Paper 71–9, 36 p.

Kutina, Jan, Carter, W. D., and Lopez, F. X., n.d., The metallogenic role of east-west fracture zones in South America with regard to the motion of lithospheric plates (with an example from Brazil). Submitted to the Djalma Guimaraes Volume, Boletim, Universidade de Brasilia.

Lapham, D. M., 1970, Triassic magnetite and diabase of Cornwall, Pennsylvania, *in* Ridge, J. D., ed., Ore deposits of the United States 1933–1967: Am. Inst. Mining Engineers, v. I, p. 72–94.

Le Pichon, X., 1968, Sea floor spreading and continental drift: Jour. Geophys. Research, v. 73, p. 3661–3697.

Morgan, W. J., 1968, Rises, trenches, great faults and crustal blocks: Jour. Geophys. Research, v. 73, p. 1959–1982.

Regan, R. D., Cain, J. C., and Davis, W. M., 1975, A global magnetic anomaly map: Jour. Geophys. Research, v. 80, p. 794–802.

Root, S. I., 1970, Structure of the northern terminus of the Blue Ridge in Pennsylvania: Geol. Soc. America Bull., v. 81, p. 815–830.

Sclater, J. G., and McKenzie, D. P., 1973, Paleobathymetry of the South Atlantic: Geol. Soc. America Bull., v. 84, p. 3203–3216.

Sheinmann, Yu. M., 1973, The new global tectonics and reality [in Russian]: Bull. Moscow Soc. Naturalists, Geol. Ser., v. 78, no. 5, p. 5–28.

Sillitoe, R. H., 1972a, A plate tectonic model for the origin of porphyry copper deposits: Econ. Geology, v. 67, p. 184–197.

——— 1972b, Relation of metal provinces in western America to subduction of oceanic lithosphere: Geol. Soc. America Bull., v. 83, p. 813–817.

Sims, S. J., 1970, The Grace magnetite deposit, Berks County, Pennsylvania, *in* Ridge, J. D., ed., Ore deposits in the United States 1933–1967: Am. Inst. Mining Engineers, v. I, p. 108–124.

Stewart, J. H., 1976, Late Precambrian evolution of North America: Plate tectonics implications: Geology, v. 4, no. 1, p. 11–15.

U.S. Geological Survey, 1974, Mosaic of imagery from Earth Resources Technology Satellite–1 of the conterminous United States: in cooperation with the U.S. Department of Agriculture, Soil Conservation Service, 1:5,000,000.

PROCEEDINGS OF
THE FIRST ANNUAL WILLIAM T. PECORA MEMORIAL SYMPOSIUM,
OCTOBER 1975, SIOUX FALLS, SOUTH DAKOTA

Landsat Data Contributions to Hydrocarbon Exploration in Foreign Regions

By F. P. Bentz,
Vice President, Santa Fe Minerals, Inc., Dallas, Texas 75219
and S. I. Gutman,
Geophysicist, Santa Fe Minerals, Inc., Orange, California 92668

ABSTRACT

Foreign exploration frequently requires that large areas of relatively unexplored territory be evaluated in the most expeditious and informative manner. The selection of areas with the greatest potential would normally start with the least expensive reconnaissance tools like photogeology, field work, and aeromagnetics before proceeding to the more costly and possibly more definitive techniques such as gravity, seismic, and, eventually, drilling. In many areas, however, this ideal sequence of evaluation can no longer be followed due to shortened exploration periods and other restrictive government regulations.

Santa Fe Minerals' past experience with Landsat has proved that the ready accessibility of multispectral imagery provides for quick and inexpensive reconnaissance of foreign exploration areas. Firstly, it allows the construction of geographic base maps which are often more accurate than any existing maps. Secondly, Landsat imagery is an invaluable source of geologic information; if used in conjunction with existing published data, it will, in most cases, improve the accuracy of geologic mapping and understanding of an area. In addition, it has been found that the imagery complements and aids in the interpretation of aeromagnetic and gravity data; this relationship is reciprocal.

Santa Fe Minerals has successfully experimented with Landsat multispectral imagery, and, as a consequence, now routinely integrates Landsat data into its exploration efforts.

Exploratory work in Egypt and Yemen serves to illustrate how Landsat imagery is used; some results are presented.

INTRODUCTION

The purpose of this paper is to present some of the major contributions of Landsat data to Santa Fe Minerals' hydrocarbon exploration in foreign areas.

Explorationists find themselves today in a highly competitive environment, complicated by shortening exploration periods and increasingly restrictive governmental regulations. For these reasons it is not always possible to follow a normal foreign exploration sequence, which is essentially a process of isolating and identifying targets with hydrocarbon potential from a large and relatively unexplored area. This process usually begins with reconnaissance tools such as aeromagnetometry, SLAR (side-looking airborne radar), and photogeology and proceeds to the more costly and time consuming (but hopefully more definitive) methods such as seismic surveys and drilling. Landsat data, because of their ready accessibility, help significantly in shortening the early reconnaissance stage of operations. In addition, Landsat imagery is, because of its low cost per unit area, one of the best data buys the explorationist can make.

Landsat has proven itself to be a valuable source of geological information. It has invariably improved the contact and spatial relationships of outcrops in poorly or sparsely mapped areas. The mapping of linears helps to define a structural fabric or framework in the exploration area. This fabric is often indistinct or invisible at the surface but, nonetheless, strongly influences hydrocarbon accumulations. With few exceptions, the pattern of linears is highly regular and can often be related to stress analysis. Subtle color and tonal anomalies have been observed which

are believed to be of significant exploration importance.

Significant relationships between gravity and magnetic data and alinements or trends have been observed in Landsat imagery. Initial conclusions suggest that the basement and intersedimentary structures, which are routinely interpreted from the potential field data, have greater (but subtle) surface expressions than we had previously anticipated.

Because it has been successful, Landsat data are now routinely integrated into Santa Fe's foreign exploration programs. It aids in planning geophysical surveys and allows the creation of exploration base maps onto which the results of literature searchers and available data can be posted; one is now able to begin the data acquisition and interpretation process almost immediately.

Exploratory work in Egypt and Yemen will serve to illustrate some of the contributions that Landsat data have made to our foreign exploration program. The choice of Egypt and Yemen was made because they essentially represent opposite ends of the information spectrum available to the explorationist.

The permit area in Egypt has well-exposed surface geology, portrayed on relatively detailed geologic maps. In addition, there are subsurface data available from nearby wildcat tests as well as Bouguer gravity and residual magnetic intensity maps. In contrast, the onshore exploration area in Yemen is covered with alluvium. There are no well data available from the five dry holes previously drilled there in the early 1960's nor is there an adequate or reliable geological map of the area. Despite the current interest in the southern Red Sea (as a consequence of the new global tectonics), there is little in the published literature concerning the onshore geophysics of the Yemen Arab Republic.

LANDSAT DATA CONTRIBUTIONS TO HYDROCARBON EXPLORATION IN EGYPT

The East Cairo concession straddles the Cario to Suez highway and encompasses about 1 million acres (fig. 1). It is bounded on the east by the Great Bitter Lake and on the west by the Damietta Branch of the Nile River where it comprises a small portion of the highly cultivated and densely populated Nile Delta. The rest of the concession area consists of gently rolling gravel desert bounded to the south by east-west trending limestone escarpments of Eocene age.

These physiographic provinces are an expression of the geology, as shown on figure 2, a geologic sketch map reproduced with permission from Said's *The Geology of Egypt* (Said, 1962). The 30th parallel (crossing the map in the center) forms the southern boundary of Santa Fe's permit.

The bulk of the escarpment-forming Eocene limestones lie south of the 30th parallel. Most of the concession is characterized by east-west trending outcrops of Oligocene to recent age, with Eocene rocks showing only in a few anticlines. Exposures of Cretaceous sediments are reported from Gebel Shabrawet overlooking Great Bitter Lake. The east-west trending outcrop pattern is indicative of the apparent folding axes; the main pattern of faulting, shown on the map, has a northwest-southeast direction.

Figure 3 (p. VIII) is a Landsat mosaic which encompasses a much larger area than the geologic map. One can orient oneself by Cairo at the neck of the delta in the west, the Suez Canal and Great Bitter Lake on the east, and the Mokkattam limestone escarpment forming the southern concession boundary to the south.

Quite a number of geologic features shown on Said's map can be readily identified on the Landsat image mosaic; for instance, the Eocene horst of Gebel Oweibid. Interestingly, there are many other geologic patterns which are more visible on the Landsat imagery than on the surface geologic map. As an example, note the almost circular syncline southwest of Gebel Shabrawet which is rather inadequately represented on the geologic map.

A great number of major and minor linears can readily be observed on the Landsat mosaic, as shown in figure 4. Close scrutiny reveals that these linears

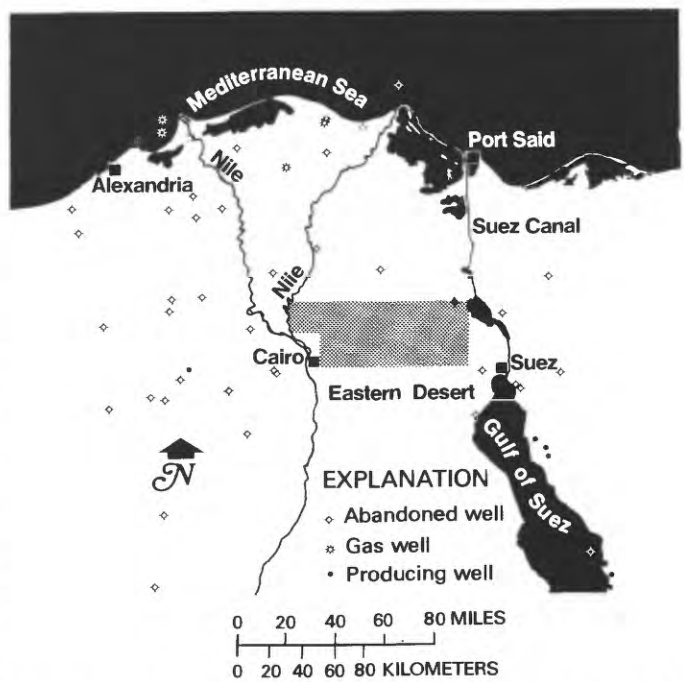

FIGURE 1.—Index map of northern Africa showing Santa Fe Minerals, Inc., exploration area.

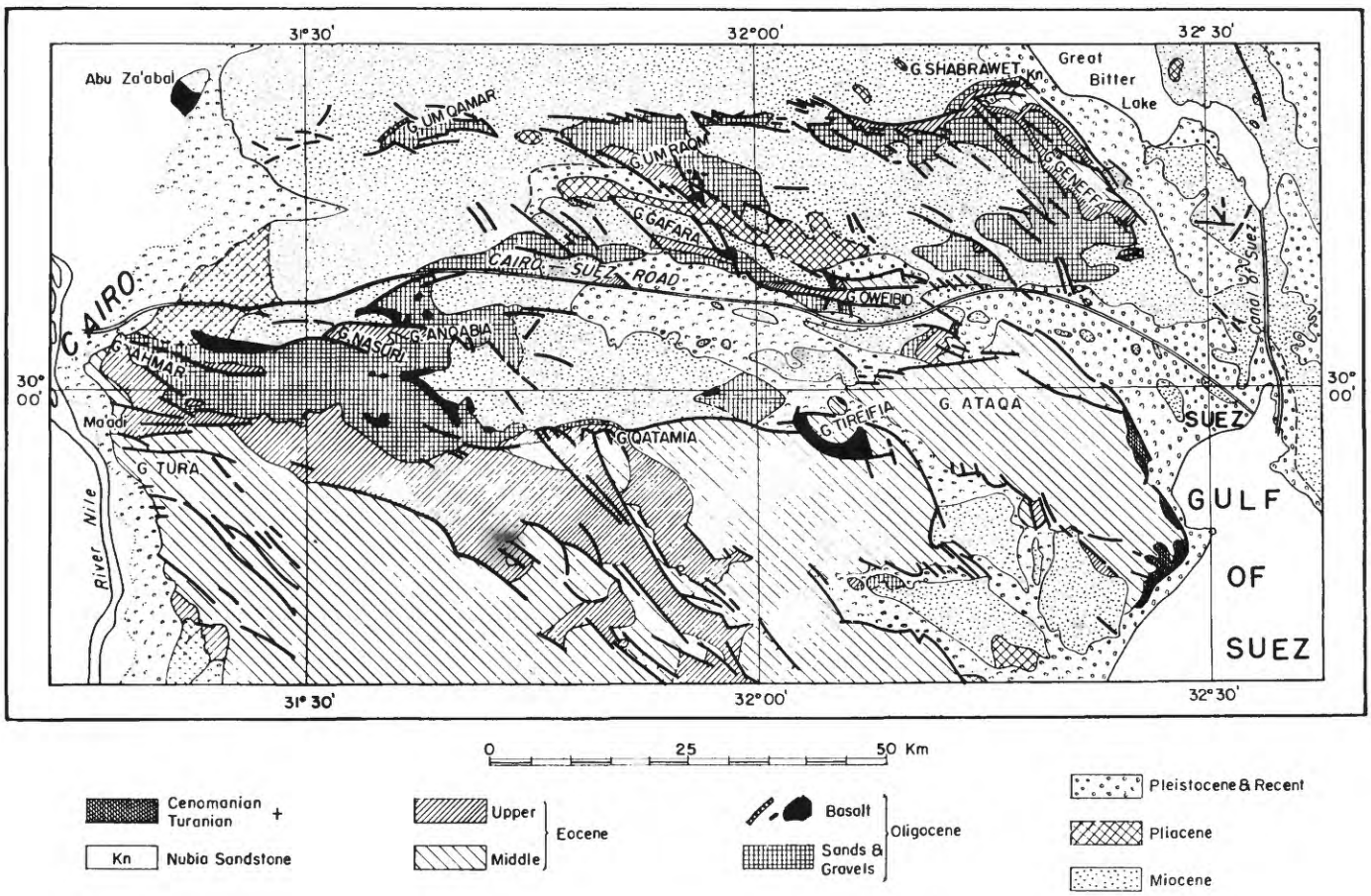

FIGURE 2.—Geology of Cairo-Suez District (after Said, 1962).

statistically represent a limited number of trends.

A presentation in the form of a star diagram not only enhances their regularity but also shows that they are intersecting each other at angles of approximately 15°, 30°, and 60° (fig. 5). These are the expected angles for shear sets of a strain ellipse, and they can also be related to Moody and Hill's wrench-fault tectonic scheme (fig. 6) first published about 20 years ago (Moody and Hill, 1956).

This does not imply that the Cairo-Suez area is governed entirely by wrench faults. In an area that lies at the junction of several important crustal plate boundaries which separate the African continent from the Mediterranean crust to the north and from the Sinai and Arabian blocks to the east, one can expect that divergent movements of these crustal blocks created a forceful stress system. This was likely relieved by a complex pattern of shear zones, compressional features, and tensional rifts.

The major structural units are illustrated in a simplified manner in a regional tectonic sketch (fig. 7).

The Gulf of Suez–Red Sea system is one of the most outstanding features in this area. It likely consists of a combination of tensional rifting and strike-slip movements (left lateral wrench faults). Initial block faulting occurred toward the end of Oligocene time and was associated with widespread volcanism.

If sea floor spreading is indeed a factor in the later history of this area, it was restricted to the Red Sea proper and did not penetrate the Gulf of Suez.

The Gulf of Aqaba–Dead Sea shear zone is equally impressive in its magnitude. It is probably along this left lateral wrench fault that any plate movement caused by Red Sea spreading occurred.

A distinct N. 50° W. trend occurs at a 15° angle to the N. 35° W. Gulf of Suez–Red Sea trend. Said combines the two trends under the name "Erythrean or African faulting"; and, indeed, the shorelines of the Gulf of Suez and the Red Sea are controlled by segments of both of these two trends (Said, 1962, p. 33). The N. 50° W. direction appears to be much older since it is expressed in shears within the Precambrian shield (Abdel-Gawad, 1969). In addition, the N. 50° W. direction was certainly rejuvenated in more recent times causing some of the more prominent right lateral shears in our area of interest.

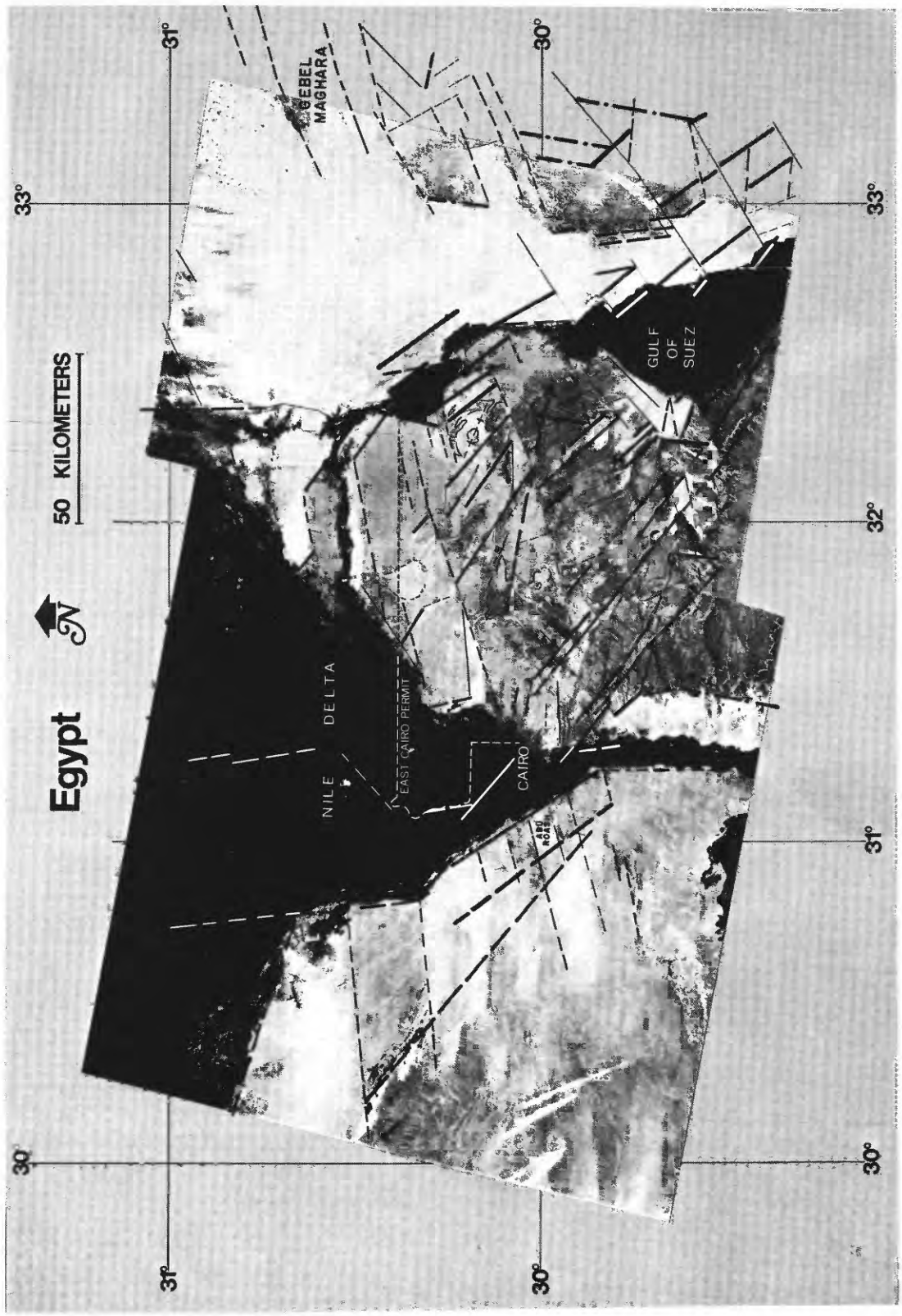

FIGURE 4.—Lineament interpretation of Landsat mosaic of Egypt.

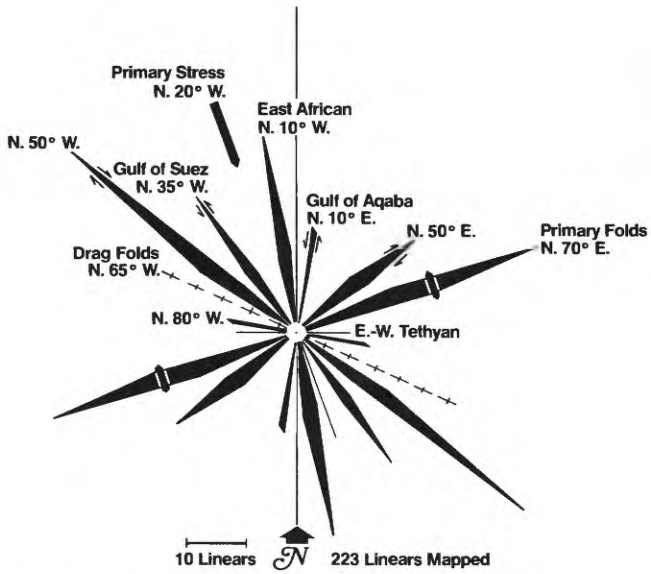

FIGURE 5.—Star diagram illustrating relationships between mapped lineaments.

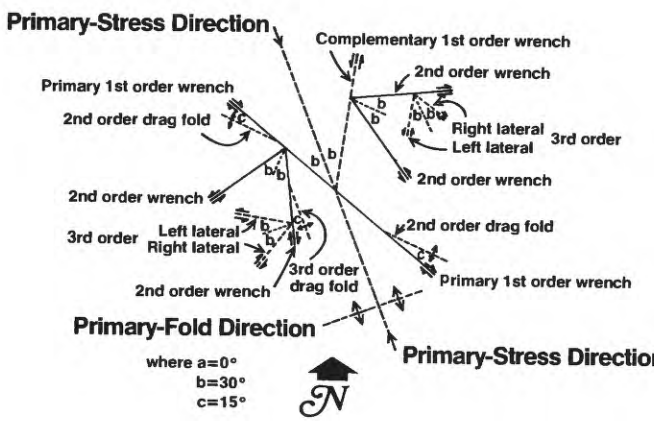

FIGURE 6.—Wrench fault tectonics as related to lineament interpretation.

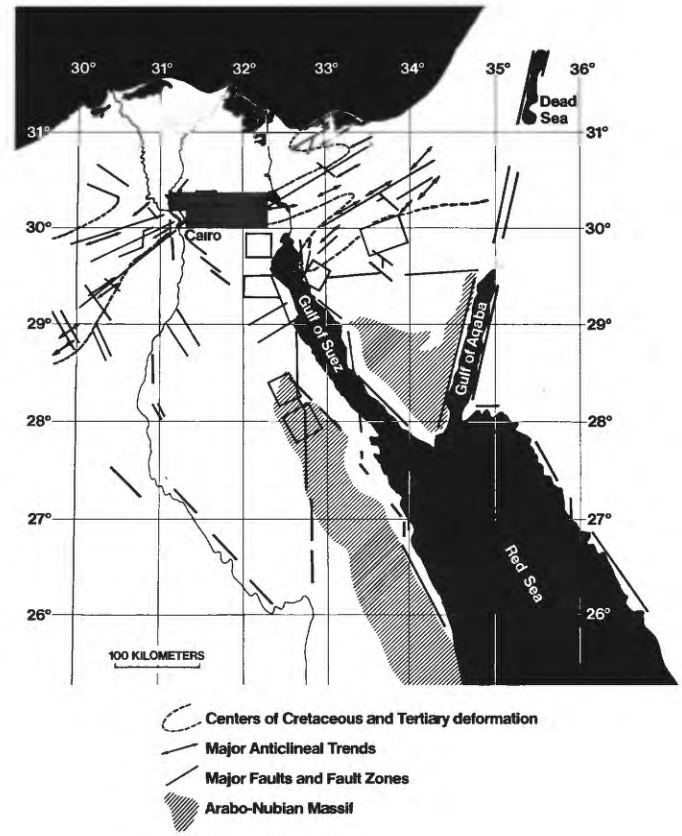

FIGURE 7.—Regional tectonics of Northeast Africa. (Adapted from Said, 1962.)

The north-south or "East African" trend is described by Said as "the old grain of Egypt" (Said, 1962, p. 32), yet it still seems to have played an important role in more recent geologic events, being responsible for deflections of the Gulf of Suez shorelines and of the Nile River.

An east-west trend related to the "Tethyan" direction is prominent in Sinai and crosses the concession area in several places. At Gebel Oweibid it can be interpreted as a right lateral wrench fault based on the outcrop configuration shown on the geologic map.

A major folding axis, described as the Gebel Maghara–Abu Roash line, crosses our area in a N. 70° E. direction, at right angles to the primary stress oriented at about N. 20° W. This primary fold axis is not obvious from the surface geologic map of our concession area; however, the magnetic intensity (fig. 8, p. IX) and the Bouguer gravity map (fig. 9, p. X) do reflect this structural orientation.

Considering the regional aspects of this main axis, one can discern a southwesterly plunge from the Jurassic outcrops at Gebel Maghara in the Sinai to the Middle Cretaceous outcrops at Gebel Shabrawet near the Great Bitter Lake and to the Lower Cretaceous and Jurassic encountered 2,000 ft below the surface in the Abu Roash wells.

At right angles to the primary stress lies also the direction of greatest tension which could, at least in part, be responsible for the rifting of the Gulf of Suez. And while a number of the mapped lineaments are probably related to strike-slip movements, others are associated with block faulting and tilting. It is believed that the major movement along the Gulf of Suez trend was a vertical displacement along normal faults resulting in tilted fault blocks. This can be illustrated by the uplifted Middle Cretaceous sedimentary rocks at Gebel Shabrawet west of the Great Bitter Lake. A similar uplift along the same direction of faulting probably occurred at Abu Roash west of the Nile Valley near Cairo. This set of block faults

would result in a steepening of the southwestward axial plunge across the area.

Evidence for horizontal displacements is illustrated by a set of drag folds that forms a distinctive pattern in the center of the concession area.

In the course of our work, we have observed a surprising correspondence between gravity and magnetic data and Landsat imagery. It usually is in the form of close associations of linears and lineaments with high gradients and magnetic accidents (fig. 8, p. IX). The magnetic anomalies which are essentially reflecting the configuration of the magnetic basement dramatically confirm the substance of the N. 70° E. regional trend that was first observed on the Landsat imagery. Please note the departure of the field from this trend in the south-central portion of the permit area. We have interpreted this as the reorientation of the basement along a major left lateral strike slip fault seen in Landsat data. This is an excellent example of how the potential field data and the Landsat imagery complement each other to arrive at a unified and consistent geological picture.

The correspondence of the Bouguer gravity anomalies (fig. 9, p. X) with the surface geology (fig. 2) is quite good. Note the roughly east-west alignments of gravity highs over the folded and faulted Oligocene sedimentary rocks in the north and observe that a broad, regional trend of N. 70° E. is disturbed by high frequency anomalies associated with contacts and structures, particularly in the center of the area. In the west, where there is a total absence of geologic outcrops due to the vegetative cover of the Nile Delta, we have a broad, elongated gravity low which trends north-south.

The Landsat interpretation highlights the contact and fault relationship inherent in the gravity data as well as the regional N. 70° E. trend which we feel is quite important to hydrocarbon accumulations east of the Nile Delta. Please observe that jogs in the course of the Nile are associated with flexures in the gravity anomalies and the extensions of lineaments mapped outside the delta. We conclude that not only is the present course of the Nile largely fault controlled but that these faults influenced the development of a gorge of Grand Canyon proportions which formed at the end of Miocene. This gigantic 10,000-ft deep erosion channel (discovered by Santa Fe's seismic reflection work) helps to explain the conspicuous north-south gravity low mentioned above.

LANDSAT DATA CONTRIBUTIONS TO HYDROCARBON EXPLORATION IN YEMEN

The Yemen Arab Republic lies on the southwestern tip of the Arabian Peninsula (fig. 10). The area in which Santa Fe Minerals was interested encompasses more than 5.7 million acres, of which close to 4 million acres are located onshore. A rather restricted exploration option of 8 months required us to survey this vast area in the most expeditious and cost effective manner. For this purpose, an abbreviated exploration program was undertaken consisting of an offshore seismic survey combined with marine gravity and magnetics. An aeromagnetic survey and Landsat interpretations were conducted over the onshore portion.

The Landsat mosaic (fig. 11, p. XI) gives an indication of the nature and quality of the data as well as a feel for some of the interpretation problems that were encountered.

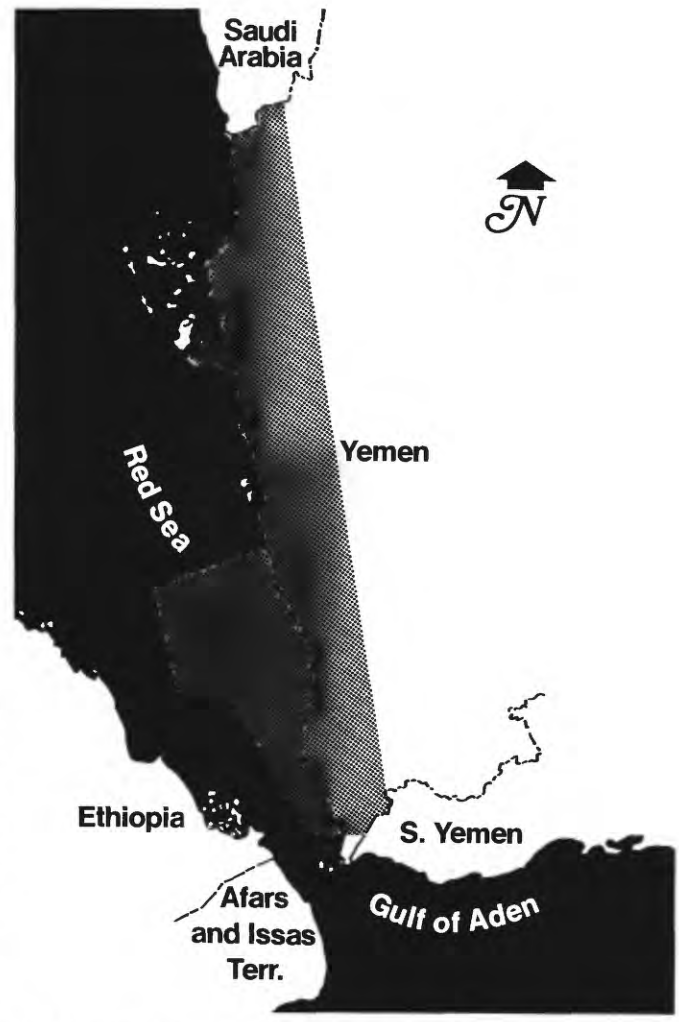

FIGURE 10.—Index map showing Santa Fe Minerals, Inc., exploration area in Yemen.

The Tihama Plain extends 400 km north to south along the Red Sea Coast. This coastal plain gently dips to the west from a mountain front which dramatically rises to heights of more than 8,000 ft. Although faulting, fracturing, and jointing are clearly visible in the mountains, at first glance there appeared to be an almost total lack of these features in the plain due to the thick alluvial cover. On closer inspection, however, it was observed that despite the lack of outcrops in the Tihama Plain, there are a profusion of subtle color or tonal streaks as well as circular anomalies visible from orbit which are totally indistinct either on the ground or in the aerial photos (fig. 12).

Lineaments in the mountains define a structural fabric which is relatable to the stresses that this area has been subjected to as a result of regional upwarp or arching during the Oligocene and rifting during the early and middle Miocene. Linears in the coastal plain echo the structural fabric of the mountains lending support to the possibility that these color and tonal anomalies reflect in some way the configuration of the subsurface, specifically fault blocks and attendant structures.

Subtle circular anomalies are observed in the Landsat images and appear to be concentrated north of lat 14°30′N. Salt is being mined from outcrops of Miocene age which have surfaced along the Red Sea Coast, particularly around Salit (El Shazly, 1967). It is also understood that an oil company had drilled several of its wells on gravity lows, suggesting that salt domes were its exploration targets (privileged communication, 1975). The aeromagnetic survey revealed that no magnetic anomalies are directly associated with these features. As a consequence, it is confidently felt that some of the circular anomalies reflect salt diapirs. Their concentration north of lat 14°30′N. suggests a thickening of the section in that area, strengthening the results of the aeromagnetic interpretation.

The subtle circular anomalies (such as those targeted on fig. 13) are best seen in band 7 images and in stretched false-color composites. While most of the anomalies appear as breaks in the tonal pattern of the plain, some are associated with vegetation occurrences.

Of the five wells drilled by an oil operator in the early 1960's, three of them are located on circular anomalies. It is observed that all of the wells drilled on circular anomalies lie on the flanks rather than on top of structural basement highs as interpreted from the aeromagnetic data, further supporting the contention that these circular anomalies reflect the presence of numerous diapirs.

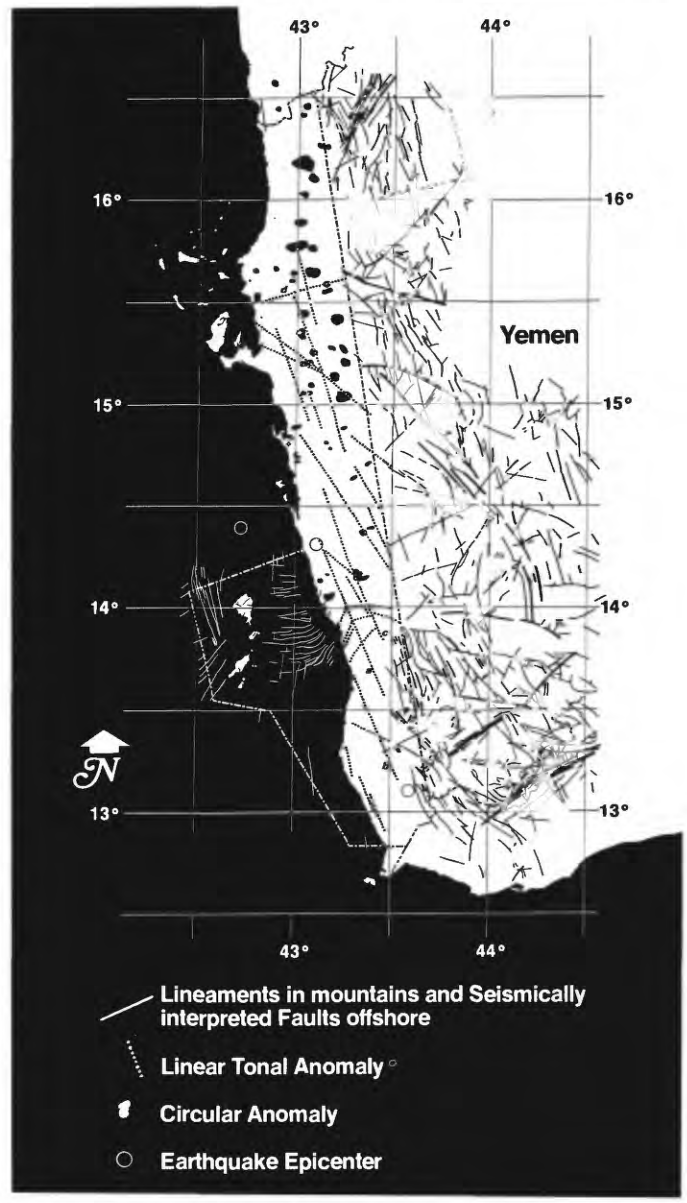

FIGURE 12.—Interpretation of lineaments, circular and tonal anomalies from Landsat data.

The color or tonal anomalies to which we alluded are highlighted in a portion of Landsat–1 scene 1117–06562 (fig. 14). The streaks, trending southwesterly appear to be related to the onshore extension of faulting as interpreted from our offshore seismic program. We feel that these represent a reorientation of the drainage patterns as a consequence of southwest tilting of the section along these faults.

The alinement of northwesterly trending streaks suggests that they may be the expression of faulting parallel to the Red Sea rift axis. Stream offsets along one such tonal anomaly indicate approximately 3 km of right lateral offset. The association with earthquake

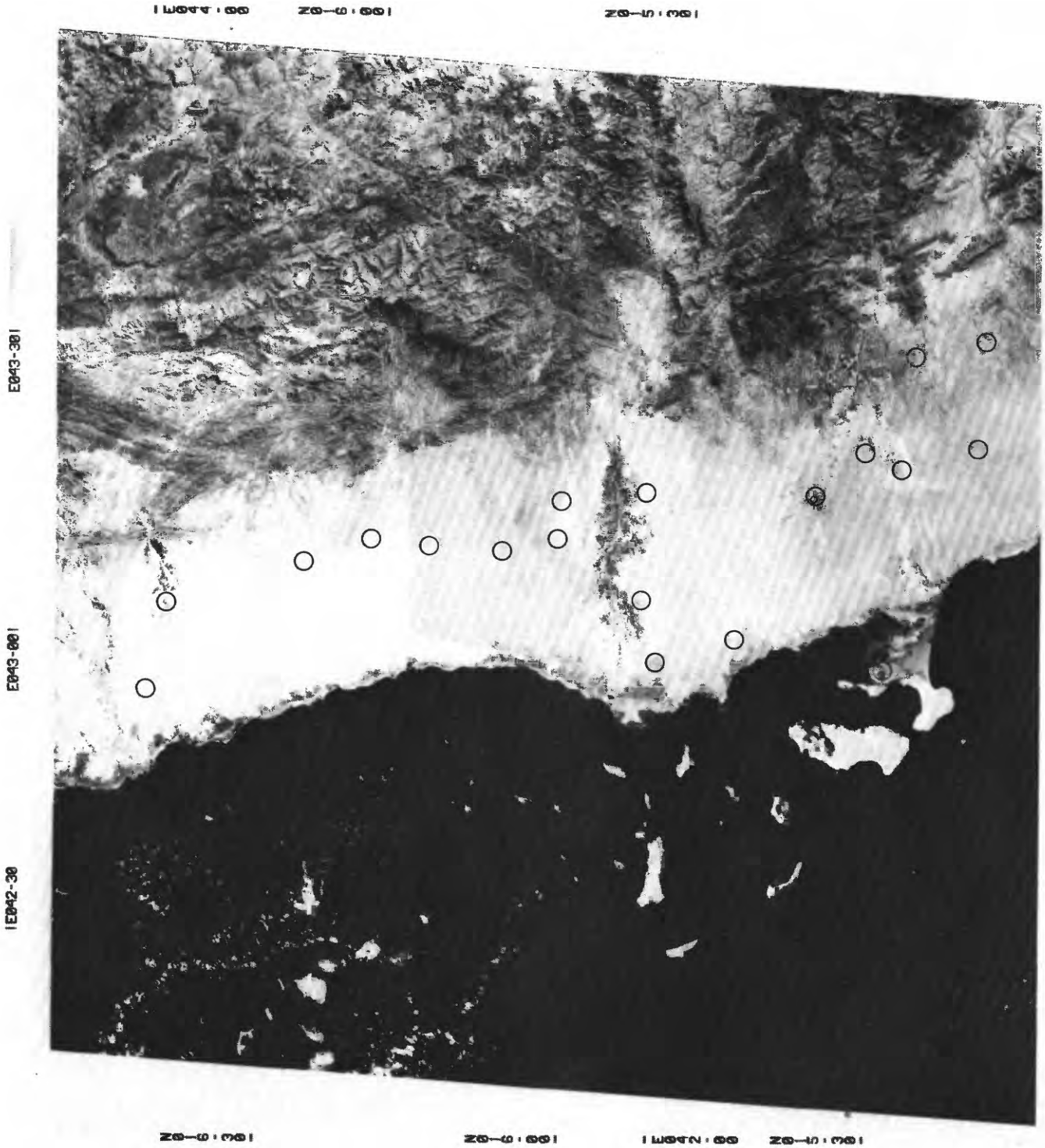

FIGURE 13.—Circular anomalies and well locations originally identified on a photographically enhanced false-color composite. Landsat–1 image 1082–07011, October 13, 1972.

FIGURE 14.—Detail of streaks and tonal anomalies on Yemen coastal plain, Landsat–1 image 1117–06562, bands 4, 5, and 7, November 17, 1972.

epicenters (Fairhead and Girdler, 1970) further indicates that these streaks are the surface expressions of faulting (fig. 12).

Compagnie Général de Géophysique (CGG) flew a 4,600-km aeromagnetic survey for this exploration effort in April 1975. The results of this survey were very gratifying because they not only confirmed the results of the offshore work but made many of the features seen in the Landsat imagery understandable in a structural context. A few of our observations may serve to illustrate this point.

A north-northwest-trending fault system (interpreted by CGG) parallels the mountain front and some of the linears observed within and at the foot of the mountains.

The extensions of some lineaments from the mountains onto the Tihama Plain coincide with high magnetic gradients not initially defined as faults. This aids in amplifying the interpreted fault pattern.

Conversely, magnetic events interpreted as basement faults coincide with stream courses emerging from the mountains, suggesting structural control of some of the drainage patterns.

The flanks and basinal axis of a 3-km deep magnetic anomaly are reflected by surface linears.

Numerous other interrelationships between magnetic data and linears in the Tihama Plain assist in deciphering the structural development of the area.

It is of particular interest to note that Landsat-observed linears are not solely related to fault and fracture patterns but often reflect deep-seated structural trends and a variety of geologic phenomena.

Considering its demonstrated versatility, low cost, and ready access, Landsat imagery deserves to be applied to all integrated exploration efforts, foreign or domestic.

ACKNOWLEDGMENTS

We wish to express our appreciation to Santa Fe International Corporation for encouraging us to prepare this paper. Our thanks to Dr. M. K. El Ayouty of EGPC for permitting us to present our findings in Egypt and to Elsevier Publishing Company for permission to reproduce Said's geologic map. We also thank Peter Coberly and Michael Wallace of Custom Color Labs in North Hollywood, California, who produced our Landsat false-color composites and Santa Fe's Art Department which produced the illustrations for this paper. Special appreciation is due to Dr. William A. Fischer and Donald Orr of the USGS EROS Program for inviting us to publicize our work with Landsat imagery.

REFERENCES

Abdel-Gawad, M., 1969, New evidence of transcurrent movements in Red Sea area and petroleum implications: Am. Assoc. Petroleum Geologists Bull., v. 53, no. 1, pp. 1466–1479.

El Shazly, E. M., 1967, Oil shows in Yemen and oil bubbles in rock salt: Arab Petroleum Congress, 6th, Baghdad 1967, Paper no. 40 (B–3).

Fairhead, J. D., and Girdler, R. W., 1970, The seismicity of the Red Sea, Gulf of Aden and Afar triangle: Royal Soc. London Philos. Trans., ser. A, v. 267, no. 1181, pp. 49–74.

Moody, J. D., and Hill, M. J., 1956, Wrench fault tectonics: Geol. Soc. America Bull., v. 67, pp. 1207–1246.

Lowell, J. D., Genik, G. J., Nelson, T. H., and Tucker, P. M., 1975, Petroleum and plate tectonics of the southern Red Sea, *in* Fischer, A. G., and Judson, S., eds., Petroleum and global tectonics: Princeton Univ. Press, pp. 129–153.

Said, R., 1962, The geology of Egypt: Amsterdam, Elsevier Publishing Co.

PROCEEDINGS OF
THE FIRST ANNUAL WILLIAM T. PECORA MEMORIAL SYMPOSIUM,
OCTOBER 1975, SIOUX FALLS, SOUTH DAKOTA

Measurement of Luminescence of Geochemically Stressed Trees and Other Materials

By W. R. Hemphill,[1] R. D. Watson,[2] R. C. Bigelow,[3] and T. D. Hessen,[3]
U.S. Geological Survey

ABSTRACT

The Fraunhofer line discriminator (FLD) is an airborne electro-optical device which operates as a nonimaging radiometer and permits detection of solar-stimulated luminescence several orders of magnitude below the intensity detectable with the human eye. Procedures employing a laboratory fluorescence spectrometer permit prediction of the FLD detectivity of a material prior to mounting an airborne test. Luminescence spectra of the material are corrected for wavelength variation in spectrometer source and detector sensitivity and solar illumination. By comparing these results with the luminescence of a rhodamine WT dye standard, the luminescence of the material may be expressed in terms of rhodamine dye equivalency at the wavelengths of several Fraunhofer lines. The FLD detectivity may be assessed at each Fraunhofer line, and the optimum line for field observation of the material may be selected.

Airborne tests of a redesigned FLD permitted measurement of differences in the luminescence of trees growing in soils containing geochemically anomalous concentrations of copper (near Denver, Colorado) and molybdenum (near Gardnerville, Nevada) from trees growing in background areas nearby. In the tests near Denver, luminescence contrast between background and stressed trees tended to be higher during periods when cloud cover was less than 10 percent; in most cases, contrast was insignificant when cloud cover exceeded 10 percent. Although diurnal variations were also observed, these do not appear to be predictable or systematic. In other airborne tests, the FLD distinguished luminescing phosphate rock and gypsum from sandstone and siltstone near Pine Mountain, California, and dispersal of oil in a natural seep from seawater in the Santa Barbara Channel.

INTRODUCTION

Laboratory and field study of the measurement and interpretation of luminescent materials began in 1964 using an active [4] ultraviolet imaging system (Hemphill and others, 1965; Hemphill and Carnahan, 1965). This work led to the development of a prototype Fraunhofer line discriminator (FLD), an airborne remote-sensing tool for measuring luminescence. The FLD was designed to operate on the Fraunhofer line depth principle (Kozyrev, 1956; Grainger and Ring, 1962) which uses the Sun as an excitation source and permits detection of luminescing materials under daylight conditions. Experiments with the instrument showed that selected materials, such as luminescing tracer dyes could be detected in very small quantities (Hemphill and others, 1969; Stoertz and others, 1969). For example, rhodamine WT dye was detected in the Pacific Ocean west of the Golden Gate in California in concentrations of less than 5.0 ppb (parts per billion). Attempts to measure the luminescence of other materials were not successful because (1) the prototype FLD operated at 589.0 nm (nanometres), the wavelength of the sodium D Fraunhofer line, and many materials luminesce at other wavelengths and (2) the sensitivity was an order of magnitude less than required for detection of some of these materials.

In order to predict optimum wavelength and sensitivity requirements for detection of materials other than rhodamine WT, luminescence of a variety of

[1] Reston, Virginia; [2] Flagstaff, Arizona; [3] Denver, Colorado.

[4] An "active" system uses an artificial source, in this case a cathode ray tube, to stimulate luminescence.

materials was measured with a laboratory fluorescence spectrometer in terms of rhodamine WT, used as a laboratory standard. These results, coupled with those obtained with the prototype FLD, were used as a basis for redesigning an FLD with an order of magnitude increased sensitivity. This redesigned model, built by the Perkin-Elmer Corporation,[3] operates at three discrete Fraunhofer lines, hydrogen β at 486.1 nm, sodium D at 589.0 nm, and hydrogen α at 656.3 nm and has the sensitivity to detect rhodamine WT dye in concentrations as low as 0.1 ppb in 0.5 m of water at 20° C.

The objectives of this report are (1) to present the results of laboratory and field measurement of luminescence of geochemically stressed trees, phosphate rock, and crude oil and (2) to demonstrate how the laboratory measurement of luminescence can be used to predict and interpret field measurements with the FLD.

Since 1971, development of the redesigned FLD by the Perkin-Elmer Corporation, as well as associated laboratory and field studies, has been supported by the Advanced Applications Flight Experiments (AAFE) Program of NASA (NASA Order L–58,514), the Earth Resources Observation Systems (EROS) Program of the Department of the Interior, and the Geologic Division of the U.S. Geological Survey.

FRAUNHOFER LINE DEPTH METHOD

Fraunhofer lines are dark lines in the solar spectrum caused by selective absorption of light by gases in the relatively cool upper part of the solar atmosphere. Line widths range from less than 0.01 nm to several tenths of a nanometre, and the central intensity of some lines is less than 10 percent of the adjacent continuum. The lines are sharpest, deepest, and most numerous in the near ultraviolet, visible, and near-infrared regions of the electromagnetic spectrum.

The Fraunhofer line-depth method of measuring luminescence involves observing a selected Fraunhofer line in the solar spectrum, and measuring the ratio of the central intensity of the line to a convenient point on the continuum a few tenths of a nanometre distant; this ratio is compared with a similar ratio of a conjugate spectrum reflected from a material that is suspected to luminesce. Both ratios normally are identical, but luminescence is indicated where the reflected ratio exceeds the solar ratio. Variation of reflectivity with wavelengths is negligible for most materials over spectral ranges of only a few tenths of a nanometre; therefore, reflectivity differences between the central intensity of the Fraunhofer line and the adjacent continuum can generally be ignored. Equations illustrating the relation of Fraunhofer line depth ratios to luminescence are presented in the *Manual of Remote Sensing* (Am. Soc. Photogrammetry, 1975, p. 116–118).

LABORATORY PREDICTION OF THE FRAUNHOFER LINE DETECTIVITY OF LUMINESCENT MATERIALS

In order to assess the sensitivity required to detect luminescing materials, Hemphill and Stoertz (1971) and Watson and others (1973, 1974) used a laboratory fluorescence spectrometer (fig. 1) to measure the luminescence intensity of materials at six Fraunhofer lines (396.8, 422.7, 486.1, 518.4, 589.0, and 656.3 nm) in terms of equivalent luminescence of specific concentrations of rhodamine dye. The spectrometer was operated so as to produce excitation spectra; that is, the excitation monochromator was scanned, exciting the sample with monochromatic light in the near ultraviolet and visible spectrum, while the emission monochromator was stationary at the wavelength of a specific Fraunhofer line. This arrangement provided a system in the laboratory analogous to an FLD in the field, where the broadband excitation of the Sun produces an emission in a luminescent material, the intensity of which is monitored at one or more Fraunhofer lines. The spectrometer, equipped with a

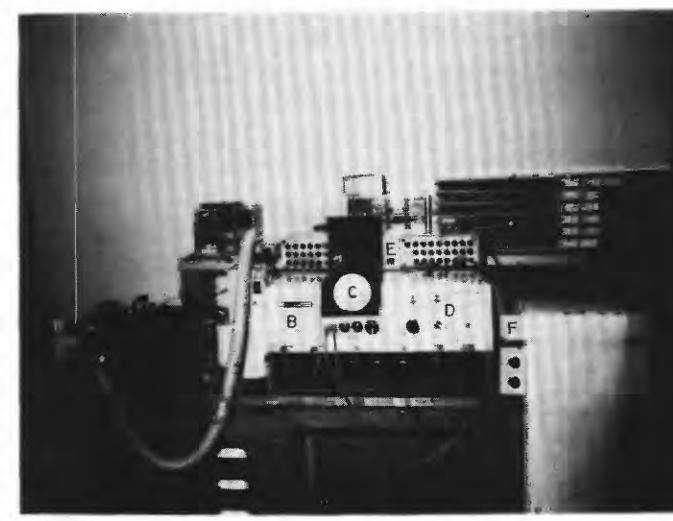

FIGURE 1.—Laboratory fluorescence spectrometer. Source (A), excitation monochromator (B), sample compartment (C), emission monochromator (D), corrected spectra attachment (E), and recorder (F).

[3] Use of trade name in this paper is for description purposes only and does not constitute an endorsement of the product by the U.S. Geological Survey.

corrected spectra attachment, automatically adjusted for the wavelength dependence of the source and detector and produced a corrected distribution of excitation intensity.

To relate all luminescence spectra to one set of conditions, rhodamine WT was used as the reference "standard" prior to each measurement. When the area under the curve of the excitation spectra of the sample was compared to the area under the curve for rhodamine WT dye (at a specific dye concentration), a relative equivalent rhodamine WT concentration was obtained. For example, a sample having an integrated excitation intensity of 50 was compared to a rhodamine WT concentration of 10 ppb, which also has an integrated excitation intensity of 50; the sample is said to have had an equivalent luminescence of 10 ppb rhodamine WT. This standardization makes it possible to correct for instrument response variations during measurement and to assess results achieved in the laboratory in terms of whether or not the same material in the field would be within the sensitivity range of an airborne FLD.

To obtain the same wavelength and intensity dependence of luminescence in the laboratory as would be observed in an FLD measurement, the source-detector corrected spectra must be convoluted with the spectral intensity of total solar radiation (direct sunlight plus diffuse skylight). A further correction is required when adjusting the standard of rhodamine dye as measured in a centimetre quartz cell in the spectrometer to that measured in the field, where sunlight penetrates the material and stimulates luminescence at a depth that is a function of the material's absorption. Descriptions of the solar and depth corrections are presented by Watson and others (1974) and by the American Society of Photogrammetry (1975, p. 118–120).

DESCRIPTION OF THE FRAUNHOFER LINE DISCRIMINATOR

The FLD consists of an optical head, electronic console, and light collector as shown in figure 2. The main components in the optical head are two telescopes, one Earth-looking and one sky-looking; a rotating optical chopper wheel; three replaceable optical filter sets; and a photomultiplier with its power supply. Sunlight and skylight falling on the diffuse surface of the light collector are reflected by a mirror into the telescope of the sky-looking channel. The Earth-looking telescope observes the target whose reflectivity and luminescence are to be measured. Light from the two telescopes is sequentially routed through two different paths by the rotating chopper wheel. In one path, light passes through a filter which is centered at a specific Fraunhofer line but whose bandpass is several hundredths nanometres wider than the Fraunhofer line. This signal constitutes the light intensity measured on the solar continuum adjacent to and including the Fraunhofer line and is designated signal "*a*" in the sky-looking channel and signal "*d*" in the Earth-looking channel. In the other path, a Fabry-Perot interference filter, with half-width of less than 0.07 nm, passes light coincident with the intensity of the central part of the Fraunhofer line; this signal is designated signal "*b*" in the sky-looking channel and signal "*c*" in the Earth-looking channel. These signals are fed to a mini-computer that generates luminescence and reflectance by solving the following equations: $\rho = (d-c)/(a-b)$; $\varepsilon = (d/a) - \rho$, where ρ is reflectance and ε is the luminescence coefficient. Both ρ and ε are displayed as four-digit numbers (from 0000 to 9999 counts) on the front panel and are fed to a digital printer for permanent record; hence, 100 counts for ε implies a luminescence of 1 percent. Reflectance values are displayed and recorded as percent directional reflectance. Inasmuch as displayed and recorded luminescence are only proportional to true luminescence for each substance measured, the luminescence count is referenced to the count from a standard (such as a dye sample or a photographer's gray card), permitting relative luminescence measurements to be made. Reflectance and luminescence values are presented in this paper in terms of their mean, plus or minus the standard deviation of the mean (Hoel, 1965, p. 139).

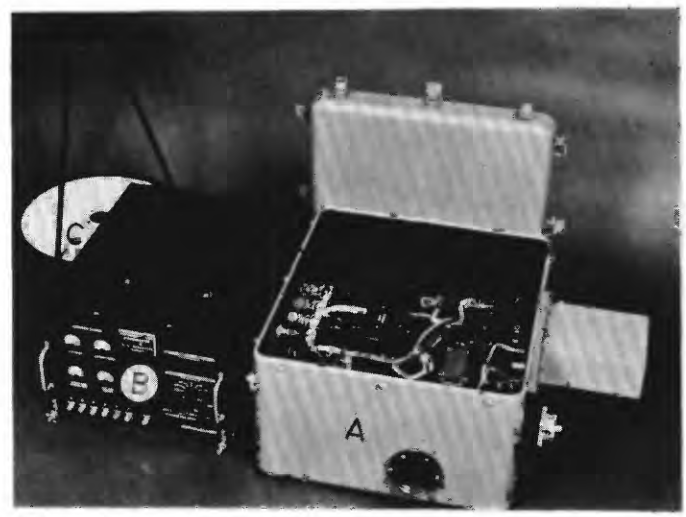

FIGURE 2.—Perkin-Elmer FLD, showing the optical head (A), electronic console (B), and light collector (C).

An automatic gain control is used to monitor and maintain the a-signal at a nearly constant level by varying the gain of the photomultiplier tube (PMT) detector. This permits measurements under a wide range of illumination and allows the PMT to operate at full gain under low illumination. Three sets of Fabry-Perot filters are available, permitting measurement at the 656.3-, 589.0-, and 486.1-nm Fraunhofer wavelengths. Additional filters can be made at other Fraunhofer wavelengths, including 396.8, 422.7, and 518.4 nm.

Ground tests show that rhodamine WT dye can be detected at the 589.0-nm Fraunhofer line in 0.5 m of water under clear sky conditions in concentrations as low as 0.1 ppb; however, sensitivity under field conditions is generally considered to be 0.25 ppb. The relationship between dye concentration and luminescence measured by the instrument is approximately linear, with 1.32 ppb equating to 100 FLD counts. Luminescence measurements were about 25 percent higher under clear sky conditions than under overcast conditions.

Figure 3 shows the FLD optical head and light collector installed in a basket atop the landing skid and adjacent to the fuselage of a helicopter. The system also includes (1) a television camera with a remotely controlled focus and zoom lens for monitoring the target measured with the FLD, (2) a second television camera which monitors a bank of light emitting diodes displaying reflectance and luminescence data that are continually updated by the digital output of the FLD, (3) a tape recording system for recording the data from both cameras and additional voice description, and (4) a television monitor on which is displayed in real time the target scene upon which is superimposed the reflectance and luminescence counts. Boresighting of the viewing system is achieved by positioning a luminescence panel on the ground and marking the position of the panel on the television screen by the luminescence indicated while hovering over the panel. The viewing system has proven dependable and permits discrimination of small luminescence targets which would otherwise be lost in data reduction. It also permits storage of both video and digital data in a form which can be replayed and analyzed in the laboratory.

Current operational procedures for airborne measurements with the FLD are as follows:

1. Optical filter and electronic warmup—30 minutes.
2. Preflight calibration using reflectant and luminescent chips.

FIGURE 3.—FLD optical head and light collector installed in a basket mid-ship of a Bell Jet *Ranger* helicopter.

3. Inflight systems check using a ground-deployed luminescent panel.
4. Airborne luminescence and reflectance measurements over target area.
5. Postflight calibration using reflectant and luminescent chips.

Air temperature, extent of cloud cover, and other meteorological parameters, as appropriate, are recorded throughout the day.

GEOCHEMICALLY STRESSED VEGETATION

The relationship between luminescence and photosynthesis in plants is complex, but, in general, factors that both impede and enhance photosynthesis can modify luminescence (Hollaender, 1956). Several such factors exist in nature. Based on the air pollution work of O'Gara (1922), Thomas (1961, p. 236–237) ranked cultivated and native plants according to resistance to sulfur dioxide fumigation. Thomas noted substantial

variability in sulfur dioxide susceptibility of some species, including conifers, but others were relatively constant. Alfalfa, barley, and cotton were most sensitive. Using alfalfa as unity, elm, birch, sumac, and poplar were about 2.5 times more resistant, pine 7–15 times more resistant, and live oak 12 times more resistant. Thomas (1961, p. 253) also noted that 3- to 4-month-old ponderosa needles were sensitive to hydrogen fluoride fumigation but that old needles were resistant.

Another such factor is geochemical stress, where abnormally high concentrations of one or more metallic elements may subject plants to chemical and physiological changes. Copper and zinc are toxic if present in large quantities (Kramer and Kowlowski, 1960, p. 225–226) and are reported to produce symptoms closely resembling iron chlorosis (Sauchelli, 1969, p. 65). J. E. McMurtrey (in Sauchelli, 1969, p. 156) notes that copper in excess of 0.1 ppm stunted tobacco plants. F. A. Gilbert (in Sauchelli, 1969, p. 158) states that growth of tomatoes in nutrient solution was reduced by as little as 1 ppm copper. Sauchelli (1969, p. 112) cites zinc having a toxic effect in some cereal grains where levels exceed 150 ppm and in citrus where levels exceed 220 ppm. K. C. Beeson (in Sauchelli, 1969, p. 133 and 138) reports that concentrations of molybdenum in plants may vary from less than 0.1 ppm to more than 300 ppm without adverse effect on growth. Press (1974, p. 374–375) reports that bean plants grown in solutions containing varying concentrations of lead exhibited chlorosis and that spectral reflectance at 550 nm ranged from 15 percent for 1 ppm (part per million) lead to more than 30 percent for 500 ppm lead.

Watson, Hemphill, and Hessin (1973) grew bean plants hydroponically and treated the nutrient solutions with varying metal concentrations, including molybdenum, copper, zinc, and lead, to demonstrate that luminescence is an indicator of geochemical stress produced by metal toxicity. Measurements were made both in the early stage of growth and at full maturity. Table 1 shows luminescence differences observed for 10 plants, 5 nonstressed and 5 stressed with 10 ppm sodium molybdate ($NaMO_4$). Both groups were grown in a Hoagland No. 2 solution. Differences in luminescence at 2 weeks are reversed at 5 weeks. The reversal not only occurs between stressed and nonstressed plants but also between large and small leaves. The difference in luminescence is reduced at 5 weeks for the large leaves. These results illustrate the complexity of luminescence during various stages of growth and tend to support the observations of Thomas (1961, p. 253) in his plant fumigation experiments noted above.

To investigate the luminescence of needles of *Pinus ponderosa*, trees growing in a copper- and zinc-rich soil near Malachite Mine, Jefferson County, Colorado (fig. 4), were measured in the field using the laboratory fluorescence spectrometer and were compared to measurements of needles from background trees. Country rock where trees grow includes biotite schist and hornblende gneiss, and younger pegmatite dikes; all are of Precambrian age (Huff, 1963).

Figure 5 shows the copper anomaly in the Malachite Mine area and the location of background and geochemically stressed tree groups. Measurements were made both diurnally (every 4 hours over a 24-hour period) and seasonally (every 4–5 weeks, July-November 1973 and April-May 1974). Data during the period from December 1973 through March 1974 could not be obtained because of heavy snow. Four twigs were collected from each of seven background and seven geochemically stressed trees making a total of 56 samples that were measured. The needles were removed from the twigs, placed on a black-matte nonluminescent surface, and measured in the front-surface mode in the spectrometer. The 4-hour spacing between separate collection runs was determined by the time required for sample collection, measurements, and logistical considerations, but it was verified that the period of as much as 2 hours between time of collection and completion of measurement did not alter the luminescence of the needles beyond experimental error.

Subsequent measurement of copper and zinc in the ash of the needles was by standard analytical techniques, and table 2 shows the results of chemical analyses of samples collected during late summer and autumn of 1973. Mean copper content of ash from stressed trees on four dates exceeds the mean copper

TABLE 1.—*Luminescence (source-detector, solar, and depth corrected) of 10 bean plants expressed in terms of rhodamine WT equivalency (ppb). The plants were grown hydroponically in Hoagland #2 nutrient solution; five of these plants were geochemically stressed with 10 ppm sodium molybdate ($NaMO_4$).*

Description	Stressed		Nonstressed	
	2 weeks	5 weeks	2 weeks	5 weeks
Top surface, large trifoliate leaves	0.62	1.05	0.45	1.19
Top surface, small trifoliate leaves	.67	.64	.49	.98

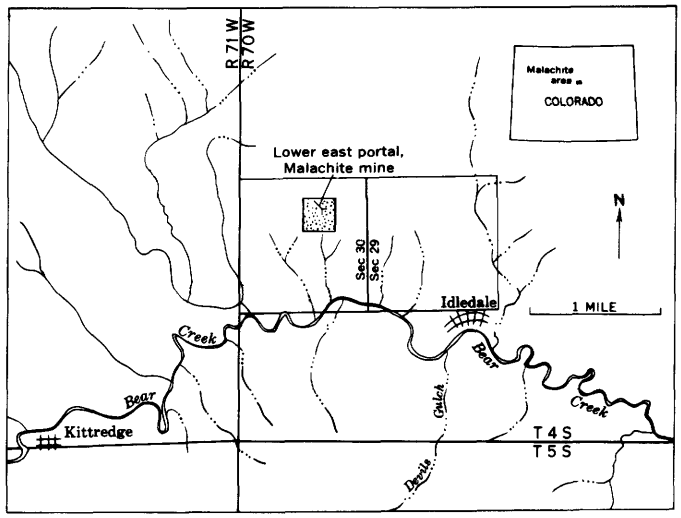

FIGURE 4.—Location of Malachite Mine area, Jefferson County, Colorado. Stipple pattern shows area of figure 5. (From Huff, 1963.)

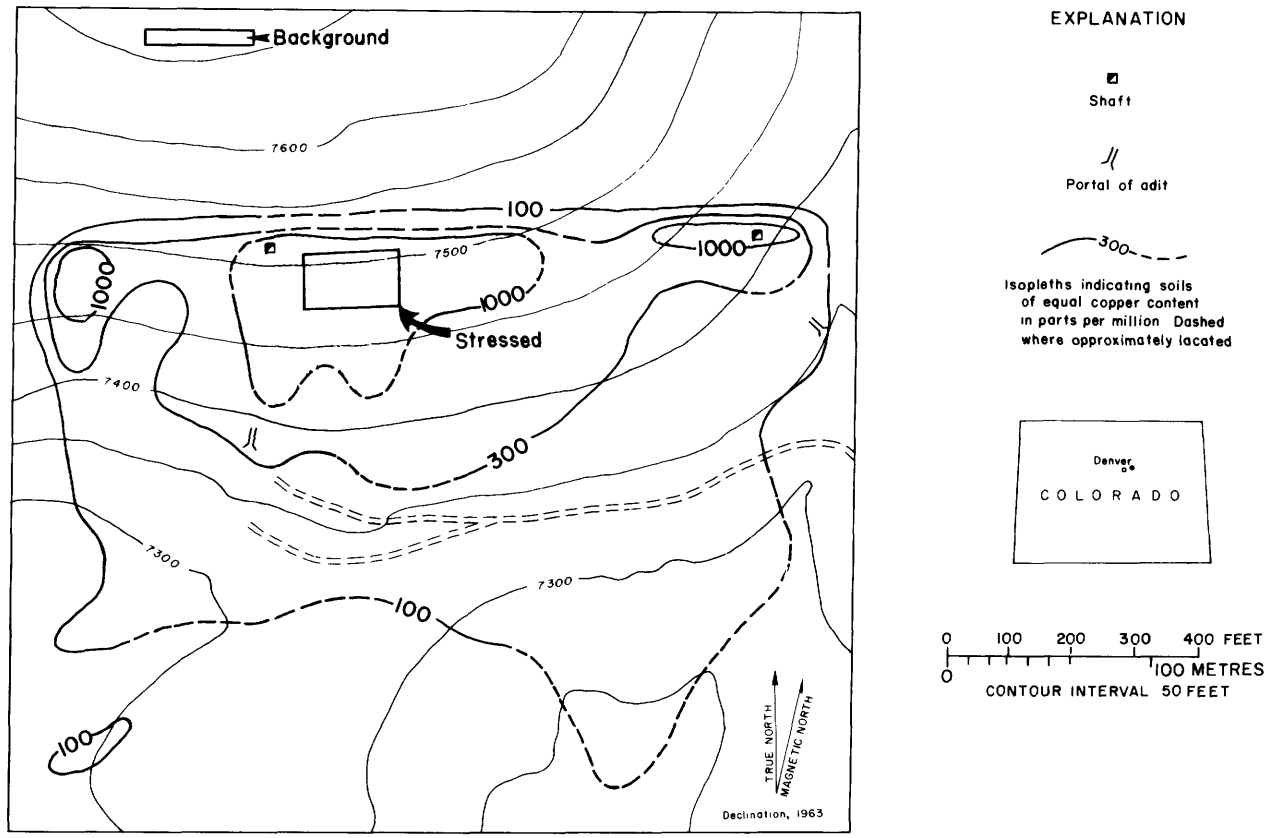

FIGURE 5.—Distribution of copper in soil and location of sample trees growing in background and anomalous soils. (Modified from Huff, 1963.)

TABLE 2.—*Mean and standard deviation of copper and zinc content (ppm) of needle ash from 13* Pinus ponderosa *growing in geochemically anomalous and background soils*

Sample Date	Seven stressed trees		Six background trees	
	Copper	Zinc	Copper	Zinc
July 26, 1973	175±16	>2000	110±7	730±35
Aug. 30, 1973	180±8	2180±77	115±4	1130±30
Oct. 18, 1973	125±5	2330±36	100±7	700±84
Nov. 12, 1973	140±7	2080±35	100±4	880±30

content of the background tree ash by factors of 1.2 to 1.6. Mean zinc content of stressed tree ash exceeds the background trees by factors of 1.9 to 3.3. Distribution of copper in the soil in the vicinity of the mine is given by Huff (1963). Additional ash analyses for copper content of 16 trees in the area are given by Howard, Watson, and Hessin (1971). These analyses show that copper content ranges from 280 ppm to 660 ppm for eight stressed trees and from 120 ppm to 180 ppm for eight background trees.

Figure 6 shows the spectral excitation curves ob-

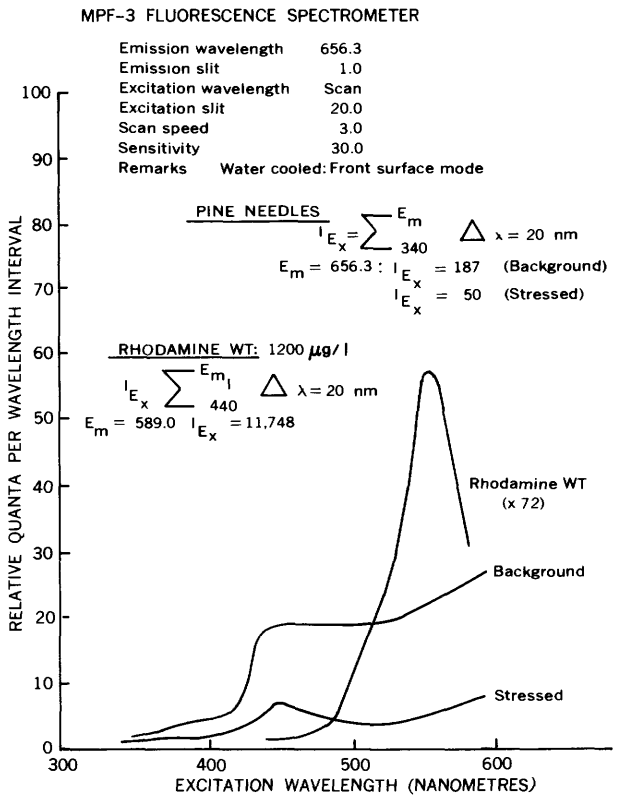

FIGURE 6.—Excitation spectra of *Pinus ponderosa* needles from geochemically stressed and background trees, Malachite Mine, Jefferson County, Colorado, as measured with a laboratory fluorescence spectrometer (source-detector corrected only). Integration of the area under each excitation spectrum permits comparison with the excitation spectra of a rhodamine WT standard.

tained in March 1973 for both groups of trees and also for rhodamine WT dye at a concentration of 1,200 ppb. The integrated excitation intensity is significantly greater for the background than for the stressed trees; solar-corrected rhodamine WT equivalents are 19 ppb and 5 ppb, respectively. Solar- and depth-corrected rhodamine WT equivalency is 0.4 and 0.2 ppb, respectively.

In order to test the sensitivity of the FLD to chlorophyll luminescence of stressed and nonstressed *Pinus ponderosa*, twigs were collected from seven stressed and seven background trees at the Malachite Mine site in early March 1974. Luminescence measurements were made within 2 hours outdoors at the Denver Federal Center and referenced to a nonluminescent gray-card standard. Mean and standard deviation of the mean of FLD luminescent counts was 107±0.5 for background trees and 90±3.0 for stressed trees.

Following this initial experiment, the FLD was used from a helicopter to measure the luminescence of stressed and nonstressed *Pinus ponderosa* trees at the Malachite Mine, both on a diurnal and seasonal basis for the period of September 1974 through July 1975.

These results, combined with the results acquired with the fluorescence spectrometer during summer and autumn 1973 and spring 1974, indicate that luminescence contrast between background and anomalous trees was independent of air temperature, relative humidity, and wind speed, but maximum contrast, ranging from 1.4 to 2.2, tended to occur during parts of 6 days when cloud cover was less than 10 percent and the sun was not obscured by clouds (fig. 7).[6] On 6 days when cloud cover exceeded 10 percent, the diurnal luminescence trace of both groups tended to be similar and contrast did not exceed 1.4 (fig. 8).[6] Data collected on September 26, 1973, September 24, 1974, and April 22, 1975, are exceptions (fig. 9).[6] A maximum contrast of 2.7 at 11:45 a.m. on September 26, 1973, was obtained during a period of 100-percent cloud cover. Contrast on April 22, 1975, does not

[6] Standard National Weather Service nomenclature: relative humidity in percent, wind speed in miles per hour, and cloud cover in percent.

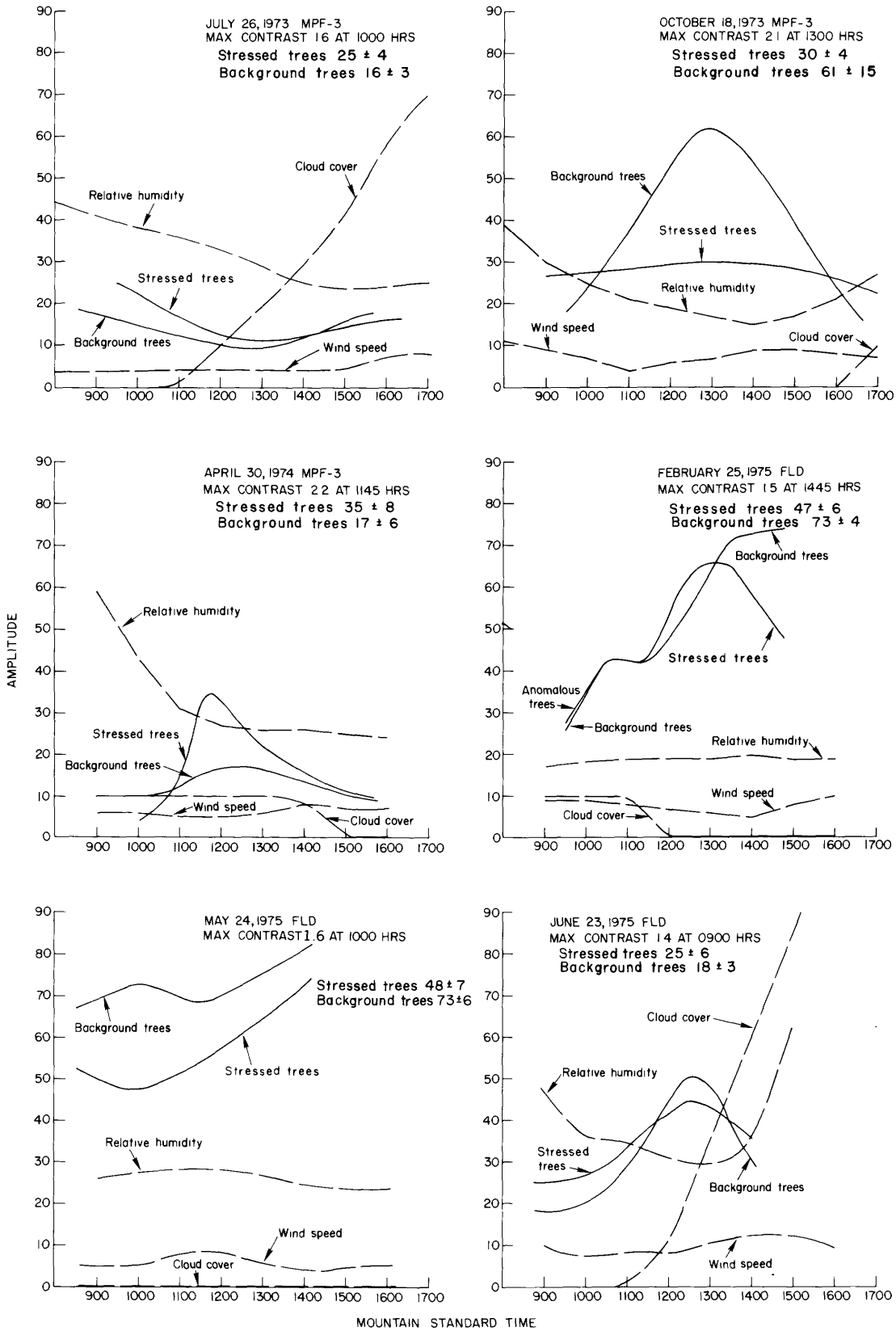

FIGURE 7.—Temporal luminescence of *Pinus ponderosa* and meteorological parameters. Maximum luminescence contrast between background and anomalous trees tends to occur during periods of minimum cloud cover. Standard deviation of the mean, computed for the time of maximum contrast, is at the 95-percent confidence level.

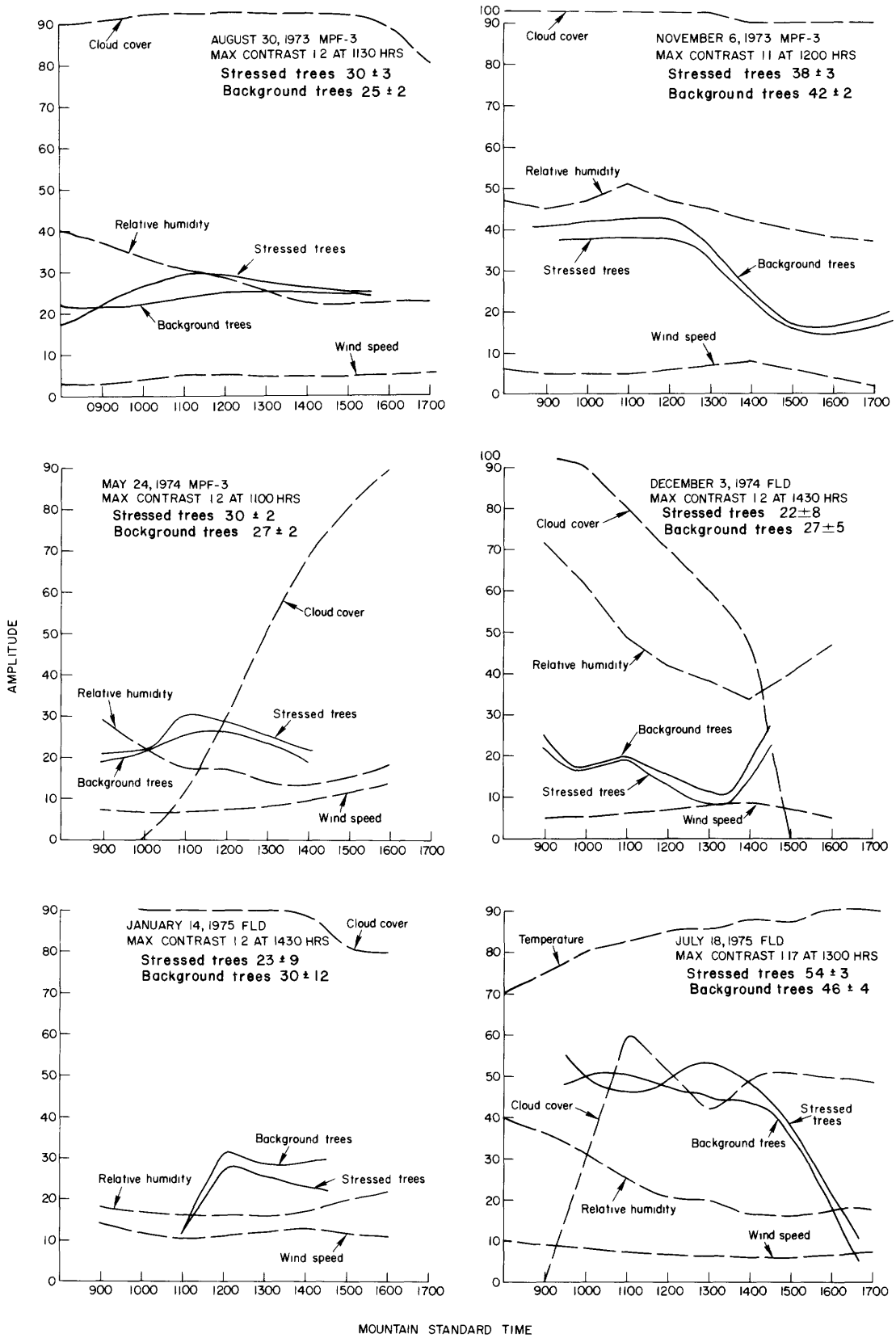

FIGURE 8.—Temporal luminescence of *Pinus ponderosa* and meteorological parameters. Minimum luminescence contrast between background and anomalous trees tends to occur during periods of maximum cloud cover. Standard deviation of the mean, computed for the time of maximum contrast, is at the 95-percent confidence level.

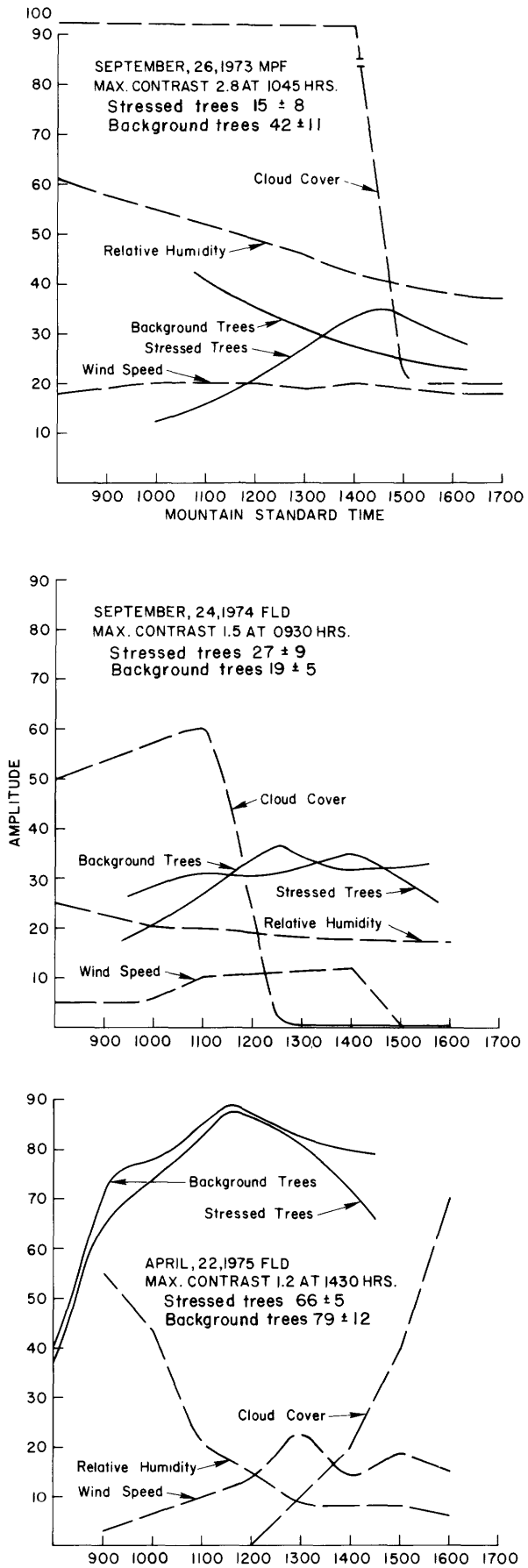

FIGURE 9.—Temporal luminescence of *Pinus ponderosa* and meteorological parameters. Luminescence contrast of background and anomalous trees do not correlate with cloud cover conditions cited in figures 7 and 8. Standard deviation of the mean, computed for the time of maximum contrast, is at the 95-percent confidence level.

exceed 1.2 despite cloud cover of less than 20 percent prior to 2 P.M. Contrast of 1.3 at 3:30 on September 24, 1974, is during a period of no cloud cover.

Standard deviation of the mean for FLD ground measurements of twig samples from *Pinus ponderosa* at the Denver Federal Center in March 1974 (see above), as well as for the fluorescence spectrometer measurements of trees during 1973 and 1974 at the Malachite Mine site ranged from less than 1 percent to 3 percent of the mean. However, standard deviation of the mean of airborne FLD measurements during 1974 and 1975 were frequently somewhat higher. This was due to the relatively sparse foliage of the *Pinus ponderosa* (which permitted bare ground to be observed through the foliage at relatively high frequency), whereas, pine needles completely filled the field of view in both the spectrometer and ground based FLD measurements. This experience suggests that a smaller standard deviation may be assured in airborne measurements by avoiding species or individual trees with sparse foliage.

In addition to *Pinus ponderosa*, airborne FLD measurements were also made July 25, 1974, and May 6, 1975, on trees growing in soils containing background and anomalous concentrations of molybdenum 17 km southeast of Gardnerville, Nevada (fig. 10). Country rock includes limestone, monzonite, and volcanic rocks of Triassic to Jurassic age. Trees in the area are limited to pinon pine *(Pinus monophylla)* and juniper *(Juniperus utahensis)*. In the 1974 measurements, the standard deviation of the mean of FLD luminescence counts for pinon pine commonly exceeded 50 percent of the mean; this is also attributed to viewing background soil and grass through the low-density pine foliage similar to the experiment at the Malachite Mine described above. By restricting FLD observations on both dates to denser junipers, standard deviation rarely exceeded 7 percent of the mean. Molybdenum content in plant ash of 32 juniper trees in figure 10 are shown in table 3. Figure 11 shows a linear regressive analysis correlating luminescence counts on both dates with molybdenum in concentrations of 20 to 300 ppm. Correlation coefficients of 0.73 for the July 1974 data (17 trees) and 0.80 for the May 1975 data (24 trees) are significant at confidence levels of 99.97. Luminescence measurements were not performed on all 32 trees because of small size and low foliage density of some individuals and because some grew in places difficult to approach with the helicopter.

The 1975 data were measured at 1000 hours. Repeated measurements on 12 stressed and background trees at 1200 and 1500 hours showed marked diurnal consistency. For example, mean FLD count for background trees increased from 53 at 1000 hours to 58 at noon, and decreased to 49 at 1500 hours. Mean FLD count for stressed trees showed even less variation, increasing from 37 at 1000 hours to 39 at noon and decreasing to 35 at 1500 hours. The 1974 data also appear to be diurnally consistent, although, because of high winds and helicopter power problems, earlier data were not acquired sequentially and the time of each measurement was not recorded. Both the 1974 and 1975 data show a decrease in luminescence of juniper with an increase in molybdenum content up to 300 ppm.

It is possible that luminescence may vary diurnally and seasonally with species; for example, although *Pinus ponderosa* repeatedly showed marked diurnal variability, *Juniper utahensis* was remarkedly consistent during the 2 days these trees were observed. A

TABLE 3.—*Location, molybdenum content (ppm) in ash, and luminescence, expressed in rhodamine WT equivalence (ppb), of geochemically stressed and background juniper trees in the Alpine Mill area. Background trees are arbitrarily denoted as those containing 70 ppm molybdenum or less*

Tree No.	Molybdenum content	Luminescence
1	150	0.69
2	50	1.60
3	300	.73
4	500	.56
5	500	(Not measured)
6	300	.20
7	500	.74
8	20	(Not measured)
9	30	(Not measured)
10	70	1.02
11	50	.87
12	200	.33
13	500	.53
14	500	.26
15	70	.92
16	50	(Not measured)
17	100	(Not measured)
18	500	0.18
19	150	.33
20	200	.38
21	500	.57
22	500	.58
23	100	.62
24	200	.51
25	70	(Not measured)
26	150	0.27
27	200	.88
28	30	1.09
29	70	.75
30	30	.87
31	20	(Not measured)
32	50	(Not measured)

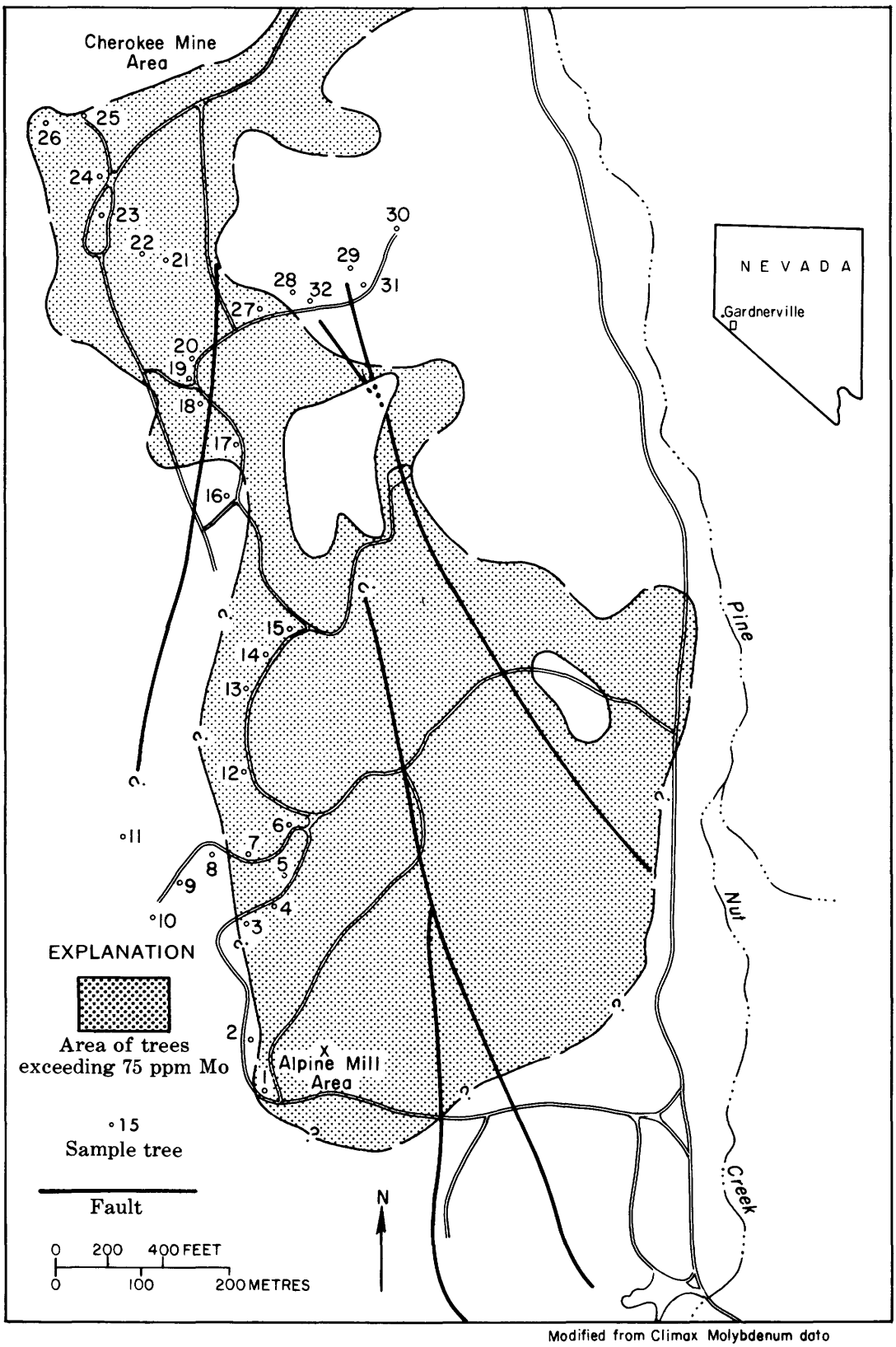

FIGURE 10.—Location of geochemically stressed and background trees in the Alpine Mill area, about 17 km southeast of Gardnerville, Douglas County, Nevada. Background trees are arbitrarily denoted as those containing 70 ppm molybdenum or less.

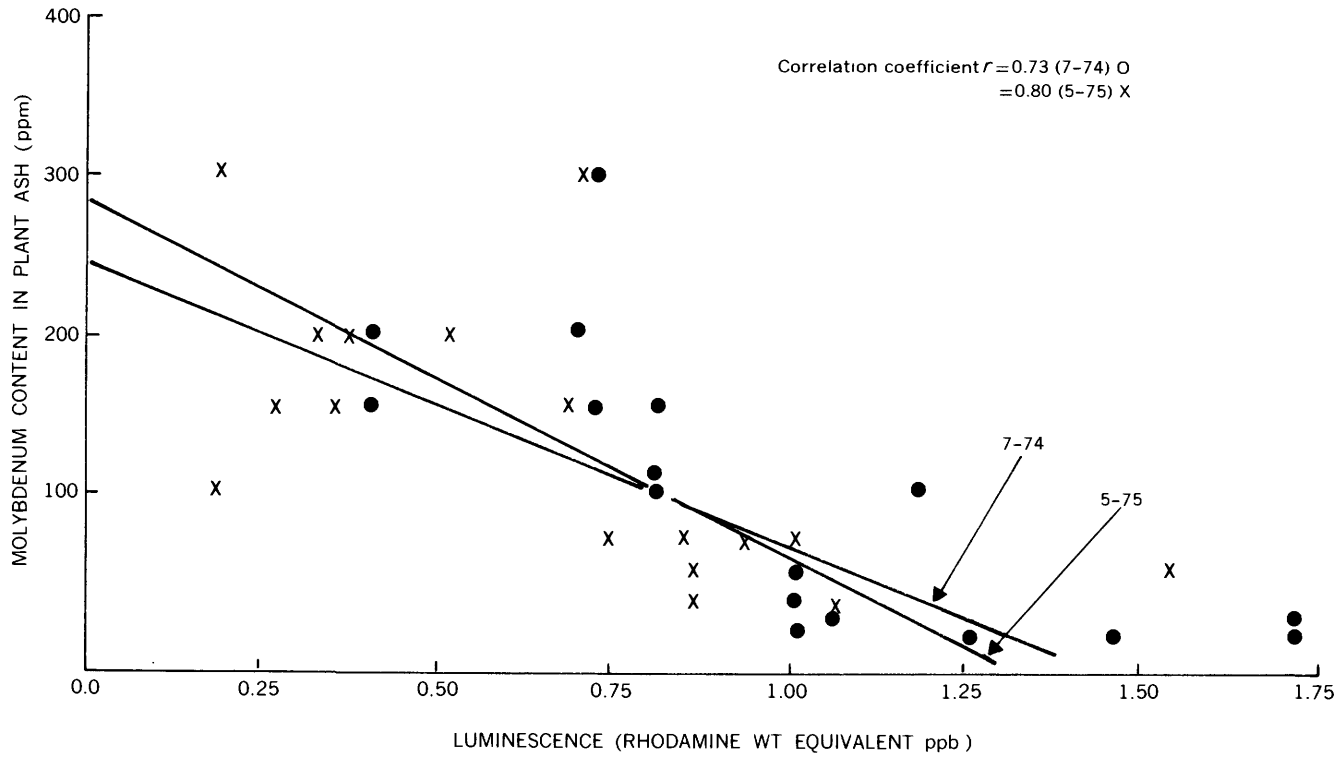

FIGURE 11.—Linear regressive analysis correlating FLD luminescence counts for trees with molybdenum concentrates from 20 to 300 ppm.

practical approach may be to restrict measurement of luminescence of geochemically stressed plants to single specie areas or to one or two species in mixed groups. Additional work is required to understand variation of diurnal and seasonal luminescence with species.

PHOSPHATE ROCK

Small hand-carried ultraviolet lamps have been used to stimulate luminescing minerals and rocks, but these methods of prospecting are limited because the lamps are low powered and effective range is limited to a metre or less. The work must be conducted at night because the low-intensity luminescence is obscured by bright sunlight. To assess the use of the FLD in prospecting for phosphate rocks, the luminescence of 10 samples of sedimentary phosphate rocks from several geographic locations, measured on the laboratory fluorescence spectrometer, at the 486.1-nm Fraunhofer line, are shown in table 4. All samples luminesced within the sensitivity range of the FLD and pointed to the need for a field test.

Several deposits of commercial-grade phosphate occur in southern California (Gower and Madsen, 1964). One of the highest grade deposits occurs near Pine Mountain, northeast of Santa Barbara, in the upper part of the Santa Margarita Formation of

TABLE 4.—*Luminescence of 10 phosphate samples measured with the laboratory fluorescence spectrometer at 486.1 nm in terms of rhodamine WT equivalence (source-detector, solar, and depth corrected)*

Sample	Luminescence (ppb)
Blue apatite from Brazil (low F, high rare earths)	8.0
Cunday, Colombia, Cretaceous (25% P_2O_5, 2% F_2, 100 ppm rare earths)	7.9
Monterey, California, pelletal phosphate (25% P_2O_5, 2–3% F_2, rare earths present)	6.5
Tennessee brown phosphate (30%+P_2O_5, 3% F_2, rare earths unknown)	5.4
Diammonian phosphate-aqueous $NH_4O_4 + H_3PO_4$ (N(15%), P(53%), K(0%), Ø F_2	3.8
Cook Hollow, Tennessee (reprecipitable phosphate, low rare earths)	2.9
Triple super phosphate $Ca_4H_2PO_4$ (N(0%), P(48%), K(0%) some F_2)	2.8
Homeland Mine, Florida (35% P_2O_5, 3.5% F_2, 200–300 ppm rare earth)	1.6
Manatee County, Florida, red phosphate (30% P_2O_5, 3% F_2)	.7
North Carolina heavy fraction (30% P_2O_5, 3.5% F_2, 200 ppm rare earths)	.4

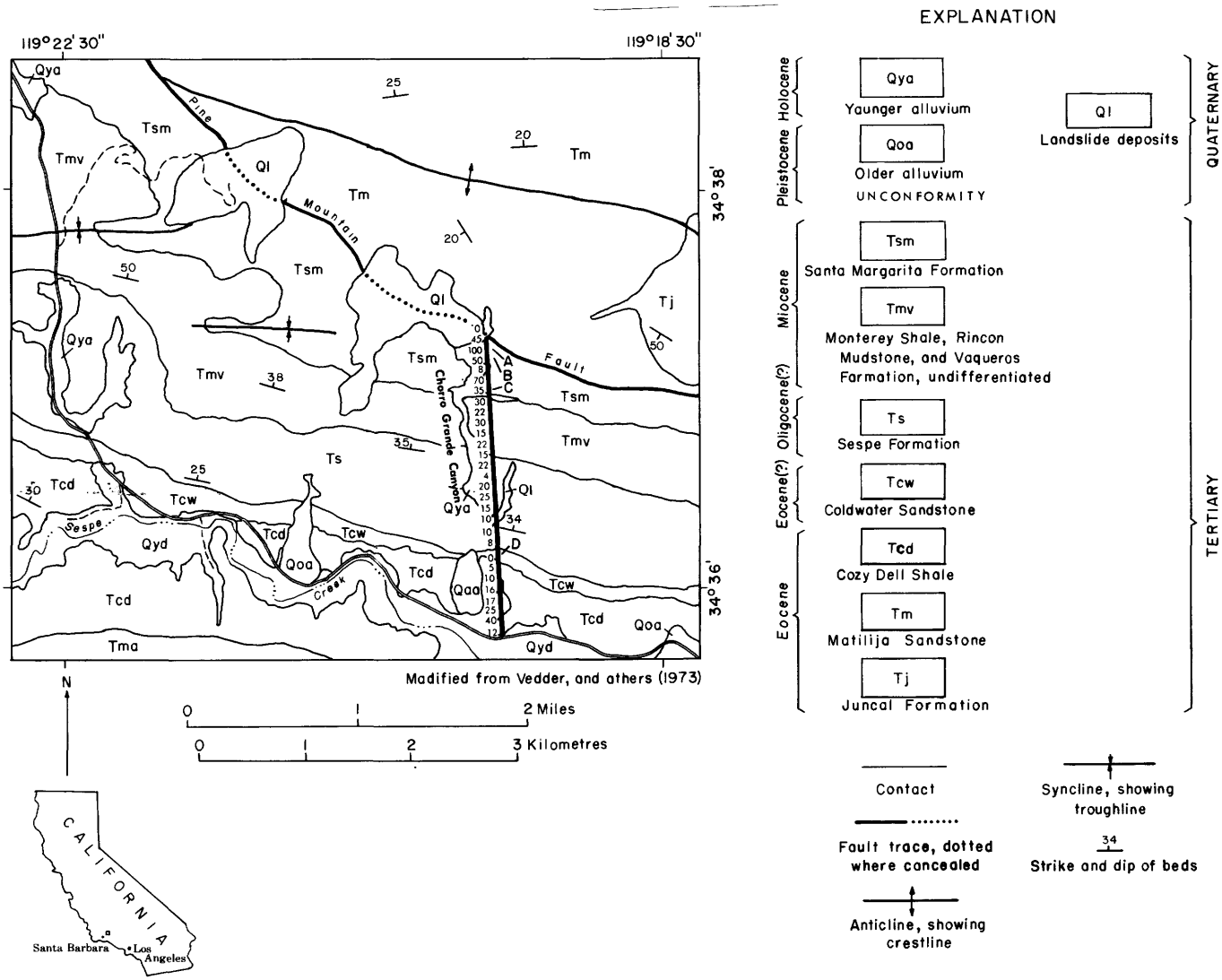

FIGURE 12.—Geologic map of part of the Sespe Creek area showing location of a helicopter traverse (solid line east of Chorro Grande Canyon) and helicopter hovers (A through D). Numbers along traverse are FLD luminescence measurements in terms of rhodamine dye equivalency.

Miocene age (fig. 12) where a phosphate zone more than 24 m thick occurs in siltstone and siliceous shale.

Excitation spectra of gypsum and phosphate rock and soil samples from the Santa Margarita Formation measured on the laboratory fluorescence spectrometer show that luminescence at the 486.1-nm Fraunhofer line exceeds luminescence measured at 589.0- and 656.3-nm lines. Table 5 shows that the luminescence of the phosphate and gypsum samples appear to be within the sensitivity limits of the FLD.

Two experiments were conducted to measure these materials in the field. Through a cooperative arrangement with the Geological Survey's Water Resources Remote Sensing group in Prescott, Arizona, the FLD was flown abroad their *HU1B* helicopter over the Sespe Creek area on November 26, 1974, at a hover altitude of 50 m. Reflectance and luminescence of gypsum, phosphate rock and soil, background soil,

TABLE 5.—*Luminescence of phosphate and gypsum samples, collected from the Santa Margarita Formation near Pine Mountain, California, and measured with the MPF–3 at 486.1 nm in terms of rhodamine WT equivalence (source-detector, solar, and depth corrected)*

Sample	Luminescence (ppb)
Phosphate pellets	0.37–1.05
Phosphate soil	0.33
Gypsum	.65
Gypsum soil	.53
Assorted samples from non-phosphatic rocks (Tmv and Ts, fig. 12)	.22–0.34

TABLE 6.—*Reflectance, FLD counts, and luminescence in terms of rhodamine WT equivalency (source-detector, solar, and depth corrected) of phosphate, gypsum, and background reference materials. Field FLD measurements were performed in November 1974*

Sample	Reflectance	FLD counts	Luminescence (ppb)
Gypsum	0.2253	68 ± 5 (66 ± 2)	1.16
Phosphate rock and soil	.0471	52 ± 3 (43 ± 2)	.95
Gray card	-----	0 ± 3 (0 ± 1)	.26
Background soil and vegetation	-----	3 ± 0.4	.30
Average of 10 readings from Tmv and Ts (fig. 12)	-----	16 ± 4	.46

and vegetation along Chorro Grande Canyon are shown for the 486.1-nm Fraunhofer line in table 6. Although both gypsum and phosphate are luminescent, the two are significantly different in reflectance so that it is possible to distinguish them.

Values in parentheses in table 6 were obtained by placing samples of the phosphate and gypsum under the FLD in a static ground measurement test. Agreement between the flight and static techniques is reasonably good, with a larger standard deviation occurring in the airborne helicopter measurements because of the nonhomogeneity of outcrops, soil, and vegetation in the FLD field of view. A calibration figure of 1.32 ppb/100 counts was used to convert airborne counts to rhodamine WT equivalence.

This experiment was repeated May 8, 1975, with a commercial rental helicopter at altitudes of 35 m for hover and 150 m for traverse. FLD counts for a single traverse are shown along the bold north-south line in figure 12. The counts are substantially higher in the Santa Margarita Formation than in the less phosphatic older rocks. In addition, luminescence and reflectance of gypsum, phosphate rock, phosphate soil, background sandstone, and background grass

TABLE 7.—*Reflectance, FLD counts, and luminescence in terms of rhodamine WT equivalency of phosphate, gypsum, and background materials. Airborne FLD measurements were performed May 8, 1975*

Sample	Run 1			Run 2		
	Reflectance	FLD counts	Luminescence rho. WT (ppb)	Reflectance	FLD counts	Luminescence rho. WT (ppb)
Gypsum (hover A)	0.111	97 ± 5	1.54	0.0948	92 ± 15	1.47
Phosphate rock and soil (hover B)	.06	77 ± 7	1.28	.051	72 ± 8	1.21
Phosphate soil (hover C)	.042	56 ± 6	1.0	.045	64 ± 8	1.10
Sandstone (hover D)	.082	41 ± 4	0.80	.147	50 ± 11	0.90
Background grass and soil	.041	35 ± 2	0.72	.052	21 ± 3	0.52
Gray card	-----	0 ± 5	0.26	-----	0 ± 4	0.26

and soil were determined by hovering over each material along Chorro Grande Canyon (points A, B, C, and D, fig. 12) and collecting approximately 50 data points for each material. Reflectance, FLD counts, and rhodamine WT equivalent luminescence for two hover runs over Chorro Grande Canyon are shown in table 7.

Comparison of Tables 6 and 7 shows that relative values of reflectance and luminescence for gypsum and phosphate correlate well for both dates, although the 1975 data are higher; background grass and soil are substantially higher. These increased levels of luminescence could be due, in part, to greater insolation in May than in November. The differences could also be attributed to the fact that 1974 and 1975 hovers were in the same area but over slightly different outcrops. Comparison between values of rhodamine WT equivalents calculated from FLD counts (tables 6 and 7) and those values based on measurements with a laboratory fluorescence spectrometer show that higher values were obtained for luminescence of phosphate from the spectrometer than with the FLD. This is probably caused by phosphate content of the pellet sample measured in the spectrometer in the laboratory being higher than the bulk phosphate rock measured with the FLD in the field. It is not understood why the luminescence level of gypsum measured with the FLD exceeds the level measured with the spectrometer by nearly a factor of 2.

In addition to the measurements noted above, phosphate rock was measured with the FLD during a

TABLE 8.—*FLD counts and luminescence in terms of rhodamine WT equivalency of associated phosphate and gypsum materials in the Lakeland, Florida, area*

Source	FLD counts	Luminescence rho. WT (ppb)
Gray card	0 ± 2 (overcast)	0.26
	2 ± 3 (clear sky)	.29
Phosphate venier in dredged pit	65 ± 12 (overcast)	1.12
Phosphate rock pile (Royster plant)	116 ± 4 (overcast)	1.79
	143 ± 4 (clear sky)	2.15
Gypsum pile	137 ± 11 (overcast)	2.04
	189 ± 15 (clear sky)	2.75

series of airborne experiments in the Lakeland, Florida, area. The materials measured had been mined and are, therefore, not representative of weathered surfaces on natural outcrops as was the case in the California experiment. Luminescence of these materials is shown in table 8. Comparison of the gray card, phosphate rock pile, and gypsum measurements shows that the FLD performs adequately under overcast conditions, although rhodamine WT equivalency for these three materials is reduced 10, 17, and 26 percent, respectively.

OIL SEEPS

Riecker (1962, p. 60–75) analyzed 103 crude oil samples from California, Colorado, Wyoming, and Alberta with a laboratory spectrometer; he found that all of them exhibited luminescence peaks in the visible region between 444 and 630 nm. Twelve percent of the samples peaked in the red at 630 nm, 54 percent peaked in the yellow at 578 nm, and 34 percent peaked in the blue at between 482 nm and 442 nm. Fantasia, Hard, and Ingrao (1971) used a pulsed ultraviolet laser installed at dockside to discriminate several oils on seawater by measuring the ratio of their luminescence through narrow band filters centered at 433 and 533 nm.

In order to quantify the luminescence of selected oils in terms of rhodamine WT equivalence, the excitation spectra of 29 crude oils were measured with the laboratory fluorescence spectrometer by Watson and others (1974). The integrated excitation intensities, corrected for source-detector, solar, and depth effects are shown in table 9. The crude oils exhibit a peak rhodamine WT equivalency at Fraunhofer wavelengths of 518.4 nm or shorter, with 19 samples (65 percent) having a maximum at 518.4 nm. Luminescence of 28 of the 29 samples exceeds 0.25 ppb rhodamine WT equivalency and appears to be within the sensitivity range of the FLD.

Specific gravity of the 29 crude oils ranges from 0.7317 to 0.9677. The dependence of bulk oil luminescence on specific gravity is shown in figure 13. A regressive analysis was performed on the 29 crude oil samples to obtain the best least-squares fit to the data points, with both the correlation coefficient and the standard error determined for six selected Fraunhofer lines throughout the visible spectrum. Correlation coefficients range from 0.34 at 656.3 nm to 0.77 at 396.8 nm and indicate that the best correlation between luminescence and specific gravity occurs at 396.8 nm.

Natural fractures in the ocean floor of the Santa Barbara Channel, California, permit oil of varying densities to seep to the surface. Throughout the channel, patches of oil films at various times can be seen with the naked eye. At times heavy crude seeps from narrow filaments near Coal Oil Point that extend for several miles parallel to the shoreline.

To measure the luminescence of crude oil with the prototype FLD, a sample of oil from the Santa Barbara Channel was poured into a tank of water; luminescence of the resulting film was not detected (Hemphill and others, 1969) because (1) the emission peak of the Santa Barbara oil is at a shorter wavelength than 589.0 nm where the prototype FLD operated and (2) sensitivity of the prototype FLD was inadequate.

Luminescence of oil seeps off Coal Oil Point were measured during the week of November 24, 1974, with the redesigned FLD operating from a helicopter at the 486.1-nm Fraunhofer wavelength. Data obtained on November 30 are shown in figure 14. Luminescence intensities of small lakes several miles inland from the coast average 20–40 counts less than the counts of so-called "clear" Santa Barbara Channel water, suggesting that small amounts of oil or other luminescing material is present in the channel.

TABLE 9.—*Integrated excitation intensity of crude oils at specific Fraunhofer wavelengths in terms of equivalency with rhodamine WT. Samples are ordered by decreasing intensity at the 486.1–nm Fraunhofer line and corrected for source-detector, solar, and depth effects*

Description			Specific	Wavelength (nanometres)					
Sample	No.	Location	gravity	396.8 (ppb)*	422.7 (ppb)*	486.1 (ppb)*	518.4 (ppb)*	598.0 (ppb)*	656.3 (ppb)*
1C	19327	Michigan	0.8327	4.88	12.95	34.62	36.36	20.62	5.95
2C	17394	Wyoming	.7866	4.16	11.51	29.33	30.46	15.90	6.26
3C	31473	Wyoming	.8098	4.86	13.64	26.86	26.36	12.44	3.33
4C	26294	Nigeria	.8163	6.63	12.33	25.80	22.17	8.76	3.87
5C	24563	Colorado	.8172	3.16	8.84	22.19	22.63	11.24	4.07
6C	17636	Louisiana	.8834	5.84	11.12	16.54	14.84	3.40	2.24
7C	29350–5	Denmark	.7790	1.21	3.45	14.68	18.16	12.32	5.91
8C	24461	Mississippi	.7932	2.91	6.74	10.93	10.58	5.90	2.36
9C	31316	California	.8532	5.52	8.98	8.49	6.91	2.23	0.58
10C	28212	Mississippi	.8455	1.30	3.28	6.39	5.93	2.74	1.90
11C	31317	California	.8377	0.71	1.84	6.34	7.77	5.65	2.43
12C	26241	Trinidad	.8318	0.76	2.03	6.31	7.22	3.48	1.86
13C	30534–1		.7317	0.93	2.48	6.16	6.89	4.29	1.84
14C	32219	California	.7713	0.87	2.59	5.76	6.48	3.47	2.16
15C	24569	Colorado	.8574	1.18	3.74	5.45	10.64	5.19	2.21
16C	27358	Libya	.8350	0.88	2.02	5.41	5.66	3.32	1.44
17C	13786	Mississippi	.8045	0.66	1.74	5.07	6.40	6.93	2.22
18C	27458	Canada	.7735	1.56	2.80	3.81	3.78	1.90	0.87
19C	31851	Bahrain	.8695	0.43	1.16	3.27	3.95	3.44	2.02
20C	30229–1	Alaska	.8654	0.35	0.78	2.50	2.91	2.35	0.59
21C	13588	Wyoming	.9110	1.80	2.42	2.33	2.29	1.76	1.09
22C	25968–2	Wyoming	.8430	0.23	0.70	2.10	2.52	1.72	1.27
23C	25179	Iran	.8854	0.21	0.62	1.74	1.97	1.64	0.84
24C	27173	Bahrain	.8370	0.29	0.59	1.72	2.25	2.74	1.23
25C	29619	California	.8639	0.29	0.66	1.63	1.90	1.44	0.77
26C	27360	Libya	.8481	0.41	0.89	1.45	1.60	1.01	0.26
27C	14525	Venezuela	.8752	0.28	0.58	1.43	1.06	0.72	0.30
28C	17112	Canada	.9677	0.09	0.19	0.60	0.78	0.88	0.47
29C	17556	Libya	.9312	0.05	0.09	0.22	0.26	0.51	0.05

* Rhodamine WT equivalency.

CONCLUSIONS

Conclusions are as follows:

1. Laboratory techniques have been developed and refined to permit the quantification of luminescence materials in terms of rhodamine WT dye equivalency and to predict reliably the detectivity of these materials with an FLD in the field.
2. The FLD has sufficient sensitivity to detect rhodamine WT dye at a concentration of 0.1 ppb in 0.5 m of water at 20° C; however, sensitivity under field conditions is generally considered to be 0.25 ppb.
3. Tests of the redesigned Perkin-Elmer FLD show luminescence measurements during clear sky conditions are about 25 percent higher than under overcast conditions.
4. Airborne tests of the redesigned FLD have led to the development of a bore-sight television system which permits precision identification of ground features and correlation of these features with measured luminescence and reflectance.
5. Fluorescence spectrometer and FLD measurements of *Pinus ponderosa* over a 2-year period show significant differences in the luminescence of background trees and trees geochemically stressed by copper and zinc in the soil. Maximum luminescence contrast tends to occur dur-

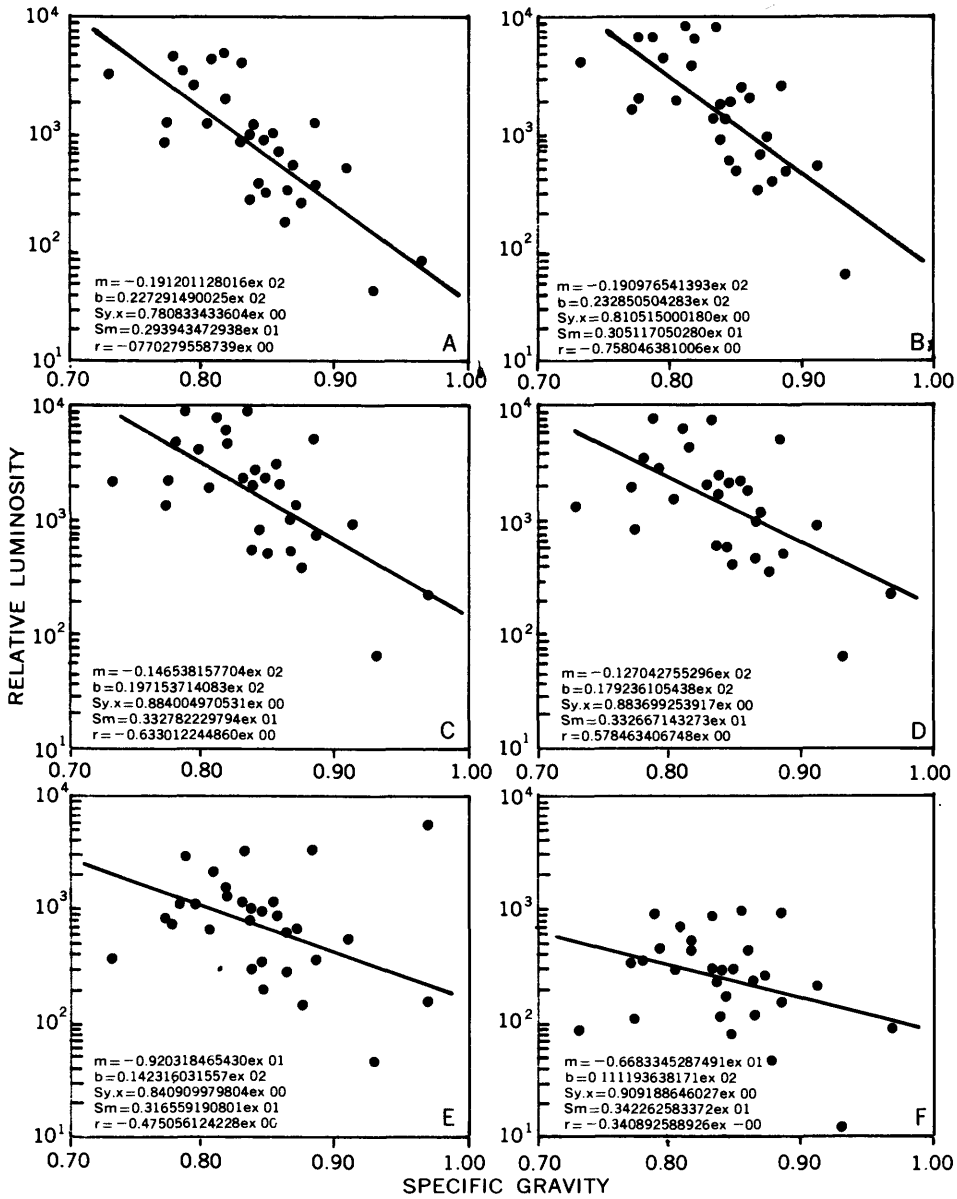

FIGURE 13.—Statistical plot showing correlation between relative luminescence and specific gravity of 29 crude oils at the following Fraunhofer lines: A, 396.8 nm; B, 422.7 nm; C, 486.1 nm; D, 518.4 nm; E, 589.0 nm; and F, 656.3 nm.

ing those periods when cloud cover was less than 10 percent.

6. FLD measurements of juniper showed significant correlation between molybdenum intake and luminescence for values up to 300 ppm molybdenum in plant ash.
7. Airborne FLD measurements in the Sespe Creek area, California, show that contrast between luminescing gypsum and phosphate rock outcrops, and older non-phosphatic sedimentary rocks, ranges from 1.5× to 3×.
8. Of 29 crude oils measured in the laboratory, 28 luminesce within the sensitivity range of an airborne FLD; laboratory work also shows correlation between thickness of an oil film (such as would occur in a marine oil spill) and luminescence for oils of specific gravity of 0.8327 or less.
9. Airborne FLD measurements in the Santa Barbara Channel show that luminescence of thicker, nearshore layers of oil from the marine seep exceeds "clear water" by a factor of 10; luminescence of thinner layers which have dispersed seaward are marginally detectable.

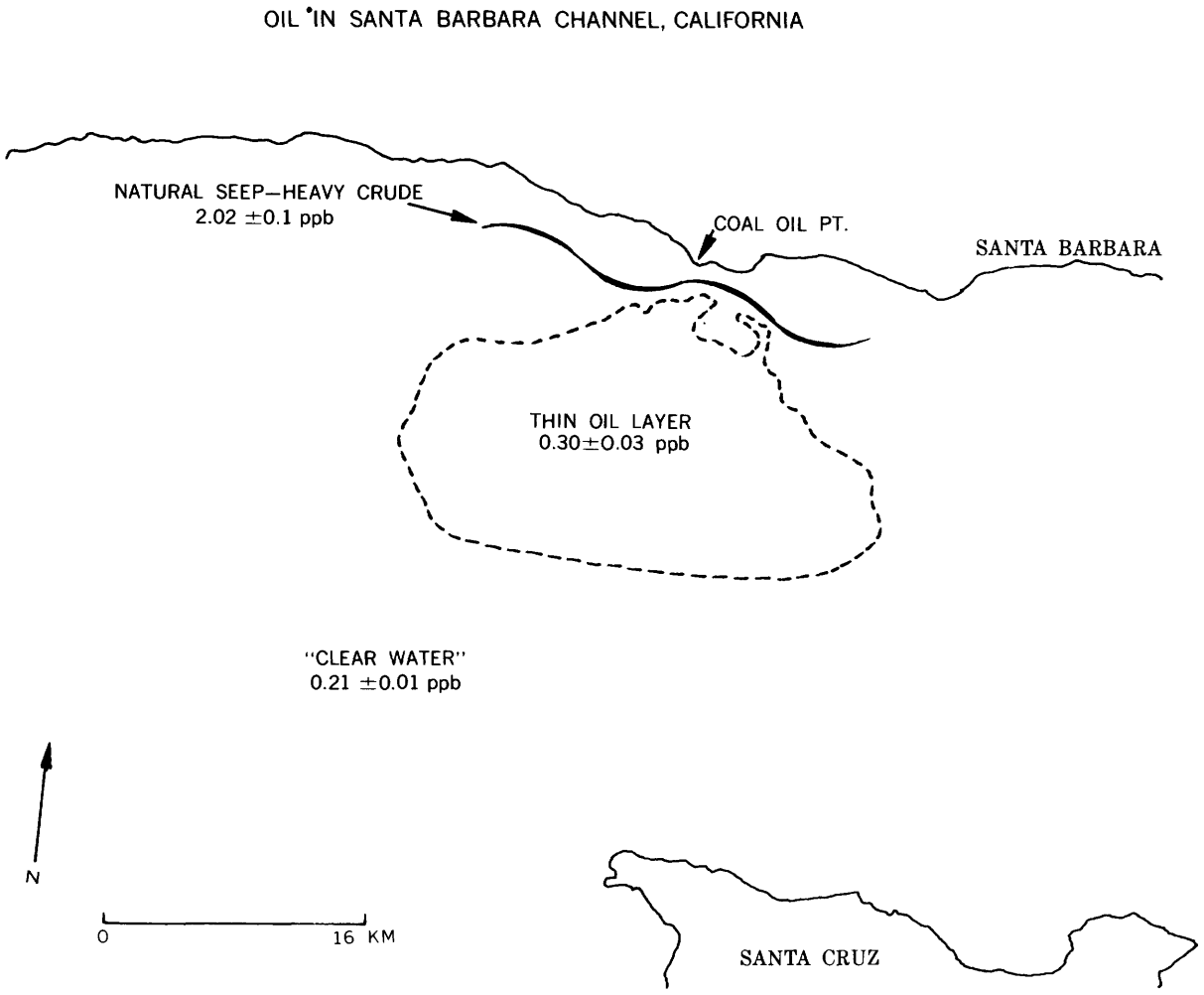

FIGURE 14.—Map showing: (1) Dispersal of oil from natural seep off Coal Oil Point, Santa Barbara Channel, and (2) FLD luminescence responses from clear water, thin oil film, and heavy crude filament.

REFERENCES

American Society of Photogrammetry, 1975, Manual of remote sensing: Falls Church, Virginia, 2,144 p.

Fantasia, J. F., Hard, T. M., and Ingrao, H. C., 1971, An investigation of oil fluorescence as a technique for the remote sensing of oil spills: Natl. Tech. Inf. Service PB 203585.

Gower, H. D., and Madsen, B. M., 1964, The occurrence of phosphate rock in California: U.S. Geol. Survey Prof. Paper 501–D, p. 79–85.

Grainger, J. F., and Ring, J., 1962, Physics and astronomy of the moon, *in* Kopal, Zdenek, ed., The luminescence of the lunar surface: New York, Academic Press, p. 385–405.

Hemphill, W. R., Fischer, W. A., and Dornbach, John, 1965, Ultraviolet investigations for lunar missions: Advances in the Astronautical Science, v. 20, pt. 1, p. 379–415.

Hemphill, W. R., and Carnahan, S. U., 1965, Ultraviolet absorption and luminescence investigations: U.S. Geol. Survey Tech. Letter NASA–6, 27 p., 53 figs.

Hemphill, W. R., Stoertz, G. E., and Markle, D. A., 1969, Remote sensing of luminescent materials, *in* Internat. Symposium on Remote Sensing of Environment, 6th, Ann Arbor, Michigan 1969, Proc., p. 565–583.

Hemphill, W. R., and Stoertz, G. E., 1971, Fraunhofer line discriminator progress report: Principal Investigator's Review, Advanced Applications Flight Experiments, NASA Langley Research Center, Proc., p. 171–185.

Hoel, P. G., 1965, Introduction to mathematical statistics: New York, John Wiley and Sons, 427 p.

Hollaender, A., 1956, Radiation biology: New York, McGraw-Hill, p. 765.

Howard, J. A., Watson, R. D., and Hessin, T. D., 1971, Spectral reflectance properties of *Pinus ponderosa* in relation to copper content of the soil—Malachite Mine, Jefferson County, Colorado, *in* Internat. Symposium on Remote Sensing of Environment, 7th Ann Arbor, Michigan 1971, Proc., p. 285–297.

Huff, L. C., 1963, Comparison of geological, geophysical, and geochemical prospecting methods at the Malachite Mine, Jefferson County, Colorado: U.S. Geol. Survey Bull. 1098–C, p. 161–179.

Kozyrev, N. A., 1956, The luminescence of the lunar surface and intensity of the solar corpuscular radiation: Izvestia Krymskoi Astroizitcheskoy Observatorye, v. 16, p. 148–161.

Kramer, P. J., and Kowlowski, T. T., 1960, Physiology of trees: New York, McGraw-Hill, Botanical Science Series.

O'Gara, P. J., 1922, Sulfur dioxide and fume problems and their solutions: Industrial Engineering Chem., v. 14, p. 744.

Press, N. P., 1974, Detecting the toxic effects of metals in vegetation from Earth observation satellites: British Interplanetary Soc. Jour., v. 27, p. 373–384.

Riecker, R. E., 1962, Hydrocarbon fluorescence and migration of petroleum: Am. Assoc. Petroleum Geologists Bull., v. 46, no. 1, p. 60–75.

Sauchelli, Vincent, 1969, Trace elements in agriculture: D. Van Nostrand Reinhold, Co., 248 p.

Stoertz, G. E., Hemphill, W. R., and Markle, D. A., 1969, Airborne fluorometer applicable to marine and estuarine studies: Marine Technology Soc. Jour., v. 3, no. 6, p. 11–26.

Thomas, M. D., 1961, Effects of air pollution on plants: New York, Columbia Univ. Press, World Health Organization Monograph, no. 46.

Vedder, J. G., Dibblee, T. W., and Brown, R. D., 1973, Geologic map of the upper Mono Creek-Pine Mountain area, California: U.S. Geol. Survey Misc. Geol. Inv. Map I–752.

Watson, R. D., Hemphill, W. R., and Hessin, T. D., 1973, Quantification of the luminscence intensity of natural materials, *in* Am. Soc. Photogrammetry, Symposium for the Management and Utilization of Remote Sensing Data, Sioux Falls, South Dakota, Proc., p. 364–376.

Watson, R. D., Hemphill, W. R., Hessin, T. D., and Bigelow, R. C., 1974, Prediction of the Fraunhofer line detectivity of luminescent materials, *in* Internat. Symposium on Remote Sensing of Environment, 9th, Ann Arbor, Michigan 1974, Proc., p. 1959–1980.

PROCEEDINGS OF
THE FIRST ANNUAL WILLIAM T. PECORA MEMORIAL SYMPOSIUM,
OCTOBER 1975, SIOUX FALLS, SOUTH DAKOTA

Use of ERTS–1 (Landsat–1) Images for Engineering Geologic Applications in North–Central Iran

By Daniel B. Krinsley,
U.S. Geological Survey, Reston, Virginia 22092

INTRODUCTION

Most of the Iranian population lives adjacent to the margins of the interior desert basins because of the availability of flat land and moderate supplies of ground water at relatively shallow depths. The basins are potentially valuable sources of water and chemicals and could be utilized for the emplacement of roads and inexpensive airfields. The basins have not been fully utilized to date because of the lack of adequate knowledge concerning the seasonal changes in their surface and ground water hydrologies and in the physical properties of their sediments. Most desert basin investigations have been conducted during the summer when the surficial sediments are dry and have sufficiently high bearing strengths to support men and vehicles.

The repetitive coverage of ERTS–1 (all images used are ERTS–1 and to avoid confusion that designation will be used in this paper) is ideally suited to provide seasonal images of the Iranian basins from which changes in the areal extent and morphology of the surficial materials may be recorded in conjunction with contemporaneous or previous ground truth studies of actual surficial conditions. Data derived from the analyses of ERTS–1 images can provide a rational basis for planning the economic utilization (salts or water extraction and agriculture) and engineering development (roads and airfields) of these desert basins.

ERTS–1 images used in this study have been examined in single bands and in false-color composites of several band combinations.

PHYSICAL SETTING OF THE IRANIAN DESERT BASINS

The Elburz and Zagros Mountains (fig. 1) were compressed against the relatively older inflexible block of the Iranian Plateau to the east during the Pliocene-Pleistocene phase of the Alpine orogeny. Lower but nevertheless rugged mountains that formed along Iran's eastern border divide the plateau into a major eastern basin in Afghanistan and a major western basin in Iran. Within the western basin are several lesser mountain chains and isolated mountains as well as extensive desert plains. The lowest depressions in these deserts are occupied by smaller desert basins (fig. 1).

Approximately half of Iran consists of basins from which there are no outlets and from which the collected drainage is removed by evaporation. Moist winds bring considerable precipitation during the winter half of the year to the northern slopes of the Elburz Mountains which effectively bar movement of moisture to the south. Similarly, the Zagros Mountains act as a barrier to the moisture-laden westerlies. Rainfall is quickly reduced in amount southward and eastward so that the interior lies within a vast rain shadow and becomes increasingly arid from west to east and from the north to south. There is exterior drainage only along the north, west, and south margins of the country; the remainder has interior drainage.

There is a considerable water deficit in the interior during all seasons, and streams that do reach the basin sumps are generally fed by ground water. The upper aquifers in the alluvial fans are phreatic, but towards the center of the basin artesian conditions develop as a result of confining clay layers (Issar, 1969, p. 94). The uppermost aquifer does remain phreatic to the margin of the basin sump (playa), where the water from the toe of the fan spills out over the playa surface creating a "wet zone." Evaporation through the capillary zone from the phreatic aquifer results in salinization of the water. Salinization is accentuated in the north-central basins that are underlain by Miocene evaporites.

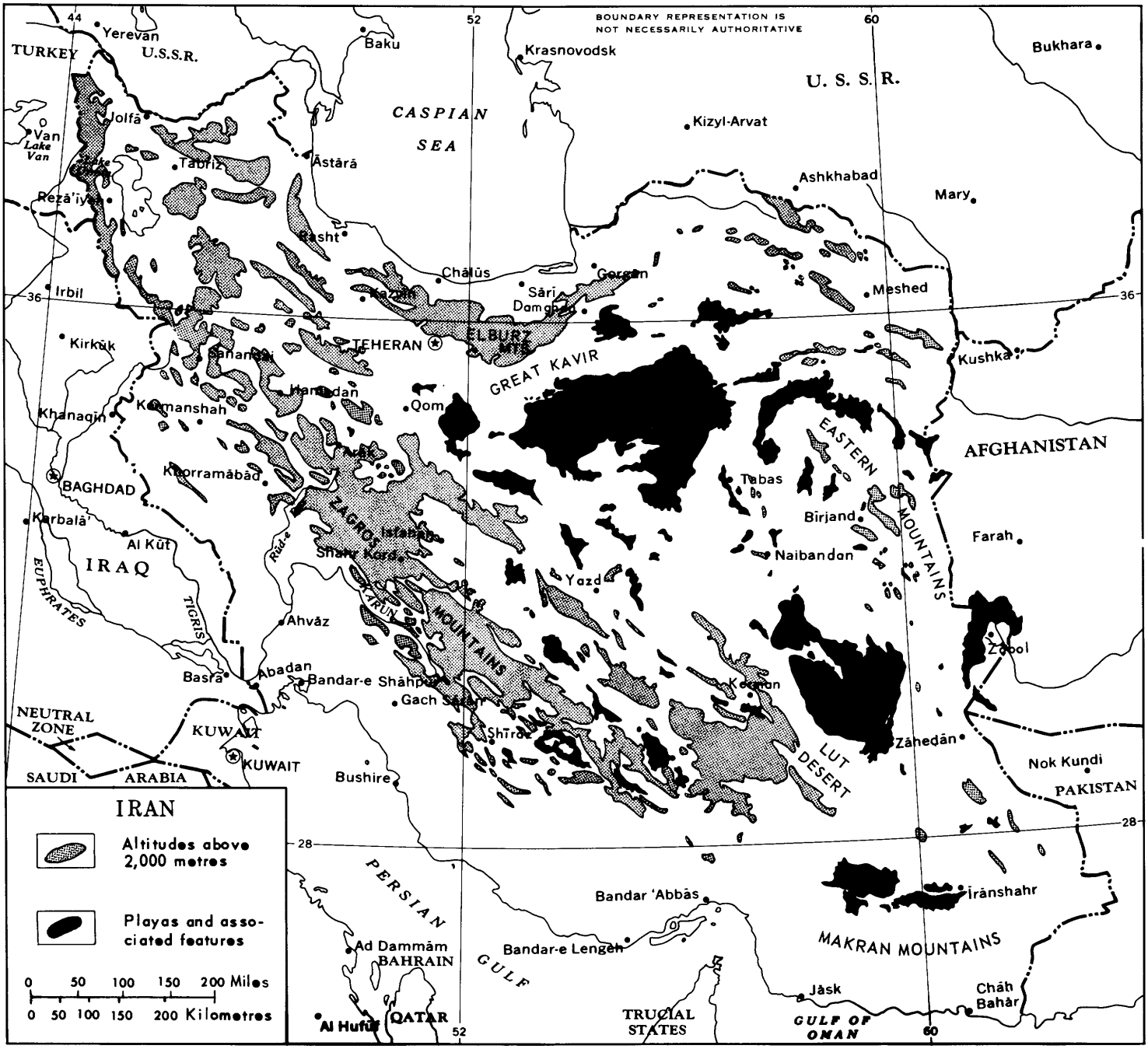

FIGURE 1.—The relationship of the desert basin sumps (playas) and associated features to relief in Iran.

Although man has severely altered the natural vegetation by extensive cutting, it is doubtful that vegetation within the inner plateau seriously affected the amount and intensity of overland flow during the Pleistocene. It seems more likely that increased cold during the glacial periods more than counteracted any relative increase in humidity that might have been favorable to growth. Significantly, no evidence has been found in any of the upper Pleistocene sediments, along the inner mountain flanks or in the playas, of buried trees or other vegetative debris (Krinsley, 1972b, p. 116).

GREAT KAVIR WATERSHED

The Great Kavir watershed (fig. 2) occupies an area of 200,747 km^2 in the northeastern quadrant of Iran. The northwestern divide, in the Elburz Mountains, has

FIGURE 2.—Interior watersheds of Iran: the Great Kavir and the superposed boundary of the ERTS–1 (Landsat–1) images.

summit altitudes which decrease from 4,002 m in the west to about 3,000 m in the east. The southwestern and southeastern divides have summit altitudes which generally range from 1,500 to 2,000 m with a few peaks just under 2,400 m along the southeastern divide. Within the watershed the lowest altitudes are found at the surface of the salt crust basins, and the lowest of these lies at an altitude of 650 m.

GREAT KAVIR

The central and lowest area of the Great Kavir watershed is occupied by the Great Kavir, a desert area of 52,800 km^2 (fig. 3). In Iran, the term "kavir" is a generic name for playa. The Great Kavir contains numerous depressions occupied by true kavirs which have imparted their character to the entire desert.

The annual precipitation decreases from a maximum of 300 mm near the divide, but within the rain shadow of the Elburz Mountains, to less than 100 mm in the Great Kavir. Mountains along the northeast divide benefit from moisture-laden air skirting the southern shore of the Caspian and penetrating the valleys and lower passes northeast of Damghan (fig. 1). Precipitation in this eastern area ranges from 100

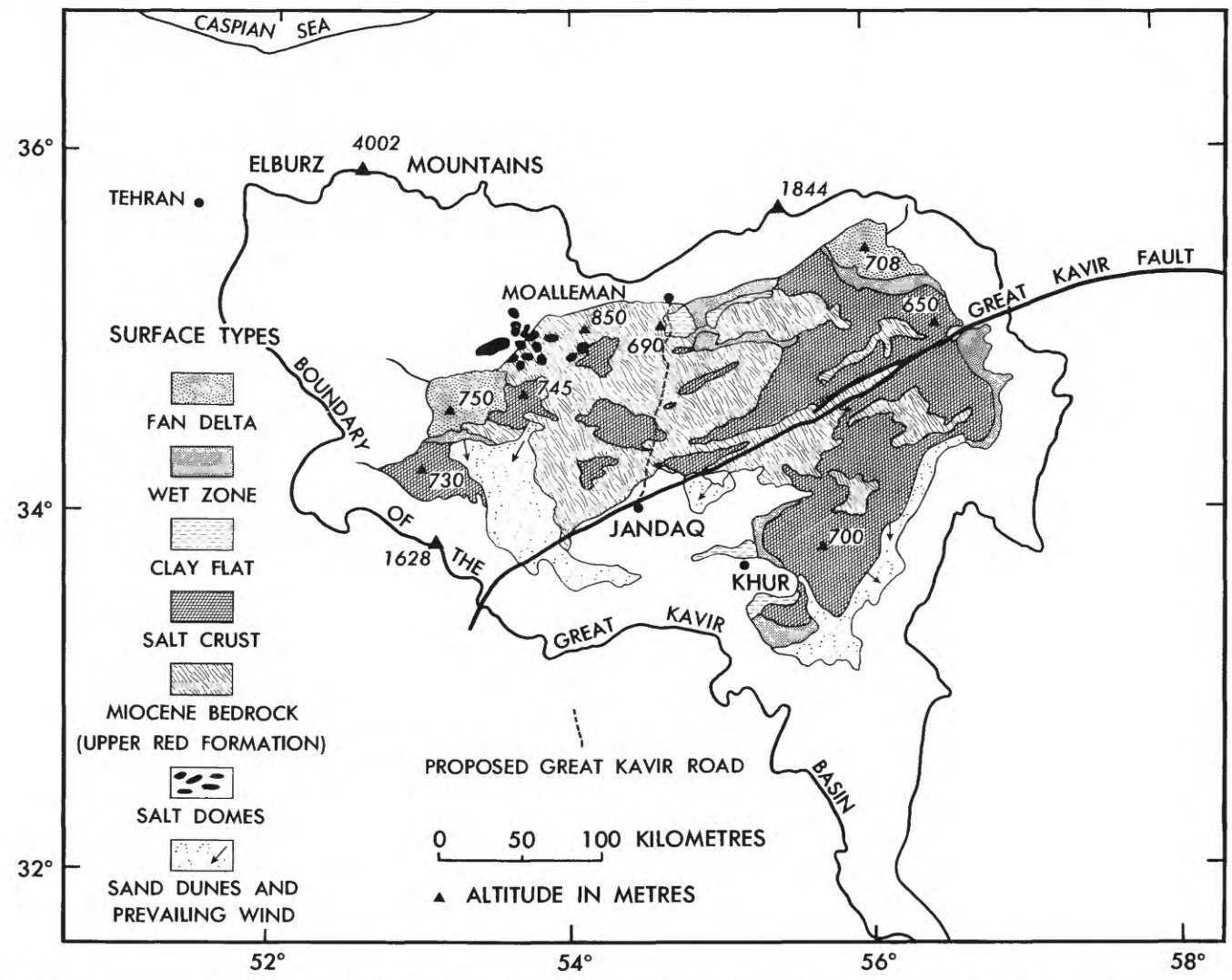

FIGURE 3.—Elements of the Great Kavir. Map based on author's fieldwork and photointerpretation and on the Geological Map of Iran (National Iranian Oil Company, 1959).

to 150 mm in the mountains, but there is considerably less in the adjacent lowlands.

In spite of the rapid decrease in precipitation southward, broad valleys with underfit and intermittent streams, below the mountain front, attest to the past erosional effectiveness of the southward flowing streams. Coarse alluvium including gravel beds, which are interbedded with clay, extends farther into the basin with increasing depths in the section. This stratigraphic relationship suggests previously greater streams. Coarse alluvium, including gravel beds, which materials farther from their source.

The surface of the Great Kavir ranges in altitude from 850 m in the northwestern part to 650 m near the northeastern boundary. It is underlain by Miocene rocks of the Upper Red Formation (Gansser, 1955, p. 291). These intricately folded siltstones, marls, anhydrites, and salt beds have been eroded to a peneplain where they are exposed over an area of 19,300 km^2.

The Great Kavir may be subdivided into eastern and western basins separated by the uplifted peneplain cut into the Miocene rocks. Three central areas of salt crust in a north-south alinement (fig. 3) approximate the peneplain divide. The location of this divide near the western boundary of the peneplain and the development of two east- to northeast-trending troughs (occupied by linear wet zones) in the eastern half of the peneplain indicate that the regional slope has long been toward the east. It is likely that currently active streams flowing westward into the western basin will eventually breach the divide by headward cutting and shift the divide eastward. The present stream cutting is due to increased gradients resulting

from recent tectonism. The Miocene rocks and the younger sediments are cut by currently active northeast-trending faults, the principal one of which is the Great Kavir fault (fig. 3).

SURFACE TYPES WITHIN THE GREAT KAVIR

The surface types within the Great Kavir are the Miocene rocks, locally pierced by salt domes, dune fields, fan deltas, wet zones, clay flats, and salt crusts (Krinsley, 1970, p. 107). The areas occupied by these surface types have been generalized at a scale of 1:2,500,000 and then reduced in figure 3. Small areas of these types which appear in ERTS–1 images (scale 1:1,000,000) may not be shown in figure 3.

Miocene rocks consisting of evaporites and other generally saliferous sediments occupy 35 percent of the area of the Great Kavir. At the peneplained surface of these rocks is a thin regolith of clay, silt, and sand with up to 47 percent halite. As a consequence of repeated dissolution of the salt in winter rains and crystallization upon the evaporation of surface moisture, or the summer evaporation of capillary water, the regolith has been churned into a rough surface resembling a plowed field. Across this vast almost flat surface, narrow drainageways terminate in the wet zones or salt crusts. Salt domes, which have locally pierced the Miocene rocks, are similarly cut by the peneplain.

The dune fields occupy 13 percent of the Great Kavir and are situated along its southern and southeastern borders. Fan deltas are large alluvial fans which transgress other surface types. The toes may be completely inundated during the principal runoff period, with the result that peripheral deposition occurs in water, as at a delta. The two large fan deltas in the Great Kavir occupy 5 percent of its area.

The wet zone is a transitional zone which is periodically inundated and always wet. It commonly borders the toes of alluvial fans and fan deltas, but it also occupies linear basins or narrow troughs within the area immediately underlain by Miocene rocks. The linear wet zones have surface gradients of less than 1 degree, sloping toward the salt crust areas. Wet zones constitute 4 percent of the kavir surface. The clay flat, which occupies only 2 percent of the area of the kavir, is a generally firm surface underlain by dry clay and silt, with variable amounts of salt. It is distinguished from the wet zone, with which it is pedologically identical, on the basis of its higher position above the dry-season water table. The salt crust occupies 41 percent of the kavir surface in basins in the east, center, and west. The eastern basins are generally continuous but are locally interrupted by Miocene outcrops in the form of northeast-trending ridges. The surface of the southern basin in the eastern area is 50 m higher than the northern salt surface adjacent to the fan delta. There is thus significant gradient northward toward the fan delta. Three salt-crust basins in the central area of the kavir occupy downwarps in the Miocene rocks. The salt crusts of these basins lie at different levels, and they are probably hydrologically independent. The larger middle basin surface is estimated to be at an altitude of approximately 850 m.

In areas of thick, white salt crusts and seasonally high water tables, the wet briny muds beneath the crusts may be more thermally expanded than the crusts. This process is facilitated by the transparency of pure salt to infrared rays and by the heat absorption of the black mud. Occasionally, the plastic muds are forced from beneath the salt plates outward and upward through the peripheral cracks. Rapid evaporation of the mud brines results in the formation of black salt dikes along the polygonal cracks. Grooves and scratches preserved in the solidified dike that were cut by preexisting crystallized salt during extrusion of the mud attest to the rapidity of the solidification.

The uneven extrusion of the briny mud frequently results in the tilting of the polygonal salt plates. Eventually, the area becomes a rough, jumbled mass of sharp and angular black salt blocks with ridges and pinnacles (fig. 4). Wind-driven rain and silt tend to modify and sharpen the rough surface features of these salt fields. Aeolian or alluvial silt added to the old salt, already darkened by the admixed black mud from beneath the crust, imparts a dark matte appearance to this grotesque surface. Relief among the salt pinnacles and ridges ranges from 30 to 50 cm.

Salt crusts and related surface features are primarily a reflection of the hydrologic regime within a basin. The crusts tend to buckle when they are thin, darkened by silt and underlain by light-colored sediments and a seasonally depressed water table. Saline muds are more likely to be extruded when they are black, and water saturated, beneath a relatively thick, white salt crust (Krinsley, 1972a, p. 173).

POTENTIAL FOR ENGINEERING DEVELOPMENT

Almost all materials produced in northern and central Iran are exchanged by means of trucks moving along the east-west and northwest-southeast road that passes through Tehran (fig. 5). Goods from the north destined for the region immediately south of the Great Kavir must travel more than 900 km rather than the

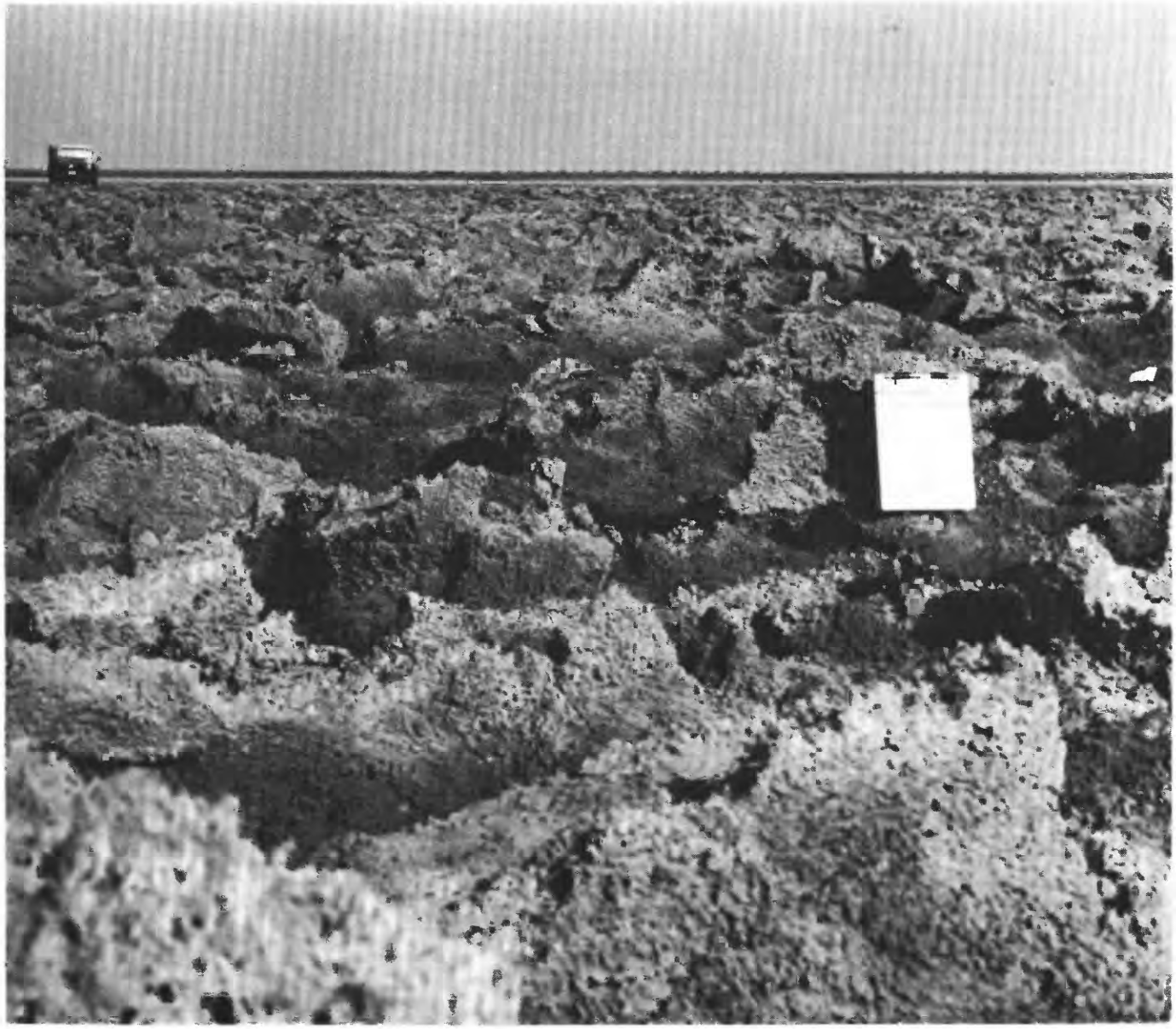

FIGURE 4.—Rough black salt ridges and pinnacles adjacent to the dry-season road across the Great Kavir, 40 km south of Moallem. Local relief ranges from about 30 to 50 cm, view northwest, date September 2, 1966.

200 km that would be required if an all-weather road existed across the desert. Less dramatic but nevertheless significant savings in time and in transportation costs could be achieved with such an all-weather road terminating at Nain farther to the southeast (fig. 5). Trucks traveling from Damghan to Nain cover the 750 km in 9 hours; the route across the Great Kavir would be 450 km and require 6 hours.

Rough dry-season roads of gravel and dirt exist for caravans or 4-wheel drive vehicles along the route indicated in figure 5, between Damghan and Nain. Engineering procedures associated with the construction of an all-weather road across the Great Kavir would be concerned with stabilizing, strengthening, or constructing a subgrade over the saliferous surficial materials and installing culverts and bridges to permit normal drainage across the route of the eventual road alinement. This section of the report is concerned with the use of ERTS–1 scenes in the selection of a preliminary road alinement through the Great Kavir.

ANALYSIS OF THE ERTS–1 IMAGES OF THE GREAT KAVIR

The basis for the analyses of the ERTS–1 images of the Great Kavir is familiarity with its actual ground

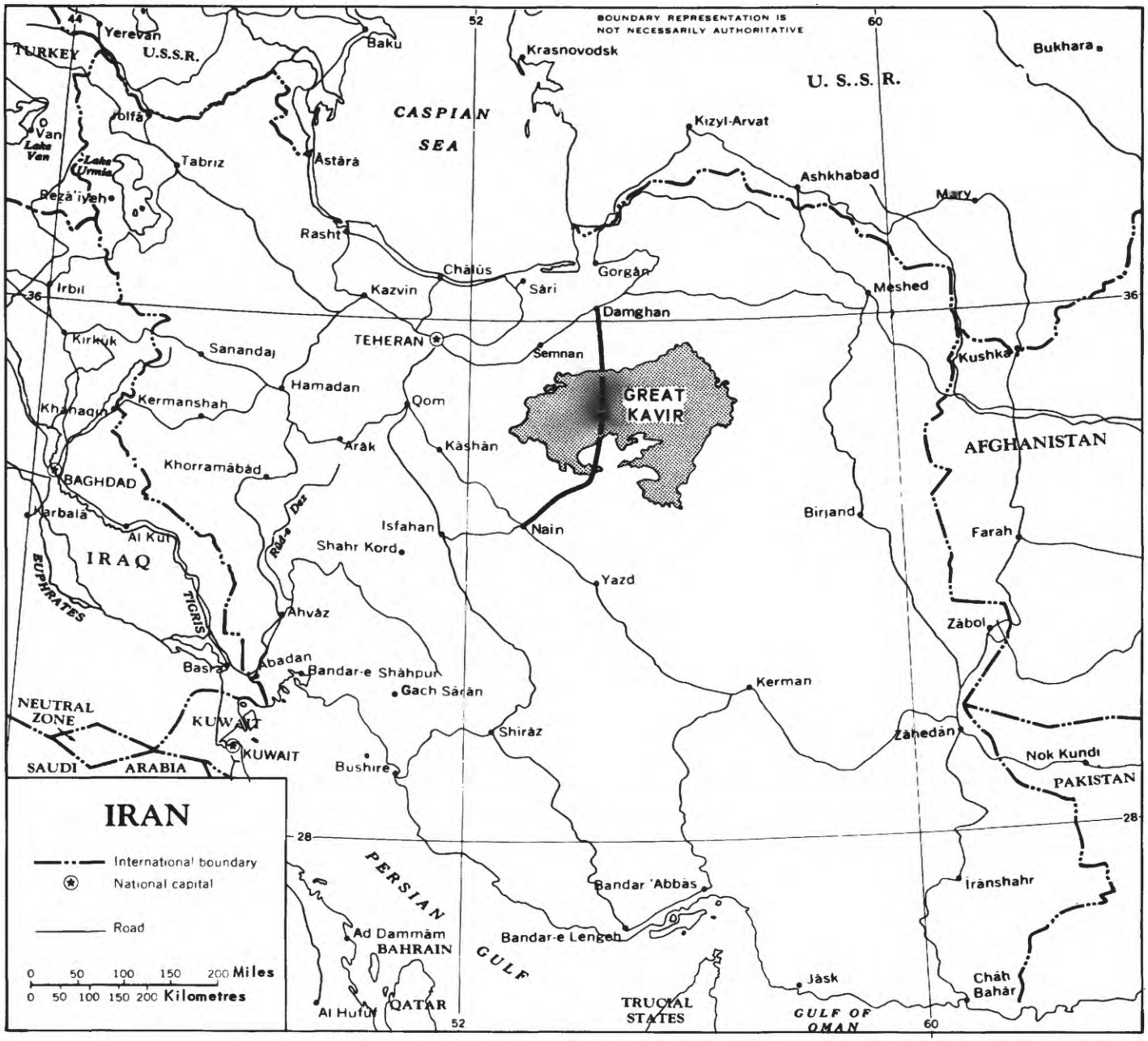

FIGURE 5.—Existing Iranian road net and the proposed Great Kavir road, which is shown by a bold dashed line. The north and south extensions of the proposed road are shown by solid bold lines.

conditions and sediments during the summer and autumn of 1965, 1966, and 1974. In addition to ground control, this area was viewed from low-flying aircraft, and many of its details were compiled from aerial photos at scales of 1:30,000 and 1:60,000.

Initially, false-color diazo transparencies were prepared from positives of ERTS–1 images. Yellow, red, and blue were used for MSS bands 4, 5, and 7 respectively. These three colors were then composited to form a false-color transparency. The composite was then compared to actual ground and aerial photos and interpreted in the light of the investigator's experience. The false-color illustrations used in this report are products of a subtractive color system. The dyes used in this system are magenta, yellow, and cyan, but the resultant pure colors are red, green, and blue.

In the false-color composites, water is blue, salt is white and the saliferous silt and clay regolith of the Miocene sediments is buff to light brown. The purity

or intensity of these colors reflect differences in the composition, hydrology, or morphology of the surface materials. With increasing depth, water ranges in color from aquamarine to dark blue to black. With increasing saturation, the salt crust ranges in color from pure white to aquamarine. With increasing roughness or microrelief, the salt crust ranges in color from pure white (smooth crust) to black (rough salt ridges; figs. 4 and 6, p. XII). Combinations of wet, silty and rough salt crust result in mixed false colors which require special considerations in their correct interpretation. In the ERTS–1 scene of September 20, 1972 (fig. 6, p. XII), white areas are smooth salt crust and black areas, adjacent to the dry-season road, are rough black salt ridges and pinnacles (fig. 4). There is no standing water, in that area, at that time of year. In the ERTS–1 scene of May 12, 1973 (fig. 7, p. XIII), the black areas adjacent to kilometres 75 and 90 are white salt crusts covered by water (compare figs. 6, p. XII, and 7, p. XIII).

SELECTION OF A PRELIMINARY ROAD ALINEMENT THROUGH THE GREAT KAVIR

The area of the Great Kavir most suitable for the construction of an all-weather road lies entirely within one ERTS–1 scene (figs. 2 and 6, p. XII). The center point of the September 20, 1972, image of that scene is 34°35′N.; 55°12′E. False-color diazo composites were prepared from positives of ERTS–1 images taken of the Great Kavir on September 2 and 20, 1972, December 19, 1972, February 11, 1973, March 1, 1973, and May 12, 1973. The route of the existing dry-season road was overlain on each diazo composite, and the seasonal hydrologic conditions along four critical segments of that route south of Moalleman were recorded (table 1).

The four critical road segments represent areas that are subject to soil saturation by water or even local flooding and thus require special engineering considerations. The road segment from kilometres 25 to 50

TABLE 1.—*Hydrologic conditions along critical segments of the dry-season road across the Great Kavir as inferred from ERTS–1 images*

Identification of ERTS–1 image*	Distances in kilometres south from Moalleman			
	25–50	60–63	90–100	110–116
Sept. 2, 1972, 34°35′N., 55°09′E., 8104106265.	Moist surface at km 40	Moist surface at km 62	Dry salt crusts	Moist surface at km 113.
Sept. 20, 1972, 34°35′N., 55°12′E., 8105906265 Figure 6.	Moist surface at km 40	----do	Dry salt crusts	Do.
Dec. 19, 1972, 34°35′N., 55°09′E., 8114906273.	Wet surface at km 40; dissolution of salt crusts.	----do	Moist to wet salt crusts; dissolution of salt crusts.	Moister surface at km 113.
Feb. 11, 1973, 34°35′N., 55°05′E., 8120306274.	Wet surface at km 40; dissolution of salt crusts.	Obscured by cloud	Wet soil and salt crusts; dissolution of salt crusts.	Obscured by cloud.
Mar. 1, 1973, 34°36′N., 55°01′E., 8122106275.	Wet surfaces at km 32 and km 40; dissolution of salt crusts at km 40.	Partly obscured by cloud, probably wet.	Wet soil and salt crusts; dissolution of salt crusts; standing water.	Wet surface at km 113.
May 12, 1973, 34°43′N., 54°56′E., 8129306274 Figure 7.	Wet surfaces at km 32 and km 40; dissolution of salt crusts at km 40.	Wet surface at km 62	Wet soil and salt crusts; dissolution of salt crusts; standing water.	Wet surface at km 113.
	Summary			
	Alinement to west with culverts probably required over wet areas.	Bridge or raised roadbed required.	Raised roadbed and bridge required.	Alinement to west around wet area.

*Date, location, identifier (EROS Data Center identification number), and figure number in this report.

lies in the area underlain by Miocene bedrock (fig. 3). It is always moist along a narrow drainageway at kilometre 40 during the dry season, but this area becomes wet by mid-December. Dissolution of the local salt crust parallel to the drainageway suggests saturation of the surficial materials. By March, the surface in a slight depression is also wet at kilometre 32. The road from kilometres 25 to 50 can be alined inexpensively to the west on good natural subgrade to avoid the two wet areas (fig. 7, p. XIII); culverts will be required along drainageways.

The segment from kilometre 60 to 63 lies in a depression within the area underlain by Miocene bedrock (fig. 3). It is always moist at kilometre 62 during the dry season and becomes moister by mid-December. This segment is wet by mid-May and a bridge or raised roadbed would be required at kilometre 62 (fig. 7, p. XIII).

The segment from kilometres 90 to 100 lies in an area that is occupied principally by salt crusts (fig. 3) which undergo significant changes in their surface conditions during the seasons. Salt crusts are dry during September but become moist by mid-December with some dissolution. By early February, both soil and salt crusts are wet with continuing dissolution of the salt. Standing water is present by March 1, and its areal extent has increased by mid-May. This segment is the most difficult and would require both a raised roadbed and a bridge. Although an alinement to the east would avoid the wettest areas, the costs of engineering for the poor subgrade over the increased length of the road (up to 30 km) would be prohibitive (fig. 7, p. XIII).

The segment from kilometres 110 to 116, which lies within the area underlain by Miocene bedrock, is always moist at kilometre 113 during the dry season, and becomes moister by mid-December. By March 1, the surface is wet at kilometre 113, and this condition continues into May. This area can be avoided by a short alinement to the west (fig. 7, p. XIII).

The use of ERTS–1 images provides a method for examining areas that are seasonally inaccessible in order to determine hydrologic changes that affect soil conditions and thus their engineering properties. There must be some knowledge of actual ground conditions in order to correctly interpret the ERTS–1 images, and the eventual determination of the location of any engineering project such as a road alinement should be based on a longer record of observation and on-site investigation.

POSTSCRIPT

The author met with His Excellency Javad Shahrestani, Minister of Roads and Transport of Iran, on September 24, 1974, at the latter's invitation for the purpose of discussing the construction of an all-weather road across the Great Kavir. Further information was provided to Minister Shahrestani by the author in November 1974 and during January and March 1975.

In August 1975, the Ministry of Roads and Transport of Iran awarded a contract to a joint venture company, Peyma-Harland (Harland Bartholomew and Associates International, Inc., of Washington, D.C., and Peyma Consulting Engineers of Tehran, Iran) to provide consulting engineering services for a feasibility and location study for a highway that will begin in the vicinity of Damghan (fig. 5) and terminate in the vicinity of Nain. The first phase of this project will be to delineate the exact route of the highway. This phase will be completed in approximately 7 months, at the end of February 1976. The second phase, which will require 18 to 24 months, will involve the final design and contract documents for the highway construction. The final construction phase will require approximately 2½ to 3 years and should be completed no later than February 1981.

REFERENCES

Gansser, A., 1955, New aspects of the geology in central Iran, *in* World Petroleum Congress, 4th, Rome 1955, Proc., sec. I, Geology Geophysics, p. 279–300.

Issar, A., 1969, The ground water provinces of Iran: Internat. Assoc. Sci. Hydrol. Bull., v. 14, no. 1, p. 87–99.

Krinsley, D. B., 1970, A geomorphological and paleoclimatological study of the playas of Iran: U.S. Geol. Survey Interagency Rept. Military–1, 329 p., 4 plates, 155 figs., 17 tables.

———1972a, Dynamic processes in the morphogenesis of salt crusts within the Great Kavir; north-central Iran, *in* Internat. Geol. Cong., 24th, Montreal, Proc., sec. 12, p. 167–174.

———1972b, The paleoclimatic significance of the Iranian Playas, *in* Zinderen Bakker, E. M. Van, ed., Palaeoecology of Africa: Cape Town, A. A. Balkema, v. 6, p. 114–120.

National Iranian Oil Company, 1959, Geological map of Iran (1:2,500,000) with explanatory notes: Zurich, Orell Fussli.

PROCEEDINGS OF
THE FIRST ANNUAL WILLIAM T. PECORA MEMORIAL SYMPOSIUM,
OCTOBER 1975, SIOUX FALLS, SOUTH DAKOTA

Applications of Remote-Sensing Technology for Powerplant Siting

By Leo Eichen and Richard F. Pascucci,
Dames & Moore, Cranford, New Jersey 07016

INTRODUCTION

Remote sensing as a practical service consists of acquisition of various data acquired remotely, e.g., satellite observations and aerial overflights; the interpretation of the source data in the context of the problems involved, e.g., geotechnical evaluations and environmental assessment; and the presentation of the results in suitable format to facilitate later phases of an investigation, e.g., planning detailed field surveys and the layout of bore-hole drilling programs.

It should be noted that remote sensing is never a solution in itself but rather a significant tool to assist the investigator in his basic skills. For example, the analysis of imagery acquired from satellites or aircraft from which specific information is sought (geologic mapping or environmental assessment) is best performed by scientists trained in these disciplines. Assistance, where required, in the techniques of image enhancement or computer-assisted analysis can be provided by remote-sensing specialists.

DATA ACQUISITION

Remote sensors generally provide the following advantages:

- When carried aboard aircraft or spacecraft, they offer a synoptic overview not achieved by ground survey methods. Observations of the total scene recorded as an image present a visual set of data patterns not merely a group of data points as would have been provided by ground methods.
- The sampling technique is an unobstrusive way of gathering data. The mere presence of a ground survey team, for example, investigating potential sites for development may result in the spread of unfounded rumors and cause unwarranted adverse reactions that may hinder further evaluation of the site.
- Images have a very high information density compared with graphic, textual, or electronic storage media.
- Remote-sensor observations provide a more comprehensive picture of the terrain than do field methods. Although the level of detail recorded by a sensor may not be so detailed for a small area as ground observations, the sensor record affords a valuable overview in a manageable form. The cost/benefit ratio between overhead coverage and ground traverses for a given area greatly favor the remote sensing approach except in cases where investigation of only a very small area is required.

TYPES OF REMOTE-SENSING DATA

Satellite-Acquired Data—Landsat and Skylab

For broad, regional coverage requirements (e.g., site selection and regional tectonics) the use of satellite imagery from NASA's Landsat and Skylab programs has proven to be an invaluable aid.

In July 1972, NASA launched the first unmanned satellite specifically designed to acquire Earth resources information. Since then a second vehicle was launched in January 1975, with a third scheduled for 1977. A fourth vehicle is planned for 1978–79 with insertion into Earth orbit from NASA's Space Shuttle.

The capabilities of the Landsat systems currently in operation provide for imaging the entire globe in 100×100-nautical-mile increments from an orbital altitude of approximately 500 nautical miles (fig. 1). This orbit was designed so that sensing is always conducted at a constant sun angle (approximately 9:30

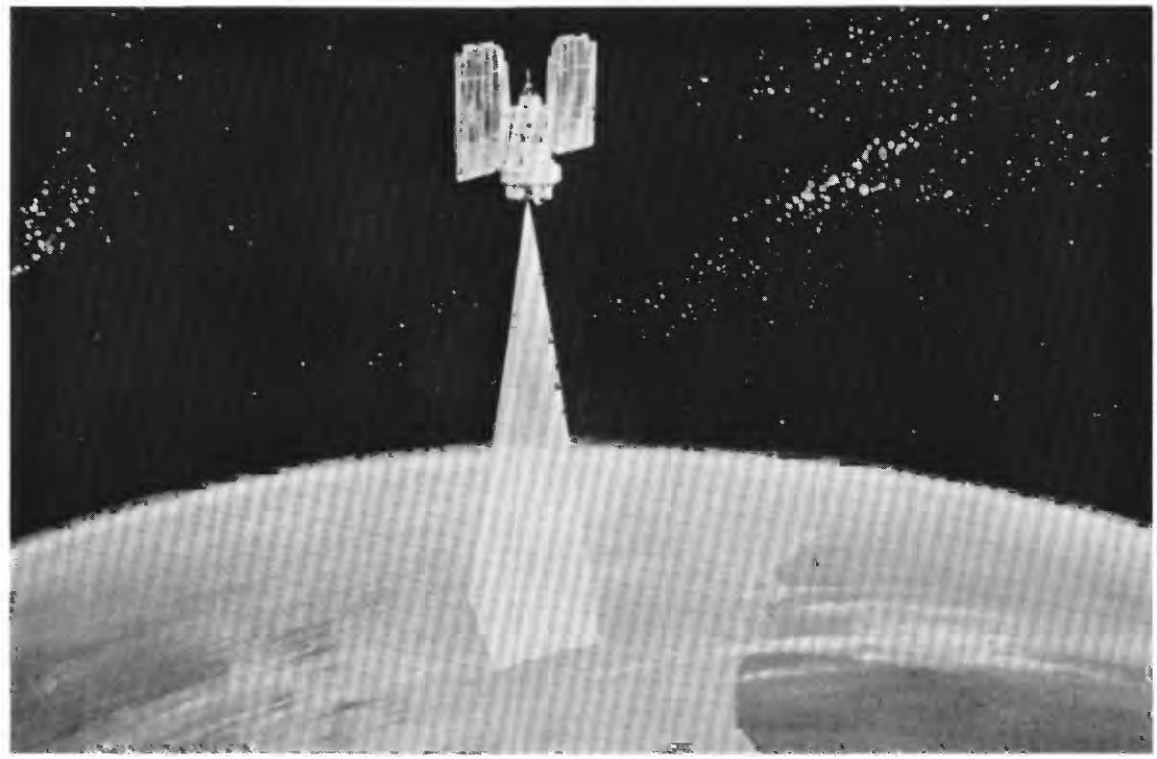

FIGURE 1.—Landsat satellite.

a.m. local time). The only deviation in illumination occurs as a result of the seasonal variations in sun elevation.

Each satellite repeats coverage of any given swath of the United States every 18 days, and, with both satellites operating, each swath is covered every 9 days. This allows changes on the surface to be monitored regularly. Overseas coverage is obtained on a selected area basis. The sensor system aboard the satellites consists of a multispectral line-scanner. This system generates individual scenes, with each scene scanned in four different wavelengths to produce four similar images simultaneously, as follows:

Green Band . . . records in the 0.5 to 0.6 μm range
Red Band . . . . . records in the 0.6 to 0.7 μm range
IR Band . . . . . records in the 0.7 to 0.8 μm range
IR Band . . . . . records in the 0.8 to 1.1 μm range

As the vehicle travels along its orbit, each frame overlaps the previous one by about 10 percent so as to provide continuous coverage. Adjacent parallel orbits are spaced so that side-lap coverage is about 10 percent at the Equator with greater side-lap nearer the poles.

The observations of the Earth are transmitted to ground receiver antennae as electrical signals and are subsequently converted to facsimile images in the laboratory. Figure 2 is an example of such imagery.

The three Skylab missions were provisioned with two film camera systems. The astronauts photographed swaths of the Earth's surface with different film-filter combinations (black and white, color, color-infrared photography) in two photo scales. Exposure intervals were cycled to accomplish stereoscopic coverage. Under good photographic conditions, it has been reported that ground resolutions approximating 30 ft (10 m) have been obtained.

Airborne-Acquired Data

A vast amount of remotely sensed data is acquired by aircraft, including inexpensive light aircraft, using hand-held, 35-mm cameras or mapping cameras over open ports in the floor of the plane. For broader regional coverage, more sophisticated imaging systems are carried aboard multiengined prop and jet aircraft (including the *RB–57* and the *U–2)* for moderate- and high-altitude missions.

Aerial cameras with different capabilities are designed for different photographic missions utilizing a wide range of film and filter combinations. The most common cameras are those employed by aerial survey firms where metric data are required for high precision applications such as in contour mapping or

FIGURE 2.—Landsat image of New York City and vicinity.

FIGURE 3.—Thermal infrared image recording of surface heat emissions. (Daedalus Enterprises, Inc.)

compiling volumetric quantities, etc. These cartographic cameras are designed to provide low image distortion with high illumination tolerances to maintain photometric quality. The most common cartographic cameras provide 9×9-inch image frames on rolls of aerial film. Image scale factors can be altered by varying (1) the flight altitude or (2) the camera's focus through the use of interchangeable lens cones of varying focal lengths. Stereoscopic photography is accomplished by selecting exposure intervals so that successive frames overlap each other by 50 to 60 percent.

Thermal Infrared Scanners

An improved remote-sensing device which detects heat emissions from the surface of terrain or water bodies employs an optical scanning technique to record observations beyond the visual range (thermal infrared, see fig. 3). These observations are accomplished by virtue of surface phenomena which illustrate a "thermal contrast" with respect to its background, e.g., warmer outfall effluent into a colder stream.

Scanners are configured with single or arrayed detectors which sense the incoming signal from a collector optic (scanning mirror). Scanners look at a single "spot" of ground at any given instant in time. The "spot" is scanned laterally to produce a line of imagery. The forward motion of the aircraft "collects" successive lines to produce a swath of the scene. The incoming optical signal image is converted to a modulated electrical signal which can be either recorded on tape for later reproduction or used inflight to vary a point source of illumination to photographically record the image on film.

Side-Looking Airborne Radar (SLAR)

SLAR is an active sensor which can obtain images either during the day or at night and through most cloud cover. The system carries its own "illumination" source that transmits a radar beam off to the side of the aircraft, normal to the flight path (hence the term "side-looking") and detects the back-scattered radar from ground objects. These signals modulate a light source (cathode ray tube sweep), through focusing

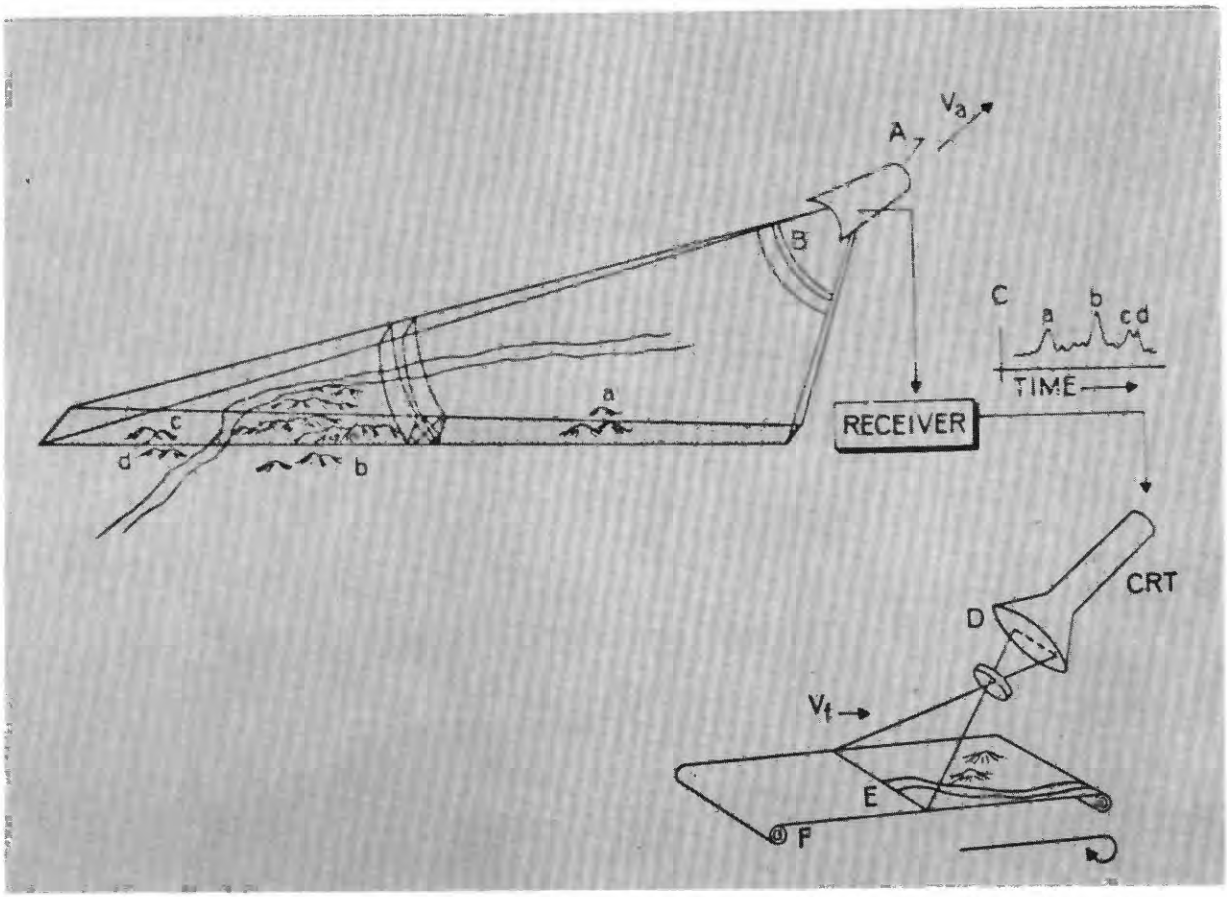

FIGURE 4.—Sketch diagram, typical side-looking airborne radar system. (Modified from Westinghouse Electric Corp., 1967, Side Look Radar.)

optics, and onto a film recorder (fig. 4). Imagery obtained from this system depicts the terrain in a way unlike conventional photographic records. Gray shades in SLAR images are a function of several terrain characteristics, such as object roughness and the basic electrical properties of the materials. The moisture content of soils also affects the film record. Due to the low gazing angles of the system's "illumination" sources, especially toward the horizon, SLAR images highlight terrain relief features so as to create the impression of a "three-dimensional" display. This rendition often emphasizes subtle relief features, as in a scene illuminated by the sun at a low angle. These enhancement characteristics are often most useful in detecting fractures, faults, stream patterns, and other terrain relief features of significance in geologic studies (fig. 5).

Aeromagnetics

Airborne aerial magnetic surveys measure the differences in magnetic susceptibilities of rock types over a study area. A series of parallel and perpendicular flights is designed to provide a complete set of "gamma" profiles recorded by the magnetometer and referenced to a common magnetic datum. The data are processed to produce magnetic contour plots from which geophysicists interpret anomalous zones associated with geologic structures (fig. 6).

The interpreted magnetic map is often used in conjunction with overlays generated by image analysis showing lineaments. These overlays are superimposed over the aeromagnetic map and provide corroborative evidence of significant geologic structures, such as fault and fracture zones.

Ground-Acquired Data

To supplement information derived from overhead coverage, geological and geophysical ground surveys are performed to provide details over specific site locations (e.g., suspect areas which may impact in the location and design of nuclear power generating facilities).

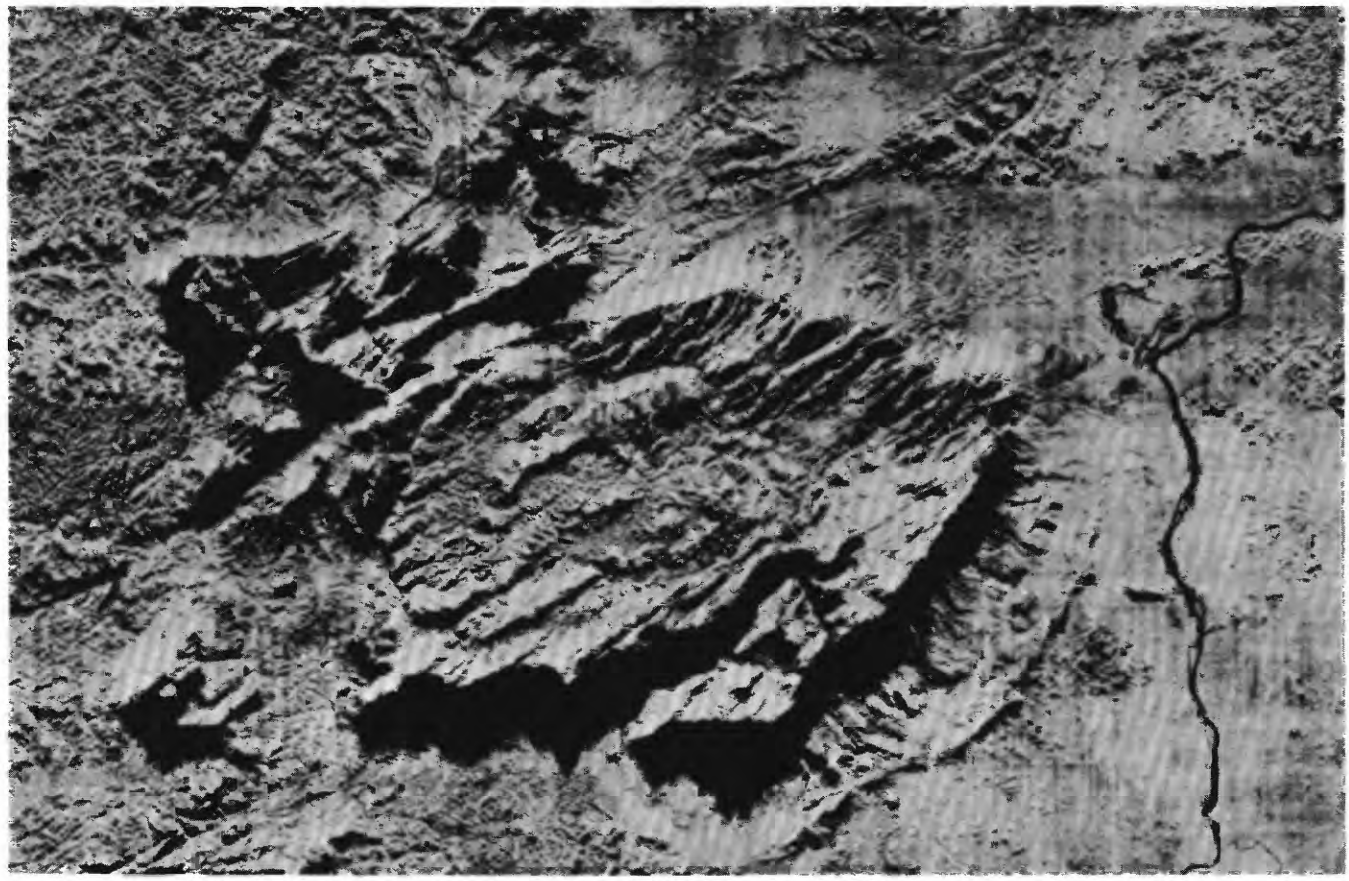

FIGURE 5.—Side-looking airborne radar image by International Aeroservices Corp. and Goodyear Aerospace Corp.

For these purposes, portable ground magnetometer, gravity meter, and seismic surveys are conducted.

DATA ANALYSIS AND SYNTHESIS

In most site investigations, the analysis of remotely sensed data is limited to Landsat imagery and off-the-shelf aerial photos for reasons of cost effectiveness. The cost of these data sources, where purchased from the Federal or State government, ranges from a few tens to a few hundreds of dollars. Interpretation and analysis costs rarely exceed $10,000 to $15,000, and a considerable quantity of structural information usually results. Other sources of remotely sensed data are not often used if they have not previously been acquired. However, in order to illustrate the methods and procedure of remote-sensor data analysis, it will be assumed that data from all of the previously described sensors exist (i.e., Landsat, Skylab, SLAR, aeromagnetics, gravimetrics, aerial photos, and thermal infrared).

In general, the procedure of analysis begins with small-scale formats and progresses to larger scales. The Landsat imagery, typically at a scale of 1:500,000, is usually analyzed first; followed by SLAR, typically at a scale of about 1:250,000; and proceeding on to aerial photos at about 1:25,000 and a thermal infrared scan at a scale of 1:10,000 or larger. The aeromagnetic and gravimetric data are interpreted separately at about the same time as Landsat and SLAR. The following describes the methods and criteria employed in the analysis and interpretation of each remote-sensor data product:

- Satellite Analysis—The interpretation of Landsat imagery is usually performed on spectral bands 5, 7, and the color-infrared composite. Supplementary coverage from Skylab where available is included. The principal effort is directed toward the detection and delineation of linear features that are neither manmade nor caused by bedding or foliation (fig. 7). It is evident, by the process of elimination, that such features are very likely to be either faults or fractures at the surface of the Earth or surface expressions of deep-seated dislocation. Each lineament is interpreted as being either a "probable fault" or a "possible fault."

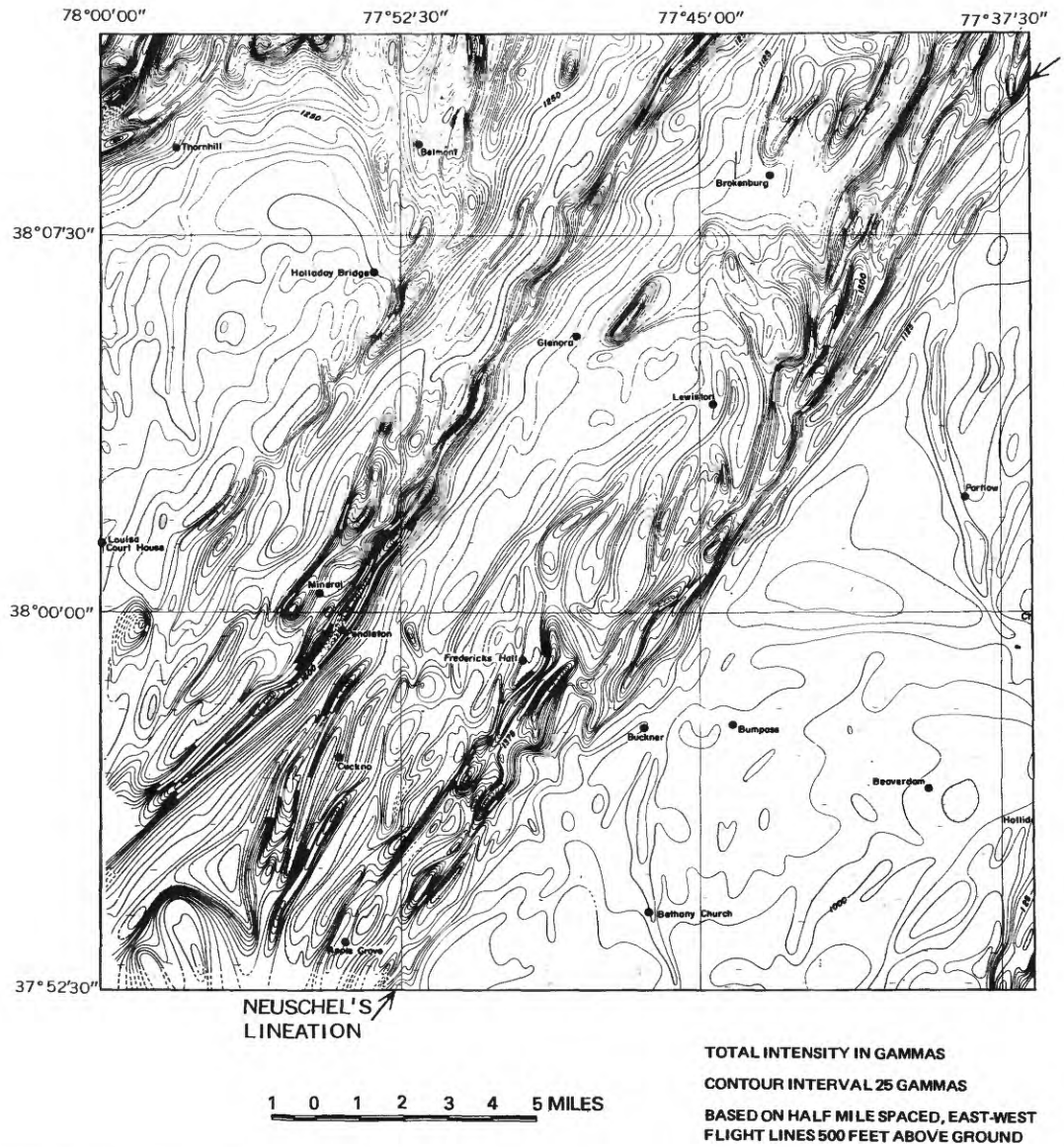

FIGURE 6.—Typical aeromagnetic map, Mineral, Virginia. (Modified from Neuschel, S. K., 1970, Correlation of aeromagnetics and aeroradioactivity with lithology in the Spotsylvania area, Virginia: Geol. Soc. America Bull., v. 81, p. 3575–3582, fig. 2.)

An example of a "probable fault" is offset bedding or an offset ridgeline. An example of a "possible fault" is a very straight stream segment, which may have developed by headward erosion along a fault or which may simply be a consequent stream following the original slope of the surface upon which it developed.

All of the lineaments are selected on the basis of satisfying one or more of the following criteria:

1. Alignment of drainage. This refers to a rectilinear segment of a stream, river or lake. If a valley is observed, but not the stream itself, criterion number 3—alignment of geomorphic features—is used.
2. Alignment of lithology. A rectilinear interface between two lithologic types assumed to be evidence of a "possible fault."
3. Alignment of geomorphic features. This includes straight ridgelines and valleys that do not appear to be caused by bedding.
4. Alignment of vegetation. This criterion includes rectilinear interfaces between vegetation types as well as long, straight

FIGURE 7.—Lineament analysis of Landsat image (1072–15190). (From Withington, C.F., 1973, Lineaments in coastal plain sediments as seen in ERTS imagery, *in* Natl. Aeronautics and Space Admin. Goddard Space Flight Center, Symposium on Significant Results obtained from Earth Resources Technology Satellite–1, 2d, New Carrollton, Md., March 1973, Tech. Presentations, v. 1, p. 517–521.)

narrow bands of vegetation, such as those bordering a watercourse.

5. Alignment of optical density (tone). This criterion is employed when the cause of an observed alignment could not be identified further; that is, when only a rectilinear tonal difference could be seen.
6. Offset of drainage. This refers to a rectilinear, lateral displacement of a stream.
7. Offset of lithology. A rectilinear discontinuity in the strike of a contact is regarded as evidence of a "probable fault." In most instances, lineaments that are probably caused by an offset in lithology were identified as offset or geomorphic features. This is due to the fact that the interpretation of geomorphic features is virtually certain while the interpretation of lithologic types is conjectural.
8. Offset of geomorphic features.
9. Offset of vegetation. (When interpreted as not being the work of man.)
10. Offset of optical density (tone).

In general, but by no means always, criteria 6 through 10—offset—are regarded as "probable faults," while criteria 1 through 5—alignments—are regarded as "possible faults" unless the alignment is very rectilinear and well-defined. The suspected faults are delineated on a transparent overlay registered to the Landsat image.

- Analysis and Interpretation of SLAR—The same procedure is followed, and the same criteria are employed as in the analysis and interpretation of Landsat imagery; that is, the analyst searches for evidence of alignment and offset. The SLAR is first examined for evidence corroborating the lineaments found in the Landsat imagery and is then searched for evidence of additional lineaments. As with the results of the Landsat analysis, the suspected faults found in the SLAR imagery are delineated on a transparent overlay registered to the SLAR. Figure 8 is an example of SLAR analysis.
- Analysis and Interpretation of Aeromagnetic Data —The aeromagnetic contour maps are interpreted without consulting the Landsat or SLAR data. The criteria used for recognizing aeromagnetic "lineaments" include:
  1. Termination of highs.
  2. Termination of lows.
  3. Changes in gradient.
  4. Linear contour patterns.
  5. Alignments of highs and lows.
  6. Long, linear "alteration" lows.
  7. A combination of the above criteria.

  Lineaments that conform to these criteria are delineated on a transparent overlay registered to the aeromagnetic contour map.
- Analysis and Interpretation of Gravimetric Data—The gravity contour map is interpreted in conjunction with the magnetic map. Differences in map construction introduce small errors in the alignment of the interpreted gravity lineaments and magnetic lineaments, but these displacements do not invalidate the existence of anomalies.

  Gravity lineaments are interpreted according to the same criteria used in interpreting the magnetic lineaments described above. The results are delineated on an overlay registered to the gravity contour map.
- Analysis and Interpretation of Aerial Photos—The principal difference between analyzing aerial photos and satellite (or SLAR) images is that the synoptic overview of the latter is exchanged for the stereoscopic view of the former. In other words, the integrating effect of the large-area, small-scale data set is supplemented by the great

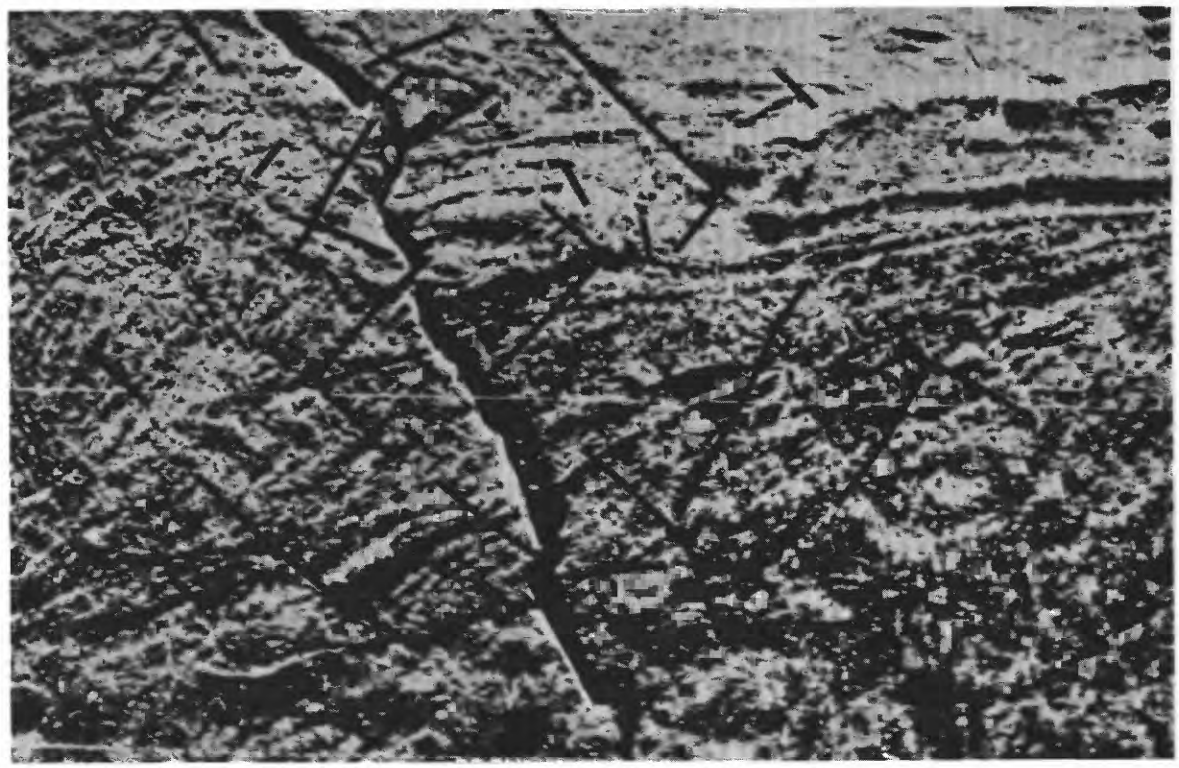

FIGURE 8.—Lineament analysis of SLAR imagery.

density of detail provided by the large-scale, three-dimensional format of the photo. The analytical criteria remain the same, however, in that the analyst is searching for evidence of alignment and offset. The principal function of the photointerpretation phase is to detect corroborative evidence of lineaments found on Landsat and SLAR and to locate smaller lineaments that Landsat and SLAR failed to detect.

- Analysis and Interpretation of Thermal Infrared Imagery—Thermal infrared imagery is seldom used in site investigations unless it has been previously acquired for some other purpose. This is because it is generally believed to be noncost effective in investigations of this kind, where it is unlikely to detect structures that have not already been detected less expensively through the use of Landsat and aerial photos. However, if thermal imagery exists and can be purchased at low cost, or, if the site is underlain by a limestone terrain in which near-surface cavities can be expected, it is well worth the additional cost.

  Unlike thermal pollution studies, site investigations do not require that the thermal imagery be calibrated so as to give accurate temperature readings. The only requirement is that temperature differences and anomalies be observable and caused, for the most part, by differences and anomalies in soil moisture or vegetation, which in turn may be caused by faults and near-surface cavities.

  Figure 9 (p. XIV) shows a machine-aided analysis of thermal imagery in which the colors represent preselected temperature ranges. For example, faults serving as ground-water conduits may cause the superjacent soil to be wetter (cooler) than the surrounding soil, and cavities may drain the overlying soil causing it to be dryer (warmer).

- Synthesis of Remotely Sensed Data—When the interpretation and analysis of all of the remote sensor records have been completed, a transfer scope is used to plot all of the delineated features of structure and lithology at a common scale and format on separate transparent overlays. These are registered to a common base map on which known faults have been delineated. Superimposition of the several transparent overlays results in an effective synthesis of the separate data sets contributed by each of the remote sensors that were employed. A synthesized overlay is then prepared which combines all of the geological features from the separate overlays. The separate structural features are

indicated by different line weights and patterns—one weight or pattern indicating that the feature was observed on all sensors and on the "ground truth" map, another weight indicating that the feature was seen on all of the sensors but one, and so on down to those features that were observed on one sensor only. Figure 10 (p. XIV) shows a synthesis of Landsat, aeromagnetic and and gravimetric data.

APPLICATIONS

Nuclear Powerplant Siting Studies

Dames & Moore routinely utilizes satellite and aerial imagery to support investigations for the location of potential plant sites and as an integral part of studies for the safety analysis of selected sites.

The interpretation of these images is performed to extract information relating to the regional geology and tectonics.

Utilizing imagery from the Landsat and Skylab Programs, analyses are conducted to delineate regional lineaments from which indications of faulting and major fracture patterns can be assessed. This information is presented on overlays to standard 1:250,000 maps of the project area. Correlations are made between the linears interpreted from the overhead coverage and known faults as shown on existing geologic maps. Linears which may have been erroneously compiled as manmade features (i.e., roads or railroads) are corrected (eliminated); existing fault traces which appears on geologic maps may be extended. By virtue of the broad (synoptic) view afforded from satellite altitudes, new lineations, heretofore undetected, add to the store of geologic information about the region.

In addition to the linear compilation, annotations showing geologic contacts in greater detail can be compiled and correlated to formational units from existing geologic mapping. By this means the final overlays will have provided investigators with lithologic and soils maps of significantly more comprehensive information.

As a complement to the satellite data, Dames & Moore has acquired available SLAR coverage for a number of projects. SLAR imagery has been used as correlative information and has been found to be extremely useful in that subtle surface linears are enhanced by SLAR, thereby facilitating detection.

Another data input applied to the geologic analysis is aeromagnetic mapping. Often these data are not available; however, where costs are justified, new surveys have been executed and the results indicative of subsurface structure are applied to those lineament features obtained by visual analysis. Regional magnetic anomalies, where found, can be matched to the scale of the linear compilation and often highlight zones for priority field checking at later stages of a siting program.

The procedures described above constitute an initial reconnaissance phase from which a "first-cut" evaluation of desirable sites can be made. Once this decision is made, a followup analysis utilizing high- and low-altitude aerial coverage is conducted. The higher resolution aerial photography provides the greater ground resolution from which detailed geologic mapping of localized areas can be performed.

The resulting products (annotated maps, photographs) are useful in orientating field crews and directing them to outcrop locations, suspected faulting, et cetera. These are supplied to the project field offices and utilized in the field for planning detailed surveys.

In addition to remote-sensing analysis for geologic/tectonic information, Dames & Moore has performed visual image interpretation and computer processing for land use mapping and ecological assessment.

Digital magnetic tape data have been used to create land-use maps for several siting studies using computer-interactive techniques. Figure 11 shows such a map, in which four categories of use have been identified. Parcels of land down to about 1 acre in size are shown. Where secondary or tertiary levels of detail or higher ground resolution are required, aerial photography and visual interpretation methods are employed along with ground truth surveys to delineate these subgroup requirements.

The land use thematic maps output, from the multispectral processing, may be compiled in a variety of formats. Different themes or categories may be displayed as alphanumeric characters, colors, or shades of gray.

Projects where similar requirements are applicable include: environmental impact reports, wetlands mapping, agricultural and forest stand inventories.

The same techniques employing electronic processing for land use data are also extremely useful in surface water mapping. Using color-infrared data, accurate delineation of land/water interfaces can be made down to the highest resolution of the data. In some cases, physical and chemical pollutants can be identified and traced back to their sources both in estuarine and marine environments. Using thermal infrared data, surface temperature differences of less than 1°F can be mapped, providing an excellent tool for mapping differential thermal effluents, spotting

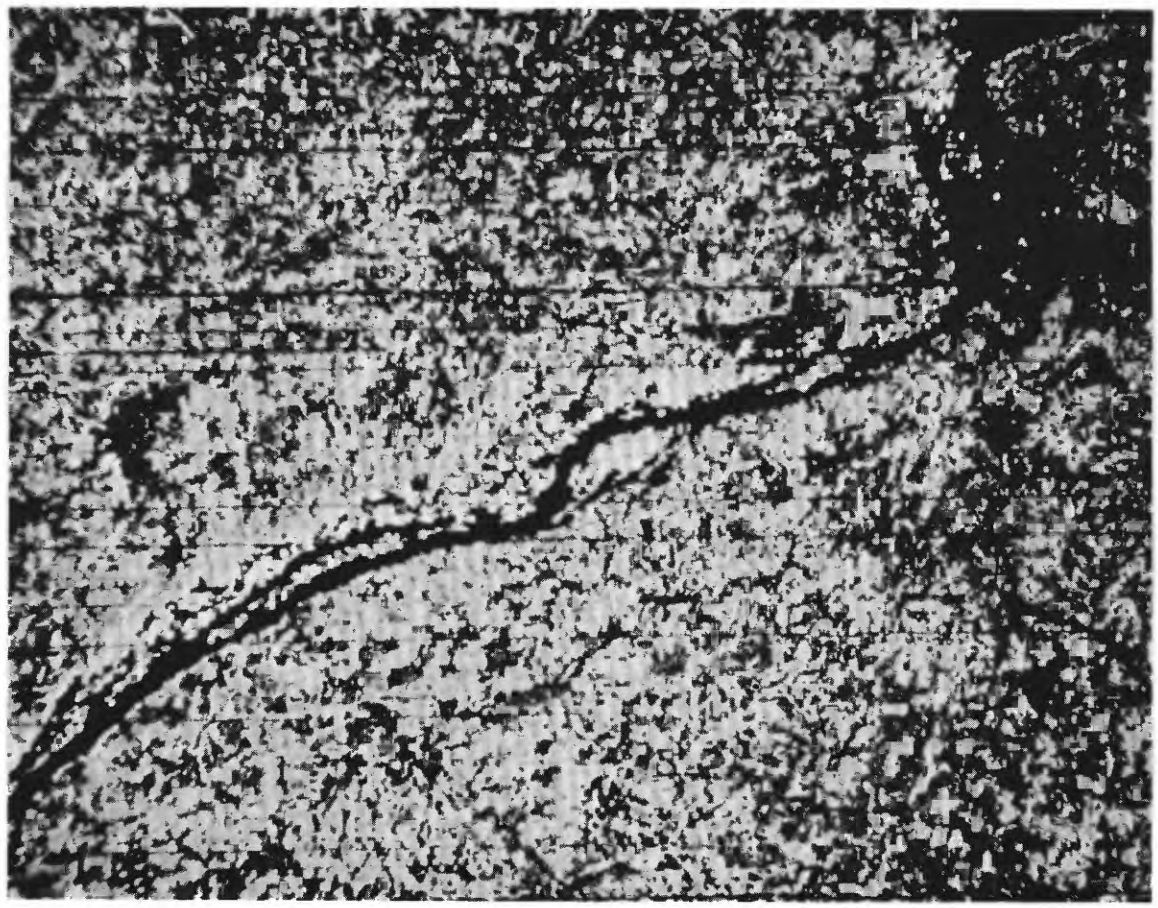

FIGURE 11.—Digitally processed land use data from Landsat observation.

water seepage, or freshwater sources on the terrain surface.

EXAMPLES

A brief description and illustrations of three nuclear powerplant studies involving typical tasks performed by Dames & Moore employing remotely sensed data and techniques are as follows:

Site Selection, South Carolina—A preliminary investigation utilizing Landsat imagery (bands 5 and 7) was conducted to ascertain major regional lineaments over the State of South Carolina. This "front-end" survey was performed to delineate indicators of subsurface structure which provided initial information as to:

1. Areas that might be eliminated on the basis of potential fault-related zones.
2. Where other suitability factors favored plant siting near these zones, further studies could be planned to direct subsequent ground investigations to these areas.

- Site Assessment/Regional Tectonics, Ameri and Bandar Bushehr, Iran—The area circumscribed by a 200-mile radius which originates at each of these two sites was evaluated and supported by Landsat image analysis. The analysis provided overlays upon which observed lineaments and existing fault traces were compiled. These products were correlated with a plot of epicenter locations to determine subsequent requirements for geologic field investigations. At a later stage, critical areas were analyzed in detail using 1:50,000-scale aerial photos, in stereo, and utilized in field surveys to verify faulting.
- Site Specific Investigation, Fulton, Pa.—The result of a regional tectonic study via Landsat visual interpretation detected a number of lineaments within a 10- to 20-mile radius of the site area. Corroborative information was achieved from SLAR, high-altitude U–2 overflights and detailed aerial photos at a relatively large scale. In addition, an aeromagnetic survey was performed so that the synthesis of all source outputs provided

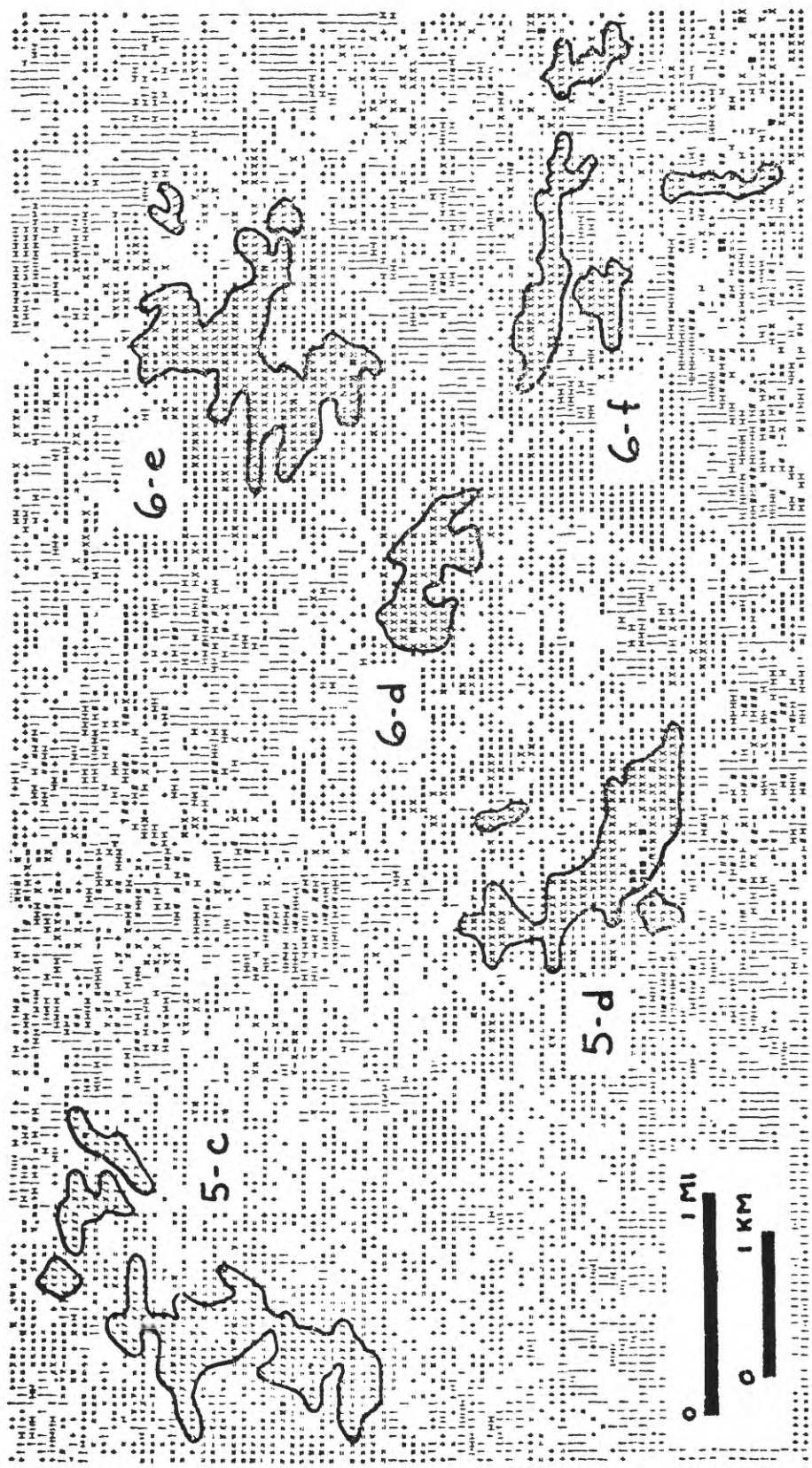

FIGURE 13.—Multispectral computer processed classification map of an area west of Koh-i-Dalil, Pakistan, showing five areas classed as "mineralized." Reconnaissance field checks showed that some hydrothermal alteration and sulfide mineralization is present in each area. (Adapted from Schmidt, R. G., Clark, B., and Bernstein, Ralph, 1975, Search for sulfide-bearing areas using Landsat-1 data and digital image-processing techniques, in Natl. Aeronautics and Space Admin. Earth Resources Survey Symposium, Houston, Tex., June 1975, Proc., v. 1B, p. 1013–1028.)

isolated areas to be used in planning ground magnetic surveys, seismic investigations and ultimate verifications by bore-hole drilling. Figure 12 (p. XV) shows lineament data from three sources: Landsat, SLAR, and U–2 photos.

- Uranium Exploration—We are witnessing a new surge in exploration activities for increased sources of uranium to support the projected needs of the nuclear power industry. Remote-sensing techniques have been developed which now afford cost-effective means for surveying vast areas and mapping zones which may contain potential new deposits.

  Two methods which are employed utilize satellite and aerial photography along with geophysical survey data, as follows:

  1. Visual interpretation for lineaments coupled with aeromagnetic and gravity data reductions and correlated with geologic maps and known deposits provide an overview to delineate areas of potential mineralization which may be associated with faults and fractures. Figure 10 (p. XIV) shows areas in which lineaments derived from Landsat data, aeromagnetic data, and gravimetric data are coincident (dark swaths), and areas in which Landsat lineaments are coincident with either aeromagnetic or gravimetric lineaments (light swaths). Areas of known mines (shown as light dots) show a high degree of correlation with these areas of coincident lineaments.
  2. Multispectral computer processing to delineate potential mineralized zones which may be associated with surficial features (such as halos) and which show a unique spectral response (signatures) on Landsat multichannel scanner data (fig. 13).

  By these procedures an area survey may be accomplished to delineate potential mineralized zones whose occurrences may be related to deposition in faults/fractures or in sedimentary structures.

PROCEEDINGS OF
THE FIRST ANNUAL WILLIAM T. PECORA MEMORIAL SYMPOSIUM,
OCTOBER 1975, SIOUX FALLS, SOUTH DAKOTA

Landsat–1 Image Studies as Applied to Petroleum Exploration in Kenya

By John B. Miller,
Chevron Overseas Petroleum, Inc., San Francisco, California 94105

ABSTRACT

The Chevron-Kenya oil license, acquired in 1972, covers an area at the north end of the Lamu embayment. Immediately after acquisition, a photogeologic study of the area was made followed by a short field inspection. As geophysical work got underway, an interpretation of Landsat–1 (ERTS–1) images was completed as a separate attempt to improve geological knowledge. This paper describes the method used in the image studies, the multispectral characteristics of rock units and terrain, and the observed anomalous features seen in the Landsat imagery.

The observed lineaments seem to be part of the regional fracture system associated with East Africa rifting and crustal expansion. A trend intersection at the north end of the Lamu embayment might be interpreted as a failed, immature triple junction, with one postulated arm opening into the Rudolf trough and a second arm into the Ogaden basin. The Lamu embayment is viewed as a possible aulacogen.

A feature of some significance to the geologic interpretation is an early Quaternary depositional summit surface formed from merging alluvial fans. The surface is slightly cut by shallow modern valleys eroded into the top part of Pliocene sedimentary deposits just beneath. Absence of a fan near the northwest license corner and a swampy area along the Ewaso N'Giro drainage suggest subsidence along what may be a structural trough or downwarp.

The postulated local trough along the Ewaso N'Giro is confirmed by the results of magnetometer and gravity surveys over the area and some early results of reflection seismic studies. The geophysical results also support certain predictions made from the photogeology and image studies relative to the basin boundaries and larger lineaments. For example, anomalies are found along the Lagh Choichuff, Lagh Bogal, Ewaso N'Giro, and Hagadera-Liboi lineaments.

However, convincing geophysical evidence of the Habaswein-Wajir Bor lineament has failed to materialize. Postulated fault relief along the trend, downdropped to the south, seems to be present relative to a structural block of basement rock at and west of Wajir but is not apparent relative to the sedimentary units and underlying basement farther east, toward the Somali border. Something of a puzzle in interpreting the geology of this northeast corner of the license area is the fact that the sedimentary section north of the lineament as indicated from the preliminary geophysics is very much thicker than the section measured in surface exposures.

Anomaly A, a large circular feature seen in the Landsat imagery, partly coincides with the apparent "basinal" (thick sedimentary) area east of Wajir. The real nature of this anomaly is not yet apparent.

The Landsat imagery yielded a surprising amount of information in this flat, relatively featureless area. The success obtained strongly supports Landsat studies as a valid exploration tool. Such image studies and photogeologic work nicely complement one another.

The study has helped to define the relationship of the Lamu embayment and its internal structure with surrounding regional features, such as the East Africa rifting, the Rudolf trough, the Bur-Acaba structural ridge, and the Ogaden basin.

INTRODUCTION

When Landsat–1 (ERTS–1) was launched by the National Aeronautics and Space Administration in July 1972, a door was opened toward a new type of information, quick and inexpensive to use. Among many

uses, the information can assist in exploring for oil, gas, and minerals.

The task of Landsat–1, also Landsat–2 and future units, is to provide an orderly array of pictorial images over what eventually may be most of the Earth's surface. Already the coverage is large and in many instances repetitive through time and changing seasons, snow, flood, and drought.

Many geologists who have made serious and well-informed efforts to use Landsat imagery have obtained good results. Also, they have recognized some of the limitations of such work. These things have been reported principally through the NASA ERTS–1 symposia, especially those of March and December 1973.

Several things contribute to a rather unique value of the Landsat imagery as it applies to exploration. One is the coverage that is already great and promises to be all but worldwide. Also, the multispectral capability, supplementing what can be seen on conventional airphotos, helps the geologist to distinguish different types and combinations of rock, soil, and vegetation and to find anomalies. The orthographic exactness and scale uniformity of Landsat imagery is of special value. An important application of the data is to provide quickly useful planimetric and geologic maps in areas where information is sparse. Inaccuracies in existing maps can be corrected while posting the maps with additional new information visible on Landsat images.

The Landsat–1 imagery is of two types: MSS (Multispectral Scanner) data and RBV (Return Beam Vidicon) data. However, the bulk of Landsat–1 data and all the Kenya imagery is MSS.

The Landsat imagery of Kenya was not obtained in time to be helpful in selecting the initial Chevron acreage. It was obtained soon afterward, however, and was used in making an early appraisal of the area and in planning a work program. Also, it was part of the basis for filing later on a smaller additional optional block which adjoins the initial block at its northwest boundary and corner.

At each stage after its original presentation in Cairo, Egypt, additions have been made to this paper [1] to keep abreast of the progress in acquisition and exploration. This revision adds geophysical information not previously given.

[1] Updated and slightly edited from a paper which was presented November 1974 at the Fourth Exploration Seminar, Egyptian General Petroleum Corporation, Cairo; in February 1975 at the Research Conference on Remote Sensing, University of Kansas, Lawrence; and in June 1975 at the NASA Earth Resources Symposium, Houston.

GEOLOGIC BACKGROUND

The Chevron oil exploration license covers the northern part of the basinal feature of the Kenya coast known as the Lamu embayment (fig. 1). That much was known in 1972 when the exploration right was acquired. But not much was known about the exact basin shape, its limits, and structural nature.

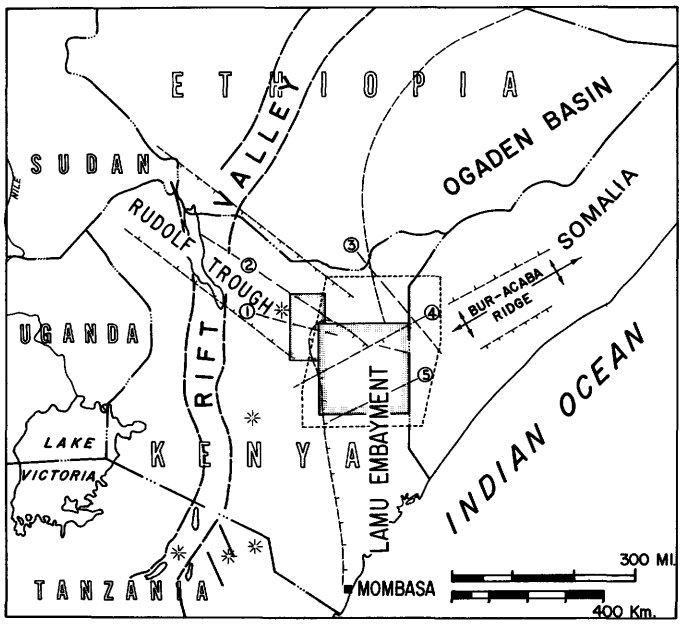

FIGURE 1.—Index map showing regional features and areas of the Chevron exploration license and option (shaded line). Lineaments are numbered: (1) Lagh Bisika, (2) Lagh Bogal, (3) Lagh Katulo, (4) Habaswein-Wajir Bor, and (5) Hagadera-Liboi. Area of Landsat image mosaics, figures 2 and 3, shown as dashed line.

Previously, British Petroleum–Shell had held an oil lease over a large part of the Lamu embayment, including some of the ground taken by Chevron. Most of the BP–Shell rights had been relinquished, leaving only a relatively small area along the Kenya coast.

BP–Shell had explored extensively and drilled 16 "dry" wildcat wells in the Lamu embayment. Only three of these—Meri–1, Waligero–1 and Wal Merer–1—are on the Chevron tract. These were enough to demonstrate the presence of more than 12,000 ft (3,660 m, approximately) of sedimentary rocks within the land acquired by Chevron. Several other wells of substantial depth were known to exist some distance to the east, in neighboring Somalia.

But while information on the embayment itself was sketchy, certain information on surrounding areas was well documented by the Geological Survey of Kenya. In the area west and north of Mombasa, Caswell

(1953, 1956), Sanders (1959), Thompson (1956), and Williams (1962) reported a thick section of sedimentary rocks. This includes Karroo-type red beds (mainly continental sandstones, Carboniferous and Permian through Triassic), a section of marine shales and local shelf-type limestone (Jurassic and Cretaceous), and locally along the coast onlapping marine deposits of Tertiary age. The aggregate section of Karroo-type beds totals about 22,000 ft (6,700 m, approximately). The Jurassic section totals 6,600 ft (2,010 m). The Cretaceous is incompletely represented in exposures by only about 300 ft (90 m) of section.

In the area north of the license area, extending to the Ethiopia border, the stratigraphic column begins with Triassic strata and ranges through the Lower Cretaceous. These rocks have also been described by geologists of the Kenya Geological Survey, particularly in reports by Thompson and Dodson (1958), Baker and Saggerson (1958), Saggerson and Miller (1957), and Matheson (1971). As compared with sedimentary rocks at Mombasa, the thickness is much less and the lithology is somewhat changed. The Triassic again is a Karroo-type facies, but the exposed thickness is only 2,000 ft (610 m). The Jurassic strata, roughly 5,500 ft (1,680 m) thick, are mainly dense, gray shelf-type limestones. About 2,500 ft (760 m) of Cretaceous section consists mostly of shallow-water sandstone and some interbedded marine shale.

Contrasts both in thickness and lithology are found when the stratigraphic units north of the license area are compared with those observed near Mombasa. However, it is not clear where and why the changes occur nor what may be their significance to the possible presence of commercial hydrocarbons.

Available maps show most of the surface in the license area as Quaternary alluvium. Jurassic limestones abut and enter the area east of Wajir, some late Tertiary volcanic rocks occur in the northwest corner, and Precambrian metamorphic rocks crop out in the southwest. Several small Jurassic exposures are reported just outside the area, north of Mado Gashi. Preliminary investigations have shown that, over much of the area, erosion has cut very shallow valleys into underlying clays considered of Pliocene age. While the exact age of these is subject to question, the clays are mainly older than sands and soils found on the undissected summits, and older by yet another stage than the alluvium in the modern streamflats. They appear to be the top part of a fairly thick Miocene-Pliocene section known in much of the Lamu embayment.

A complex, sloping plateau rises from an altitude of about 1,200 ft (370 m) above the sea at the west margin of the Lamu embayment north of Garissa to a structural swell reaching a height of more than 6,000 ft (1,830 m) along the Kenya (Gregory) Rift Valley. This is mainly an area of Precambrian rocks, including a variety of metamorphic and intrusive rocks, but there are also great areas of volcanic rocks and several large volcanic peaks. The more resistant crystalline masses stand as prominent inselbergs. Many belts of hills representing old topography occur within and between the valleys. In this terrain are well-preserved parts of three planation surfaces, produced by denudation after principal stages of structural uplift associated with the African rift system. The plateau area was tilted seaward in Late Cretaceous, middle Tertiary, and late Tertiary episodes of domal uplift (Saggerson and Baker, 1965; Matheson, 1971; Baker and Wohlenberg, 1971).

Two geologic papers containing new, important information relative to the Lamu embayment were published in 1973. One of these, by Walters and Linton of BP–Shell (1973) provides subsurface information on the Lamu embayment. The other, by Gulf Oil geologists Beltrandi and Pyre (1973), described the geology of adjoining basinal areas in Somalia. Although these add substantially to available knowledge, they provide incomplete answers about basinal structure, bounding limits, and stratigraphy.

GEOLOGICAL INTERPRETATION

METHODS

To conduct this study, Chevron purchased 70-mm positive transparencies of all four spectral bands of the required Landsat–1 imagery. These were composited into color, using an early model International Imaging System (I^2S) additive-color viewer then available at the Chevron Oilfield Research Laboratories at La Habra, California. Several color arrays were recorded as 35-mm color slides on Ektachrome high-speed film. For interpretation of the imagery, the 35-mm slides and also the 70-mm black and white images were projected on the wall of a darkened room. A sheet of white drafting paper fastened to the wall served as a projection screen and as a base for annotating the geology and other photographic detail.

Since completion of this work, Chevron Overseas has obtained, at its home office, an improved I^2S viewer. This eliminates dependence on color slides, and makes it possible to annotate on a transparent medium directly over the screen of the compositor. This is done at a favorable scale of 1:500,000. During annotation, the image is examined with a binocular

headpiece which provides 1½ X and 2½ magnification.

Just prior to the Landsat study, even predating the availability of the Landsat imagery, I conducted a photogeologic study of our area (airphoto scales partly 1:40,000; partly 1:80,000) and made a 6-day trip into the field. This work extended from September into early November 1972. This experience in Kenya was most fortunate as a prelude to the work on the Landsat images. Of course, such experience is never amiss. As background toward evaluating a new and unfamiliar type of imagery, it proves to be especially helpful. It is a framework for judging the physiographic and geologic phenomena as registered by the Landsat sensors and for evaluating the usefulness of the data.

Two Landsat image mosaics are used to illustrate this paper. These copy fourth-generation products from the 70-mm positive transparencies acquired from the EROS Data Center at Sioux Falls, South Dakota. The first step was to photographically enlarge the images into a set of negatives at 1:1,000,000 scale, produced on 9×9-inch film. Contact prints from these formed the original mosaic, which then was reproduced into a single mosaic negative and into photographic prints.

The remainder of this paper is an appraisal of information recovered from the interpretation of the Landsat images. Comparisons are made, from time to time, with detail as seen on airphotos and occasionally as seen on the ground. A comparison is made also with geophysical data obtained since the Landsat analysis was completed.

PHYSIOGRAPHY

Much of the drainage pattern is seen on the Landsat images with remarkable clarity, even into the headwaters of relatively minor drainage courses. In viewing the Landsat images, this is almost the only evidence of relief. An impression of relief is better when there are ground shadows, but very few slopes in the area are steep enough to produce shadows. The exceptions are the cuestas of Triassic sandstones roughly 80 km north of Wajir, several lava features west of Wajir, the Bur Wein anticline south of El Wak, and inselbergs of basement. All of these hills are small, even at the scale used during the interpretation. At the reduced size of the present mosaics and maps (figs. 2–5) they become all but invisible.

The drainages are gullies and wide, flood-washed channels in a semi-arid terrain. These are seen clearly in Landsat images and can be drawn accurately. The drainages that originate on the plateau and enter the region from the west have relatively wide streamflats. The Tana River carries a good flow of water. Through the use of the infrared image particularly, the dark meandering line of this can be followed readily (fig. 2). The other streams are seasonal. The Ewaso N'Giro spreads and much of its flow is arrested at the Malka Galla swampy area north of Mado Gashi. Lush vegetation at the "swamp" produces high response in the infrared as compared to the green and red band response, so that a false-color image registers flaming hues of red. Below this spot, the Ewaso N'Giro drainage channels become narrow and dispersed, and, while borders of the streamflat are sharply defined, the channels within it are indistinct. The same is true for other similar streams. For example, a 15-km segment of Lagh Katulo as sketched differs from the main stream course marked from airphotos, but the difference is inconsequential in small-scale mapping amid shifting channels.

The relief, indeed, is low. Except for an escarpment along the Yamicha area lava bench, the only hills with substantial sloping profiles are either west or well to the north of the Chevron license. Although there is about 180 m of slope in 220 km from the west edge of the license to the southeast corner, the horizon, as seen on the ground, is commonly flat. The most rugged ground generally consists of a gentle, faintly rilled slope into a shallow valley, a low-cut bank, and then an equally gentle rise to a low, broad summit. In perhaps half of the license, these slopes are so slight as to be imperceptible during ordinary stereoscopic study of airphotos. They are defined mainly by directions of rainwash and drainage rather than visible relief. Remarkably, much of the drainage of these insubstantial slopes is seen almost as clearly on Landsat images as on the airphotos.

ROCK SIGNATURES

Quite a number of boundaries between rock types can be traced on the Landsat images even though the nature of the lithology is not clear. To some degree, even the approximate nature of the lithology can be surmised. In this text, the visible characteristics of units will be reviewed in successive order of decreasing age. Many of the characteristics are not seen in figures 2 and 3 because these are much smaller than the images employed for interpretation.

The migmatitic character of the basement rocks seems to be subtly evident. A peculiarity of folia is that they show on many scales, which range from microscopic size into the outcrop and then to a textural grain seen on airphotos. In the Kenya

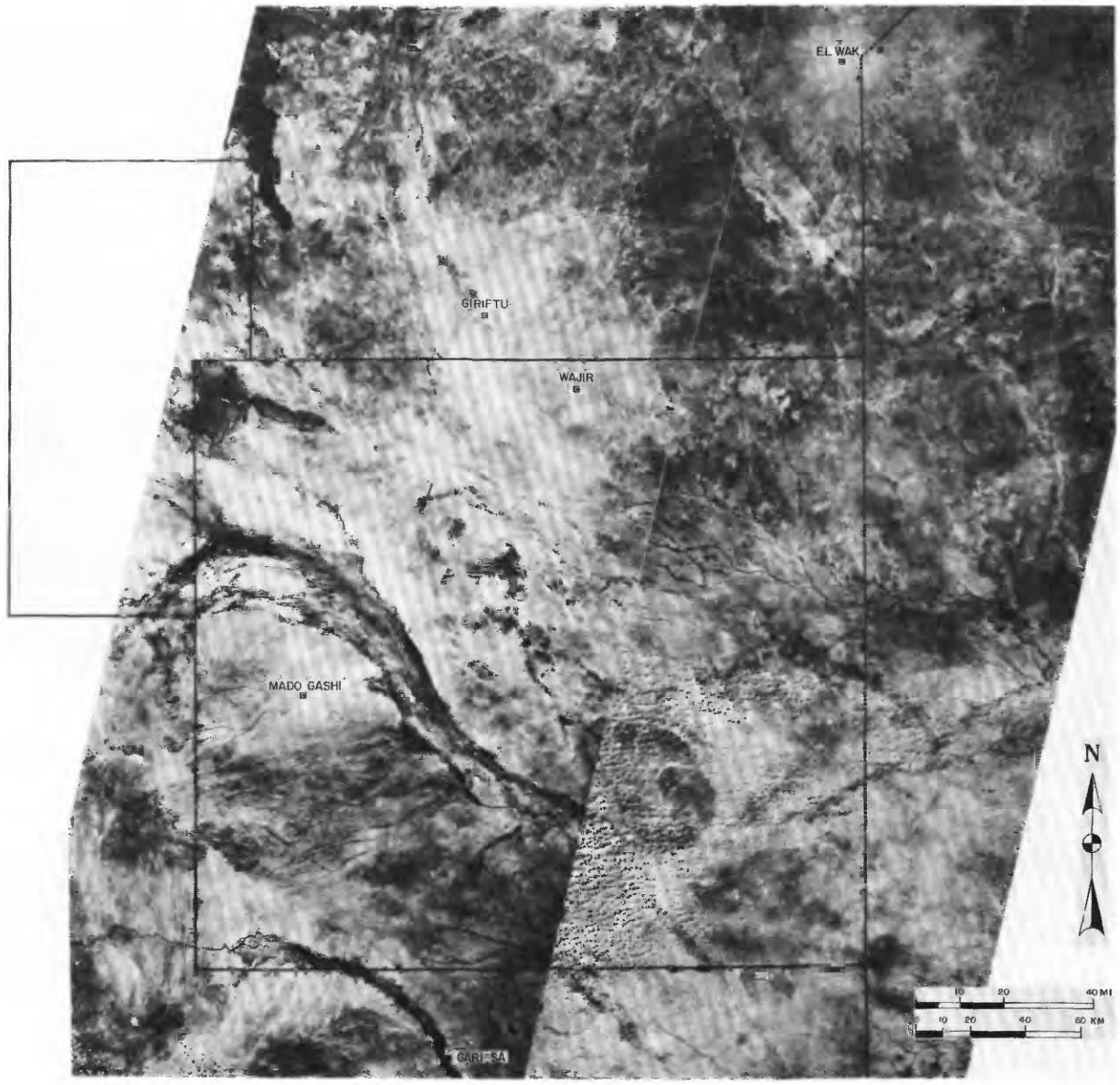

FIGURE 2.—Landsat image mosaic Garissa-Wajir-El Wak area, Kenya, band 7 scenes. The lines where the images are matched show as sharp, straight boundaries parallel and normal with the slant margins. The dark Jurassic limestones northeast of Wajir, transected by the Lagh Katulo alluviated valley and fault line, are clearly visible. The Hagadera Liboi lineament is also prominent. The white flecks in the lower right hand scene and at extreme lower left are clouds. Landsat images 1190–07052 (upper left), 1189–06593 (upper right), 1190–07054, 1189–07000, 1190–07061, and 1153–07003.

migmatites, some of the foliated grain is reproduced even in the Landsat images. It appears as faint, shadowy bands, probably representing rock and topography and interwoven layers of differing lithology. In places, there are inselbergs indicating resistant rock. A wide color range, from eggshell and flesh tones into green and gray very likely represent composition ranges from light-reflective bands of quartzose rocks and feldspar through rocks of intermediate composition, mantling residual material rich in iron oxides, into belts of relatively fresh rock containing unoxidized femic minerals, gray slate, and, locally, marble.

The Triassic conglomerate and sandstones north of Wajir stand out from the metamorphic complex mainly because of their sharp, arcuate- and irregular-shaped cuestas. The well-stratified and resistant character of the rocks is revealed by the erosional form of the

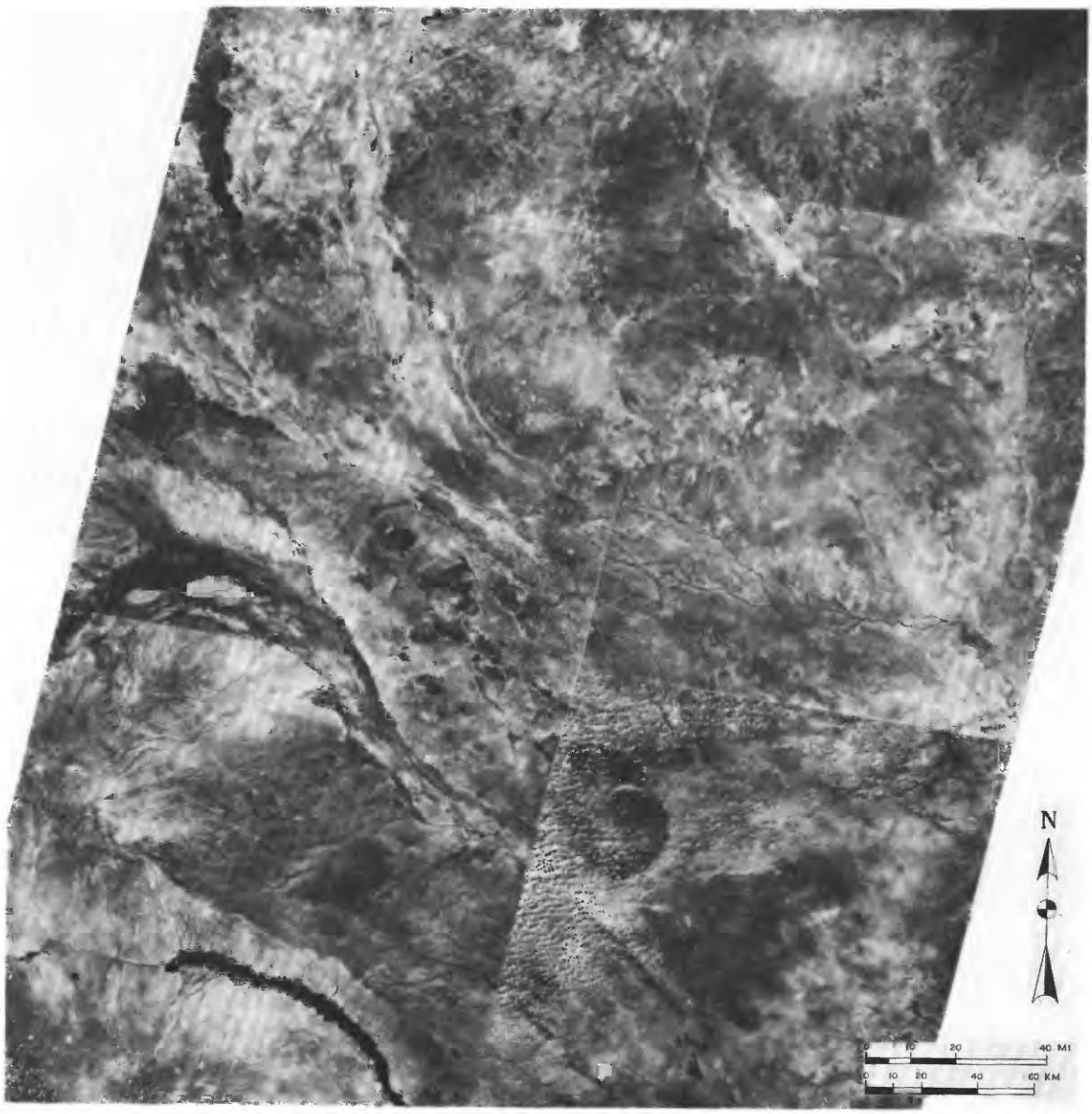

FIGURE 3.—Landsat image mosaic, Garissa-Wajir-El Wak area, Kenya, band 5. The Lagh Bisika, Lagh Bogal, Lagh Bor, and at least part of the Wajir Bor lineaments are quite apparent. The Pliocene-Pleistocene depositional surface is better defined by band 5 than band 7 (fig. 2). The expanding wedge of "upper" Merti can be found by comparing band 5 with band 7 imagery; it is seen in mainly the Tana River valley wall north of Garissa. With apex near the metamorphic rocks and expanding as a narrow wedge eastward, the unit contrasts sharply with the rim of darker duricrust, just north. Its base, seen as a contrast with the lighter colored "lower" Merti, shows better on the band 7 imagery of figure 2.

ridges. The low dip present in the strata can be construed from down-dip expanse of the dip slopes.

A basal boundary of the Jurassic limestone can be followed only inexactly. The limestones appear quite dark in bands 6 and 7, somewhat less dark in bands 4 and 5, and show as dark gray partly flushed with red in the composite image. The red is a response from a combination of thin soils and sparse vegetation.

Cretaceous sedimentary units show in the extreme northeast as sharply defined ridges and cuestas. The direction of dip is generally discernible.

Pliocene and Quaternary volcanic rocks, mainly basalts, are present in the northwest part of the area. In fresh outcrop, these register darkest in all color bands, and, in the color composites, they show as nearly black. There is a weathered surface and some soil across the basaltic mass at Yamicha, but, in its

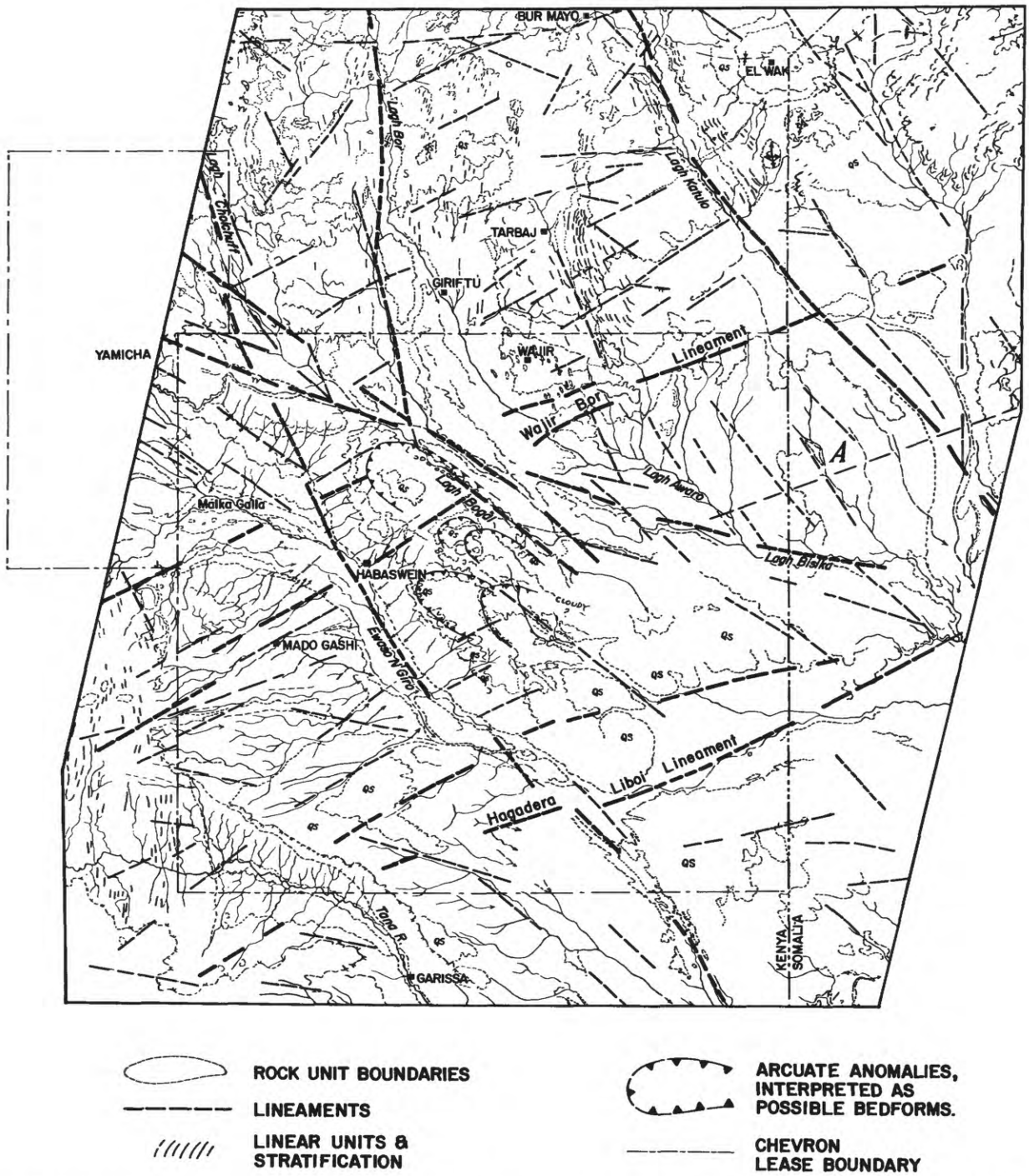

FIGURE 4.—Lineaments, rock unit boundaries, and other features as interpreted from the Landsat imagery. The Qs symbol designates part of the Pliocene-Pleistocene summit depositional surface, regarded primarily as Quaternary material. Centered at A and near its margins by a circular pattern of drainage is Anomaly A. Scale 1:2,500,000.

southern escarpment, which probably marks an original flow edge, the volcanic rocks are very fresh. Farther north, a virtually unweathered volcanic flow is defined both by its lobate form and nearly black color.

Of somewhat the same age are the Pliocene-Pleistocene clastic deposits. These show the most varied color signatures of all—a greater range than are accounted for by known differences in lithology. The Pliocene part can be locally divided into two

FIGURE 5.—Rock unit distribution, broadly defined from Landsat imagery and other sources.

parts. At the top and probably Quaternary in age is a depositional surface and calcrete (fig. 5).

The main unit, the Merti sands and clays named in Kenya geological literature, is regarded as late Pliocene. These sediments fill a late structural sag along the Lamu embayment. The observed relationships strongly suggest faulting along the western basin margin, because the "End Tertiary" erosion surface extends across basement rocks at elevations of 600 ft (182 m) or more west of Mado Gashi but drops beneath the Merti in the basin. As shown by the thickness of Merti beds in the Dera borehole, near the basement rock boundary—240 ft (73 m) to top of basalt; 408 ft (124 m) to base of volcanic debris: Matheson, 1971, p. 19—the "End Tertiary" surface seems to drop structurally at least 250 ft (76 m) in crossing the basement boundary.

The boundary of the Merti deposits with basement rocks is plainly seen on Landsat–1 imagery at the Tana River. The basement appears banded. The adjoining Merti is finely rilled and, especially in band 7, has a lighter tone (fig. 2). Extrapolating from topographic maps, the thickness of Merti beds exposed in the valley slope near the basement boundary is about 600 ft (180 m).

Above this, and within my knowledge recognized only on the Landsat–1 imagery, is a second unit. It begins at the basement boundary and thickens wedge-like into the basin. It is slightly darker in bands 5, 6, and 7 than the sediments beneath. I distinguish this wedge-shaped unit tentatively with the name "upper Merti," but suppose it may not be readily separated from the underlying part of the Merti except in the Tana Valley. Saggerson and Baker (1965, p. 57) mention 300 ft (90 m) of Merti sediments at Garissa. On the basis of the Landsat–1 image, at least 200 ft (61 m) of these seem to belong to the "upper Merti." Seemingly they will entirely overlie the estimated 600 ft (183 m) of Merti beds exposed near the basement boundary.

The distinguishing tonal difference of the "upper" Merti from underlying beds is clearly seen in the color image and in the longer wavelengths of bands 5, 6, and 7. It is seen hardly at all in band 4. The smaller sensitivity of shorter wavelengths to these lithic divisions may explain why the divisions were not recorded during work on conventional airphotos. Coupled with this is another reason: The sediments are unconsolidated. They are intricately scored by rilled drainage, and small masses of the material have moved downslope through the action of crumbling and mudflow. The boundary, as seen on the airphoto, has probably been softened and blurred by this action. On the other hand, as seen in the overview of the Landsat image, the boundary is relatively sharp and conspicuous.

Above the Merti is a thin unit of sand, marl, and calcrete deposits or "caliche." This tends to form a duricrust with thickness commonly ranging from 1 ft to perhaps 8 ft (about 2 or 3 m). The top surface, probably Pleistocene, is a thin layer of soil thinly mantled with sand. Near the town of Wajir, the Quaternary deposits—about half sand and shale, and the top half mainly calcrete—thicken to as much as 100 ft (30 m) and contain a substantial amount of ground water. Calcrete outcroppings in this area appear on the Landsat images as white patches.

The depositional surface of the Quaternary duricrust (mapped Qs) has been cut and partly destroyed by the modern system of streams. Nevertheless, there are numerous remaining patches. The distribution of these bears on several aspects of the geology, including the reconstruction of previous drainage and a definition of lineaments.

Remnants of the surface, as seen on airphotos, have a relatively dark gray cast and slight, benchland-type rims. Commonly there is a pattern of widely spaced "pits" that appear to be subtle, periodically wet depressions. Where the surface has been destroyed, there are rilled slopes or an expansive surface of clay which is broken, probably along jointing, into polygons or prisms. Each polygon has an almost imperceptible hummock and central cluster of brush (as confirmed on the surface) surrounded by bare clay and a wash of white sand.

The depositional surface stands out quite well on the Landsat imagery, although a color composite is needed for most effective mapping. It supports grass and significantly more trees than are found over most adjoining rock units. Consequently, in addition to a darker cast than most surrounding rock units except limestone and basalts, the false-color images rendered by the surface are distinctly reddish. A response that comes from grass and trees, the reddish tint is probably somewhat seasonal, dependent on rains.

Examination of the surface suggests two main parts, a sloping plain from the north-northwest, and what may be called the Tana fan from the southwest. Judged from valley entrenchment and airphoto stereoscopy, there is a definite easterly slope to the Tana fan. Also, the plain beyond the Ewaso N'Giro tends to undulate slightly across axes parallel to the present drainage. As judged from the distribution, destruction of some of the surface, e.g., the northwesterly part and a belt along the Ewaso N'Giro, seems to have

started before development of the southern part of the surface was complete.

Examination of the Landsat images reveals several elements within the plain that were not noticed on airphotos. Located between the Ewaso N'Giro and Lagh Bogal (fig. 4), these can be effectively defined only on the color image (fig. 6, p. XVI). They show as four or possibly five differing arcuate bands of color. Their shapes suggest giant bedding structures. Preserved parts of the Quaternary depositional summit coincide with the associated arcuate forms, indicating these might be anchored by resistant layers among somewhat complex stratigraphic forms just beneath the surface. For example, they could mark the upper edges of several shallow, trough-shaped features related to erosion and depositional patterns. Although probably not sensitive to structural trends, these might be significant to the distribution of possible shallow ground water.

LINEAMENTS

As used in this paper, the term lineament refers to apparently natural lines, bands, and anomalous zones generally more than 10 km (6 mi) long. These lines and linear bands are associated variously with straight or slightly arcuate drainage courses, tonal lines, aligned erosional breaks in the Quaternary depositional surface, and occasionally other phenomena.

A set of linears aligned about N. 50°–60° E. probably is paired with another set aligned N. 45°–60° W. Representatives of the northeasterly set are the Habaswein-Wajir Bor and Hagadera-Liboi lineaments. Trends in the northwesterly set are along the Lagh Katulo, Lagh Bogal and a segment of the Ewaso N'Giro. Considered as conjugate directions, the intersection angles generally fall between 60° and 80°.

Another set of lineaments (e.g., Lagh Choichuff, Lagh Bor) commonly bears about N. 10° W.–N. 20° W. Probably conjugate with this is the Lagh Bisika and several smaller trends bearing N. 70° W. The intersection angle ranges between 50° and 65°.

A number of lineaments, accentuated in figure 4, are discussed below. Among the many linear features present, these seem to relate, as seen in figure 1, to geologic phenomena well beyond the figure 4 map boundary.

HABASWEIN-WAJIR BOR TREND

This wide, subtly defined linear anomaly (lineament) crosses the license area at its middle west boundary and, east of Wajir, continues into Somalia. The anomaly forms a band distinguished in part by sparsity (a result of erosion) of the Quaternary duricrust.

The trend is defined by two bounding linear features comprised of separate, aligned, but not quite continuous, lineaments. Parts of these are formed by straight stream courses and other parts by tonal changes occurring, for example, along straight edges of remaining areas of the duricrust where fractures are probably a controlling factor in the erosion.

The ending of ridges where Jurassic limestone is exposed northeast of Wajir seems to be part of the tonal change along part of the lineament. This suggests that the trend, in this sector, may be an expression of a fault that steps the limestones downward into the basin where they may then be overlain by younger sediments.

An easterly extension of the Habaswein-Wajir Bor trend may play a part in an offset in basement rocks along the north flank of the Bur-Acaba structural ridge in Somalia. This is mentioned further in later paragraphs.

In the southwesterly direction, the Habaswein-Wajir trend extends toward distant Mt. Kenya, a major volcano.

Some 60 km south of the Wajir Bor trend is a parallel Landsat lineament, mainly tonal. It is not named, but on the map passes nearly through the center of the feature called Anomaly A (fig. 4). The lineament may play a part in the tectonic scheme and therefore will be mentioned again.

HAGADERA-LIBOI LINEAMENT

About parallel to the Habaswein-Wajir Bor feature, the Hagadera-Liboi lineament crosses the southern part of the license and then extends into Somalia. Much of it is defined by drainage along a southerly leg of the Ewaso N'Giro (locally called Lagh Dera) past the Liboi military post. Toward the west, it runs along lesser drainage courses and finally extends along the south margin of the Tana River valley. In this segment, it partly outlines the edge of the preserved Quaternary surface.

As it is traced eastward on Landsat–1 imagery, the Hagadera-Liboi lineament aligns directly along the southerly edge of the Bur-Acaba structural ridge. This ridge, in Somalia, is a major uplift exposing an area of granite and metamorphic basement. The local geology indicates that at least its southern flank is faulted. The Habaswein-Wajir Bor and Hagadera-Liboi linear features were first defined through the Kenya photogeology. Their exact coincidence, when projected by means of Landsat imagery into Somalia, with the boundaries of the Bur-Acaba structural ridge is considered geologically significant.

CHOICHUFF, BOR, AND EWASO N'GIRO LINEAMENTS

The Lagh Choichuff and its companion trend, Lagh Bor, trend southward across the license boundary along drainage courses bearing these names.

Just within the license, each is crossed by southeastward features—the Lagh Bogal and Lagh Bisika lineaments. The Lagh Bor feature is not seen southward of its juncture with these features. The Choichuff trend meets the valley of the Ewaso N'Giro and—if structural aspects are continuous—changes in trend from S. 20° E. to a new direction of S. 25°–30° E.

The apparent bend along the Ewaso N'Giro apparently is caused by an interaction between trends and by structural slivering. When viewed with the aid of a regional map, the Choichuff lineament is found to align with a segment of seacoast north of Malindi and the lower stream course of the Tana River. This suggests a deeply rooted fracture nearly parallel to the fault which bounds the west margin of the basin.

LAGH BOGAL AND LAGH BISIKA LINEAMENTS

These two trends cross the northern part of the license area and intersect at a narrow angle. Some structural interference may occur where the two trends meet. There is a hint of left-lateral displacement of the Lagh Bogal feature, but exact placement of the lineaments and definition of offset are uncertain.

The Lagh Bogal lineament is about axial relative to a structural-morphologic feature called the Rudolf trough by Brock (1965, p. 101–102). From a regional standpoint, it might be appropriate to name the lineament from North Island in Lake Rudolf because it can be traced this far to the northwest (fig. 1) and probably is responsible for the North Island volcanic center. It is also associated with a concentration of volcanic craters northeast of Mount Marsabit. The Lagh Bisika feature also passes northwestward, but lies slightly askew to the trough. This trend flanks the south side of Mount Marsabit and merges with a bounding linear of the trough about at the south end of Lake Rudolf. Along the Kenya-Ethiopia border, linears flanking the north side of the Rudolf trough are seen on the Landsat imagery.

LAGH KATULO FAULT

A fault displacement of Jurassic sediment along the Lagh Katulo can be detected both on Landsat imagery and on the Kenya airphotos. The displacement can be seen in the structural attitudes, also in the distribution and expanse of Mesozoic rock units. The faulted lineament can be traced northwestward into Ethiopia, also southeastward into Somalia.

OTHER ANOMALIES

ANOMALY A

This anomaly is partly within the license area. It centers east of the international border, in Somalia, and is a large anomaly of relatively pale tone and color, outlined by a circular drainage pattern. Its eastern edge is marked by a prominent deviation of the Lagh Katulo stream course. A northern boundary is the Wajir Bor lineament; a southern boundary is the Liboi lineament. The feature therefore may be related structurally to the Bur-Acaba structural ridge which apparently develops astride this same trend and structural block, farther east.

In a fold regime, such an anomaly is suggestive of a domal uplift. Within this extension regime amid a strongly developed fracture system the domal implication becomes much less forceful. The stream systems seemingly are deflected across major fracture lines, then follow along polygons of fracturing. The anomaly as a whole is outlined by a rimlike margin of the preserved Quaternary duricrust, reduced by sapping action to a circular outline.

Whatever the difficulties in exact interpretation, the anomaly probably is related in one way or another to the conditions of subsurface structure.

MALKA GALLA AREA

The periodic collection of water over the Ewaso N'Giro streamflat is not strinkingly abnormal at sites such as this where extensive drainage from highlands empty into arid plains. Yet it does suggest a break in the stream gradient and a possible structural sag.

Possibly more significant than the "swamps" is the apparent absence, in this sector, of any large alluvial fan coincident with the Ewaso N'Giro. The Quaternary duricrust developed mainly over fans entering from the southwest (Tana River sector) and north (Lagh Choichuff and Lagh Bor, and similar drainage).

The absence of a substantial fan on the Ewaso N'Giro may be construed as evidence of structural subsidence. Acting as a sediment trap, substantial subsidence would arrest the movement of sediment and minimize the growth of fans.

Construed in this way as a discrete structural sag filled with young clastic sediments, the area may be ideal for large, relatively shallow supplies of ground water.

BUR WEIN

The Bur Wein anticline (Baker and Saggerson, 1958) lies within Cretaceous outcrops about 40 km south of El Wak. This feature, a sharply defined domal up-

lift, shows in the Landsat image as a unique feature. Its steep flanks, clearly visible, set it apart from all other recognized features. The characteristics of the Bur Wein anticline, as contrasted with the surrounding geology, suggest it as a diapiric feature possibly developed over an igneous plug.

ANALYTICAL REVIEW

Four basic directions have been described in the pattern of lineaments. Three of the directions are coincident with major rift directions mapped in East Africa. The examples, classified roughly in terms of regional direction groups, are northward, parallel to the Gregory Rift Valley (Choichuff), northwestward (Lagh Bogal-Rudolf), and northeastward (Habaswein-Wajir Bor)—the northwestward and northeastward systems parallel regionally to the Rukoban and Ruaha fracture sets in Tanzania. Except for local minor deviations, the directions are remarkably consistent. Not only the younger Cretaceous and post-Cretaceous rifts but also the older basins filled with Karroo-phase sandstones as old as Permian conform with this pattern. The rift and fracture system tends to divide the continental block into entire and partial hexagonal prisms.

The regional tectonics apparently are dominated by vertical movements and tensional stress. The Lamu embayment, which contains a succession of sedimentary rocks beginning with Karroo sandstones, is postulated as an extension basin of possible failed-arm type. Any compression-type structures within the embayment are probably of secondary importance.

Evidence of downfaulting of Pliocene sediments at the basement boundary west of Garissa is construed from the geometry of bedding and sedimentary fill (observed in the Landsat image) as these combine with known relief. The faulting suggests this line as a main, if not necessarily a unique western boundary to the basin, rather than as a less important line of sedimentary onlap and tilting.

The anticipated northern limit of the Lamu embayment, east of Wajir, is the line of postulated fault relief across the Habaswein-Wajir Bor lineament. North of this, Triassic sandstones and Jurassic carbonates are found in outcrop, resting on metamorphic basement. South of it, one might expect a much thicker section, ranging to Tertiary age.

Westward from Wajir, the situation changes. It is possible to relate three separate phenomena and conclude from them that an apex of the basin may extend into the northwest corner of the license area—its margin staggered, perhaps, between several intersecting faults: (1) the semi-swamps of the Ewaso N'Giro, (2) an absence of a clearly defined "Quaternary surface" fan, as previously discussed, combine to indicate an active structural sag, and (3) Jurassic outcrops reported in this area, stepped far to the west of the Jurassic boundary northeast of Wajir. These outcrops must be preserved in a downwarped or down-dropped block and suggest a major offset or displacement of the basin margin.

Construed from this evidence is the idea that a somewhat discrete trough or graben may extend to the northwest corner of the Chevron holding.

A number of lineaments converge within the northern part of the tract. These may relate partly to the termination of the Lamu embayment if the embayment is, in fact, an aulacogen or failed arm. The northerly trend of the Lamu embayment combined with two lesser branches may form a triple junction. One of these, behaving as a carbonate shelf northwest and landward from the Bur-Acaba ridge, goes into the Ogaden basin of Ethiopia and Somalia.

The other, the narrow grabenlike trough toward Lake Rudolf, seemingly could have been a Mesozoic valley which directed Mesozoic river drainage into the Lamu embayment. This could bring about major changes in sedimentary thickness and facies—changes not yet known, but possibly important to oil occurrence—within the Chevron holding. Possibly, also, the trough could have held a short-term arm of the sea.

GEOPHYSICAL PROGRAM

During 1973, an airborne magnetometer survey and helicopter-mounted gravity survey were made. These surveys were planned with the benefit of photogeologic knowledge. The work was already in progress during the Landsat study. A seismic program, which benefits from all previous work, is going forward in 1974 and 1975.

There is a limited correlation between the geophysical results and the analysis made from Landsat images and the airphotos (fig. 6, p. XVI; figs. 7, 8). At this preliminary stage, neither the coincidence of anomalies where coincidence occurs, nor a lack of coincidence is very well understood. The best correlations are these:

1. A good magnetic definition, and a modest gravity definition closely matching the construed fault along the western basin boundary. The data do not suggest a single profound structural drop-off, but instead one that is stepped or, most likely, involves an element of tilt as well as faulting.
2. Defined in all geophysical results is a troughlike feature in the northwest part of the license area

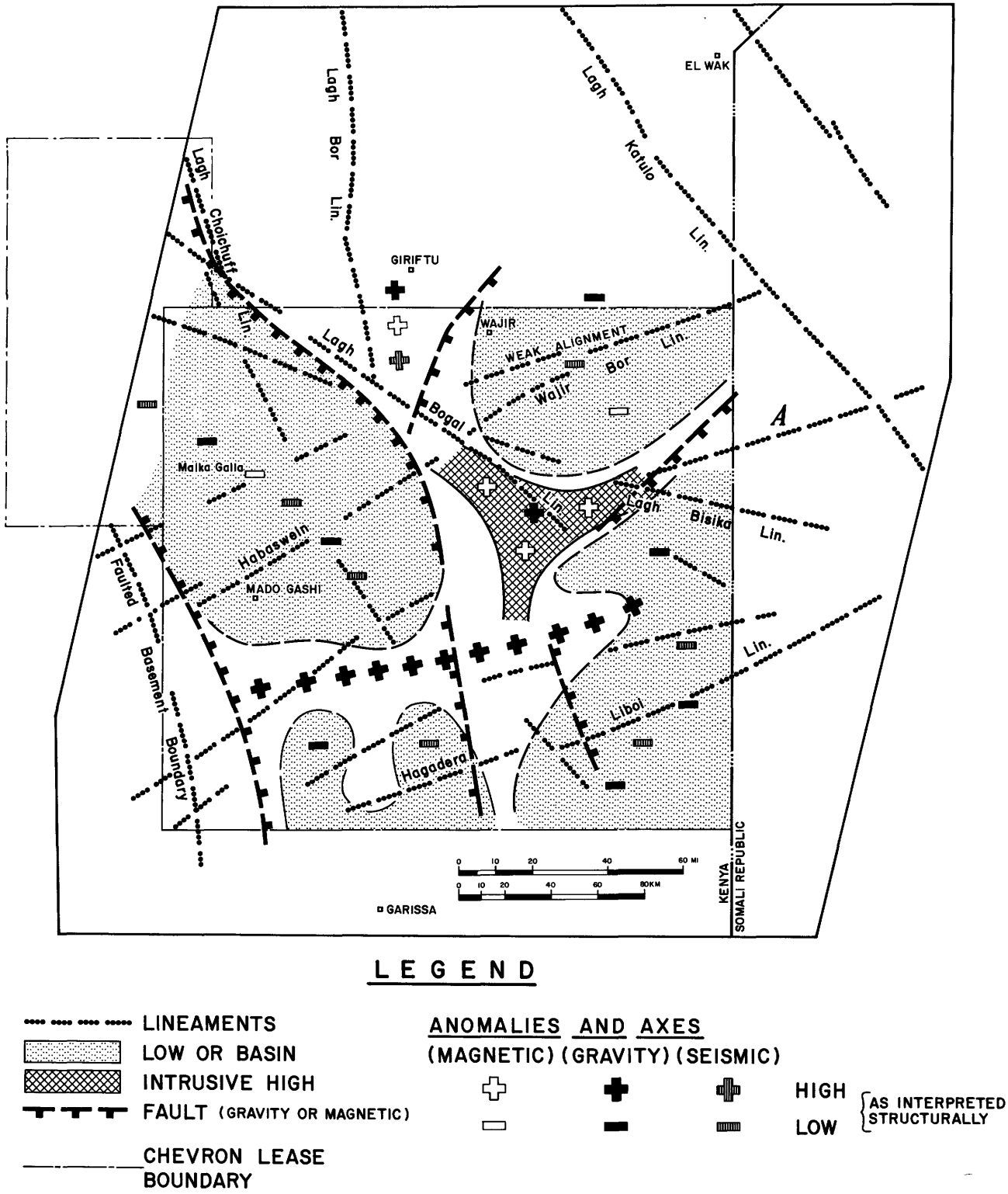

FIGURE 7.—Comparison of Landsat imagery structural features with crudely represented geophysical data.

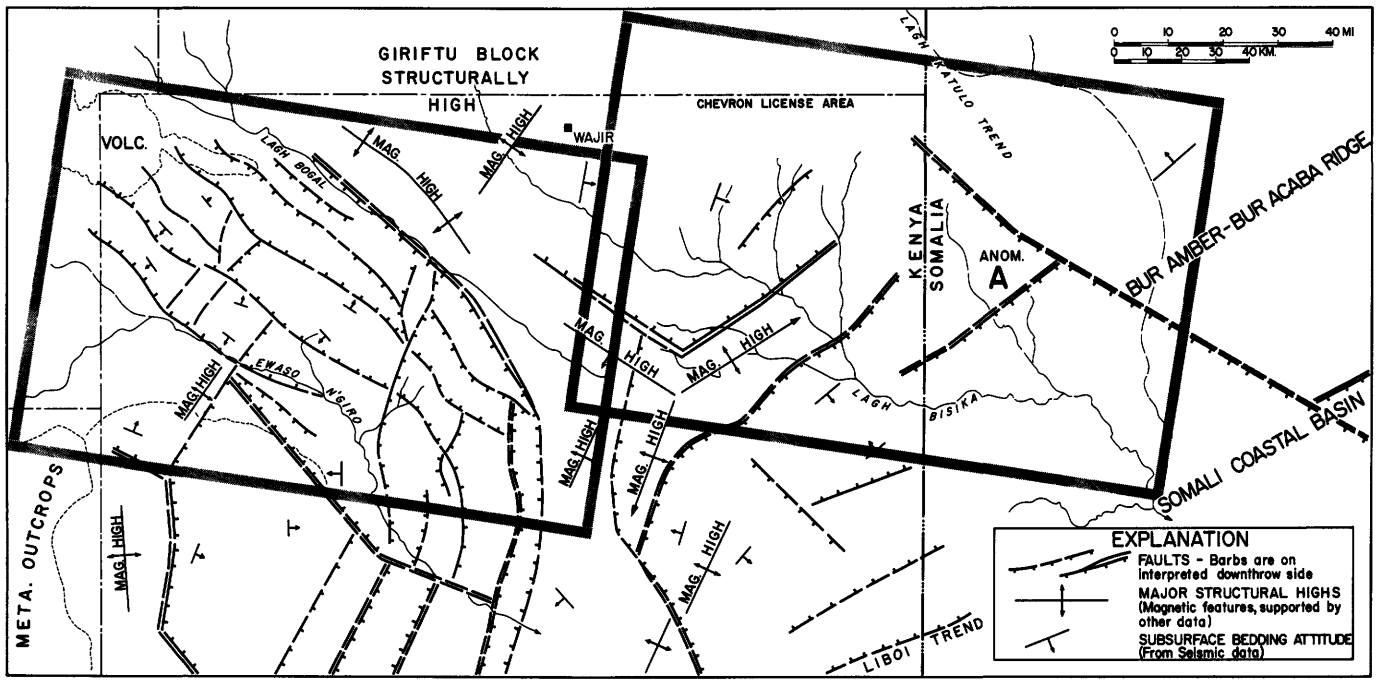

FIGURE 8.—Structural pattern derived from geophysical data over the northern part of the initial Chevron license. In Somalia, a less detailed pattern is located as well as possible from the small-scale published maps of Beltrandi and Pyre (1973). The shaded outlines define the position of the colored Landsat images reproduced in figure 6. These permit a comparison with imagery, maps, and descriptions given in this paper. The position of Anomaly A, in right part of map, is indicated.

Magnetometer and gravity data spread rather uniformly over the area of the Chevron license. There is also a grid of seismic lines over the whole area, but the principal density of seismic data is in the west. Very apparent is the triangular anomaly formed around the magnetic high in the eastern half of the Chevron holdings, caused evidently by a relatively shallow body of igneous rock, probably mainly intrusive. This anomaly appears as a central point within a distinct three-way branching of structure. The details shown within Chevron holdings are adapted from interpretations of geophysical data by Chevron geophysicists R. F. Flege and R. M. Wright.

There is insufficient information on structural control in Somalia to properly evaluate this part of the map. The differences in geology from the Kenya to the Somalia side of the border may well be caused by the relative spacing and position of data points. For example, inspection of the Landsat imagery, not all shown here, suggests the southeastward-trending fault which passes the Bur Amber-Bur Acaba ridge in Somalia as a probable extension of the Lagh Katulo fault. It is simply a little askew, as shown, and poorly located in the sector near the Kenya border.

more or less coincident with the inferred structural sag along the Ewaso N'Giro. A northeast and east boundary of this feature is evidently a fault. For a considerable distance, the fault lies along the Lagh Bogal lineament. About at the juncture of the Lagh Bor lineament it turns south through an area where there is no distinct, matching linear. It tends to die away near the center of the Chevron holding.

3. Rocks having high seismic velocities and the magnetic properties of basement project slightly into the license area in the Giriftu structural block, just east of the Lagh Bor lineament.
4. Shallow magnetic basement, probably igneous, lies along the Lagh Bogal and Lagh Bisika lineaments southeast of their juncture and about 80 km southeast of Wajir. A tonal Landsat lineament parallel to the Wajir Bor lineament extends northeastward from this point and bisects the feature called Anomaly A. As noted by geophysicist R. F. Flege, the magnetic and gravity anomalies which signify the presence of the igneous body are roughly triangular. Their shapes correspond with magnetic linearity in three directions about parallel to the Wajir Bor, Rudolf trough and Lamu embayment directions of structure. Conceivably, the magnetic anomaly may represent an igneous mass related to triple junction spreading.
5. The area north of this basement high, over part of Anomaly A and the entire northeast corner of the license area, has a thick section of sediments. This relatively basinal feature is confirmed by early results of seismic work.
6. A general gravity high trend crosses the area along a line just north of the Hagadera-Liboi

lineament. A magnetic high trend follows this in a general way. Basement along the crest of this feature, as compared to the flanks of the feature, appears relatively shallow.

Some differences and things yet unexplained are apparent also:

1. There appears to be no distinct downstepping of the basin from the carbonate shelf northeast of Wajir toward Anomaly A. Also, the apparent depth to basement within and immediately adjacent to the Jurassic outcrops is at least twice what it should be as judged from the stratigraphic measurements of the surface sections reported by Thompson and Dodson (1958), Joubert (1963), and others. Why this is so is not yet clear.
2. No substantial geophysical anomaly has been found along the Habaswein-Wajir Bor lineament. The Giriftu basement block seems to end near the lineament probably through downfaulting. West of the Lagh Bor lineament, no geophysical anomaly at all seems to be associated with the Habaswein-Wajir lineament. East of the town of Wajir, gravity data fail to detect the lineament. Magnetic and seismic data show a local, minor feature which seems to have neither great displacement nor continuity.
3. The transverse basement high aligned parallel to the Hagadera-Liboi lineament seems to terminate the structural trough which extends along a part of the Ewaso N'Giro. This trough, which lies in the northwest part of the license area, tends to end against the northwest flank of the high.
4. From geophysical evidence (fig. 8), the central structural depression along the Ewaso N'Giro is not directly along the valley of this stream as my foregoing analysis implies. Instead, it lies farther to the north and east, about at the Ewaso N'Giro–Lagh Bogal drainage divide. Possibly the present stream valley is eroded in softer ground where the duricrust was thin or along a line where faulting has weakened it.
5. Low velocity beds that seemingly would be Tertiary do not commence just southward of the Wajir Bor lineament, as predicted. Their first appearance is approximately at Lagh Bisika, some 70 or 80 km farther south.
6. Although phenomena coinciding with many of the major imagery lineaments are seen in the geophysical data, the features generated along a single lineament are often highly varied. A substantial number of the individual elements among these are elongated in direction of the lineament identified on airphotos. Yet from the geophysical evidence alone, one generally would not integrate them as a structural trend.

The idea that the Lamu embayment may have originated as an aulacogen, even though unproven, is partly supported by gravity data. Readings over the embayment are consistently higher than strongly negative readings generally obtained over the outcropping Precambrian rocks to the west. The readings are not anomalous to what is commonly regarded as a normal crustal thickness for continents.

Significant, however, is a three-way alignment seen among the structural components of the basin. This is quite apparent in figure 7 as well as in detail added by figure 8.

CONCLUSIONS

The results of the Landsat image study are analyzed here as they fit within an evolving program of exploring for oil in Kenya. They start with a review of geological knowledge initially available, progress through a comparison of Landsat image analysis with photogeology, and finally compare the results with what has been learned during the beginning and intermediate stages of geophysical exploration.

The Landsat information assists the geological program in two ways:

1. By helping to define an oil license area and the end of the Lamu embayment relative to a regional geological setting, and
2. By improving the definition of anomalies and lineaments significant to interpreting structure and stratigraphy. The area provides a severe test of the use of Landsat data, because surface geological differences within the license area are few and the relief very low. Almost all the important basin geology is concealed by young, flat-lying Pliocene and Quaternary fill. Useful ideas have sprung from the information extracted, and this is counted as progress.

In addition, the Landsat studies contributed evidence for suspecting subsidence along the Ewaso N'Giro near Malka Galla and suggested a branching arm of the basin toward the Rudolf trough. When supported by geophysical evidence, this led to filing on an option area adjoining the original Chevron license, thus extending the Chevron holdings.

Several of the anomalies are defined better on the Landsat images than on the airphotos. The Lagh Bisika lineament, as a distinct fracture direction, was

defined only from Landsat data. On the airphotos it might be thought of simply as a sub-fracture parallel to the Lagh Bogal lineament. The Hagadera-Liboi lineament and the Lagh Katulo fault are defined more completely on Landsat images than on airphotos. Anomaly A was not covered completely in airphoto work and did not become apparent until the Landsat images were examined.

On the other hand, substantial evidence in support of the Habaswein-Wajir Bor trends comes from the pattern of smaller fractures observed only on airphotos. In the Landsat imagery, this lineament—mainly seen as a tonal band—has its best expression northeast of Wajir extending into Somalia. Its coincidence with the north flank of the Bur-Acaba structural ridge appears more than coincidental. I believe the lineament is an important, valid structural feature and do not understand why the geophysical data in Kenya do not show it clearly.

The similarities of trends mapped by means of geophysics with many features of the Landsat and airphoto interpretation suggests that a great number of the chosen anomalies and lineaments are structurally valid. The directions are generally alike, even when the positions differ. Many Landsat lineaments are wide bands—10 km and more—where the position of the annotation or drawn line is rather arbitrary. There is also the chance of fault-line anomalies: surface traces shifted laterally from the phenomena that cause them.

The complex overall associations point to complex rather than simple geology. They are not conducive to an early and complete understanding.

During the Landsat image study, evidence was found of a previously unrecognized lithologic division within Pliocene deposits west of Garissa and also an internal depositional structure within Pliocene-Pleistocene deposits along a summit east of the Ewaso N'Giro. These proved helpful in understanding structural and basinal depositional patterns and in reconstructing basin history. And significantly, they show how Landsat images can function as a separate source of information.

In the Landsat interpretation, I have used a modified form of the usual techniques and skills of photogeology. The Landsat studies give an overview predisposed to finding regional anomalies, while airphotos more effectively look at local detail. The Landsat and airphoto work logically should go hand-in-hand, neither of them separately and alone, because each of them may lose the things most easily seen by the other. Landsat imagery adds multispectral data that are geologically useful. Most significant of all, Landsat studies have the advantage of very quick interpretation over new areas and regions. Such work saves time and money and gives a substantial basis for new ideas.

REFERENCES

Baker, B. H., and Saggerson, E. P., 1958, Geology of the El Wak-Aus Mandula area: Nairobi, Geol. Survey of Kenya, Report no. 44, 48 p.

Baker, B. H., and Wohlenberg, J., 1971, Structure and evolution of the Kenya Rift Valley: Nature, v. 229, p. 538–542.

Beltrandi, M. D., and Pyre, A., 1973, Geological evolution of Southwest Somali, *in* Blant, G., ed., Sedimentary basins of the African coasts: Paris, Assoc. of African Geol. Surveys, p. 159–178.

Brock, B. B., 1965, The Rift Valley Craton, *in* The World Rift System, International Upper Mantle Project: Geol. Survey of Canada Paper 6614, p. 99–123.

Caswell, P. V., 1953, Geology of the Mombasa-Kwale area: Nairobi, Geol. Survey of Kenya, Report no. 24, 69 p.

Caswell, P. V., 1956, Geology of the Kilifi-Mazeras area: Nairobi, Geol. Survey of Kenya, Report no. 34, 54 p.

Joubert, P., 1963, Geology of the Wajir-Bor area: Nairobi, Geol. Survey of Kenya, Report no. 57, 34 p.

Matheson, F. J., 1971, Geology of the Garba Tula area: Nairobi, Geol. Survey of Kenya, Report no. 88, 30 p.

National Aeronautics and Space Administration, Goddard Space Flight Center Earth Resources Technology Satellite Symposium, 2d, New Carrollton, Md., 1973, Abs.

——— Earth Resources Technology Satellite Symposium, 3d, Washington, D.C., 1973, Summary of Results.

Saggerson, E. P., and Baker, B. H., 1965, Post-Jurassic erosion surfaces in Eastern Kenya and their deformation in relation to rift structure: Geol. Soc. London Quart. Jour., v. 121, p. 51–72.

Saggerson, E. P., and Miller, J. M., 1957, Geology of the Takabba-Wergudud area: Nairobi, Geol. Survey of Kenya, Report no. 40, 42 p.

Sanders, D. L., 1959, Geology of the Mid-Galana area: Nairobi, Geol. Survey of Kenya, Report no. 46, 50 p.

Thompson, A. O., 1956, Geology of the Malindi area: Nairobi, Geol. Survey of Kenya, Report no. 36, 63 p.

Thompson, A. O., and Dodson, R. G., 1958, Geology of the Kerkali-Melka Murri area: Nairobi, Geol. Survey of Kenya, Report no. 43, 35 p.

Walters, R., and Linton, R. E., 1973, The sedimentary basin of coastal Kenya, *in* Blant, G., ed., Sedimentary basins of the African coasts: Paris, Assoc. of African Geol. Surveys, p. 133–158.

Williams, L. A. J., 1962, Geology of the Hadu Fundi-Isa area: Nairobi, Geol. Survey of Kenya, Report no. 52, 62 p.

PROCEEDINGS OF
THE FIRST ANNUAL WILLIAM T. PECORA MEMORIAL SYMPOSIUM,
OCTOBER 1975, SIOUX FALLS, SOUTH DAKOTA

Regional Linear Analysis as a Guide to Mineral Resource Exploration Using Landsat (ERTS) Data

By R. A. Hodgson,
Gulf Research and Development Company, Pittsburgh, Pennsylvania

ABSTRACT

The direct association of commercial mineral deposits with geologic features having a linear surface expression, such as faults and fracture zones, has long been known. Landsat data, displayed in appropriate formats, comprise a remarkably effective tool for recognizing and mapping several orders of such features in considerable detail. The data also allowed the definition of complex fracture-lineament systems over significantly large regions.

Regional fracture-lineament systems mapped to date show patterns that appear to be reasonably consistent with those predicted by theories which postulate such fracture patterns result from stresses generated by systematic and nonsystematic changes in the Earth's shape and/or shifts of the lithosphere with respect to the geographic pole.

As sufficient detailed data become available for large regions with respect to the areal distribution and nature of the various orders of linear features, it will become possible to evaluate better present fracture-tectonic theories as well as to establish empirically significant spatial relations between various types of mineral deposits and elements of the fracture network. Perhaps at that point it may become possible to develop a valid genetic theory for predicting in advance the location of environments specifically favorable for mineral deposits.

INTRODUCTION

The direct association of commercial mineral deposits with several orders and types of linear structural features such as faults, fracture zones, and joint systems has long been established. The fact that such structures commonly have a systematic spatial disposition has been well documented for over a century. Many mineral deposits occur along or at the intersection of linear structures where geologic conditions are favorable. Thus, any new technique should be investigated which promises to aid in the delineation of the spatial relations and structural characteristics of the various orders of linear features. The Landsat spacecraft provides a new platform for observation of such features and a very effective digital-analog system for the recording, display, and analysis of data.

The use of Landsat data to delineate and analyze regional linear features is, of course, quite recent. The Landsat system was not designed specifically for such a job but, as it turns out, has several features which make it particularly well suited for the purpose. The most important of these features from the standpoint of analysis are:

1. Synoptic nature of the imagery.
2. Temporal character (capability of recording the same scene every 18 days or every 9 days where both Landsat–1 and –2 are operational).
3. Very extensive areal coverage.
4. Capability for both digital and analog enhancement of images.
5. Unrestricted availability and low cost of raw data.
6. Variety of useful formats for analysis and display of data.

The Landsat system operates within a well-defined digital-analog framework and, therefore, imposes a specific approach in the analysis of the data by the investigator. Figure 1 is a flow chart showing the various steps and options in the use of Landsat data for minerals exploration.

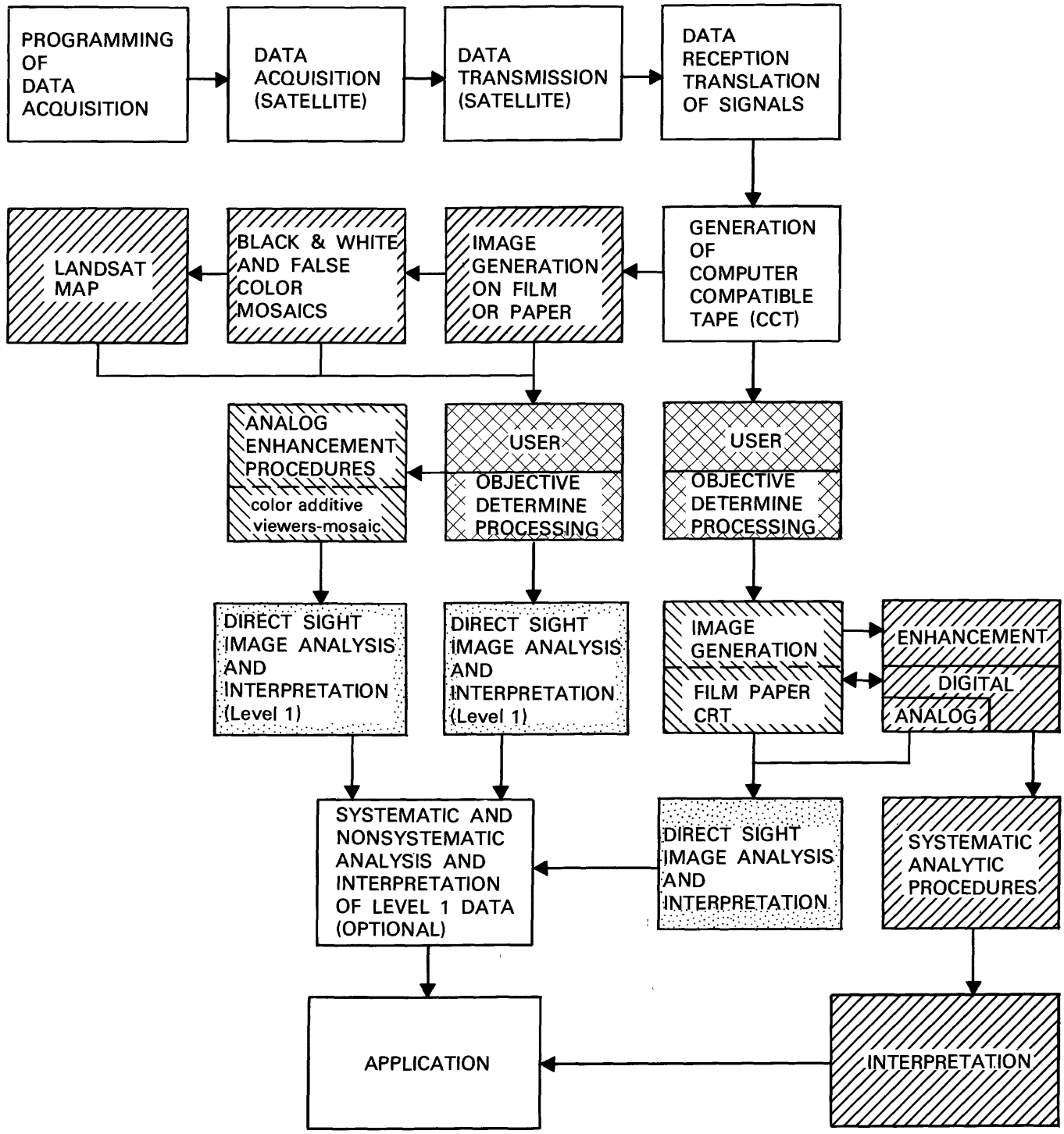

FIGURE 1.—Chart showing sequence of Landsat data flow from acquisition to application in minerals exploration.

PRIMARY FACTORS IN ANALYSIS

Before undertaking the analysis and interpretation of linear geologic features from Landsat images a number of factors should be considered which individually and together determine the effectiveness and validity of the results. These factors are outlined in figure 2.

The hardware and software characteristics of the Landsat system are most important in that they determine the ultimate resolution of any data acquired

1. CHARACTERISTICS OF DATA ACQUISITION SYSTEM
2. FORMATS OF DATA PRESENTATION
3. METHODS OF DATA ANALYSIS
   (METHODS MUST BE APPROPRIATE TO DATA)
4. METHODS OF DATA INTERPRETATION
   - LEVEL I—DIRECT SIGHT DELINEATION FROM PHOTOGRAPH
   - LEVEL II—APPLICATION OF THEORETICAL CONCEPTS
5. APPLICATION (EXPLORATION OBJECTIVES)
   - EXPERIENCE
   - THEORY

FIGURE 2.—Primary factors considered in use of Landsat data for analysis and interpretation of regional linear geologic features.

as well as the various data formats available for analysis and interpretation.

Analytic data handling procedures differ with digital and analog formats even though the objectives may be entirely similar. More detailed information resides in the computer compatible tape (CCT), for example, than in the photographic images for the same scene. With respect to regional linear analysis more information often can be gained from mosaics composed of the images of several scenes than from a single scene even though the scale and definition of the two photographic representations are the same.

It is important that the methods used to analyze Landsat data be appropriate to the nature of the data. This implies a working knowledge of the data systems as well as a knowledge of the geological parameters involved. For example, because of the synoptic nature of the imagery, the areal pattern of linear features can be established more effectively by direct inspection of the image than by a statistical treatment of data from a series of observations at points over the image.

The various options on digital enhancement operations should be considered carefully as some are more useful than others for enhancement of linear features. Inspection of images shows that the linear features are represented by a series of tonal or morphological events which can be visually integrated into a single large-order feature. Mathematical analytic procedures such as linear stretching and edge enhancing of the data tend to magnify or emphasize the changes in reflectance which identify linear features. Procedures such as clustering may help establish significant but not obvious areal differences in reflectance across a linear feature suggesting it may mark a fault zone or a geologic boundary, etc.

There are two distinct levels of interpretation involved in using the imagery to investigate regional linear features. The first level involves the identification and delineation of the various orders of linear features from the raw data. This may be accomplished by direct sight interpretation of photographic images or may involve a complex technology of data enhancement and viewing techniques. The end result is usually a map showing directly the structural character and spatial relations of the features sought.

At the second level of interpretation, theoretical concepts can be applied to the "observed" data and various established analytic techniques used to study some portion of the data content of specific interest. For example, one might consider that areal changes in angles of intersection of a certain class of linears is important or that a certain spacing or azimuth is critical. The results of such systematic analyses can be presented using contour maps, graphs, etc.

Where analysis and interpretation are being done for a specific exploration purpose, the exploration objectives must be kept in mind and the methods of investigation designed to abstract as much as possible of the desired information from the imagery. How the results are applied to the problem at hand depends, of course, on the experience and theoretical views of the user.

LANDSAT DATA ACQUISITION SYSTEM

Of particular interest to the interpreter are the main elements of the Landsat data acquisition system, inasmuch as the primary limitations on the use of Landsat data for regional linear analysis appear to reside primarily in the Landsat system itself and have to do with parameters such as spatial resolution, spectral bands recorded, the Earth's atmosphere, and data handling formats.

Landsat is a remote-sensing system that operates in limited and specific wavebands. It has a lower limit of spatial resolution which is significant from the standpoint of the interpretation of linear features. The manner in which the system records and transmits data determines to a great extent the digital and analog formats in which the data can be presented for analysis. The basis for these formats should be understood at least in outline so that unwanted bias is not introduced into the interpretation of linear features from the imagery.

The Landsat–1 spacecraft, from which the imagery discussed in this paper was derived, has two image acquisition subsystems. These are the Return Beam Vidicon, or RBV, and the Multispectral Scanner, or MSS. All the data used here for analysis are from the MSS. Figure 3 shows the main features of the MSS subsystem.

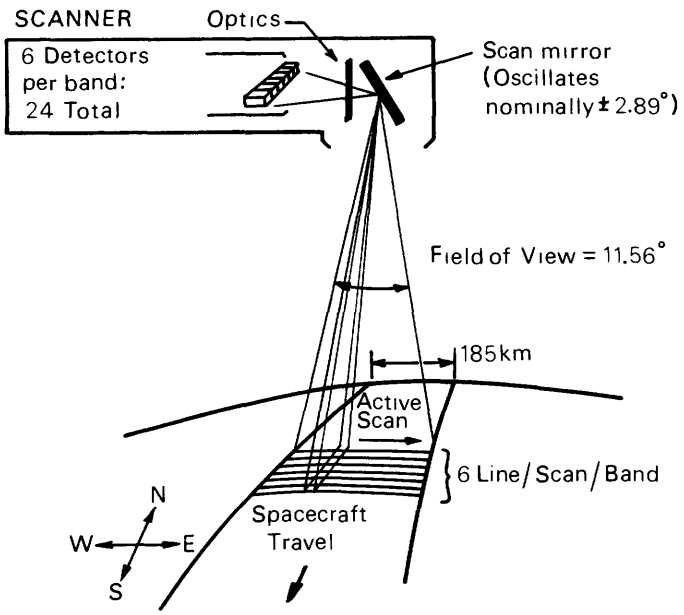

FIGURE 3.—Main features of the Landsat–1 MSS subsystem.

The MSS is a four-band scanner which operates in the solar-reflected spectral region from 0.5 to 1.1 μm. The four spectral bands are 0.5 to 0.6 μm, 0.6 to 0.7 μm, 0.7 to 0.8 μm, and 0.8 to 1.1 μm. There are six detectors for each of the four bands, and the spectral bands do not overlap. Scanning is accomplished by means of an oscillating flat mirror placed between the ground scene and a double reflector telescopic optical chain.

The video outputs from each of the detectors are sampled, commutated, and multiplexed into a modulated stream so that the data can be encoded and transmitted to a ground receiving station. At the receiving station, the raw data are compiled on video tapes which are transmitted to the NASA Data Processing Facility at the Goddard Space Flight Center.

At this point the data are converted into computer compatible tapes and 70-mm film images through the Initial Image Generating Subsystem, shown schematically in figure 4. These two products are the basic material which is used in one form or another for the mapping, analysis, and interpretation of geologic features.

A single Landsat scene comprises about 34,000 km^2 on the ground and the ground resolution of the system is about 80 m from the operational altitude of 918 km. As shown schematically in figure 5, any given

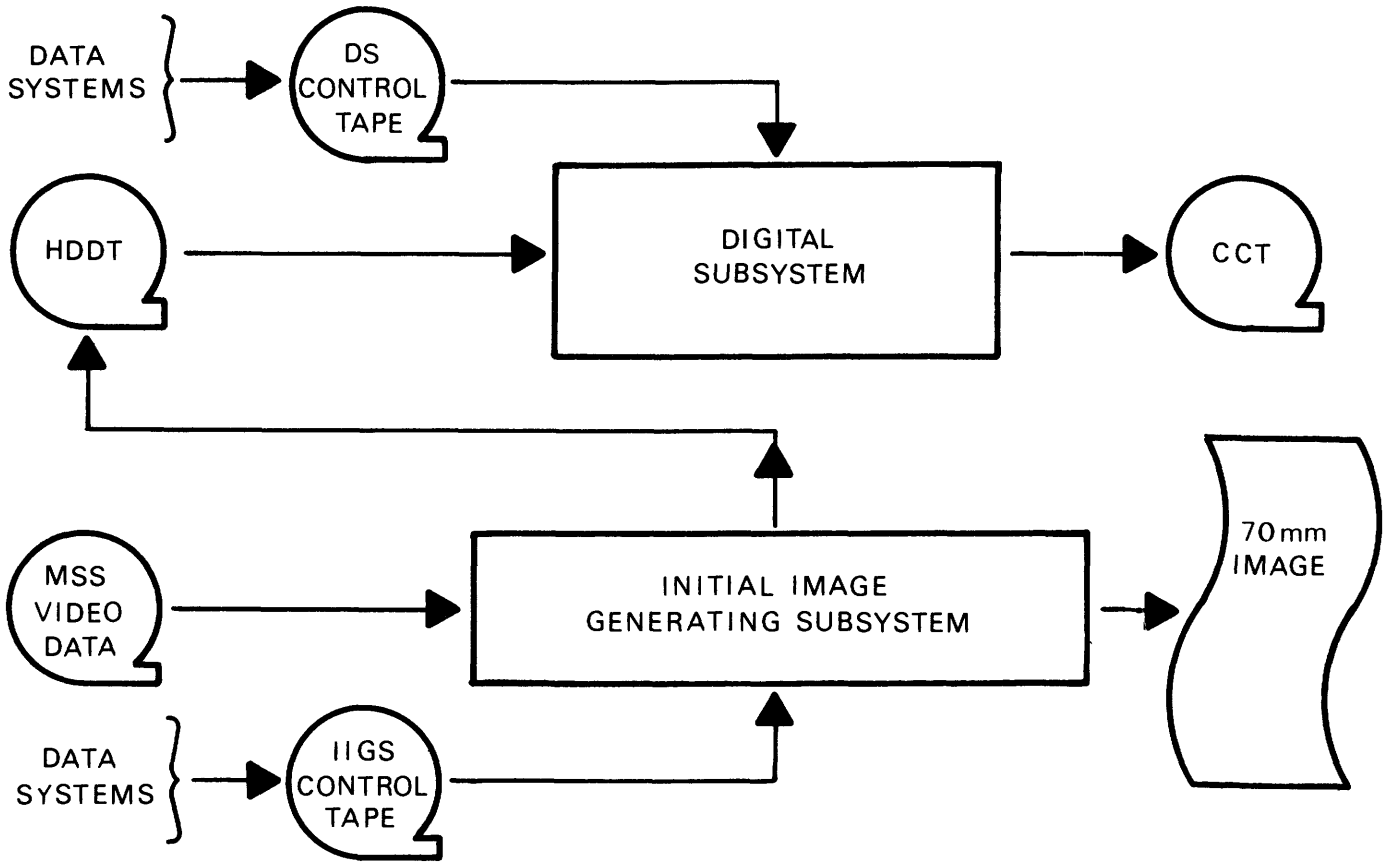

FIGURE 4.—Diagram showing configuration of the Initial Image Generating Subsystem.

image is composed of parallel scan lines each containing a large number of video data points. A film image of a scene can be generated from the MSS video data where the radiance levels recorded on the tape can be projected on 70-mm film at successive points along a scan line to produce pixels, or picture elements, in specified intensities or levels of gray. The resulting image looks very much like an aerial photograph from which, however, it differs significantly in several obvious respects.

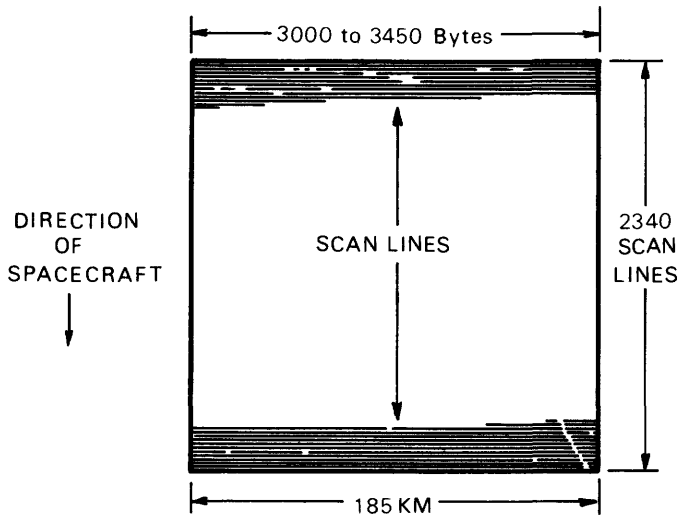

FIGURE 5.—Diagram showing the main elements comprising a Landsat image.

DEFINITIONS

The term "linear" as used by photogeologic interpreters has acquired some specific connotations with respect to length which are *not* implied where the term is used in this discussion. The term is used here in the general descriptive sense as defined by Webster; that is, the term pertains to a line or lines, consisting of lines, in a straight direction, resembling a line, narrow, long, and uniform in width.

In general, the regional linear features of the Earth's surface as seen on Landsat imagery can best be described by the technical term "lineament" as originally defined by William Herbert Hobbs (1904, 1911). Lineaments are generally found to be composite geomorphic and structural features when examined in detail and as shown schematically in figure 6.

The term "fracture zone" is used here to describe linear structural features (other than known faults) which have a direct expression on the Landsat imagery and can be reasonably inferred to be a direct expression of fracturing.

The term "planetary" is used to describe those regional or super-regional lineaments which are of a length, width, and linearity which would indicate they extend to great depths in the lithosphere. They are azimuthally distributed in systems that reasonably can be inferred to reflect their generation by the body forces of the Earth. In addition, they show morphologic similarities to equavalent features on the other

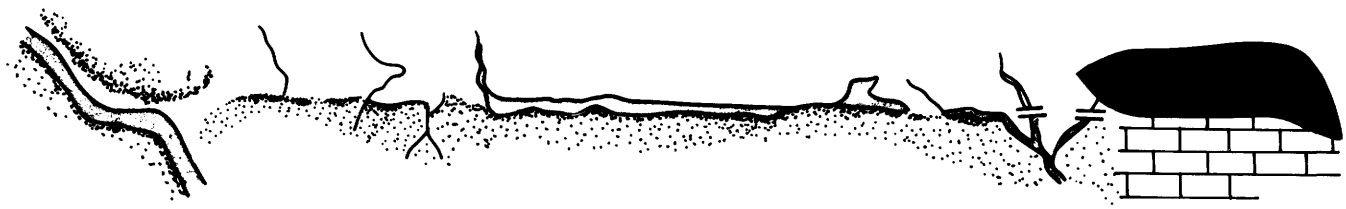

SCHEMATIC DIAGRAM INDICATING THE COMPOSITE EXPRESSION OF A LINEAMENT after HOBBS (1911)

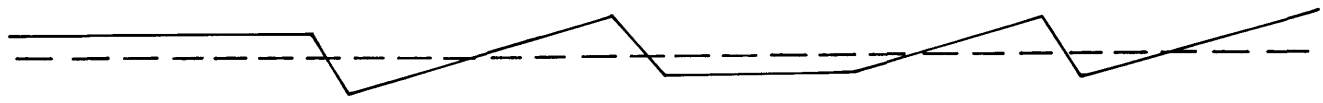

SCHEMATIC DIAGRAM INDICATING THE COMPOSITE NATURE OF DISLOCATION LINES after HOBBS (1904)

FIGURE 6.—Schematic diagrams showing the composite structural and physiographic aspects of lineaments.

terrestrial planets and so may be features which are common to all such planets and which are generated initially by similar forces.

BASIC TYPES OF GEOLOGIC STRUCTURES

The study of the nature of geologic structures suggests that there are two basic types which can be classed as continuous or discontinuous and distinguished on the basis of their distribution in time and space. The types of structures and the main characteristics which distinguish them are outlined in figure 7. The major linear features viewed on Landsat imagery clearly fall into the category of continuous structures. This is of great importance to minerals exploration as the universal and remarkably uniform distribution of these features as well as their persistence across all other structures of whatever age suggests some level of constant or intermittent structural activity along their length and at their intersections. As a result we may expect to find structures favorable for mineralization distributed more or less uniformly around the Earth in rocks of all types and ages.

BASIC TYPES OF STRUCTURES	
CONTINUOUS	DISCONTINUOUS
SYSTEMATIC JOINTS	FAULTS
MASTER JOINTS	FOLDS
JOINT ZONES	CLEAVAGE
LINEAMENTS	VOLCANIC
BELTS OF LINEAMENTS	CRYPTOVOLCANIC IMPACT
MAIN CHARACTERISTICS	MAIN CHARACTERISTICS
1. UBIQUITOUS OCCURRENCE IN ROCKS OF ALL TYPES AND AGES—NONREVERSIBLE	1. ISOLATED STRUCTURAL EVENTS IN TIME AND SPACE
2. MAINTAIN UNIFORM AREAL PATTERNS OVER VAST AREAS	2. NONUNIFORM AREAL DISTRIBUTION
3. UNIFORM SPACING MAINTAINED BETWEEN ELEMENTS OF EACH ORDER	3. CLEAVAGE AND FLEXURES—NONREVERSIBLE—EPISODIC
4. REGIONAL AND PLANETARY ORDERS CROSS *ALL* OTHER STRUCTURAL FEATURES WITHOUT DEVIATION OR OFFSET	4. FAULTS—REVERSIBLE (?)—EPISODIC
5. ALL SYSTEMATIC LINEAR FEATURES CROSS EACH OTHER WITHOUT DISCERNIBLE OFFSET	5. VOLCANIC—EPISODIC
6. LARGER ORDERS—COMPLEX STRUCTURES	6. CRYPTOVOLCANIC AND IMPACT—UNIQUE—NONREPEATED

FIGURE 7.—Basic types of geologic structures.

ORDERS OF SYSTEMATIC LINEAR FEATURES

Linear features seen at the Earth's surface occur in several distinct orders and, individually, range from a few metres to hundreds of kilometres in length. Within each order, they tend to occur in well-defined sets or systems which extend quite uniformly over very large areas. The main orders of systematic linear features are listed in figure 8.

The two largest classes of linear features are the subject of discussion here, but it is useful to consider that they may be end members in a continuous or intermittent series of genetically related structures at the other end of which is the systematic joint.

A field example of regional linear feature is the Florence Pass lineament (Hodgson, 1965). This feature is some 100 km in length and crosses the center of the Big Horn Mountain Range in Wyoming. The lineament is marked along its length by a series of deep valleys in Precambrian terrane where it crosses the highest part of the mountain. It is expressed as a monoclinal flexure in the sedimentary rocks on the gentle west flank of the range. These characteristics are shown in figure 9. Some normal faulting is present along the line of the lineament at the very crest of the range. A lineament of this magnitude is usually a complex structure of some width as was recognized long ago by Hobbs. Field examples of smaller orders of linear structures are shown in figure 10.

ORDERS OF SYSTEMATIC LINEAR FEATURES	
1. PLANETARY	DISTINCTION MAY BE BASED ON LINEAR EXTENT AS WELL AS CHARACTER
2. REGIONAL	
3. LOCAL	
FRACTURE ZONES	
MASTER JOINTS	
SYSTEMATIC JOINTS	

FIGURE 8.—Orders of systematic linear features.

FIGURE 9a.—Aerial view west along Florence Pass lineament showing physiographic expression of the structure. (Sketch after photo by R. A. Heimlich *in* Hodgson, 1965). See figure 9b, p. 162.

Figure 11 shows graphically the order of linear features which we are likely to see on Landsat images considering the ground resolution of the system as 80 m. As indicated in the figures, we can see only the widest of fracture zones directly, and then only under favorable lighting and environmental conditions. It is possible, however, to infer the presence and even the spatial relations of smaller orders of linear features indirectly. This is because of the distinctive reflectance signatures of vegetation and soils above fractures where the environmental conditions are slightly different from those in the immediately adjacent areas. Topographic features which develop preferentially along such linear fractures also reveal their presence. Obviously, there is no difficulty in seeing regional linear structures in Landsat imagery.

INTERPRETATION

Regional lineaments are not identified by a unique spectral signature but rather by a series of signatures. It is the difference in spectral signatures between any point or area along or within the lineament and that of areas immediately adjacent that makes the lineament visible.

The prominence of a given lineament may vary according to the spectral band in which it is viewed, but the larger lineaments are usually visible in all bands primarily because they are identified by differences rather than uniformity of spectral signatures and so may be marked by a wide spectral band of reflectances.

Digital data enhancement procedures, where used, should be designed to emphasize local spectral differences. This can be done by a number of mathematical operations such as linear stretching, edge enhancing, or by developing signatures and themes for areas along a lineament which, by inspection, appear favorable for defining the total extent of the feature. Analog enhancement procedures involve the use of color additive viewers, changing of scales and total area viewed, and the selective use of printing screens in making black and white photographic copy. The screen technique is particularly useful in that detail of the image is eliminated or de-emphasized without significant loss in distinction among gray levels. The end result is the enhancement of the larger linear features by increasing the apparent contrast between them and their surroundings.

The order, or size, of linear features recognized in direct viewing of images and mosaics is a function of the maximum ground resolution of the imagery which, of course, is the limiting factor in the ultimate amount of detail which can be seen and so determines the smallest order of linear structure which can be mapped. The two parameters of the imagery which can be varied within wide limits are scale and total area of the Earth's surface presented in a single view. Features not at all apparent, or seemingly poorly defined in a single scene, may show clearly on a mosaic at the same scale and in the same spectral band but depicting a much larger area. Decreasing scale tends to enhance the appearance of increasingly larger linear features as scale is reduced.

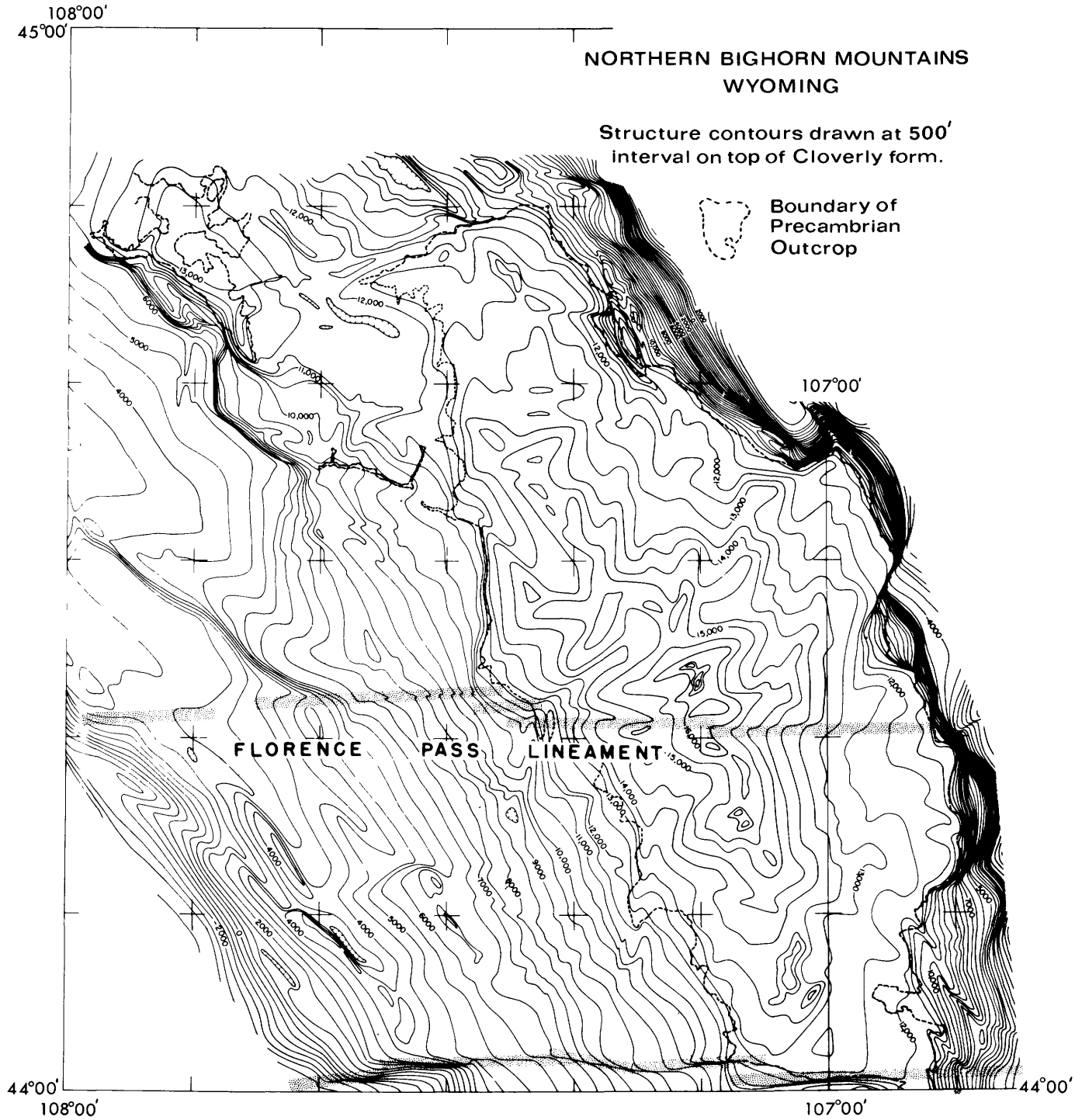

FIGURE 9b.—Structure contour map of the northern Big Horn Mountains, Wyoming, showing location and structural geometries of the Tensleep and Florence Pass lineaments. (After Hodgson, 1965.)

These observations and principles can be illustrated by showing examples of regional and planetary lineaments.

Figure 12 (p. XVII) shows a color composite image of a Landsat scene in the Great Basin and includes the area around Twin Falls, Idaho, and the region to the south. Looking at the image itself one can see a narrow but very distinct linear feature extending diagonally across the top of the image from left to right just to the south of the predominantly red area. From the changes in the colors of the surficial material and the fabric of the topography, it is evident that the lineament crosses a variety of physiographic and geologic features. It extends unbroken for a distance of nearly

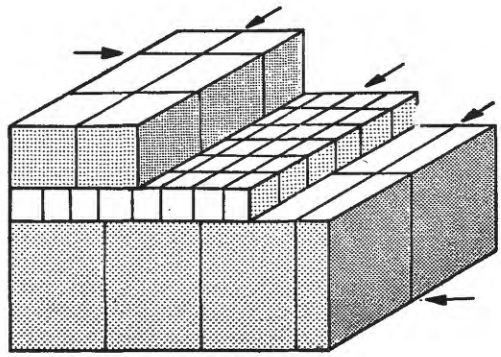

SYSTEMATIC JOINTS

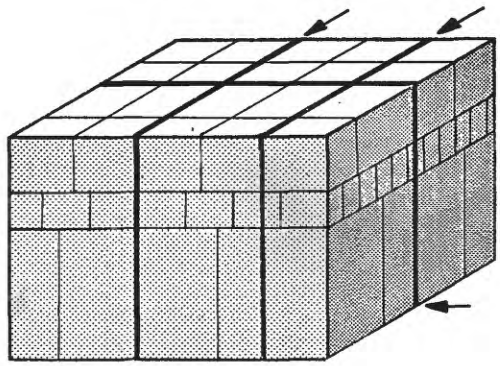

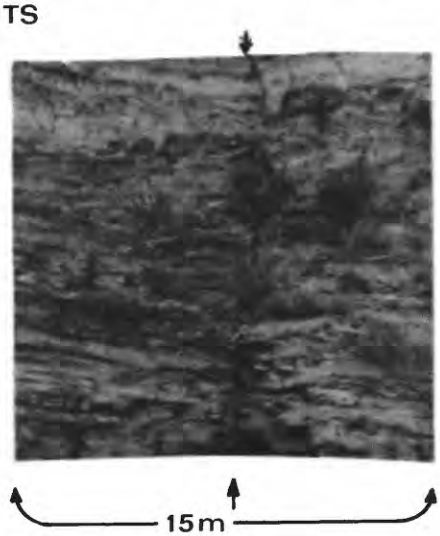

MASTER JOINTS

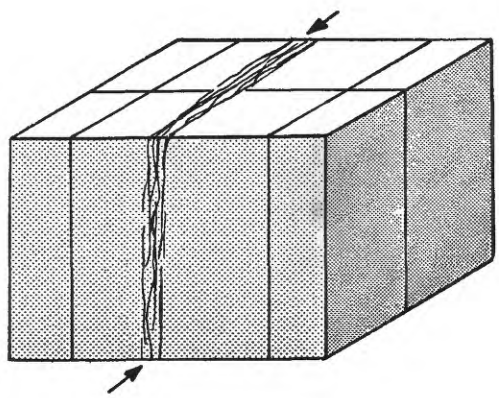

Joint zone deforming graywakes of the Lower Carboniferous strata dips about 25°- a quarry NE of Olomouc, Czechoslovakia. (Photo by Miroslav Plička)

FRACTURE ZONES

FIGURE 10.—Smaller orders of linear geologic structures.

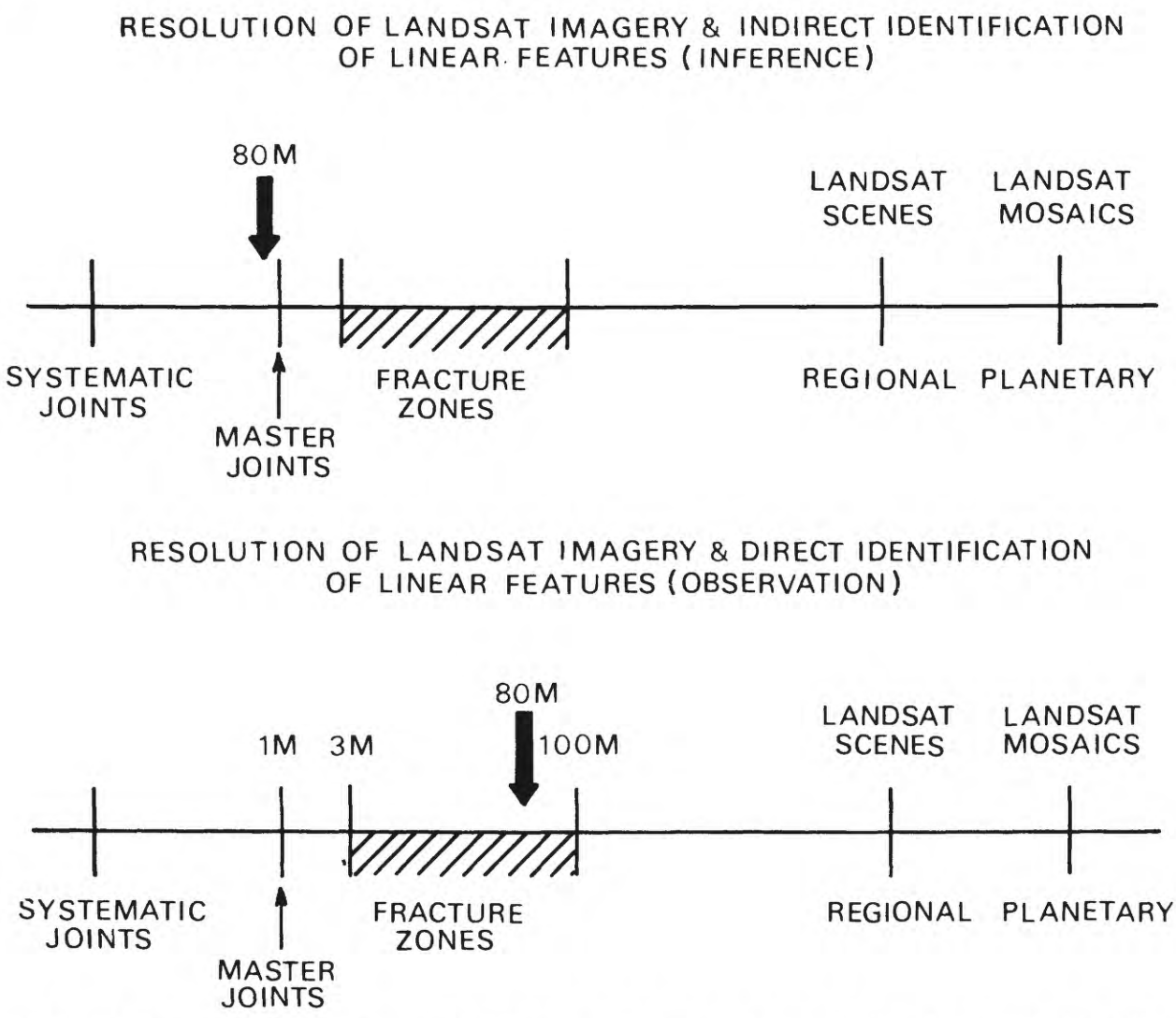

FIGURE 11.—Smallest order of linear geologic structure seen on Landsat imagery by direct observation or by inference.

a hundred miles in this scene. To determine how much farther it may extend in either direction would require enlarging the area viewed. The feature itself appears to be a wide fracture zone and may well include a number of normal faults. It maintains its remarkably straight course through mountainous terrain as well as flat lowlands and so must be essentially vertical in nature and extend to great depth.

Figure 13 (p. XVIII) shows the same lineament mapped to scale on the "Tectonic Map of the United States" (USGS and AAPG, 1961). The feature follows the trend direction of mapped faults and, in places, is coincident with them. It appears from the lineament that the structural trend of the west limb of the Snake River downwarp continues far to the southeast of Twin Falls. The fact that the Landsat feature shows so plainly is a good indication of recent tectonic movements along it. This also is information which can be readily checked in the field.

By increasing the size of the area viewed without losing essential detail, it becomes possible to map similar features to their full extent and to delineate larger features which cannot be defined initially on a single image. Figure 14 shows the western United States as depicted by the band 7 U.S. Department of Agriculture Landsat mosaic at the scale of 1:5,000,000. Less than half the visible lineaments have been mapped here, but enough are marked to illustrate the remarkable parallelism among sets of lineaments over very great distances. The light lines show individual linear features which appear to belong to a given set but are generally more irregular in their course than their neighbors. Note also the remarkable uniformity of spacing in places between members of the same

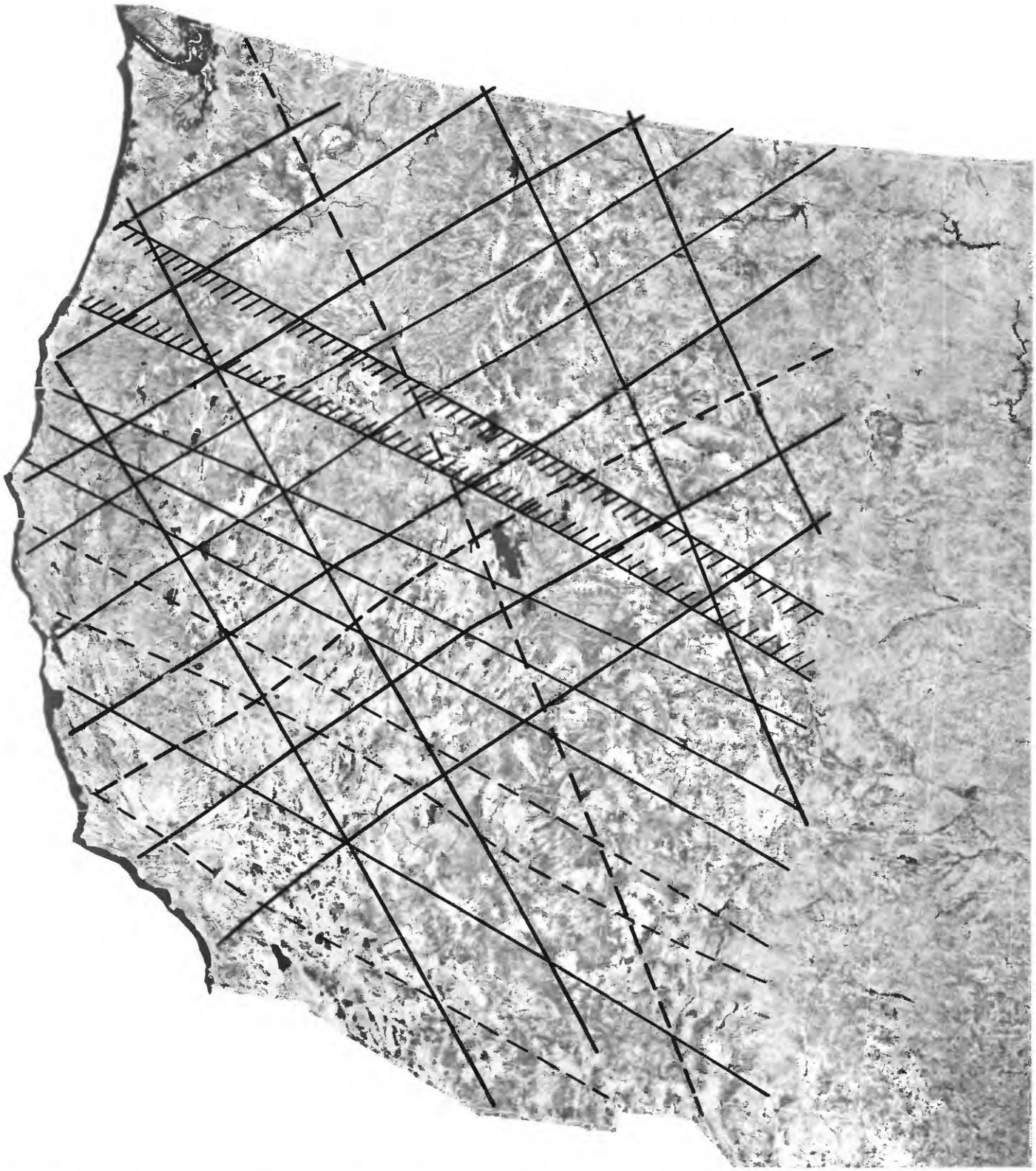

FIGURE 14.—Sets of major lineaments identified on the 1974 band 7 USDA Landsat mosaic of the United States at scale 1:5,000,000.

FIGURE 15.—First-order lineaments of the United States taken from the band 5 Mosaic of the United States as published in the July 1974 issue of Geotimes.

set and the orthogonal spatial relations between at least two of the sets. Of great tectonic significance is the apparent lack of offset of one great lineament by another where they cross each other and the lack of significant deviation where they cross major fold belts.

The broad band delineates a wide zone of several closely spaced parallel lineaments which, taken together, may comprise the largest order of lineaments.

One can continue to reduce scale and increase the area viewed to define larger and larger linear features, if they exist. As noted previously, the printing screen can be used to enhance the contrast of the larger features. Figure 15 shows the results of mapping lineaments which have a transcontinental extent (or at least a transmosaic extent) on the band 5 mosaic of the United States published as the center fold in July 1974 issue of Geotimes. (This is an example where the dot screen used in making the plate for printing the mosaic resulted in an enhancement of the largest linear features.) Several of the east-west lineaments show an excellent correspondence in geographic position with the great east-west fracture zones of the Pacific such as the Murray, Pioneer, and Mendocino suggesting they are in fact single continuous structures of global significance.

In detail, most of the major features recognized are composed of a connected series of structural phenomena along their length such as fault zones, fracture zones, linear folds and fold belts, and edges of regional features such as downwarps and upwarps, all constituting narrow, linear zones of deformation when considered at the viewing scale. A few lineaments are marked by what appears to be a single well-defined suture along their length. There is a generally systematic distribution for all orders of linear features. As a generalization, one can say they are distributed azimuthally in sets following approximately NE, NW, E–W, and N–S directions over very large regions.

At this point one can take the data derived from this first level interpretation of the imagery and use it directly to pinpoint areas which, on the basis of previous experience, promise to be prospective. One may, however, wish to proceed to the second level of interpretation in which the observed data are con-

sidered, not only in the context of previous experience, but also within the context of one or more hypotheses concerning the origin and significance of linear structural features and the manner in which they may exert control on the location and genesis of ore deposits. Thus, at the first level, the interpreter must decide on the nature and extent of the features which he has detected in the imagery and present the data in some form of direct use such as a map. At the second level, he may apply systematic analysis to the data and interpret this within the context of some hypothesis. As a result, the theoretical views and experience of the interpreter have a strong influence on the nature of the second level interpretation.

The observed systematic areal pattern of the major lineaments is reasonably compatible with that predicted by theories which postulate large-scale systematic fracturing in the lithosphere as a result of global deformation caused by systematic and nonsystematic changes in the rotation of the Earth or the position of its axis of rotation relative to the lithosphere.

The several theories that postulate crustal fracture patterns similar to those we observe on the Landsat imagery have been reviewed in detail in the literature by Sonder (1947), Vening-Meinesz (1947), and Belousov (1962). As a result of the investigations outlined here, it can be concluded that the tectonic forces which first produced the great Earth lineaments are global in nature and have to do with tidal forces and changes in the Earth's shape caused by changes in the rate of rotation of the Earth. These forces can be considered to act today at essentially the same level they did in the beginning, and the major lineaments have existed since then and have maintained a continuous low level of tectonic activity.

This hypothesis, if true, is significant in that it states that linear features have always existed in the Earth's crust as we see them today and, therefore, could have acted as channelways for mineralization at any time in geologic history.

If such uniform structural conditions for mineralization persisted through geologic time, has there been a uniform distribution of mineralization, or has there been any preferential mineralization along lineaments having certain azimuths? Are there ore belts along which we might expect certain types of minerals to be more plentiful than others? These possibilities have been considered, of course, and figure 16 shows a map by Nikolai Thamm in which he has marked the Silver Line of Spurr, noting incidentally that it follows closely a great circle. Thamm has also noted that

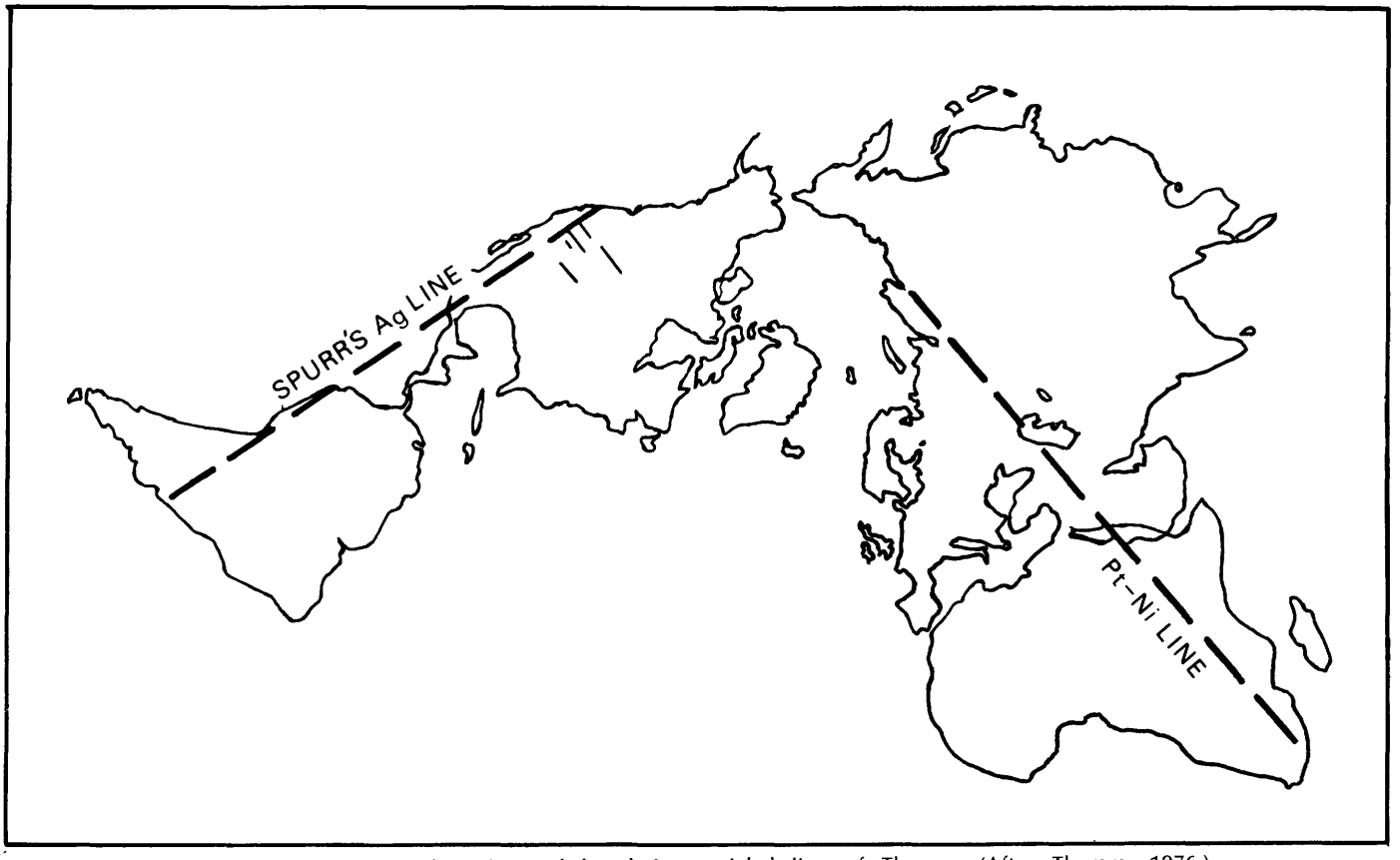

FIGURE 16.—Spurr's Silver Line and the platinum–nickel line of Thamm. (After Thamm, 1976.)

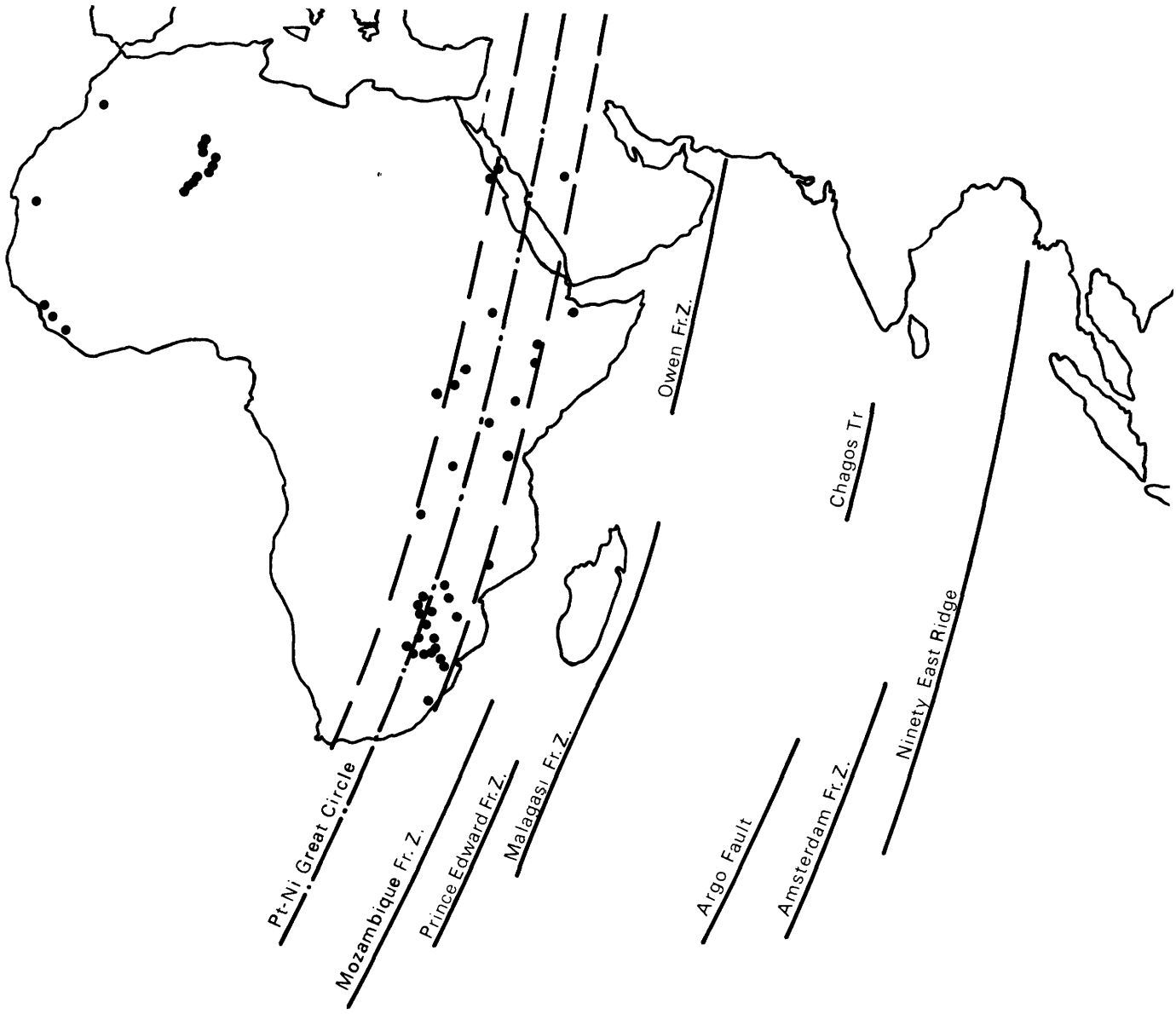

FIGURE 17.—Zonal distribution of platinum–nickel deposits along a Great Circle in eastern Africa. Note correspondence in azimuth with fracture zones and ridges of the Indian Ocean. (After Thamm, 1976.)

there appears to be a preference for the occurrence of platinum and nickel along a similar line or belt through Africa and the Middle East, Middle Europe and Siberia. This too follows a great circle. Figure 17 shows the southern portion of this zone in Africa where Thamm has noted a remarkable coincidence in trend and extent between the ore belt and the great fractures traversing the Indian Ocean. Thus, it seems that great ore channels may exist and follow the azimuths of great lineament belts. Within these belts we may find that actual mineral deposits are preferentially associated with a particular class or order of linear feature as suggested diagrammatically in figure 18. They may occur preferentially along a given set of lineaments within an ore belt, at or near lineament intersections, et cetera.

As a working hypothesis, we might start with Thamm's statement in his last paper (1976) that "All such zones, lines or belts seem to originate at considerable depths and more often than not, bear no relation to any surface structures. Just as with jointing, the existence of mineral-bearing zones is a permanent phenomenon, i.e., it re-appears with its identical mineralization after long periods of time and and after structural disturbances in an independent manner."

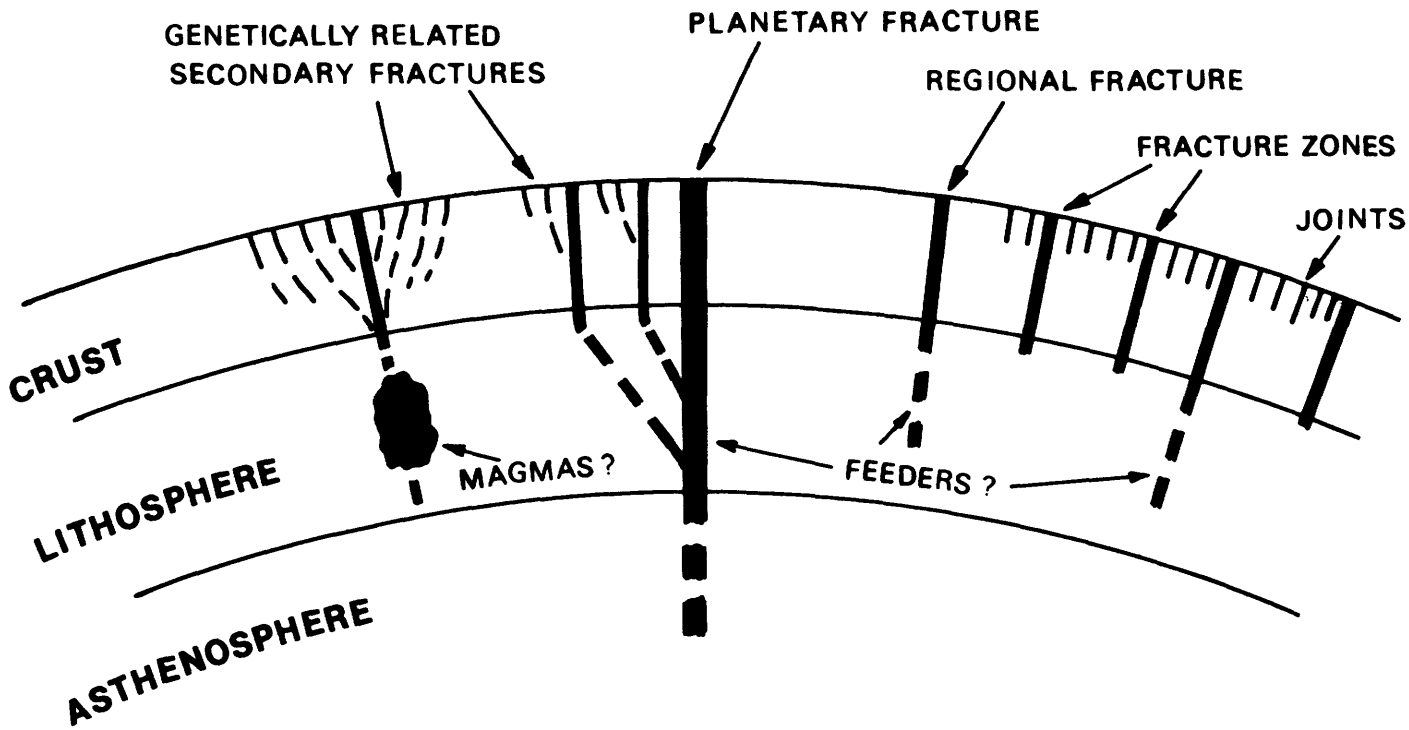

FIGURE 18.—Sectional diagram showing various orders of fractures which may be genetically related and which may control the location of mineral deposits.

CONCLUSIONS

In conclusion one can say that Landsat imagery offers a new and powerful tool for the delineation in detail of regional linear structures. It serves as a guide to pinpoint areas of direct interest to minerals exploration which can then be further investigated with conventional means.

The synoptic aspect of Landsat imagery, coupled with the amount of detail shown, largely eliminates the need for the statistical approach in mapping regional linear features. Their identification is direct and, in many examples, unequivocal. Systematic analytic methods should be directed primarily toward enhancing or abstracting some particular aspect of interest from the total observed data content.

The remarkably straight course of regional lineaments over tens to hundreds of kilometres shows they are vertical and must extend far into the lithosphere if not entirely through it in some cases. They may serve as channelways for mineral producing solutions from the greatest depths.

Persistence of regional linear structures across all other structures suggests some level of continuous structural activity along the lineaments. The possibility of periodic increases in the level of such activity must be considered.

It may be, however, that such activity, while promoting the upward movement of mineralizing solutions from great depths, may inhibit the formation of mineral deposits along the lineament itself near the surface. More favorable environments might be found along associated secondary orders of linear structures as suggested by Wertz (1976) and as diagrammed in figure 18.

We must consider that geologic features occurring along the same lineament, although separated by tens or hundreds of kilometres may, in fact, be genetically related and time equivalent.

Mineralization could occur in connection with the lineaments at any time in geologic history, at successive intervals along the same lines or belt and, involve the same mineral suites each time.

Detailed information on the location and nature of existing mineral deposits over large regions is needed to test the various existing hypotheses of the regional associations of mineral deposits and regional lineaments. Once such associations are established, it will increase our ability to extrapolate favorable conditions for mineralization into new areas and so decrease the costs of regional exploration by making the exploration programs more efficient.

SELECTED REFERENCES

Belousov, V. V., 1962, Basic problems in geotectonics (Eng. ed., J. C. Maxwell, ed.): New York, McGraw-Hill, 816 p.

Blanchet, P. M., 1957, Development of fracture analysis as exploration method: Assoc. Am. Petroleum Geologists Bull., v. 41, p. 1748–1759.

Gay, S. P., Jr., 1973, Pervasive orthogonal fracturing in Earth's continental crust: Am. Stereo Map Co. Tech. Pub. no. 2, 121 p.

Haman, P. J., 1961, Lineament analysis on aerial photographs exemplified in the North Sturgeon Lake area, Alberta: West Canadian Research Pub., sec. 2, no. 1, 20 p.

———1975, A lineament analysis of the United States: West Canadian Research Pub. Geology and Related Sciences, Series 4, no. 1, 27 p.

Hobbs, W. H., 1904, Lineaments of the Atlantic border regions: Geol. Soc. America Bull., v. 15, p. 483–506.

———1905, The correlation of fracture systems and the evidence of planetary dislocations within the Earth's crust: Wis. Acad. Sci., Arts and Letters Trans., v. 15, p. 15–29.

———1911, Repeating patterns in the relief and in the structure of the land: Geol. Soc. America Bull., v. 22, p. 123–176.

Hodgson, R. A., 1961a, Regional study of jointing in Comb Ridge-Navajo Mountain area, Arizona and Utah: Assoc. Am. Petroleum Geologists Bull., v. 45, p. 1–38.

———1961b, Reconnaissance of jointing in Bright Angel area, Grand Canyon, Arizona: Assoc. Am. Petroleum Geologists Bull., v. 45, p. 95–97.

———1965, Genetic and geometric relations between structures in basement and overlying sedimentary rocks, with examples from Colorado Plateau and Wyoming: Assoc. Am. Petroleum Geologists Bull., v. 49, p. 935–949.

Isachsen, Y. W., Fakundiny, R. H., and Forster, S. W., 1973, Evaluation of ERTS-1 imagery for geological sensing over the diverse geological terranes of New York State, *in* NASA Goddard Space Flight Center Symposium on Significant Results Obtained from Earth Resources Technology Satellite–1, 2d, New Carrollton, Md., Mar. 1973, Tech. Presentations, v. 1, sec. A, p. 223–230.

Kjerulf, Theodor, 1880, Die Geologie des sudlichen and mittleren Norwegen: Bonn, Gurlt, 350 p.

Krebs, Wolfgang, 1975, Formation of southwest Pacific Island arc-trench and mountain systems: Assoc. Am. Petroleum Geologists Bull., v. 59, p. 1639–1666.

Kutina, Jan, 1975, Tectonic development and metallogeny of Madagascar with reference to the fracture patterns of the Indian Ocean: Geol. Soc. America Bull., v. 86, p. 582–592.

Lillestrand, R. L., and Hoyt, R. P., 1974, The design of advanced digital image processing systems: Photogrammetric Eng., v. 40, p. 1201–1218.

Mollard, J. D., 1957, Aerial mosaics reveal fracture patterns on surface materials in southern Saskatchewan and Manitoba: Oil in Canada, v. 9, p. 26–50.

Pariiskii, N. N., 1960, Earth tides and the Earth's inner structure: Akad. Nauk SSSR Vestnik, no. 6, p. 61–69.

Pilger, A., 1976, The importance of lineaments in the tectonic evolution of the Earth's crust and in the occurrence of ore deposits in Middle Europe, in Internat. Conf. on the New Basement Tectonics, 1st, Salt Lake City 1975, Proc.: Utah Geol. Assoc. Pub. no. 5.

Polyakov, M. M., and Trukhalev, A. I., 1975, The Popigay volcanotectonic ring structure (Eng. ed.): Internat. Geology Rev., v. 17, p. 1027–1034.

Prucha, J. J., Graham, J. A., and Nickelsen, R. P., 1965, Basement controlled deformation in Wyoming province of Rocky Mountains foreland: Assoc. Am. Petroleum Geologists Bull., v. 49, p. 966–992.

Sonder, R. A., 1947, Discussion of shear patterns of the Earth's crust by F. A. Vening-Meinesz: Am. Geophys. Union Trans., v. 28, p. 939–945.

Spencer, E. W., 1959, Geologic evolution of the Beartooth Mountains, Montana and Wyoming, pt. 2, Fracture patterns: Geol. Soc. America Bull., v. 70, p. 467–508.

Stovas, M. V., 1957, The irregularity of the Earth's rotation as a planetary geomorphological and geotectonic factor: Geol. Jour. of the Ukrainian S.S.R., v. 3, p. 58–69.

Thamm, Nikolai, 1969, Great circles—The leading lines for jointing and mineralization in the upper Earth's crust: Geol. Rundschau, v. 58, p. 667–696.

———1976, The distribution of oil and natural gas deposits in the Earth's crust in relation to the mineralization with Ni, Pt, and Cr along Great Circles (abs.): Internat. Conf. on the New Basement Tectonics, 1st, Salt Lake City 1975, Proc.: Utah Geol. Assoc. Pub. no. 5, p. 617.

U.S. Geological Survey and American Association of Petroleum Geologists, 1961, Tectonic map of the United States, exclusive of Alaska and Hawaii: U.S. Geol. Survey, 2 sheets, scale 1:2,500,000 (1962).

Vening-Meinesz, F. A., 1947, Shear patterns of the Earth's crust: Am. Geophys. Union Trans., v. 28, p. 1–61.

Wertz, J. B., 1976, Detection and significance of lineaments and lineament intersections in parts of the North Cordillera, *in* Internat. Conf. on the New Basement Tectonics, 1st, Salt Lake City 1975, Proc.: Utah Geol. Assoc. Pub. no. 5, p. 42–53.

Wise, D. U., 1958, The relationship of Precambrian and Laramide structures in the southern Beartooth Mountains, Wyoming: Billings Geol. Soc., 9th Am. Field Conf., Guidebook, p. 24–30.

———1964, Microjointing in basement, middle Rocky Mountains of Montana and Wyoming: Geol. Soc. America Bull., v. 75, p. 287–306.

———1976, Sub-continental sized fracture systems etched into the topography of New England, *in* Internat. Conf. on the New Basement Tectonics, 1st, Salt Lake City 1975, Proc.: Utah Geol. Assoc. Pub. no. 5.

PROCEEDINGS OF
THE FIRST ANNUAL WILLIAM T. PECORA MEMORIAL SYMPOSIUM,
OCTOBER 1975, SIOUX FALLS, SOUTH DAKOTA

The Application of Remote Sensing Technology to Assess the Effects of and Monitor Changes in Coal Mining in Eastern Tennessee

By A. E. Coker, A. L. Higer, and R. L. Rogers,
U.S. Geological Survey, Tampa, Florida; Miami, Florida;
Roswell, New Mexico

ABSTRACT

In response to significant increases in coal mining activity expected in the Appalachians, an area with limited available data and rugged terrain, remote-sensing techniques are used to monitor and assess coal mining changes for investigating the effect of mining on water quality, sedimentation, and stream flow in this region. Digitally rectified and rescanned Landsat data were integrated with existing maps at a scale of 1:24,000. The images, acquired between February 1973 and March 1975, were used to analyze mining activities during this period. The processed data are also used to delineate land-water cover type including vegetation species and agriculture and water areas. These data are useful for updating maps of strip mining activity, updating assessments of coal reserves, and surface mine detection and monitoring. The mapping techniques utilized the Bendix MDAS (Multispectral Data Analysis System) system. Thermal imagery data are used to delineate ground-water outflow, acid mine drainage, ponding on strip-mining benches, storm runoff, and surface-water flow. These remote-sensing data provide information to aid development of a digital and pictorial data base.

PROCEEDINGS OF
THE FIRST ANNUAL WILLIAM T. PECORA MEMORIAL SYMPOSIUM
OCTOBER 1975, SIOUX FALLS, SOUTH DAKOTA

Exploration by Petroleum Independents Using Imagery and Photos from EROS and Manned Space Surveys

By R. W. Worthing, Consulting Geologist,
The Reserve Petroleum Company, Oklahoma City, Oklahoma

My early evaluation of the Landsat program was that it would be a high-cost through-put for the independent. I was wrong. The U.S. Geological Survey and Goddard Space Flight Center have made it available for the "poor-boy" oil company.

Nevertheless, problems exist. For example, the lack of ability to extract information from this wonderful aid to exploration results in a "hit and miss" approach, due to lack of training of independent geologists and engineers. This will soon disappear as user education increases. I hope soon that small company management or funders quit saying that "this erudite program is not for us."

This paper is concerned largely with lineaments as they relate to brecciation and improved carbonate petroliferous reservoirs, such as chalk, oölitic lime, dolomite, and clay-silica limes. The existence of these lineaments, containing hairline fractures, joints, or megashears, increases the rate of oil production from reservoirs of these types that account for more oil, over the world, than the sandstones.

The Landsat program and related underflights have been directly responsible for renewed interest in shear patterns on the Earth's surface because they have revealed anomalies that had been forgotten or perhaps had not been previously revealed. The extent of such shear patterns as seen on Landsat data has been noted frequently. In many areas, matching sets or pairs of shears are present at approximately right angles. These sets of shears at right angles are often recognized although one set may be more obscure than the other. What is less well known in areas, such as Oklahoma and the Illinois and Michigan basins, is that there are sometimes secondary and tertiary rectilinear joint sets, which are only clear locally and which are not widely recognized or accepted, although they are sometimes described as joint patterns. What is far more important to this presentation is the fact that new spectral bands of surveying have picked up secondary and otherwise very obscure joint sets, even sets that have been missed in previous geological data gathering.

Let us examine the newly recorded evidence of these phenomena which may be discerned at least faintly across the major portion of Oklahoma's Anadarko basin (Landsat image 1347–16462).[1] To me, these are indications of previously undetected regional tectonic directions. The well-known primary fracture sets in Oklahoma are N. 70°W. and N. 14°E.

It is also significant that the newly detected lineaments reveal a graben 5 miles wide and approximately 35 miles long not previously known and possibly of considerable importance in western Oklahoma. Only the previously known Seneca graben in northeastern Oklahoma approaches this in size. Needless to say, I intend to pay close attention to "Landsat" lineaments in the future and I believe their study will become a major chapter in the basic structural geology texts of the future.

In a different application, impressive work has been coming recently from West Coast studies of faulting and (or) earthquakes. The Landsat color print of San Francisco Bay (image 1075–18173) shows parts of the Calaveras, Hayward, and San Andreas (the Granddaddy) faults. On an image produced by combining bands 5 and 7 in black and white and enlarging the

[1] Copies of referenced images may be obtained from the EROS Data Center, Sioux Falls, South Dakota 57198.

image to approximately 1:125,000 scale, shear features are shown. I am told that Landsat has recorded many lineaments along which strain and (or) faulting has occurred in the California mobile belts. These are of considerable importance as a contribution to new earthquake knowledge. Incidentally, the association of this tectonic belt to second order anticlines containing very valuable oilfields has been pointed out in the literature by Moody and Hill (1956) and others.

Studies applying this type of tectonic analysis to the Michigan basin suggest that the Scipio-Albion field is a "baby" San Andreas structure. Scipio was discovered with the help of a crystal ball gazer. If this embarrasses the geologists, think of the evaluation engineers who said the wells would not pay—only to watch 140,000,000 bbl flow out between 1959 and 1968. The decline curve is still straight and very flat.

Some geologists agree that the Scipio-Albion field lies over a basement shear zone and more agree that the Trenton Limestone reservoir is not broken by faulting. A possibility of rock flow associated with strain or a strain lineament has been noted. The possibility of post-glacial movement of perhaps 1 mile does coincide with a lineament detected on Landsat imagery. The economic importance attached to lineament tectonics in the Michigan basin is impressive. Every oilfield in the Michigan basin with an accumulation of 10,000,000 bbl of crude oil (actually $100,000,000 of products at present prices) can be closely associated with such tectonic patterns.

Landsat images of the Saginaw Bay area (image 1320–15525) show three important geologic controls which mark the Michigan Thumb fault running from the Bay City area and controlling the southeast side of this fresh-water basin. On these images, the Arenac shelf can be seen protruding into Saginaw Bay as a result of movement along the Bay Rifle River lineament. The Arenac shelf lineaments come to the surface and are known to cause fracturing in the Bayport Limestone of Mississippian age; far more importantly, these lineaments have been associated with productivity in Arenac County amounting to as much as 1,600,000 bbl per 40-acre well and recoveries in the Deep River Pool are at least 40,000 bbl per acre. These are extremely high productivities for the U.S. oil industry.

Cores from reservoirs developed in fractured shear zones are typical of secondary dolomitization. The sharp black areas are high-permeability through-put channels that make these reservoirs excellent, and there is a coincidence of these zones with linear features expressed on Landsat data.

The Nisson anticline in the Williston basin is similar to the Scipio feature and has a string of pools with an expected production of 500,000,000 bbl. I think it is very important that there are two or three features that appear to be of similar mechanical origin in the Illinois and Michigan basins, and they are untested.

In an entirely different mineralized situation, let's look at the southern Illinois and Kentucky fluorspar districts which produce approximately 150,000 tons of fluorspar per year. The economic importance of this mineral may be measured by prices of $109 per ton and up for calcium fluoride (wet cake) and indications that prices may rise in a tight market. It now appears that a half dozen mining companies are active in the area and producing fluoride valued at up to $15,000,000 per year from an area with most unusual lineaments. These producers and possibly some of those prospecting, in the west, might take stock of these patterns and look for similar structures elsewhere.

There are at least six different directions of shear disturbances visible on Landsat data of the Illinois basin. One set, at least, appears to be important to the accumulation of highly productive oil pools found in the pre-Pennsylvanian carbonate rocks and seems to be closely allied with a similar pattern of major shear zones throughout the mid-continent area as well as the southern, middle, and northern Rocky Mountains. Oil and gas fields, in this area, are spatially coincident with these shear zones, and the same type of shear lineaments appear to be significant in the State of California where second order anticlines associated with these shear patterns are, quite obviously, controlled by the regional pattern. The major shear belts of the Rockies also seemingly control second order tectonic features which in turn may partly control the orebodies of the Colorado mineral belt.

The gross continental orientation of lineations, such as those shown in an analysis of major lineations of the United States, undertaken by W. D. Carter (*in* Fischer and others, 1976), may have far reaching scientific implications. In Carter's analysis, the orientation of the primary pair of shears appears to rotate clockwise as they approach the western edge of the continent; is this a reflection of continental mobility?

I would like to emphasize that the science of exploration may have experienced a new dawning in July 1972 and that as yet the new sun has not come up over the horizon. This is only a personal opinion, but I would like to restate that early skepticism on the part of individuals in the oil industry as to the value of the new imagery was premature, often resulting

from (1) poor images or mosaics, (2) lack of understanding, and (3) incorrect experimentation. Further, the independent exploration geologist lacks experience in putting the computer to work to realize the full value of the data. There is perhaps much disillusionment based upon not seeing that "particularly favorite crustal structure or geomorphic anomaly." Take heart; there can be a reason for this!

REFERENCES

Fischer, W. A., Angsuwathana, Prayong, Carter, W. D., Hoshino, Kazuo, Lathram, E. H., and Rich, E. I., 1976, Surveying the Earth and its environment from space: Am. Assoc. Petroleum Geologists Mem. (in press).

Moody, J. D., and Hill, M. J., 1956, Wrench-fault tectonics: Geol. Soc. America Bull., v. 67, p. 1227.

POSTSCRIPT

The ABC's of Discovery

A for Alluvial Deposition, Areal Geology, etc.
B for Below Surface Mining & Drilling Data, etc.
C for Color Photos—Computer Printouts, etc.
We can now say: *ABCD's of Discovery—ADD "D"*
D for *Determinations* and *Discovery* from *Space*

PROCEEDINGS OF
THE FIRST ANNUAL WILLIAM T. PECORA MEMORIAL SYMPOSIUM,
OCTOBER 1975, SIOUX FALLS, SOUTH DAKOTA

Tectonic Deductions from Alaskan Space Imagery

By Ernest H. Lathram and Robert G. H. Raynolds,
U.S. Geological Survey, Menlo Park, California

ABSTRACT

Inductive analyses (reasoning from specific data to general conclusions) based on compilations of detailed mapping postulate numerous tectonic and metallogenic lineaments. Landsat, NOAA, and Nimbus images provide successively more regional and general views, which permit direct observation of significant lineament patterns. Deductions based on these patterns are in accord with many inductively derived patterns and solutions and provide new insights into tectonics and metallogenesis.

Most major space image lineaments reflect zones of weakness, many of which have persisted since Precambrian time, and most of which reflect major tectonic discontinuities. These lineaments display coherent patterns throughout the North American Cordillera suggesting a consistent regional stress field. Subparallel sets of lineaments 1,000 km or more in length trend dominantly northwest, northeast, east and north. The pattern of these lineaments is considered to represent the surface trace of the boundaries of a mosaic of crustal blocks.

In Alaska, some lineaments (e.g., northwest-trending Yentna lineament) reflect differential movement of crustal blocks in response to contemporary forces of plate convergence. Others coincide with portions of sutures that reflect earlier plate interactions, and still others traverse successively accreted belts of continental crust, suggesting that continental masses and materials accreted to them react to the stresses of plate convergence by accommodation along lines of weakness preexisting in the continents.

Many inductively derived metal "province" outlines reflect lineament trends, and some areas of metal fecundity occur at lineament intersections. The use of space image lineament to define crustal block boundaries and the analysis of the metallogenic character within the area of single blocks may be a fruitful exploration tool.

INTRODUCTION

Lineament studies of continental masses have a common foundation in the work of Sonder (1947) proposing a "global regmatic shear" pattern for Earth, and of Katterfel'd and Charushin (1970) for Earth and other planets as well; a pattern resulting from stresses induced by the rotation of a planet on its axis. Moody and Hill (1956) modified this thesis and developed "wrench fault tectonics," later applied by Moody (1973) to petroleum exploration. Alinements of mineral deposits led Heyl (1972) and Snyder (1970) to postulate lineaments along the 36th, 38th, and 41st parallels in the United States and Kutina (1969) to formulate an empirical "shear stress net" of mineralizing lineaments in the western United States. Many others, among them Thomas (1974), Roberts (1964), Sikabonyi and Rodgers (1959), Tweto and Sims (1963), Maughan (1966), Haites (1960), and Ozoray (1972) point to more local systems of fractures, believed to be crustal in origin and to have controlled the site or origin of oil or mineral deposits.

The most fascinating lineament studies in the past have been those dealing with features of the ocean floor. The combined work of many authors, summarized in the maps of Pitman, Larson, and Herron (1974), display a lineament system of oceanic ridges and nearly orthogonal fractures or transform faults. These have become a cornerstone of the new global tectonics. The discovery of concentrations of metal-rich brines and sediments along spreading plate boundaries has led to metallogenic concepts in these areas sim-

ilar to the concepts basic to lineament studies on the continents.

All of the above studies have one element in common—the derivation of general hypotheses through the synthesis of specific details, i.e., inductive reasoning. Even the quantum-jump from the hypothesis of sea-floor spreading to the theory of plate tectonics is inductive, resting as it does on the synthesis of scattered data developed through oceanographic study.

The advent of polar-orbitting satellite imagery, particularly that of Landsat, has for the first time permitted application of deductive methods through lineament study. For the first time, lineaments can be observed directly over large areas of the Earth, their pattern defined, and their geologic and metallogenic significance examined and amplified by specific study. Lineament studies from Landsat imagery have been pursued by many researchers and are reported primarily in Proceedings of various Landsat symposia (Freden and others, 1973, 1974; Smistad, 1975), the First International Symposium on the New Basement Tectonics (Hodgson, Gay, and Benjamins, 1976) and the First William T. Pecora Memorial Symposium (this volume). Most of these Landsat studies have concentrated on areas the size of several states or smaller, and many have been concerned with analyses of the number and concentration of linears, i.e., "linear populations." To our knowledge, only three studies (Carter, 1974; Haman, 1975; and Hodgson, oral commun., 1975) have treated the distribution of Landsat lineaments throughout the conterminous United States.

Metallogenic modeling has occupied the attention of many earth scientists. Earlier models based on the classical geosynclinal theory generally related exogenic deposits to crustal downwarping, plutonism, and associated hydrothermal activity, primarily in mobile zones. Most recent models (see Guild, 1972), based on contemporary plate tectonic theory, associate exogenic deposits with subduction or mantle upwelling along plate margins. Repeated tectonism or plutonism, changes in the rate of subduction, or the development of new plate margins are believed to generate differing epochs of mineralization. As Kutina (oral commun., 1975) and others point out, however, many deposits occur in continental interiors distant from mobile zones or plate boundaries, under conditions difficult to reconcile with either tectonic theory, despite application of "intracratonic," "platform," "intraplate," "small-plate," and "migrating plume" theories.

Lineament studies of continental masses have generally presumed exogenic deposits to be related to crustal fractures, or zones of weakness, which have provided pathways for mineralizing agents to rise from a general source in the lower crust or upper mantle and form deposits wherever host conditions were propitious.

Our approach to metallogenic modeling combines the new dimension of space image lineament study with tectonic knowledge and theory to develop new insights into continental tectonics. Through these additional parameters, we attempt to identify viable new rationales for mechanisms of mineral concentration and favorable locales for mineral exploration.

We have chosen to concentrate our attention, not on linear populations, but on the location and pattern of continental-sized lineaments—those 1,000 km or more in length—and their geologic, tectonic, and ultimately metallogenic significance. We have also chosen not to limit our study to Landsat imagery. If our conclusions (Lathram and Albert, 1976) are correct, that abundant, short, sharp linear features reflect the youngest deformation of the upper lithosphere and tend to mask less abundant, longer, and more diffuse lineaments marking deeper crustal structures, and the conclusions of Shapiro (1971) that all imagery contains comparable *quantities* of data and only the level of generalization changes with altitude and scale of viewing, imagery from other satellites will assist in regional lineament study. This is analogous to the practice in airborne magnetometry in which the flight altitude is increased to observe deeper magnetic fields. Accordingly, we have analyzed imagery taken by Nimbus (1,100-km altitude, ~3.7-km resolution) and NOAA (1,500-km altitude, 1-km resolution) as well as Landsat (900-km altitude, 80-m resolution) satellites. All analyses have been by visual examination of photographic prints and mosaics, primarily the Landsat mosaics of the U.S. Department of Agriculture and of the Canadian Department of Energy, Mines and Resources. We have examined geologic, tectonic, magnetic, and gravity maps and reports, and all the lineaments represented can be shown to coincide with known alinements or discontinuities in the character of lithospheric materials.

We have concentrated on space image lineaments in Alaska. However, because data on Precambrian and Paleozoic geologic history is sparse in Alaska, we have made a general examination of imagery of the western parts of Canada and the conterminous United States, where such data exist. We believe that conclusions as to the antiquity and recurrent nature of structures whose trace is marked by lineaments in these areas can be extrapolated directly to similar lineaments in Alaska along whose trace geologic, tec-

tonic, and geophysical anomalies or discontinuities indicate significant changes at depth.

Our studies suggest that a pattern of continental-sized lineaments, recognized in Alaska, extends over the entire North American Cordillera and probably over the entire continent. These lineaments reflect major crustal boundaries, and higher or more synoptic satellite views seem to reveal deeper and more fundamental structures. We believe that knowledge of the nature and history of these lineaments is not only important in unraveling the tectonic history of a region but is critical to understanding how continental masses react internally to the stresses of plate movement. This knowledge can lead to the development of even more fundamental tectonic theories than those of today, theories that reconcile both mobilistic and stabilistic evidence of lithospheric deformation. To us a lineament network as a guide to a "plumbing system" is too simplistic; we view the lineament pattern as a plan of a mosaic of crustal blocks (similar to that of Garson and Krs, 1976) whose horizontal and vertical jostling through geologic time has guided tectonic relief to Earth stresses and, concomitantly, has guided the emplacement of orebodies.

LINEAMENT PATTERN

Study of a 1971 Nimbus IV image resulted in identification of a number of previously unknown very long lineaments in Alaska (Lathram, 1972). Subsequent study of Landsat images and mosaics (Lathram and Albert, 1976; Lathram and Raynolds, 1975) revealed not only most of these lineaments and others as well, but also a possible geometric pattern. Further examination of the Nimbus and Landsat images and mosaics, and of images from NOAA 3 satellite has disclosed even more lineaments (fig. 1).

The lineaments identified occur as alinements of surface geologic structures, linear valleys or ridges, and linear changes in tonal contrast marking differences in soil type, soil moisture, or vegetation. Most of the major lineaments are composed of combinations of some or all of these. Most are broad and diffuse, some being poorly identifiable for short stretches along their length. Parts of the trace of many of the lineaments coincide with the trace of known major faults in Alaska of Cretaceous or younger age (Grantz, 1966), which are primarily strike-slip in character.

The number of large lineaments identifiable on space imagery of Alaska (fig. 1) increases from Nimbus (fig. 1A) to NOAA (fig. 1B) to Landsat (fig. 1C) views, i.e., from smaller scale, low-resolution images to larger scale, higher resolution images. Most lineaments visible on Nimbus and NOAA images can be identified on Landsat images, but on the smaller scale images they tend to be more diffuse and can be less accurately located. The more synoptic view of the smaller scale images, however, permits recognition of a greater length for some of the lineaments than that shown on the Landsat mosaics and also shows that some shorter, individual, alined lineaments are probably segments of a longer lineament that is only intermittently discernible. On the other hand, the sharpness of features in the higher resolution images may lead to selection of unrelated younger tectonic elements as representatives of the lineament, and cause its mislocation. Some lineaments visible on the low-resolution images are less easily recognized on Landsat mosaics. Examples are the curvilinear and circular features shown on the NOAA image (fig. 1B). They are recognizable on the Landsat mosaic but were identified only after they were recognized on the NOAA image.

It is also apparent that, at the scale and resolution of the Landsat imagery, the number of lineaments discernible, and their varied trends, tend to obscure a regular pattern (fig. 1C). This suggests that for the purpose of broad, regional tectonic study, the optimum scale and resolution may lie between that of the NOAA and Landsat imagery. This observation is supported by our increased ability to discern broad lineament systems in the conterminous United States by examining a lithograph print of the Department of Agriculture 1:5,000,000-scale Landsat mosaic (U.S. Geological Survey, 1974) and comparing it to the original 1:1,000,000-scale mosaic. Carter (1974) also had good success in identifying many of these lineaments by direct study of the 1:5,000,000-scale mosaic.

Identification of a systematic pattern of lineaments in Alaska (fig. 1D) required the elimination of a large number that constitute a concealing background. The lineaments shown on the Nimbus and NOAA images display a pattern, and we have found that they are marked by significant geological or geophysical anomalies or discontinuities along much of their length. These lineaments were used as guides in identifying the lineament pattern.

We are aware of the degree of subjectivity involved in the selection of individual lineaments forming the resulting pattern. Many other lineaments are parallel, or nearly so, to those selected, and through future study may be shown to be of greater tectonic significance. The number selected was determined by the scale of this study, to illustrate the pattern clearly and its existence elsewhere as well. A broadly comparable spacing is apparent (fig. 1D); Albert (oral commun., 1975) has noted in more detailed studies in

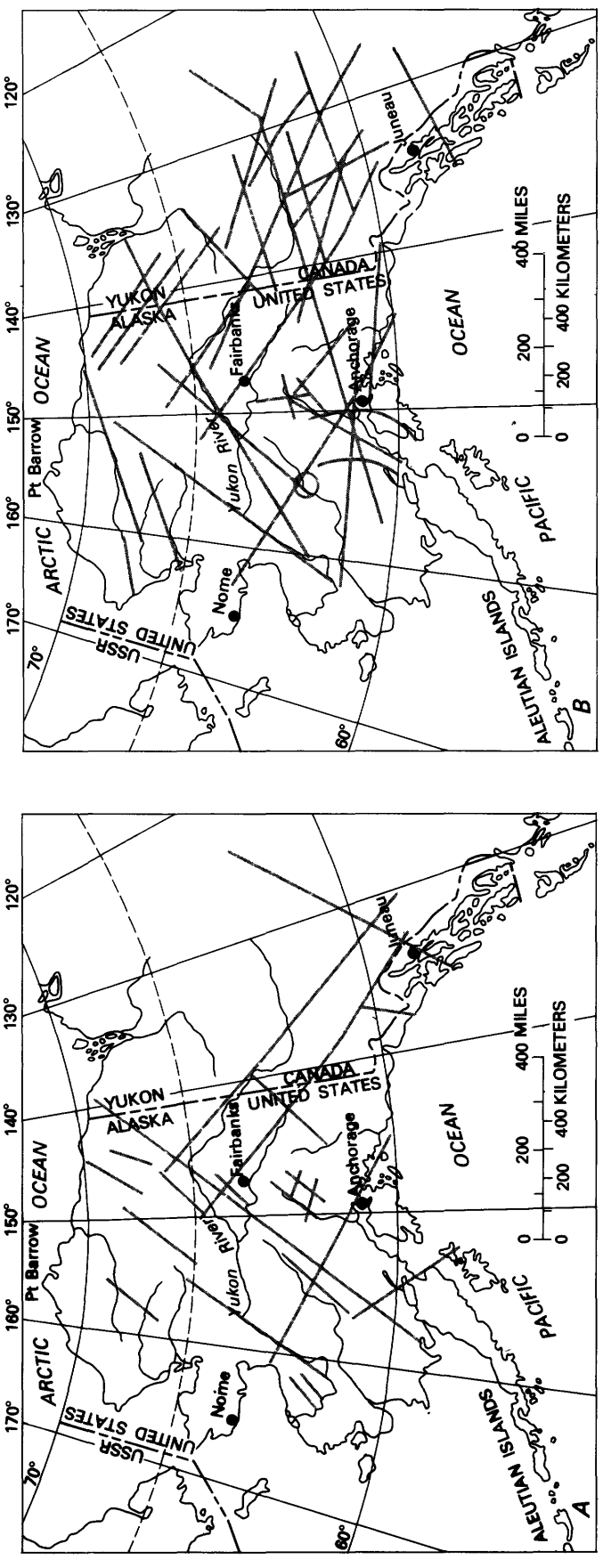

FIGURE 1.—Space image lineaments in Alaska. *A*, Nimbus satellite. *B*, NOAA satellite. *C*, Landsat satellite. *D*, Landsat lineament pattern. (See text for explanation of symbols on figure 1*D*.)

Alaska that major lineaments parallel to those shown occur with a general spacing of multiples of about 30 km.

It is tempting to assign firm compass measurements to the trends of these lineaments; however, the trend of most is not sufficiently consistent, and the orientation of the overall pattern seems to change slightly from area to area. This may be partly due to problems of map projection, but, if these lineaments do reflect crustal block boundaries and the blocks have moved differentially, one would not expect sharp, straight boundaries. Further, no persuasive model has yet been proposed to explain the mechanism of propagation of crustal features through overlying younger material. Hence, we are unsure how later tectonic movements would affect the trends of lineaments marking deep crustal features. For example, a number of the lineaments are transected by faults known to have significant lateral displacements, i.e., the Denali fault system, but are not themselves offset, suggests that later tectonic movements either had little effect or some mechanism exists whereby the lineament readjusts its trace. In order to permit some comparison of these lineaments with those in other distant areas, their trends in central Alaska are approximated to be roughly N. 40°E., N. 60°E., N. 50°W., N. 80°W., and N.

Previous study (Lathram and Albert, 1976) showed that lineaments having trends parallel to those of the pattern in Alaska also characterized the western United States. Examination of Nimbus and NOAA imagery, the new Landsat mosaics of western Canada and the Landsat mosaic of the western United States substantiates this conclusion and shows that the pattern recognized in Alaska extends throughout the North American Cordillera (fig. 2).

GEOLOGICAL AND GEOPHYSICAL EVIDENCE

It is impractical to discuss in this paper all of the geological and geophysical features that characterize the lineaments identified in the pattern (figs. 1D, 2). Consequently, we shall discuss briefly some selected lineaments in Alaska, mention some others elsewhere in the North American Cordillera for which evidence of antiquity and persistent movement is known, and compare the space image lineament pattern to lineaments or linear crustal fractures recognized in some previous inductive studies.

It is also impractical to include adequate geographic, geologic, or geophysical detail in the figures. Most of our data appear on the Tectonic Map of North America (King, 1969) and the Bouguer Gravity Map of Alaska (Barnes, 1976), which should be used in conjunction with this paper. Data that do not appear on these maps are referenced to the appropriate paper.

Examination of the supporting data will show that, whereas most lineaments are discernible throughout their length, many do not coincide with linear changes or disruptions in surface geology and/or subsurface geophysical data throughout their length. Portions of lineaments marking significant tectonic or geophysical changes are adjacent to portions that show none. We have no explanation for this, other than that the sensible adjustment on the boundary occurred prior to emplacement of the earth materials yielding the geologic or geophysical data. Therefore some mechanism must exist for the propagation of these lineaments through overlying strata.

Lineament A, the Tanana lineament of this paper (fig. 1D), trends along the Tanana River and northwest to Cape Lisburne in northern Alaska. At the Canadian Border, it separates the dominantly polymetamorphosed Precambrian(?) and Paleozoic Yukon-Tanana terrane from the Permian and younger arc-trench representatives to the southwest. In the Fairbanks area, it transects the southern margin of the metamorphic terrane but coincides with a marked change in structural trends within the terrane, a series of saddles in otherwise north-trending magnetic anomalies (Brosgé and others, 1970), and a zone of shallow microseisms (Gedney and others, 1972). Throughout this area the lineament separates two regimes of significantly disparate gravity anomalies. Through the Ray Mountains, between Fairbanks and the Koyukuk River area, structural trends are nearly orthogonal to the lineament, and no disruption in them or change in Permian and younger tectonic elements is evident, but the lineament follows a line marking a regional change in gravity measurements. In the Koyukuk area, it coincides with, and may have governed the location of, an anomalously northwest-trending Cretaceous basin in the Yukon-Koyukuk Volcanic Province of Patton (1973). Between the Koyukuk area and Cape Lisburne, the lineament marks a structural warp in mid-Paleozoic Brooks Range strata, a line dividing distinctive gravity anomalies under the Brooks Range from disparate anomalies to the south and southwest, and a line of change in structural style in Jurassic and Cretaceous formations northwest of the Delong Mountains (Lathram, 1974). If extended to the northwest under the Chukchi Sea, the lineament would coincide with the fault boundary between the extension of the thrust-faulted Paleozoic strata of the

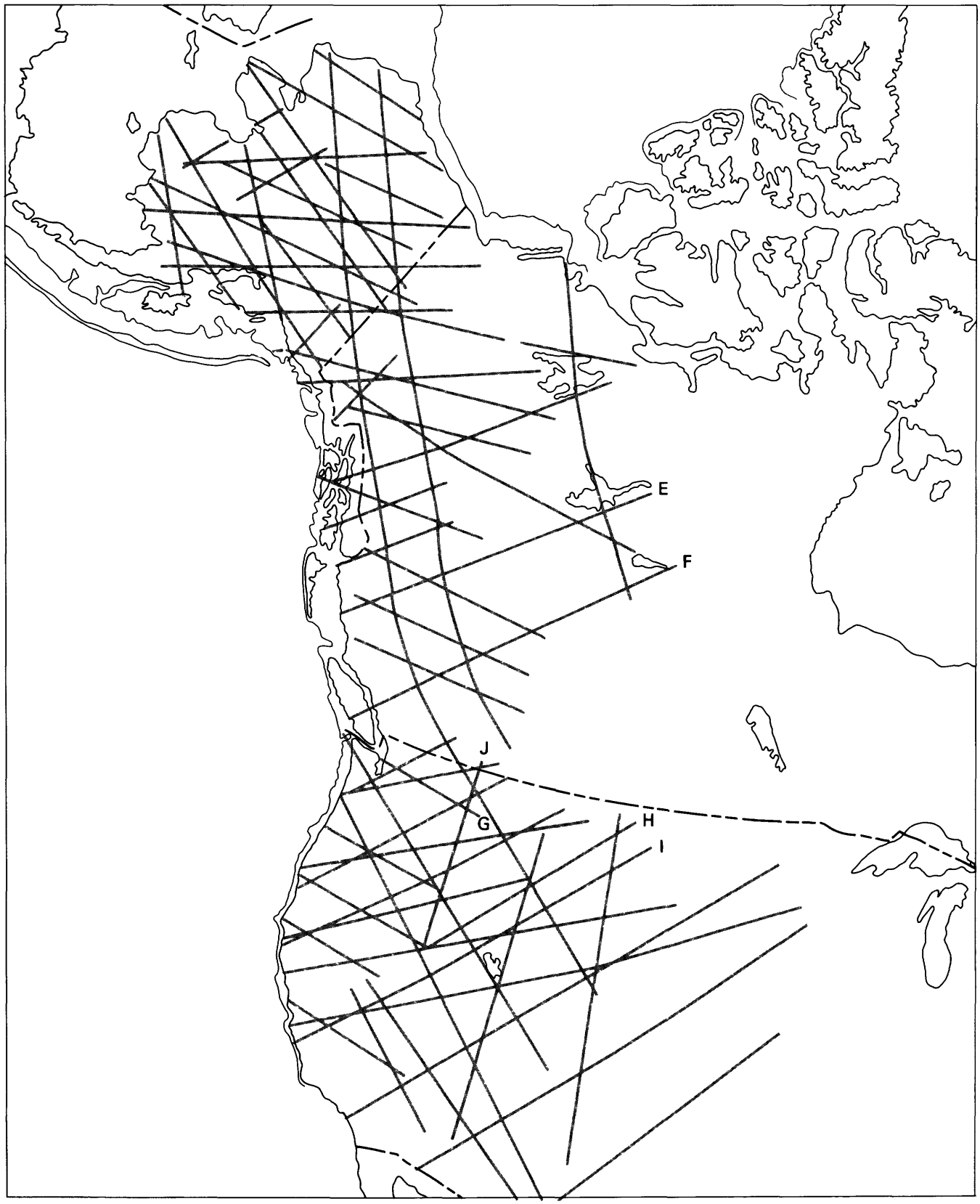

FIGURE 2.—Space image lineament pattern in North American Cordillera. (See text for explanation of symbols.)

Brooks Range orogen and the Mesozoic basin to the northeast (Grantz and others, 1975).

Lineament B (fig. 1D) coincides with the Tintina fault in Yukon Territory and extends northwest to Icy Cape. In the southeast, the lineament separates the unmetamorphosed Yukon stable block (Lathram, 1973) and MacKenzie Mountain thrust belt from the Yukon-Tanana metamorphic complex, and is followed by a series of magnetic lows (Brosgé and others, 1970) and an alinement of excursions in gravity contours. To the northwest, it marks the eastern termination of the Kobuk trench, the point of inflection of the Paleozoic schist and ophiolite rim of the Yukon-Koyukuk Volcanic Province, and a pronounced offset in the low gravity anomaly underlying the Brooks Range. Between the Range and the coast, the lineament parallels Mesozoic facies lines (Detterman, 1973) and bisects a broad gravity low.

Lineament C (fig. 1D), described by Lathram (1972) and Lathram and Albert (1976), may represent an early Paleozoic continental margin throughout much of its length, and is characterized by a series of gravity highs and alined gravity gradients.

Geologic and tectonic features along lineament D (fig. 1D) were detailed by Lathram and Raynolds (1975). Briefly, in the east, the lineament coincides with a fundamental fault separating Paleozoic and Mesozoic strata. In the Cook Inlet area, it marks significant changes in physiographic and magnetic features, is the northern terminus of the Aleutian Volcanic Arc and the northern boundary of the Jurassic intrusive core of the Alaska Peninsula. In the west, a young pluton is anomalously foliated parallel to the lineament on the Bering Sea coast. A pronounced line along which gravity contours change trend and strong linear anomalies terminate or seem to be offset follows the lineament through much of its length.

Elsewhere in the North American Cordillera, the lineaments are characterized by features whose nature and history are better known. Lineament E (fig. 2) is marked by the MacDonald or East Arm fault system and coextensive Hay River fault and Skeena Arch believed to have exhibited persistent movement since Precambrian time (Haites, 1960; Sikabonyi and Rodgers, 1959; Sutherland-Brown and others, 1971). Lineament F (fig. 2) coincides with the Athabasca-Peace River lineament, active since the Precambrian and particularly in the late Paleozoic (Sikabonyi, 1967). Lineament G (fig. 2) lies along and is a continuation of the Lewis and Clark line which, in the eastern Washington and Idaho area, has been persistent since the Precambrian (Sales, 1968). Lineaments H and I (fig. 2) correspond to postulated basement structures Eaton and others (1975) believe controlled the emplacement of the basalts of the Snake River Group. Lineament J (fig. 2) marks the line described by Yates and others (1966) and Taubeneck and Armstrong (1974) as the western boundary of Precambrian basement.

A compilation was made of the lineaments and crustal fractures proposed by a number of other authors through inductive analysis (fig. 3). The pattern of space image lineaments correlates well with many of these features, in general orientation, if not in specific compass trend, and many individual space image lineaments correspond to mineralizing crustal fractures. Although many of the long lineaments of the compilation (fig. 3) are based on physiographic expression, some of the long and most of the short linear elements are based on geological, geophysical, or tectonic evidence.

TECTONIC CONSIDERATIONS

The existence of a systematic pattern of space image lineaments 1,000 km or more in length and evidence that many (1) coincide with faults known to have been persistent since Precambrian time, (2) correspond to systems of mineralizing crustal fractures recognized locally, (3) mark significant changes in gravity and magnetic fields, and (4) bound fundamental tectonic elements suggest to us that these lineaments reflect boundaries between crustal blocks. Vertical and horizontal adjustments along these boundaries in response to Earth stresses have resulted in each block possessing different properties and a different history. This accords with the principal conclusions reached by Garson and Krs (1976) who recognized crustal block tectonics in the Red Sea area, reasoning primarily from geophysical data but also noting the coincidence of some Landsat lineaments with geophysical lineaments.

Recognition of the possible existence of a mosaic of crustal blocks in Alaska, each with a varied history of vertical or horizontal adjustment, helps to explain the known varied character and disjunctive distribution of basement rocks in the State.

A number of the lineaments evident in the North American Cordillera transect boundaries that have been considered to coincide with former ocean/continent interfaces without notable deviation in trend. Garson and Krs (1976) discussed the rifting of a continent to generate a spreading ridge (e.g., the Red Sea and Atlantic Ocean) and concluded that ancient crustal fractures determine the form and posi-

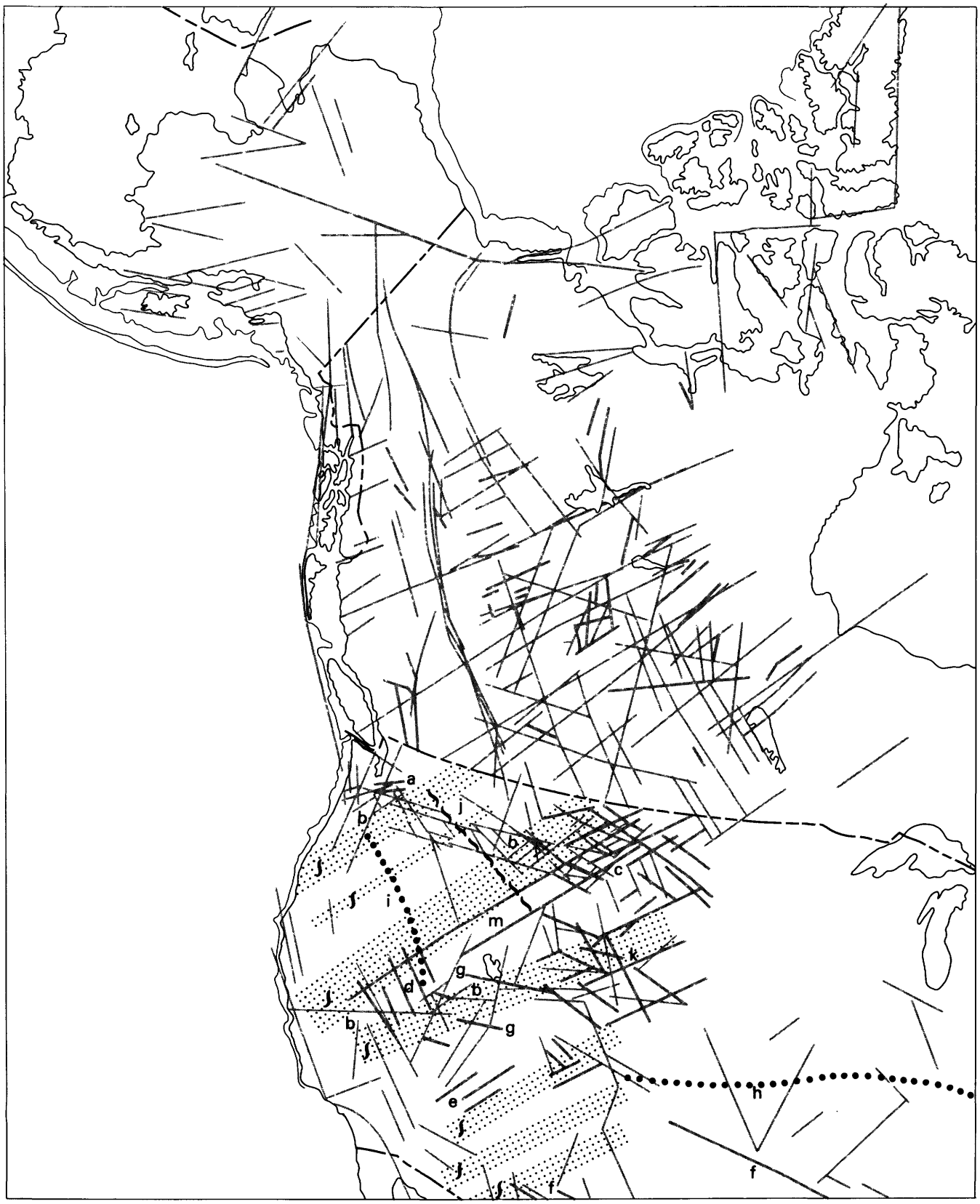

FIGURE 3.—Lineaments and crustal fractures suggested in selected inductive analyses. Compiled from: Moody (1966) and Ozoray (1972), (most long lineaments, fine line); and (a) Grant (1969), (b) Zietz and others (1969, 1971), (c) Thomas (1974), (d) Roberts (1964), (e) Shoemaker and others (1974), (f) Muehlberger (1965), (g) Cook (1957), (h) Heyl (1972), (i) Stewart and others (1975), (j) Yates (1968), (k) Maughan (1966), (l) Landwehr (1967), (m) Eaton and others (1975), (in western Canada) Haites (1960).

tion of the ridge and of the transform faults that transect it. In consequence, continental crustal fractures are traceable across passive continent/ocean boundaries into major transform faults. This conclusion does not hold for active continent/ocean margins, in which the two are decoupled, and for members of different plates. Indeed, in the Pacific Ocean, ringed by active margins, few transform faults have been demonstrated to be coextensive with either continental fractures or space image lineaments.

Our studies suggest that oceanic crust with active margins, whose spreading is not directly associated with continental rifting and whose structures may trend at angles to continental structures, will react with continental crust in a manner such that failure will occur along or parallel to lines of weakness preexistent in the continental crust. Accordingly, the preexisting lines of weakness in the continents will be reactivated, and extensions of these lines of weakness will develop in the products of the interaction as they are accreted to the continents. Sympathetic parallel lines of weakness will also develop in the accreted materials. This mechanism helps to explain the propagation of lineaments near active plate margins but does not explain their vertical propagation along passive margins nor within continental interiors.

From the foregoing, it is evident that the study of space image lineaments can provide insight into the nature of ocean/continent interactions and their effects within continental interiors. The Yentna lineament is an instructive example.

The Yentna (Y, fig. 1D) and parallel Tanana lineaments (A, fig. 1D) played a significant role in the interaction between the Pacific (oceanic) plate and continental Alaska in late Cenozoic time. The Yentna lineament forms the northeast boundary of a zone of pronounced change in trend of structures in the continental shelf (Von Huene and Shor, 1969), the northeast boundary of the segment of ocean floor warped in the 1964 Alaska earthquake (Plafker, 1969), the northeast boundary of the major interarc basin of Cook Inlet (Grantz and Kirschner, 1975), and the northeastern termination of the late Cenozoic volcanic arc of the Aleutian Islands and Alaska Peninsula. The lineament parallels the direction maintained by the oceanic plate vector in the Gulf of Alaska over the last 40 million years (Grow and Atwater, 1970). In the Alaska Range, the lineament coincides with the Yentna lineament of Van Wormer and others (1974) along which a warp occurs in the northwest-dipping Benioff zone, or zone of inclined earthquake foci. According to these authors, northeast of the Yentna lineament the Benioff zone is more steeply inclined and dips more northerly. The Benioff zone continues northeast beyond Mt. McKinley and terminates near the Tanana lineament.

These data suggest that movement of the Aleutian Arc-Trench system in the last 40 million years has been essentially translatory northwestward past the more resistant main continental mass of Alaska. The stress of plate interaction has been successively accommodated along crustal block boundaries parallel to and southwest of the Tanana lineament. The change in the Benioff zone at the Yenta lineament is suggestive of drag resulting from dextral shear. Southwestward of the Yentna, the volcanic chain of the Alaska Peninsula is segmented in plan, segment boundaries coinciding with lineaments at Lake Iliamna and at Controller Bay which trend northwest parallel to the Yentna and Tanana lineaments. To the west, a similar segmentation of the Aleutian Volcanic Arc has been noted (Jordan and others, 1965). The Tanana lineament also coincides in part with an earlier suture of Permian-Triassic age (Richter and Jones, 1973).

From the above phenomena, we conclude that adjustments in continental crust as a result of oceanic plate convergence have occurred along zones of weakness already existing in the continental crust. Continued adjustments have occurred successively along other zones of weakness parallel to these preexisting zones of weakness. We believe that the tectonized remnants of the Permian to early Cenozoic arcs and basins owe their present shape to accretion against a northern buttress formed of a northeast-trending early and middle Paleozoic continental shelf on the northwest and a remnant northwest-trending Precambrian and Paleozoic remnant volcanic arc complex in the northeast (Yukon-Tanana Upland). Northward compressive stresses which successively collapsed these arcs and basins against the continental mass (Richter and Jones, 1973; Jones and others, 1970) were relieved by decoupling along northeast- and northwest-trending fractures already existing in the continental crust, parallel to the trends of the buttress. Two of these fractures are now visible as northeast- and northwest-trending lineaments which mark the trace of parts of the Denali fault system in eastern and western Alaska.

Short, convex-east curvilinear features were noted in the area south of the Denali fault system on examination of the NOAA images (fig. 1B). They are less apparent, but present, on Landsat images and apparently are enhanced by the distortion of the NOAA images. These curvilinears do not accord with any of the lithologic or tectonic trends in the area, except the slightly convex-east arcuate pattern of volcanoes

from Lake Iliamna to the Yentna lineament. The Denali fault system exhibits a history of dextral movement since Cretaceous time, but there is also evidence of vertical movement in the segment west of the Nenana River (Grantz, 1966). The vertical movement in this area would accord with the presumed northwest shortening in response to crowding from the Tertiary arc complex, but the dextral movement is less easily understood. Clague and others (1975), studying the age of volcanic rocks dredged from the Hawaiian Ridge and Emperor Seamounts, recapitulated the case for the Hawaiian-Emperor bend forming as a result of a change from north to northwest in the movement of the Pacific plate over a melting spot in the mantle and added supporting evidence of progressive changes in age of volcanism that would ensue were this hypothesis valid. They conclude the age of the bend is 41 to 43 m.y. If such a vector change occurred, it would have impressed a counterclockwise rotation on the area south of the Denali fault system, engendering a dextral stress release along it. The curvilinear features may reflect this distortion and, therefore, be young and temporary.

METALLOGENIC SIGNIFICANCE

In an earlier study, Lathram and Gryc (1973) related some of the space image lineaments to the distribution of mineralized areas, and compared. this with the conclusions of Sutherland-Brown and others (1971) that areas of mineral concentration in British Columbia were related to the intersection of major through-going orthogonal structures. Preliminary comparison of the full pattern of lineaments developed in this paper to the distribution of mineral deposits in Alaska has as yet revealed no significant additional relationships. However, comparison of this pattern of lineaments to the empirical "shear-stress network" developed by Kutina (1969) in the western United States reveals that a large number of lineaments cross a number of highly mineralized areas, a large number of lineament intersections coincide with metal-rich areas (as do Kutina's "shear-stress" lines), and there is a striking correlation between the two patterns in orientation and spacing of individual elements. Further, the trends and spacing of lineaments of the space image pattern correspond closely to the trends and spacing of "deep-seated tectonic zones" recognized by Garson and Krs (1976) in the Red Sea area. Garson and Krs showed these zones to be related not only to mineral deposits in the continental crust but also to brine pools in the Red Sea. Further study of the pattern in Alaska, or modifications to it, should be fruitful for mineral exploration.

Many metallogenic experts, especially Clark and others (1974) in Alaska and Sutherland-Brown (1974) in British Columbia have also pointed to broad areas or zones of like mineralization which seem uncontrolled by major structures. Sutherland-Brown (1974, p. 54) in particular studied the regional distribution of metals as shown by geochemical sampling and concluded that the similarity between the pattern of mineral deposits and metal background means that the deposits owe their origin to the level of background in the terrane they inhabit—"the rocks have the ore deposits they deserve." On the other hand, Sillitoe (1974) has examined the known linear zonation of mineral deposits in the Andes and, using geologic discontinuities transverse to the length of the zones, has subdivided the Andes into tectonic segments, each with a metallogenic character different from that of its neighbors.

From the foregoing, we suggest that mineral concentrations may be expected along or at the intersection of space image lineaments that mark significant crustal block boundaries. We also suggest that the identification of major crustal block boundaries through the study of space image lineaments and the analysis of the tectonic history, geochemistry, and mineralization within each block (as opposed to broader regions or zones) may also be fruitful in mineral exploration. In fact, the differing history experienced by individual blocks as the result of relief of internal as well as external plate stresses may be a more significant determinant of the mineral fecundity of an area. A possible example is the lower Kuskokwim area, rich in mercury deposits as compared to the rest of Alaska. Although individual deposits seem controlled by local faults, the area of mineralization is not related to a single lineament but is largely confined between two northeast-trending lineaments (Lathram and Gryc, 1973) and two northwest-trending ones, the Yentna and one parallel to it south of Lake Iliamna.

CONCLUSIONS

We conclude that:

1. Most space image lineaments 1,000 km or more in length are the surface expression of major changes in the character of the lithosphere resulting from persistent movement, vertically and/or horizontally along zones of weakness in the crust.

2. A systematic pattern exists in these lineaments and represents a systematic pattern of boundaries of a mosaic of crustal blocks.
3. Differing vertical and/or horizontal adjustments from block to block in response to plate stresses result in differing tectonic histories and, hence, differing geological and geophysical characteristics in the lithosphere of each block.
4. The response of continental crust to forces of plate convergence or divergence and of oceanic crustal materials accreted to the continents during plate convergence is guided by accommodation along these preexisting crustal block boundaries.
5. Metal concentrations may not only be controlled by these crustal block boundaries and their intersections, as felicitous channels for the migration of mineralizing agents but may also be governed by greater or lesser mineral fecundity within individual blocks, as determined by differences in tectonic history.
6. The study of very long space image lineaments and their geologic significance provides a powerful new tool for tectonic and metallogenic analysis.

SELECTED REFERENCES

Barnes, D. F., 1976, Bouguer gravity map of Alaska: U.S. Geol. Survey Open-File Rept. 76–70, 1: 2,500,000.

Brosgé, W. P., Brabb, E. E., and King, E. R., 1970, Geologic interpretation of reconnaissance aeromagnetic survey of northeastern Alaska: U.S. Geol. Survey Bull. 1271–F, p. F1–F12.

Carter, W. D., 1974, Tectolinear overlay of the United States: U.S. Geol. Survey Open-File Rept., 1: 5,000,000.

Clague, D. A., Dalrymple, G. B., and Moberly, Ralph, 1975, Petrography and K-Ar ages of dredged volcanic rocks from the western Hawaiian Ridge and the southern Emperor Seamount chain: Geol. Soc. America Bull., v. 86, p. 991–998.

Clark, A. L., Berg, H. C., Cobb, E. H., Eberlein, G. D., MacKevett, E. M., Jr., and Miller, T. P., 1974, Metal provinces of Alaska: U.S. Geol. Survey Misc. Inv. Map I–384, 1:5,000,000.

Cook, D. R., ed., 1957, Geology of the East Tintic Mountains and ore deposits of the Tintic mining district: Utah Geol. Soc. Guidebook to the geology of Utah, no. 12, 183 p.

Detterman, R. L., 1973, Mesozoic sequence in Arctic Alaska, *in* Pitcher, M. G., ed., Arctic geology: Am. Assoc. Petroleum Geologists Mem. 19, p. 376–387.

Eaton, G. P., Christiansen, R. L., Iyer, H. M., Pitt, A. M., Mabey, D. R., Blank, H. R., Jr., Zietz, Isidore, and Gettings, M. E., 1975, Magma beneath Yellowstone National Park: Science, v. 188, p. 787–796.

Freden, S. C., Mercanti, E. P., and Becker, M. A., eds., 1973, Symposium on significant results obtained from the Earth Resources Technology Satellite-1, v. I: Technical presentations: Natl. Aeronautics and Space Admin. Spec. Pub., SP 327, 2 sections, 1,730 p.

———1974, Third Earth Resources Technology Satellite-1 symposium, v. I: Technical presentations: Natl. Aeronautics and Space Admin. Spec. Pub., SP 351, 2 sections, 1,994 p.

Garson, M. S., and Krs, Miroslav, 1976, Geophysical and geological evidence of the relationship of Red Sea transverse tectonics to ancient fractures: Geol. Soc. America Bull., v. 87, p. 169–181.

Gedney, L., Shapiro, L. H., Van Wormer, J. D., and Weber, F. L., 1972, Correlation of epicenters with mapped faults, east-central Alaska, 1968–1971: U.S. Geol. Survey Open-File Rept. 1,768 p.

Grant, A. R., 1969, Chemical and physical controls for base metal deposition in the Cascade Range of Washington: Washington Div. Mines and Geol. Bull. 58.

Grantz, Arthur, 1966, Strike-slip faults in Alaska: U.S. Geol. Survey Open-File Rept. 852, 82 p.

Grantz, Arthur, Holmes, M. L., and Kososki, B. A., 1975, *in* Yorath, C. J., Parker, E. R., and Glass, D. J., eds., Canada's continental margins and offshore petroleum exploration: Canada Soc. Petroleum Geologists Mem. 4, p. 669–700.

Grantz, Arthur, and Kirschner, C. E., 1975, Tectonic framework of petroliferous rocks in Alaska: U.S. Geol. Survey Open-File Rept. 75–149, 29 p.

Grow, J. A., and Atwater, Tanya, 1970, Mid-Tertiary tectonic transitions in the Aleutian Arc: Geol. Soc. America Bull., v. 81, p. 3715–3722.

Guild, P. W., 1972, Metallogeny and the new global tectonics, *in* Internat. Geol. Cong., 24th, Montreal 1972, Proc., Sec. 4, Mineral deposits, p. 17–24.

Haites, T. B., 1960, Transcurrent faults in western Canada: Alberta Soc. Petroleum Geologists Jour., v. 8, p. 33–79.

Haman, P. J., 1975, A lineament analysis of the United States: West Can. Res. Pub., ser. 4, no. 1, 27 p.

Heyl, A. V., 1972, The 38th parallel lineament and its relationship to ore deposits: Econ. Geol., v. 67, p. 879–894.

Hobbs, W. H., 1968, Geologic setting of metallic ore deposits in the northern Rocky Mountains and adjacent areas, *in* Ridge, J. D., Ore deposits in the United States: Am. Inst. Min. Eng., p. 1352–1371.

Hodgson, R. A., Gay, S. P., and Benjamins, J. Y., eds., 1976, Proceedings of the First International Conference on the New Basement Tectonics: Utah Geol. Assoc. Pub. 5, 636 p.

Jones, D. L., MacKevett, E. M., and Plafker, George, 1970, Speculations on late Mesozoic tectonic history of part of southern Alaska (abs.): Am. Assoc. Petroleum Geologists Bull., v. 54, p. 2489.

Jordan, J. N., Lander, J. F., and Black, R. A., 1965, Aftershocks of the 4 February 1965 Rat Island earthquake: Science, v. 168, p. 1323–1325.

Katterfel'd, G. N., and Charushin, G. V., 1970, Global fracturing on the earth and other planets: Geotectonics, no. 6, 1970, p. 333.

King, P. B., comp., 1969, Tectonic map of North America: U.S. Geol. Survey, scale 1:5,000,000.

Kutina, Jan, 1969, Hydrothermal ore deposits in the western United States: a new concept of structural control of distribution: Science, v. 165, p. 1113–1119.

Landwehr, W. R., 1967, Belts of major mineralization in western United States: Econ. Geol., v. 62, p. 494–501.

Lathram, E. H., 1972, Nimbus IV view of the major structural features in Alaska: Science, v. 175, p. 1423–1427.

——— 1973, Tectonic framework of northern and central Alaska, *in* Pitcher, M. G., ed., Arctic geology: Am. Assoc. Petroleum Geologists Mem. 19, p. 351–360.

——— 1974, Geologic applications of ERTS imagery in Alaska, *in* Freden, S. C., Mercanti, E. P., and Becker, M. A., eds., Third Earth Resources Technology Satellite-1 Symposium Volume I: Technical Presentations: Natl. Aeronautics and Space Admin. Spec. Pub., SP 351, Addendum-Technical Presentation G3–1, 12 p.

Lathram, E. H., and Albert, N. R. D., 1976, Significance of space image linears in Alaska, *in* Hodgson, R. A., Gay, S. P., and Benjamins, J. Y., eds., Proceedings of the First International Conference on the New Basement Tectonics: Utah Geol. Assoc. Pub. 5, p. 11–26.

Lathram, E. H., and Gryc, George, 1973, Metallogenic significance of Alaskan geostructures seen from space: Internat. Symposium on Remote Sensing of Environment, 8th, Ann Arbor, Mich. 1973, Proc., p. 1209–1211.

Lathram, E. H., and Raynolds, R. G. H., 1975, Final report on significance of giant linears in Alaska, pt. II: Geologic differences along selected giant linears: U.S. Geol. Survey Open-File Rept., p. 29–43.

Maughan, E. K., 1966, Environment of deposition of Permian salt in the Wulliston and Alliance Basins, *in* Northern Ohio Geol. Soc. Symposium on Salt, 2d, Cleveland, Ohio 1965, Proc., v. 1, p. 35–47.

Moody, J. D., 1966, Crustal shear patterns and orogenesis: Tectonophysics, v. 3, p. 479–522.

——— 1973, Petroleum aspects of wrench-fault tectonics: Am. Assoc. Petroleum Geologists Bull., v. 57, p. 449–476.

Moody, J. D., and Hill, M. J., 1956, Wrench-fault tectonics: Geol. Soc. America Bull., v. 67, p. 1227.

Muehlberger, W. R., 1965, Late Paleozoic movement along the Texas lineament: New York Acad. Sci. Trans., v. 27, p. 385–392.

Ozoray, G. F., 1972, Tectonic control of morphology on the Canadian interior plains, *in* Adams, W. P., and Helleiner, F. M., International geography 1972: Res. Council Alberta, Canada Contr. 547, p. 51–54.

Patton, W. W., Jr., 1973, Reconnaissance geology of the northern Yukon-Koyukuk province, Alaska: U.S. Geol. Survey Prof. Paper 774A, 17 p.

Patton, W. W., Jr., Lanphere, M. A., Miller, T. P., and Scott, R. A., 1976, Age and tectonic significance of volcanic rocks on St. Matthew Island, Bering Sea, Alaska: U.S. Geol. Survey, Jour. Research, v. 4, p. 67–73.

Pitman, W. C., III, Larson, R. L., and Herron, E. M., 1974, The age of the ocean basins: Geol. Soc. America, 2 charts and summary statement.

Plafker, George, 1969, Tectonics of the March 27, 1964, Alaska earthquake: U.S. Geol. Survey Prof. Paper 543–I, p. 11–174.

Richter, D. H., and Jones, D. L., 1973, Structure and stratigraphy of eastern Alaska Range, Alaska, *in* Pitcher, M. G., ed., Arctic geology: Am. Assoc. Petroleum Geologists Mem. 19, p. 408–420.

Roberts, R. J., 1964, Economic geology, *in* Mineral and water resources of Nevada: Nevada Bur. Mines Bull. 65, p. 39–45.

Sales, J. K., 1968, Crustal mechanics of cordilleran foreland deformation: a regional and small-scale approach: Am. Assoc. Petroleum Geologists Bull., v. 52, p. 2016–2044.

Scholl, D. W., Buffington, E. C., and Marlow, M. S., 1975, Plate tectonics and the structural evolution of the Aleutian-Bering Sea region, *in* Forbes, R. B., ed., The geophysics and geology of the Bering Sea region: Geol. Soc. America Special Paper 151, p. 1–32.

Shapiro, L. H., 1971, Comparison of information content of space photography and low altitude aerial photography: U.S. Geol. Survey Interagency Rept. USGS–229, 40 p.

Shoemaker, E. M., Squires, R. L., and Abrams, M. J., 1974, The Bright Angel and Mesa Butte fault systems of northern Arizona, *in* Karlstrom, T. N. V., Swann, G. A., and Eastwood, R. L., eds., Geology of northern Arizona with notes on archeology and paleoclimate, pt. I: Geol. Soc. America Rocky Mt. Sect. Mtg., Flagstaff, Arizona, p. 355–391.

Sikabonyi, L. A., 1967, Major tectonic trends in the Prairie region of Canada: Alberta Soc. Petroleum Geologists Jour., v. 5, p. 23–28.

Sikabonyi, L. A., and Rodgers, W. J., 1959, Paleozoic tectonics and sedimentation in the northern half of the West Canadian Basin: Alberta Soc. Petroleum Geologists Jour., v. 7, p. 193–216.

Sillitoe, R. H., 1974, Tectonic segmentation of the Andes: implications for magmatism and metallogeny: Nature, v. 250, p. 542–545.

Smistad, Olav, coord., 1975, Proceedings of the NASA Earth Resources Survey Symposium, June, 1975, v. I: Technical session presentations: Natl. Aeronautics and Space Admin. Tech. Mem., TM X–58168, 2 sections, 1,497 p.

Snyder, F. G., 1970, Structural lineaments and mineral deposits (abs.): Mining Eng., v. 22, p. 36.

Sonder, R. A., 1947, Discussion of "Shear patterns of the Earth's crust" by F. A. Vening Meinesz: Am. Geophys, Union Trans., v. 28, p. 939–945.

Stewart, J. H., Walker, G. W., and Kleinhampl, F. J., 1975, Oregon-Nevada lineament: Geology, v. 3, p. 265–268.

Stone, D. B., 1974, Plate tectonics and Alaska-crustal motions: Univ. Alaska, Geophys. Inst., Ann. Rept. 1973–74.

Sutherland-Brown, A., 1974, Aspects of metal abundances and mineral deposits in the Canadian Cordillera: Canada Inst. Min. Metal. Trans., v. 77, p. 14–21.

Sutherland-Brown, A., Cathro, R. J., Panteleyev, A., and Ney, C. S., 1971, Metallogeny of the Canadian Cordillera: Canada Inst. Min. Metal. Trans., v. 74, p. 121–145.

Taubeneck, W. H., and Armstrong, R. L., 1974, The Precambrian continental margin in western Idaho (abs.): Geol. Soc. America Abs. with Program, v. 6, p. 477–478.

Thomas, G. E., 1974, Lineament-block tectonics: Williston-Blood Creek Basin: Am. Assoc. Petroleum Geologists Bull., v. 58, p. 1305–1322.

Tweto, O. L., and Sims, P. K., 1963, Precambrian ancestry of the Colorado mineral belt: Geol. Soc. America Bull., v. 74, p. 991–1014.

Van Wormer, J. D., Davies, J., and Gedney, L., 1974, Seismicity and plate tectonics in south central Alaska: Seismol. Soc. America Bull., v. 64, p. 1467–1475.

Von Huene, Roland, and Shor, G. G., Jr., 1969, The structure and tectonic history of the eastern Aleutian Trench: Geol. Soc. America Bull., v. 80, p. 1889–1902.

Yates, R. G., 1968, The trans-Idaho discontinuity, *in* Internat. Geol. Cong., 23rd, Prague, 1968, Proc., sec. 1, Upper mantle (geol. processes): Prague, Academia, p. 117–123.

Yates, R. G., Becraft, G. E., Campbell, A. B., and Pearson, R. C., 1966, Tectonic framework of northeastern Washington, northern Idaho, and northwestern Montana: Canada Inst. Min. Metal. Spec., v. 8, p. 47–59.

Zietz, Isidore, Bateman, P. C., Case, J. E., Crittenden, M. D., Jr., Griscom, Andrew, King, E. R., Roberts, R. J., and Lorentzen, G. R., 1969, Aeromagnetic investigation of crustal structure for a strip across the western United States: Geol. Soc. America Bull., v. 80, p. 1703–1714.

Zietz, Isidore, Hearn, B. C., Jr., Higgins, M. W., Robinson, G. D., and Swanson, D. A., 1971, Interpretation of an aeromagnetic strip across the northwestern United States: Geol. Soc. America Bull., v. 82, p. 3347–3372.

PROCEEDINGS OF
THE FIRST ANNUAL WILLIAM T. PECORA MEMORIAL SYMPOSIUM,
OCTOBER 1975, SIOUX FALLS, SOUTH DAKOTA

Computer-Enhanced Landsat Imagery as a Tool for Mineral Exploration in Alaska

By Nairn R. D. Albert,
U.S. Geological Survey, Menlo Park, California,
and Pat S. Chavez, Jr.,
U.S. Geological Survey, Flagstaff, Arizona

ABSTRACT

Recent work in the Nabesna and McCarthy quadrangles, Alaska, indicates that computer-enhanced Landsat imagery shows many of the known mineral deposits and can help in the prediction of potential mineral occurrences. False color, "simulated natural color," and color ratio techniques, were used successfully in conjunction with a black and white, single band image mosaic of Alaska. Computer techniques involved two stages of digital image processing (1) atmospheric and Sun-elevation corrections, noise removal, computer mosaicking, and change of the data format and (2) image enhancement, involving data manipulation for maximum discrimination of surface materials and structure. Application of a new technique called a "sinusoidal" stretch gave information not available in other products having standard contrast stretches. We identified several orthogonal sets of linears and found parallel linears to be regularly spaced at approximately 30 to 35-km intervals. The locations of known mineral occurrences correlate well with the linears. Extensions of known faults and possible locations of hidden intrusive bodies were identified. Analysis of numerous areas of anomalous light reflectance showed that whereas most are associated with known mineral occurrences, altered zones, or geochemical anomalies, some are not and may represent unexplored altered zones or mineralized areas worthy of future exploration.

INTRODUCTION

Recent work carried out in the Nabesna and McCarthy quadrangles, Alaska, under the Alaskan Mineral Resource Assessment Program (AMRAP) indicates that Landsat data can significantly help detect and predict mineral occurrences, when used in conjunction with geologic mapping, geochemical sampling, and aeromagnetic and gravimetric data. Landsat data can provide additional information on geology and structure relevant to mineral exploration that cannot be or may not have been acquired by other methods.

This report presents the results of Landsat data interpretation in the Nabesna quadrangle, Alaska (Albert, 1975), and the preliminary results of similar interpretations in the McCarthy quadrangle, Alaska, and their significance for mineral exploration.

LOCATION

The Nabesna and McCarthy quadrangles are in south-central Alaska (fig. 1) bounded on the north and south by the 63°N. and 61°N. latitudes and on the west by 144°W. longitude. The eastern boundary is the Alaska-Canada border (141°W. longitude).

PHYSIOGRAPHY

Topographic extremes in the area studied range from a low of about 305 m (1,000 ft) in the western part of the McCarthy quadrangle to a high of more than 5,000 m (16,400 ft) in the southeastern part. The area can be divided into three types of terrain: (1) Plains and lowlands from about 305 m (1,000 ft) to 1,220 m (4,000 ft) with heavy to moderate vegetation and few outcrops; (2) low mountains from about 915 m (3,000 ft) to 1,830 m (6,000 ft), with heavy to light vegetation and numerous outcrops in the higher

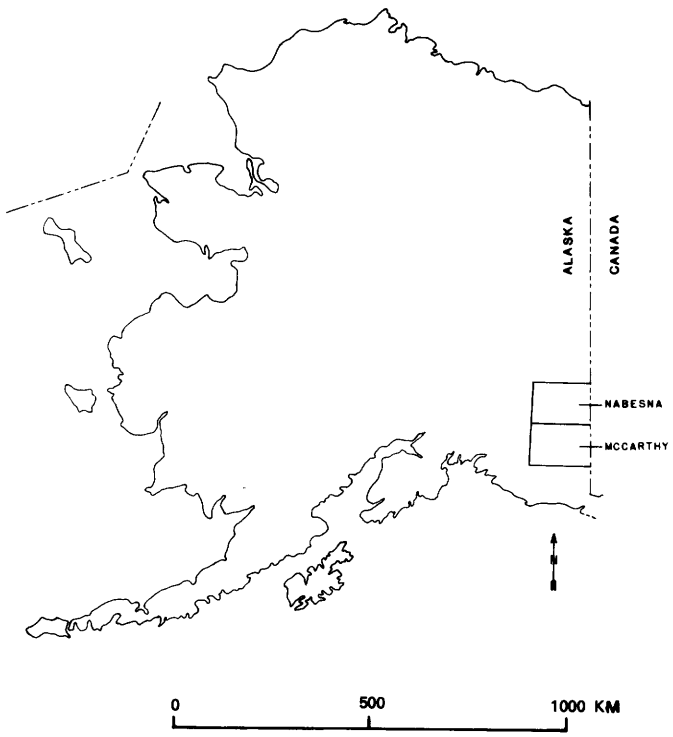

FIGURE 1.—Map of Alaska showing location of the Nabesna and McCarthy quadrangles.

elevations; and (3) high rugged mountains from about 915 m (3,000 ft) to peaks of 5,000 m (16,400 ft), with moderate to no vegetation, numerous glaciers, heavy snow cover and extensive outcrops.

Temperatures in these quadrangles range from highs above 38°C (100°F) during the summer to lows below −57°C (−70°F) during the winter. Much of the area is underlain by discontinuous permafrost.

BRIEF GEOLOGIC DESCRIPTION

The Nabesna and McCarthy quadrangles are underlain by three general geologic terranes that are separated by the Denali and Border Ranges faults (fig. 2). North of the Denali fault are mainly regionally metamorphosed lower Paleozoic sedimentary and subordinate igneous rocks. South of the Denali fault and north of the Border Ranges fault, there are three assemblages of extensive andesitic volcanic and associated sedimentary and intrusive rocks: Upper Paleozoic, Upper Mesozoic, and Upper Cenozoic. South of the Border Ranges fault are extensive Mesozoic flysch-type sedimentary deposits.

Most mineral production in the Nabesna and McCarthy quadrangles, chiefly copper, gold, and silver (Richter and others, 1975; MacKevett and Cobb,

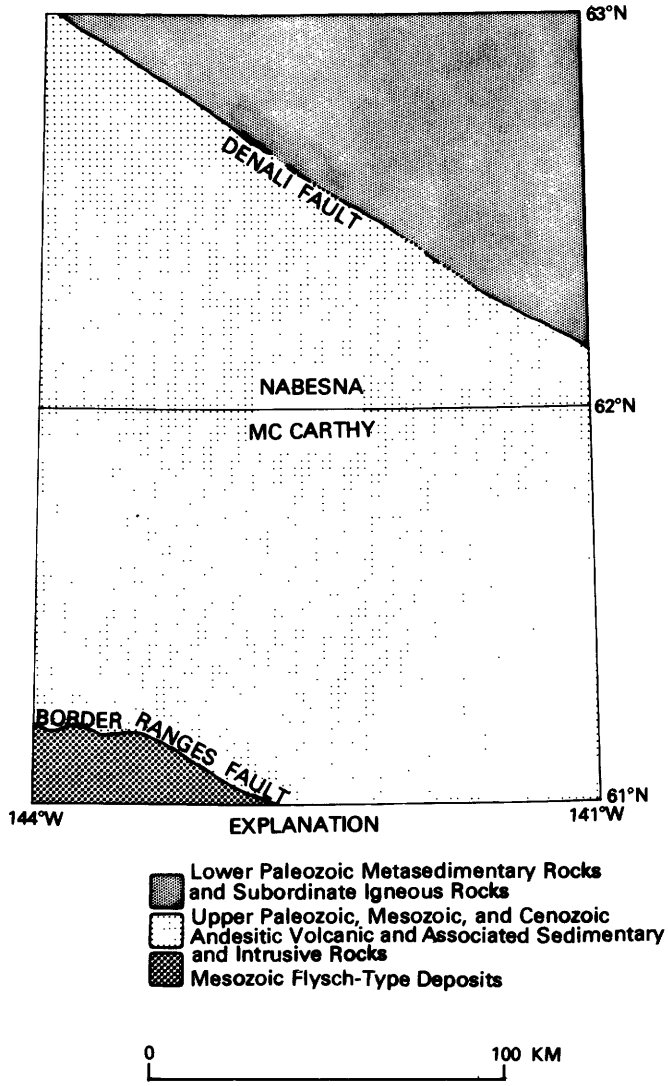

FIGURE 2.—Map of the Nabesna and McCarthy quadrangles showing generalized geologic terranes.

1972), has been in the area between the Denali and Border Ranges faults.

INTERPRETATION OF IMAGERY

The study of three kinds of computer-enhanced Landsat imagery in conjunction with a single-band, black and white Landsat image mosaic of Alaska, resulted in (1) the identification of linear and circular features and their correlation with known geology, mineral occurrences, and geophysical data and (2) the identification of mineral occurrences and numerous potential targets for future exploration.

LINEAR FEATURES

One of the types of imagery used in this study was the Alaskan Landsat mosaic constructed in 1973 by

the Soil Conservation Service, U.S. Department of Agriculture, using band 7 images generated without computer enhancement. Because of the synoptic perspective and low Sun-angle of the non-summer images used, the mosaic was most useful for identifying linear and circular features. Additional linear and circular features were identified on the computer-filtered imagery discussed below.

Three nearly orthogonal sets of linears were identified in the Nabesna and McCarthy quadrangles (fig. 3). The predominant set trends approximately N. 43° W. and N. 48° E., the subordinate sets approximately N. 72° W. and N. 20° E. and N. 87° E. and north. Parallel linears trending N. 43° W., N. 48° E. or N. 87° E. are spaced approximately 30–35 km apart.

East-trending linear features seen clearly on Landsat imagery (figs. 3 and 4) suggest the existence of major east-trending concealed structures in the Nabesna quadrangle south of the Denali fault. Aeromagnetic (Griscom, 1975) and gravimetric (Barnes and Morin, 1975) data support the Landsat interpretations. These east-trending structures can also be seen in the McCarthy quadrangle (figs. 3 and 5) on Landsat imagery and should be substantiated by future aeromagnetic and gravimetric studies.

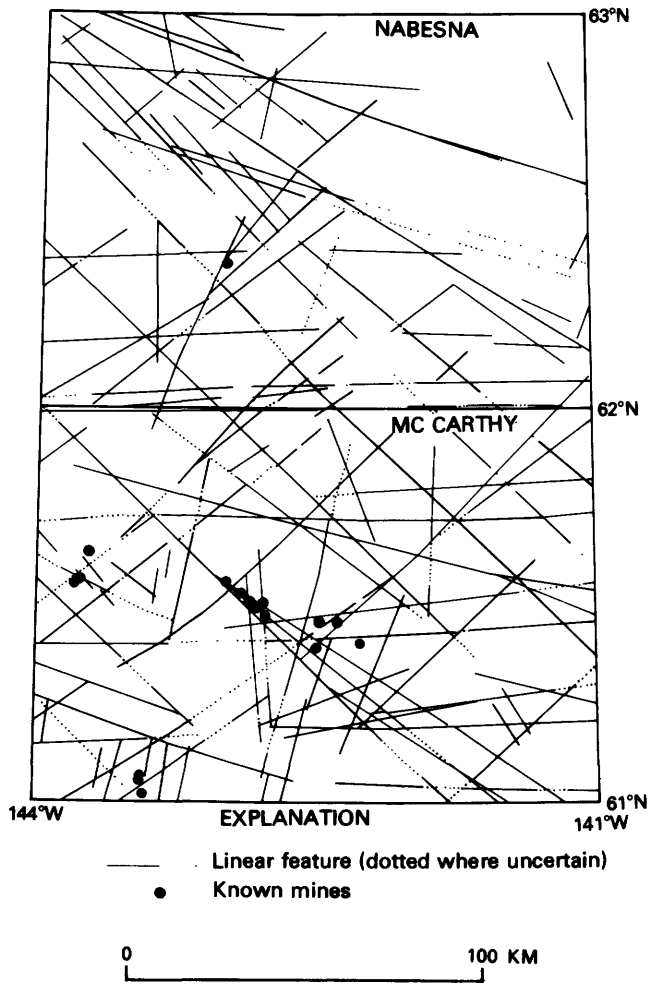

FIGURE 3.—Map of the Nabesna and McCarthy quadrangles showing linear features and mine locations.

The correspondence of known mineral occurrences to linear features in the Nabesna and McCarthy quadrangles is very good. Of 257 known mineral occurrences (Richter and others, 1975; MacKevett and Cobb, 1972; MacKevett, written communication), 141 (55%) occur within 1 km of linear features. One hundred twenty-four occurrences are prospects or mines, 78 (63%) of which occur within 1 km of linear features. Of the 17 mines, 14 (82%) occur within 1 km of linear features (fig. 3). These correlations suggest a strong relation between linear features and the more significant mineral occurrences.

Statistically, the different mineral commodities in the McCarthy quadrangle appear to be related to the trend of specific orthogonal linear feature directions (table 1). For example, 34 of 85 copper prospect and mine deposits occurring within 1 km of a linear feature are associated with northwest-trending linears. Subordinately, 18 copper deposits are associated with northeast-trending linears. This orthogonal relation appears to apply for silver, molybdenum, and, possibly, antimony. Gold, on the other hand, occurs primarily near linears with north-northeast and northeast directions and subordinately near linears with northwest trends. Chromium, iron, zinc, and nickel, not shown, also appear to have preferred orthogonal linear direction associations.

Evaluation of significant mineral occurrences in each linear direction reveals three groupings: (1) northwest and northeast-trending linears to which most mineral occurrences are related, (2) north-northwest, north-northeast, and east-trending linears, and (3) west-northwest, east-northeast, and north-trending linears to which the fewest mineral occurrences are related. Although the information is preliminary and incomplete, these trends are suggestive of the relations resulting from the Moody and Hill (1956) model for primary, secondary, and tertiary fault and fold development in regions of wrench-fault tectonics.

CIRCULAR FEATURES

Numerous circular features were identified in the Nabesna and McCarthy quadrangles (figs. 4 and 5). North of the Denali fault, these circular features can be correlated with aeromagnetic and geologic data suggesting that they may be related to concealed in-

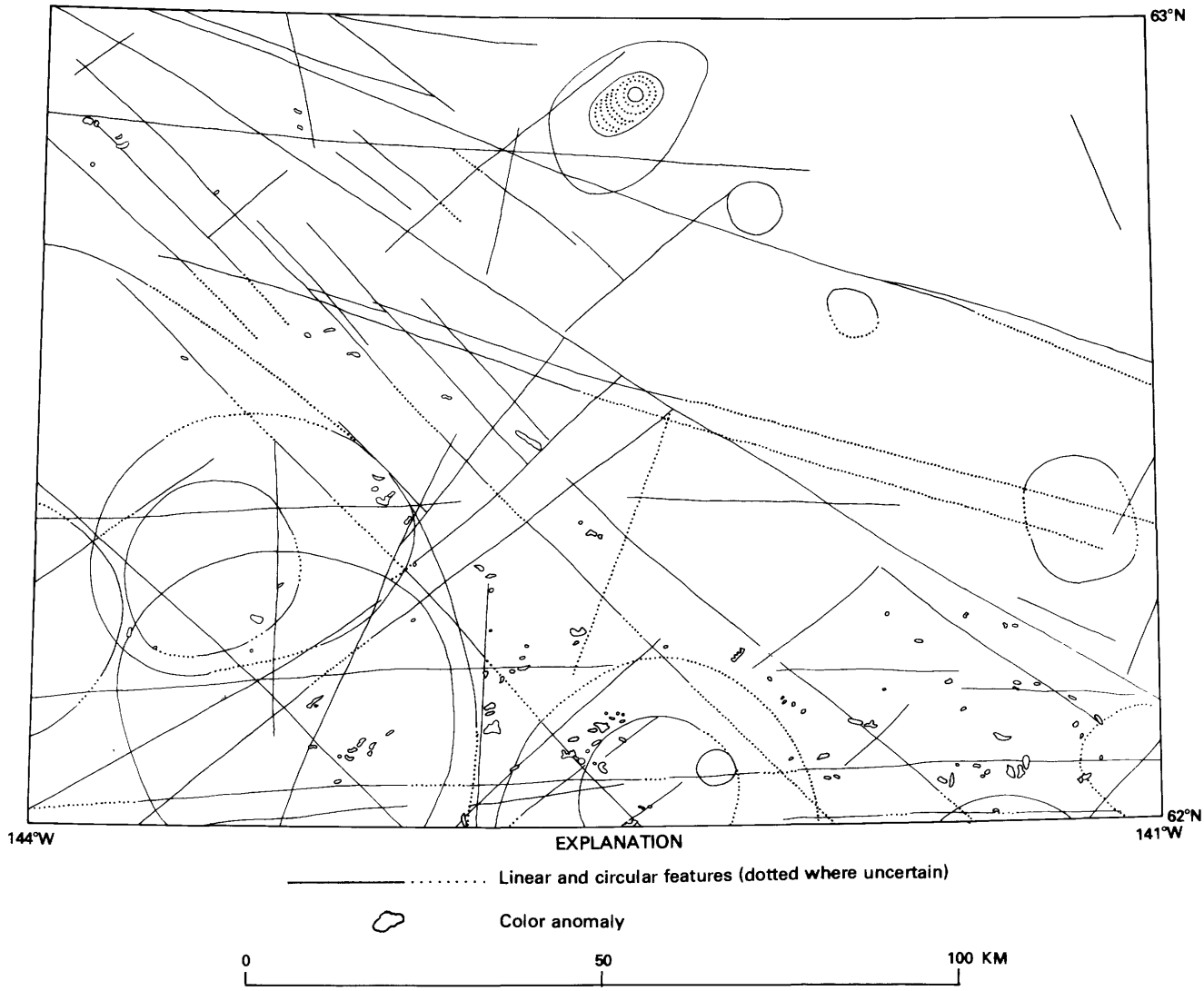

FIGURE 4.—Map of the Nabesna quadrangle showing linear and circular features and color anomalies observed on computer-enhanced Landsat imagery. (From Albert, 1975.)

TABLE 1.—*Number of significant mineral occurrences (mines and prospects) in the various linear directions in the McCarthy quadrangle, Alaska*

Linear direction	E	WNW	NW	NNW	N	NNE	NE	ENE
Antimony	---	---	3	---	---	---	---	---
Copper	11	5	34	5	2	6	18	4
Gold	---	---	3	1	---	6	5	2
Molybdenum	---	---	2	1	---	---	---	---
Silver	---	---	9	3	---	---	3	1
Total	11	5	51	10	2	12	26	7

trusive bodies. Those circular features observed between the Denali and Border Ranges faults, some nearly 200 km in diameter, appear to be related to volcanic activity. The relation of circular features to mineralization is not yet clear.

COMPUTER-ENHANCED IMAGERY

Three types of computer-enhanced Landsat imagery were used successfully to locate mineral occurrences in the Nabesna quadrangle: (1) color ratio,

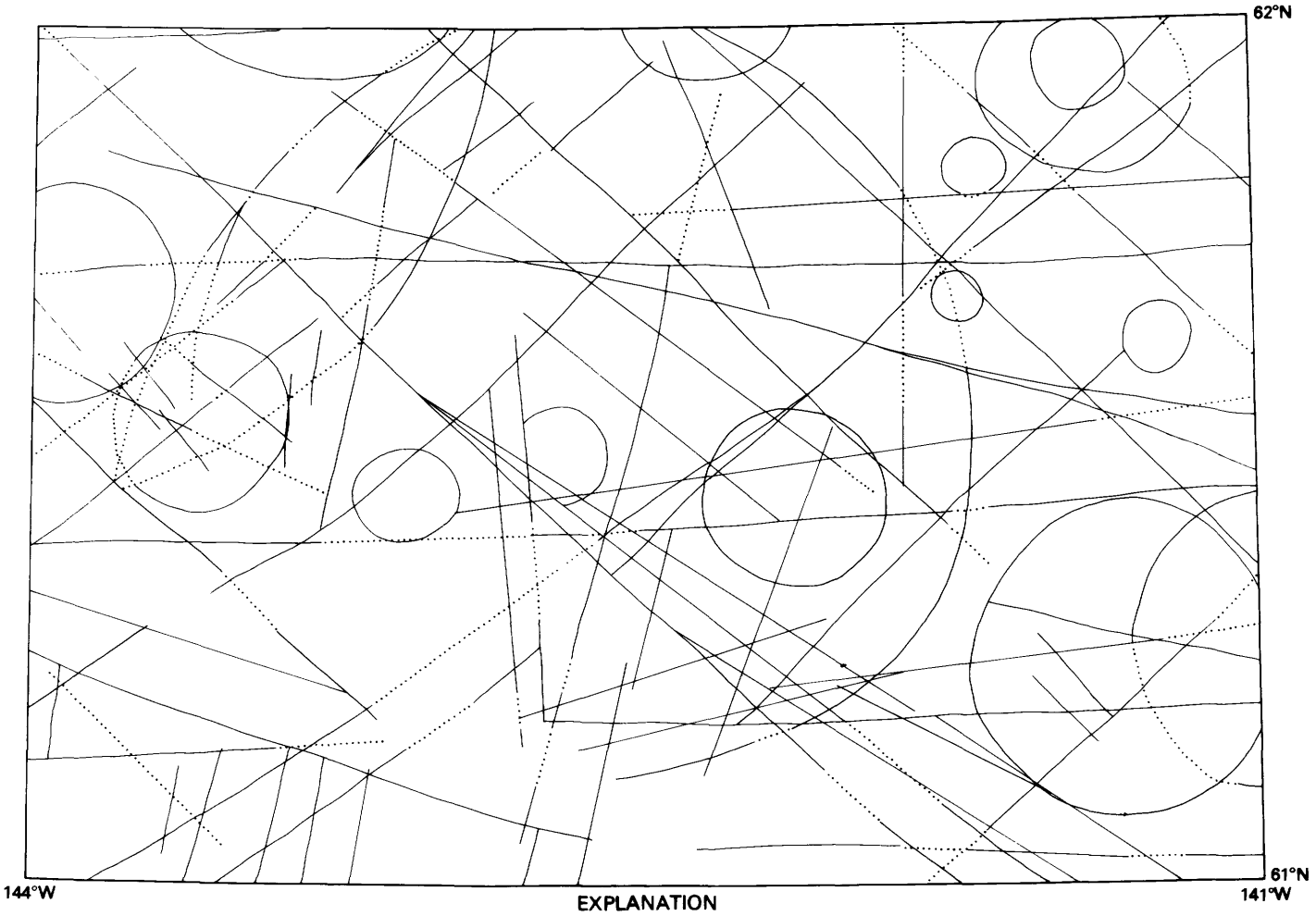

FIGURE 5.—Map of the McCarthy quadrangle showing linear and circular features.

(2) standard false color, and (3) simulated natural color. An additional enhancement technique called a "sinusoidal" stretch is being used on imagery of the McCarthy quadrangle. Analysis of these "sinusoidally" stretched images is still in progress, but preliminary observations indicate that they can supply information not available on other types of images.

Digital image processing can be separated into two stages, the preprocessing or "clean-up" stage and the actual image enhancement stage. The output of the clean-up stage is called a data base and is used as input to the different image-enhancement techniques.

The preprocessing stage includes noise (striping) removal, haze and Sun-elevation corrections, and a geometric correction (Chavez, 1975). The final step in the preprocessing stage is to mosaic by computer the different images needed to cover the area of interest. For the 3-degree quadrangles in Alaska, it usually means mosaicking parts of three or four images. Four data-base tapes are then generated, each containing one of the four Landsat bands that cover the entire area of interest.

The several enhancement techniques used in this study can be separated into the following types: contrast stretches, color ratios, structural and linear enhancements, simulated natural color, and a "sinusoidal" stretch that maximizes the color variations within an image.

The first type of enhancement, contrast stretch, is a standard false color composite made by using three of the four Landsat bands to which linear stretches have been applied. For this study, band 4 was filtered with blue light, band 5 with green, and band 7 with red. The second type of enhancement, color ratios, involves the division of spectral values of one band by those of another band and the application of linear

stretches to the subsequent ratios. In the Nabesna quadrangle, the color-ratio image was generated by filtering bands 5/4 with red light, 6/4 with green, and 4/5 with blue.

Structural and linear enhancement is generated by the use of a high-frequency filter that removes most of the albedo information in order to bring out structural and linear information. In this study, the structural and linear information obtained by this method was added to that observed on the Alaskan image mosaic.

Another type of enhancement is the simulation of natural color (Eliason and others, 1974). In this technique, a pixel (picture element) is classified into one of three general categories, vegetation, rocks and soils, and water, using the ratio of band 5 to band 6 after haze removal. Once the pixel has been classified, a different algorithm is used for each category to extrapolate a theoretical value for the blue region of the spectrum. This new band is then used to generate a color composite with colors approximating those that might be seen without atmospheric effects from satellite altitude (fig. 6, p. XIX).

A recently developed enhancement technique, the "sinusoidal" stretch, is applied to any three bands used to generate a color composite having maximum color variation (fig. 7, p. XX). Most dissimilar materials show up as dissimilar colors in the composite except where materials have the same spectral response in all three bands selected. The sinusoidal stretch extends multiple-input spectral reflectivity values over the entire output spectral range such that the color changes are gradual for small differences of gray levels. This new stretch enhances not only large spectral differences within the image but also very subtle differences not usually enhanced by other methods.

Color anomalies identified on Landsat imagery were found to correspond well with known mineral deposits and geochemical anomalies. A color anomaly is considered to be a variation in tone or color observed on the images that differs significantly from the local background color, indicating a reflectivity difference on the ground.

In the Nabesna quadrangle, 120 color anomalies were identified on the standard false color and simulated natural color images. Of these, 72 and 69 were identified respectively on the standard false color and simulated natural color images. Twenty-one were identified on both. No color anomalies were identified on the color-ratio image.

Of the 120 color anomalies, 39 correspond to known mineral occurrences. Of the 81 that do not, 17 correspond to geochemical anomalies (fig. 8). Of the 64 color anomalies that correspond to neither known mineral occurrences nor geochemical anomalies, 27 were in areas that were not geochemically sampled. Thus, at least 56 (47%) of the color anomalies observed on Landsat imagery of the Nabesna quadrangle appear to be related to mineralization. (Many others are thought by Richter [oral comm., 1975] to correspond to unmapped altered zones). In addition, 27 color anomalies may be related to unknown mineral occurrences and should certainly be targets for future exploration.

Studies of computer-enhanced Landsat imagery in the McCarthy quadrangle are still in progress. Three types of imagery are being used: (1) simulated natural color, (2) color ratio with bands 5/4 in blue, 6/7 in green, and 7/4 in red, and (3) false color using sinusoidal stretches, with the various bands expressed in different color combinations.

One of the advantages of the sinusodal stretch is that snow, a major ground cover in Alaska, does not have to be displayed in white, as it does in standard

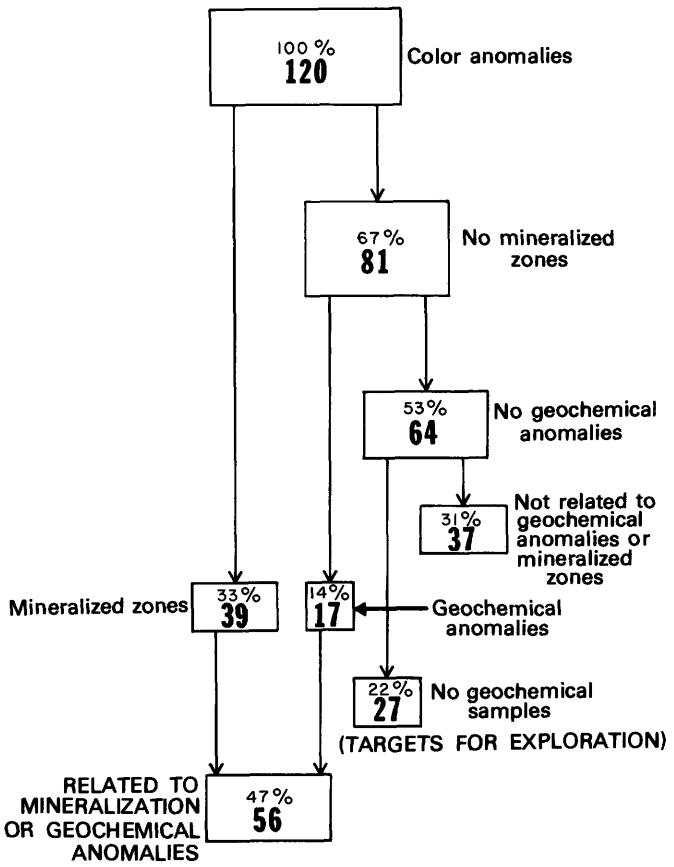

FIGURE 8.—Breakdown of color anomalies seen on computer-enhanced Landsat imagery and their association with mineralized areas and geochemical anomalies in the Nabesna quadrangle.

false-color and simulated natural-color images (fig. 7, p. XX). Photographically, the white, snow-covered areas tend to "bleed" over into adjacent non-snow areas, reducing reflectivity discrimination of rock, soil, or vegetation differences.

By superimposing mapped faults in the McCarthy quadrangle over a sinusoidally stretched image with bands 5 in green, 6 in blue, and 7 in red, it was possible to draw numerous extensions of these faults based on linear and curvilinear features visible in the image (fig. 9). The true nature of these extensions and their relation to mapped faults is uncertain. Their actual surficial expressions have not been observed by field geologists (MacKevett, oral comm., 1975) and may be detectable only by high-altitude imaging systems. Additional data on the existence and nature of these extensions may soon be available upon completion of an aeromagnetic map of the McCarthy quadrangle.

Further studies of the Landsat imagery of the McCarthy and other Alaskan quadrangles now in progress will make possible a more thorough evaluation of sinusoidally stretched imagery and its usefulness in mineral exploration.

CONCLUSIONS

Landsat data have furnished significant geologic and structural information to mineral resource appraisal studies of the Nabesna and McCarthy quadrangles, Alaska. Information of this type, when used in conjunction with geologic, geophysical, and geochemical data, is a modern tool that should be con-

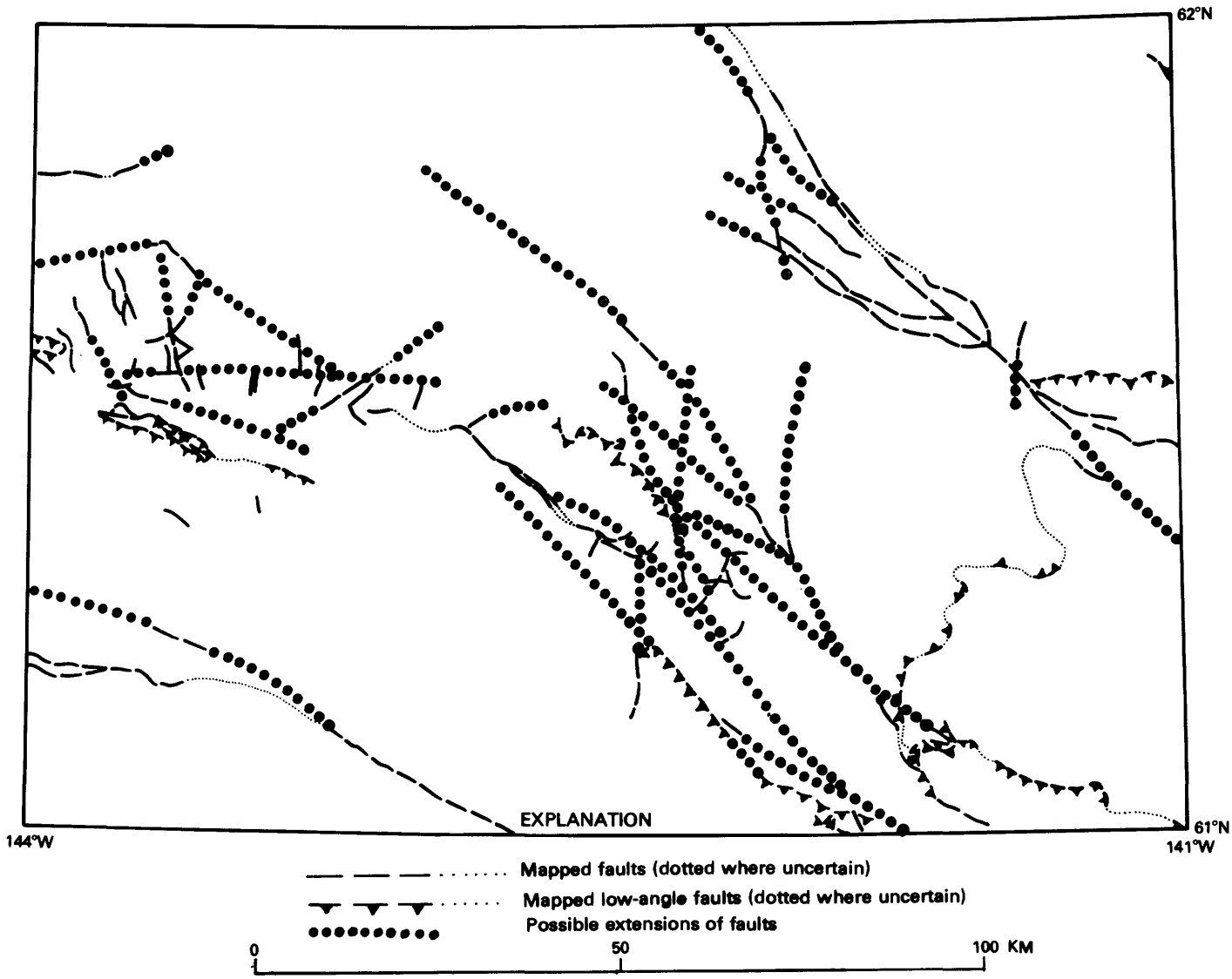

FIGURE 9.—Map of the McCarthy quadrangle showing known faults and their possible extensions as determined by linear and curvilinear features visible in the sinusoidally stretched false-color Landsat image of the McCarthy quadrangle.

sidered essential to effective regional mineral exploration.

REFERENCES CITED

Albert, N. R. D., 1975, Interpretation of Earth Resources Technology Satellite imagery of the Nabesna quadrangle, Alaska: U.S. Geological Survey Misc. Field Studies Map MF–655J, 2 sheets, scale 1:250,000.

Barnes, D. F., and Morin, R. L., 1975, Gravity map of the Nabesna quadrangle, Alaska: U.S. Geological Survey Misc. Field Studies Map MF–655I, 1 sheet, scale 1:250,000.

Chavez, P. S., Jr., 1975, Atmosphere, solar, and MTF corrections for ERTS digital image (abs.): American Society of Photogrammetry, Fall Convention, Phoenix, Ariz. Oct. 1975, Proc., pp. 69–69a.

Eliason, E. M., Chavez, P. S., Jr., and Soderblom, L. A., 1974, Simulated true color from ERTS: Geology, v. 2, no. 5, pp. 231–234.

Griscom, Andrew, 1975, Aeromagnetic map and interpretation of the Nabesna quadrangle, Alaska: U.S. Geological Survey Misc. Field Studies Map MF–655H, 2 sheets, scale 1:250,000.

MacKevett, E. M., Jr., and Cobb, E. H., 1972, Metallic mineral resources map of the McCarthy quadrangle, Alaska: U.S. Geological Survey Misc. Field Studies Map MF–395, scale 1:250,000.

Moody, J. D., and Hill, M. J., 1956, Wrench-fault tectonics: Geol. Soc. America Bull., v. 67, pp. 1207–46.

Richter, D. H., Singer, D. A., and Cox, D. P., 1975, Mineral resources map of the Nabesna quadrangle, Alaska: U. S. Geological Survey Misc. Field Studies Map MF–655K, 1 sheet, scale 1:250,000.

PROCEEDINGS OF
THE FIRST ANNUAL WILLIAM T. PECORA MEMORIAL SYMPOSIUM,
OCTOBER 1975, SIOUX FALLS, SOUTH DAKOTA

Evaluation of Improved Digital-Processing Techniques of Landsat Data for Sulfide Mineral Prospecting

By R. G. Schmidt,
U.S. Geological Survey, Reston, Virginia
and Ralph Bernstein,
International Business Machines Corporation, Gaithersburg, Maryland

ABSTRACT

A relatively simple method of digital computer classification of multispectral scanner data was tested at an ideal porphyry copper deposit in a very arid part of Pakistan and was then successfully applied to mineral exploration in an adjacent region. The surface expressions of the already known porphyry copper deposit and the five new prospects discovered in this experiment are all characterized by abundant light-toned sulfate minerals and do not seem to contain much pigmentation by iron oxides.

Digital multispectral classification was performed at the IBM Digital Image Processing Facility by using reformatted computer-compatible tapes of one scene. A test area of 55 km^2 was selected in the Saindak, Pakistan, area, which included a well-mapped porphyry copper deposit. A "supervised" classification table was prepared of high and low limits of acceptable reflectance in each of the four spectral bands for each surface type by using control areas selected from a geologic map. The first classification table was revised several times until it was deemed capable of giving information useful in mineral exploration, even though we expected that many of the rock identifications would be incorrect. This revised table was applied to evaluation of 2,100 km^2 in the Chagai District, Pakistan. Of 50 sites classified as "mineralized" by the digital-processing program, 23 were selected as possibly similar to the control area and therefore deserving of inspection in the field. Nineteen of these were visited in October 1974; five of the sites, constituting a total area of 4.7 km^2, contain sulfide-bearing hydrothermally altered rock that is mostly quartz-feldspar porphyry. Parts of all five sites are believed to represent parts of porphyry copper systems. The presence of copper beyond trace amounts has been established at two points, and the prospects are under investigation by the Government of Pakistan.

It may be important when using remote-sensing methods in some geologic environments to seek altered parts of porphyry copper deposits that are not specifically enriched or pigmented by iron oxides.

Our experiment indicates that simple methods of digital classification of Landsat data can aid in the location of mineral deposits in desert terrain. These methods can complement conventional methods of mineral exploration.

A major problem in identifying the sulfide-bearing areas is the overlap of reflectance values of mineralized areas with the reflectance values from other high-albedo areas, such as parts of drywashes and, most commonly, areas of windblown sand. In an effort to solve this problem, new classification tables using several classes for each rock type have been prepared. Each class has relatively close high/low limits; several classes are therefore needed to cover the full range of albedo that can be expected from each major surface type, as for example, from similar rock occurring on slopes of different orientation to the Sun. The narrowed reflectance limits increase the possibility of discrimination between materials of generally similar reflectance values. Recent tests of these more sophisticated classification tables suggest that we can now achieve better discrimination of mineralized areas than we did in the evaluation study in 1974. Future satellite-borne sensors having higher sensitivity, wider

spectral range, narrower spectral bands, and greater resolution should help to alleviate the reflectance-overlap problem.

Our experiment used high-albedo areas associated with intense quartz-sericite alteration as guides to sulfide mineralization although some of the control areas do contain some hematitic and some jarositic pigmentation. Attempts to use strongly red stained areas in the outer pyrite zone as control areas resulted in no satisfactory delineation of the area of mineralization. All prophyry copper deposits may not include areas of light-toned sulfate and/or clay alteration; also, not all known deposits have "red-thumbs" or areas of strong red iron oxide pigmentation derived from decomposition of pyrite.

INTRODUCTION

The concept of using remote-sensing methods at the Saindak porphyry copper deposit predated Landsat–1 by almost 10 years, for it was discussed by the geologists during field mapping from 1961 to 1966, and some simple spectral tests were made at that time using ordinary color photography and colored filters (Schmidt, 1968, p. 59). Two investigations that have sought a simple method of identifying sulfide deposits using Landsat multispectral scanner data have used the Saindak deposit as a test site because the deposit is large, has well-developed alteration zones, and scant vegetation and is well exposed and undisturbed (fig. 1). The deposit has been mapped in detail at a scale of 1:6,000 (Khan, 1972), and the senior author was familiar with the deposit and region. Both investigations used image 1125–05545 (Nov. 25, 1972) and the first experiment also used image 1090–05595 (Oct. 21, 1972) and 1124–05491 (Nov. 24, 1972). In the first experiment, false-color composites were visually examined to locate possible favorable areas; in the second, favorable areas were

FIGURE 1.—Index map showing the Chagai District and Saindak, Pakistan.

selected by digital computer classification. The near-winter solstice date of these images and the resultant low Sun illumination angle was probably an advantage in the first experiment and a disadvantage in the second.

Both experiments were designed to test relatively simple methods of utilizing Landsat multispectral scanner (MSS) data in mineral exploration. Simplicity is considered important because we are looking for a method that may find wide usage in both government and private sector mineral exploration applications.

For the first experiment, false-color composites were made using NASA system corrected MSS images of three scenes over a very arid and vegetation-free part of the western Chagai District, Pakistan. Later, a color composite was also prepared from MSS bands 4, 5, and 7 by computer processing of the taped data to produce an image that was geometrically corrected for systematic errors and radiometrically adjusted (fig. 2, p. XXI). These composites were visually examined for tonal features resembling the known porphyry copper deposit at Saindak (Schmidt, 1974). Seven areas were selected for prospecting, and three of these were field checked. None of the three contained significant mineralization. Later analysis of the results indicated that too few areas were selected by visual examination and that this method must be considerably modified for greatest effectiveness in mineral exploration. Some further testing in which more light-toned areas are selected should be made before the results of this experiment can be considered final.

In the second experiment, machine processing was used. Digital multispectral classification was experimentally performed on the reformatted computer-compatible tapes of one scene. The IBM Digital Image Processing Facility was used for image correction, image enhancement, and multispectral classification (fig. 3). A 55-km^2 area in the Saindak vicinity was extracted and displayed in photographic form using the imagery printer, and a test area was selected which included known porphyry deposits. Areas representing specific rock types were identified, and their reflectance values were extracted for MSS bands 4, 5, 6, and 7. Provisional classification tables were prepared for given geological units; each table was used to classify the test area, and the tables were modified upon comparison of these results with the known geology. The cycle was repeated five times until a classification table was developed that could, it was hoped, provide information useful in mineral evaluation. High accuracy of identification was not considered to be necessary for success of the method, and was not expected.

Then the multispectral classification program, using the classification table already prepared, was used to evaluate 2,100 km^2 east of the test area, and a partial field check of the results was conducted. By evaluating the resultant digital classification map, 23 prospecting targets were selected as being similar to the Saindak altered rock area, and 19 of these were visited in the field. Of these 19, 5 localities constituting a total area of 4.7 km^2 contain hydrothermally altered rock, mostly quartz feldspar porphyry. A program for evaluation of these new prospects has been prepared by the Government of Pakistan.

Despite the apparent success of the 1974 application experiment, it used classification tables that were relatively simple. While the number of sites falsely classified as mineralized was not unreasonable when compared to other standard field methods of mineral prospecting, we had reason to believe that our method could be refined. This would result in more distinct delineation of mineralized areas, fewer areas falsely classified as mineralized, and perhaps improvement of quality of mapping of other surficial materials. This refinement has been the goal of our continuing experimentation.

Acknowledgments.—The original color composite experiment conducted by the U.S. Geological Survey was partly supported by the National Aeronautics and Space Administration. Financial support for part of the digital processing experiment and for the travel expenses of the field checking was provided by the EROS Program, and logistical support in the field was furnished by the Resource Development Corporation, a Pakistan Government corporation. The extraction of reflectance data for several sites in the experiment area by Jon D. Dykstra of Dartmouth College, using computer facilities and algorithm of the NASA Goddard Institute of Space Studies, New York, is gratefully acknowledged.

GEOLOGY OF THE EXPERIMENT AREA

The general geology of the western Chagai District is portrayed on 1:253,440 photogeologic maps (Hunting Survey Corporation, Ltd., 1960). The rocks of the region consist of marine and terrestrial sedimentary and volcanic rocks of Cretaceous to Holocene age, and a few shallow intrusive bodies. The influence of widespread volcanism is continuous in the geologic record from Cretaceous time to the present. The highest mountains in the area are the dormant volcanoes Koh-i-Sultan in Pakistan and Kuh-e-Taftan in nearby Iran.

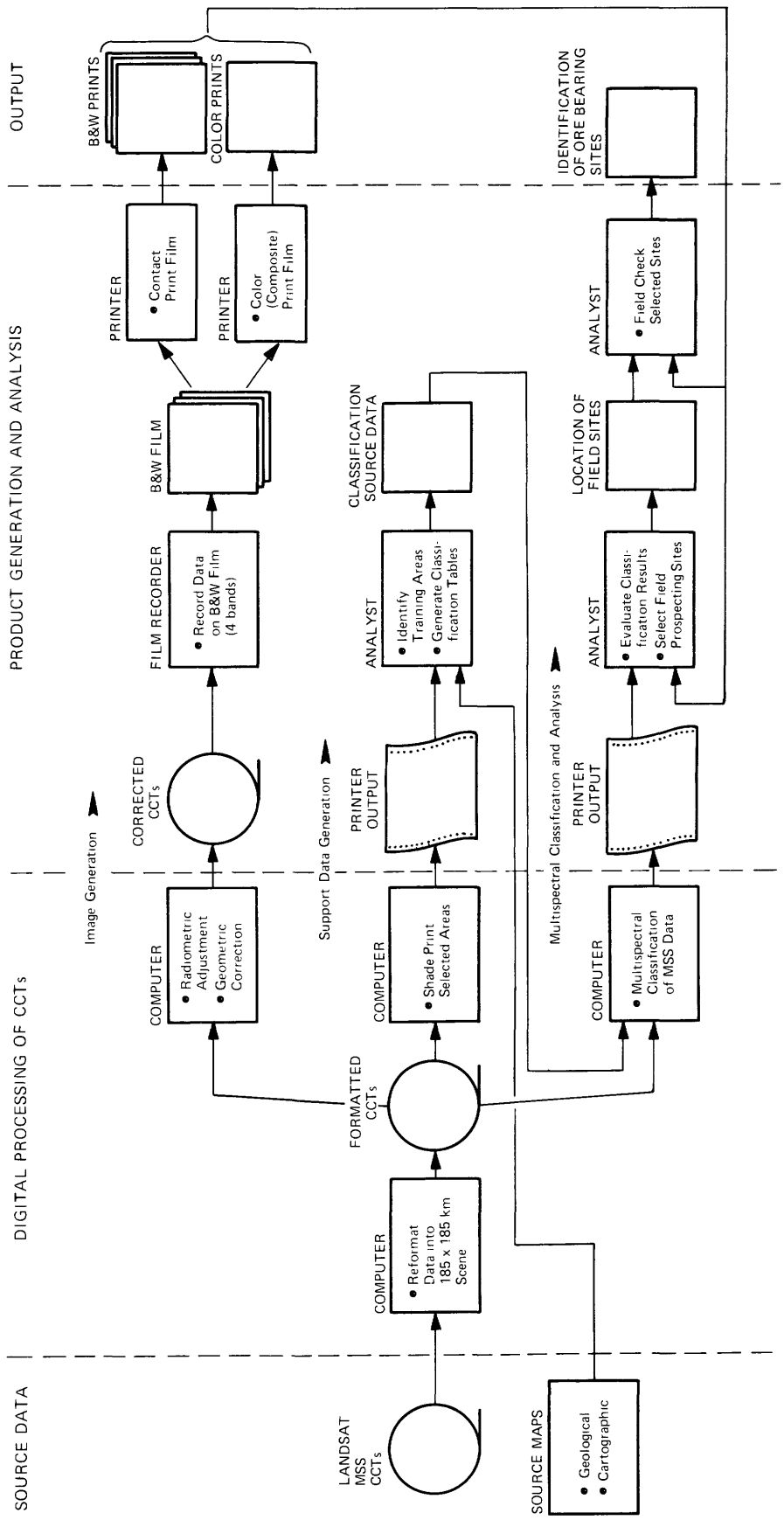

FIGURE 3.—Graphic summary of digital processing and data analysis performed in the experiment.

The Mirjawa range area, where the known porphyry copper deposit, Saindak, is located, has mostly folded and much faulted (along northwest trends) sedimentary and volcanic sedimentary strata. Except for a group of large and extensive pre-Tertiary sills, intrusive and extrusive volcanic rocks make up but little of the total outcrop area, but volcanic material is common in sedimentary strata. Cretaceous rocks represent a wide variety of marine and continental depositional environments; lower Tertiary rocks are mostly shallow marine deposits, and upper Tertiary and Quaternary strata are largely of continental origin.

The Mashki Chah region can be considered geologically as a western extension of the Chagai Hills, west of the volcano, Koh-i-Sultan. In this extension, gently folded Cretaceous and undeformed Tertiary volcanic rocks with low dips (probably initial) are common and widespread, and intrusive rocks, especially stocks, are more abundant than in the Mirjawa ranges. Faults are widespread. The folding lacks the strong linear pattern characteristic of the Mirjawa ranges, and the two areas are dissimilar structurally. Recently dried or still weakly flowing sinter-depositing saline springs, plus small weak fumaroles on Koh-i-Sultan, indicate that there is still a little hydrothermal activity.

ECONOMIC GEOLOGY

Several large areas of the Chagai District contain volcanic rocks of intermediate and felsic composition, within which small bodies of hypabyssal intrusive rocks may be considered to have a good potential for large sulfide deposits of the porphyry copper type. Mineral reconnaissance in the Chagai District has been spotty and mostly for high-grade deposits. Small copper occurrences are widespread in the region, but none had been known within several miles of the new prospects identified in this experiment.

At Saindak, a group of small copper-bearing porphyritic quartz diorite stocks cut northward across the folded lower Tertiary stratigraphic section (Ahmed, Khan, and Schmidt, 1972). The stocks may be cupolas on a single barely exposed granitic body 8 km (5 mi) long and as much as 1.5 km (1 mi) wide or separate but related intrusive bodies. The group of stocks is surrounded by zones of intense hydrothermal alteration very similar to those of the ideal model described by Lowell and Guilbert (1970). At Saindak, the innermost area seen at the surface is a zone of potassic alteration containing hydrothermal biotite (Shahid Noor Khan, oral communication). This is surrounded successively by zones of quartz-sericite alteration and finally a 1- to 3-km zone of propylitic alteration in which pyroclastic rocks in particular are altered to a hard, dark epidote-rich hornfelsic rock.

Copper mineralization is probably restricted to the potassic alteration zone and the inner part of the quartz-sericite zone, both mostly but not entirely located in the intrusive quartz diorite porphyry. The copper-bearing zone is in turn enclosed in a sulfide-rich zone that contains as much as 15 percent by volume pyrite (locally pyrrhotite), probably limited to the outer part of the quartz-sericite alteration zone. Mineralization in the propylitic zone is limited to lean lead-copper-silver veins (Ahmed, Kahn, and Schmidt, 1972, p. A19–A20) and local hematite and pyrrhotite skarns formed by replacement of limestone beds (Ahmed, Khan, and Schmidt, 1972, p. A19).

The pyrite-rich peripheral zone and the innermost quartz-sericite and potassic zones have been eroded to form a cross-structural valley in which the surficial materials are light toned and highly reflective. Soils related to certain parts of many porphyry copper deposits the world over have distinct red and orange anomalies, and this is true at part of the Saindak deposit as well, especially over the pyrite-rich zone in the valley north of the main areas of mineralization. The amount of red and yellow coloration in the most central part of the alteration zone at Saindak seems less than in some peripheral areas but, unfortunately, this has not been measured quantitatively. Alluvial and windblown materials cover part of the light-toned soil, and it is necessary to use much care in selecting specific control areas for any remote-sensing experiment.

COMPUTER-AIDED INFORMATION-EXTRACTION EXPERIMENTS

Computer-aided information-extraction experiments were conducted to identify potential sulfide-ore-bearing localities. The experimental approach is summarized in figure 3. Shown here are the source data used, the digital processing applied to the source data, the products generated, the analysis conducted, and the final products. By a combination of digital image processing and information extraction, and visual analysis and evaluation, three processing operations were performed: digital image generation, support data generation and analysis, and multispectral classification and analysis.

Digital image generation.—The uncorrected Landsat multispectral scanner (MSS) data were reformatted into band separated 185 km x 185 km areas, and each band was radiometrically (intensity) adjusted and systematically geometrically corrected (Bernstein,

1974). The resulting computer-compatible tape (CCT) data were then converted to an image on film from which black and white and color composite prints were made. These prints were used as aids in the selection of the field prospecting sites during the evaluation of the classification results and also during the field checking.

Support data generation and analysis.—The formatted but uncorrected CCT's were used for analysis, especially preparation of classification tables, prior to the multispectral classification operation. Shade prints (computer printouts providing the reflectance values in each spectral band) for selected areas were prepared and used as a geographic reference for precise location of individual data samples or picture elements (pixels) relative to known ground features and rock types. Numeric data for the four MSS bands were extracted for each pixel in the known areas, and maximum and minimum sensed-reflectance limits were chosen for each rock type. A known highly altered and copper sulfide-bearing part of the deposit at Saindak was the source of data used to prepare the classification tables. Five revisions were made and tested, and one alternate classification table was tried, resulting finally in classification table "B" shown on table 1. Table 1 shows three general types of materials: (1) *Mineralized rock*, including intensely hydrothermally altered (quartz-sericite zone) quartz diorite, and pyritic rock, (2) *Alluvial and eolian materials*, recently moved dry-wash alluvium and eolian sand being the materials most likely to be confused with the first group, and (3) *A loose category of dark surfaces* that includes both hornfels-type bedrock and many areas of desert-varnished lag gravels (especially in class 10). These tables of reflectance limits were then used on an interactive basis to classify a nearby region within the same Landsat scene in which copper sulfide-bearing areas were suspected but in which no deposits were known (application area).

Multispectral classification and analysis.—A spectral-intensity discrimination program was used for multispectral classification on the application area using the tables prepared for the Saindak deposit. The program tested the reflectance of each pixel within the application area against the maximum and minimum reflectance limits in the table and determined into which surface class (rock type) the pixel belonged. The symbol for that class was printed as part of a classification map. When the observed values fit more than one class (when classes were set up with overlapping limiting values), a pixel was placed in the class that was considered first in the search sequence.

The digital classification method using table "B" was used to evaluate an area of 2,100 km^2 near Saindak considered to have good potential for porphyry copper deposits (fig. 4). The results were printed out in 13 computer-generated vertical strip maps. These maps were examined for groups of pixels classified as one of the four mineralized classes (two classes each of mineralized quartz diorite and pyritic rock), and about 50 groups or concentrations were identified. Each was then evaluated for probability of correct classification, relationship to concentrations of other classes, and comparison with known rock types and known occurrences of hydrothermal mineralization. From this examination, 30 localities most deserving reconnaissance checking in the field were chosen. The locations of these targets were marked on an enlarged (1:253,440 scale) digitally enhanced image of MSS band 5 in order to simplify location on aerial photo-

TABLE 1.—*Digital classification table "B" used in 1974 mineral evaluation in the Chagai District, Pakistan*

Class number	Rock type			Symbol	Reflectance limits of multispectral scanner bands			
					4	5	6	7
1	Mineralized rock	Quartz diorite	High reliability	0	46–50	52–60	50–60	18–22
2			Low reliability	⊠	44–45	52–60	45–49	18–19
3		Pyritic rock	High reliability	¥	41–45	47–54	39–44	16–17
4			Low reliability	X	41–45	47–54	39–44	16–19
5	Dry-wash alluvium		High reliability	=	39–46	39–46	35–44	14–17
6			Low reliability	-	41–45	46–51	42–49	18–19
7	Boulder fan			+	33–40	39–46	30–35	9–16
8	Eolian sand		High reliability	.	38–44	46–54	42–51	18–22
9			Low reliability	,	45	46–127	42–127	18–63
10	Various dark surfaces including hornfelsic rock outcrops, desert-varnished lag gravels, and detrital black sand			I	33–36	28–38	29–35	11–15
11				#	24–35	19–27	20–32	8–12
12				H	29–36	28–38	20–28	9–14

TABLE 2.—*Revised classification table "SSD" prepared in April 1975*

Class Number	Rock type	Symbol	Reflectance limits of multispectral scanner bands			
			4	5	6	7
1	Detrital black sand	,	27–30	26–28	23–26	9
2		,	28–32	27–31	25–27	10
3	Dry wash alluvium	-	38–44	39–44	35–38	13–16
4		=	43–48	44–48	38–43	15–18
5	Eolian sand	.	49–54	59–66	54–62	23–27
6		.	43–48	50–58	46–55	19–24
7		.	37–43	41–50	38–47	15–20
8		.	33–38	35–42	32–39	12–16
9	Mineralized rock	0	39–42	41–45	33–38	14–16
10		θ	41–44	44–48	37–41	16–18
11		θ	43–46	47–51	41–45	17–20
12		0	44–46	50–53	45–48	18–20
13		θ	46–49	53–56	48–51	19–21
14		Ø	49–52	56–59	51–54	20–22
15	Dark surfaces, except detrital black sand	I	33–36	28–38	29–35	11–15
16		#	24–35	19–27	20–32	8–12
17		H	29–36	28–38	20–28	9–14

TABLE 3.—*Revised classification table "S" prepared in September 1975*

Class number	Rock type	Symbol	Reflectance limits of multispectral scanner bands			
			4	5	6	7
1	Detrital black sand	,	27–30	26–28	23–26	9
2		,	28–32	27–31	25–27	10
3	Dark pebble desert	"	35–36	34–38	31–34	12–13
4	Dry-wash alluvium	-	35–39	37–42	31–36	13–15
5		=	39–43	41–46	35–41	15–17
6		=	43–47	46–50	41–46	17–19
7	Eolian sand	.	37–43	41–50	38–47	15–20
8		.	43–48	50–58	46–55	19–24
9		.	49–55	59–68	54–63	23–27
10		.	54–60	67–76	62–70	27–30
11		.	60–66	76–85	70–78	30–33
12	Unmineralized felsic intrusive rock	F	48–52	55–60	50–54	21–24
13		F	44–48	51–56	47–51	19–21
14		F	40–44	46–51	43–47	17–19
15	Mineralized rock, pyritic	P	39–42	41–45	33–38	14–16
16		P	41–44	44–48	37–41	16–18
17		P	43–46	47–51	41–45	18–19
18	Mineralized rock, sericitic	Q	46–49	51–55	45–49	19–21
19		Q	48–51	54–58	49–53	21–22
20		Q	50–53	57–62	52–57	22–24
21	Dark surface, except detrital black sand	I	33–36	28–38	29–35	11–15
22		K	24–35	19–27	20–32	8–12
23		H	29–36	28–38	20–28	9–14

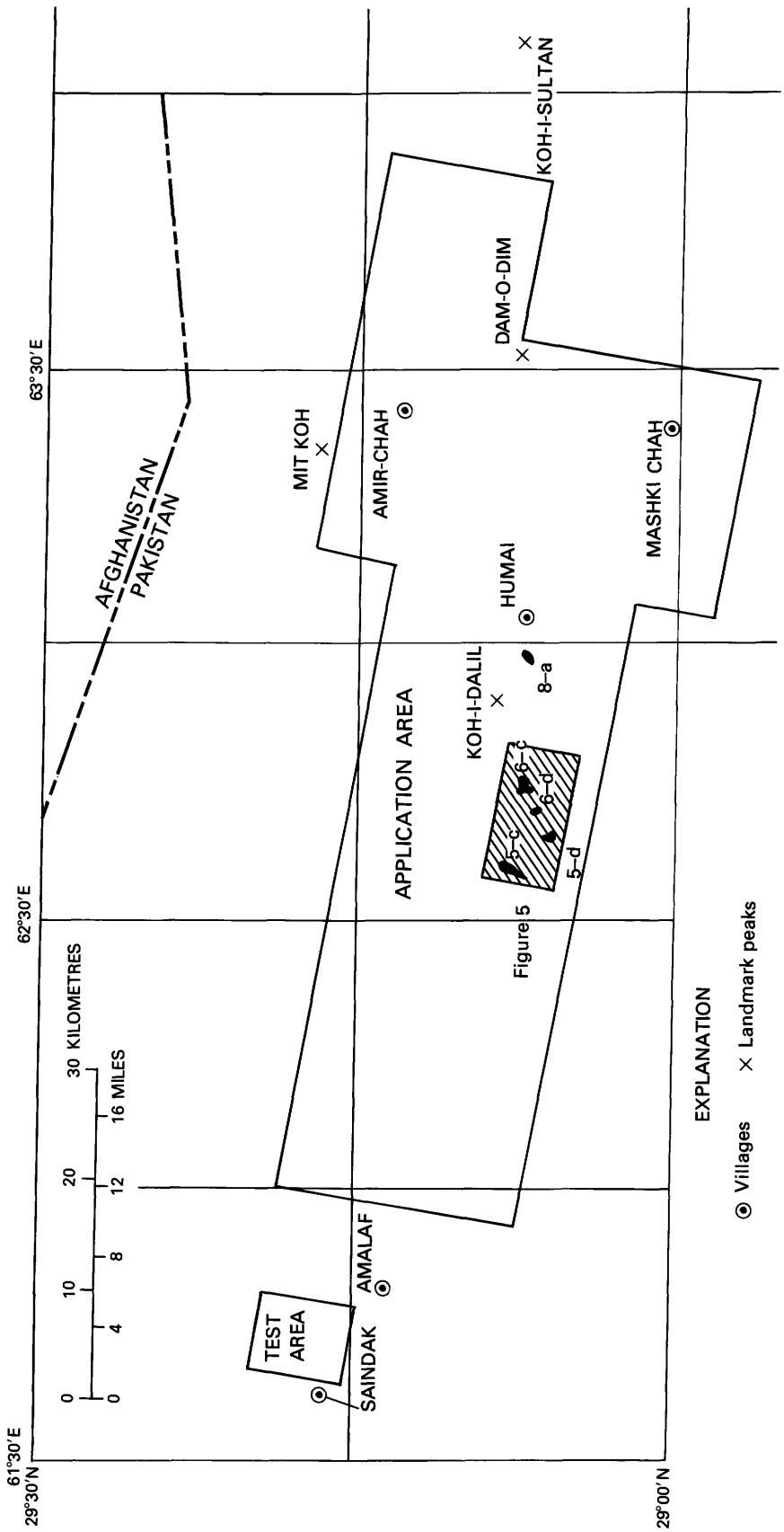

FIGURE 4.—The Saindak–Mashki Chah area of the western Chagai District, Pakistan, showing the control area near Saindak and the area where the digital-classification method was applied. The numbered locations are newly discovered mineralized prospect sites.

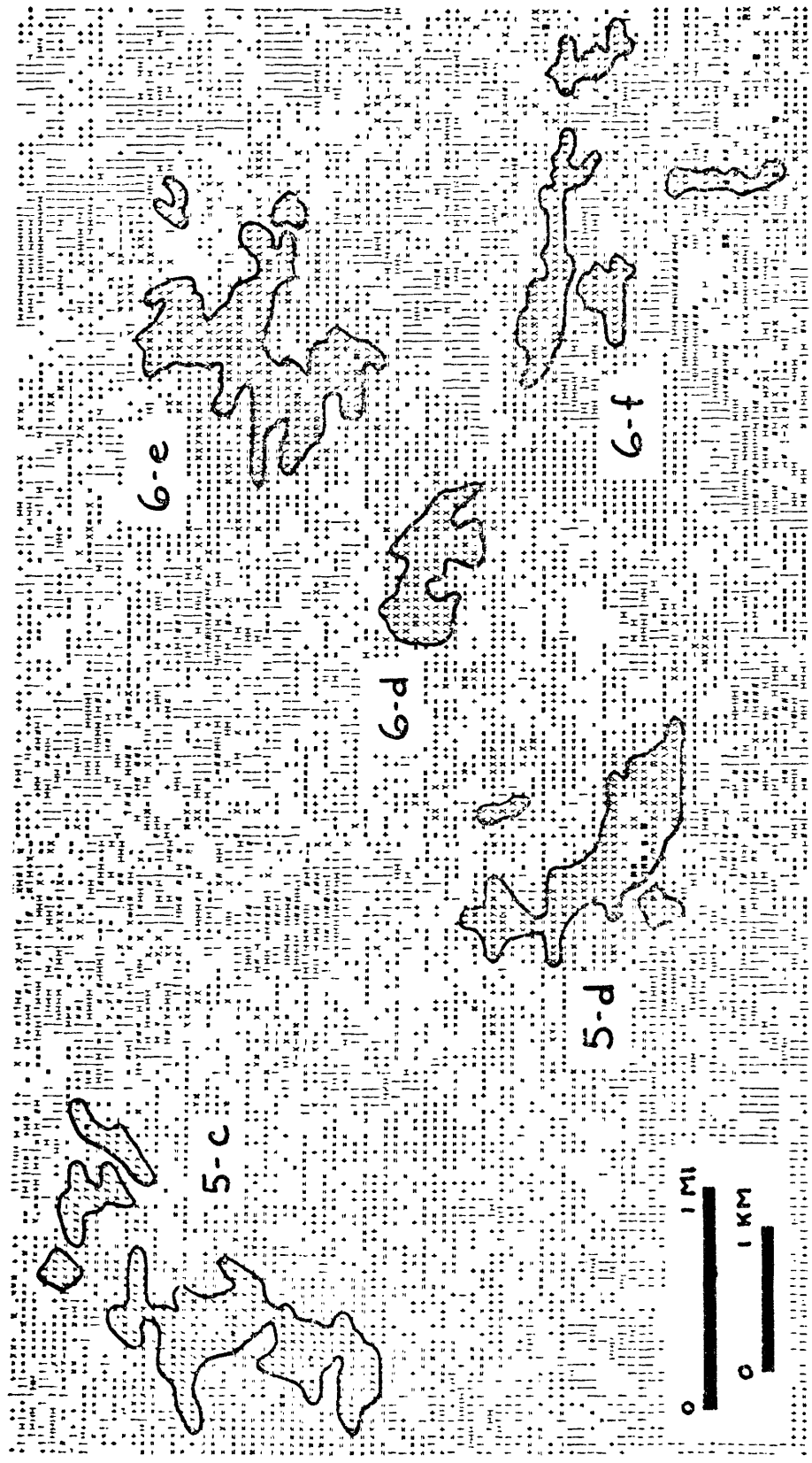

FIGURE 5.—Classification map of an area west of Koh-i-Dalil (fig. 4) showing five areas classed as "mineralized," using table "B." Reconnaissance field checks showed that some hydrothermal alteration and sulfide mineralization is present in each area. Area 6-d seems the most promising for further study. The northeast end of 5-c, the west end of 6-f, and the northeast end of 6-e were not adequately field checked. The east end of 6-f is mostly dune sand.

graphs and in the field. As part of the field check all anomalous areas were first examined on stereoscopic pairs of 1:40,000-scale aerial photographs. At this point, it was possible to reject seven more areas as probably related to windblown sand.

Nineteen sites were examined in the field, and four desirable sites were not reached in the field checks. Five sites were found to be extensive outcrops of hydrothermally altered sulfide-rich rock (figs. 4 and 5). Two additional sites contain altered rock with some sulfide but seem less attractive for prospecting at this time.

EVALUATION OF RESULTS

Classification using table "B".—In the evaluation using table "B," mineralized rock is believed to have been generally identified correctly, but much other light-toned surface was also classified as mineralized. Alluvium was mostly classified accurately, but some gravel fans derived from light-toned rocks were not. Perhaps only 25 percent of dune sand was correctly identified by means of table "B," most sand having been classified as mineralized rock. Classification of areas of dark rock outcrops and several types of lag gravels yielded different combinations of classes 10, 11, and 12 and made it possible to differentiate among some of these materials, and some of these differentiations were made among surfaces having surprisingly subtle differences.

In classification table "B," four of the main surface types are each represented by a high and low reliability class. The high reliability or more restrictive class has reflectance limits in at least one band that made it exclusive from all other high reliability classes; the secondary class has reflectance limits that overlap the limits of at least one other class. The classes of two reliability levels have not been used in later tables. The classification map made by using table "B" is compared with a geologic map (fig. 6).

In building table "B," as the acceptable reflectance limits of a class were narrowed, fewer matches were found. In classes 1 and 2 (mineralized quartz diorite, table 1), for example, if we chose limits that included most pixels in the training areas and also many pixels in all the areas of known mineralization, we also got false classifications in dry-wash material. The limits were subjectively adjusted wider or narrower so that enough points were classified correctly in the areas of known mineralization to call attention to those areas and the false classifications were reduced to an acceptable level. Because revisions to the tables are time-consuming and successive revisions generally achieve diminishing improvement, table "B" as used in this experiment was revised only a few times.

The three dark-surface classes were established on the basis of small samples of particular rock formations in training areas, but the classes were very unsatisfactory in discriminating among the three formations. The classes would have been abandoned except that various combinations of the three classes delineate areas of dark rock outcrops and lag gravels. The printout of class 11 (symbol #) in particular resulted in abundant pixel groups just inside the perimeter of the propylitic zone at Saindak (no similar propylitic zone in volcanic sedimentary rocks, as at Saindak, was found near the new prospects).

Classification using table "S".—The data collected in the field check made it possible to evaluate the accuracy of identification of all of the surface types, not the mineralized rock alone, and to revise the tables to improve accuracy. A new style of table evolved, having several relatively narrow classes spanning the expected albedo range for each rock type but no high and low reliability classes, resulting in classification table "SSD" (table 2) and finally classification table "S" (table 3). The limiting values for each class span relatively narrower ranges than those in table "B" and more classes are required. The use of several classes for a range in albedo from similar surface types is designed as a simple way to compensate for variations in reflectance angles, especially those caused by southeast- and northwest-facing slopes, and also albedo-related systematic changes in color balance of similar surfaces, regardless of their cause. Classification using table "SSD" was performed to reevaluate part of the application area. An area of 170 km^2 was tested that includes four of the new prospects. The results are very encouraging.

The area tested using table "SSD," included 13 of the groups of "mineralized"-class pixels originally evaluated using table "B." Of the 13 pixel groups, 7 had been selected as possibly mineralized rock and worth field checking, 5 were subsequently visited during the field check, and 4 were found to contain some mineralization. Evaluation of the same area using table "SSD" resulted in the delineation of only 5 areas as "mineralized;" 4 of these were known from earlier field checking of table "B" targets to have mineralization, 1 was identified in the earlier evaluation but not chosen as deserving a field check, and one was not delineated by the table "B" evaluation. (The latter two sites, not chosen for checking in the earlier study, have not had field examinations). One mineralized site identified using table "B" was omitted by the table "SSD" evaluation. Table "SSD"

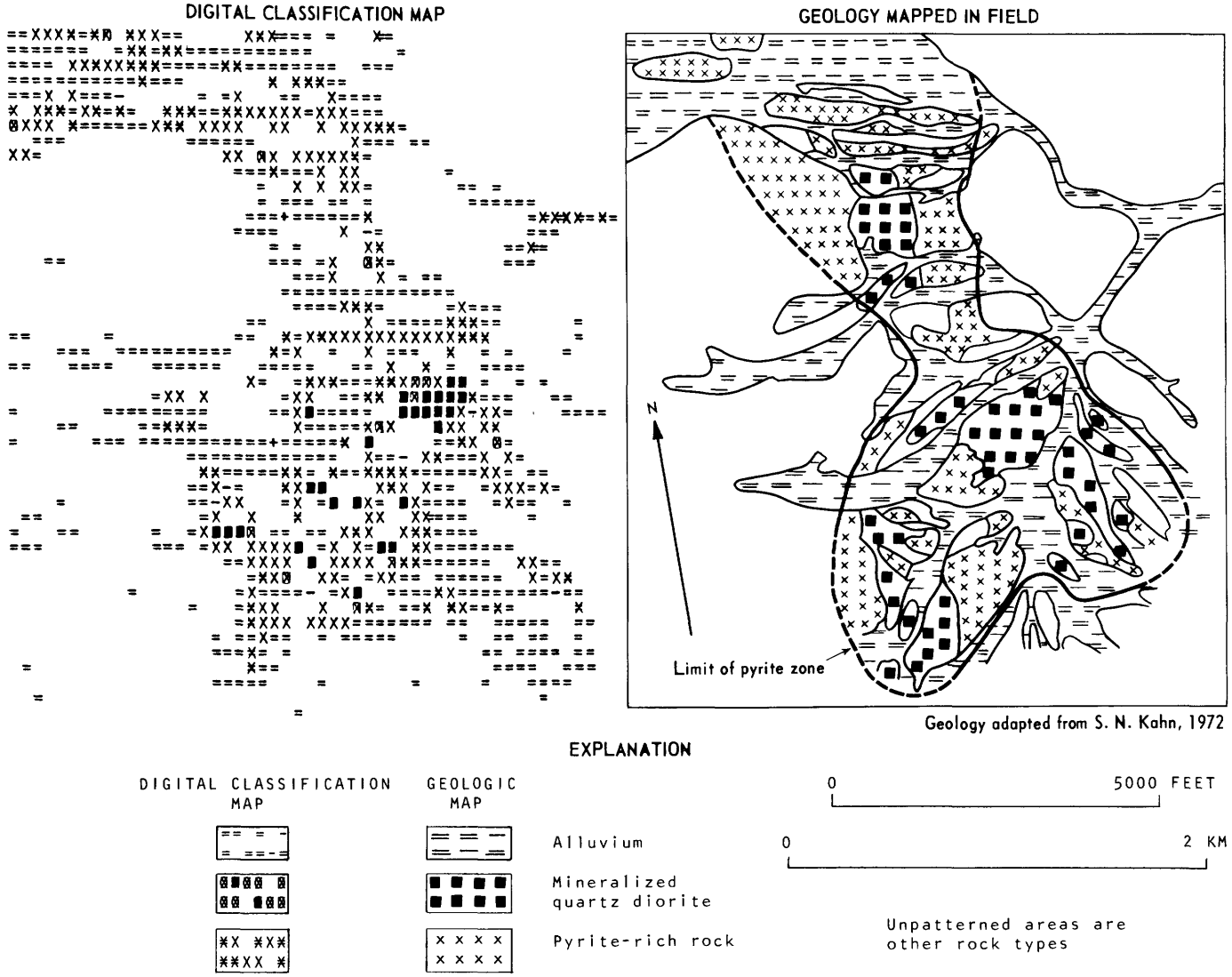

FIGURE 6.—Comparison of digital-classification map made by using table "B" and geology mapped in field, Saindak porphyry copper deposit, Pakistan.

does a much more effective job of separating mineralized areas from other light-toned materials, largely eliminating the need for human evaluation of a large number of "false" tonal anomalies. Omission of one of the best areas of mineralization points to the need for slight revision of the mineralized rock classes.

Revisions to table "SSD" have yielded table "S" which includes classes to cover sands of higher albedo and dry-wash material of lower albedo than were included in table "SSD," classes for dark pebble desert and unmineralized felsic rock (rock types not included in earlier tables), and modified reflectance limits for part of the mineralized rock classes. Only a few preliminary tests have been made of this new table.

SUMMARY

Visual evaluation of false color composites and a relatively simple method of digital classification were tested as aids to mineral exploration by using areas of known hydrothermal alteration and mineralized and altered intrusive stock as control areas. Both methods seem to be useful exploration tools, and greatest advantage is probably gained by using them together. The simple classification method was applied to evaluate 2,100 km^2 of area regarded as having a high potential for deposits of the porphyry copper type, leading to the discovery of five sizable areas of hydrothermally altered rock containing abundant sulfide, disseminated or in stockwork veins. Although

the classification method used was relatively simple and unrefined, and 14 prospecting targets proved to be false leads, the number of sulfide-bearing areas identified was outstanding, and the falsely classified areas were not so many as to require an unreasonable amount of field checking. Further experimentation indicates that better discrimination of mineralized areas than we used in the field test can be achieved. Our study indicates that simple methods of digital classification of Landsat data can aid in exploration for mineral deposits in desert regions, and these methods can complement conventional exploration techniques.

REFERENCES CITED

Ahmed, Waheeduddin, Khan, S. N., and Schmidt, R. G., 1972, Geology and copper mineralization of the Saindak quadrangle, Chagai District, West Pakistan: U.S. Geol. Survey Prof. Paper 716–A, 21 p.

Bernstein, Ralph, 1974, Scene correction (precision processing) of ERTS sensor data using digital image processing techniques: Third Earth Resources Technology Satellite–1 Symposium, v. 1: Technical Presentations Section B, NASA SP–351, Dec. 10–14, 1973, p. 1909–1928.

Hunting Survey Corporation, Ltd., 1960, Reconnaissance geology of part of West Pakistan; a Colombo Plan Cooperative Project: Toronto, 550 p. (Report published by Government of Canada for the Government of Pakistan).

Khan, S. N., 1972, Interim report on copper deposit of Saindak, Chagai District (Baluchistan), Pakistan: Pakistan Geol. Survey, Saindak copper report no. 1.

Lowell, J. D., and Guilbert, J. M., 1970, Lateral and vertical alteration-mineralization zoning in porphyry ore deposits: Econ. Geology, v. 65, no. 4, p. 373–408.

Schmidt, R. G., 1968, Exploration possibilities in the western Chagai District, West Pakistan: Econ. Geology, v. 63, p. 51–60.

———1974, The use of ERTS–1 images in the search for large sulfide deposits in the Chagai District, Pakistan: U.S. Dept. of Commerce, Natl. Tech. Inf. Service, E74–10726, 38 p.

PROCEEDINGS OF
THE FIRST ANNUAL WILLIAM T. PECORA MEMORIAL SYMPOSIUM,
OCTOBER 1975, SIOUX FALLS, SOUTH DAKOTA

A Deeper Look at Landsat–1 Images of Umiat, Alaska

By Andre F. Maurin
Compaignie Française des Pétroles, Paris, France,
and Ernest H. Lathram,
U.S. Geological Survey, Menlo Park, California

ABSTRACT

Discussion of subjective evidence for visual identification of previously unrecognized lake lineations shown on Landsat–1 (formerly ERTS–1) image 1004–21395 (Fischer and Lathram, Oil and Gas Journal, May 28, 1973) led the senior author to undertake more precise geomorphic mapping. The use of a new statistical tool, the Texture Analyser, has provided a mathematical control for lake lineations as they were first sketched by Fischer and Lathram. The structural pattern has been developed into a full map of the area covered by thaw lakes. Enlarged pictures of an almost similar image taken by Landsat–1 earlier in the spring confirm the meteorological origin, but with an underlying tectonic influence for the most conspicuous (north) trend in lake shores. A second trend, east-northeast, is demonstrated to result from a complex elliptical pattern caused by numerous closed structures. Further details are given on the potential of the Texture Analyser for cuesta mapping and fault enhancement through discrimination of certain values of grays, although this last method is not as accurate as other computerized programs such as gray stretching. Its instant reading makes it very valuable for geomorphic applications in numerous domains.

INTRODUCTION

The Arctic Coastal Plain of Alaska is characterized by thousands of thaw lakes. Many are oriented; elongated rectilinear shorelines trend approximately N. 9° W., nearly perpendicular (~85°) to the prevailing wind direction. Most authors ascribe the orientation of these lakes to elongation of shorelines through wind-induced erosion (Black and Barksdale, 1949; Carson and Hussey, 1962; Price, 1968; Black, 1969).

In many of the elongated lakes, short shorelines are straight and orthogonal to long ones, suggesting to Rosenfeld and Hussey (1958) a possible structural control. In addition, in the Umiat area, individual lakes are aligned in a direction perpendicular to the elongation, as are linear areas betweeen lakes, and some groups of lakes, lines of lakes and lines of interlake areas form oval or circular cluster-shapes. These observations led Fischer and Lathram (1973) to suspect that the lake orientation results from control by concealed structural patterns.

The features noted above are consistent with patterns noted in other areas and ascribed to block-faulting (Bostock, 1948; Price, 1968). In particular, the alignment of individual lakes and the linear pattern of interlake areas seem more logically to be the result of structural control, as wind influence generally initiates a random distribution pattern, acting only on individual shapes. With respect to oval or circular cluster shapes, it is interesting to note Bostock's illustration of an "oval basin shape developing" within an area of oriented lakes strongly affected by block faulting (Price, 1968, p. 794).

The purpose of this paper is to present the method and preliminary results of a mathematical analysis of lake distribution and orientation in northern Alaska (fig. 1) designed to provide an objective and rigorous basis for geomorphic interpretations and for inferences of structural control. The method combines the regional (34,000 km ^{2}) view and orthoplan representation of Landsat images with the statistical analysis capability of the Texture Analyser (Leitz-Ecole des Mines de Fontainebleau, France), originally developed

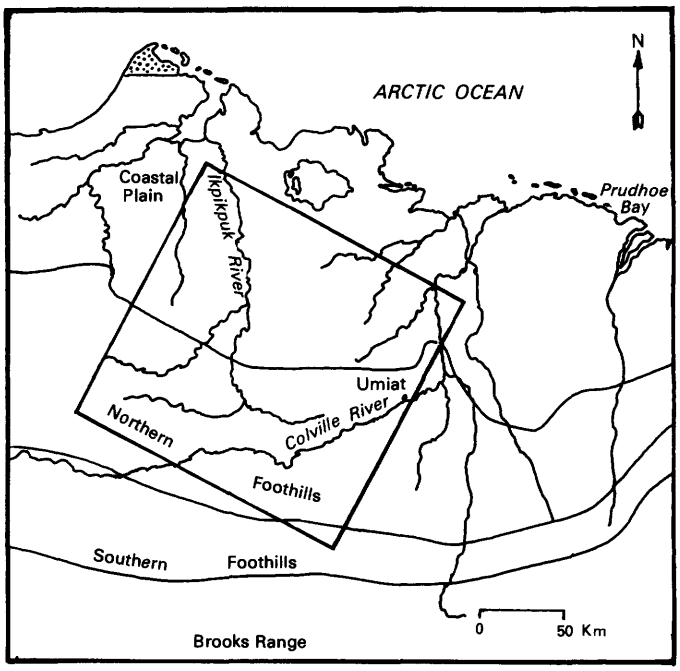

FIGURE 1.—Index map of northern Alaska showing physiographic provinces, the area covered by Landsat image 1004–21395, and the area of oriented lakes previously studied by Carson and Hussey (1962).

for analysis of microscopic textural fabrics. Landsat–1 image 1004–21395 (fig. 2), the basis for Fischer and Lathram's interpretations, is admirably suited for the purpose. All of the geomorphic features described above are included on a single scene. Further, the band 7 image (0.8–1.1 μm) presents a high contrast between land and water and a sharp definition of the form and distribution of lakes, because this part of the light spectrum is absorbed by water.

The method assists in geomorphic analysis by assessing the statistical value of each character and provides a more firm basis for naturalistic interpretations but, *like other such computer-like systems, should not be substituted for human interpretations.*

Computer enhancement of the quantitative values produced by Landsat multispectral sensors has previously been employed for several purposes. Values of light reflectance, grouped by computer as to type of natural or manmade feature having a characteristic reflectance or group of reflectances, have been used to determine land cover by class, and type and species of vegetation (Ellefsen and others, in press; Hall and others, 1974). Ratios, or augmentations, of reflectances in different wavelength bands have been utilized to identify rock types, alteration products, and soil types (Rowan and others, 1974; Albert, 1975). In addition, gratings, with parallel or concentric ruling, have been used to augment the appearance of linear or curvilinear features and to determine qualitatively the trends and patterns of Earth features. The method here employed permits the objective measurement of the trend of linear or curvilinear features and of the form and shape of Earth features and of their *quantification* by ADP methods. In short, it provides a *statistical* basis for geometrical description of Earth features, a *fundamental step* in the study of structures and their significance in the exploration for mineral and mineral fuel resources.

MATHEMATICAL APPROACH

The mathematical basis for and geometric rationale of the use of structural elements in texture analysis is given in Serra (1972). The description of a prototype Texture Analyser and its use is given by Klein and Serra (1972). Since their paper, an operational model has been built from the prototype. Most applications for the Texture Analyser and previous quantifying instruments have been directed toward study at microscopic scales (grain distribution in cement and in ground ore, ore mineralogy and metallurgic study in polished section, porosity distribution, cytology, etc). The application reported here represents a quantum jump in the scale of study.

For clarity some mathematical terms employed herein require a simplified definition:

1. *Erosion.*—an elementary geometrical operation for filtering, resulting in the "smoothing" of boundaries (grain contours, patches, etc.) such as suppression of peaks. (Presumably high band-pass spatial filtering, ed.—)
2. *Dilatation.*—complementary process to erosion, addressing intergrain geometry (e.g., porosity). (Presumably low band-pass spatial filtering, ed.—)
3. *Opening.*—the result of both erosion and dilatation processes designed to improve, through simplification, the structural meaning of a geometrical pattern. Because of the possibility of varying the size of the hexagonal element (the geometric figure employed to analyse patterns), such a pattern provides great flexibility in observation.
4. *Closing.*—the reverse function of opening; e.g., a closing to simplify grain pattern is an opening with respect to the porosity pattern.

GRAY DISCRIMINATION

This is the basic step in use of the Texture Analyser. As the analyser makes statistical counts of white

FIGURE 2.—Landsat image 1004–21395, band 7, of the Umiat area. Lakes are in black.

or black dots, contrast in the image must be high, and intermediate gray levels suppressed. The unenhanced positive transparency from Landsat band 7 provides sufficient contrast for a direct read-out. However, increased contrast was obtained by making a simple ozalid print of the positive transparency (fig. 3) and by making a high-speed Ektachrome slide for microscopic use.

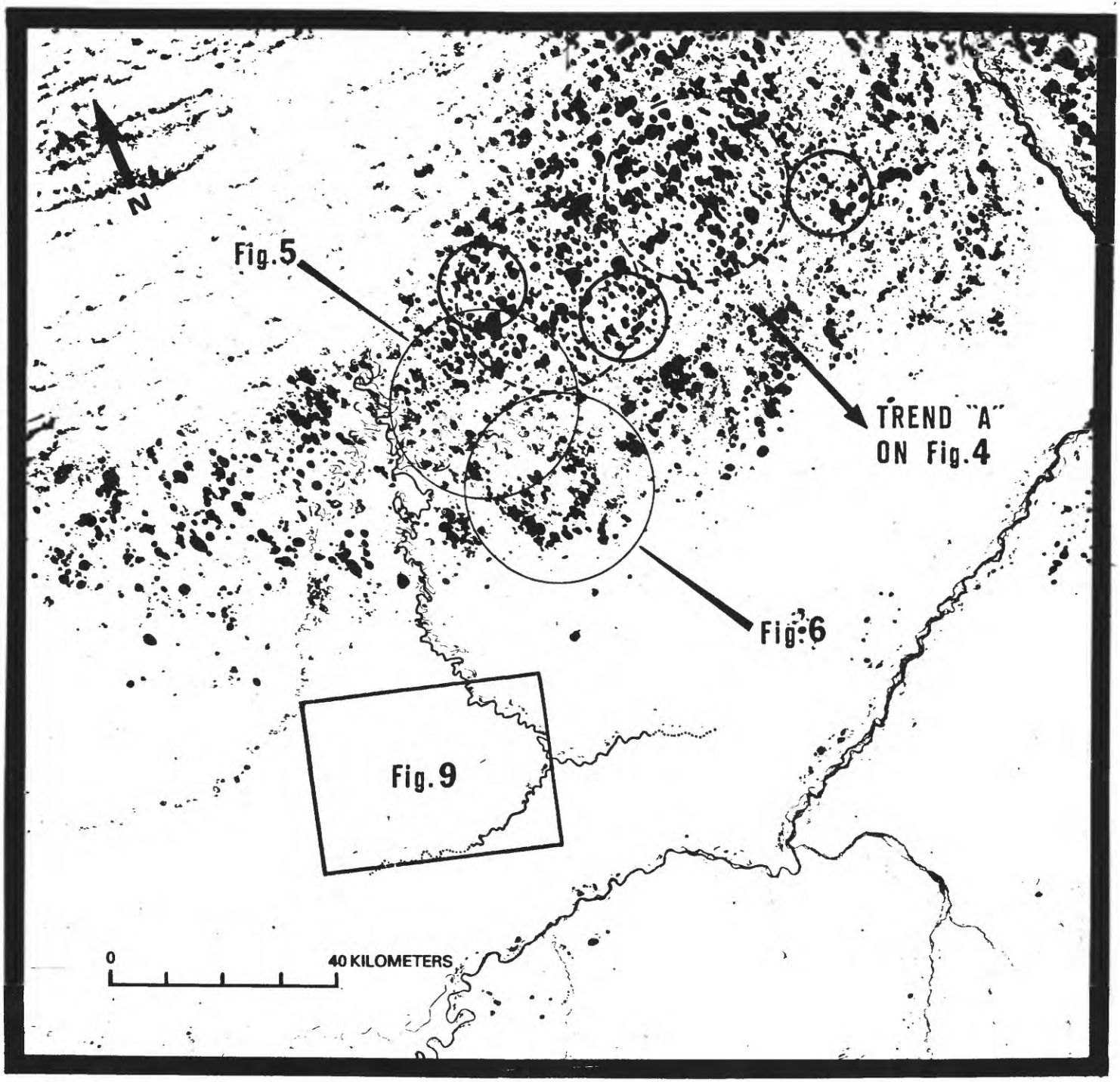

FIGURE 3.—Ozalid print of positive transparency of Landsat image 1004–21395, band 7, showing contrast enhancement and location of detailed figures. Two dashed circles represent the areas in which average lake lengths were measured automatically. Three small heavy circles are the three zones studied to produce the direction diagram in figure 4.

AVERAGE LENGTH OF LAKES

An automatic survey of the length of lakes was made on the analyser. This was accomplished by computing the average length of linear groups of uninterrupted black dots recognized by the analyser along selected diameters of circular fields of observation. Two large circular areas were surveyed providing a

count of more than 100 lakes. Trend A (fig. 3) was chosen arbitrarily parallel to the major trend in lake shores and dry paths (linear interlake areas) with a similar direction. The average length of lakes along Trend A is 1.426 km. A measurement perpendicular to Trend A yields 1.406 km, while counts at 20°, 40°, and 60° from Trend A give 1.102, 1.147, and 1.246 km, respectively.

(Because this computation involves a complicated statistical function, requiring nearly 2 hours for hand calculation of these five measurements, a hardware connection is under development to permit instant computation.)

TRENDS OF PREFERENTIAL ALIGNMENTS

A reduced photographic slide of the lake area was observed through the microscopic apparatus using programmed rotations of the "electronic rotating stage." Six circles were analysed at high speed. Each circle was studied by "Hit or Miss Transformation" (Serra, 1972) of black versus white lengths, every 2°. The computation for one circle required about 60 seconds. The direction diagram (fig. 4) shows these measurements integrated in 4° segments.

Out of the six circles, three give apparently random diagrams (not represented in fig. 4), but three seem to give rather significant results. Figure 4 is a diagram composed from mixing the three last results. This diagram is *qualitative* and provides two families of trends.

The first family is composed of two clear trends which form a narrow angle bisected by Trend A (figs. 3 and 4). The second family is composed of a number of lesser trends, subtending a greater angle (40°), bracketed by two major trends; the bisectrix of the second family we designate as Trend B. It should be stressed that in no way is this rose diagram influenced by the length of lakes. Following Serra's (1972, p. 95–96) consideration, these trends represent the proportion of black (lake) versus white (land) segments in a given direction. By the same token, this measurement provides an indication of preferential rectilinear alignments either of lakes or of paths.

At this point in the investigation, it is clear that it is not possible to apply to the Umiat area the conclusions of Carson and Hussey (1962) resulting from their field study near Point Barrow, north of the Umiat area. Normal winds could initiate a narrow forked pattern such as that of Trend A by interference in wind directions (Carson and Hussey, 1962, figs. 3, 4, and 5), but Trend B and the anomalous length computed in average length counting must originate through another process. It is logical to expect a greater influence of tectonics in the Umiat area as compared to the Point Barrow vicinity, as it is common for structures to decrease in intensity from the

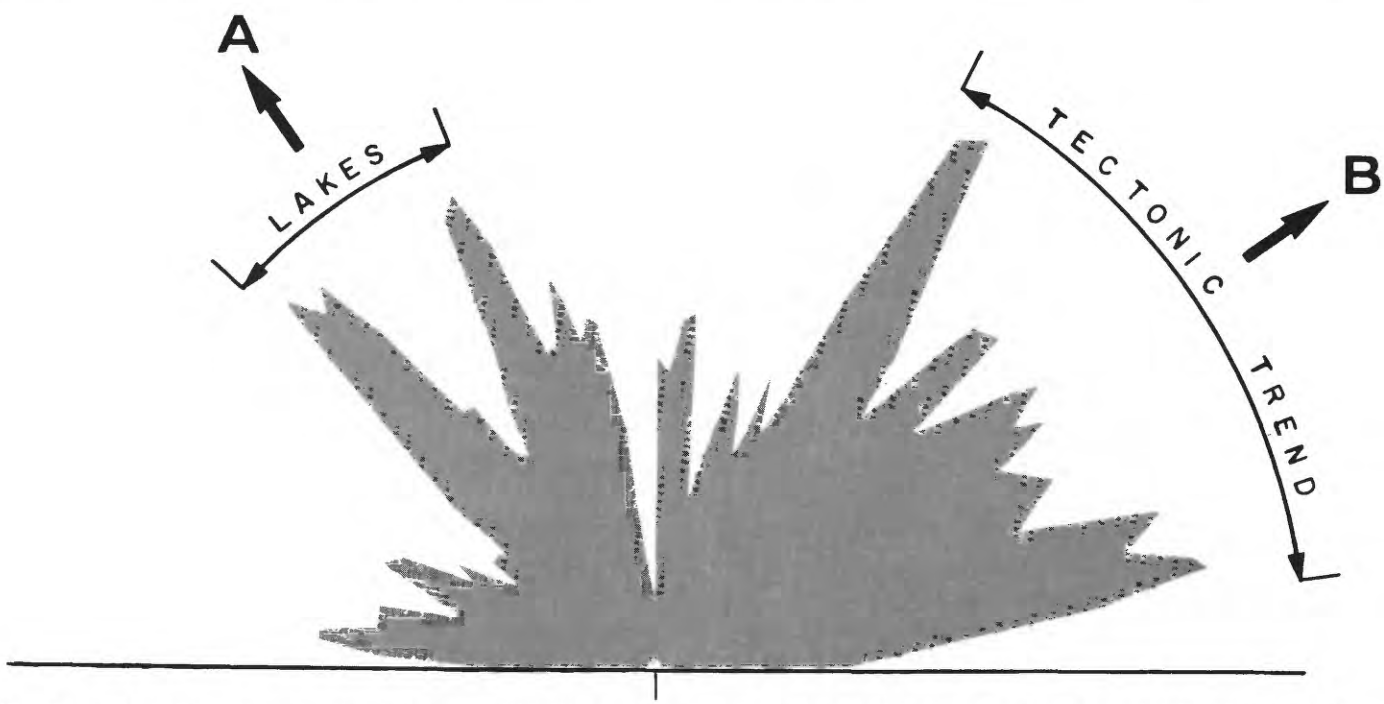

FIGURE 4.—Direction diagram computed from the three heavy small circles of figure 3. *A* and *B* are significant trends discussed in the text.

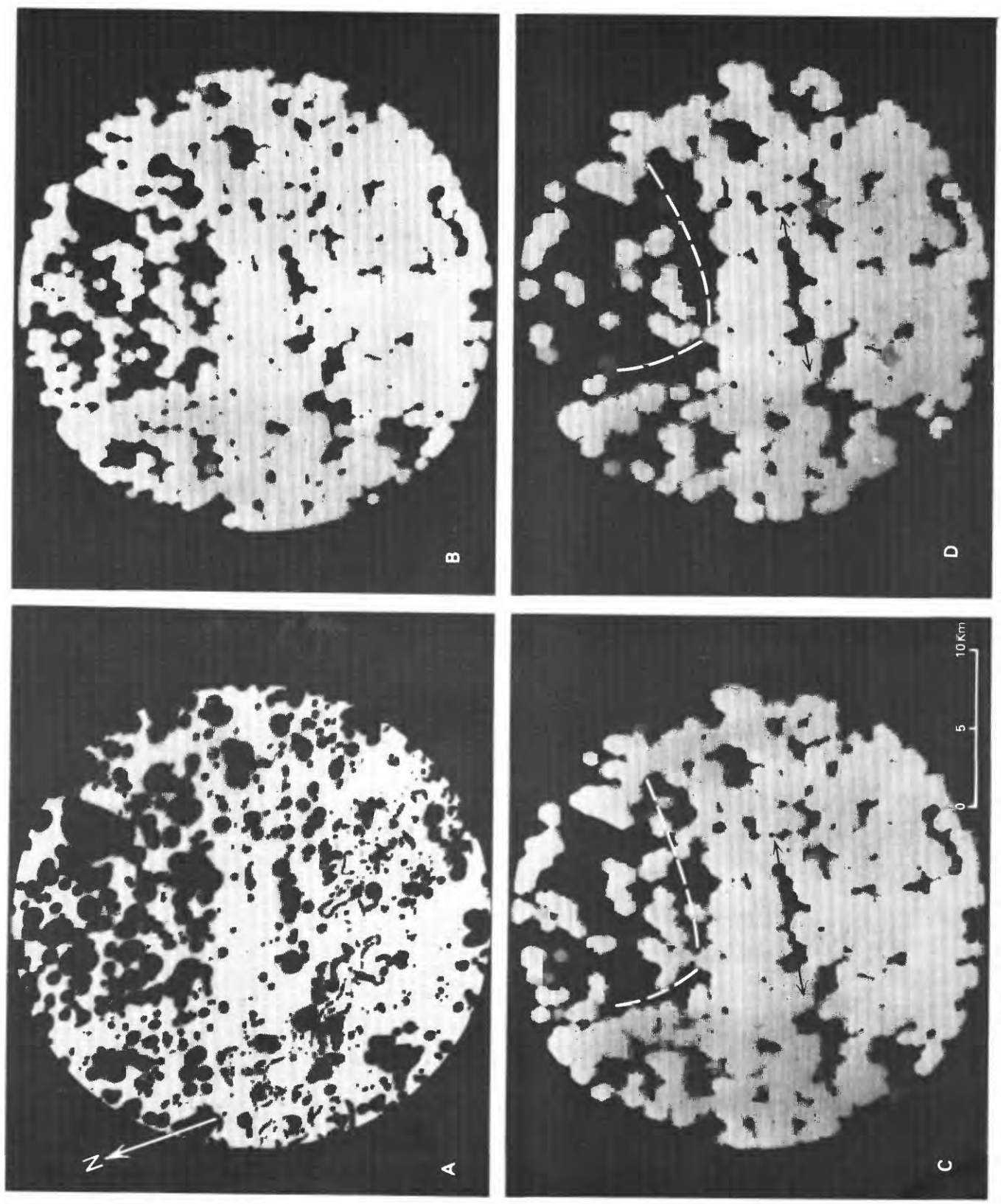

FIGURE 5.—Steps in *erosion* and *opening* process. *A*, circular area investigated with gray discrimination; note that the outer zone of the control screen is not discriminated. *B*, hexagonal *erosion* of blacks (black spots); shape of hexagons is apparent. *C* and *D*, hexagonal *opening* of blacks with two standard sizes of hexagons. A rectilinear pattern is indicated by arrows, the nested curvilinear trends are shown by dashed lines, and an offset is apparent. Analysis of unenhanced positive transparency of Landsat band 7 image.

inner to outer zones of foothills and toward the plains, as in northeast British Columbia.

Observing trends along the Ikpikpuk River extending some 15 miles southward from the Point Barrow area, Rosenfeld and Hussey (1958) inferred a structural influence, and suggested an additional east-northeast lineation (i.e., Trend B). It is obvious that the smaller scale and wider observation offered by Landsat images allow instant perception of a greater span of anomalous trends.

HEXAGONAL TRANSFORMATIONS

Klein and Serra (1972) describe the Texture Analyser as an apparatus able to "measure forms, sizes, and patterns." Sizes and forms have been partly investigated in the two preceding sections. Hexagonal logic allows the analysis of the structural pattern (this logic may also be introduced into the first two steps).

The circular areas shown on figure 3 were analysed through hexagonal transformation (figs. 5 and 6). Each figure exhibits the control image, after gray discrimination (electronic suppression of intermediate levels of gray) of the exact area of survey. Then, this image is transformed into a set of patches made of individual *hexagons* (fig. 5*B*). These patches are the result of a mathematical *erosion* (Serra, 1972) determined by the size of individual hexagons (notice that the hexagon is the most complex polygon which allows a complete coverage of a bidimensional surface without overlap; such an overlap would be embarrassing for statistical purposes). The next processing is *opening* of black patterns. Klein and Serra (1972), and Serra (1972) demonstrate the structural value of such a mathematical process, and complete references to earlier works are contained in their papers.

Figures 5*C* and *D* exhibit an ENE–WSW trending linear set and a near-circular feature made of two crescentic anomalies of possible morphological value. Such circular or elliptical lineations of lakes deserve a lot of attention. Coupled with crescentic lineations, they are believed to be the subtle expression of a mini-cuesta system, e.g., erosional breaks formed on very gently sloping beds within the Pleistocene Gubik Formation.

Figure 6, converted into the hexagonal pattern and *opened* (comparable to 5*D*), shows a crescentic imbrication of prime significance in geomorphic mapping. It is located close to the most northerly Foothills anticline axis (Lathram, 1965; Fischer and Lathram, 1973, fig. 3) and provides a basis for geomorphic mapping.

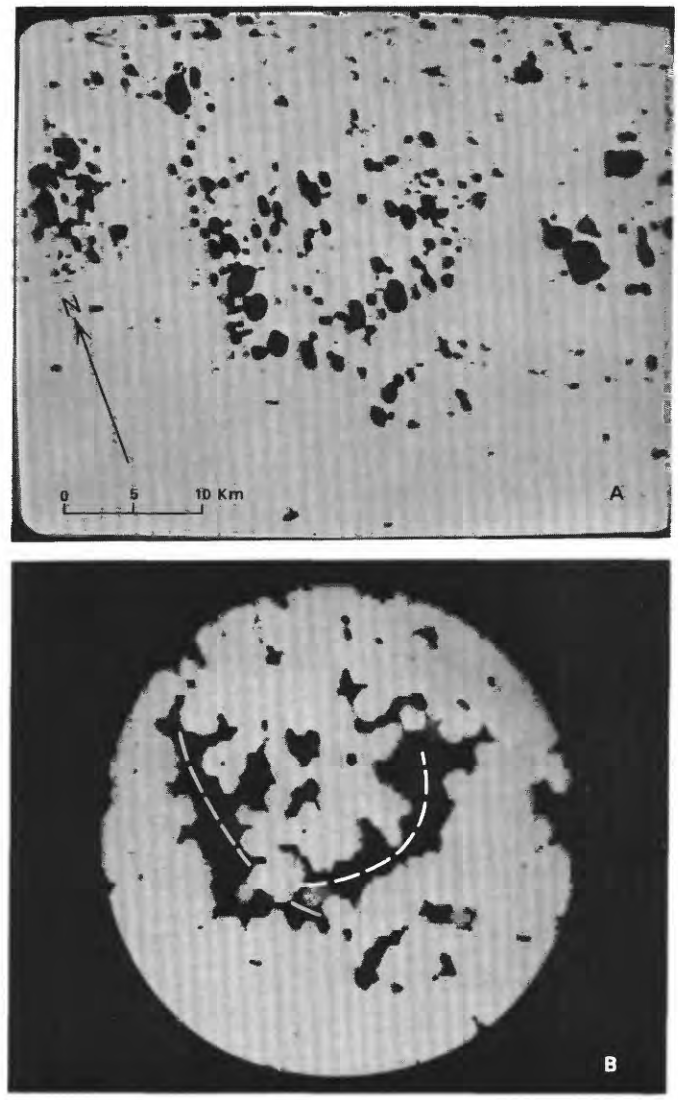

FIGURE 6.—Another area studied using the *erosion* and *opening* process. *A*, control screen without gray discrimination. *B*, *eroded* and *opened* cluster zone. Analysis of unenhanced positive transparency of Landsat band 7 image.

GEOMORPHIC MAPPING

We believe the foregoing mathematical data indicate a structural origin for both Trends A and B (figs. 3 and 4). With respect to B, the angular array of high values, broader than the array for Trend A and with many intermediate trends, may originate from a different tectonic cause than that of A. The Trend A array may be caused by intercepts with narrowly diverging rectilinear paths or lines of lakes, whereas the B array may reflect numerous broadly divergent intercepts controlled by the curved outline of the ellipses. Logically, intercepts with a rectilinear zone would be narrow, but intercepts tangent to the outline of an ellipse would be broadly divergent. By the same reasoning,

the more narrow angular display of Trend A may represent both a wind-induced preferential shore direction and a structural element. This element may have lesser impact on morphology than the ENE–WSW trending ellipses.

Unfortunately, the Texture Analyser is not designed at present to analyze and compare curved elements, but only to compare and measure straight ones. A program to analyze and compare the radii of curved image features is being developed and will be operational in late 1975.

Accordingly, conventional methods of geomorphic interpretation, guided by the foregoing data and reasoning, were used to develop a structural map of the area (fig. 7). Using the surface anticline (Lathram, 1965) closest to the Coastal Plain as a standard, deflections and bends of the north-flowing Ikpikpuk River are considered to be produced by anticlinal plunges, with apexes located east of the river. West of the most southerly bend in the river on the Coastal Plain, three sets of lakes arranged in three crescentic patterns appear to be the remnants of the bend as the river was displaced erosionally to the east.

ENE–WSW lineations between lakes (paths) are clearly bent and follow lines of elliptical anomalies. These lines are considered to be anticlinal axes; the chaplets of apexes create elliptical patterns. The three more northerly axes are drawn on less sure grounds but are suggested by the lines of ellipses.

The long clear lineament along the east bank of the river (fig. 7) is one of several linear anomalies lying parallel to Trend A. However, its special bearing on tectonic interpretation deserves some discussion. Axes on the west, aligned along the centers of crescents, are displaced from those on the other side of this lineament. The lesser number of lakes and elliptical anomalies on the west side may indicate that this is a down-thrown block. However, this feature is interpreted herein as a transverse fault. Other lineaments parallel to this fault or Trend A could also represent minor fracturing. We note that the lineament shown on figure 7 is an extension of the transverse trend of the Maybe Creek "low" recognized by Brosgé and Whittington (1966, p. 583).

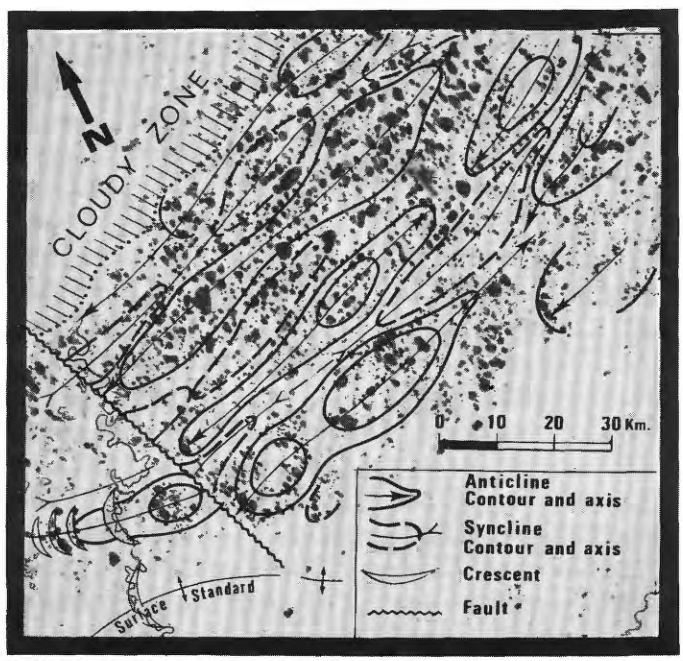

FIGURE 7.—Structural interpretation by conventional geomorphologic study using outcropping anticline as a standard and the elliptical "path" concept.

ADDITIONAL OBSERVATIONS FROM THE LANDSAT IMAGERY

Additional observations have been made which substantiate our interpretations and provide additional support for the mathematical approach. At the same time, the incredible amount of information displayed on Landsat imagery is demonstrated.

OBSERVATIONS ON METEOROLOGIC EFFECTS ON THAW-LAKES

About 20 percent of the lakes investigated in this study are oriented according to the definition of Carson and Hussey (1962) and Black (1969). This permits a thorough test of their concepts. On Landsat–1 image 1004–21395, the east-west banding of clouds provides an instant meteorological indicator of the wind direction they derived from many historical records. Further, an almost similarly located image (1345–21344, band 7) taken by Landsat–1 on July 3, 1973, (almost 1 month earlier than the previous one) exhibits partially frozen lakes (fig. 8). Some of the elongated lakes contain mushroom-shaped ice cakes which substantiate the observations of Carson and Hussey (1962) as shown on their figures 10a, b, and c (Ikroavik Lake) and support their meteorological interpretation. The symmetrical pattern of the ice cakes and the bulbous shape of the distal wings indicate a dominant wind blowing westwardly and counter-rotational lake currents as they suggest. The repetitive views of Landsat provided a time dimension they were not afforded in the field, i.e., Landsat observations every 18 days and their field work once per summer.

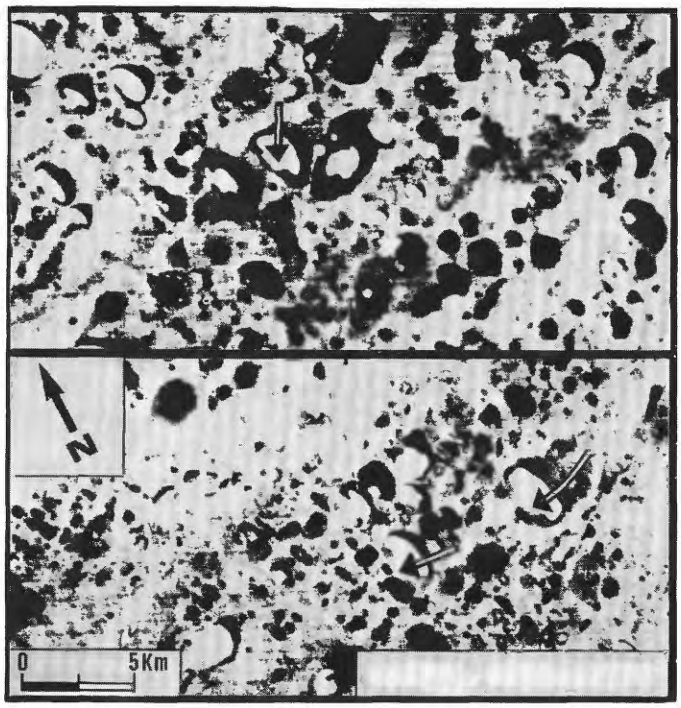

FIGURE 8.—Two selected areas of Landsat image 1345–21344, band 7, with common orientation showing mushroom ice cakes (arrows) in black lakes.

APPLICATION OF THE TEXTURE ANALYSER TO STRUCTURE IN THE FOOTHILLS

Although the topic of this paper is centered around the thaw-lakes area, some observations in the Foothills south of the Coastal Plain will help understand the anticline-transverse faulting pattern in the Coastal Plain. Once again, information is derived from Landsat–1 image 1004–21395, proving the wealth of information provided by such small-scale imagery. Near the big bend of the Ikpikpuk River, the map of Lathram (1965) indicates a number of anticlines within the area of figure 9 (location on fig. 3).

After gray discrimination, a further process eliminates, through thresholding, some specific grays from the control scale (right of fig. 9*B*). This helps in delineating dip slopes and displacements by enhancing shadows and triangular facets. Hexagonal transformation with minimal erosion strongly enhances such displacements. Cross faults appear very sharply (fig. 9*C*). It is interesting to note that most of these faults are parallel to Trend A.

Analysis of the Foothills zone on image 1004–21395 exhibits two groups of faults (with dextral and sinistral offsets) belonging certainly to a transverse fault system. These observations support the structural map (fig. 7) of the thaw-lake area.

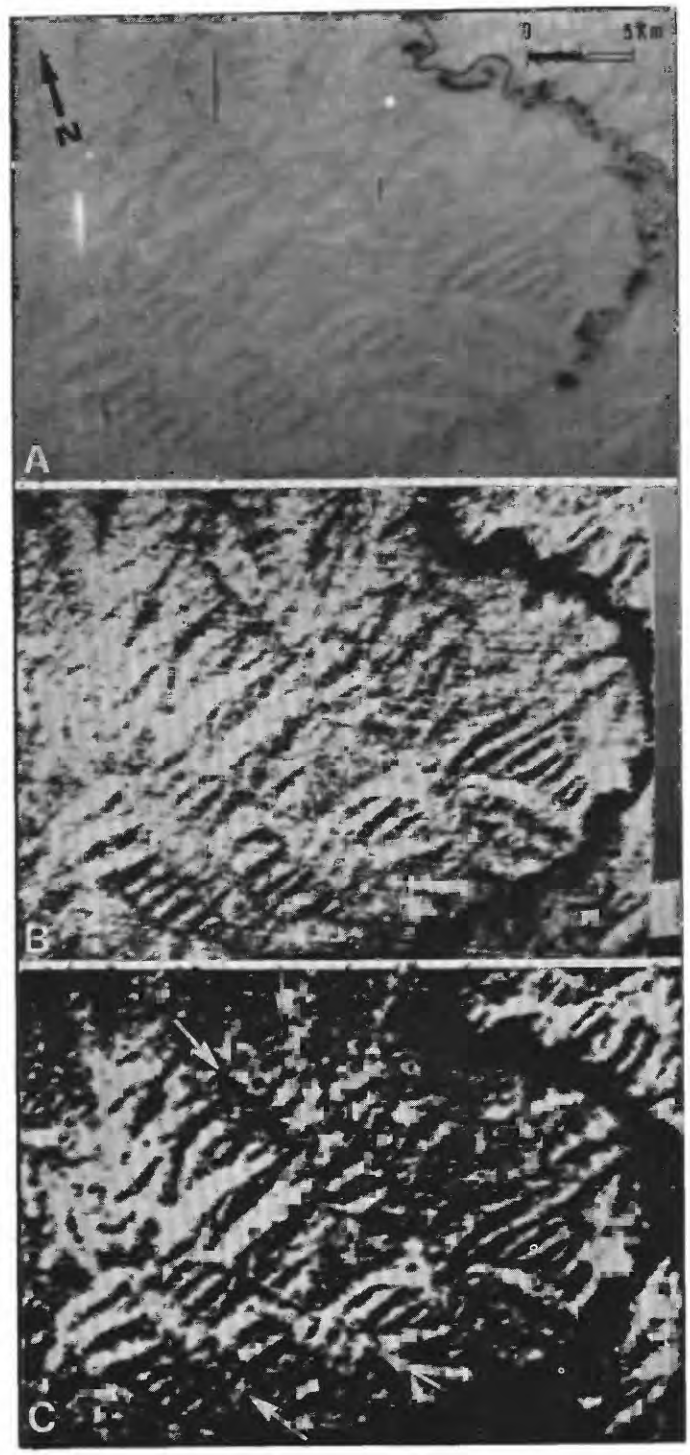

FIGURE 9.—Experimental processing of part of the Northern Foothills shown on Landsat image 1004–21395.
A, Control image. See figure 3 for location of surface anticlinal axes. *B*, Same image after thresholding of penultimate gray level of the analyser, scale shown on right margin without level 1 (white). *C*, Hexagonal transformation of the black and white information of figure *B*, with minimal erosion. Note that in *C* shadows which may be cuestas are more strongly enhanced. Faults are enhanced and clearly shown by linear disruptions (see arrows); in some cases offsets along the faults can be quantified by the analyser.

CONCLUSION

The morphologic value of both Landsat imagery and the use of the Texture Analyser have been demonstrated.

In such an area as the Arctic Coastal Plain, where technical problems of resource exploration (ecology, costs, etc.) are very stringent, the method can provide a maximum of information without environmental stress, can be evaluated with a minimal amount of conventional checks, and provide guides to the optimum location of such checks. The structural map may be greatly improved and become an actual operational tool.

These results are sufficiently encouraging to pursue the same approach west and eastward. To the east the Prudhoe Bay area will provide the type of checking and control required. Precise angular measurements are needed in order to separate tectonic effects from those of dominant winds in those areas where both directions are not parallel or perpendicular, and work on these is proceeding.

The use of only two sequential Landsat images of the same scene has permitted observations to be made in three domains, the conciliation of the two main genetic theories for the origin of thaw-lakes, and a suggestion of even more fundamental ideas:

1. The Foothills domain in which faulting is normal to anticlinal axes.
2. The thaw-lake area in which nearly perpendicular linear trends point toward a structural pattern, and ice cakes in many of the lakes conform to meteorological theories of the formation of oriented lakes.
3. The cloudy zone in which banding is parallel to the general direction of the mountains.

From these observations we believe that meteorological conditions, mainly dominant winds over the Coastal Plain, are a topographic consequence of the Range and Foothills system. Further, the structural pattern within the Plain is a weak but subsequent image of the tectonic style in the Foothills. If these conclusions are valid, then a perfect similarity should exist between wind-induced shore patterns and cross faulting through an anticlinal area of great petroleum potential.

ACKNOWLEDGMENTS

Publication of this paper has been authorized by Compagnie Française des Pétroles (Paris and Calgary). We thank Messrs. Klein and Serra for kindly providing mathematical precision and *Centre de Morphologie Mathématique* of Ecole des Mines, in Fontainebleau, France (Co-owner with IRSID, of the patent on the Texture Analyser, manufactured by Leitz, Germany), for experimental access to the Texture Analyser. J. M. Fonck and M. Riguidel, CFP, Paris, provided much information on previous and future use of the machine.

REFERENCES

Albert, N. R. D., 1975, Interpretation of Earth Resources Technology Satellite imagery of the Nabesna quadrangle, Alaska: U.S. Geol. Survey Misc. Field Studies Map MF–655J, 2 sheets, scale 1:250,000.

Black, R. F., 1969, Thaw depressions and thaw lakes, a review: Biul. Peryglacjalny, no. 19, pp. 131–150.

Black, R. F., and Barksdale, W. L., 1949, Oriented lakes of Northern Alaska; J. Geol., v. 57, pp. 105–118.

Bostock, H. S., 1948, Physiography of the Canadian Cordillera, with special reference to the area north of the fifty-fifth parallel: Geol. Survey Can. Memoir 247, 106 p.

Brosgé, W. P., and Whittington, C. L., 1966, Geology of the Umiat—Maybe Creek region, Alaska: U.S. Geol. Survey Prof. Paper 303–H, 638 p.

Carson, C. E., and Hussey, K. M., 1962, The oriented lakes of Arctic Alaska: J. Geol., v. 70, pp. 417–439.

Ellefsen, R., Gaydos, L., Swain, P., and Wray, J., New techniques in mapping urban land use and monitoring change for selected U.S. Metropolitan areas: an experiment employing computer-assisted analysis of ERTS–1 MSS data, *in* Internat. Soc. of Photogrammetry, Commission VII Symposium, Banff, Alberta, Oct. 1974, Proc. (in press).

Fischer, W. A., and Lathram, E. H., 1973, Concealed structures in Arctic Alaska identified on ERTS–1 imagery: Oil and Gas J., v. 71, no. 22, pp. 97–102.

Hall, F. G., Bauer, M. E., and Malila, W. A., 1974, First results from the crop identification technology assessment for remote sensing: West Lafayette, Indiana, Purdue University, Laboratory for Application of Remote Sensing, LARS Information Note 041874.

Klein, J. D., and Serra, J., 1972, The Texture Analyser: J. Microsc., v. 95, pp. 349–356.

Lathram, E. H., 1965, Preliminary geologic map of Northern Alaska: U.S. Geol. Survey open-file map, scale 1:1,000,000.

Price, W. A., 1968, Oriented lakes, *in* Fairbridge, R. W., ed., The encyclopedia of geomorphology: Reinhold Book Corp., pp. 784–796.

Rosenfeld, G. A., and Hussey, K. M., 1958, A consideration of the problem of oriented lakes: Iowa Acad. Sci. Proc., v. 65, pp. 279–287.

Rowan, L. C., Wetlaufer, P. H., Goetz, A. F. H., Billingsley, F. C., and Stewart, J. H., 1974, Discrimination of rock types and detection of hydrothermally altered areas in South-central Nevada by the use of computer-enhanced ERTS images: U.S. Geol. Survey Prof. Paper 883, 35 p.

Serra, J., 1972, Stereology and structuring elements: J. Microsc., v. 95, p. 93–103.

PROCEEDINGS OF
THE FIRST ANNUAL WILLIAM T. PECORA MEMORIAL SYMPOSIUM,
OCTOBER 1975, SIOUX FALLS, SOUTH DAKOTA

Why Landsat? A Management View

By J. Robert Porter, Jr., President,
Earth Satellite Corporation, Washington, D.C.

Earth Satellite Corporation has provided substantive geological consulting services to over 100 projects in which Landsat imagery has been utilized. To the best of my knowledge, this is considerably more exploration experience with Landsat than any other commercial or governmental group has had to date. Today, I thought you would be interested in some of the conclusions we have made, considering these projects as "case studies" from which one can generalize about the learning curve corporations and individuals experience in working with Landsat data. For the purpose of this presentation, I am only going to address the oil and gas applications of EarthSat and exclude our hydrological and geothermal activities.

Two years ago, the initial decision to utilize Landsat (then ERTS) imagery was generally made either at the top or the bottom of the corporation. The reason for this was quite simple, and can be related to the time frame in which a person's job is evaluated. A corporate president or vice president of exploration in a medium to large company is primarily focusing his attention on attaining his corporate goals over a 2- to 10-year period. He was interested in understanding, first and foremost, how Landsat and/or other remote-sensing techniques may affect his corporate strategy. Further, he was interested in introducing new technology to his exploration groups from the standpoint of developing a "training" familiarity which may pay off in a few years. In brief, he expected very little in the short term but felt a "little money ought to be put into this to see what's there."

At the bottom of the organization are the geologists and engineers who are basically interested in preparing themselves and their company for the future, even if the new technology is not of proven worth initially.

In the middle sits the exploration manager for a district or a region, who has a very tight, well-defined exploration budget and who must obtain results within a short period of time or be considered a failure. Understandably, he was initially not interested in Landsat because there was no one in his organization, or elsewhere, who could convince him 2 years ago that this would save him time or money and help him meet his corporate objectives with more certainty. During the last 2 years a significant change has taken place and Landsat is becoming an exploration tool which will soon be routinely a part of the budget controlled by this exploration manager. The use of Landsat imagery has moved from research to operations.

The reason for this is simple. The technology works! There is no question but that a new "quality" of information is available. I say "quality" because its contribution to the investment decision is quite different, for example, than aerial photography.

The way a corporation utilizes Landsat imagery varies considerably with its familiarity and experience. Almost every group I know went through an initial "gee whiz" phase in which they bought or were shown a few photographs from Sioux Falls and noted with interest that several features they were familiar with could be seen in the imagery. Alternatively, they may have been impressed by a false-color rendition of some salient or subtle feature exhibited by a commercial vendor.

The second phase is characteristically much more professional but not yet commercial. At this point, geologists and engineers are looking at Landsat imagery as though it were a low resolution aerial

photo. Naturally they became more interested in technique development which, in a sense, from their view at this time, is a means of compensating for the "limited resolution" inherent in Landsat. During this phase, several important mental limitations still exist. Primarily, they do not really understand what is different in the scene they view which wouldn't be better perceived by an aerial photograph if they had it. The principal attraction is low cost and newness. Nonetheless, at this point, Landsat imagery starts to be a tool in which features are identified and related to one another so that it becomes incorporated, somewhat traditionally, into ongoing operational programs.

In the third phase, by combining a model of resource occurrence (based on theory and previous work) with the large area relationships visible in orbital imagery, data from satellite platforms become a powerful exploration tool.

The unique ability of satellite systems to acquire imagery that portray large portions of the Earth's surface enables geologists to characterize large, widely separated regions (such as shield areas or extensive sedimentary sequences) and compare known mineralized areas with as yet unexplored areas as an important first step in the search for mineral deposits. Moreover, once having located an area of general interest (a proper geologic environment), investigators have mapped the tectonic style of the area and delineated those subareas which generally favor economic accumulations of minerals—for example, sedimentary basins, greenstone belts, and fold mountain belts. In several instances, the Landsat imagery enabled the geologists to proceed a step further and identify and map structural features as lithologic associations within the subareas which might serve as keys to economic accumulations of minerals, petroleum, ground water, or geothermal resources—for example, salt domes, anticlines, intrusions, ultramafic rocks, and fracture intersections. At this level of detail, the geologist is able to correlate known economic deposits with lithologic and structural features perceived in the imagery and draw additional inferences about factors controlling and localizing economic deposits, thus refining his initial exploration model.

There is some evidence that space imagery can lead to the direct detection of certain geologic resources by virtue of recognizing such features as gossans, peculiar tonal-textural features that are strongly correlated with oil and gas production, depressions under the icecaps that mark possible geothermal heat sources, or terraces along streams known to carry gold. However, most often the contribution of space-acquired data is based on inferences drawn from experiences or from a particular exploration model. In these circumstances, the strength of space data as an exploration tool is greatly increased by the inclusion of ground data in combination with data from other exploration devices such as airborne magnetometry. Several exploration groups are now doing just this. The space imagery is used to locate the favorable structural setting, and then airborne electromagnetic and gravity data are used to refine the details of the model. Targets thus identified are followed up on the ground using geochemistry, resistivity, conventional mapping techniques, and, finally, drilling.

Several geologists have used Landsat and Skylab imagery to tentatively locate structural features of interest to petroleum exploration. In Alaska, near the Umiat oilfield, Fischer and Lathram (1973) spotted a peculiar arrangement of lakes that geophysical data corroborated as an attractive structural feature for petroleum exploration. Further, Saunders and others (1973), related lineaments seen in Landsat imagery to oil and gas occurrences in west Texas. Based on the relationships they saw in the imagery, they have identified several prospective areas.

In the Anadarko basin, we found that many of the known oil and gas producing structural features could be identified on Landsat and Skylab imagery. In addition, we reported that, as yet unexplained, tonal-textural features, called "hazy anomalies," are strongly correlated with oil and gas production. Upon examining the pervasive pattern of lineaments seen in the space imagery and correlating these with geophysical and well data, we concluded that faulting has played a much larger role in the origin and development of the basin than was previously suspected. Based on the study of Landsat imagery in the Basin and Range province of the western United States, we noted a complex interrelationship between faulting, intrusion, and mineralization. Interrelationships noted can be used to guide further exploration even in this relatively well explored area. We also noted that there seems to be a regular spacing of lineaments (fractures) that control mineralization and that the highest potential for mineralization is at the intersection of two such regularly spaced sets.

The savings in time and money realized from these applications is already substantial and will increase as they are used more widely and as these tools are more completely integrated into exploration programs.

Phase three could be called the "commercial phase" in which the technology is better understood and the product is both incorporated into ongoing commercial strategy and becomes a stimulus to the change

in corporate strategy. In my opinion, to equate Landsat imagery with aerial photography is to miss the point almost completely and to lose much of the enormous commercial edge Landsat can provide. Landsat sees geological features in a way aerial photography doesn't.

First, its perspective is different. It is not a substitute. It is different. Not always better. But always different. It avoids the distortion of wide-angle viewing and permits the application of computerized techniques to areas of meaningful geological size where the illumination levels and Sun angle are uniform. The net effect of this is that in Landsat imagery features can be detected and often identified which are totally unrecognizable in conventional aerial photography. Further, it has been our experience, and the experience of our clients, that in virtually every case, even those in which extensive ground work and aerial photography had been previously done, significant new geological features were revealed through the utilization of Landsat imagery.

Second, its spectral coverage is different from any existing film system and its output format on digital tape provides analysts with many more levels of spectral intensity variation to evaluate and manipulate.

Third, traditionally companies have been restricted as a practical matter strategically to areas in which they already had a substantial base of geological information. *The use of Landsat as a means to evaluate rapidly new areas changes the cost equation dramatically and makes it possible for a company to consider an entirely new exploration strategy.* For example, in a number of projects in which we have been associated, prospective concession areas were rapidly and effectively evaluated so that the exploration costs of alternative prospects could be evaluated for less money and with greater certainty than was ever possible previously. Consequently, the companies were not dependent on limited photography or secondhand geological interpretations based on limited information. Further, a consistency was added to the evaluation not previously possible, and new options have been made available at very modest cost in dollars and in time.

So what is next? There is no question in my mind that within 5 years Landsat will be a standard medium used by the oil and mining industries. Unquestionably coincident with this would be greatly improved enhancement techniques taking advantage of digital tapes and repetitive looks during different seasons to identify different features. (One of the great misconceptions during the second phase of development mentioned above is the approach that one picture does it. This is just not so and repetitive coverage under different seasonal and weather conditions makes a significant difference.)

Further, one must consider the context of the times. The advent of Landsat technology is certainly timely: First, because the demand factor for new oil, gas, and mineral reserves is inordinately high and great pressure is being put both from the economic and a nationalistic standpoint on finding new reserves. Second, associated with this, companies are very much of a mind to spread their bets and diminish their risk, in part because they recognize that the political climate of the world is such that it is not possible to predict which situations will be stable from an economic standpoint over the period required to attain a reasonable return on investment. Further, this economic unpredictability does not correlate simply with traditional indicators of political stability as is shown by the fact that even well-established and "stable" governments have become increasingly aggressive in regulation and taxation under the pressures of the energy crisis. Finally, of great consequence, is the fact that new exploration models must be developed. The ability of satellite systems to provide an uninterrupted view of the regional geology of large areas, coupled with the new concepts of plate tectonics, provide many opportunities for perceiving interrelationships that previously had gone unrecognized. These types of perceptions have far-reaching consequences, both for geologic exploration and the development of geologic hypotheses on the origin and evolution of major portions of the Earth's crust. For example, in some of our work using Landsat imagery, we have observed that a constant spacing in major fractures in the Earth's crust appears to be characteristic of specific crust blocks. Geologic theory has long held that the emplacement of intrusive bodies of igneous rocks, some of which may carry economically valuable minerals, is controlled largely by pre-existing fractures. Thus once the fracture spacing pattern is determined and a few economic deposits are found in a particular area, one has a powerful tool for searching for other deposits in the same region.

Another promising area of research and one which will undoubtedly receive increasing attention as mineral exploration increases over the next few years, is the field of geobotany. While this work certainly pushes the state-of-the-art of Landsat resolution, nevertheless Landsat affords a needed opportunity to obtain repetitive coverage at low cost so that correlation can be established and new geobotanical exploration models developed.

Finally, a significant edge will be gained by those organizations which are able to restructure their exploration strategy to take advantage of this technology over the next 3 years. All pictures and all people are not equal, and the merging of high-quality enhancement techniques coupled with high-quality geological minds will be a telling combination. On the other hand, I would like to close with a note of caution. We are just now at the beginning of a commercial phase where we are starting to understand critical subtleties of the technology with which we work. Oil and mineral exploration is a damn tough business. Answers are not spewed out of black boxes run by aerospace "whiz kids." Rather, valuable information is provided which must be evaluated within the context of a sound exploration model. As was the case with all other new exploration techniques, the state-of-the-art will always be stretched and challenged beyond its reasonable limits, and the ability of black boxes to provide answers, as always, will be oversold. Nonetheless, this is an exciting time because what we are seeing is a revolution in access and perception which will tax us all over the next 5 years in just applying the current state-of-the-art. On the other hand, there is a lot of profit to be made, and a lot of losses which could be avoided, if we get on with it aggressively.

REFERENCES CITED

Fischer, W. A., and Lathram, E. H., 1973, Concealed structures in Arctic Alaska identified on ERTS–1 imagery: Oil and Gas Jour., May 28, 1973.

Saunders, D. F., Thomas, G. E., Kinsman, F. E., and Beatty, D. F., 1973, ERTS–1 imagery use in reconnaissance prospecting—Evaluation of the commercial utility of ERTS–1 imagery in structural reconnaissance for minerals and petroleum: Type III Final Report to Natl. Aeronautics and Space Admin. Available from U.S. Dept. of Commerce Natl. Tech. Inf. Service as E74–10345.

PROCEEDINGS OF
THE FIRST ANNUAL WILLIAM T. PECORA MEMORIAL SYMPOSIUM,
OCTOBER 1975, SIOUX FALLS, SOUTH DAKOTA

Regional and Global Geological Studies Using Satellite Magnetometer Data

By Robert D. Regan,
U.S. Geological Survey, Reston, Va.

ABSTRACT

A global magnetic anomaly map derived from satellite measurements offers a new perspective in regional and global geologic studies. Preliminary correlation with tectonic and geologic maps indicates that in addition to reflecting obvious large-scale features such as continental shields, the map also reveals many unexplained structures. Particularly striking are the lack of anomalies in the Pacific Ocean, with the exception of a pair (+6 gammas and −6 gammas) near the 180° meridian in the area where the Emperor Seamount and the Hawaiian Island chain intersect, a broad magnetic low over the Gulf of Mexico, and several highs in the central United States.

Also evident is a major magnetic anomaly in central Africa that does not directly correlate with any known tectonic feature. This anomaly, termed the Bangui anomaly, was discovered in the satellite data and confirmed by aeromagnetic measurements. The anomaly is over an area of thick continental crust and has been interpreted as a massive crustal intrusion that may be related to crustal thickening. Many major mineral deposits are associated with this body.

Although much more work is needed to completely interpret the map and to determine the causes of all the anomalies, the initial results show the utility of a satellite magnetometer as a geological/geophysical tool.

The global magnetic anomaly map and a complete discussion of its derivation are published in the Journal of Geophysical Research, v. 80, no. 5, p. 794.

PROCEEDINGS OF
THE FIRST ANNUAL WILLIAM T. PECORA MEMORIAL SYMPOSIUM,
OCTOBER 1975, SIOUX FALLS, SOUTH DAKOTA

AIRTRACE™—An Airborne Geochemical Exploration Technique

By A. R. Barringer,
Barringer Research Limited,
Rexdale, Ontario, Canada, M9W 5G2

ABSTRACT

The AIRTRACE™ system is a new airborne geochemical technique for collecting and analysing atmospheric particulate material and relating this to the underlying geology and geochemistry. The technique depends upon the existence in the atmosphere of a dispersion of particulate material which covers a broad range of particle sizes. The coarser material above 10 μ in diameter tends to be localized to such an extent that if this size fraction is used the effects of manmade pollution are not a problem in most exploration areas. In temperate and tropical regions vegetation is a prime source of the particulates utilized in the system and laboratory research with radioactive traces as well as field surveys has demonstrated the important role played by vegetation in releasing particulates carrying heavy metals and other trace elements.

Special techniques have been developed for separating particulates of local derivation from the general ambient background by specifically isolating the material in rising thermal plumes. Good results have been obtained in test surveys over orebodies covered by glacial overburden and heavy vegetation. Elements detected include Cu, Zn, Ni, Mn, Fe, Cr, Cd, Al, Mg, Ca, Ti, Si, and C. Techniques for measuring uranium are under development. Tests have also been carried out over an oil and gas field, and it has been demonstrated that airborne anomalies correspond with the location of the field as well as surface rock and soil anomalies in carbon isotopes and manganese. The equipment is being flown in helicopters and fixed winged aircraft.

INTRODUCTION

In the conventional approach to geochemical exploration samples of soil, stream sediment, rocks, or plant material are gathered on a reconnaissance basis or on a close grid in order to determine the regional or detailed distribution patterns of mineralization. The methods of sampling and analysis have been studied over a period of more than 25 years and have led to the establishment of geochemical exploration as a prime mineral exploration method (Hawkes and Webb, 1962; Levenson, 1974). Considerable research has also been carried out in hydrocarbon geochemistry; however, the techniques of geochemical exploration for oil and gas appear to have found widespread application only in Russia (Kartsev and others, 1954).

In the work reported in this paper investigations have been made of the use of atmospheric particulate geochemistry as an exploration tool for both minerals and hydrocarbons, with the aim of supplementing ground geochemical methods and providing techniques for low-cost, large-scale airborne reconnaissance.

An early proponent of the use of atmospheric particulates for airborne geochemical applications was Weiss (1967). Weiss initially employed a filter method for sucking in air and an X-ray analytical technique for analysing particles on the filters. Subsequently, he has used a system of towed filaments that are dragged through the air in order to collect particles on their surfaces. These filaments are periodically wiped, and the material subsequently analysed. Weiss has referred to the atmospheric aerosols as containing mineral particles and has stated that the method is not applicable where the terrain is covered by heavy vegetation (Weiss, 1971).

In the present investigations, attempts have been made to develop new particle collection techniques that are capable of separating and collecting particles that have risen from underlying terrain and rejecting particles that have travelled substantial distances

laterally. Investigations have also been carried out on the contribution of vegetation to the generation of meaningful geochemical responses in the atmosphere, and, in addition, there has been substantial analytical chemical research to develop appropriate methods for use in atmospheric geochemistry.

SOURCES OF ATMOSPHERIC PARTICULATES AND AEROSOLS

The sources of atmospheric particulates and aerosols are both manmade (anthropogenic) and natural, the former being a source of interference in airborne geochemical studies. Anthropogenic pollutant sources associated with urban and industrial areas generate very high loadings of atmospheric particulates, the effects of which tend to be localized in the giant particle sizes (plus 10 μ) but carry great distances under some meteorological conditions in the small particle size range. In urban environments the mean residence time in the atmosphere of submicron particles in the absence of precipitation is in the order of 100 to 1,000 h (Esmen and Corn, 1971). Pollutant particles of greater than 10 μ in diameter will, therefore, have mean residence times of less than 10 h and will be generally localized to the vicinity of urban and industrial areas. Studies of easily recognized carbon and flyash spherules over the North Atlantic confirm that these pollutant particles do not exceed 6 μ in diameter over open ocean and reach larger sizes in only a very small percentage of the total mass of particulates in ocean areas close to pollutant sources such as the Bay of Maine (Parkin and others, 1970). It has been estimated that the mean residence time of particles in the lower troposphere is about 4 days (Poet and others, 1972), and it is, therefore, clear that in the absence of precipitation there can be widespread migration of the mean particulate burden over distances that can on occasion amount to hundreds of miles or more. The fine particle component is the fraction that migrates, and it is this fraction which contains the highest concentration of trace metals (Lee and others, 1967). Approximately 45 percent of the mass of particles in nonurban air close to the ground lies in the size range above 10 μ in diameter (Noll and Pilat, 1971), and it is essential to consider only this size range if the effects of urban and industrial pollution are to be minimized when studying the atmospheric geochemistry of nonurban areas.

The existence of high concentrations of heavy metals in atmospheric particulates is observed even in regions remote from civilization (Rahn and Winchester, 1971); this is frequently cited as evidence of an all-pervading influence of anthropogenic pollution. However, the presence of high concentrations of heavy metals in atmospheric particulates is by no means a proven indicator of the influence of pollution, since it has been found that particulates rich in heavy metals can be released from vegetation by a phenomenon that parallels the release of water by transpiration (Beauford and others, 1975). Once again the effects of large-scale migration of particulates from vegetation sources can be minimized by considering only particles of greater than 10 μ in diameter. The release of heavy metals from vegetation and particle localization will be dealt with in greater detail later.

Additional natural terrestrial sources of particulates and aerosols include the weathering of geological materials to produce soil particulates at the surface, the effects of wind erosion (Hilst and Nickola, 1959), the formation of aerosol particles derived from naturally occurring hydrocarbons produced by plants (Went, 1964, 1967), the generation of condensation aerosols by homogeneous gas reactions (Walter, 1973), the formation of condensation nuclei by evaporation processes in semiarid terrains (Twomey, 1960); and the production of organic particulate material by the decay, biodegradation, and weathering of plant material.

The oceans also provide a significant source of particulates in the atmosphere. Ocean derived particulates are generated by dehydration of windblown spray and the bursting of air bubbles entrained by wave action or rain (Woodcock and Gifford, 1949; Blanchard and Woodcock, 1957; Junge, 1972). Particulates of marine origin can contain up to 20 percent of organic carbon (Hoffman and Duce, 1974) and in some areas can contain even higher percentages of organic material. This anomalously high concentration of organic substances in marine particles is derived from the organic layer on the ocean surface (Garrett, 1967; Barger and Garrett, 1970). Aerosols generated by bursting bubbles are coated with the organic material (Blanchard, 1963, 1964, 1968; Garrett, 1967; Williams, 1967). Microorganisms can also be injected into the atmosphere from the ocean surface by the bubble-bursting mechanism (Carlucci and Williams, 1965; Blanchard and Syzdek, 1972), and airborne marine microorganisms have been observed by the author and his colleagues as well as other researchers (ZoBell and Mathews, 1939; Stevenson and Collier, 1962).

RELEASE OF HEAVY METALS IN PARTICULATE FORM FROM NATURAL SURFACES

The transfer of elements into the atmosphere from vegetation is of special interest in relation to the application of atmosphere geochemical methods in vegetated terrain. Movement of elements into the atmosphere from coniferous trees has been studied (Curtin and others, 1974), and it has been suggested that volatile exudates are the carrier. It has also been suggested that aerosols may be formed subsequently by agglomeration processes from the volatiles and that they could be used for geochemical sampling purposes. Recent work, however, with laboratory plants using radioactive zinc 65 and lead 210 as tracers in the plant nutrients has indicated that the initial release takes place in particulate form (Beauford and others, 1975). Some of this work, as yet unpublished, has shown that particulates in small laboratory plants are released dominantly in the submicron range. However, in the natural environment particles labelled with radioactive tracers can be released through a size range that is collected through all stages of a multistage particles impactor. It is of particular significance to the present study to note that radioactively labelled particles in size ranges up to at least as large as 10 μ in diameter can be released under free convection even in the absence of any wind.

The release of radioactive materials from vegetation that has been sprayed with a solution containing strontium 89 has been reported; it has been shown that there is a steady loss of radioactivity to the atmosphere (Moorby and Squire, 1963). It was suggested that the release might be taking place during the shedding of cuticular waxes, but the work was not continued by Moorby and Squire to verify this concept. Cuticular waxes abound on the leaves of most plants in the form of small wax platelets which provide the leaves with a water shedding surface. These platelets are continuously released by abrasion and the rubbing of leaves against each other and, in many instances, are able to renew themselves (Eglinton and Hamilton, 1967; Martin and Juniper, 1970). The use of various solvents on particulates that have been released from vegetation, clearly indicates that they carry only a small wax content and an analysis of the solvent extracts also shows that the waxes do not appear to be the major carrier of metals.

In considering the mechanisms of elemental release from plant surfaces it is important to note that such surfaces contain salts that can be readily leached out by rain or dew (LeClerc and Breazeale, 1908; Long and others, 1956; Clement and others, 1971). Whereas most studies are concerned with the leaching of major elements such as K, Na, and Cl, the writer and his colleagues have confirmed (to be published) that the heavy metal trace elements such as copper, lead, and zinc may also be leached from the surface of leaves with simulated dew or rain. It seems highly probable that the deposition of elements at the surface of leaves is related to the transpiration process in which soil solutions carrying dissolved salts are taken up by the plant roots, but the evaporation from the leaf surfaces is confined to the release of essentially pure water. Some of the salts in upward migration through the plant are utilized in the normal metabolic processes of the plant; however, certain elements may be enriched in the vicinity of the leaf surfaces.

A preliminary study is being carried out using newly available equipment on the distributions of 19 elements in soils, plants, and vegetative particulates on two sites in the Bancroft area of Ontario, Canada. The region is one of Pre-Cambrian geology, and one of the sites carries pegmatitic uranium mineralization while the other has only background values in uranium. Analyses of the A and B soils, bark, needles, and branches of conifers and deciduous trees were studied as well as the particulates generated by this vegetation. Particulates were sampled by filling large plastic bags with vegetation material and collecting the particulate material released by agitating the bags. High-volume suction sampling methods were used employing a small cyclone thereby providing sufficient material for precision multielement analysis.

Results are shown in table 1 and indicate certain interesting features. For example, the concentration of many elements in the particulates released from branches and needles is comparable with the concentration of these elements in soil. However, in the case of Fe, Al, Ti, and U, these elements are substantially depleted in the plants with respect to the soil concentrations, but the particulates released by the plants in general are enriched in comparison with the plant concentrations. It seems as if the vegetation minimizes the uptake of these elements and at the same time tends to further eliminate them by shedding enriched particulates. These elements belong to the nonbiogenic class that occupies a certain restricted area in an ionic radius/ionic charge diagram (Hutchinson, 1943; Brook, 1972).

It will also be observed that uranium mineralization is more readily detected in the particulate material than in the vegetation from which it is derived.

TABLE 1.—*Analyses of soils, plants, and vegetative particulates*
(Figures quoted are parts per million dry weight)

	Cd	Zn	Ni	Cr	Co	Cu	Ag	Mo	Mn	Fe*	Sr	Ca	Mg	K	Na	Al*	Ti*	P	U*
SAMPLE SITE 1—URANIUM ANOMALY																			
Soil A Zone	9.4	84.2	13.7	64.1	5.5	9.7	1.6	19.7	250	32290	11.1	1695	1689	2000	353.7	10896	1500.8	472.5	4.8
Soil B Zone	12.5	52.5	5.9	74.3	7.6	7.9	1.6	27.5	134	43552	5.5	727	1434	2800	375.0	13572	1932.7	503.8	13.5
Conifer Bark	0.9	45.9	6.0	6.6	ND	5.0	ND	ND	288	102	17.4	5437	396	1200	ND	109	0.3	310.7	<.1
Conifer Bark Particulates	2.9	35.9	7.3	ND	3.9	3.2	1.6	3.0	176	119	8.7	2746	254	1200	122.2	77	ND	205.3	<.1
Conifer Needles	1.5	74.1	24.2	56.1	1.3	3.2	0.8	3.3	716	314	30.2	10159	768	2800	149.1	199	3.4	600.0	0.1
Conifer Needle Particulates	8.0	66.1	18.4	13.6	4.4	22.6	4.6	4.3	61	1643	5.0	532	328	800	108.0	605	32.0	382.4	0.6
Deciduous Bark	4.1	122.4	5.6	7.3	1.1	11.1	1.1	3.9	173	476	47.5	10865	435	3200	207.4	308	24.6	305.3	0.2
Deciduous Bark Particulates	0.4	126.8	ND	9.2	9.6	4.1	3.2	7.7	112	297	34.3	8169	474	3600	11.4	96	0.3	206.1	<.1
Deciduous Branches	1.8	58.9	37.1	71.2	6.2	2.3	2.1	4.7	92	204	12.0	2983	184	1200	130.7	ND	ND	127.5	<.1
Deciduous Branch Particulates	14.4	105.1	ND	19.5	8.7	25.8	3.4	5.9	117	929	23.3	6340	392	2400	137.8	469	18.5	282.4	1.6
Forest Litter	2.5	79.8	8.8	7.3	2.1	7.0	1.0	2.8	737	195	29.1	8804	1157	2400	81.0	135	1.7	236.6	<.1
Forest Litter Particulates	2.0	70.5	ND	21.8	6.6	11.1	1.9	6.3	433	723	27.7	7595	940	2800	44.0	405	29.3	287.0	0.8
SAMPLE SITE 2—BACKGROUND SITE																			
	Cd	Zn	Ni	Cr	Co	Cu	Ag	Mo	Mn	Fe*	Sr	Ca	Mg	K	Na	Al*	Ti*	P	U*
Soil A Zone	3.5	35.2	8.5	29.6	3.9	4.1	1.0	7.3	134	12445	8.5	1403	1685	1600	348.0	7056	809.1	382.4	0.4
Soil B Zone	4.3	35.2	16.2	51.4	4.6	3.8	0.8	8.9	190	13944	7.6	1158	1596	2000	240.1	8436	868.7	358.8	<.2
Conifer Bark	1.6	48.8	ND	ND	ND	4.7	ND	2.4	190	136	25.5	5938	442	1600	ND	173	1.0	296.9	<.1
Conifer Bark Particulates	2.6	56.0	5.4	3.3	1.8	5.0	0.4	2.2	223	187	27.9	6600	464	1600	76.7	186	10.4	304.6	<.1
Conifer Needles	0.9	33.8	ND	ND	3.2	2.9	1.6	10.1	261	76	18.1	4507	525	2400	39.8	135	ND	278.6	<.2
Conifer Needle Particulates	13.7	65.4	12.7	12.6	0.5	43.5	2.7	2.8	59	1687	6.6	702	460	ND	144.9	904	60.4	526.7	0.3
Deciduous Bark	4.0	51.0	10.5	7.3	3.4	12.0	2.6	5.5	81	451	72.4	15707	314	4000	71.0	302	8.8	229.0	0.2
Deciduous Bark Particulates	0.6	40.2	ND	9.2	7.1	4.7	2.1	7.7	98	221	97.4	18027	367	5600	2.8	167	3.0	177.1	0.1
Deciduous Branches	1.6	15.1	10.9	ND	7.8	4.1	2.6	6.7	17	ND	6.2	800	69	1200	161.9	ND	4.4	94.7	<.2
Deciduous Branch Particulates	15.6	46.7	3.9	22.5	9.8	15.2	3.8	8.3	60	937	24.2	4784	342	2400	62.5	411	23.2	195.4	0.4
Forest Litter	3.2	82.0	7.6	ND	3.2	5.9	1.6	4.5	653	102	30.5	9543	1059	2800	275.6	77	1.7	232.8	<.1
Forest Litter Particulates	4.2	61.8	12.4	49.3	7.9	12.0	2.7	8.3	226	4154	23.0	4878	1212	2800	133.5	1979	243.2	318.3	0.4

*Elements depleted in plants with respect to soils and enriched in particulates compared to plants.

A further example of this phenomenon was noted in some tests over a small deposit of massive sulfides carrying copper and zinc in the Pre-Cambrian shield of Manitoba. There was a moderate geochemical anomaly in the soils, but conventional biogeochemistry for copper and zinc in the vegetation gave no indication of the anomaly while there was positive indication in particulates released from vegetation collected in large plastic bags. Further studies are continuing to gather more case histories on the relationship between element concentrations in soil and vegetation and the particulates released by that vegetation.

The role of vegetation is likely to be a very significant factor in any approach to airborne geochemistry, since plant surfaces cover an area many times their area as seen on an aerial photograph. Even in sparsely vegetated terrain, the total plant surface area can represent a sizable proportion of the land/air interface and in temperate regions having moderate to heavy vegetation cover, the interface is dominated by plants. Since this plant cover projects into the boundary layer and is exposed to the microclimate of circulating convective currents and surface winds, it provides a major contribution to the total particulate burden in vegetated temperate and tropical regions. Furthermore, although some of the organic content of atmospheric particulates in the small size range is derived from the condensation and exudation of plant volatiles such as terpenes (Went, 1967), 20 percent or more of the atmospheric particulate burden is normally composed of nonvolatile organic material (Neumann and others, 1959). It is the plus 10 μ fraction of this nonvolatile organic material that is the main information carrier for the AIRTRACE™ system in vegetated regions.

With regard to the sources of inorganic particulate material in the atmosphere in relation to metals and mineralization, it is obvious that weathered and dusty soil surfaces are a prolific source. The geochemistry of some of these surface particulates has been studied, and figure 1 shows analyses for metal and copper in the top few millimetres of surface dust sampled in a traverse across the nickel orebody at Agnew in Western Australia.

A number of case histories have been studied of surface dust sampled across mineral deposits. Where residual soils are present there is invariably an anomaly which more or less parallels the conventional B zone geochemical anomaly. However, the problem of obtaining a ground sample, in areas of even modest vegetative cover, that is truly representative of airborne particulates is difficult because of the unknown mix between soil surface derived particles and plant surface derived particles. Furthermore even in the case where the soil surface dominates, there may be a certain bias imposed by the selective winnowing of particles according to their aerodynamic shape and density.

Heavy metals are also released from the ocean surface by the bubble bursting mechanism due to the trace metal enrichment in the sea organic microlayer (Piotrowicz and others, 1972; Szekielda and others, 1972; Barker and Zeitlin, 1972). However, not all of the trace metals in the marine atmosphere are derived from the ocean surface, since the finer metal carrying particles may originate from land sources (Hoffman and others, 1972). It is not known whether the trace metal content of surface organic films and of overlaying atmosphere particulates will increase in the presence of mineral deposits located beneath shallow water.

METEOROLOGICAL FACTORS AND CONTROLS

When carrying out atmospheric sampling of particulates for airborne geochemical purposes it is essential to ensure that particles being collected are of local derivation and that they have not been transported long distances. This requirement can be met partially by collecting only giant particles of greater than 10 μ in diameter, but this in itself is not completely satisfactory since particles can still be collected that have travelled many miles. Special techniques can be used for obtaining a highly localized sample providing that there is strong vertical mixing and the air is vigorously lifting particles from the atmospheric interface to appropriate sampling altitudes. These conditions tend to arise when there is sunshine and adiabatic or superadiabatic conditions in which the temperature decreases adequately with increasing altitude. Low-level inversions in which normal lapse of the temperature is reversed provide very unfavorable conditions which give rise to suppression of mixing and the trapping of atmospheric particulates at the inversion layer.

Under the correct survey conditions of sunshine and light winds, convective plumes are formed which are basically nonrotating columns of rising warm air which travel at a lower velocity than the mean wind speed (Taylor, 1958; Kaimal and Businger, 1970; Businger, 1972). These plumes are tilted in a downwind direction and show maximum vertical flux on their leading edge (fig. 2). Flights made with a low-flying aircraft carrying equipment for measuring temperature fluctuations, vertical acceleration, and

CONCENTRATION OF ELEMENTS IN SOILS, PLANTS, AND PLANT

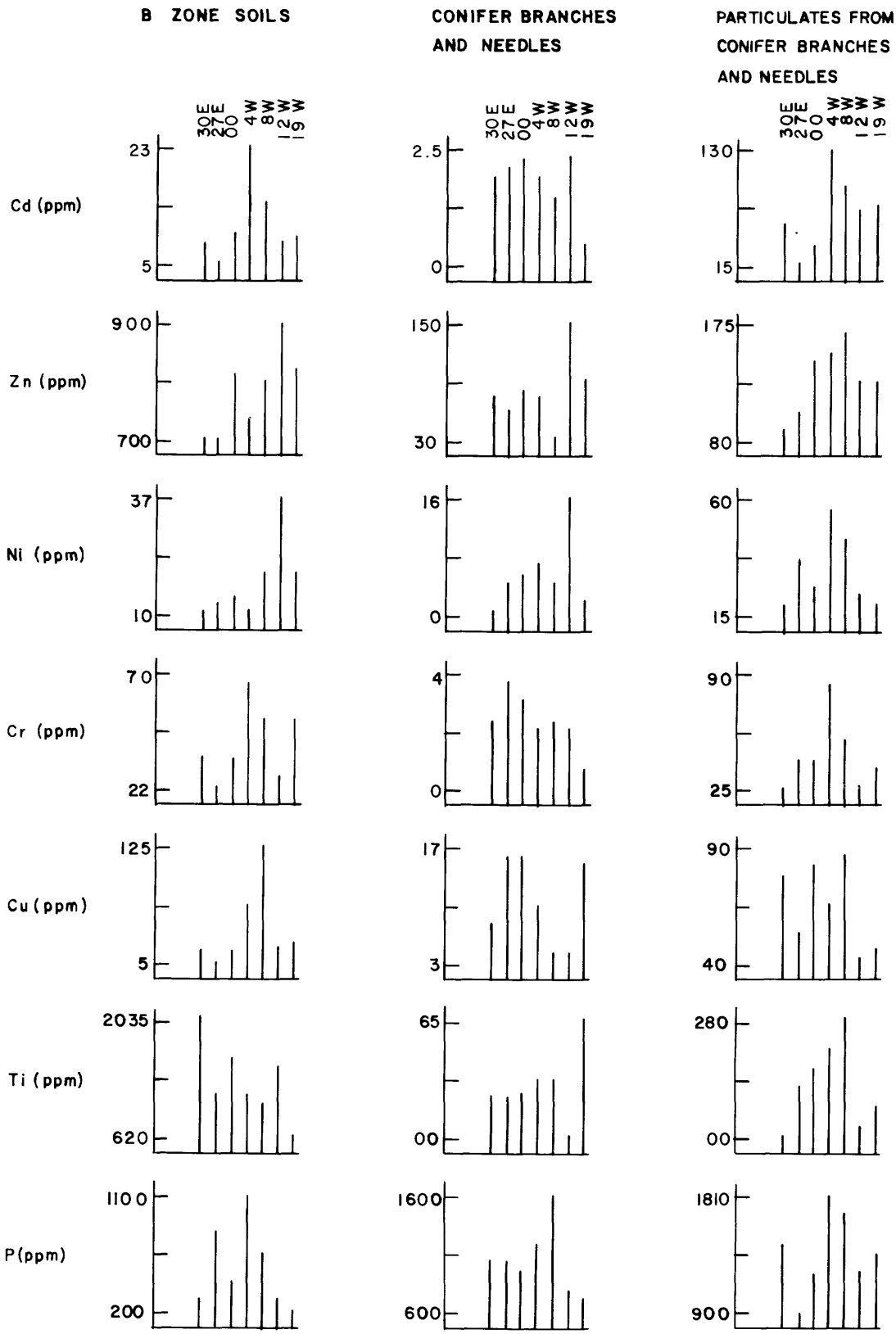

PARTICULATES, OVER Zn MINERALIZATION, DEER LAKE, ONTARIO

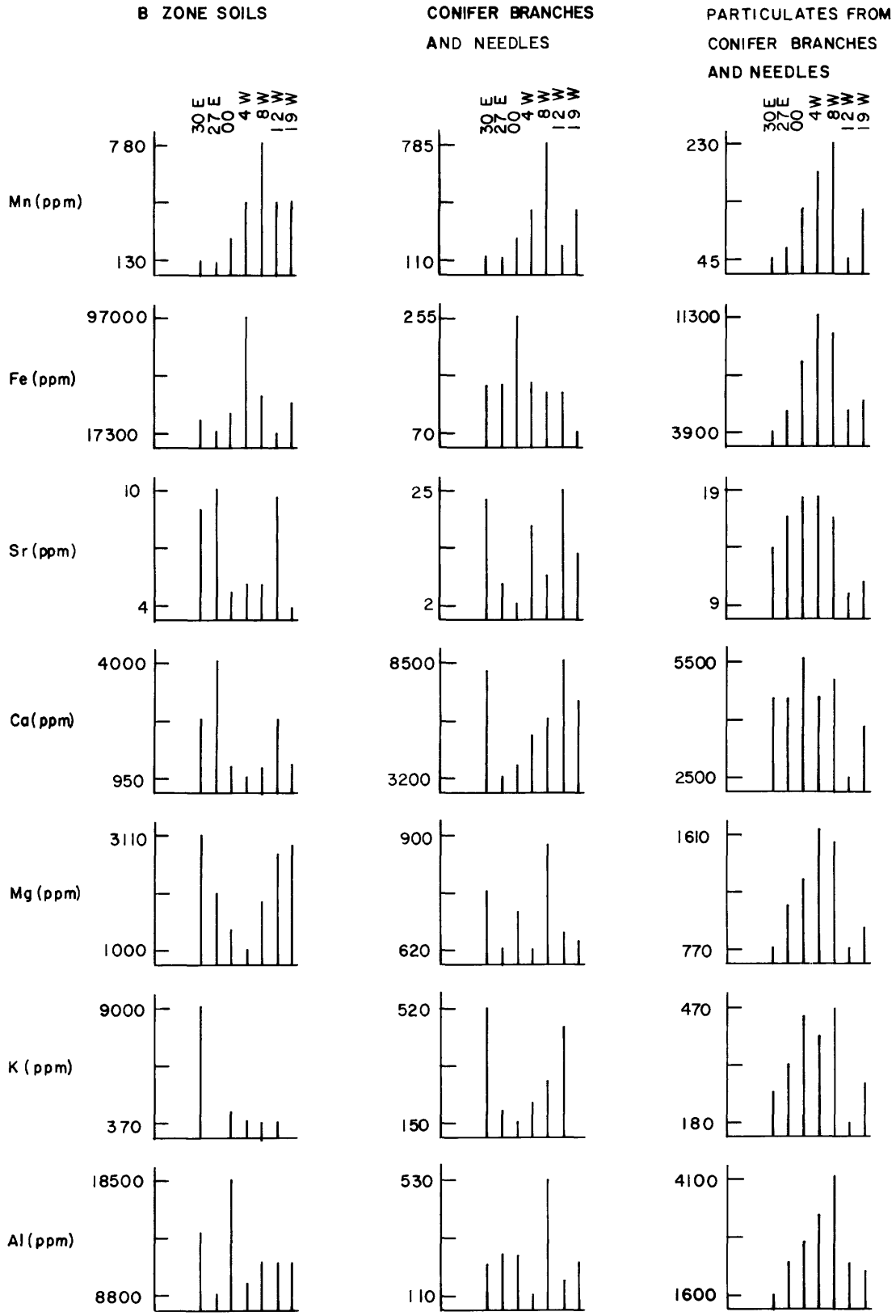

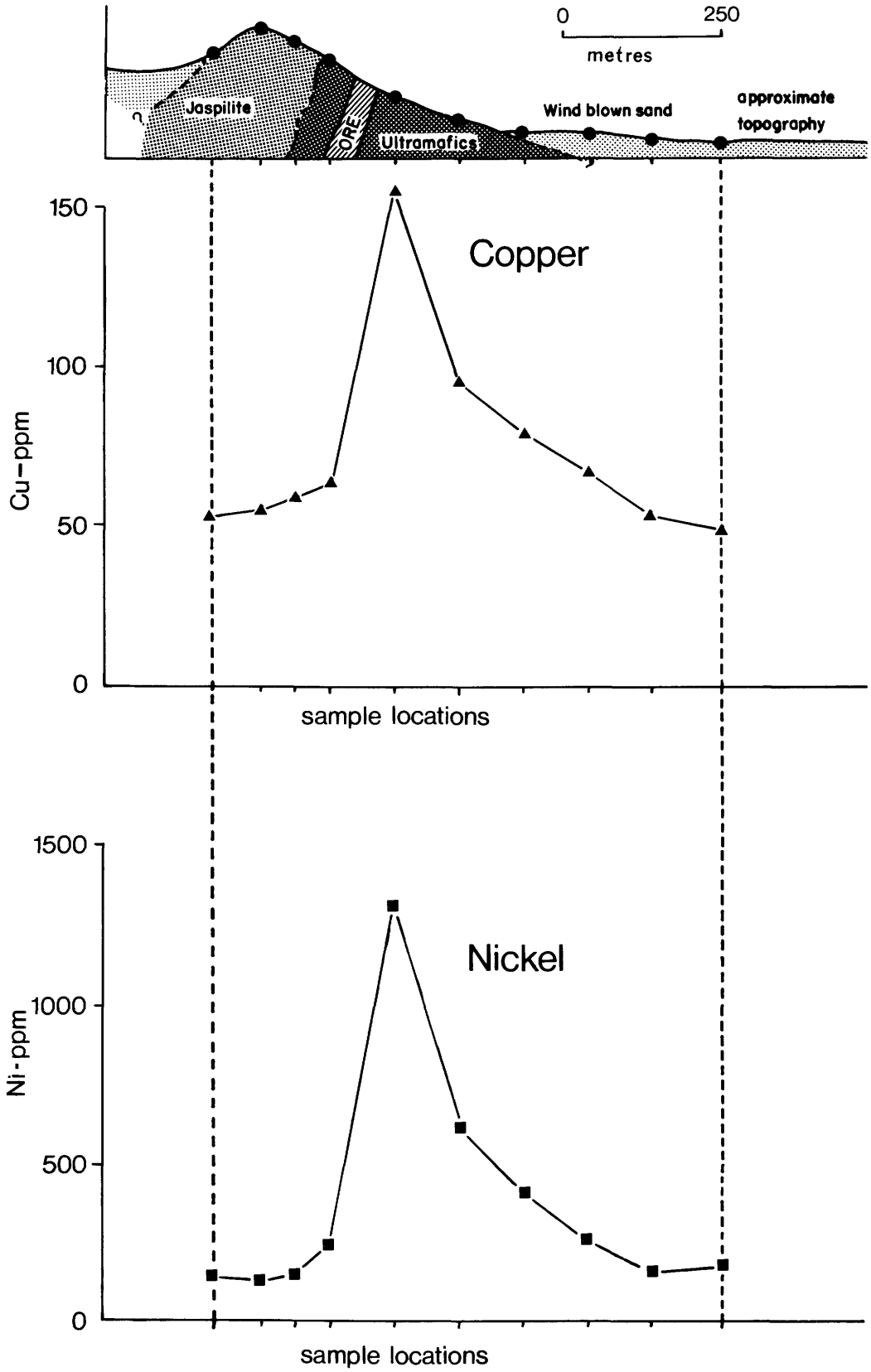

FIGURE 1.—Nickel and copper in surface dust, Agnew, Western Australia.

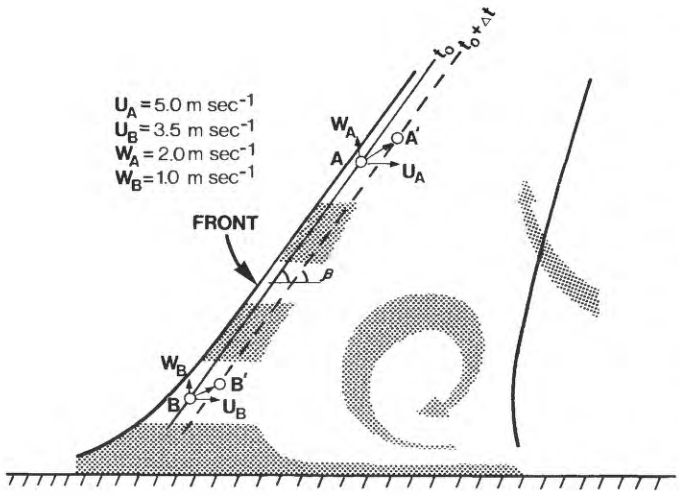

FIGURE 2.—Two-dimensional model of the convective plume. (From Kaimal and Businger, 1970.)

particulate loading show close correlation between all of these parameters (fig. 3). Temperatures were measured at two levels, with one sensor in the aircraft and the other 100 ft below in a towed bird. These sensors show the extent of vertical structure in the warm thermal peaks, and they also indicate that heavy dust loading are carried aloft by these rising vertical thermal structures. It has also been noted that when flights are made over a lake the thermal structures passing with the wind from land to water, tend to smooth out within 1,000 ft of the shoreline. Clusters of dust particles however can retain coherence for distances of at least 1 mile. This strongly suggests that when pockets of concentrated particulates are closely associated with parcels of warm air, then these particles have moved only a short distance from their ground source. Support for the concept that the mixing zone contains parcels of particulate matter of predominantly local origin surrounded by particulates from more distant sources is in part provided by the independent observation that the size distribution spectra of particles can vary widely in immediately adjacent air samples (Graedel and Franey, 1974).

In the AIRTRACE equipment, major emphasis has been placed on the development of methods for separating the particulates in rapidly rising warm air from the particulate burden in the cooler surrounding air. A very satisfactory thermal switching sampling technique has been evolved, and this is outlined in the section describing the AIRTRACE airborne equipment.

When the thermal switching and sampling system is used, it immediately becomes apparent that there are often pronounced differences in the chemical composition of the adjacent warm and cool air samples. Geochemical anomalies will appear on both sets of data, but there is often a displacement downwind of the anomalies derived from cool air particulates, the displacement being a function of the terrain clearance and wind velocity.

The overriding need for some means of selectively sampling predominantly local material and rejecting the ambient background becomes obvious if one examines the mechanisms that contribute material to the near surface particulate loadings. There is a small global or continental background that occurs entirely in the minus 10 μ fraction that is derived from fallout of material that has spread in the stratosphere and upper troposphere. There is also a regional background that falls out from the middle troposphere in a size range mostly within the minus 10 μ range. Finally there is a local background generated in the zone of mixing which covers the entire size range up to 100 μ (fig. 4). The ratio of regional to local background material is strongly controlled by meteorological conditions. In covering the climatic range from stagnant air through moderate mixing to strong mixing, the contribution of local background to the total burden increases drastically (fig. 5). At the same time the increasing thermal plume activity creates columns of particulates rich in very local material that is sampled by the AIRTRACE equipment as described above.

In addition to day-to-day variations in mixing conditions, there is also a marked diurnal cycle. At nighttime, when convective mixing ceases and still air conditions prevail, there is a steady settling of particulates within the lower troposphere. In the morning if the sun is shining and adiabatic or superadiabatic conditions prevail, active mixing will commence, building up by midmorning to high levels. This will raise particles into the air in thermal plumes at velocities which can amount to several metres per second, and there will be a continuous increase in the particulate burden. The upward flux of particles during active mixing is much greater than the downward flux since the latter is controlled substantially by sedimentation. By early afternoon even some of the giant particles may have moved considerable distances laterally making it imperative to reject the background material if sampling resolutions of fractions of a mile are to be achieved.

In general the great variability of the conditions which effect the contribution of regional material to the local particulate burden indicates the difficulties of gathering reliable data unless a thermal plume sampling technique is employed.

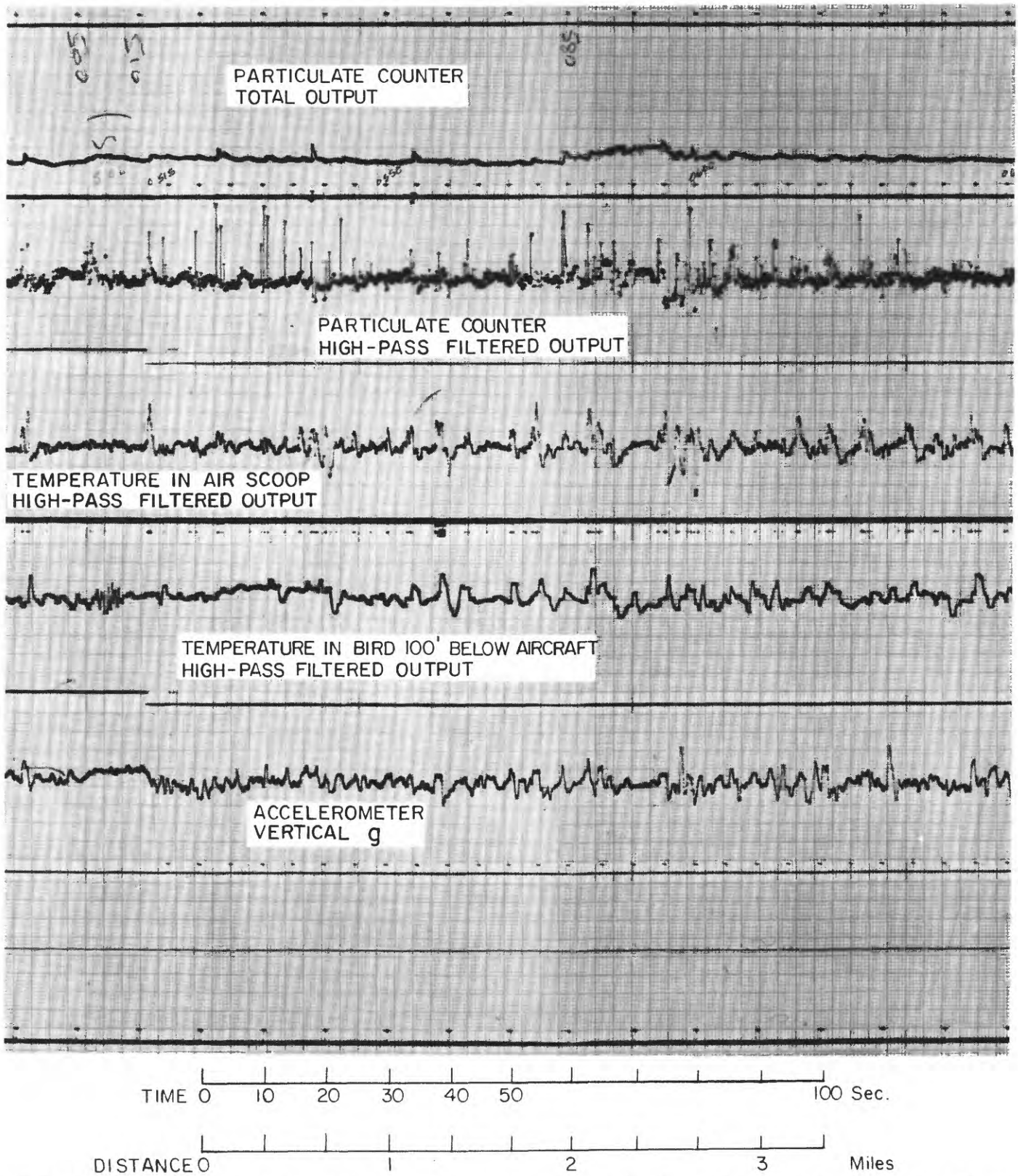

FIGURE 3.—Inflight analog record of particulate count, temperature, and vertical g, Arizona, February 6, 1975, flying height 80 m.

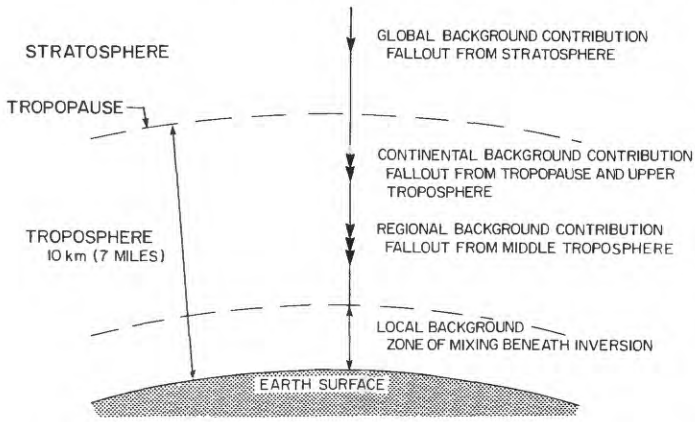

FIGURE 4.—Contributions of global, continental, regional, and local backgrounds to near-surface particulate loadings.

Turning to the seasonal meteorological constraints placed upon the AIRTRACE system, these depend upon the region of operations. Whereas strong mixing can occur at all times of the year in warm climates, there are areas where much of the winter is unsuitable. However, satisfactory operations have been achieved in Canada at temperatures well below zero fahrenheit with total snow coverage on the ground. It appears that if sunshine is present strong mixing can occur even under these winter conditions, and an adequate particulate burden for airborne geochemical surveys can be provided by evergreens and the branches of deciduous vegetation.

The meterological constraints are of course far less onerous if the AIRTRACE system is used for assessing regional geochemistry. This approach, however, has only limited applications.

AIRBORNE EQUIPMENT FOR THE AIRTRACE SYSTEM

Particulate collection is carried out in the AIRTRACE system with inertial devices and both cyclones and louvred collectors are employed (Stern, 1968). Lightweight cyclones can be manufactured to handle several hundred cubic feet of air per minute with good collection efficiency for the requisite particle sizes and louvred collectors can readily handle air volumes of as much as 12,000 ft^3/min in an airborne system. In one embodiment of the system particles are concentrated into an airstream and passed to a device which transfers them into an argon carrier gas (Barringer, 1974a). Spectroscopic analysis is then carried out directly inflight on the particles (Barringer, 1973a, 1973b). This technique is primarily applied to the measurement of volatiles such as hydrocarbons and mercury.

One of the principal methods used is to impact the particles onto a special tape and to analyse this tape on a post-flight basis. The key factor in the system is the aforementioned separation of the incoming stream of particles into rising and falling air components (Barringer, 1974b). This selection is achieved by the

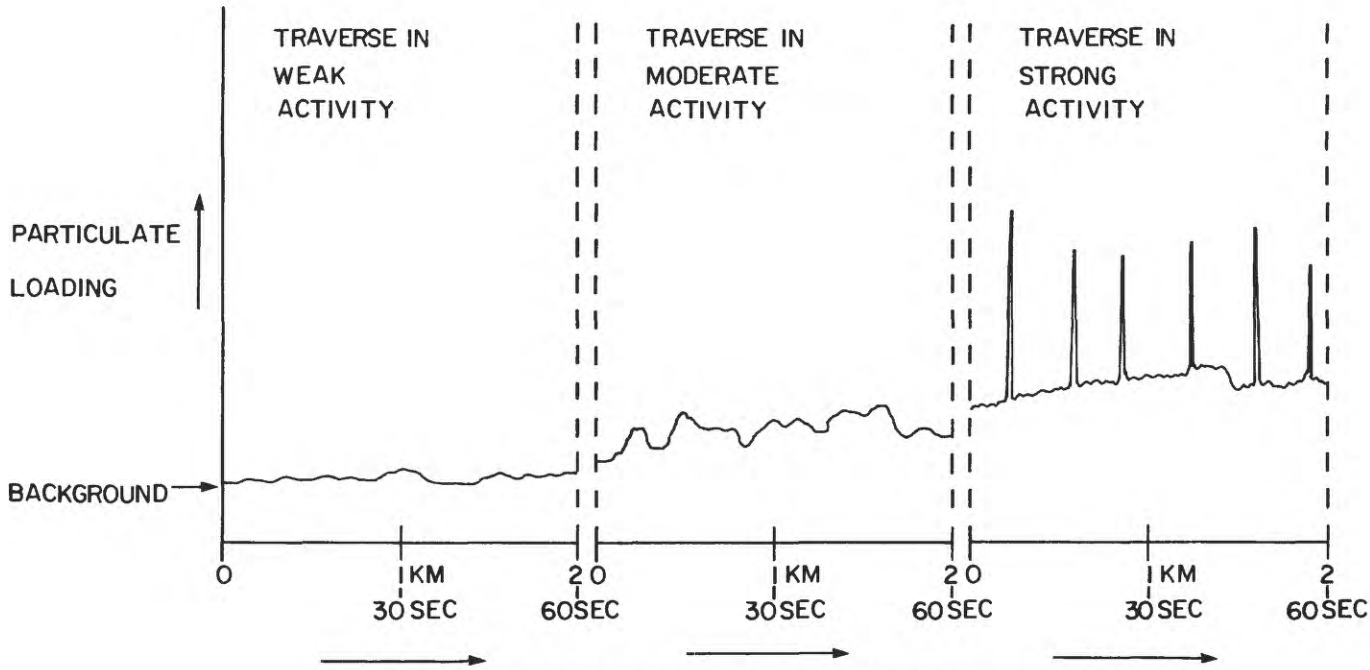

FIGURE 5.—Effect of mixing activity on particulate loading.

use of fast response thermal detectors at the air scoop inlets in conjunction with a suitable electrical filter, a digital delay line system and solenoid valve switching. Delays are adjusted appropriately so that switching of the particle stream can be accurately timed in relation to the transit delay for the particles passing through the piping of the system. This technique enables very small air parcels to be sampled with a resolution in the order of 5 ft. Samples are integrated into hot and cold spots on the tape using collection intervals that can be selected at either 5 or 10 s.

The effectiveness and precise resolution of this plume sampling technique is a function of the choice of the lower level of particle size collected, the selection of the wave filter functions applied to the temperature sensor, and the sensitivity settings of the thermal switching thresholds. The optimization of these parameters has to be based upon extensive experimentation.

The equipment is usually mounted on a helicopter (fig. 6), and surveys are carried out at altitudes of 20 or 30 ft above the treetops. This altitude turns out to be quite practical and is in fact used very commonly in crop spraying operations. Navigation of standard grid surveys at a quarter-mile spacing, for example, can be achieved in most terrains using conventional navigation from a photomosaic, providing that the navigator is skilled. Alternatively electronic navigation can be employed.

The equipment is also being operated in fixed-wing installations where surveys are carried out at 200 ft altitude. At this altitude the equipment is well suited for climates where there is very strong mixing such as in South Africa or Australia.

FIGURE 6.—AIRTRACE™ equipment mounted on a *206B Jet Ranger*.

The basic AIRTRACE system is employed in conjunction with other geophysical equipment such as magnetometers in helicopters and an EM system in the case of a fixed-wing installation. Inflight monitoring is provided by a multichannel analog recorder for optical measurements of the particle stream, thermal monitoring, etc.

ANALYTICAL SYSTEMS

One of the problems of airborne geochemistry is the very small amount of material that is collected. This makes it necessary to use extremely sensitive analytical techniques. Relatively simple equipment has been developed that provides inflight analysis of absorbed hydrocarbon and mercury, and there are some valuable applications for this approach. However, as research on airborne geochemistry has proceeded, it has become obvious that a system capable of analysing for a large number of elements would provide the optimum. Specifications for such a system include multielement capability, very high sensitivity, wide dynamic range, and high speed of operation. These requirements are extremely difficult to meet in real-time analytical equipment due to the problems of weight, power consumption, complexity, and the difficulties of operation and maintenance in an aircraft. It was, therefore, decided to develop a post-flight analytical system.

In considering possible systems, one approach that at first seems obvious would be the use of X-ray fluorescence analysis. Unfortunately, however, even the most advanced of these systems have inadequate sensitivity for the particulate levels that are encountered under some climatic and terrain conditions, and, furthermore, the time taken for sample analysis tends to be long in comparison with the time taken to collect samples.

The solution that has been employed is the use of laser vaporization in conjunction with inductively coupled plasma spectroscopic analysis. These two techniques used together provide a very wide dynamic range, high sensitivity, simultaneous multielement capability for more than a dozen elements, good linearity, and an analysis time of seconds per sample. The operational equipment is capable of functioning in a fully automatic mode, and the output is on magnetic tape where it is directly available for use in the preparation of maps by computerized methods.

All readings on the equipment bear a fixed relationship to the mass of each element present on the analytical tape so that any pair of elements can be ratioed. The linearity of the system is demonstrated by figures 7 and 8 which show the plots of silicon versus titanium and zinc versus titanium in a minus 200 mesh soil sample through a 40:1 range of loadings. This degree of precision is duplicated for most of the elements that are recorded and applies to both organic and inorganic matrices. Elements currently being analysed include Cu, Zn, Ni, Cr, Mn, Fe, Ti, Mg, Ca, Na, K, Cd, Si, and C. It is hoped to expand this list shortly and to include uranium as well as certain volatile elements.

With regard to data handling, in a simple approach it is possible to plot the ratios of a given element pair such as copper and titanium to look for copper anomalies. However, in practice a more sophisticated method is used in which linear regressions are employed to plot the variations of elements such as copper against six other preselected elements. This provides a very satisfactory approach that is giving good results, but a number of other possibilities remain to be tested. These include statistical methods such as factor and cluster analysis.

FIELD RESULTS

An interesting example of the early research work carried out with the system was in a truck-mounted version of the equipment which was traversed across a small orebody at Limerick, Ontario. This mineralization was substantially covered by trees with very little exposed soil present. An important feature of the area was the presence of a seepage zone located to one side of the mineralization and which provided a strong cold extractable anomaly in the soils. The truck traverse results, which were obtained with an atomic absorption analytical system, are presented in figure 9. It will be noted that the main AIRTRACE anomaly occurs over the seepage zone and that the anomalies were present both in the absolute concentrations of metals in the atmosphere and also in the copper/zinc metal ratio. Since the area is heavily vegetated, it seems almost certain that the anomaly must be mainly biogeochemical in origin. Bulk collections of aerosol that were subject to sink and float separation in carbon tetrachloride (density 1.60) indicated a very high proportion of organic material being present. This substantiated the biogeochemical nature of the particulate anomaly.

An example obtained with the current equipment operating under very difficult geochemical conditions is shown in figures 10 and 11. This survey was flown over a deposit recently discovered with the INPUT airborne EM system by Selco Mining Corporation and Pickens Mather Incorporated in Brouillan township in Northern Quebec. The deposit is reported to comprise three separate zones with an unofficial combined

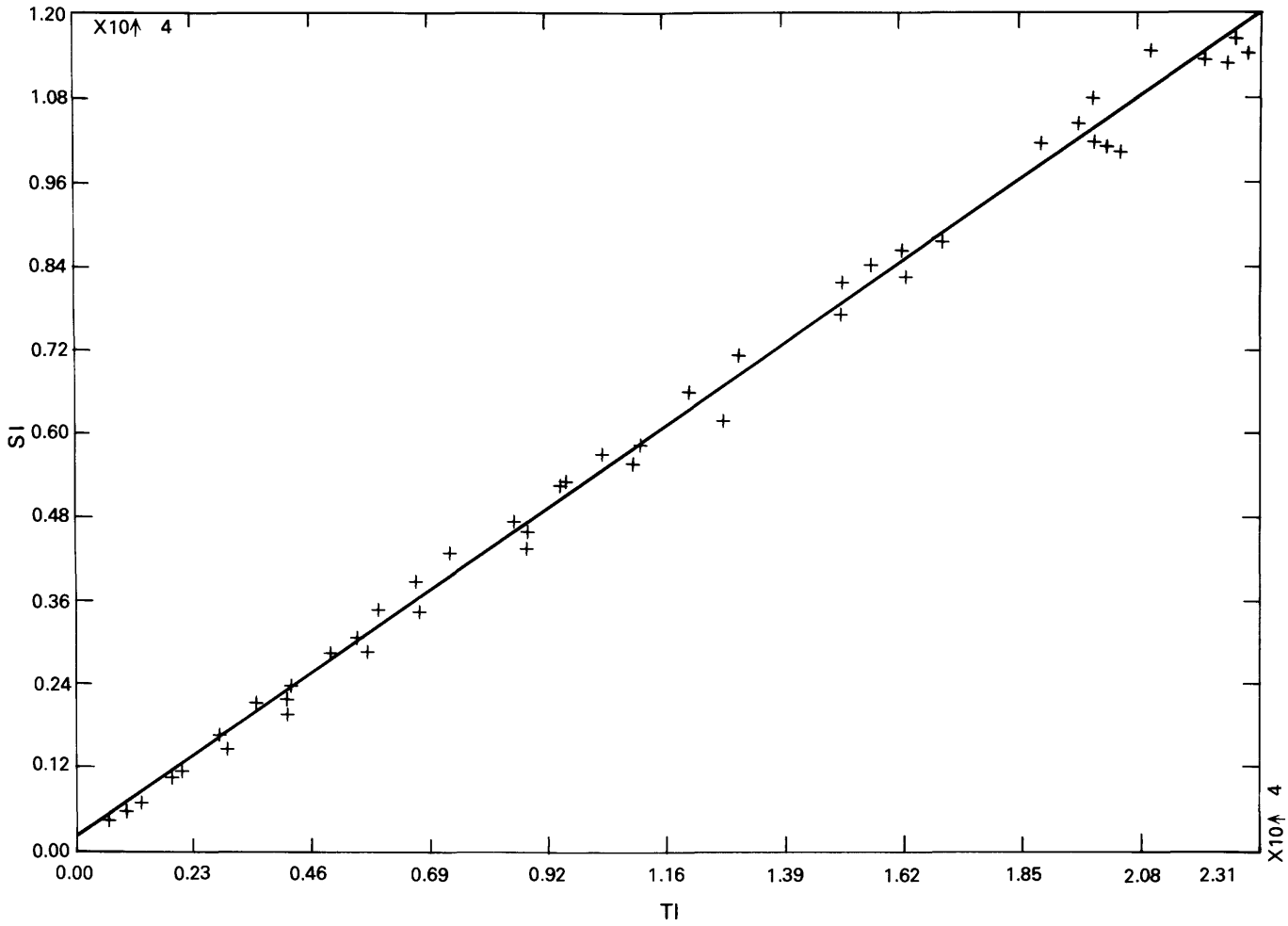

FIGURE 7.—A test of linearity of laser analytical system for variations in loadings of USGS soil (XRG-6), silicon versus titanium. Date: 7/10/75.

tonnage in excess of 50 million tons. The first zone discovered contains an estimated 35,400,000 tons of ore averaging 0.39 percent copper, 2.30 percent zinc, 1.04 oz silver, and 0.009 oz gold and lies beneath a minimum of 30 ft of glacial overburden. Ore grades in the other two zones are reported to be much higher in copper than the first zone, and they occur at greater depths.

The anomaly map was derived by a multiple regression technique carried out on a line by line basis for copper and zinc, and, in addition, spatial filtering was employed to smooth out noise and generate a contoured map.

The area was flown twice, both times under far from ideal weather conditions, since in this region weather conditions are frequently rather poor. Nevertheless, clear-cut delineation of an anomalous zone was obtained on both flights, in each case somewhat displaced but clearly relating to the location of the airborne EM conductor. These results taken in conjunction with airborne geophysical data provide a definite indication of a drilling target in a region which contains large numbers of barren EM conductors that normally have to be disproven by expensive drilling.

An interesting example of the AIRTRACE system applied to a hydrocarbon target is shown in figure 12. This traverse was chosen to cross a geochemical anomaly in carbon isotope ratios identified by T. Donovon of the U.S. Geological Survey (Donovon, 1974). The survey covered the Cement field in Oklahoma which is named for the cementation by carbonate of the surface rocks over part of the oilfield. These surface rocks not only show anomalous C^{13}/C^{12} values but also a manganese anomaly. A ground truth survey carried out by collecting fine particulate material from the surface on a traverse line indicated a definite anomaly in the manganese/iron ratio across the oilfield, and this was subsequently duplicated in airborne

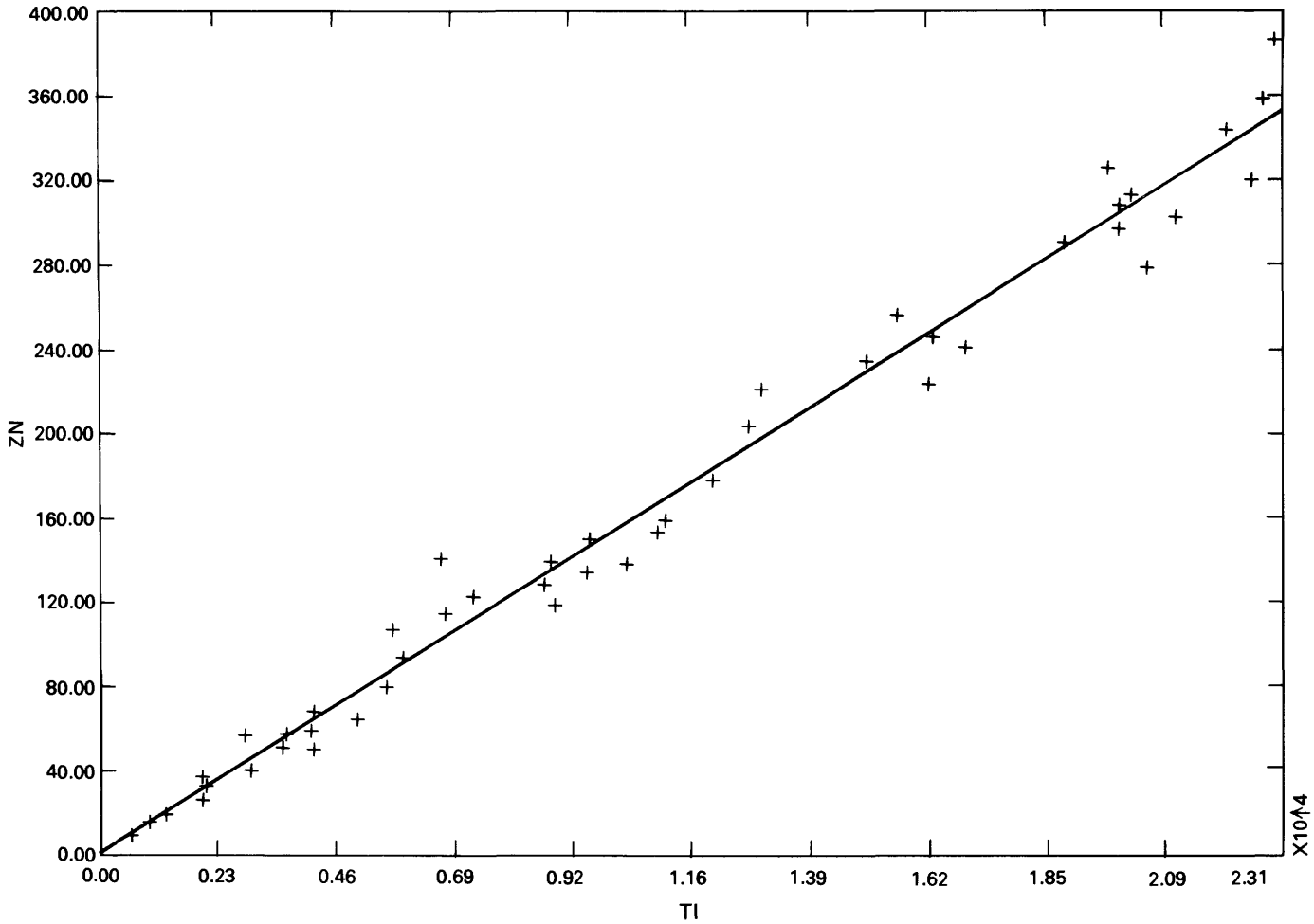

FIGURE 8.—A test of linearity of laser analytical system for variations in loadings of USGS soil (XRG–6), zinc versus titanium. Date: 7/10/75.

traverses with the AIRTRACE system. Additional tests have been carried out over other oilfields using the AIRTRACE technique for hydrocarbon volatiles Barringer, 1973a), and strong, highly localized anomalies have been observed—some apparently relating to faults and other structures over oilfields.

CONTINUING RESEARCH

A programme of research on botanical aspects of airborne geochemistry is continuing in the Botany Department of Imperial College, London, under a post-doctorate fellowship agreement with W. Beauford, a post-graduate scholarship with M. Luton, and with consulting assistance from J. Barber, Reader in the department. Current work is on the factors affecting the release of particulates from vegetation in situ as related to seasonal and diurnal factors, meteorological conditions, plant growth conditions, etc.

Research is also continuing on the atmospheric geochemistry over oilfields and the application of the AIRTRACE techniques to hydrocarbon exploration. On the analytical side, new methods of fingerprinting using spectro-fluorometric and mass spectrometric approaches are being studied in the laboratories of Barringer Research.

OPERATIONAL PLANS

The AIRTRACE equipment is now being used operationally in parallel with continuing testing over an increasing range of environments. Certain promising applications remain to be tested, including the use of the system for uranium, coal, and kimberlite exploration.

The system is being operated by Minsearch Surveys Limited for minerals and Barringer Hydrocarbons Limited for hydrocarbon exploration. Both companies

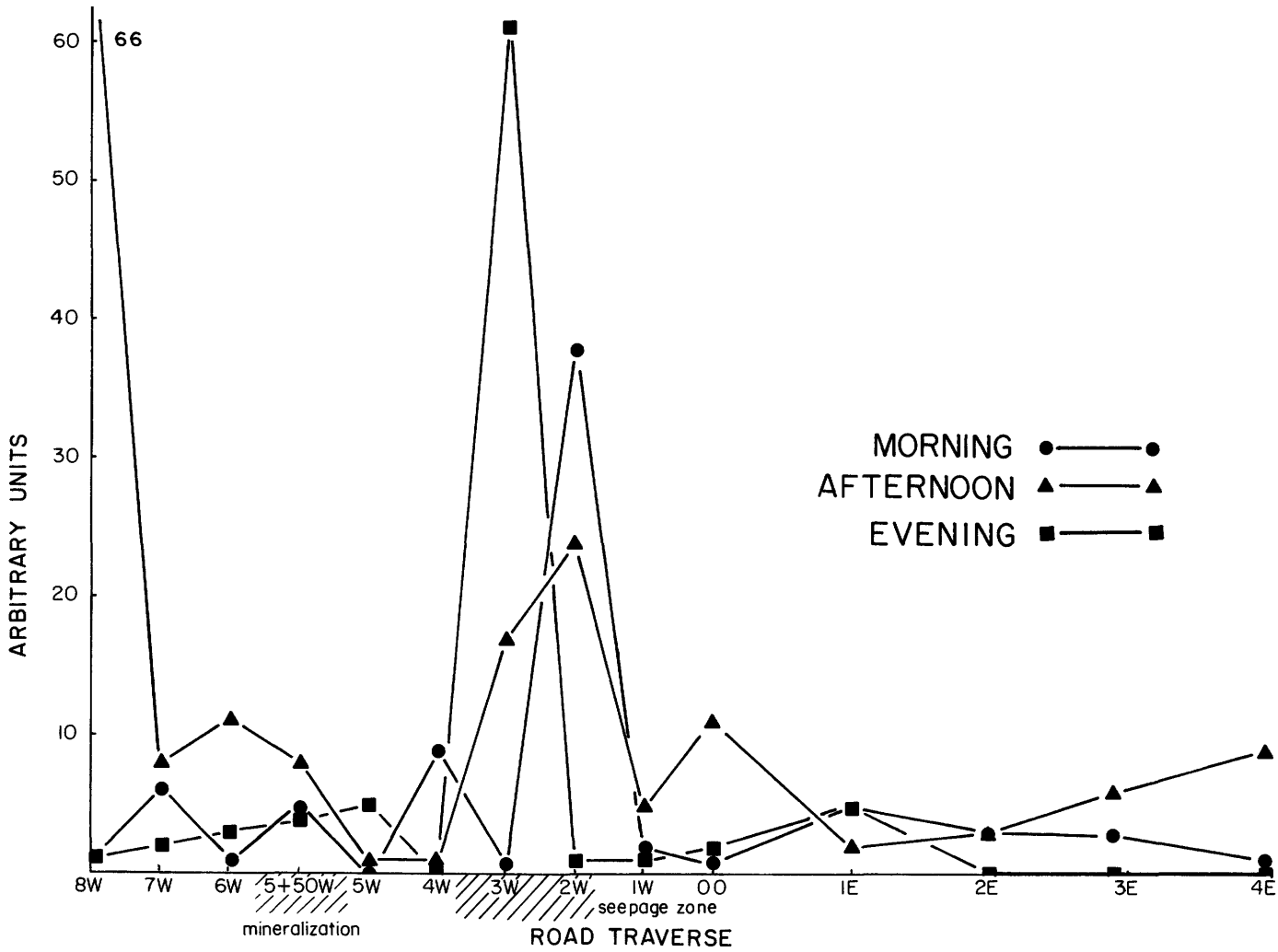

FIGURE 9.—Limerick prospect, near Bancroft, Ontario, AIRTRACE™ Mk III—copper.

are joint ventures between Anglo American Corporation and Barringer Research Limited.

CONCLUSIONS

The AIRTRACE system for airborne geochemical prospecting has been evolved over a period of years in a series of parallel research programmes on particulates collection and sampling techniques, meteorological controls near the ground, analytical methods, biogeochemical studies, and ground truth geochemical programmes. Some of the earlier field studies and case histories programmes have been made obsolescent by the later development of greatly improved collection methods, thermal switching techniques, multielement analyses, etc. There is an immediate necessity therefore to gather a great deal more data with all of the new technology. Nevertheless a scientific basis has been established for the development of multielement particulate anomalies over areas that are partly or completely covered by vegetation as well as in the more obvious regions of soil exposure. Surveys carried out over known mineral deposits in areas covered by glacial overburden and vegetation have yielded positive results. Furthermore the possibilities for atmospheric geochemistry being of value not only for mineral exploration but also for hydrocarbons has been demonstrated and anomalous effects have been seen in both organic and inorganic parameters over known oil and gas fields.

One of the more obvious potential applications of atmospheric geochemical exploration could be in the areas having difficult access such as tropical rain forests. It will be a great interest for example to see the effects of deep taproots and high transpiration rates on the overlying atmospheric geochemistry.

Some recent preliminary field data indicate that the principles of biogenic enrichments and depletions

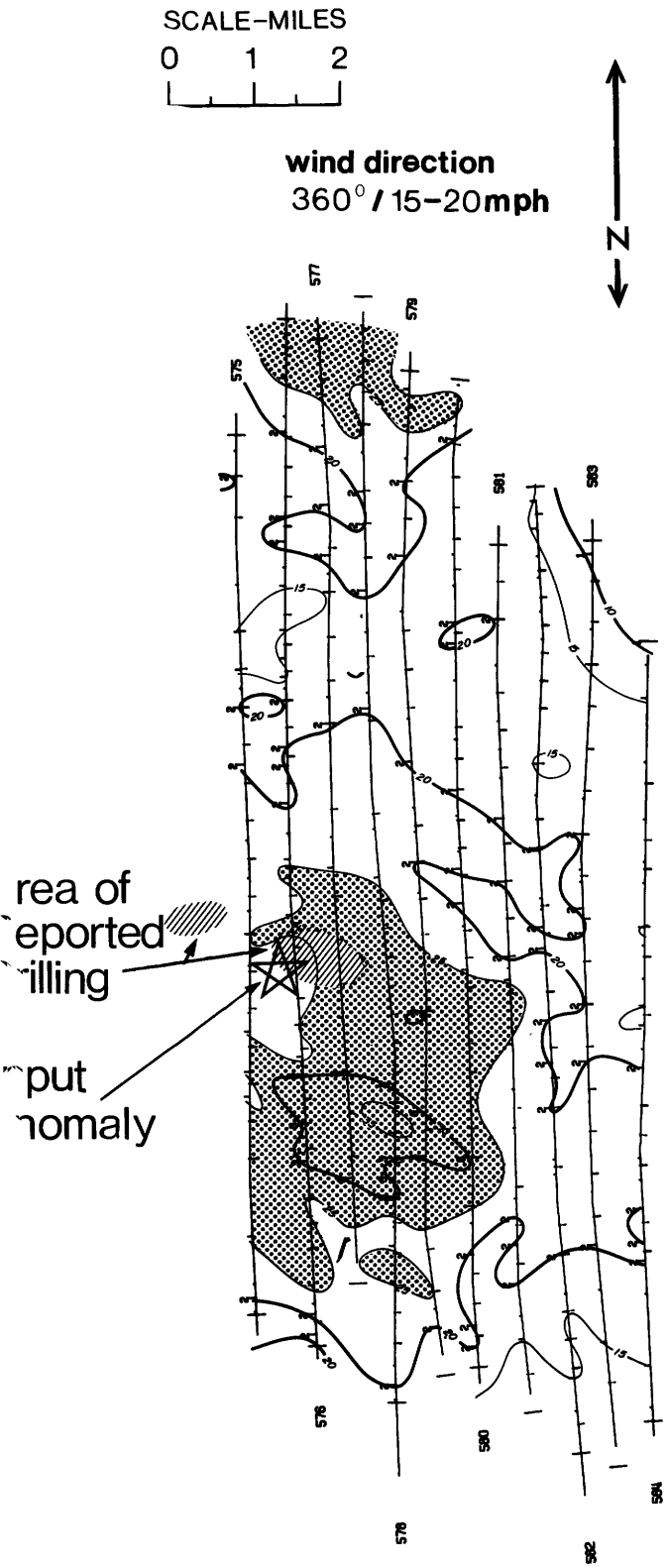

FIGURE 10.—Flight A AIRTRACE™ activity contours Cu + Zn regression.

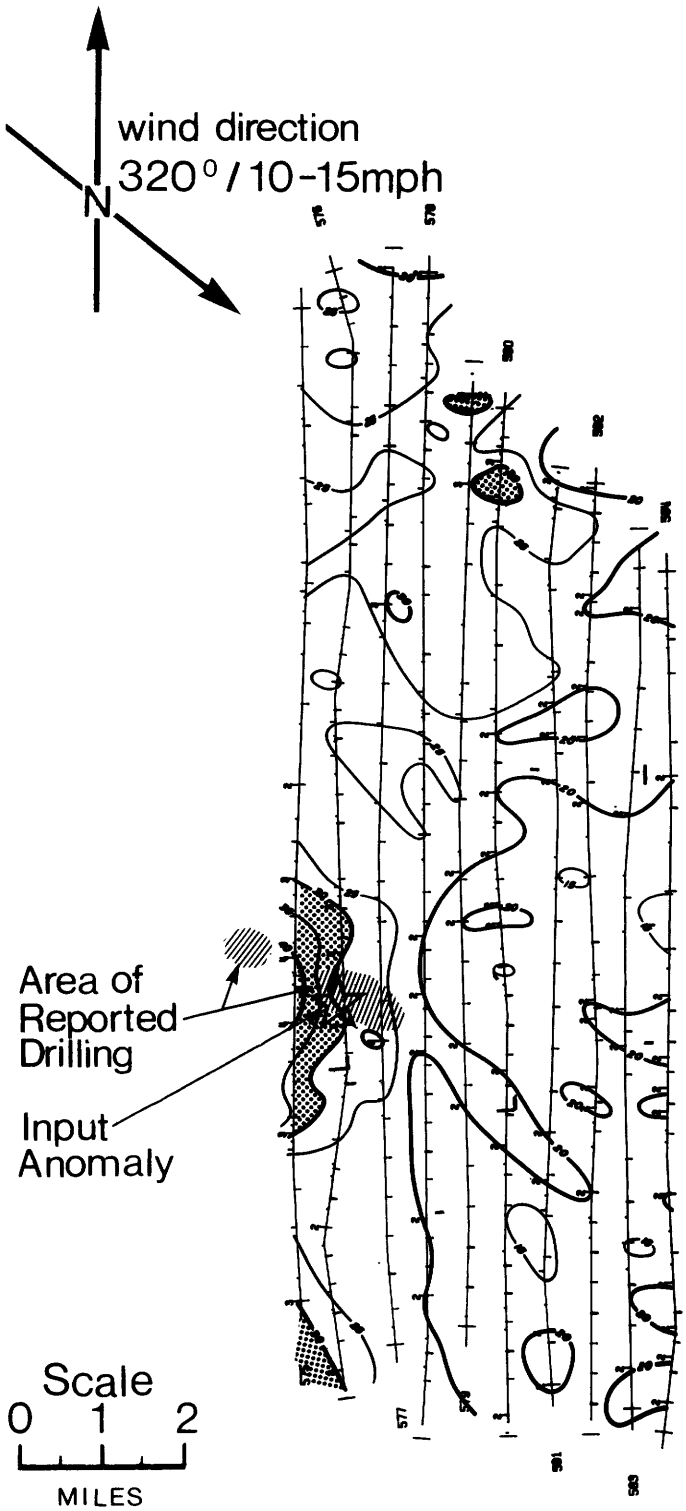

FIGURE 11.—Flight B AIRTRACE™ activity contours Cu + Zn regression.

between plants and soil have a parallel in the enrichment factors between plants and the particulates they release. A full understanding of this phenomenon should in the future allow a more fundamental approach to the interpretation of data gathered over vegetated terrain.

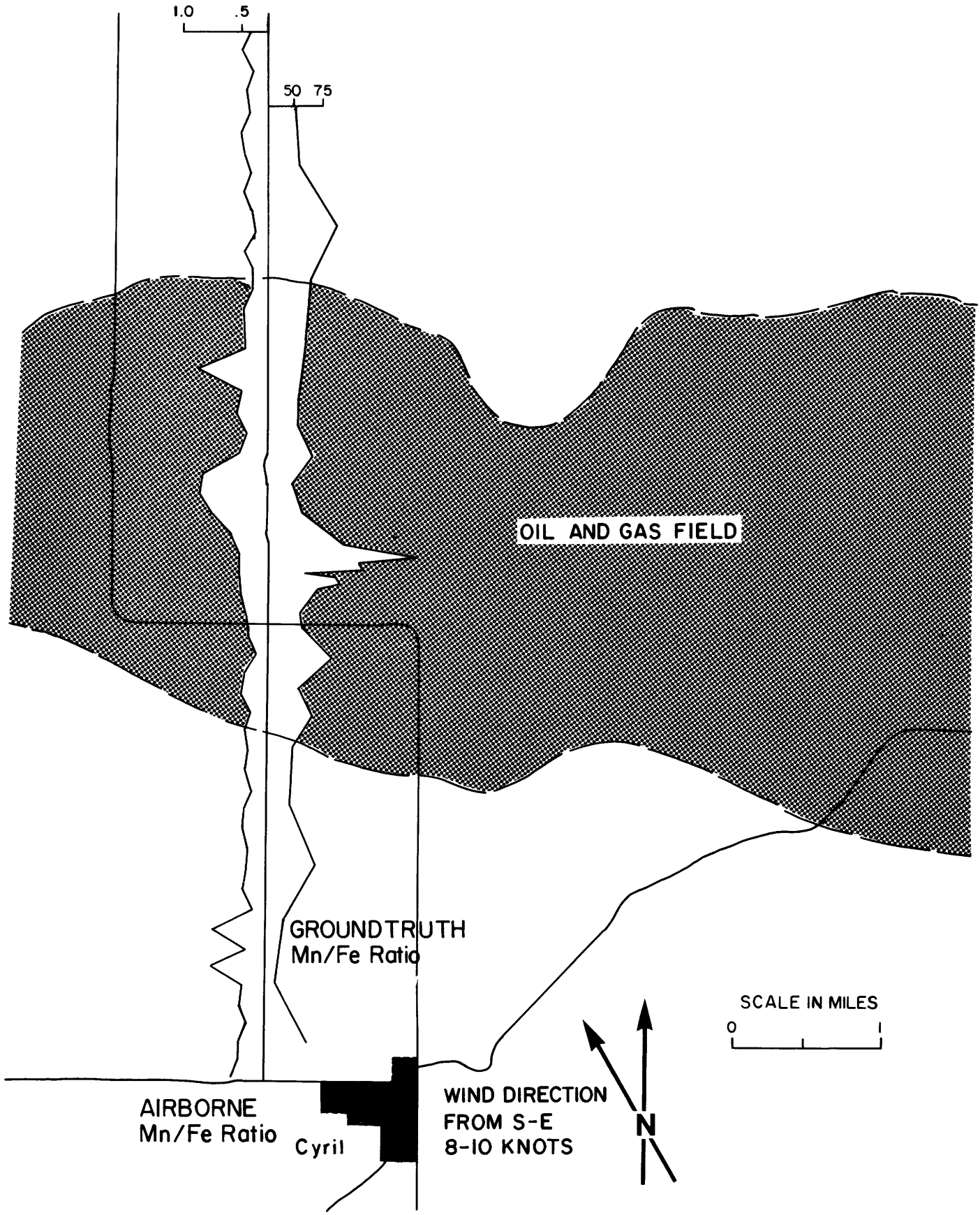

FIGURE 12.—Cement comparison of AIRTRACE™ data and ground truth.

ACKNOWLEDGMENTS

The writer has been associated with a number of colleagues within Barringer Research Ltd. who have contributed substantially to the research reported in this paper and to the development of the operational AIRTRACE system. These persons include the following. Geochemical investigations: P. M. Bradshaw, B. Smee, I. Thompson. Development of operation hardware and electronics: M. Failes,* M. Paul, F. Lanza. Analytical developments: M. Silvester, F. Abercrombie, H. Zwick. Microbiological research: A. Murray. All of the above are members of Barringer Research except as indicated.

The writer is especially indebted to Mr. D. Macourt** who has played a very important role in many phases of the AIRTRACE development programme from its inception.

Research on botanical and biological aspects has been carried out in the Botany Department, Imperial College, by J. Barber and W. Beauford.

The AIRTRACE development has only been possible through the joint efforts of all of the above together with the combined funding of Barringer Research Ltd., the Anglo American Corporation of Canada, and Hudson Bay Mining and Smelting Co. Ltd.

SELECTED REFERENCES

Barker, D. R., and Zeitlin, H., 1972, Metal-ion concentrations in sea-surface microlayer and size-separated atmospheric aerosol samples in Hawaii: Jour. Geophys. Research, v. 27, p. 5076–5086.

Barger, W. R., and Garrett, W. D., 1970, Surface active organic material in the marine atmosphere: Jour. Geophys. Research, v. 75, p. 4561–4566.

Barringer, A. R., 1973a, U.S. Patent No. 3759617. Method of apparatus for geochemical surveying.

———1973b, U.S. Patent No. 3768302. Method of apparatus for sensing substances by analysis of adsorbed matter associated with atmospheric particulates.

———1974a, U.S. Patent Pending. Method and apparatus for collecting atmospheric samples.

———1974b, Canadian Patent No. 954564. Method and apparatus for transferring particles from one fluid stream to another.

———1975, U.S. Patent No. 386822. High resolution geochemical prospecting method and apparatus.

Beauford, W., Barber, J., and Barringer, A. R., 1975, Heavy metal release from plants into the atmosphere: Nature, no. 256, p. 35–37.

Blanco, A. J., and McIntyre, R. G., 1972, An infra-red spectroscopic view of atmospheric particulates over El Paso, Texas: Atmospheric Environment, v. 6, p. 557–562.

Blanchard, D., 1963, The electrification of the atmosphere by particles from bubbles in the sea: Prog. in Oceanography, v. 1, p. 71–202.

Blanchard, D., and Woodcock, A. H., 1957, Bubble formation and modification in the sea and its meteorological significance: Tellus, no. 2, p. 145–158.

Blanchard, D. C., 1964, Sea-to-air transport of surface active material: Science, v. 146, p. 396–397.

———1968, Surface active organic material on airborne salt particles, *in* Internat. Conf. on Cloud Physics: Toronto, Proc.

Blanchard, D. C., and Syzdek, L. D., 1970, Mechanism for water to air transfer and concentration of bacteria: Science, v. 170, p. 626–628.

———1972, Concentration of bacteria in jet drops from bursting bubbles: Jour. Geophys. Research, v. 77, p. 5087–5099.

Brooks, R. P., 1972, Biobotany and biogeochemistry in mineral exploration: New York, Harper and Row.

Bussinger, J. A., 1972, Remote sensing of the troposphere: U.S. Dept. of Commerce Natl. Oceanic and Atmospheric Admin. (Univ. Colo.).

Carlucci, A. F., and Williams, P. M., 1965, Concentration of bacteria from sea water by bubble scavenging: J. Cons. Perm. Int. Explor. Mer., v. 30, p. 28–33.

Clement, C. R., Jones, L. H. P., and Hopper, M. J., 1971, The leaching of some elements from herbage plants by simulated rain: Grassland Research Inst., Hurley, Berkshire.

Curtin, G. C., King, H. D., and Mosier, E. L., 1974, Movement of elements into the atmosphere from coniferous trees in subalpine forests of Colorado and Idaho: Jour. Geochem. Exploration, v. 3, p. 245–263.

Donovon, T., 1974, Petroleum microseepage at Cement, Oklahoma: Evidence and mechanism: Am. Assoc. Petroleum Geologists Bull., v. 58, no. 3, p. 429–446.

Eglinton, G., and Hamilton, R. J., 1967, Leaf epicuticular waxes: Science, v. 156, p. 1322–1335.

Esmen, N. A., and Corn, M., 1971, Residence time of particles in urban air: Atmospheric Envir., v. 5, p. 571–578.

*M. Failes, formerly Barringer Research Limited, now Independent Consultant, Toronto.

**D. Macourt, Independent Consultant, Sydney.

Garrett, W. D., 1967, Stabilization of air bubbles at the air-sea interface by surface-active material, I, Sea surface: Deep Sea Research, v. 14, p. 661–672.

Graedel, T. E., and Franey, J. P., 1974, Atmospheric aerosol size spectra: Rapid concentration fluctuations and bimodality: Jour. Geophys. Research, v. 79, p. 5643–5650.

Hawkes, H. E., and Webb, J. S., 1962, Geochemistry in mineral exploration: Harpers Geoscience Series.

Hilst, G. R., and Nickola, P. W., 1959, On the wind erosion of small particles: Am. Meteorological Soc. Bull., v. 40, p. 73–77.

Hoffman, E. J., and Duce, R. A., 1974, The organic carbon content of marine aerosols collected on Bermuda: Jour. Geophys. Research, v. 79, p. 4474.

Hoffman, G. L., Duce, R. A., and Hoffman, E. J., 1972, Trace metals in the Hawaiian marine atmosphere: Jour. Geophys. Research, v. 77, p. 5322–5329.

Hutchinson, C. E., 1943, The biogeochemistry of aluminum and of certain related elements: Quart. Rev. Biology, v. 18, p. 1–29, 129–153, 242–262, and 331–363.

Junge, C. E., 1972, Our knowledge of the physicochemistry of aerosols in the undistributed marine environment: Jour. Geophys. Research, v. 77, p. 5183–5200.

Kaimal, J. C., and Bussinger, J. A., 1970, Case studies of a convective plume and a dust devil: Jour. Applied Meteorology, v. 9, p. 612–620.

Kartsev, A. A., Tabasarankii, Z. A., Subbota, M. I., and Mogilevski, G. A., 1954, Geochemical methods of prospecting and exploration for petroleum and natural gas: Univ. California Press.

LeClerc, J. A., and Breazeale, J. F., 1908, Plant food removed from growing plants by rain or dew: U.S. Dept. of Agriculture Yearbook, p. 389–402.

Lee, R. E., Jr., Patterson, R. K., and Wagman, J., 1967, Particle size distribution of metal components in urban air: Am. Chem. Soc. Mtg.

Levenson, A. A., 1974, Introduction to exploration geochemistry: Calgary, Applied Publishing.

Long, W. G., Swell, D. V., and Tukey, H. B., 1956, Loss of nutrients from foliage by leaching as indicated by radio-isotopes: Science, v. 27, p. 1039–1040.

Martin, J. T., and Juniper, B. E., 1970, The cuticles of plants: New York, St. Martin's Press.

Moorby, J., and Squire, H. M., 1963, The loss of radioactive isotopes from the leaves of plants in dry conditions: Rad. Botany, v. 3, p. 163–167.

Noll, K. E., and Pilat, M. J., 1971, Size distribution of atmospheric particles: Atmospheric Envir., v. 5, p. 527–540.

Neumann, G. H., Fonseluis, S., and Wahlman, L., 1959, Measurements on the content of nonvolatile organic material in atmospheric precipitation: Internat. Jour. Air Pollution, v. 2, p. 132–141.

Parkin, D. W., Phillips, D. R., and Sullivan, R. A. L., 1970, Airborne dust collections over the North Atlantic: Jour. Geophys. Research, v. 75, p. 1782–1793.

Piotrowicz, S. R., Ray, B. J., Hoffman, G. L., and Duce, R. A., 1972, Trace metal enrichment in the sea-surface microlayer: Jour. Geophys. Research, v. 77, p. 5243–5254.

Poet, S. E., Moore, H. E., and Martell, E. A., 1972, Lead 210, Bismuth 210, and Polonium 210 in the atmosphere: Accurate ratio measurement and application to aerosol residence time determination: Jour. Geophys. Research, v. 77, p. 6515–6527.

Rahn, K. A., and Winchester, J. W., 1971, Sources of trace elements in aerosols: An approach to clean air: U.S. Atomic Energy Commission. Available from U.S. Dept. of Commerce, Natl. Tech. Inf. Service as COO–1705–9.

Stern, A. C., 1968, Source control by centrifugal force and gravity, *in* Caplan, K. J., Air pollution: New York, Academic Press, v. 3, p. 359–395.

Stevenson, R. E., and Collier, A., 1962, Preliminary observations on the occurrence of airborne marine phytoplankton: Lloydia, v. 25, p. 89–93.

Szekielda, K. M., Kupferman, S. L., Klemas, V., and Polis, D. F., 1972, Element enrichment in organic films and foam associated with aquatic frontal systems: Jour. Geophys. Research, v. 77, p. 5278–5282.

Taylor, R. J., 1958, Thermal structures in the lowest layers of the atmosphere: Aust. Jour. Physics, v. 11, p. 168–176.

Twomey, S., 1970, On the nature and origin of natural cloud nuclei: L'Observatoire du Puy de Dome Bull., January-March, no. 1, p. 1–19.

Walter, H., 1973, Coagulation and size distribution of condensation aerosols: Aerosol Science, v. 4, p. 1–15.

Weiss, O., 1967, U.S. Patent No. 3309518. Method of aerial prospecting which includes a step of analysing each sample for element content, number and size of particles.

———1971, Airborne geochemical prospecting. *CIM Special* Vol. 11: Geochem. Explor., p. 502–514.

Went, F. W., 1964, The nature of Aitken condensation nuclei in the atmosphere: Botany, v. 51, Natl. Acad. Sci. Proc., p. 1259–1267.

———1967, Formation of aerosol particulates derived from naturally occurring hydrocarbons produced by plants: Air Pollution Control Assoc. Jour., v. 17, p. 579–580.

Woodcock, A. H., and Gifford, M. M., 1949, Sampling atmospheric sea-salt nuclei over the ocean: Jour. of Marine Research, v. 8, no. 1–3, p. 177–197.

Williams, P. M., 1967, Sea surface chemistry: Organic carbon and inorganic nitrogen and phosphates in surface films and sub-surface waters: Deep Sea Research, v. 14, p. 791–800.

ZoBell, C. E., and Mathews, H. M., 1939, A qualitative study of the bacterial flora of sea and land breezes: Natl. Acad. Sci. Proc., v. 22, p. 567–572.

PROCEEDINGS OF
THE FIRST ANNUAL WILLIAM T. PECORA MEMORIAL SYMPOSIUM,
OCTOBER 1975, SIOUX FALLS, SOUTH DAKOTA

An Application of Satellite Imagery to Mineral Exploration

By Mark A. Liggett and John F. Childs,
Cyprus Georesearch Company,
Los Angeles, California 90071

ABSTRACT

The application of satellite remote-sensing techniques to mineral exploration is based on the ability to recognize a variety of geologic features characteristically associated with hydrothermal alteration and related mineralization. Such features can include favorable structural settings, lithologic associations, and alteration color or topographic anomalies. Successful application of satellite imagery, however, is dependent upon the size and expression of these characteristic features and their predictive value for narrowing the area of exploration to a practical size for economical evaluation using other exploration techniques. Landsat–1 MSS imagery has been effectively used in studying the regional tectonic controls of Cenozoic volcanism, plutonism, and related gold, silver, and base metal mineralization in part of the Basin and Range province of southern Nevada, eastern California, and northwestern Arizona. Within a volcanogenic province aligned along the Colorado River south of Lake Mead, Nevada, the locations of known mineral deposits appear in satellite imagery to be spatially associated with generally east-west structural trends, transverse to the north-south structural grain typical of the province. Field reconnaissance in this area has confirmed a temporal as well as spatial relationship between mineralization and the anomalous east-west structural trends. Assuming a genetic relationship between structure and mineralization, systematic analysis of Landsat imagery and subsidiary data has provided a basis for selecting new targets for ground-based exploration reconnaissance.

INTRODUCTION

Applications of satellite remote-sensing techniques to mineral exploration have generally been based on the ability to observe characteristics of mineralization, associated alteration or other related features in synoptic imagery of relatively low resolution. Such characteristic features can include alteration color and topographic anomalies, distinctive lithologic associations, favorable structural settings, and vegetation changes caused by soil geochemical anomalies. The relative value of these features as exploration guides often varies with the genetic type of mineralization, geologic terrane, and climatic setting. The economic advantages of using satellite imagery depend both on the success of detecting these features and the costs of obtaining comparable information using alternate methods.

In the western United States, direct surface expressions of alteration and mineralization are likely to have been recognized long ago by conventional means. In such well-explored areas, it is necessary that the exploration methods used lead to the detection of blind or poorly exposed mineralization. One approach to reconnaissance exploration for such ore deposits is the selection of preliminary targets on the basis of favorable structural settings or other regional geologic associations.

This paper summarizes a study in which Landsat–1 imagery was used in studying the regional structural settings of known gold, silver, and base metal deposits in part of the Basin and Range province of southern Nevada, eastern California, northwestern Arizona and southwestern Utah as shown in figure 1. The synoptic overview of regional geology and the identification of specific structural features expressed in the Landsat–1 imagery has led to the development of a regional model for the tectonic control of Cenozoic volcanism, plutonism, and genetically related epithermal mineralization within a portion of the study area.

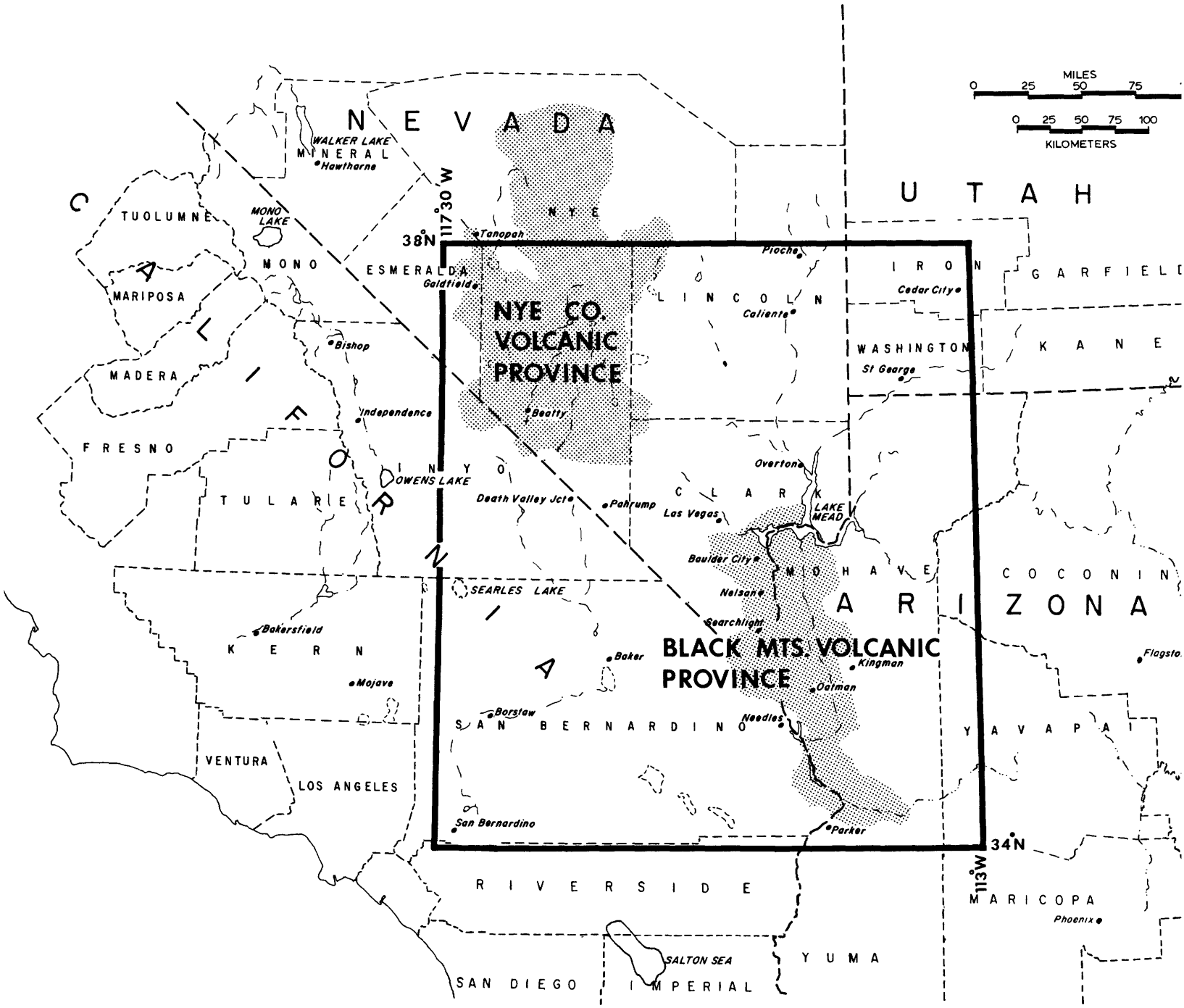

FIGURE 1.—Location map for the area of study. The generalized positions of the Black Mountains and Nye County volcanic provinces are shown with the stippled pattern. The area of the Landsat mosaic of figure 2 (p. XXII) is outlined with a heavy line.

LANDSAT–1 IMAGERY

A false-color mosaic of Landsat–1 multispectral scanner (MSS) composites which covers the area of study is shown in figure 2 (p. XXII). The individual Landsat–1 frames used in this mosaic are identified in figure 3. The false-color composites were prepared from black and white MSS transparencies using a technique developed by MacGalliard and Liggett (1973).

The false-color composites used in figure 2 were produced with the following combination of MSS bands and printing filters:

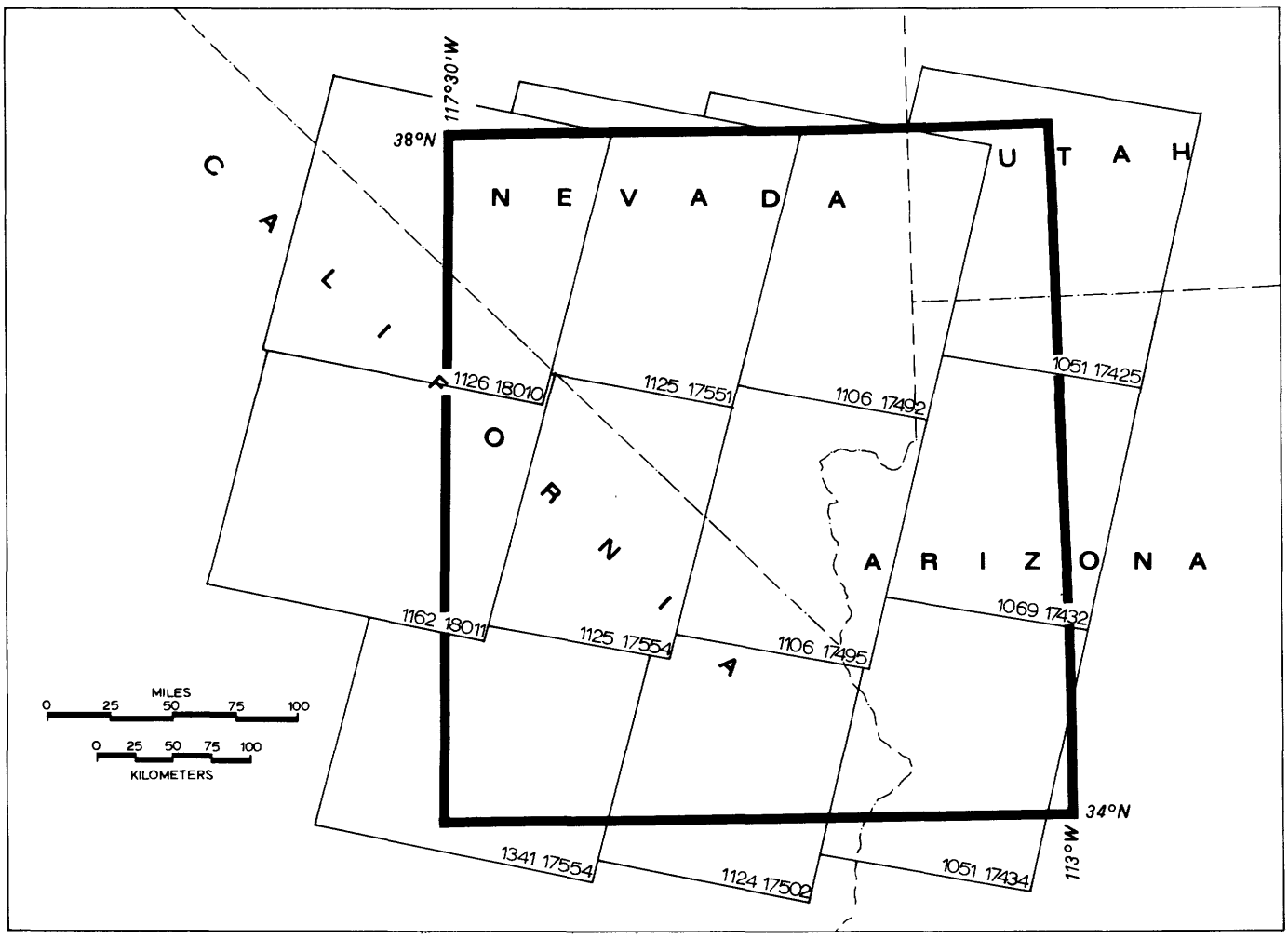

FIGURE 3.—Index map showing the locations and identification numbers of the Landsat–1 MSS frames used in the false-color mosaic of figure 2 (p. XXII). Area of study is outlined.

MSS band	Spectral range	Printing filter
4	Green and yellow (0.5–0.6 μm)	Blue
5	Red (0.6–0.7 μm)	Green
7	Near-infrared (0.8–1.1 μm)	Red

As a result of this MSS band-filter combination, green vegetation appears as intense red due to the high reflectance of vegetation in the near-infrared portion of the spectrum. Most buff-to-brown rock or soil units in the composites reproduce in approximately their natural colors. Neutral colored igneous and sedimentary rocks appear with gray to slightly blue coloring; dark igneous and metamorphic rocks reproduce with dark-brown to steel-gray coloring. Red, iron-rich sedimentary rocks and iron oxide staining associated with hydrothermal alteration appear as yellow coloring, sometimes varying between greenish yellow and orange, depending on the mineralogy and moisture content of the surface material. Water bodies appear dark blue or black due to water's high absorption in the spectral range recorded by the three MSS bands.

Individual Landsat–1 images in the form 1:500,000-scale false-color composites and spectral ratio images (Liggett and research staff, 1974) were studied in comparison with the geologic and structural maps referenced in the bibliography. Analysis of the satellite imagery focused primarily on structural lineaments considered to be possible faults of Cenozoic age. These structures were systematically compared with available geologic maps or checked in the field. The tectonic map of figure 4 is a compilation of those lineaments identified as faults or fault zones which have undergone Cenozoic movement. For the purpose of clarity, faults having traces less than 5 km in length have been eliminated from the compilation.

A map of Cenozoic volcanic and plutonic rocks (fig. 5) was compiled from the referenced published

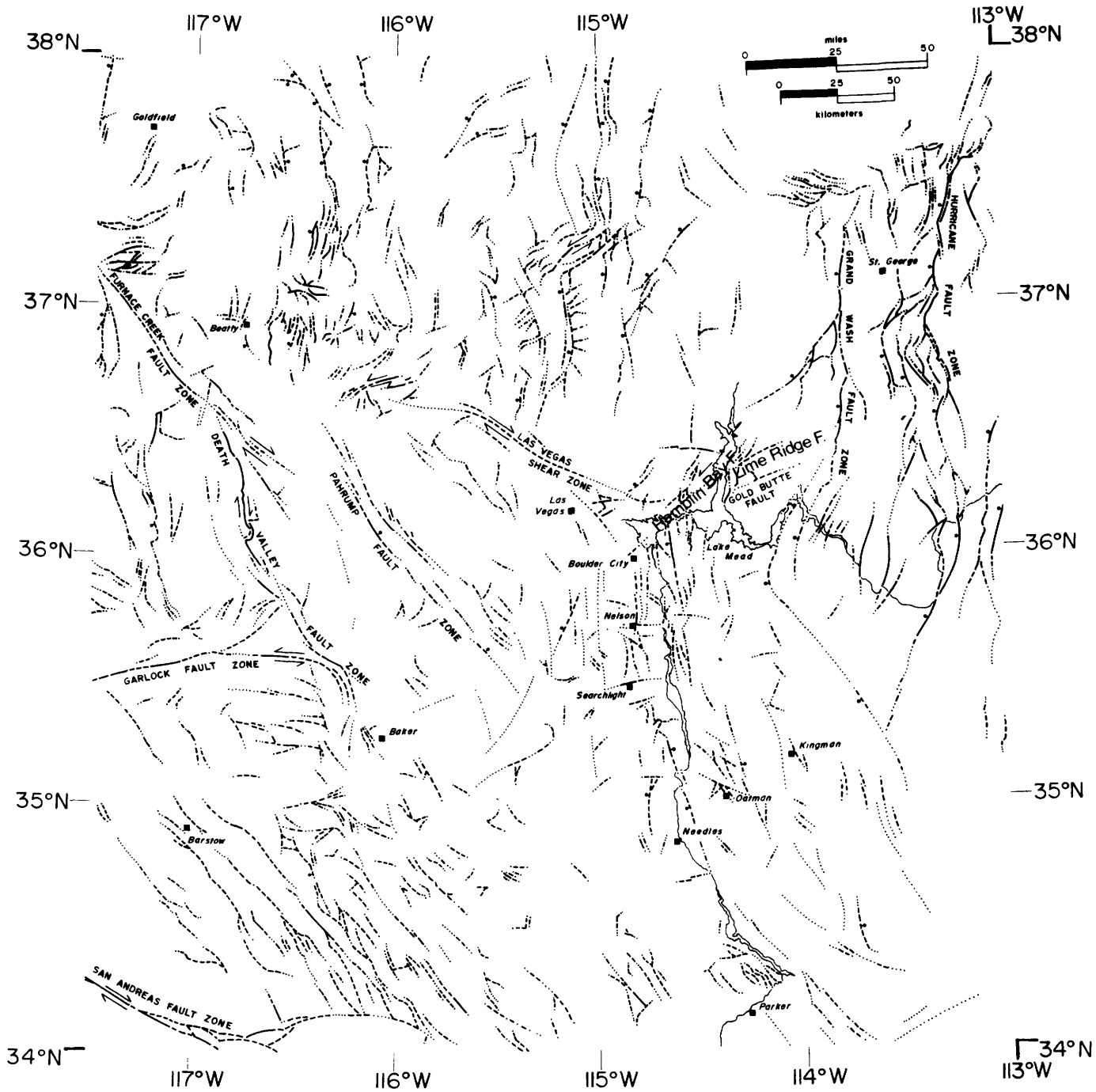

FIGURE 4.—Generalized map of the major Cenozoic fault systems visible in the Landsat–1 imagery of figure 2 (p. XXII). Sense of movement on major strike-slip faults is indicated by arrows; bars and balls are on the down-thrown sides of major normal faults.

sources and from reconnaissance mapping guided by analysis of Landsat–1 imagery. The mapped distribution of volcanic rock types has been generalized to distinguish between those of predominantly silicic to intermediate composition (rhyolite and trachyte through andesite) and those of predominantly basaltic composition (olivine andesite and basalt). Plutonic rocks shown in figure 5 range in composition from granite to gabbro although most are of intermediate composition.

REGIONAL GEOLOGIC SETTING

The area shown in the Landsat–1 mosaic of figure 2 (p. XXII) is located along the border between the

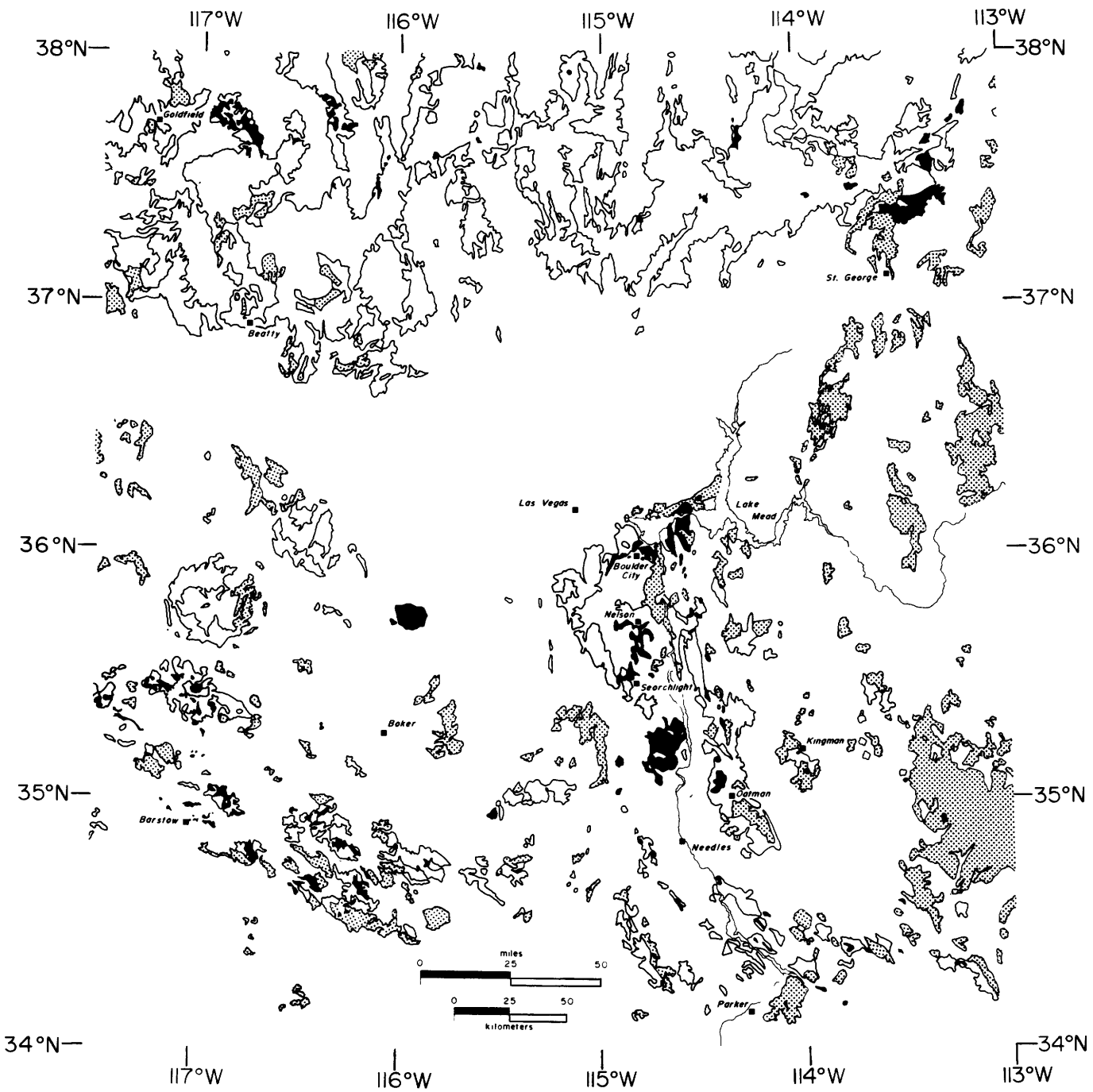

FIGURE 5.—Generalized map of the Cenozoic volcanic and plutonic rocks in the study area. Solid black areas are plutonic bodies of predominantly intermediate composition; the outlined areas are volcanic rocks of generally silicic to intermediate composition; and the stippled areas are volcanic rocks of predominantly basaltic composition.

Basin and Range province to the west and the Colorado Plateau to the east. The physiography of the Basin and Range province, as expressed in the Landsat–1 imagery, is characterized by systems of northerly trending mountain ranges separated by deep alluvial valleys. The province forms a distinct physiographic and structural terrane that can be traced from southern Oregon into northern Mexico.

Much of the Basin and Range province is underlain by Precambrian, Paleozoic, and Mesozoic rocks which were deformed during several orogenies of late Paleozoic and Mesozoic age (Armstrong, 1968). The

formation of the characteristic Basin and Range physiography began in mid-Tertiary time with the onset of regional normal faulting and widespread volcanic and plutonic activity which followed a 60-million-year period of relative crustal stability.

The Cenozoic structure of the province is characterized by northerly trending systems of complex grabens, horsts, and tilted blocks bounded by normal faults (Stewart, 1971). Major range-front faults typically dip at approximately 60° toward the basins with the angle of dip decreasing at depth (Hamilton and Myers, 1966). However, range-front faults having large displacements and dips of less than 25° are not uncommon in the Basin and Range province (Longwell, 1945; Anderson, 1971; Liggett and Ehrenspeck, 1974).

Within the area of study, much of the late Cenozoic volcanic activity is concentrated within two generalized areas referred to here as the Black Mountains and Nye County volcanic provinces (figs. 1 and 5). The volcanic rocks of these provinces are generally silicic to intermediate in composition and were erupted from fissure systems and caldera structures which are closely associated with the normal faults that characterize the Basin and Range province.

Within the Black Mountains volcanic province, erosion has exposed several large, late Cenozoic intrusive bodies which are genetically related to the widespread silicic and intermediate volcanic rocks (fig. 5). In several areas, massive dike swarms are exposed which cut both the crystalline basement and overlying volcanic rocks. These swarms are believed to have been feeders for at least some of the volcanic rocks, and their emplacement can be shown to be both temporally and spatially related to Basin and Range normal faulting (Liggett and Childs, 1974).

Systems of right- and left-lateral strike-slip faults are mapped within the Basin and Range province, generally striking at high angles to the northerly trends typical of the province. The estimates of lateral displacements on these fault systems range up to tens of kilometres. An example is the Las Vegas Shear Zone which can be traced from the southern margin of the Nye County volcanic province to the northern margin of the Black Mountains volcanic province, a distance of nearly 150 km (fig. 4).

Various theories which have been proposed to explain the origin of Basin and Range structure are discussed in excellent summaries by Nolan (1943), Gilluly (1963), Roberts (1968), and Stewart (1971). Most concepts can be separated into the following three categories:

1. Basin and Range structure has resulted from the collapse of the upper crust caused by such mechanisms as lateral transfer of lower crustal material (Gilluly, 1963) or eruption of huge volumes of volcanic rocks (Le Conte, 1889; Mackin, 1960).
2. Basin and Range structure has formed en echelon to movement on deep-seated, conjugate sets of right- and left-lateral strike-slip faults (Shawe, 1965; Sales, 1966).
3. Basin and Range structure is the result of regional crustal extension in an east-west direction (Cook, 1966; Hamilton and Myers, 1966; Roberts, 1968; Stewart, 1971). This process is believed to have occurred by plastic extension of the lower crust, perhaps accompanied by intrusion of plutons beneath Basin and Range grabens (Thompson, 1966). The net amount of crustal extension has been estimated to be as great as 300 km, or 100 percent of the former width of the province (Hamilton and Myers, 1966).

Most current theories of Basin and Range structure presume net crustal extension within the province during late Cenozoic time. Although the causes, mechanisms, and amounts of extension in the province remain controversial, evidence of extension has been documented by geologic mapping and geophysical studies.

TECTONIC MODEL

Based on analysis of Landsat–1 imagery and data published by Fleck (1970a), a tectonic model was proposed by Liggett and Childs (1974) in an attempt to explain the temporal and spatial relationships observed for strike-slip deformation on the Las Vegas Shear Zone and normal faulting, plutonism, volcanism, and related mineralization in the Black Mountains and Nye County volcanic provinces.

Figure 6 shows by means of a simplified model how the Las Vegas Shear Zone is believed to have functioned as an intracontinental "ridge-ridge transform fault" (as defined by Wilson, 1965) which formed in response to east-west crustal extension in the Black Mountains and Nye County volcanic provinces. The geology and chronological development of the Las Vegas Shear Zone and the two areas of inferred crustal extension are summarized below.

LAS VEGAS SHEAR ZONE

A major zone of right-lateral strike-slip deformation passing through Las Vegas Valley was first pos-

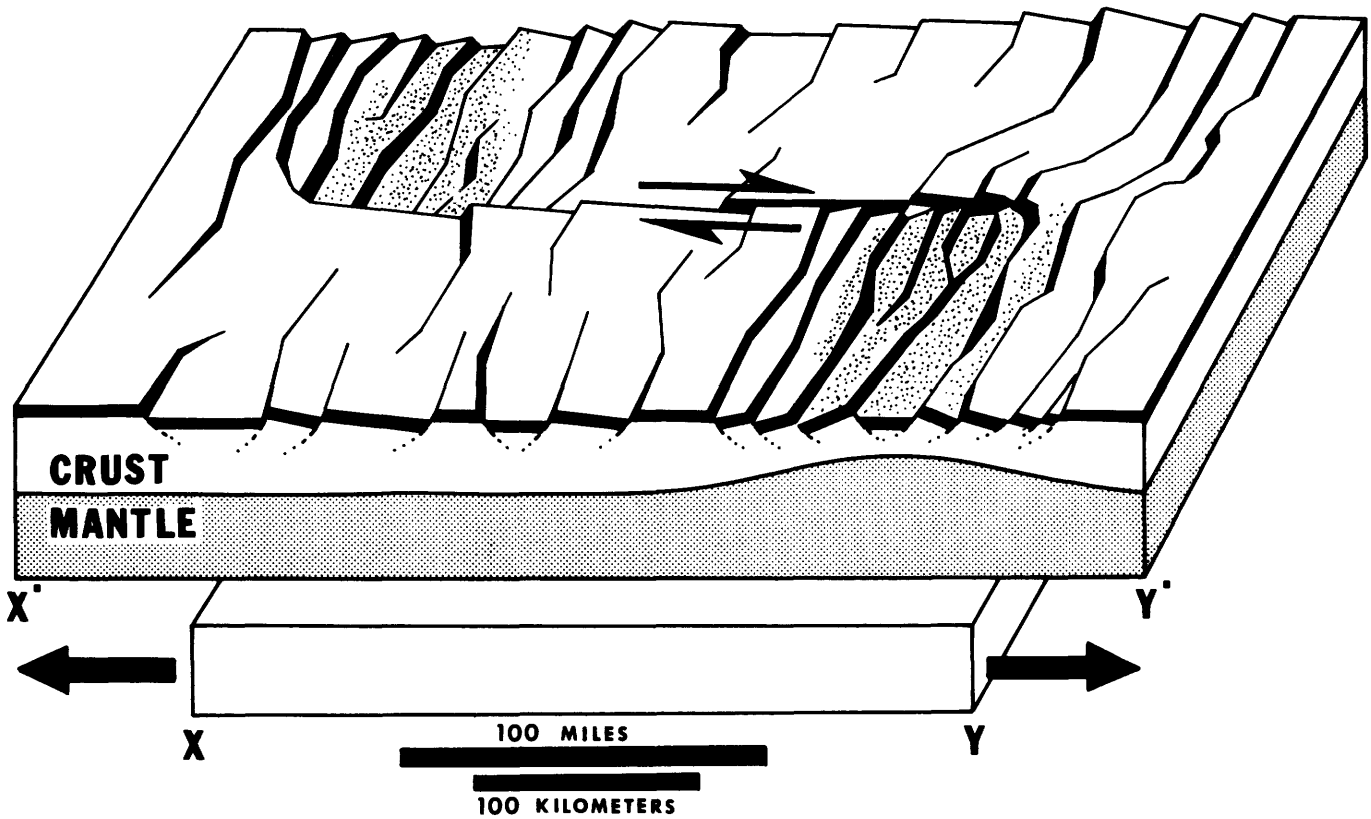

FIGURE 6.—Diagrammatic model relating right-lateral strike-slip movement on the Las Vegas Shear Zone to crustal extension in the two volcanic provinces (stippled patterns). The crustal extension is expressed in the model by major low-angle normal faulting which has caused anomalous thinning of the crust beneath the volcanic provinces. The amount of extension is represented by the increase in length of X–Y to X'–Y'.

tulated by Gianella and Callaghan (1934) in their discussion of the regional implications of the Cedar Mountain earthquake of 1932. The existence of this fault zone was supported by detailed mapping and named the Las Vegas Valley shear zone by Longwell (1960) (see fig. 4).

Indirect evidence suggesting more than 40 km of right-lateral strike-slip on this structure has been cited by several workers. These estimates have been based on displacements of stratigraphic isopachs and sedimentary facies (Longwell and others, 1965; Fleck, 1967; Stewart and others, 1968) and offset of distinctive thrust faults of the Sevier orogenic belt (Longwell and others, 1965; Fleck, 1967). At the scale of the Landsat–1 imagery, evidence for the shear zone is expressed in the flexure of the range trends immediately north and south of the zone. Compensating for the effect of flexure along the shear zone, Fleck (1967) estimated approximately 70 km of right-lateral displacement of features across the deformed belt bordering the shear zone. Of this total, a net slip of 30 km has been estimated for features along the trace of the structure.

The eastern termination of the Las Vegas Shear Zone is thought to lie in the vicinity of Lake Mead where major right-lateral slip on the shear zone gives way to a system of left-lateral oblique-slip faults (fig. 4). Immediately north of Lake Mead, Anderson (1973) has mapped two halves of a Miocene stratovolcano which are displaced left-laterally a distance of approximately 19 km along a northeast-striking fault zone. This structure, called the Hamblin Bay Fault, strikes at a low angle to the easternmost mapped branch of the Las Vegas Shear Zone.

East of the Hamblin Bay Fault, the Gold Butte, and Lime Ridge Faults of Longwell and others (1965) are considered by Anderson (1973) to be left-lateral strike-slip faults. This hypothesis is supported by the flexure of hogback ridges observed adjacent to these faults in the Landsat–1 imagery. The amount of left-lateral strike-slip deformation in this region is poorly known, although it is believed to exceed 19 km (Anderson, 1973). The spatial relationship of these structures to late Cenozoic normal faulting, volcanism, and plutonism in the Saint George-Cedar City area of Utah, suggests that the strike-slip deforma-

tion may be mechanically related to localized crustal extension in that area (figs. 4 and 5). An alternate model which involves differential subcrustal flow of the mantle has been proposed by Anderson (1973).

The duration of movement on the Las Vegas Shear Zone has been estimated (Fleck, 1967) from radiometric age determinations of rock units exposed along its trace. A radiometric age date of 15 million years from deformed beds of the Gale Hills Formation suggests that significant movement has occurred on the shear zone since that time. Undeformed basalts of the Muddy Creek Formation along the shear zone have been dated at 10.7 million years. From these dates and field evidence, Fleck (1967) concluded that most strike-slip movement on the Las Vegas Shear Zone probably occurred during the period from 17 to 10 million years ago.

BLACK MOUNTAINS VOLCANIC PROVINCE

The Black Mountains volcanic province is a distinctive igneous and structural terrane which extends southward along the Colorado River from Lake Mead, Nevada, to near Parker, Arizona (figs. 1 and 5). Reconnaissance maps of portions of this region have been published by Longwell (1963), Longwell and others (1965), Wilson and others (1969), and Volborth (1973). Detailed studies of mining districts within the province have been published by Schrader (1917), Ransome (1923), Callaghan (1939), Hansen (1962), Anderson (1971), and Thorson (1971).

The Black Mountains volcanic province is characterized by thick deposits of ignimbrites, flows, and volcaniclastic sediments of generally silicic to intermediate composition, although thin basalt flows are locally widespread. Near Nelson, Nevada, the composite thickness of the late Tertiary volcanic sequence is estimated to be over 5 km (Anderson and others, 1972).

The volcanics were deposited on an erosional surface developed on a crystalline basement of Precambrian gneiss and granite. In parts of the province, the Precambrian basement may have been subjected to metamorphism during a Jurassic orogeny (Volborth, 1973). Both the pre-Tertiary crystalline basement and the overlying volcanic rocks have been intruded by plutons of Miocene age (Anderson and others, 1972; Volborth, 1973). The plutons are generally elongate north-south, and range in composition from leucocratic granite to gabbro, although granite, quartz monzonite, and quartz diorite predominate (Anderson and others, 1972).

Structurally controlled, northerly striking dikes of rhyolite, andesite, and diabase cut both the crystalline basement and the volcanic cover throughout much of the province. In the Newberry Mountains, 25 km southeast of Searchlight, Nevada, a massive swarm of dikes is especially well-exposed forming a belt over 10 km wide. These dikes form a bimodal suite consisting of porphyritic rhyolite and hornblende diabase. Near Nelson, Nevada, dikes of similar compositions are exposed in the lower portions of the volcanic cover, generally decreasing in number upward in the stratigraphic section. It is probable that these dike swarms fed much of the volcanic cover and were in part synchronous with plutonism (Lausen, 1931; Volborth, 1973; Liggett and Childs, 1974).

A close genetic relationship between Tertiary intrusive rocks and chemically equivalent volcanic facies was suggested as early as 1923 by Ransome in a reconnaissance study of the Oatman mining district, Arizona. This conclusion has been supported by more recent mapping and geochemical studies in that district by Thorson (1971). Callaghan (1939) suggested a genetic relationship for an intrusive body and adjacent volcanic rocks in the Searchlight district, Nevada. Based on detailed geochemistry and radiometric age date analysis, Volborth (1973) has proposed a genetic interrelationship for plutonism, hypabyssal dike emplacement and volcanism in nearly the entire western half of the Black Mountains volcanic province. Most of this igneous activity occurred during the period from about 18 to 10 million years before present (Thorson, 1971; Anderson and others, 1972; Volborth, 1973).

The structure of the Black Mountains volcanic province is dominated by northerly striking normal faults, many of which dip at angles of 10° to 20°. This style of deformation has been mapped in detail near Nelson, Nevada, by Anderson (1971) who attributed the low-angle faulting to extreme east-west distension of the upper crust.

Individual normal faults within the Black Mountains volcanic province are estimated to have displacements of 2 to 5 km (Anderson, 1971; Anderson and others, 1972). Within many of the uplifted blocks, erosion has removed the volcanic cover, and exposures of crystalline basement are commonly juxtaposed against thick sequences of late Tertiary volcanic rocks.

Although there is insufficient stratigraphic evidence upon which to base accurate estimates of dip-slip on most of the faults in the Black Mountains volcanic province, the frequency of major low-angle normal faults suggests that crustal extension may exceed 70 km. Estimates of similar magnitude have been made for other portions of the Basin and Range province

by Hamilton and Myers (1966); Proffett (1971), and Davis and Burchfiel (1973).

Based on a seismic-refraction profile recorded across the Las Vegas Shear Zone from near Kingman, Arizona, toward the Nye County volcanic province, Roller (1964) has suggested that an anomalously thin crust, 27 km thick, underlies the Black Mountains volcanic province. North of the Las Vegas Shear Zone, the thickness of the crust increases rapidly to 32 km. The seismic-refraction pattern is supported by the existence of a northerly trending Bouguer gravity high (U.S. Air Force, 1968) which is aligned with the trend of the Black Mountains volcanic province. The gravity anomaly suggests an upward bulge of the mantle beneath the volcanic province, possibly the result of isostatic compensation for a thin, distended crust. The high gravity anomaly, like the volcanic province, terminates north of Lake Mead along the Las Vegas Shear Zone and Hamblin Bay Fault systems.

The southern end of the Black Mountains volcanic province is complex and indefinite. The pattern of volcanism, plutonism, and normal faulting within the volcanic province appears to terminate in the vicinity of Parker, Arizona, against a broad zone of northwesterly striking faults. Although this fault system is poorly mapped, field reconnaissance by the authors near Vicksburg, Arizona, and geologic mapping of the Quartzite quadrangle, Arizona, by Miller (1970) indicate right-lateral strike-slip on many of the northwesterly striking faults. The total amount of displacement on this fault system is unknown.

NYE COUNTY VOLCANIC PROVINCE

The Nye County volcanic province lies northwest of the Las Vegas Shear Zone in southern Nye County, Nevada (figs. 1 and 5). This province contains 10 known volcanic centers, at least 5 of which are believed to have formed caldera structures (Ekren, 1968). Detailed geologic studies have been conducted in several mining areas including Rhyolite and Beatty (Cornwall and Kleinhampl, 1964) and Goldfield (Ransome, 1909; Cornwall, 1972; Ashley, 1974). Detailed mapping, stratigraphic, and geophysical studies have been conducted by the U.S. Geological Survey in the U.S. Atomic Energy Commission's Southern Nevada Test Site (Eckel, 1968).

The Tertiary ignimbrites and flows recognized within the Nye County volcanic province are estimated to have a composite thickness of approximately 9 km and a volume of over 11,000 km^3 (Ekren, 1968). Most of these rocks range in composition from dacite to rhyolite, although andesite and basalt flows are locally abundant (Anderson and Ekren, 1968; Ekren, 1968). The volcanic units unconformably overlie a basement of Paleozoic carbonate rocks, which were folded, thrust faulted and metamorphosed during pre-Tertiary time. Several Mesozoic plutons have intruded this Paleozoic basement.

Numerous small plugs, domes, and dikes which range in composition from rhyolite to andesite with minor diabase have intruded the Tertiary volcanic cover. These intrusives are similar in composition to the volcanic rocks and many are believed to have been feeders (Ekren and others, 1971). Most of the volcanism and plutonism within the Nye County volcanic province was synchronous with major normal faulting in a time span from approximately 26.5 to 11 million years ago (Ekren and others, 1968).

The Tertiary deformation within the Nye County volcanic province is dominated by Basin and Range normal faults which have produced a complex horst and graben structure similar to that of the Black Mountains volcanic province. This structural pattern is locally interrupted by caldera subsidence structures, domes, and radial faults related to separate volcanic centers in the province. Arcuate faults which rim caldera structures have displacements estimated on the basis of gravity anomalies and drill hole data to be as great as 2 km (Orkild and others, 1968). Much of the Basin and Range structure is masked by the youngest volcanic rocks, and the full extent of normal faulting is unknown. On the basis of gravity data, several basins are estimated to be filled with as much as 4.8 km of volcanic rock (Healey, 1968); structural control of these basins is suggested by the pronounced northerly trends of the gravity anomalies.

The southern margin of the Nye County volcanic province is formed by the western end of the Las Vegas Shear Zone. Within this area of complex structural intersection, several short northeast-striking faults have been mapped which are believed to have undergone left-lateral strike-slip movement of from 3 to 5 km (Ekren, 1968). No continuation of the Las Vegas Shear Zone has been recognized west of the Nye County volcanic province.

CHRONOLOGY

The structural model proposed here for late-Tertiary deformation in the southern Basin and Range province is supported by the synchronism of strike-slip movement on the Las Vegas Shear Zone and volcanism, plutonism, and normal faulting in the two areas of inferred crustal extension. The chronology of these events is summarized in figure 7.

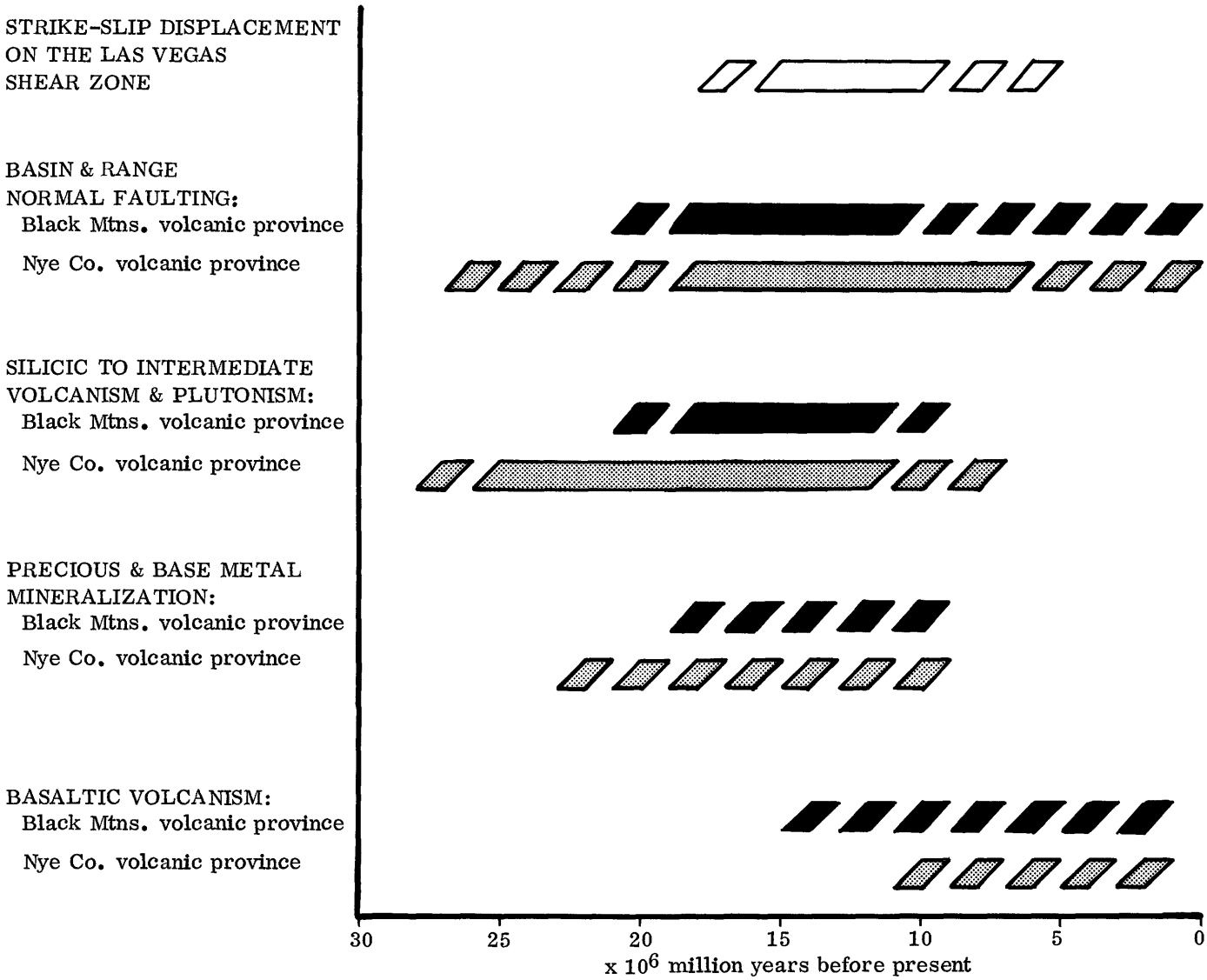

FIGURE 7.—Generalized chronology of strike-slip movement on the Las Vegas Shear Zone and normal faulting, igneous activity, and related mineralization in the Black Mountains and Nye County volcanic provinces.

Within the area of study, the folding and thrust faulting of the Sevier orogeny is believed to have been confined to a relatively brief time span between 90 and 75 million years ago (Fleck, 1970b). The Sevier orogeny appears to have been followed by a long period of relative stability and moderate erosion which by mid-Tertiary time had resulted in a broad terrane of subdued topography.

During mid-Tertiary time the area south of Lake Mead appears to have been the site of a broad arch which shed arkosic conglomerates and fanglomerates containing fragments of Precambrian rock toward the northeast. These sediments overlie an erosional surface cut in the Paleozoic rock of the western Colorado Plateau northeast of Kingman, Arizona. The sediments are conformably overlain by the Peach Springs Tuff of Young (1966) which has been variously dated at 18.3±0.6 and 16.9±0.4 million years (Young and Brennan, 1974). These relationships indicate that by Miocene time erosion had unroofed Precambrian basement in the arch south of Lake Mead and that major normal faulting had not yet separated depositional areas on the Colorado Plateau from source areas in the ancestral Basin and Range province. Following deposition of the Peach Springs Tuff, Basin and Range faulting disrupted the northeast-flowing drainage, leading to formation of a new pattern of isolated structural depressions filled by basin deposits (Lucchitta, 1972).

According to Anderson and others (1972), in the core of the Black Mountains volcanic province the oldest volcanic rocks overlying the Precambrian

crystalline basement are tuff units believed to be 18.6 million years old; the youngest volumetrically significant volcanic units in the area consist of tuffs and flows dated at 12.7 million years; and most of the epizonal plutonic rocks in the Black Mountains volcanic province range in age from 17 to 12 million years.

In the Nye County volcanic province, the chronology of volcanism and structural deformation is similar to that in the Black Mountains volcanic province. An erosional surface of low relief developed on the folded and thrust faulted Paleozoic basement in early Tertiary time. This surface was covered by a widespread welded tuff unit dated at 26.5 million years (Ekren and others, 1968). Shortly after the eruption of this tuff, normal faults with northeast and northwest strikes began to develop. The typical north-trending Basin and Range normal faults first began to form in the Nye County volcanic province after deposition of a tuff breccia dated at 17.8 million years. The present mountain ranges are believed to have been well defined prior to eruption of the Thirsty Canyon Tuff dated at 7 million years (Ekren and others, 1968), although minor normal faulting has continued to the present.

Albers and Kleinhampl (1970) have studied the genetic relationships between precious metal mineralization and spatially associated volcanic centers of Cenozoic age throughout Nevada. On the basis of radiometric age determinations these workers suggest that mineralization was at least temporally related to the late stages of igneous activity in the associated volcanic centers. The available evidence suggests similar relationships in the Black Mountains volcanic province.

In summary, the first major normal faulting, volcanism, and plutonism in the Black Mountains and Nye County volcanic provinces began in the period from approximately 26 to 18 million years ago. Right-lateral strike-slip movement on the Las Vegas Shear Zone appears to have begun about 17 million years ago and to have continued with synchronous igneous activity and extensional normal faulting in both volcanic provinces. Major strike-slip movement, igneous activity, and related mineralization ended by approximately 10 million years ago, although Basin and Range normal faulting and intermittent basaltic volcanism have continued to the present time.

STRUCTURAL CONTROL OF MINERALIZATION IN THE BLACK MOUNTAINS VOLCANIC PROVINCE

The gold, silver, and base metal mineralization of Cenozoic age in the Black Mountains and Nye County volcanic provinces is both spatially and temporally related to the igneous activity and structural deformation of these two areas. The structural control of mineralization in the Black Mountains volcanic province is of particular interest since both the regional structural setting of the province and the key structural trends which have localized mineralization are visible in the Landsat–1 imagery.

The major ore production in the Black Mountains volcanic province has come from the Eldorado and Searchlight districts in southern Clark County, Nevada, and the Oatman and Katherine districts east of the Colorado River in Mohave County, Arizona (fig. 8). Small mine workings and prospects are found throughout the province. The local geology and structural controls of mineralization in these districts are summarized below.

ELDORADO MINING DISTRICT

The Eldorado mining district is located in southern Clark County, Nevada, approximately 35 km south of Lake Mead. Most of the mines in the district are located within a 10-km radius of the town of Nelson (fig. 8). The host rocks for mineralization include Precambrian gneiss and Miocene plutonic and volcanic rocks of silicic to intermediate composition.

The structure of the Eldorado mining district is dominated by closely spaced, northerly striking normal faults, which commonly have dips of less than 30°. Anderson (1971) has attributed this system of low-angle normal faults to tensional rifting and distension of the upper crust, possibly related to the intrusion of a granitic pluton at shallow depth. In spite of the strong north-south structural grain, mineralization in the district is in almost all cases controlled by a system of steeply dipping, east-west striking faults. This transverse structural trend is well expressed in the Landsat–1 imagery.

The mineralization occurs in veins of fault breccia cemented with quartz and calcite gangue. The gold and silver are believed to have been contained in disseminated pyrite with minor galena, sphalerite, and chalcopyrite; however, the original sulfide minerals are now largely oxidized (Hansen, 1962). The veins typically show evidence of multiple episodes of fault movement followed by cementation and mineralization; many of the transverse faults along which the veins were formed are known to have undergone strike-slip movement (Anderson, 1971).

Total production from the Eldorado mining district during the period 1907–1945 is cited by Hansen (1962) as 101,522 oz gold and 2,339,353 oz silver, with minor production of copper and lead.

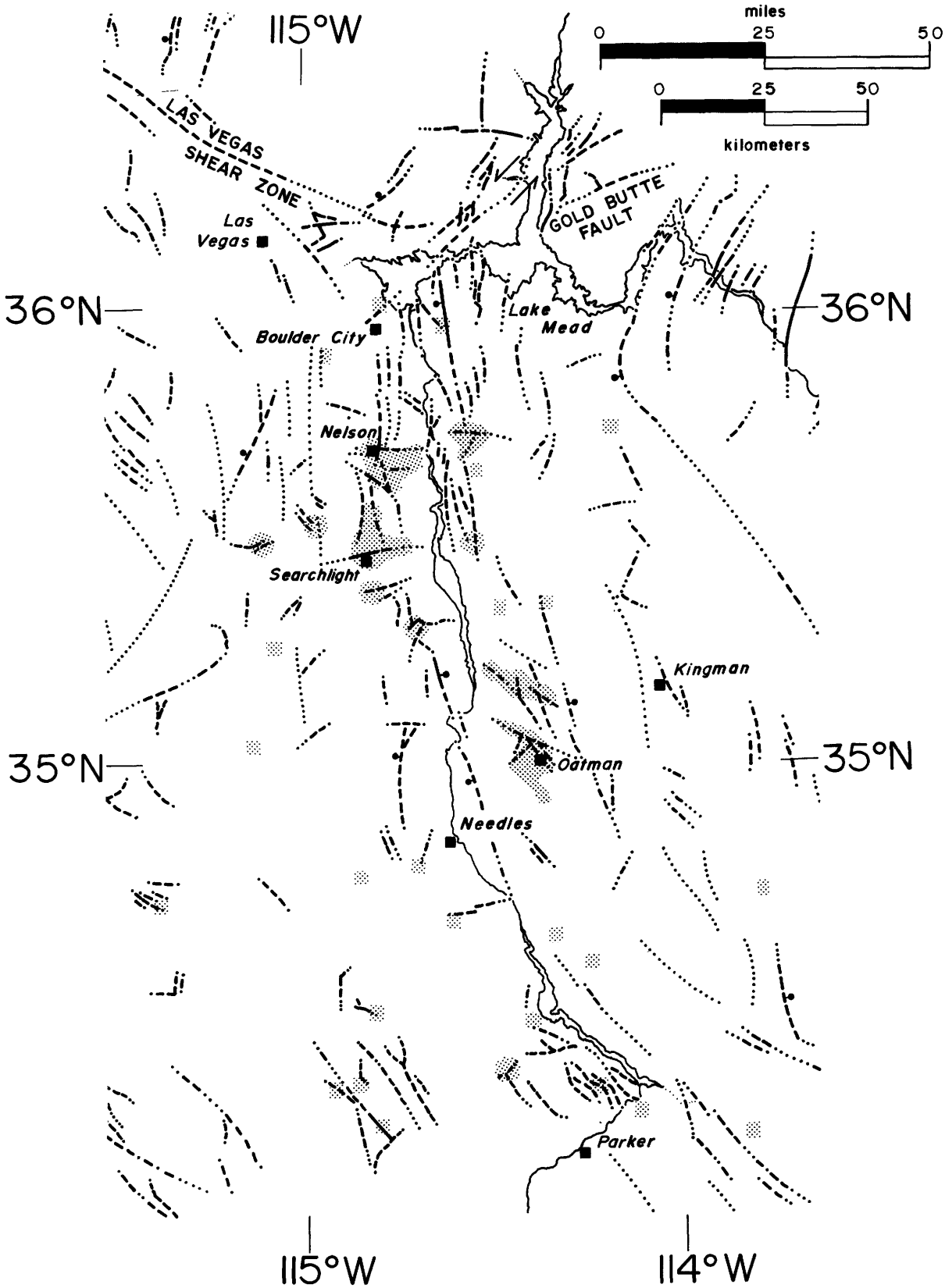

FIGURE 8.—Areas of late Cenozoic precious and base metal mineralization (stippled) in the Black Mountains volcanic province in relation to the Cenzoic fault systems visible in the Landsat imagery.

A relatively small mining area known as the Weaver district is located in the northern Black Mountains of Arizona due east of the Eldorado mining district. Like the Eldorado district, precious metals and minor copper occur in quartz and calcite vein systems which generally strike from N. 45° to 100° E., transverse to the structural grain of the province. Host rocks include Precambrian gneiss, Miocene volcanic rocks, and granites of probable Tertiary age. Although exact production figures are unavailable, total production from the Weaver district is believed to be small.

SEARCHLIGHT MINING DISTRICT

The Searchlight mining district is located at the southern end of the Eldorado Mountains, approximately 30 km south of the Eldorado mining district (fig. 8). The most prominent geologic feature of the district is a large quartz monzonite pluton of Miocene age which intruded a crystalline basement of Precambrian gneiss and granite and Tertiary volcanic rocks of intermediate composition (Callaghan, 1939). Although the shape of the pluton is generally controlled by the northerly structural grain of the Black Mountains volcanic province, the pluton is terminated on the south by a major east-west striking fault (Volborth, 1973).

Gold, silver, copper, and lead mineralization in the Searchlight district occurs in structurally controlled vein systems in and adjacent to the quartz monzonite pluton. Approximately 25 of the 34 productive veins in the district strike between N. 80° and 123° E.; most of these dip steeply to the south (Callaghan, 1939). The veins contain clasts of brecciated country rock usually cemented with quartz gangue although calcite and adularia occur locally. As in the Eldorado district, the veins show evidence of multiple episodes of fault movement followed by cementation and mineralization. Although the sense and amount of movement on the east-west striking faults is not known, these transverse structures contain the principal mineralization of the district.

Production from the Searchlight district for the period 1902–1934 is reported by Callaghan (1939) to be 207,570 oz gold, 219,596 oz silver, 650,550 lb copper, and 1,675,560 lb lead.

An area of numerous small gold and silver mines is located in Tertiary volcanic rocks east of the Colorado River, approximately 30 km east-northeast of the Searchlight district. The largest producing mine in this area is known as the Golden Door mine. The major mineralized quartz-calcite veins in the area strike generally eastward with generally steep dips; subordinate veins are irregular in strike and have shallow dips. Recent development and exploration work in the Golden Door mine area has concentrated on flat-lying volcanic units which have been preferentially silicified and mineralized.

OATMAN MINING DISTRICT

The Oatman mining district is located east of the Colorado River on the western slope of the Black Mountains, approximately 115 km south of Lake Mead (fig. 8). Most of the production from the Oatman district has come from vein systems within a thick sequence of late Tertiary volcanic rocks of silicic to intermediate composition. These volcanic rocks unconformably overlie a crystalline basement of Precambrian granite and gneiss. Both the crystalline basement and overlying volcanic rocks were locally introduced by dikes and small granitic plutons which are believed to be genetically related to the volcanic cover (Thorson, 1971).

The mineralized veins were formed within transverse fault zones, most of which range in strike from west to northwest and dip steeply toward the north or northeast. Several of the northwest-striking faults have undergone right-lateral strike-slip movement. The veins range in width from a few centimetres to several metres, and typically contain clasts of country rock cemented with a gangue of coarsely crystalline quartz and calcite with smaller amounts of microcrystalline adularia and fluorite. The veins commonly show a pronounced banding in cross section, produced by successive episodes of fault movement, cementation, and mineralization. Lausen (1931) reported five distinct stages of quartz deposition in the mineralized veins of which the later stages generally contain the highest ore values. Host rocks adjacent to the veins commonly show evidence of propylitic alteration.

A small amount of gold and silver has been produced from several mines in an area known as the Katherine mining district, located approximately 25 km north-northwest of Oatman. The veins in the Katherine district are similar in mineralogy to those at Oatman, although unlike the Oatman veins, they occur primarily within the Precambrian granitic basement which has been locally intruded by dikes and plugs of rhyolite (Lausen, 1931). The mineralized veins in the Katherine mining district generally strike at high angles to the northerly structural grain of the Black Mountains volcanic province.

The combined value of gold and silver production from the Oatman and Katherine mining districts is reported by Lausen (1931) as $35,417,926 for the period from 1897 through 1928. This is estimated to represent a metal production of approximately

1,714,000 oz t gold and 870,000 oz t silver from ore averaging approximately 0.6 oz of gold and 0.3 oz of silver per ton.

DISCUSSION

Field reconnaissance and study of geologic literature guided by analysis of Landsat–1 imagery have led to a model which relates strike-slip deformation on the Las Vegas Shear Zone to normal faulting, volcanism, and plutonism in the Black Mountains and Nye County volcanic provinces. The Las Vegas Shear Zone is believed to have functioned as a ridge-ridge transform fault, which separated these two areas of east-west crustal extension. Geochronology and field evidence indicate that the right-lateral strike-slip movement on the Las Vegas Shear Zone was synchronous with normal faulting, igneous activity, and related mineralization in both volcanic provinces.

The east-west crustal extension in the Black Mountains volcanic province is represented by northerly trending systems of normal faults, dike swarms, and shallow plutons. The pronounced north-trending structural grain of the province is locally crossed by transverse fault systems, several of which are known to have undergone strike-slip movement. These transverse structures are well expressed in the Landsat–1 imagery and have played an important role in localizing late Cenozoic precious and base metal mineralization within the volcanic province.

In several areas within the Black Mountains volcanic province a complex interrelationship has been observed between the normal and strike-slip fault systems. Many of the northerly striking normal faults terminate against transverse strike-slip faults without apparent offset. In addition, transverse strike-slip faults are frequently observed to end by turning abruptly in strike to merge with north-striking normal faults. Examples have been mapped by Anderson (1971) and Volborth (1973) in parts of the Boulder City and Nelson 15′ quadrangles. This interrelationship of strike-slip and normal faults suggests that these structures may be mechanically related as illustrated in the diagrammatic model of figure 9. This model suggests that the transverse strike-slip faults in the Black Mountains volcanic province may have formed as minor transform faults which separated areas of differential crustal extension.

The mechanisms by which the transverse faults have controlled the location of mineralization are not well understood. It is possible that the steep dips of these structures provided effective conduits for ascending hydrothermal solutions. Because each transverse fault is mechanically linked to a system of normal faults, it would remain active, and thus open to ascending solutions, over prolonged periods of extensional deformation. In contrast, individual gently dipping normal faults could be easily sealed by a variety of processes and are not likely to have afforded direct channelways for mineralizing solutions.

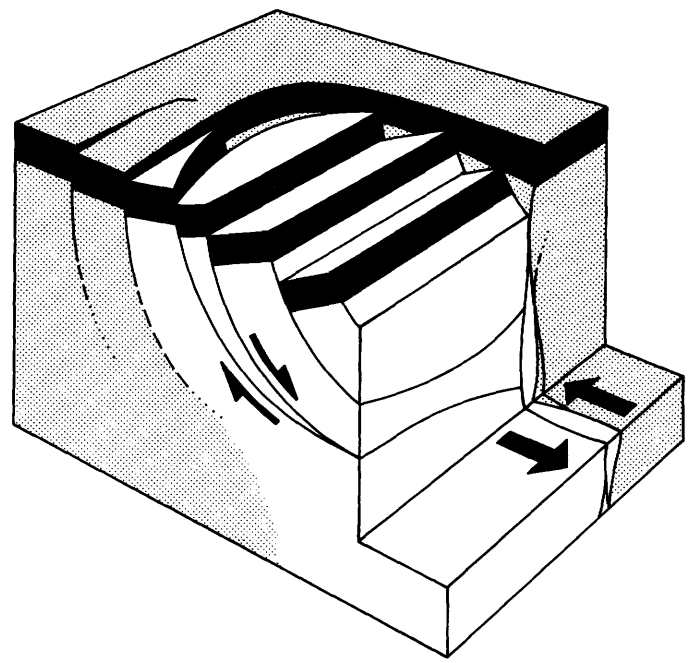

FIGURE 9.—Diagrammatic model illustrating the mechanical interrelationship of strike-slip and normal faulting believed to exist in the Black Mountains volcanic province. Note that movement on the strike-slip fault zone is mechanically linked to slip on the system of low-angle normal faults.

The model proposed here for the regional structural setting of the Black Mountains volcanic province unifies many of the temporal and spatial relationships recognized for the Cenozoic tectonics, igneous activity, and mineralization in this part of the Basin and Range province. Although many details of the structural deformation and the physicochemical controls of magma genesis and mineralization are not understood, the structural model and specific structural features expressed in the Landsat–1 imagery provide an effective basis for extrapolating mineralized trends and for selecting blind or poorly exposed targets for further investigation.

The application of satellite remote-sensing techniques to mineral exploration is not likely to replace the use of conventional methods. However, the synoptic perspective of satellite imagery can provide a valuable framework for synthesizing diverse geologic data and for guiding field research to test working hypotheses. Integrated with other exploration

techniques as part of a systematic program, satellite imagery can be a valuable tool in reconnaissance exploration.

ACKNOWLEDGMENTS

This investigation benefited greatly from the work of R. E. Anderson, R. J. Fleck, C. R. Longwell, A. Volborth, and the other individuals cited in the references. Wally MacGalliard prepared the false-color composites of Landsat–1 MSS imagery used in this investigation, and H. E. Ehrenspeck compiled much of the data presented in figures 4 and 5. The authors, however, are solely responsible for errors in fact or interpretation.

This research was supported jointly by Cyprus Mines Corporation and the National Aeronautics and Space Administration under Contract NAS5–21809.

REFERENCES CITED

Albers, J. P., and Kleinhampl, F. J., 1970, Spatial relation of mineral deposits to Tertiary volcanic centers in Nevada: U.S. Geol. Survey Prof. Paper 700–C, p. C1–C10.

Anderson, R. E., 1971, Thin skin distension in Tertiary rocks of southeastern Nevada: Geol. Soc. America Bull., v. 82, p. 43–58.

———1973, Large-magnitude late Tertiary strike-slip faulting north of Lake Mead, Nevada: U.S. Geol. Survey Prof. Paper 794, 18 p.

Anderson, R. E., and Ekren, E. B., 1968, Widespread Miocene igneous rocks of intermediate composition, southern Nye County, Nevada, *in* Eckel, E. B., ed., Nevada Test Site: Geol. Soc. America Mem. 110, p. 57–63.

Anderson, R. E., Longwell, C. R., Armstrong, R. L., and Marvin, R. F., 1972, Significance of K–Ar ages of Tertiary rocks from the Lake Mead region, Nevada-Arizona: Geol. Soc. America Bull., v. 83, p. 273–288.

Armstrong, R. L., 1968, Sevier orogenic belt in Nevada and Utah: Geol. Soc. America Bull., v. 79, p. 429–458.

Ashley, R. P., 1974, Goldfield mining district, *in* Guidebook to the geology of four Tertiary volcanic centers in central Nevada: Nevada Bur. of Mines and Geology Rept. 19, p. 49–66.

Callaghan, Eugene, 1939, Geology of the Searchlight district, Clark County, Nevada: U.S. Geol. Survey Bull. 906 D, p. 135–185.

Cook, K. L., 1966, Rift system in the Basin and Range province, *in* The world rift system: Canada Geol. Survey Paper 66–14, p. 246–279.

Cornwall, H. R., 1972, Geology and mineral deposits of southern Nye County, Nevada: Nevada Bur. Mines and Geology Bull. 77, 49 p.

Cornwall, H. R., and Kleinhampl, F. J., 1964, Geology of Bullfrog quadrangle and ore deposits related to Bullfrog Hills caldera, Nye County, Nevada, and Inyo County, California: U.S. Geol. Survey Prof. Paper 454–J, p. J1–J25.

Davis, G. A., and Burchfiel, B. C., 1973, Garlock fault: An intracontinental transform structure, southern California: Geol. Soc. America Bull., v. 84, p. 1407–1422.

Eckel, E. B., ed., 1968, Nevada Test Site: Geol. Soc. America Mem. 110, 290 p.

Ekren, E. B., 1968, Geologic setting of Nevada Test Site and Nellis Air Force Range, *in* Eckel, E. B., ed., Nevada Test Site: Geol. Soc. America Mem. 110, p. 11–19.

Ekren, E. B., Anderson, R. E., Rogers, C. L., and Noble, D. C., 1971, Geology of northern Nellis Air Force Base Bombing and Gunnery Range, Nye County, Nevada: U.S. Geol. Survey Prof. Paper 651, 91 p.

Ekren, E. B., Rogers, C. L., Anderson, R. E., and Orkild, P. P., 1968, Age of Basin and Range normal faults in Nevada Test Site and Nellis Air Force Range, Nevada, *in* Eckel, E. B., ed., Nevada Test Site: Geol. Soc. America Mem. 110, p. 247–250.

Fleck, R. J., 1967, The magnitude, sequence, and style of deformation in southern Nevada and eastern California (Ph.D. thesis): Berkeley, Univ. California, 92 p.

———1970a, Age and possible origin of the Las Vegas shear zone, Clark and Nye Counties, Nevada: Geol. Soc. America, Abs. with Programs (Rocky Mountain sect.), v. 2, no. 5, p. 333.

———1970b, Tectonic style, magnitude, and age of deformation in the Sevier orogenic belt in southern Nevada and eastern California: Geol. Soc. America Bull., v. 81, p. 1705–1720.

Gianella, V. P., and Callaghan, E., 1934, The earthquake of December 20, 1932, at Cedar Mountain, Nevada, and its bearing on the genesis of Basin Range structure: Jour. Geology, v. 42, no. 1, p. 1–22.

Gilluly, J., 1963, The tectonic evolution of the western United States: Geol. Soc. London Quart. Jour., v. 119, p. 133–174.

Hamilton, W., and Myers, W. B., 1966, Cenozoic tectonics of the western United States: Rev. Geophysics, v. 4, no. 4, p. 509–549.

Hansen, S. M., 1962, The geology of the Eldorado mining district, Clark County, Nevada (Ph.D. thesis): Rolla, Univ. Missouri, 262 p.

Healey, D. L., 1968, Application of gravity data to geologic problems at Nevada Test Site, *in* Eckel, E. B., ed., Nevada Test Site: Geol. Soc. America Mem. 110, p. 147–156.

Lausen, Carl, 1931, Geology and ore deposits of the Oatman and Katherine districts, Arizona: Arizona Bur. Mines and Geol. Series no. 6, Bull. 131, 126 p.

Le Conte, J., 1889, On the origin of normal faults and of the structure of the Basin region: Am. Jour. Sci., third series, v. 38, no. 226, p. 257–263.

Liggett, M. A., and Childs, J. F., 1974, Crustal extension and transform faulting in the southern Basin Range Province: Argus Exploration Company, NASA Rept. Inv., NASA–CR–137256, E74–10411, 54 p.

Liggett, M. A., and Ehrenspeck, H. E., 1974, Pahranagat shear system, Lincoln County, Nevada: Argus Exploration Company, NASA Rept. Inv., NASA–CR–136388, E74–10206, 12 p.

Liggett, M. A., and research staff, 1974, A reconnaissance space sensing investigation of crustal structure for a strip from the eastern Sierra Nevada to the Colorado Plateau: Argus Exploration Company, NASA Final Rept. Inv., NASA–CR–139434, E74–10705, 156 p., plus 16 appendices, 17 figures, and 8 plates.

Longwell, C. R., 1945, Low-angle normal faults in the Basin Range Province: Am. Geophys. Union Trans., v. 26, p. 107–118.

———1960, Possible explanation of diverse structural patterns in southern Nevada: Am. Jour. Sci. (Bradley Volume), v. 258–A, p. A192–A203.

——1963, Reconnaissance geology between Lake Mead and Davis Dam, Arizona-Nevada: U.S. Geol. Survey Prof. Paper 374–E, p. E1–E51.

Longwell, C. R., Pampeyan, E. H., Bowyer, B., and Roberts, R. J., 1965, Geology and mineral deposits of Clark County, Nevada: Nevada Bur. Mines and Geology Bull. 62, 218 p.

Lucchitta, I., 1972, Early history of the Colorado River in the Basin and Range province: Geol. Soc. America Bull., v. 83, p. 1933–1948.

MacGalliard, Wally, and Liggett, M. A., 1973, False-color compositing of ERTS–1 MSS imagery: Argus Exploration Company, NASA Rept. Inv., NASA–CR–135859, E74–10018, 5 p.

Mackin, J. H., 1960, Structural significance of Tertiary volcanic rocks in southwestern Utah: Am. Jour. Sci., v. 258, p. 81–131.

Miller, F. K., 1970, Geologic map of the Quartzite quadrangle, Yuma County, Arizona: U.S. Geol. Survey Map GQ–841, scale 1:62,500.

Nolan, T. B., 1943, The Basin and Range province in Utah, Nevada and California: U.S. Geol. Survey Prof. Paper 197–D, p. D141–D196.

Orkild, P. P., Byers, F. M., Jr., Hoover, D. L., and Sargent, K. A., 1968, Subsurface geology of Silent Canyon caldera, Nevada Test Site, Nevada, *in* Eckel, E. B., ed., Nevada Test Site: Geol. Soc. America Mem. 110, p. 77–86.

Proffett, J. M., Jr., 1971, Late Cenozoic structure in the Yerington district, Nevada, and the origin of the Great Basin: Geol. Soc. America, Abs. with Programs (Cordilleran sect.), v. 3, no. 2, p. 181.

Ransome, F. L., 1909, The geology and ore deposits of Goldfield, Nevada: U.S. Geol. Survey Prof. Paper 66, 258 p.

———1923, Geology of the Oatman gold district, Arizona: A preliminary report: U.S. Geol. Survey Bull. 743, 58 p.

Roberts, R. J., 1968, Tectonic framework of the Great Basin: Rolla, Univ. Missouri Res. Jour., no. 1, p. 101–119.

Roller, J. C., 1964, Crustal structure in the vicinity of Las Vegas, Nevada, from seismic and gravity observations: U.S. Geol. Survey Prof. Paper 475–D, p. D108–D111.

Sales, J. K., 1966, Structural analysis of the Basin Range province in terms of wrench faulting (Ph.D. dissert.): Reno, Univ. Nevada, 289 p.

Schrader, F. C., 1917, Geology and ore deposits of Mohave County, Arizona: Am. Inst. Mining Engineers Trans., v. 56, p. 195–236.

Shawe, D. R., 1965, Strike-slip control of Basin-Range structure indicated by historical faults in western Nevada: Geol. Soc. America Bull., v. 76, p. 1361–1378.

Stewart, J. H., 1971, Basin and Range structure: A system of horsts and grabens produced by deep-seated extension: Geol. Soc. America Bull., v. 82, p. 1019–1044.

Stewart, J. H., Albers, J. P., and Poole, F. G., 1968, Summary of regional evidence for right-lateral displacement in the western Great Basin: Geol. Soc. America Bull., v. 79, p. 1407–1414.

Thompson, G. A., 1966, The rift system of the western United States, *in* The world rift system: Canada Geol. Survey Paper 66–14, p. 280–290.

Thorson, J. P., 1971, Igneous petrology of the Oatman district, Mohave County, Arizona (Ph.D. dissert.): Santa Barbara, Univ. California, 173 p.

U.S. Air Force Aeronautical Chart and Information Center, 1968, Transcontinental Geophysical Survey (35°–39° N) Bouguer gravity map from 112° W. longitude to the coast of California: U.S. Geol. Survey Misc. Geol. Inv. Map I–532–B.

Volbroth, Alexis, 1973, Geology of the granite complex of the Eldorado, Newberry and northern Dead Mountains, Clark County, Nevada: Nevada Bur. Mines and Geology Bull. 80, 40 p.

Wilson, E. D., Moore, R. T., and Cooper, J. R., 1969, Geologic map of Arizona: U.S. Geol. Survey, scale 1:500,000.

Wilson, J. T., 1965, A new class of faults and their bearing on continental drift: Nature, v. 207, p. 343–347.

Young, R. A., 1966, Cenozoic geology along the edge of the Colorado Plateau in northwestern Arizona: Dissert. Abs., sec. B, v. 27, no. 6, p. 1994.

Young, R. A., and Brennan, W. J., 1974, Peach Springs Tuff: Its bearing on structural evolution of the Colorado Plateau and development of Cenozoic drainage in Mohave County, Arizona: Geol. Soc. America Bull., v. 85, p. 83–90.

ADDITIONAL REFERENCES USED IN COMPILING FIGURES 4 AND 5

Albers, J. P., and Stewart, J. H., 1972, Geology and mineral deposits of Esmeralda County, Nevada: Nevada Bur. Mines and Geology Bull. 78, 80 p.

Anderson, R. E., 1969, Notes on the geology and paleohydrology of the Boulder City pluton, southern Nevada: U.S. Geol. Survey Prof. Paper 650–B, p. B35–B40.

Bassett, A. M., and Kupfer, D. H., 1964, A geologic reconnaissance in the southeastern Mojave Desert, California: California Div. Mines and Geol. Spec. Rept. 83, 43 p.

Bechtold, I. C., Liggett, M. A., and Childs, J. F., March 1973, Regional tectonic control of Tertiary mineralization and Recent faulting in the southern Basin-Range Province: An application of ERTS–1 data, *in* Freden, S. C., Mercanti, E. P., and Becker, M. A., eds., Symposium on significant results obtained from ERTS–1, New Carrollton, Maryland, v. 1, sect. A, paper G–21, NASA–SP–327, p. 425–432.

Bishop, C. C., 1963, Geologic map of California, Needles sheet, Olaf P. Jenkins edition: California Div. Mines and Geology, scale 1:250,000.

Bowen, O. E., Jr., 1954, Geology and mineral deposits of Barstow quadrangle, San Bernardino County, California: California Div. Mines and Geology Bull. 165, 208 p.

Carlson, J. E., and Willden, Ronald, 1968, Transcontinental Geophysical Survey (35°–39° N) geologic map from 112° W longitude to the coast of California: U.S. Geol. Survey Misc. Geol. Inv. Map I–532–C, scale 1:1,000,000.

Childs, J. F., 1973a, The Salt Creek Fault, Death Valley, California (abs.): Argus Exploration Company, NASA Rept. Inv., NASA–CR–133141, E73–10774, 6 p.

———1973b, A major normal fault in Esmeralda County, Nevada (abs.): Argus Exploration Company, NASA Rept. Inv., NASA–CR–135859, E74–10018, 6 p.

Clary, M. R., 1967, Geology of the eastern part of the Clark Mountains Range, San Bernardino County, California: California Div. Mines and Geology Map Sheet 6.

Cook, E. F., 1957, Geology of the Pine Valley Mountains, Utah: Utah Geol. and Mineralog. Survey Bull. 58, 111 p.

———1960, Geologic atlas of Utah, Washington County: Utah Geol. and Mineralog. Survey Bull. 70, 124 p.

Dibblee, T. W., Jr., 1967, Areal geology of the western Mojave Desert, California: U.S. Geol. Survey Prof. Paper 522, 153 p.

Gillespie, J. B., and Bentley, C. B., 1971, Geohydrology of Hualapai and Sacramento Valleys, Mohave County, Arizona: U.S. Geol. Survey Water-Supply Paper 1899–H, p. H1–H37.

Gregory, H. E., 1950, Geology of eastern Iron County, Utah: Utah Geol. and Mineralog. Survey Bull. 37, 153 p.

Hall, W. E., and Stephens, H. G., 1963, Economic geology of the Panamint Butte quadrangle and Modoc district, Inyo County, California: California Div. Mines and Geology, Spec. Rept. 73, 39 p.

Hamblin, W. K., 1970, Structure of the western Grand Canyon region, *in* Hamblin, W. K., and Best, M. G., eds., Guidebook to the geology of Utah: Utah Geol. Soc. no. 23, p. 3–19.

Hewett, D. F., 1931, Geology and ore deposits of the Goodsprings quadrangle, Nevada: U.S. Geol. Survey Prof. Paper 162, 172 p.

Heylmun, E. B., ed., 1963, Guidebook to the geology of southwestern Utah: Intermountain Assoc. Petroleum Geologists, 12th Annual Field Conference, Salt Lake City, Utah, 232 p.

Hintze, L. F., 1963, Geologic map of southwestern Utah: Utah Geol. and Mineralog. Survey, scale 1:250,000.

Jahns, R. H., ed., 1954, Geology of southern California: California Div. Mines and Geology Bull. 170.

Jennings, C. W., 1958, Geologic map of California, Death Valley sheet, Olaf P. Jenkins edition: California Div. Mines and Geology, scale 1:250,000.

———1961, Geologic map of California, Kingman sheet, Olaf P. Jenkins edition: California Div. Mines and Geology, scale 1:250,000.

———1972, Geologic map of California, south half (preliminary): California Div. Mines and Geology, scale 1:750,000.

Jennings, C. W., Burnett, J. L., and Troxel, B. W., 1962, Geologic map of California, Trona sheet, Olaf P. Jenkins edition: California Div. Mines and Geology, scale 1:250,000.

Kupfer, D. H., 1960, Thrust faulting and chaos structure, Silurian Hills, San Bernardino County, California: Geol. Soc. America Bull., v. 71, p. 181–214.

Liggett, M. A., and Childs, J. F., 1973, Evidence of a major fault zone along the California-Nevada state line 35°30′–36°30′ north latitude: Argus Exploration Company, NASA Rept. Inv., NASA–CR–133140, E73–10773, 13 p.

Malmberg, G. T., 1967, Hydrology of the valley-fill and carbonate-rock reservoirs, Pahrump Valley, Nevada-California: U.S. Geol. Survey Water-Supply Paper 1832, 47 p.

Maxey, G. B., and Jameson, C. H., 1948, Geology and water resources of Las Vegas, Pahrump, and Indian Spring Valleys, Clark and Nye Counties, Nevada: Nevada Water Resources Bull. 5, 121 p.

McAllister, J. F., 1952, Rocks and structure of the Quartz Spring area, northern Panamint Range, California: California Div. Mines and Geology Spec. Rept. 25, 38 p.

———1955, Geology of mineral deposits in the Ubehebe Peak quadrangle, Inyo County, California: California Div. Mines and Geology Spec. Rept. 42, 63 p.

———1956, Geology of the Ubehebe Peak quadrangle, California: U.S. Geol. Survey Map GQ–95, scale 1:62,500.

———1970, Geology of the Furnace Creek borate area, Death Valley, Inyo County, California: California Div. Mines and Geology Map Sheet 14, scale 1:24,000.

McKee, E. H., 1968, Geology of the Magruder Mountain area, Nevada-California: U.S. Geol. Survey Bull. 1251–H, 40 p.

Noble, D. C., 1968, Kane Springs Wash volcanic center, Lincoln County, Nevada, *in* Eckel, E. B., ed., Nevada Test Site: Geol. Soc. America Mem. 110, p. 109–116.

Norman, L. A., Jr., and Stewart, R. M., 1951, Mines and mineral resources of Inyo County: California Jour. Mines and Geology, v. 47, no. 1, p. 17–223.

Rogers, T. H., 1967, Geologic map of California, San Bernardino sheet, Olaf P. Jenkins edition: California Div. Mines and Geology, scale 1:250,000.

Ross, D. C., 1965, Geology of the Independence quadrangle, Inyo County, California: U.S. Geol. Survey Bull. 1181–0, 64 p.

Schrader, F. C., 1909, Mineral deposits of the Cerbat Range, Black Mountains, and Grand Wash Cliffs, Mohave Co., Arizona: U.S. Geol. Survey Bull. 397, 226 p.

Smith, A. R., 1964, Geologic map of California, Bakersfield sheet, Olaf P. Jenkins edition: California Div. Mines and Geology, scale 1:250,000.

Smith, G. I., Troxel, B. W., Gray, C. H., and von Huene, Roland, 1968, Geologic reconnaissance of the Slate Range, San Bernardino and Inyo Counties, California: California Div. Mines and Geology Spec. Rept. 96, 33 p.

Stokes, W. L., and Heylmun, E. B., 1963, Tectonic history of southwestern Utah, *in* Heylmun, E. B., ed., Guidebook to the geology of southwestern Utah: Intermountain Assoc. Petroleum Geologists Guidebook 12, p. 19–25.

Strand, R. G., 1967, Geologic map of California, Mariposa sheet, Olaf P. Jenkins edition: California Div. Mines and Geology, scale 1:250,000.

Threet, R. L., 1963, Structure of the Colorado Plateau margin near Cedar City, Utah, *in* Heylmun, E. B., ed., Guidebook to the geology of southwestern Utah: Intermountain Assoc. Petroleum Geologists Guidebook 12, p. 104–117.

Tschanz, C. M., and Pampeyan, E. H., 1970, Geology and mineral deposits of Lincoln County, Nevada: Nevada Bur. Mines and Geology Bull. 73, 187 p.

PROCEEDINGS OF
THE FIRST ANNUAL WILLIAM T. PECORA MEMORIAL SYMPOSIUM,
OCTOBER 1975, SIOUX FALLS, SOUTH DAKOTA

Mineral Exploration Applications of Digitally Processed Landsat Imagery

By R. J. P. Lyon,
Stanford Remote Sensing Laboratory,
Stanford University, Stanford, California 94305

ABSTRACT

Enhancement processing of Landsat CCT digital data can markedly increase its application in mineral exploration in two principal ways: (1) by producing enhanced images with higher contrast and resolution, and hence higher information content for the photogeologist and (2) by pattern-recognition techniques applied by computer directly to the four-band digital spectra.

Of these, by far the greatest use will be the photogeological usage of enhanced images because of the simplicity of analysis in requiring only the mind of a creative photogeologist. The use of computers in geological analysis of these images is complicated because of the inability of the creative photogeologist to specify mathematically the decisionmaking process by which he arrives at an analysis. Algorithms can be created for some of the steps only, but by using an interactive computer display system, under the control of the geologist personally familiar with the problem and area being studied, the man-machine interaction can extract the benefits of both.

This paper describes the use of such a system (STANSORT) to mineral exploration problems, in zero vegetation cover (Yerington; Goldfield, Nev.), mixed cover of piñon pine and juniper (Pine Nut Mtns., Nev.), heavy birch forest (Karasjok, Norway), and full tropical cover (Tifalmin, New Guinea). Clearly the increasing vegetation cover makes the recognition process more complex. The inclusion of geobotanical (and biogeochemical) information in exploration is essential. Landsat data are an excellent base for this purpose, but ground information must be secured for their full application.

INTRODUCTION

Over two-thirds of the land surface of the world is covered with vegetation, of which 42 percent is forest, 24 percent is grasslands, and 21 percent comprises a cover of desertic shrubs and grasses in semiarid terrains (Draeger and Lauer, 1967). In any mineral exploration program, therefore, to neglect this obscuring cover is naive. Many of the applications of digitally enhanced Landsat data unfortunately have been made in areas devoid of vegetation cover (Pakistan, Peru, etc.) and consequently the effect of such cover has not been considered. This paper speaks to this point and shows the application of this emerging technology to areas of sparse desertic cover (Nevada), moderate cover of pines and juniper (Nevada), and full cover of birch forest (northern Norway), and rain forest-jungle (central New Guinea Highlands).

We must consider vegetation in our Landsat analysis or we will be dealing essentially with only one part of the total exploration problem. The principal measurement problem is a familiar one—sampling—and revolves around making sure that the coverage of the field equipment adequately expresses what is seen by the satellite in one pixel (0.4 ha or 1 acre) resolution. Clearly one must evolve techniques which include soils and vegetation in the right proportions, and this is difficult at ground level.

A secondary, but very real, problem is that no one technique of data enhancement (stretching, ratioing, etc.) works all the time in every area, mainly because of the variable effect of differing vegetation cover. One must use a group of techniques to obtain the maximum benefits from the computer compatible tapes (CCT's) from Landsat.

BACKGROUND

The principal attraction of the Landsat satellite system to a modern mineral exploration program is, that for the first time, a calibrated and quantitative spectrally filtered photographic system is available with coverage of almost any part of the land surface of the Earth. Unlike traditional aerial photography, one does not have to question the film type, filters, the development practices which were used, or by what means were numerical data extracted from the film-base materials. We can directly compare spectra. The spectral response is fixed and constant, the gray-scale characteristics identifiable, no matter whether we are looking at Norway or New Guinea, Australia, or Argentina. In addition, as an important corollary, any software algorithms developed to process the digital data from the satellite apply equally to any other geographic locality.

Spatially with Landsat we have to modify our thinking somewhat, as each resolution cell (the highest resolution unit possible) covers 0.4 ha (1 acre) and is seen at scales smaller than those with which we have had most of our prior experience. This can be looked at in at least two ways. Normally we use a higher resolution element—say 10 cm^2 and a scale of 1:40,000—because our decisionmaking process in photointerpretation requires this degree of spatial resolution for *shape* identification. Even when using color film we base most of our photogeological analysis on shape and neglect the discriminant power of the spectral color. This conditioned reflex has come about because our color reproduction in printing leaves much to be desired, and we have not been able to state (or remember) precisely what spectral colors we were viewing. Landsat with its quantitative reproducibility has changed much of that. Furthermore, although the pixel is 0.4 ha in area, there are still 250/km^2 (640/mi^2). If decisions can be made on the spectral information content of each pixel, then we can consider this resolution as giving 250 decisions/km^2 (640 decisions/mi^2)—a very different way of looking at data. Each Landsat scene contains about 7 million pixels covering 34,000 km^2, and any set of pixels in that or adjoining tapes can be rapidly evaluated by the same algorithm, thus markedly broadening the usefulness of this search approach in exploration.

In our work at Stanford, we have continually worked at high resolution with the Landsat data, often using only 100 pixels or so to perform analyses relating ground measurements to those of the satellite. Our basic study areas are 20 km^2 (7.6 mi^2) presented on a video-display and on paper printout at about 1:20,000 scale. For larger coverages, at the district level we prepare film images of 300–360 km^2 (125 mi^2) at a scale of about 1:220,000, to which we have

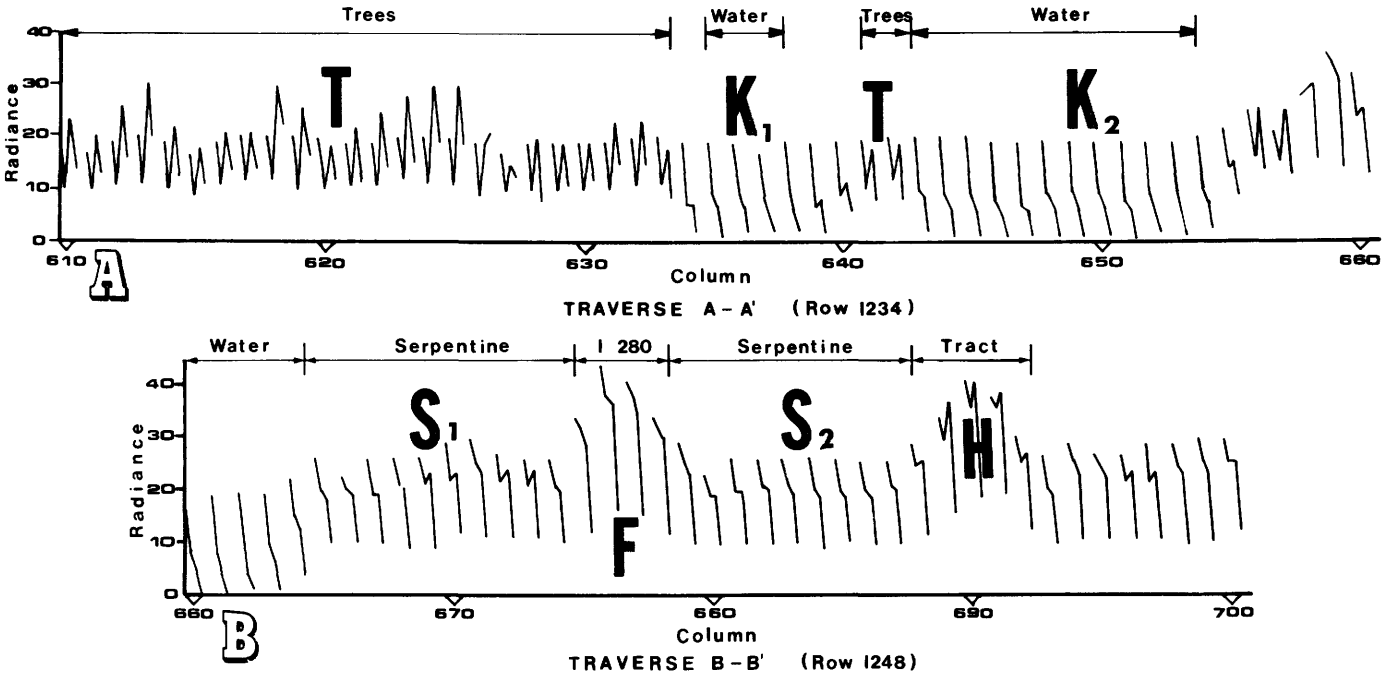

FIGURE 1.—Channel-by-channel spectral plots for picture elements (pixels) along a raster line. T=trees; K=Crystal Springs reservoir (water); S=serpentine; F=freeway (I–280); H=housing tracts. From Levine (1976).

made the required geometric correction. We thus continually remind ourselves that the field problems to which we are applying these techniques require detailed answers for 20–300 km² areas at scales between 1:24,000 and 1:100,000 to be of use in the typical exploration program.

RATIOING CONCEPTS AND ADVANTAGES

Of all the concepts presently used in enhancing Landsat digital data that of ratioing any pair of the four channels has proved the most significant. This has several immediate advantages—it tends to normalize the spectral data, removing "brightness" contrasts between any two pixels and enabling a better comparison of their hue or color. Such ratioing has been performed optically before (Whitaker, 1965) by simultaneously printing a positive transparency of one channel and a negative of the other, but many assumptions as to linearity of response of the two film records have to be made. By far the more positive and simpler task is to use the digital data and perform the single ratio step in the computer. At the same time one often stretches the data in each channel to make maximum use of the full dynamic range (0–255) before ratioing.

A small exercise is useful at this point to elucidate further the physical meaning of Landsat spectra and the ratioing process and, at the same time, to show the high resolution capabilities of spectral analysis of this system. To illustrate these points figures 1 and 2 have been taken from a more detailed analysis (Levine, 1976) of the concept initially developed by Honey and others (1974).

The upper traverse (A) in figure 1 represents a plot of 50 pixels along a single raster line (pixels 610–660;

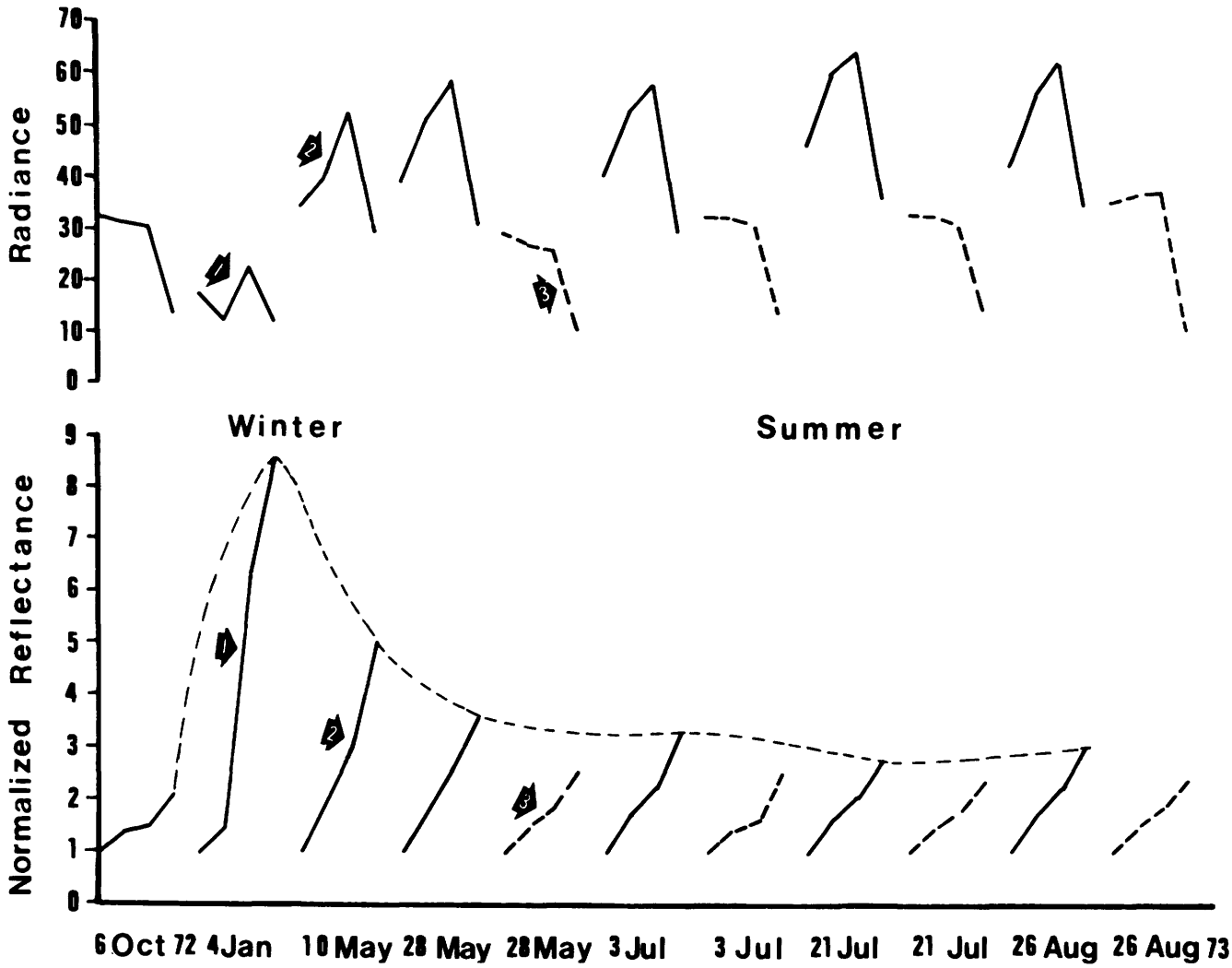

FIGURE 2.—Time series of averaged spectra and radiance (upper) and normalized reflectance (lower). Spectra for averages of 10 pixels. Dashed spectra are for burned-over areas (soil areas). From Levine (1976).

row 1234) for a San Francisco Bay scene (1075–18173). The lower traverse (B) represents a similar traverse of 40 pixels (pixels 660–700; row 1248) slightly farther to the southeast.

Each small zigzag pattern is a radiance plot of all four Landsat channel values for a single pixel, with the digital numbers joined to give a low resolution spectrum. The spectra can be easily classed into similar shapes, by passing the eye rapidly from left to right along the raster line, using the well-developed shape-recognition features of the human eye-brain system (Step 1). As Step 2, we can correlate these pattern classes precisely with mapped land-water interfaces by locating them on large-scale topographic maps (1:24,000 scale) or, preferably, if available, on orthophoto maps at the same scale. The pattern (T) could be identified with tree-covered slopes, (K_1) with the western arm, and (K_2) with the eastern arm of Crystal Springs reservoir. Similarly (S_1) and (S_2) were identifiable with patches of serpentine outcrops cut by Interstate 280 (F), and (H) as a housing tract which lay to the east.

To adapt this eye-recognition method to machine operation an automatic, unsupervised clustering algorithm was written by Honey which simulates Step 1 in the computer and forms the basis of our STANSORT program (Honey and others, 1974). Steps 1 and 2 together when performed manually help the worker gain confidence in the credibility of Landsat spectra and in possible pattern recognition processes. This part of the exercise has important teaching applications.

Atmospheric corrections, which remove the effects of back scattering of sunlight by the atmospheric column, were performed (Step 3) by subtracting the observed apparent brightness in each channel from over a large area (45 pixels) of zero-reflectivity carbon-black refinery waste lying on the south shore of Carquinez Bay (northeast of San Francisco but still on the same Landsat scene and tape; see (Lyon and others, 1975). Reduction of the atmospherically corrected values of reflectance is performed in Step 4 by observing the apparent brightness of a known reflectance target—the concrete parking aprons of Moffett Field, on the southwest edge of San Francisco Bay, in the same Landsat tape. As the bidirectional reflectance of the concrete has been measured by us (28 percent, 31 percent, 30 percent, 32 percent in each channel, 4–7) a linear interpolation between the zero-reflectance target (<0.5 percent in all channels) and the concrete "bright" target enables us to convert any other pixel spectrum to reflectance.

Figure 2 (upper) shows radiance spectra (averaged over 10 pixels) from another nearby grassy/soil area, in a time-series (plotted as the abscissa) from fall (October 6, 1972) through summer (August 26, 1973). Only the solid curves, like (1) and (2), need concern us; the dashed curves (3) are for burned-over areas of significance later in the year. By performing the ratioing (Step 5) much more familiar spectral shapes appear. Here in figure 2 (lower), Channels 5, 6, and 7 have been divided by Channel 4, although equally well any other channel, the total of all channels, etc., could be used, and particularly so if Channel 4 is noisy.

Ratioing removes the varying absolute levels of brightness (see within pattern T in fig. 1) which are from the sunlit and shaded sides of hills covered with a constant terrain material—in this case, trees. Steps 3 and 4 may be omitted if one does not require atmospheric corrections and reflectance data and comparable shadow-free "flat earth" spectral images may be made. Ratioing thus enhances the spectral-color information (Whitaker, 1966) in Landsat data by suppressing the relative brightness due solely to topography. Obviously in structural analysis this would not be an asset where shadows materially aid in the analysis, but the later discussion of applications will show the merit of ratioing for lithological differentiation. We retain both structural and lithological information by making three-color imagery, with two of the three color-guns assigned to ratio images (say Ch 7/4* = green and Ch 5/4 = blue) and with the red gun assigned to our "edge-enhancement" procedure, which produces nondirectional symbols at spectral-contrast edges in the four-channel data matrix (Honey, Prelat and Lyon, 1974). The human eye again is used to connect the edge dots into meaningful lineaments. These may or may not parallel lithologic contacts as seen in the other two ratio images in the three-color print.

APPLICATION CASE HISTORIES

Where the surface materials over a mineralized area are residual and contain alteration minerals—clays, iron oxides, etc.—typical of that style of mineralization, the techniques for use of Landsat digital data in a search mode are relatively straightforward. These have been well documented by Goetz and others (1975), Vincent (1973), and by ourselves (Lizaur, 1975; Ballew, 1975a, 1975b; Lyon and others, 1975; Lyon, 1976). However where the mineralized targets of search are covered—either by glacial debris, wind-

*Ratios may be shown as Ch 7/4 or R74, etc.

blown sand, alluvial outwash, etc., or more often, by even minimal amounts of vegetation—their discovery is much more complicated.

This selection of our case histories is oriented to these points and is arranged in order from essentially zero vegetative and surficial cover (Yerington, Nevada, pit and dumps), through light desertic cover (Singatse Range, and Goldfield, Nevada), to moderate piñon pine and juniper forest (Pine Nut Mountains, Nevada), and, finally, heavy forest of birch in an Arctic environment with a full cover of glacial till (Karasjok, Norway), and jungle at Tifalmin, New Guinea.

The localities are tabulated in table 1.

TABLE 1.—*Localities and results of case histories*

Very low to zero cover:
Yerington copper pit, dumps, and surrounding Singatse Range, Nevada. Oxidized and nonoxidized ore (sulfide) may be differentiated in the pit and the sulfide rock "discovered" in the tailings pond using Landsat data in a search mode (STANSORT/SEARCH).
Goldfield, Nevada. Alteration zones and gossans surrounding gold-alunite mineralization. Outline of alteration zone can be mapped by Landsat image enhancements.
Moderate cover:
Pine Nut Mountains, Nevada. A molybdenum-bearing skarn with a biogeochemical anomaly in the piñon pine and juniper, independently located by color-ratio images prepared from Landsat data.
Heavy cover:
Karasjok, Norway. A known copper-bearing biogeochemical anomaly was relocated by the Landsat data and now has been extensively studied in the field.
Tifalmin, New Guinea. A known set of copper-bearing intrusives under full jungle cover. So far very little success in determining any vegetative anomaly.

VERY LOW TO ZERO COVER

YERINGTON COPPER PIT AND DUMPS, MASON VALLEY, NEVADA

General description.—The simplest example which can be chosen for analysis, and which is still of significance to mineral exploration, is that of an open-pit mine and its surrounding dumps. Here, single rock type materials cover enough area as to be statistically significant (>8–10 pixels) in the pit itself (generally a single type of intrusive rock with one or two superposed alteration or oxidation mineralogies). The dumps have been carefully segregated during mining and represent waste rock, low-grade ore, and tailings from the metal extraction.

Yerington pit in Lyon County, Nevada, about 80 km south-southeast of Reno, satisfies all of these criteria. This pit, while small (2×1 km), may be considered to have an oxidized upper portion and a nonoxidized sulfide-bearing lower portion (fig. 3). The southern dumps are made up of alluvial overburden and waste rock (largely granodiorite). The northern dumps (from northwest to northeast) are respectively oxide tailings from leach ore, sulfide tailings pond (T) and low-grade mixed oxide-sulfide leachable ore. All the northern dumps represent varying grades of oxidation of the quartz monzonite and granodiorite. From the pit, to the south, the dumps are alluvial outwash and cover. The housing settlement of Weed Heights (W) and the irrigated river-bottom lands of the Mason Valley (M) and Walker River show patterns typical of vegetation (gardens, lawns, fields, etc.).

The Singatse Range (S–S) has a typical Nevadan Basin and Range topography bounded on the east by several range-front faults. The geology of the range is complex and is composed of Jurassic granodiorites and sediments to the southwest of the pit, with predominantly Tertiary volcanics (ignimbrites, etc.) to the west and northwest of Weed Heights.

The vegetated cover of the pits and dumps is zero. The cover on the Singatse Range is sparse (mainly sagebrush and other desertic shrubs) typically 3 to 5 bushes per 10 m^2. From above, less than 10 percent of the ground would be covered.

Analysis.—Single band images prepared on a line-printer, with each pixel value being encoded as a symbol (lighter toned for higher value=brighter areas, darker for lower value=darker areas) with 14 steps or gray tones, are shown in figure 4. These resemble over-enlarged photographs but are very useful as "road maps" for locating specific pixels or areas for detailed analysis.

Figure 4 shows a typical output stage of data each for 20 km^2 of Channel 5 (left) and Channel 7 (right).

FIGURE 3.—Yerington pit area, Nevada, aerial photograph from 20 km. T=tailings pond; Fe=acidified ferric sulfate leach liquor; D=dumps, D1=oxide leach waste, D2=leach dumps, low-grade oxide and sulfide; D3 & D4=mixed alluvial and waste rock, mainly granodiorite; M=Mason Valley; W=Weed Heights housing area for the mine; f–f=range-front fault; S-S=Singatse Range. In pit: 1=sulfide, 2=oxide, 3=mixed, 4=leached ore. Original copied from a color photo (RB57–MX248) taken August 11, 1973.

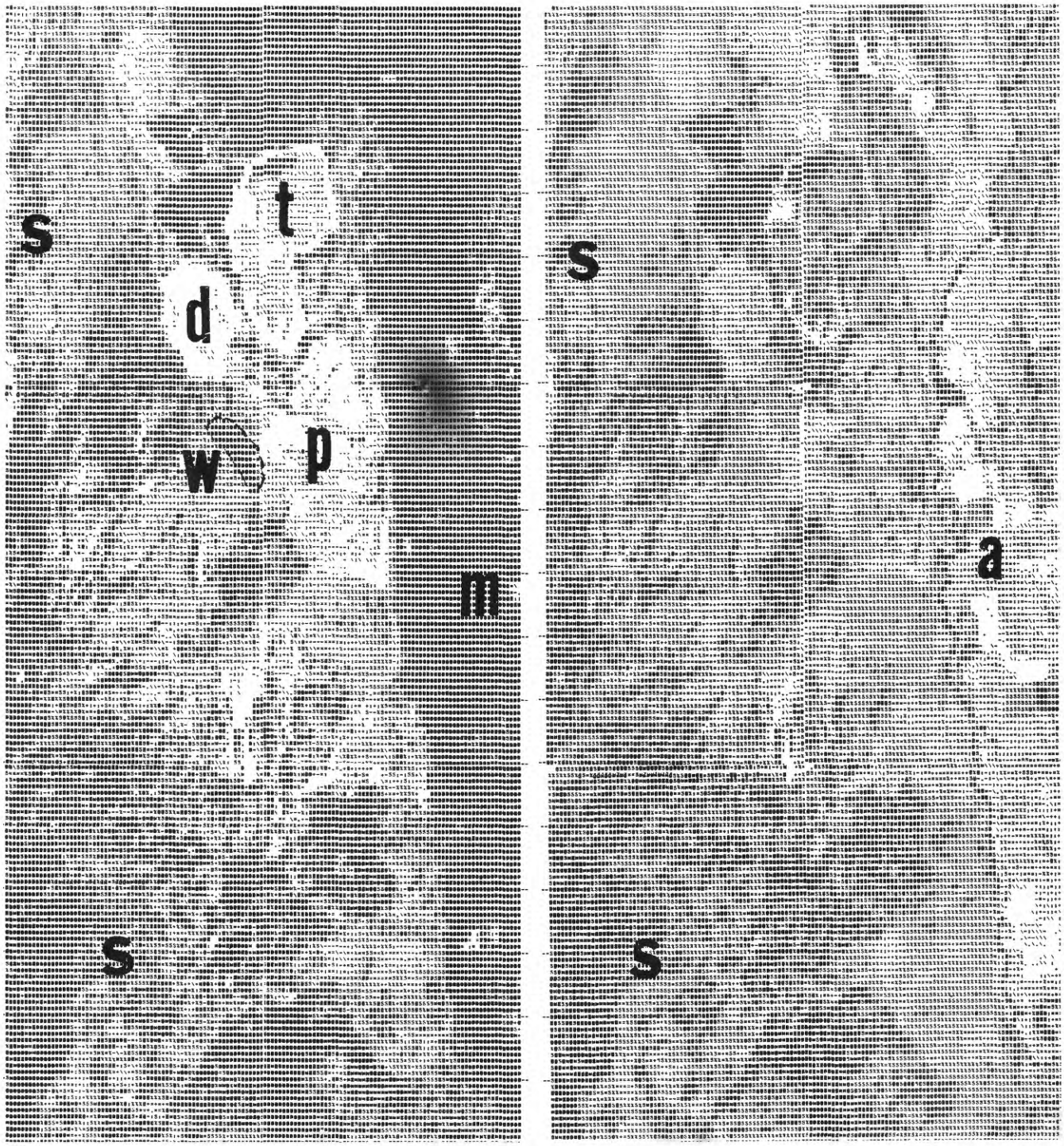

FIGURE 4.—Raw lineprinter output for channels 5 (left) and 7 (right), Yerington pit area, Nevada. t=tailings pond; d=dumps, oxide waste; p=Yerington pit; w=Weed Heights housing area; m=Mason Valley; a=agriculture along the Walker River; S-S=Singatse Range. Reduced about 5 times; approximate scale, 1:24,000.

Each figure represents a (5:1) photoreduction of raw lineprinter output.

Vegetation in the Mason Valley (m) is dark in Channel 5 (left) and lighter in Channel 7 (right), if growing well (as at a) where some field shapes can be seen. The eastern flanks of the Singatse Range occupy the left edge of each image. Weed Heights housing area (w) for the mine is also dark in Channel 5 and light in Channel 7.

The pit area (p), dumps (d) and tailings pond (t) ap-

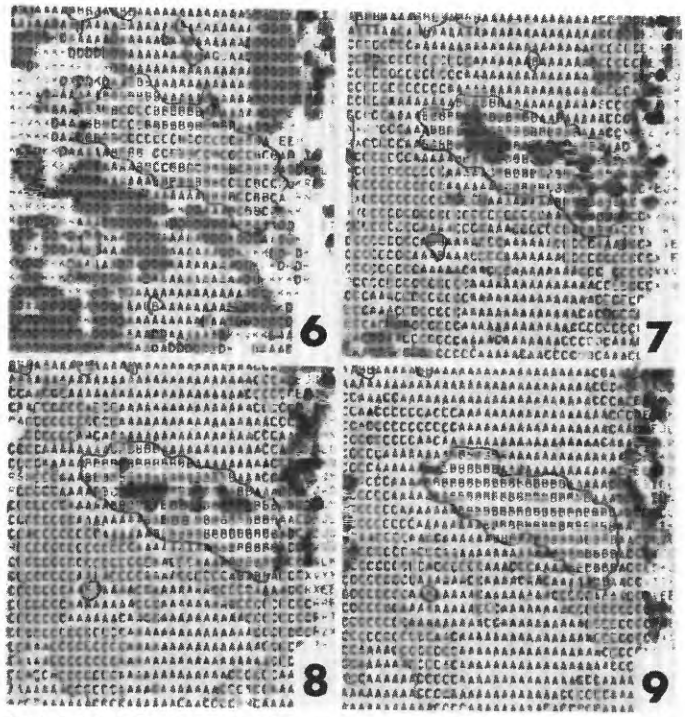

FIGURE 5.—Effect of varying the tolerance level in STANSORT/CLUSTER. Data for the immediate Yerington pit area, showing the decreasing number of classes (letters) of materials as the tolerance is increased, from 6 percent to 9 percent, thereby simplifying the pit classifications. Landsat CCT 1397–18051, smoothed.

pear in varying shades of gray in each channel. Some water (black in Channel 5 and Channel 7) lies at the north (uppermost) end of the tailings pond inside the lighter toned dikes.

This represents the simplest form of Landsat enhancement—stretching and density encoding—and is presented at an original scale of about 1:24,000.

In figure 5, the next step of classification is shown. The clustering algorithm used in STANSORT/CLUSTER (Honey, Prelat, and Lyon, 1974) operates with a gating technique to make a "like/unlike" decision on the four-band spectra of each pixel, commencing at the upper left corner of the matrix and proceeding to the lower right. The gating value is an input variable and may be modified at will by the user, in an interactive mode. Wider tolerances (say 15 percent) allow most spectra to pass into a few classes—tighter tolerance produces many classes. The system uses the 26 alphabetical symbols and then blanks for all above 26. The clustering step is very fast and takes 10–30 s. If the pattern produced on the video screen has too few symbols one closes up the tolerance—if there are too many blanks one opens the tolerance. Up to 20 km^2 may be classified at once.

The key to the method is that the operator decides which pattern best fits his knowledge of the training area he has selected. In the case shown in figure 5, of the area immediately surrounding the Yerington pit, we felt that T (tolerance) = 8 or 9 percent gave the best fit, permitting segregation of class 'B' for oxidized quartz monzonite and 'P' for unoxidized ("sulfide-bearing") quartz monzonite. Class 'A' correlates with the surface dumps, while class 'C' represented the alluvial outwash from the Singatse Range to the west.

With this best-fit decision made, the spectra are "frozen," and can be used to search the rest of the 34,000 km^2 on the tape. Figure 6 shows the subsequent

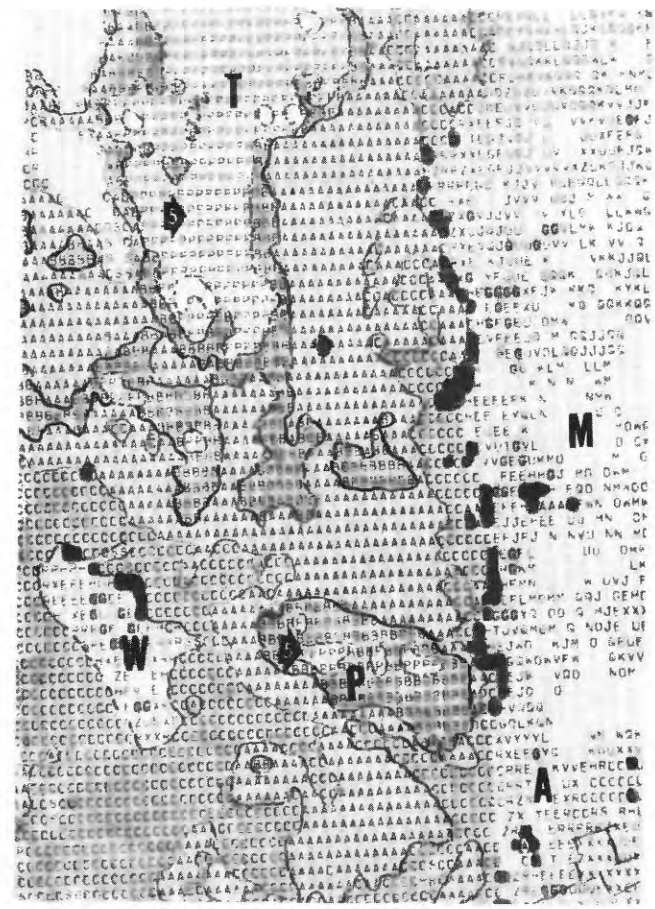

FIGURE 6.—Clustering analysis using STANSORT/SEARCH, tolerance=8 percent after training on the immediate pit area. This map starts at row 1140/col. 707, Landsat CCT 1397–18051, training area was as shown in fig. 5. T=tailings pond; P=pit; W=Weed Heights housing area; M=Mason Valley irrigated land; A=agriculture in the valley along the Walker River. Pit classification symbol "P" appears only in the tailings pond area, with symbol "B" only in the pond dikes and on some of the dumps. Most of the southern dumps have a symbol "A" which matches some of the leach residues.

patterns developed in STANSORT/SEARCH using the frozen spectra in a supervised mode of pattern recognition but retaining the same tolerance (T=8).

The following points are significant:

1. The vegetated areas of Weed Heights housing area (W) and the Mason Valley (M) and (A) are similarly identified.
2. The nonoxidized, sulfide-bearing monzonite (P, also labelled with a #5 arrow only occurs elsewhere in the tailings pond (T)—exactly where one would expect to find it after the copper-flotation step. Only a few other isolated pixels in the entire Singatse Range are so classified and are considered as noise.
3. The oxidized monzonite (B symbol), on the other hand, appears mainly on the dikes around the tailings and in patches between the pond and the pit. Elsewhere in the Singatse Range this symbol occurs principally at the dumps of the Ludwig mine off to the southwest.
4. The "low-oxide copper" and other dump materials (symbol A) occur immediately to the south of the pit, to the north near the leach liquor pond (blank), and on the east flank of the tailings pond.

Thus patterns selected in the pit (training area) can be used to classify and segregate similar materials nearby on the mine property or in the rest of the Singatse Range itself. Potentially the system can search the whole Landsat scene, covering 3.3 million ha (8.2 million acres).

A slightly different technique is shown in figure 7 (p. XXIII). Black and white enhanced images of Channels 5, 6, and 7 of Landsat data over the Yerington-Singatse Range area were combined into a color print using the Dicomed image-forming process. Digital data preprocessed for enhancement were fed sequentially into the Dicomed unit using a blue filter for Channel 5, a green filter for Channel 6, and a red filter for Channel 7. The resulting false color infrared image is shown as figure 7*B* (p. XXIII), which can be directly compared with an aerial color photograph (fig. 7A, p. XXIII) taken from 20 km (65,000 ft) 13 days earlier. A close match geometrically is evident, and the increased contrast more clearly reveals features like roads and desert washes.

To make figure 7*D* (p. XXIII), which is a color ratio print, the ratio channel data were prepared for the Dicomed unit. This time ratio R54 was coded with a blue filter, R64 with a red filter, and R74 with a green filter.

This color ratio print (fig. 7*D*, p. XXIII) differs markedly in information content from the color-infrared print (fig. 7*B*, p. XXIII), although pixel-by-pixel the data locations are the same.

The ratioing "smooths out" the topography, removing the shadowed-side effects, and emphasizing the spectral content of the data. Now irregular patches of color replace the topographic-dominance in figure 7*B* (p. XXIII) and in figure 7A (p. XXIII), too. Careful comparison with the geological map (fig. 7*C*, p. XXIII) (Moore, 1969) reveals that the ratioing has enabled a close correlation of similarly colored areas with the regional geology to be prepared using Landsat digital data alone.

We are planning a much more detailed ground measurement program in this area to relate better the geology with the ratio images, but even the initial results shown here are most significant of the role of Landsat digital processing in regional geology.

GOLDFIELD, SOUTHWEST-CENTRAL NEVADA

The old mining camp of Goldfield had its heyday around 1906 but is now becoming something of a celebrity again as a test site for Landsat analysis techniques (Rowan and others, 1974; Goetz and others, 1975; Lizaur, 1975; Ballew, 1975b). These several efforts are based upon the painstaking studies of Roger Ashley who mapped the 45 km^2 (17 mi^2) area in the 1968–1971 period under the U.S. Geological Survey's Heavy Metal Program. Ashley's geological maps (Ashley, 1971, 1974) and especially the map of the argillic alteration, which is so pervasive at Goldfield, form the ground calibration data for most of the studies. Figure 8*A* shows the typical low vegetative cover of the desert area.

Figure 9 compares three map products to emphasize their similarities. Figure 9*A* is taken from Ashley's caldera study (Ashley, 1974) and shows the premineralization structural pattern with the dominant ring fracture systems, central fractures (northeast in the northern half and swinging to southeast in the southern half of the caldera), and the tangential "taillike" fracturing extending out to the east-southeast. The premineralization intrusive centers (hatchured) are strongly clustered on the inferred ring-fault system.

Figure 9*B* is an outline map (from Ashley, 1971) of the same area at about the same scale but, with the outcrop zone of the argillic alteration in the volcanics, shaded a darker tone. This bull's-eye and tail pattern is the key to the search for ore mineralization at Goldfield, showing a strong structural control for both the alteration and mineralization stages.

The same spatial pattern (of the argillic alteration zones) can be defined directly from the Landsat digital

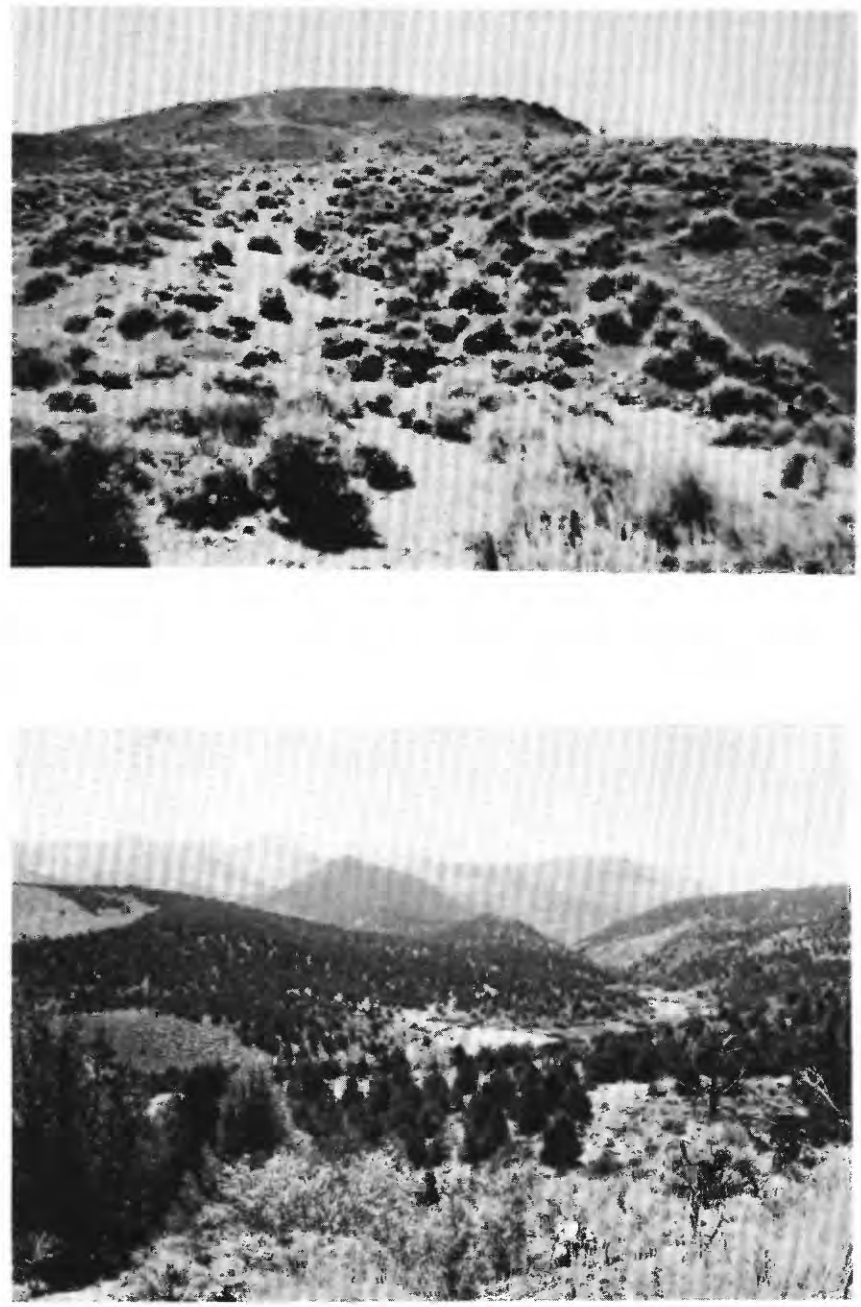

A

B

FIGURE 8.—Comparison of vegetation covers. 8*A*; Goldfield, Nevada, with sagebrush. 8*B*; Pine Nut Mountains, Nevada, with piñon pine and juniper, and some sagebrush in the foreground. This area is closer to the Sierras and has a higher rainfall, although still a semidesert.

data, by ratioing Channel 5/Channel 4, as prepared from CCT 1342–18003 (June 30, 1973, fig. 9C). This ratio (R54) may be used to emphasize iron-oxide-rich areas which show high ratios with these bands. White areas in the caldera ring and east-southeast tail have ratios above 1.20 whereas darker areas, and the Malpais basalt to the southwest, have values around 0.90–0 95 (tables 2, 3, 4, and 5).

Similar comparisons for other ratios (although not so striking) can be found in the ground-measured Goldfield data, shown in table 4A—Altered samples, and 4B—Unaltered samples.

The ratio image (R54, fig. 9C) used to emphasize iron-rich areas, shows the ring fracture (and east-southeast tail) features clearly (inside the solid black arrows), although on this image the central bull's-eye pattern is very subtle. The white patch to the northeast shows the argillic alteration and gossans of the North Diamondfield district, outside the main structure, again indicating how a pattern developed for one

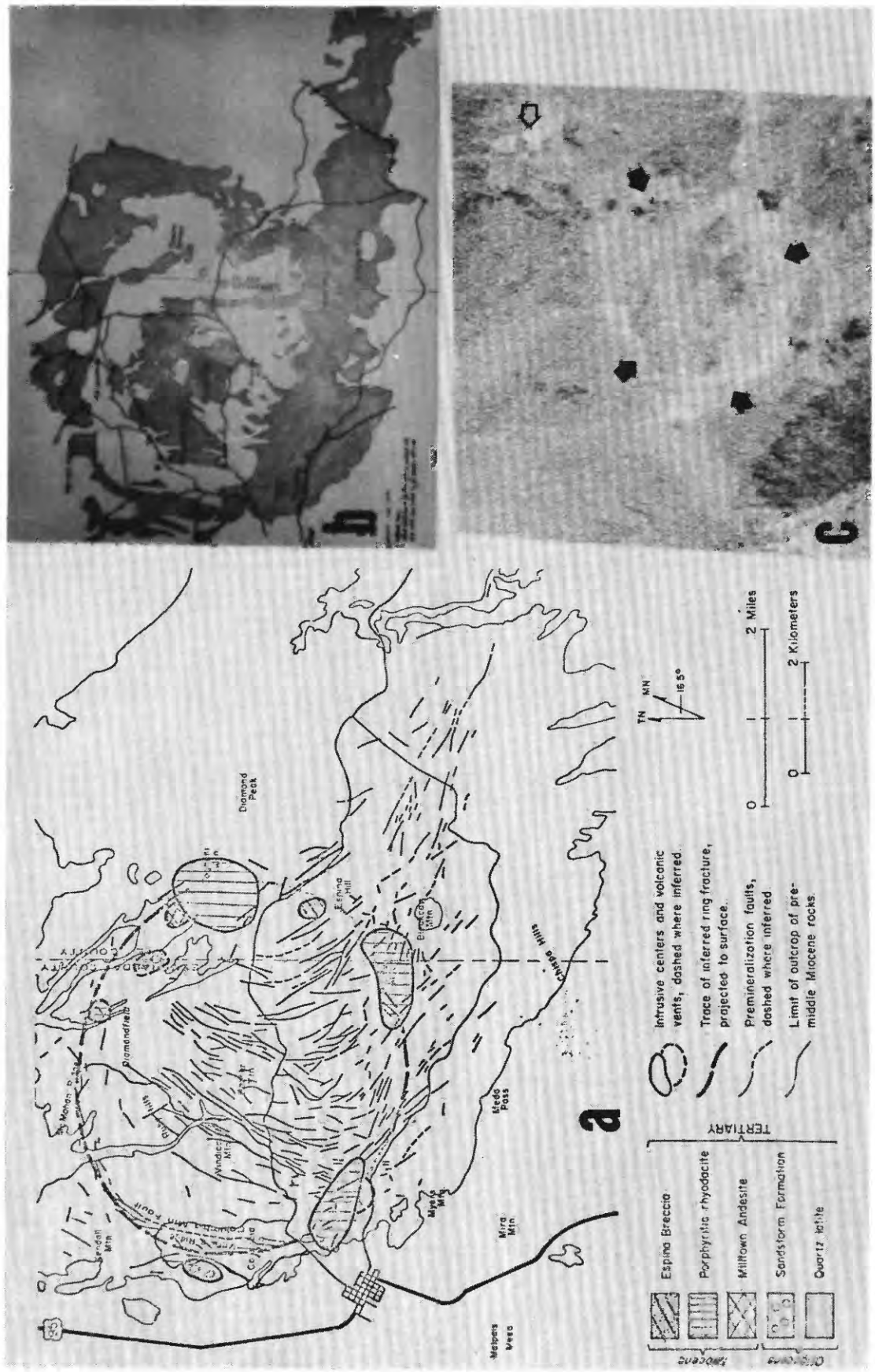

FIGURE 9.—Relation between the regional structure (a), alteration zones (b), and the Landsat R54 ratio image (c) for Goldfield, Nevada (Map a after Ashley, 1974; b after Ashley, 1971). Arrows on c indicate the ring of alteration around the caldera fracture zone. Open arrow in c indicates an alteration area to the northeast of Diamondfield, which is of interest. Landsat CCT 1342–18003, June 30, 1973, was used to make the R54 image, beginning in upper left at row 619/col. 2115.

TABLE 2.—*Typical ratio R54 values for Goldfield (after Lizaur, 1975)*

LANDSAT-derived data (1342–18003, June 30, 1973)	*Ratio*
Iron-oxide-rich areas	Above 1.20
Malpais basalt	0.90–0.95
FIELD-measurement data	
Iron oxide gossan soils	1.60±0.20
Montmorillonite soils (average)	1.22±0.13
Montmorillonite soils (selected)	1.30±0.04
Kaolinite soils (average)	1.22±0.16
Kaolinite soils (selected)	1.17±0.08
Most altered rocks (average)	1.30±0.17
Unaltered rocks (average)	1.10±0.11

TABLE 3.—*Ratio comparisons for Goldfield, Nevada (after Lizaur, 1975)*

	R54 Landsat	*R54 Ground*
Unaltered rock		
Malpais basalt	Below 0.92	Not measured
Milltown andesite	----do	1.00–1.20
Background		
Gray volcanics	1.00–1.11	1.10–1.19
Altered (targets)		
Traverse areas	Above 1.19	1.18–1.42
Gossan soils		1.48–1.74

locality can be used to locate other similar areas elsewhere.

A large map of R54 values was made by Lizaur (1975), and several background areas were selected along access roads to establish the character of these areas as seen from Landsat. Tables 2, 3, and 4 have been calculated from his field measurements over areas shown to be anomalous by R54 ratio maps prepared from Landsat data (CCT 1342–18003, June 30, 1973) and have been segregated by him to be field checked. In three traverses in sec. 4 he crossed a typical quartz-alunite (silicified) ridge, locally called a "ledge." These are usually gold ore bearing and surrounded by a kaolinite-rich selvage (15–20 m wide), grading outwards into a montmorillonite zone more than 100 m wide. Table 5 lists published data for several alteration minerals.

Of the altered rocks seen in these traverses and at localities in secs. 21, 22, the gossan soils clearly were anomalously high in R74, R65, and R64 as well as R54, although these rocks differed from the unaltered or background samples in almost every ratio.

MODERATE COVER

Geobotanical anomalies which have been carefully studied and described in the literature may be used as test targets to establish the credibility of Landsat detectability (for example, Billings, 1950). We have worked with two such areas ("copper-barrens") in Norway as well as with a mapped bio-geochemical anomaly (high molybdenum values in the leaves of vegetation) in western Nevada. Our aim was to define the correlation between (1) the anomalously high metal content in the soils, which affects the types and species-proportions of the vegetation populations near such metal deposits, (2) their reflectance characteristics as measured with Landsat bandpass equipment on the ground, and (3) the Landsat satellite data taken over the same areas. The two areas differ, as the Pine Nut Mountains area in western Nevada has a moderate cover (about 16 trees/ha) whereas the Karasjok locality in northern Norway has a total cover of birch forest or grass.

A third type of area, at Tifalmin, central western New Guinea, also with a total cover (jungle trees and grasses) did not show any evidence in the vegetation, as seen by Landsat, which would enable the detection of the copper mineralization known in the rocks and soils beneath the cover (Press and Norman, 1972).

PINE NUT MOUNTAINS, CENTRAL-WEST NEVADA

Being closer than Goldfield to the Sierra Nevada mountains of California which lie 30 km to the west, the Pine Nut Mountains enjoy a higher moisture content (mainly snowfall, about 20–25 cm/yr). The hills lie between 2,100–2,300 m in elevation and are covered with evenly mixed piñon pine (*Pinus monophylla*) and juniper (*Juniperus utahensis*), at about 16/ha (40/acre). The area between these trees is predominantly sagebrush, 1–1.5 m in height, with some rabbitbrush (*Chrysothamnus* sp.) (fig. 8*B*).

The bio-geochemical anomaly which patchily covers about 1–2 km² on the eastern flank of a low ridge of intermediate volcanics and limestones has been described in detail (Lyon, 1976). The anomaly takes the form of anomalously high (from 75–500 ppm) molybdenum levels in the ash of juniper and pine needles extending down slope from a molybdenum-bearing skarn mineralized zone in the rocks surrounding a small quartz monzonite intrusive (see stippled area, fig. 10) (De Long, 1971; Noble, 1962).

A 3–5 times larger anomalous area, covering about 4.5 km² and located centrally over the bio-geochemical anomaly, was independently found directly from the Landsat digital data, without prior knowledge of the specific location of the molybdenum-bearing vegetation pattern (Lyon and Honey, 1974). The STANSORT interactive computer program was used to identify the

TABLE 4A.—*Means and interband ratios for some altered rocks, Goldfield, Nevada*
(Data recalculated from Lizaur, 1975, using BMDO7M programs)

Group	N	Ch 4 [1]	5	6	7	RNX	RNY	R76	75	75	65	64	54
Altered samples (N=98); Traverses I, II & III (87% altered rocks)													
1. Montmorillonite zone	62	188	229	286	252	329	406	88	111	134	126	152	122
		[2](.23)	(.24)	(.24)	(.24)	(.07)	(.05)	(.10)	(.11)	(.13)	(.14)	(.12)	(.11)
Selected area	3	263	342	392	377	319	418	94	108	140	114	149	130
		(.09)	(.06)	(.06)	(.11)	(.03)	(.02)	(.08)	(.08)	(.08)	(.08)	(.10)	(.03)
2. Kaolinite zone	20	245	299	358	326	343	394	91	111	135	121	147	122
		(.18)	(.20)	(.14)	(.17)	(.06)	(.05)	(.13)	(.17)	(.17)	(.11)	(.11)	(.13)
Selected area	3	318	372	465	414	376	402	89	111	129	124	145	117
		(.11)	(.12)	(.17)	(.15)	(.15)	(.03)	(.03)	(.05)	(.05)	(.05)	(.08)	(.07)
3. Silicified zone	6	375	471	529	522	344	394	99	114	140	115	141	125
		(.18)	(.26)	(.20)	(.17)	(.10)	(.08)	(.07)	(.16)	(.12)	(.21)	(.16)	(.18)
4. Gossan soil in volcanics	4	123	196	296	247	273	424	83	126	204	151	243	160
		(.19)	(.20)	(.21)	(.18)	(.12)	(.02)	(.07)	(.07)	(.19)	(.08)	(.18)	(.13)
Group means, Altered rocks	98	252	318	388	356	331	406	91	113	147	125	163	129
		(.36)	(.31)	(.25)	(.29)	(.10)	(.03)	(.06)	(.06)	(.19)	(.11)	(.24)	(.12)

[1](Ch4–Ch7, times 10; rest, times 100).
[2]Coefficient of variability (COV)=σ/x; NX=Ch4/(Ch4+5+7); NY=Ch5/(Ch4+5+7); NX+NY+NZ=1.00.

TABLE 4B.—*Means and interband ratios for some unaltered rocks, Goldfield, Nevada*

Group	N	Ch 4	5	6	7	RNX	RNY	R76	75	74	65	64	54
Unaltered samples (N=15), excluding Milltown andesite, all picked by their R54 ratios as being background													
1. Milltown andesite ------	7	132	144	174	160	359	391	88	110	120	123	135	110
		(.27)	(.24)	(.26)	(.29)	(.02)	(.07)	(.09)	(.17)	(.06)	(.09)	(.05)	(.10)
2. Vindicator rhyolite ------	3	172	187	231	210	355	391	90	111	122	**122**	134	110
		(.19)	(.11)	(.24)	(.24)	(.05)	(.06)	(.02)	(.14)	(.10)	(.14)	(.08)	(.10)
3. Gray volcanics ---------	2	171	197	232	206	352	404	89	103	120	116	134	**115**
		(.17)	(.15)	(.27)	(.23)	(.01)	(.03)	(.04)	(.08)	(.06)	(.12)	(.10)	(.02)
4. Gray volcanics ---------	3	223	269	337	306	337	406	90	114	137	125	151	120
		(.02)	(.10)	(.04)	(.03)	(.04)	(.04)	(.03)	(.07)	(.01)	(.08)	(.02)	(.08)
Group means, Unaltered rocks ------	15	175	199	244	221	351	398	89	110	125	122	138	114
		(.21)	(.26)	(.26)	(.28)	(.03)	(.02)	(.01)	(.04)	(.07)	(.03)	(.06)	(.04)
Group means, Altered rocks --------	**98**	252	318	388	356	331	406	91	113	147	125	163	129
		(.36)	(.31)	(.25)	(.29)	(.10)	(.03)	(.06)	(.06)	(.19)	(.11)	(.24)	(.12)
Total, all samples -------	113	221	271	330	302	333	402	89	112	137	125	153	123
		(.37)	(.37)	(.33)	(.37)	(.08)	(.05)	(.10)	(.13)	(.16)	(.13)	(.21)	(.12)

TABLE 5.—*Published ratio values for some alteration minerals*

Alteration mineral	Reflectance %				x100					
	Ch4	5	6	7	R76	75	74	65	64	54
Montmorillonite	33	50	60	56	93	112	170	120	182	154
Kaolinite	67	72	73	72	99	100	107	101	109	107
Alunite	43	61	71	71	100	116	165	116	165	142
Hematitic limonite*	18	38	44	46	105	121	256	116	244	214
Goethitic limonite	5	9	12	12	100	133	240	133	240	180
Jarosite	7	10	10	7	74	74	108	100	146	146

Digitized from Rowan and others (1974, fig. 20) from data originally in several papers.
*=samples in place.

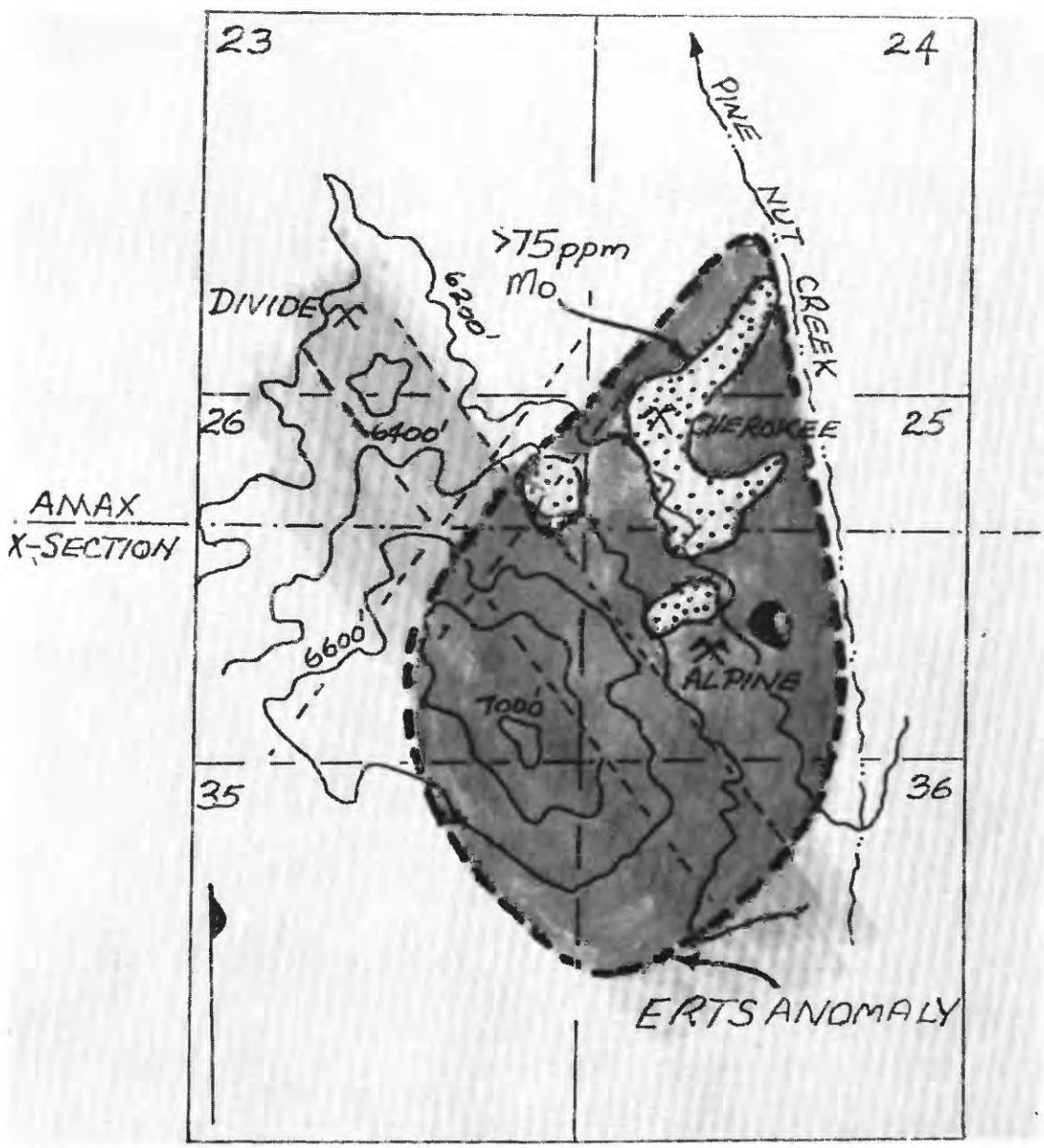

FIGURE 10.—Locality map of Landsat-detected anomaly and the Mo-anomaly in the vegetation. Sections are in T. 12 N., R. 21 E., Mt. Siegel quad, Nevada. NW-trending linears are limestone outcrops; NE-trending linears are strongly developed joints (?faults). Quartz monzonite outcrop is in solid black near the Alpine mine mill. Stippled anomaly area is 75 ppm Mo in the juniper needle ash. Landsat anomaly is outlined in heavy dashes. Divide and Cherokee mines are also shown.

features and ratio images (especially R74) mode which showed the shape and location of the anomaly.

We have performed a considerable amount of ground measurements in the field in the area, both with cut branches and with trees in place, to attempt a correlation with tree reflectance and Landsat-derived ratios. The ground data show higher ratios for vegetation inside the anomaly relative to similar trees outside the area (0.5–1 km away). These higher values are offset, however, by a lowered tree spacing per hectare inside the anomalous area (12–14/ha inside versus 16–20/ha outside). The specific percentages of trees versus sagebrush and soils has not been determined, but clearly increased sagebrush or soil coverages, with R74 ratios of 150–180 (instead of 400–500 as with the trees), would lead to a darker area on a ratio image, comparable to that which we found in the Landsat data (Lyon, 1976).

FULL COVER

KARASJOK, NORTHERN NORWAY

A locality in northern Norway in heavily birch covered glacial till areas, contains several copper sulfide bearing strata in the Karasjok group of hornblende schists (fig. 11*B*). These "copper layers" in turn produce copper-rich, ground-water springs which poison the birch trees where the springs issue beneath the till cover (Lag and Bolviken, 1974). This well-documented, poisoned area covering approximately 100 m in width by 1 km in length was successfully located on Landsat image 1365–09430, shown in figures 11*A* (Channel 5, red) and 11*C* (Channel 6, infrared). The locality is circled on the 1:250,000-scale geological map (fig. 11*B*) cut from the larger Karasjok sheet prepared by the Norwegian Geological Survey.

Channel 5 data (fig. 11*A*) show a pronounced light-gray banding to the north and east of the letter "A," which closely approximates the S-curved stratigraphic strike of the granodiorite/metasediment boundary (gd/m). Bright white patches on the inner side of the river curves are low-lying river gravels, with a sparse tree cover, but having a heavy coverage of reindeer moss, a white lichen form.

Channel 6 data (fig. 11*C*), however, show principally the patterns of vegetation and much less information on the stratigraphy. Strong ENE and SSW fracturing is brought out by thin bright lines along the drainage. Several portions of the river towards the top of the image also show the east-northeast trend.

The anomaly of Lag and Bolviken lies inside the open arrows, in figures 11*D* and *E*, and inside the open circle in figure 11*B*. Insets 11*D* and *E* are enlargements. The ground location for this was defined for us on aerial photographs at about 1:16,000 scale and referenced to topographic maps at 1:50,000 scale. Our role was to see if the patterns observed on the ground, and in large-scale airphotos, could be seen in the Landsat-imaged data. In this we were very successful. The anomaly is more clear on figure 11*E*.

Ground measurements taken in the summer of 1975 are being interpreted and will be presented in a paper submitted to the International Geological Congress, Sydney, Australia (Bolviken and others, 1976).

TIFALMIN, CENTRAL WEST NEW GUINEA

Landsat–1 multispectral scanner (MSS) data in CCT format were acquired for scene 1028–00134 which covers an area in Papua, New Guinea, containing a number of porphyry prospects. Only two of these, however, Kennecott's Tifalmin prospect and Carpenteria Exploration's Freida prospect, were sufficiently free of cloud cover during data acquisition to provide adequate data for remote-sensing investigations. Work to date has been confined to the Tifalmin prospect, since basic ground-acquired geological and geochemical data, though limited, are available for that site only (Bamford, 1974).

Data manipulations were carried out using the STANSORT computer program. Specific output generated in the current study was Channels 4, 5, 6, and 7 shadeprints; R47, R45, and R75 reflectance ratio prints (with minimum values of ratios subtracted and step intervals selected to maximize print contrast in areas of interest); and cluster analysis prints (Channels 4, 5, 6, and 7 data clustered using a ± 14 percent tolerance). A complete set of these data was derived for each of two centers of copper mineralization, the Olgal-Futik and Unfin areas of the Tifalmin prospect. A single line-print page (approximately 1:20,000 scale and covering an area about 3.8 by 5.4 km) provided adequate coverage of each mineralized area and adjacent surroundings to facilitate definition of reflectance anomalies (if any) within that area (fig. 12). All shadeprints and ratio prints in this study were color coded to aid interpretation using brown to yellow colors of graduated density. Dark colors were used for delineation of higher values. Cluster analyses were coded using progressively darker colors to define progressively smaller (more anomalous) areas.

Figure 12 shows part of data generated for the Olgal-Futik and Unfin mineralized areas. Figures 12*A* and 12*B* are uncolored MSS 7 shadeprints for these areas showing the locations of the mineralized intrusions and principal drainages. Copper geochemistry

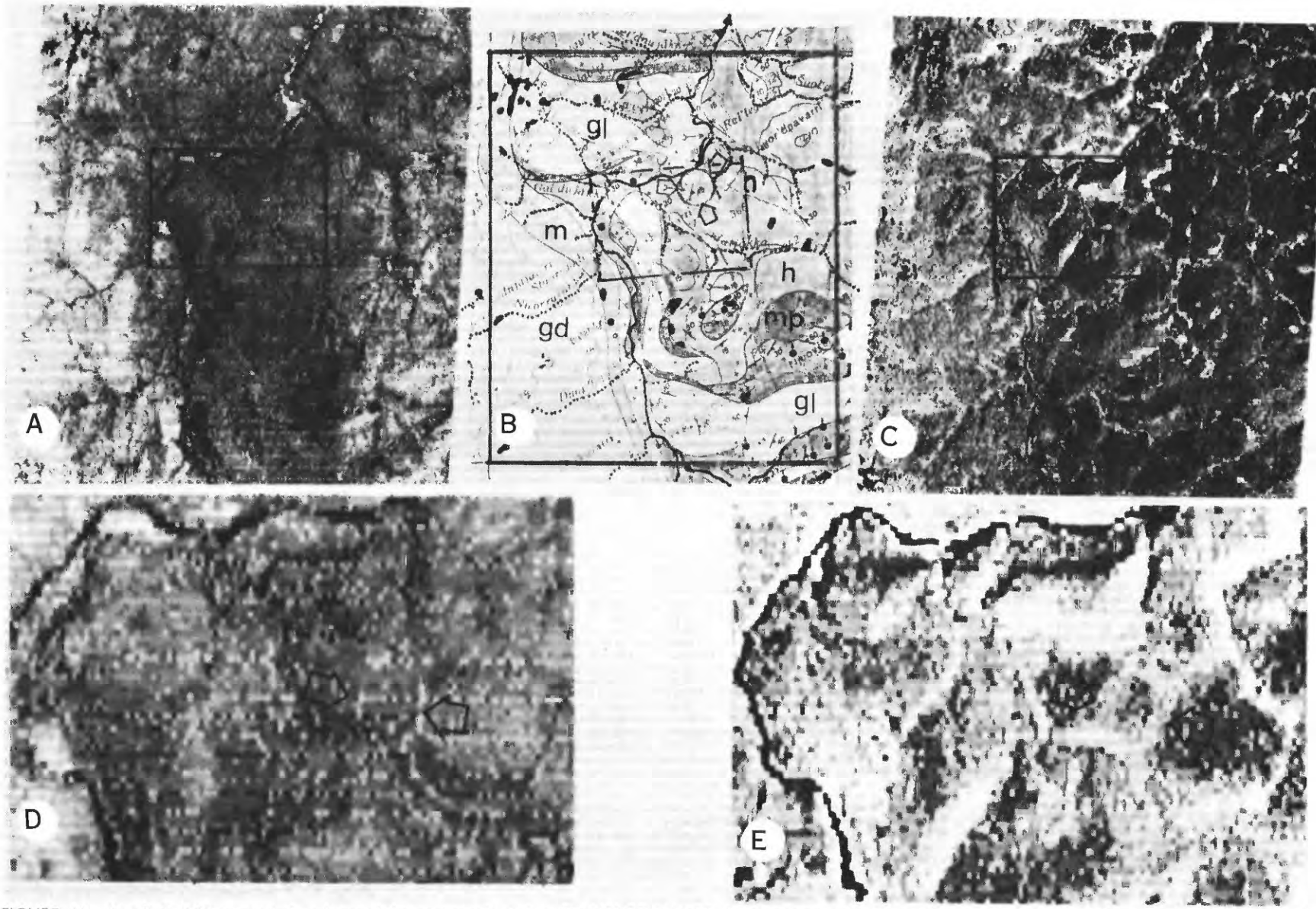

FIGURE 11.—Landsat CCT-generated enhanced images made using STANSORT/IMAGE for Channel 5 (11*A*) and Channel 6 (11C) with 4x enlargements as 11*D* and 11*E* respectively, compared with the geological map (11*B*). Notice that Ch 5 shows the closest correlation with the sweeping structural patterns of the geological map, but that the anomaly pattern is best shown in Ch 6 data. The Ch 6 pattern of the anomaly is that of a gray oval 10–12 pixels high, between the two open arrows. The Ch 5 pattern is a single "vertical" line of pixels near the point of the eastern arrow, which crosses the noisy raster lines at a high angle.

Geologic map is modified from the Norwegian Geological Survey Geological Map, Karasjok sheet; scale as shown here is 1:250,000.

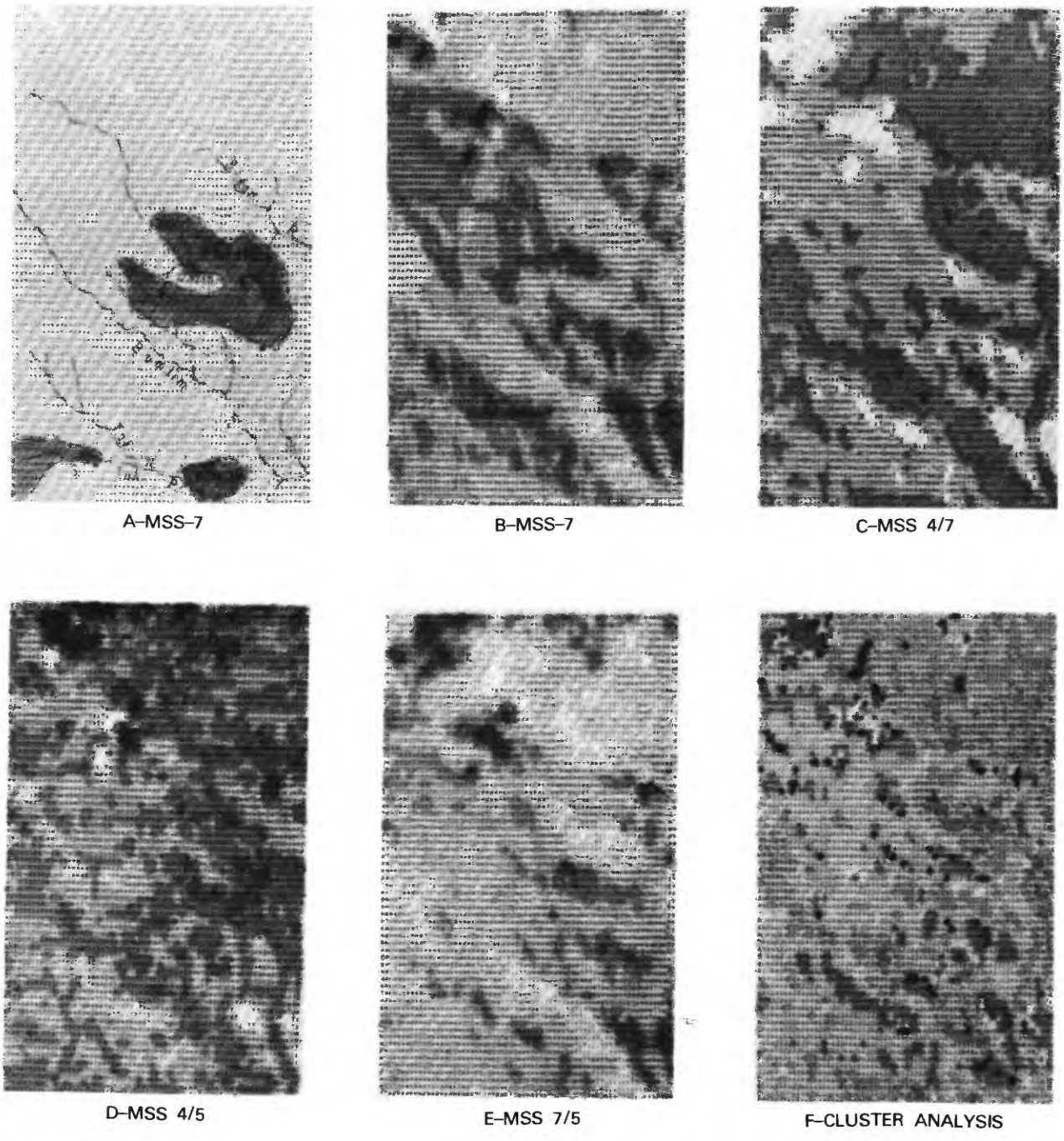

FIGURE 12.—Examples of Landsat CCT-generated lineprinter images, compared with the only geological map available (12*A*), for the Unfin area, Tifalmin prospect, New Guinea. The map shows the approximate location of mineralized intrusives (cross hatched) and the principal drainages. Figure 12*B* is an uncolored Channel 7 shadeprint, 12C a R47 ratio print, 12*D* a R45 ratio print, 12*E* a R75 ratio print, and 12*F* a normalized cluster analysis. All prints cover the same geographic area.

over the mineralized intrusions commonly averages 1,000 to 2,000 ppm in creek outcrop, rock chip samples, and about 500 ppm in ridgetop soil and rock samples which are frequently oxidized and leached. Systematic geochemical grid sampling, however, has not been completed for these areas.

The MSS raw data shadeprints, band ratio prints, and cluster analyses for the Olgal-Futik and Unfin

areas do not appear to provide evidence of correlation between reflectance and known mineralized areas.

Explanations for the lack of detection of reflectance "anomalies" include the possibilities that: (a) reflectance modifications may have taken place as suggested by previous work (Press and Norman, 1972) but are of insufficient magnitude to be resolved in Landsat–1 MSS data and (b) vegetation assemblage over the mineralized area may have adapted to the base metal-anomalous soils by survival of tolerant species only and thus may not be significantly more stressed than surrounding vegetation. Work to test these tentative explanations is desirable but not practical at present due to the remoteness of the test locality. It should also be noted that atmospheric corrections have not yet been made, hence reflectance calculations have not been attempted. Such refined data could possibly reveal reflectance anomalies not resolved by the raw data. Lack of information on areas of zero reflectance or other calibrated reflectances precluded determination of an atmospheric correction factor.

EFFECT OF VEGETATION ON INTERBAND CORRELATIONS AND RATIOS

In tables 6 and 7 various reflectances and interband ratios for 575 ground-measured spectra of four main data sets (A = Goldfield, B = 3 Spanish sites, C = Pine Nut (horizontal), and D = Norway) are compared with their cross correlations (table 6) and their individual variabilities, expressed as coefficient of variability (COV) = σ/x. The progression A–D represents increasing numbers of vegetation spectra in each total set, either as pure vegetation-only spectra (Pine Nut) or increasing leaf-cover in the field of view (Norway). Each locality is mineralized, and they form typical exploration targets. All sets contain some soils and rock spectra. Table 6 shows two partial sets of the 144 cross-correlations calculated—those of band correlations (Channels 4, 5, 6, and 7) are those of the interband ratios (R76, 75, 74, 65, 64, and 54). Solid contours serve to emphasize the higher positive value, dashed lines enclose the higher negative sets.

TABLE 6.—*Correlation between variables in data sets with increasing vegetation content*

[COV values derived using BMD02D program. Solid lines enclose higher positive values; dashed lines enclose higher negative values.]

A. GOLDFIELD (0% vegetation in set; N=113)

Ch 5	6	7	
83	80	77	4
	77	77	5
		87	6

R75	74	65	64	54	
34	30	—42	—30	06	R76
	58	70	36	—26	75
		34	81	62	74
			60	—28	65
				59	64

B. SPANISH TEST SITES (3) (29% vegetation in set; N=229)

Ch 5	6	7	
96	83	77	4
	86	78	5
		98	6

R75	74	65	64	54	
62	55	49	36	—48	R76
	95	98	90	—37	75
		94	97	—11	74
			93	—33	65
				—01	64

C. PINE NUTS (83% vegetation in set; N=151)

Ch 5	6	7	
99	91	74	4
	88	70	5
		94	6

R75	74	65	64	54	
86	88	82	84	—53	R76
	98	99	98	—66	75
		97	99	—54	74
			98	—69	65
				—55	64

D. NORWAY (85–90% vegetation in set; N=82)

Ch 5	6	7	
97	87	85	4
	83	82	5
		99	6

R75	74	65	64	54	
09	37	—17	03	26	R76
	70	96	72	—38	75
		59	93	28	74
			70	—44	65
				21	64

TABLE 7.—*Means and variability in data sets with increasing vegetation content*

	Set A Goldfield	Set B Spanish sites (3)	Set C Pine Nuts (horiz)	Set D Norway
Percentage vegetation in set	0%	29%	82%	85–90%
N	113	229	151	81
Ch4	*212(.33)	*120(.70)	96(.88)	54(.31)
Ch5	260(.36)	143(.78)	115(.96)	62(.65)
Ch6	317(.32)	208(.60)	214(.44)	159(.76)
Ch7	285(.34)	240(.59)	283(.36)	212(.76)
NX	335(.08)	307(.17)	237(.23)	267(.17)
NY	403(.05)	344(.20)	253(.30)	264(.15)
R76	900(.10)	115(.13)	137(.12)	134(.12)
R75	111(.13)	204(.65)	368(.45)	350(.35)
R74	136(.16)	226(.57)	408(.41)	413(.30)
R65	124(.13)	171(.55)	258(.38)	261(.36)
R64	152(.17)	191(.47)	287(.34)	306(.28)
R54	123(.13)	115(.19)	113(.10)	122(.30)

*Group mean values; COV in parentheses. (Ch 4–Ch 7, x10; rest, x100); coefficient of variability (COV)=σ/x; if >0.40, data are widely spread. Calculated using BMDO2D output, ungrouped within sets. NX=Ch 4/(Ch 4+R5+R7); NY=Ch5/(Ch4+R5+R7); NX+NY +NZ=1.00. Data sets presumed to be Gaussian populations.

Table 7 lists the group mean values for each of the 12 variables used and shows the variability (COV=σ/x)* in parentheses (where COV is >0.40 the data are widely spread).

Analysis—Table 6: Cross-Correlations

1. *Channel correlations* are high (>0.70) in all four data sets, but increase with vegetation content.
2. Correlations between Channels 6 and 7 are higher with increasing vegetation content.
3. Correlations between Channels 5 and 4 are high even where vegetation is dominant.
4. *Interband correlations* markedly change in value with even a slight increase (29 percent) in vegetation content (see absolute values in table 7), in some cases doubling in value.
5. High (>80 percent) vegetation sets (C and D) show varying correlation patterns, which may mean each relationship is specific for one data set only. This is being investigated.

Analysis—Table 7: Mean (Absolute) Levels of Variables

1. Variability (COV) of the values must be considered for data dispersions, when comparing means. For example, even though mean values for each channel vary sympathetically with increasing vegetation, their COV's are very high.
2. *The normalized color index* (NX, NY, NZ, where NX+NY+NZ=1, NX=Ch 4/(Ch 4+R5+R7), etc., is sensitive to vegetation, being high (330 NX: 400 NY) in altered rock (Set A) and declining to lower values (260 NX: 260 NY) with increasing vegetation. (Vigorous, green plant materials would have values as low as 150:170 respectively, for "pure" fields of view). This index is a version of the International CIE color index used for color standardization in the visible region, adapted by us for use in the near-infrared, e.g., Ch 4+Ch 5+Ch 7 are used (Lyon and others, 1975).
3. Ratios R75, 74, 65 and 64 are vegetation-sensitive (Lyon, 1976) and rapidly change with vegetation content, especially R75 and R74.
4. Ratio R54 usually drops with increasing vegetation, but also rises rapidly with bare exposures of iron-rich soils. The fact that all four sets contain these soils, as well as vegetation, somewhat obscures this effect with these data sets.
5. *Criteria of "usefulness"* (e.g., which variable is the most useful, as in table 7) such as that used successfully by Goetz and others (1975) (a high COV of a set of *group means for a variable)* must also take into account the dispersion of each population from which the means were de-

*The COV values were derived using the BMDO2D (UCLA Biomedical Division) statistical package, which examines all the spectra as a set in an ungrouped mode and differs slightly from the BMDO7M discriminant program, which also develops a correlation matrix, but uses grouped data leading to consistently higher values for σ and for the linear correlation coefficient, r. Data sets were presumed to have normal distributions.

rived. Following their practice, however, one would decide that R74 with the highest COV of 0.46 was the best ratio, although the COV for the R74 mean in Set B-Spanish was 0.57 indicating widely varying data in that total set.

CONCLUSIONS

Digital processing of Landsat data is of great significance to mineral exploration. It may be used to produce enhanced images of mosaics of large areas which by computer manipulation now have better definition or increased contrast which will aid the interpretational analyses of photogeologists.

Of much greater import is the fact that Landsat is a four-band set of radiometers which in addition to producing imagery also produce quantified and calibrated measurements of any terrain in the world. As the data are readily available on digital tape, any number of algorithms may be used to remove atmospheric scattering effects or stretch densities (both to increase contrast and, hence, interpretability) or to prepare computational products like ratios. Statistics may be calculated and search programs (like STANSORT) written to automatically locate comparable reflectances elsewhere.

At Stanford our approach to the mineral exploration applications has been concentrated in high resolution studies of small 1–100 km^2 areas testing the ultimate limits of the Landsat system because this scale of representation (1:24,000) and areal size is that most often of use in exploration.

Vegetation must become a part of mineral exploration/Landsat studies. Very few areas of interest are devoid of vegetated cover and that cover must be considered in defining the "average Landsat spectrum" of any 1 pixel area (0.4 ha). The principal problem facing us at this stage of the studies is sampling, or how we can integrate enough terrain in our "ground" measurements to be equivalent to the Landsat pixel size. Clearly the next step involves helicopter-sampling.

A second real problem is that no one technique works all the time and a group of approaches must be used. Landsat with its four-quantified channels materially broadens the usual data base available to the explorationist used to working with black and white film.

As a corollary to this, an interactive, video-display system, "driven" by the geologist who is personally familiar with the area and problem is essential to extracting the most from the Landsat system. For a while we called our program H–ERTS, because it put the geologist in the "driver's" seat. Man-machine interactions are essential in Landsat analysis, preferably the man should be the field geologist himself.

SELECTED REFERENCES

Ashley, R. P., 1971, Preliminary geological map of the Goldfield mining district, Nevada: U.S. Geol. Survey Open-File Map.

———1974, Goldfield mining districts: Nevada Bur. Mines and Geology Rept. 19, p. 49–66.

Ballew, G. I., 1975, A method for converting LANDSAT–1 MSS data to reflectance by means of ground calibration sites: Stanford Remote Sensing Lab. Tech. Rept. 75–5, p. 90.

———1976, Correlation of LANDSAT–1 multispectral data with surface geochemistry, *in* Internat. Symposium on Remote Sensing of Environment, 10th, Ann Arbor, Mich. 1975, Proc. (in press).

Bamford, R. W., 1974, Band reflectance ratio maps from ERTS–1 data over two copper prospects in New Guinea: Stanford Remote Sensing Lab. Tech. Rept. 74–13, 4 p.

Billings, W. D., 1950, Vegetation and plant growth as affected by chemically altered rocks in the western Great Basin: Ecology, v. 31, no. 1, p. 62–74.

Bolviken, B., Honey, F. R. Levine, S. L., Lyon, R. J. P., and Prelat, A., 1976, Detection of naturally heavy-metal poisoned areas by LANDSAT–1 digital data (abs.): Internat. Geol. Congress, 6th, Sydney, Australia 1976, Proc. sec. 10 B (geochemistry).

Draeger, W. C., and Lauer, D. T., 1967, Present and future forestry applications of remote sensing from space: Am. Inst. Aeronautics Astronautics, 4th Mtg., Anaheim 1967, Paper 67–765.

Goetz, A. F. H., Billingsley, F. C., Gillespie, A. R., Squires, R. L., Shoemaker, E. M., Lucchitta, I., and Elston, D. P., 1975, Application of ERTS images and image processing to regional geologic problems and geologic mapping in northern Arizona: Pasadena, Calif. Inst. Tech. Jet Propulsion Lab., Tech. Rept. 32–1597, p. 1–188.

Honey, F. R., Prelat, A., and Lyon, R. J. P., 1974, STANSORT: Stanford Remote Sensing Laboratory Pattern Recognition and Classification System, *in* Internat. Symposium on Remote Sensing of Environment, 9th, Ann Arbor, Mich., 1974, Proc., p. 857–905.

Howard, J. A., Watson, R. D., and Hessin, T. D., 1971, Spectral reflectance properties of Pinus Ponderosa in relation to copper content of the soil—Malachite mine, Jefferson County, Colorado, *in* Symposium on Remote Sensing of Environment, 7th, Ann Arbor, Mich. 1971, Proc., p. 285–296.

Lag, J., and Bolviken, B., 1974, Some naturally heavy-metal poisoned areas of interest in prospecting, soil geochemistry, and geomedicine: Norges Geol. Unders., v. 304, p. 73–96.

Levine, S., 1976, Correlation of ERTS spectra with rock/soil types in California grassland areas, *in* Internat. Symposium on Remote Sensing of Environment, 10th, Ann Arbor, Mich. 1975, Proc. (in press).

Lizaur, P., 1975, Study of the alteration zone around Goldfield mining district by means of ERTS satellite multispectral scanner data: Stanford Remote Sensing Lab. Tech. Rept. 75–3, p. 284.

Lyon, R. J. P., 1975, A comparison of observed and model-predicted atmosphere perturbations on target radiances measures by ERTS, *in* Inst. Electrical and Electronics Eng. Symposium on Application Remote Sensing Digital Imagery to Mineral and Petroleum Exploration, Houston, Tex. 1975, Proc., 6 p.

——— 1976, Correlation between ground metal analysis, vegetation reflectance, and ERTS brightness over a molybdenum skarn deposit Pine Nut Mountains, western Nevada, *in* Internat. Symposium on Remote Sensing of Environment, 10th, Ann Arbor, Mich. 1975, Proc. (in press).

Lyon, R. J. P., and Honey, F. R., 1974, Multispectral signatures in relation to ground control signature using a nested sampling approach (abs.): Natl. Tech. Info. Service (NTIS), NASA Earth Resources Survey Prog., Weekly Govt. Abs., E74–10690, p. 132.

Lyon, R. J. P., Honey, F. R., and Ballew, G. I., 1975, Evaluation of ERTS multispectral signatures in relation to ground control signatures using a nested sampling approach: Final Report, NAS 5–21884, June 1975, 600 p. (contains 16 separate reports).

Moore, J. G., 1969, Geological map of Lyon, Douglas and Ormsby Counties, Nevada: Nevada Bur. Mines Bull. 75, pl. 1.

Noble, D. C., 1962, Mesozoic geology of the southern Pine Nut Range, Douglas County, Nevada: Stanford Univ., Ph.D. thesis, 200 p.

Press, N. P., and Norman, J. W., 1972, Detection of ore bodies by remote-sensing the effects of metals on vegetation: Inst. Mining and Metall. Trans., Sec. B, v. 81, p. 166–168.

Rowan, L. C., Wetlaufer, P. H., Goetz, A. F. H., Billingsley, F. C., and Stewart, J. H., 1974, Discrimination of rock types and altered areas in Nevada by the use of ERTS images: U.S. Geol. Survey Prof. Paper 883, 35 p.

Vincent, R. K., 1973, Spectral ratio imaging methods for geological remote sensing from aircraft and satellites, *in* Symposium on Management and Utilization of Remote Sensing Data, Sioux Falls 1973, Proc., p. 377–397.

Whitaker, E. A., 1965, Colors and the meso-structure of the Maria, *in* Ranger VII, pt. II, Experimenter's analyses and interpretations: Pasadena, Jet Propulsion Lab. Tech. Rept. 32–700, p. 29–39.

———1966, The surface on the moon, chap. 3, *in* Hess, W. N., Mensel, D. H., and O'Keefe, J. A., eds., The nature of the lunar surface: Johns Hopkins Press, p. 79–98.

PROCEEDINGS OF
THE FIRST ANNUAL WILLIAM T. PECORA MEMORIAL SYMPOSIUM,
OCTOBER 1975, SIOUX FALLS, SOUTH DAKOTA

Tradeoff Considerations in Utilization of SLAR for Terrain Analysis

By Louis F. Dellwig and Richard K. Moore,
University of Kansas Center for Research, Inc.,
Remote Sensing Laboratory,
Lawrence, Kansas 66045

ABSTRACT

Optimum SLAR system parameters for terrain data extraction have been suggested by previous investigators on the basis of comparison of imagery from several different systems with a wide diversity of parameters. For some determinations this proves satisfactory. However, the determination of any optimum system parameter can best be made only on the basis of utilization of a single system, imagery of which could be generated with multiple polarizations, depression angles, look directions, or frequencies, or which could be manipulated to alter such parameters. Extraction of data from imagery showing a range of variations in such parameters by discipline-oriented interpreters has enabled us to shed some light on the effect of variations in radar system parameters on extraction of geologic, hydrologic, geographic, and botanical data.

INTRODUCTION

Following the imaging of Panama in 1967 by the U.S. Army Corps of Engineers, serious evaluation of side-looking airborne radar (SLAR) as a geologic tool was initiated. Earlier numerous small test sites throughout the United States for the NASA Earth Resources Survey Program resulted in the generation of imagery over a variety of terrains, and, with the general availability of this imagery to the geoscience community, interest in its evaluation and utilization was accelerated. Following the entrance of Aero Service, Grumman Aircraft Corp., and later Motorola Aerial Remote Sensing, Inc., into the commercial field which had been established initially by Westinghouse Aerospace Corp., imagery of several systems became available to the geoscience community and a not unexpected evaluation and comparison of these systems began. Now with the reduction of the lower limit of resolution from 35 to 10 ft (11.6 to 3 m), imagery of additional systems is becoming available to the researcher and will inevitably be competing with better known systems for the "best in show" award.

Recognizing a great diversity of capabilities and limitations, we embarked upon a study under the sponsorship of the Jet Propulsion Laboratory to determine optimum system parameters for a spacecraft radar. At about the same time we initiated A Demonstration and Evaluation of the Utilization of Side Looking Airborne Radar for Military Terrain Analysis for the Engineer Topographic Laboratories. Through the conduct of these two studies and with the availability of imagery not previously available, it had been our hope that we would be able to determine the optimum SLAR system parameters for terrain analysis. But as the projects progressed we became faced with the problem which had faced us on many occasions, optimum SLAR system parameters for what?

To a large degree the requirements for tactical military terrain analysis are those of the civilian segment of the population, only two basic requirements being critical in military terrain analysis: (1) Near or real time data acquisition and (2) target detection and identification. Many civilian uses of airborne monitoring, reconnaissance, or mapping systems also require near real time data and identification of specific or unique features in both urban and rural environments.

The optimum parameters for military or civilian operation is only one of the choices which must be made. Optimum for the geologist who prefers a wide swath width is not optimum for the city planner who wishes

to acquire as much detail as possible in a relatively small urban area. Thus recognizing that optimum for the geologist is not optimum for other geoscientists, rather than define a series of hard and fast parameters such as was done by the National Aeronautics and Space Administration (NASA) in the selection of the Landsat Multispectral Scanner (MSS) bands (and satisfying no one), it seems most reasonable to evaluate variations in parameters and not attempt to define optimum parameters for a single system. With such an approach the reader will essentially have a do-it-yourself kit and can define the parameters (including cost) which best enables him to realize maximum data content for any specified mission.

RESOLUTION

Few parameters have been devoted the attention which has been received by resolution. In an early geologic study (Dellwig and others, 1966), it was stated that there appeared to be some value in the degradation of resolution, but, in a more recent paper by Rydstrom (1970), it was pointed out that high resolution radar imagery contained not only the same but more data than did imagery of lower resolution systems. It is not the authors' intention to resurrect this problem, for sufficient data are not available for either author to pursue the point further. Rather, we would prefer to look at the needs of terrain analysts and evaluate systems on their own merit. We can begin by looking at the Phoenix, Arizona, area as imaged by the AN/APQ–152 (fig. 1A) and the AN/APS–94D (fig. 1B). There is an obvious strong contrast in resolution, but there are also other perhaps not so obvious contrasts. Both images show full swath width. For the urban planner there is an obvious advantage in the utilization of the AN/APQ–152, but for the geologist who is concerned with tracing major linear patterns or in conducting reconnaissance studies in heretofore uncharted areas, the wide swath width of the AN/APS–94D (which cannot be obtained with the AN/APQ–152) provides a more desirable format and presents him with adequate data for mapping purposes. On the coarser resolution image no difficulties are encountered in defining the urban areas and adjacent field patterns nor in the separation of industrial from residential areas. In general, swath width cannot be increased without suffering some degradation of resolution, and thus the user must consider the relative values of fine resolution and wide swath width.

In considering resolution, one must look at both spatial resolution, which we normally consider, and gray-scale resolution, which is seldom considered in photography because it is usually good, but is always important for radar. The problem is that a radar image produced with the best possible synthetic-aperture resolution has an extremely speckled appearance. This comes about because of the same phase-interference phenomenon that causes radio signals to fade, and that is particularly evident in nighttime standard-broadcast signals and in FM signals received in a car. Shine a laser on a moderately rough surface like a blackboard and you will see this speckle phenomenon dramatically displayed.

To reduce speckle and thus improve the ability to determine the average gray scale in a region, one must look at the target element many times and average the results together to make the image. This can be done with a radar by the panchromatic technique (Moore and others, 1969) as in optics, but most radars do not have this capability. A tradeoff must be made between reduced speckle (improved gray-scale resolution) and finer spatial resolution. With properly configured systems this is a direct tradeoff: doubling the two linear dimensions of the spatial resolution cell improves the standard deviation of the speckle by a factor of two. To determine gray scale within 10 percent of the mean at any point requires 100 looks, resulting in 10 times poorer spatial resolution. With 20-percent uncertainty in the gray level of a single cell, the penalty in spatial resolution is only a factor of 5. Even ± 50 percent uncertainty is often good enough, and in this case the spatial resolution is degraded only by a factor of 2. Probably one would never be satisfied with this for a single cell, but the eye does the averaging over homogeneous areas to improve the net effect to much better than ± 50 percent, and having the spatial resolution allows one to determine which areas the eye should average in a way that would not be possible if the averaging were done automatically.

The standard deviation of the gray scale turns out to be a relatively poor indicator of the interpretability of an image that has a lot of speckle; a better indicator is the ratio of the brightness exceeded 90 percent of the time to that exceeded 10 percent of the time (Moore, 1975). With most systems in use today these values can be obtained from a chi-square distribution of 2N degrees of freedom, where N is the number of samples averaged. When this definition is applied, the ratio between the resolutions required for equal interpretability with a fully coherent single-look synthetic-aperture radar and a radar with photographic quality (infinite number of looks) is found to be 4.7. That is, if 30.4 ft (10 m) resolution is required

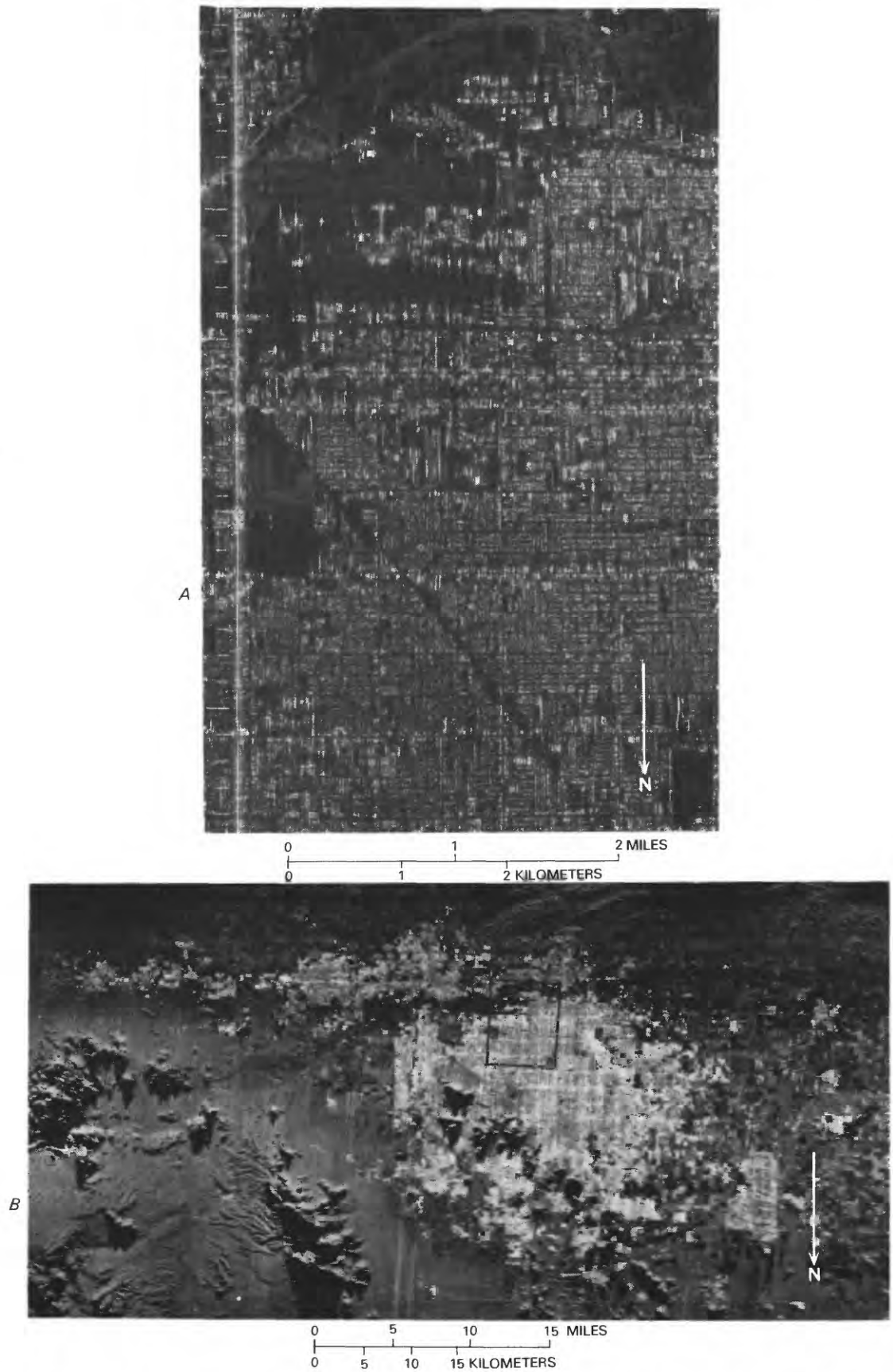

FIGURE 1.—Two radar images of Phoenix, Arizona. *A*, AN/APQ–152 (X-band) SAR (Synthetic aperature radar) imagery. *B*, AN/APS–94D (X-band) SLAR imagery. Area outlined indicates aproximate coverage of *A*. Apparent distortion of outlined area results from the transfer of one image in slant range format to another, also in slant range format.

for the single-look system, one can get by with 142.8 ft (47 m) in the photographic-quality system.

A recent study at the University of Kansas (Moore, 1975) disclosed that the numerical interpretability of an image can be related to the size of a square pixel by the relation

$$I = I_o \exp(-r^2/r_c^2)$$

where r is the pixel dimension and r_c is a critical pixel dimension for the type of application. Figure 2 illustrates how well this relation (indicated by the solid regression line) fits the experimental data for four different areas and two classes of target. Note that the critical value of resolution for the single-look picture (point of 37-percent interpretability) is at around 30 ft (10 m) for both kinds of application, and that the corresponding "Photographic" resolution is nearly 150 ft (50 m).

Another result of the study was the discovery that the area of the pixel is the key factor in its interpretability, that is, a long, narrow pixel and a square one having the same area turned out to have the same interpretability. This is illustrated, using only the fully coherent image data (fig. 3). The largest length/width ratio used was 10 in this study.

From this study, and others like it that remain to be done, the equivalent resolution required for a given mission can be calculated for any radar whose averaging characteristics are known once the single-look or photographic-quality critical resolution has been determined. One interesting result of the study is that the azimuth resolution for a radar that averages 10 looks can be 10 times as great as for a single-look system and achieve the same interpretability, provided the range resolution is the same as for the single-look system. This means that for most aircraft radar applications to earth science a real-aperture radar that is properly designed can be just as effective as a single-look synthetic-aperture system. A 3-look synthetic system, however, is significantly better than the 10-look system (synthetic or real aperture). Hence, if one really wants to determine whether a particular system can do the job, one must determine the required equivalent photographic resolution and from this calculate the capability of the system under consideration.

FREQUENCY

Currently plans are being formulated to fly a two-frequency radar aboard a shuttle mission. Defense is being mustered for an X(~3 cm)- and L(~25 cm)-band system on the basis of its capability for mapping geology. Partly in defense of this has been presented the results of an excellent study by Schaber, Berlin and Brown (1975), who have pointed out that L-band radars rather dramatically effected the separation of coarse (>2.0–3.5 cm) from fine (<2.0–3.5 cm) gravel. In a similar manner, it was pointed out in earlier studies at Pisgah Crater (Dellwig, 1969; MacDonald and Waite, 1972) that the smoothness of playa lake surface and adjacent lavas and alluvial fans in the basin and range country of the Western United States could be defined on the basis of the return from such surfaces on K(1.18–1.67 cm)- or X-band radars. From these studies it becomes quite obvious that the optimum frequency for an imaging radar is that frequency which enables the investigator to derive the necessary terrain data for his particular discipline. From the point of view of general geologic mapping, one finds difficulty in defending the utilization of an L-band system as opposed to a C(~5 cm)- or even P(77–136 cm)-band system, for geologic studies do not necessarily require the separation of material of a size range smaller than 2.0–3.5 cm from material of a size range larger than that figure. A problem of infinitely more general importance than the separation of materials of varied size ranges is the determination of soil moisture content. Studies concurrently being conducted at the University of Kansas using the Microwave Active Spectrometer (MAS) system rather dramatically demonstrate that the indication of soil moisture content which one might expect to be reflected in radar backscatter is strongly frequency dependent (Batlivala and Ulaby, 1975). Whereas the data required by geologists for the most part are not particularly frequency dependent, a wide range of earth scientists interested in soil moisture content will undoubtedly show a strong preference for radar imaging in the C-band range.

POLARIZATION

A parameter never fully investigated, and unfortunately not subject to investigation by most earth scientists due to a lack of data, is that of polarization. The evaluation of numerous AN/APQ–97 images generated during the NASA Earth Resources Survey Program flights failed to reveal any significant difference from the point of view of geologic investigation between parallel-vertically and parallel-horizontally polarized signal return in Ka(~.86 cm)-band. Comparisons between like and cross polarized images, however, showed considerable potential for the revelation of data not available in a single image. In studying a variety of rock outcrops in the Western United States, McCauley (1972) identified surface roughness as the cause of polarization reversals in a variety of rock

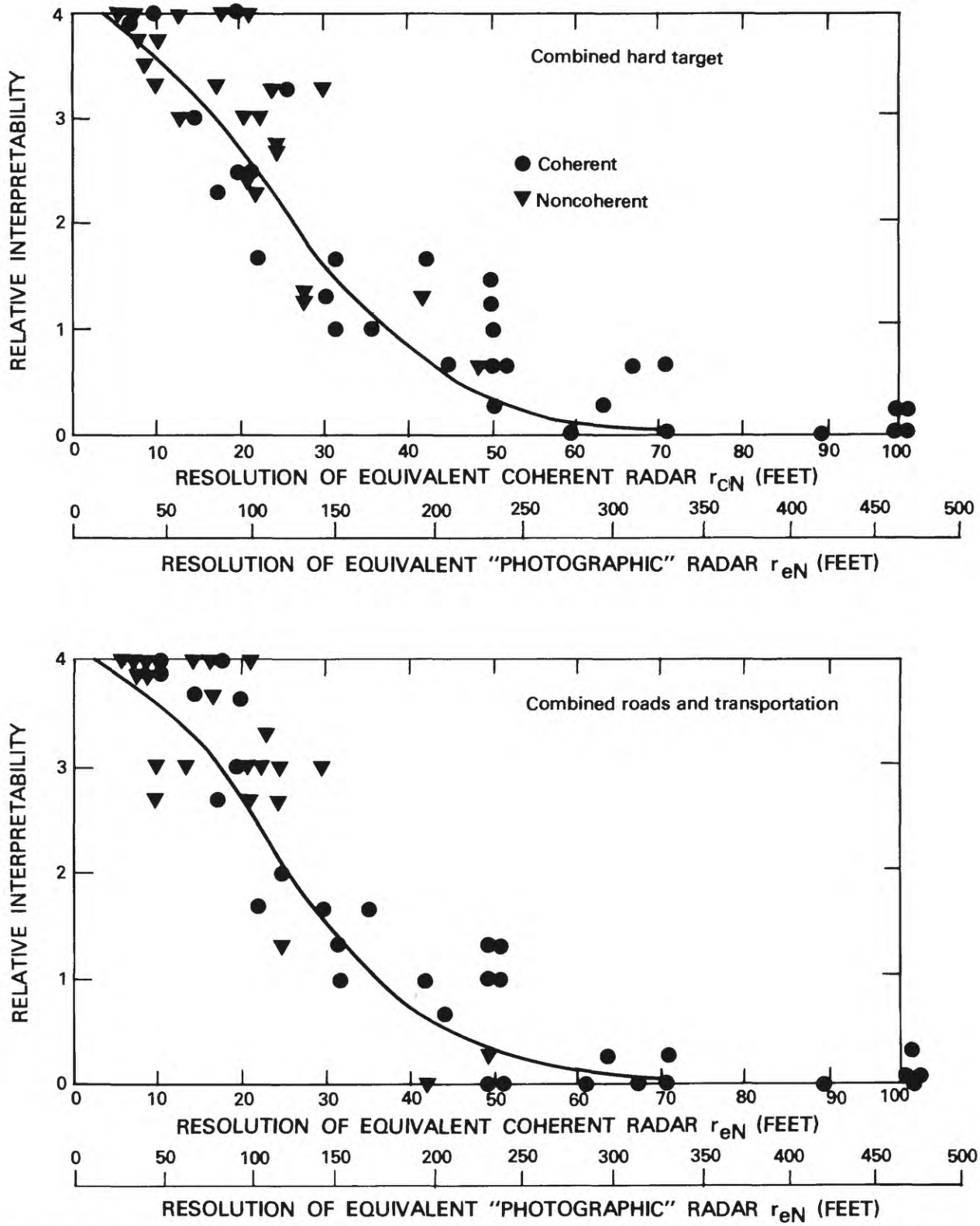

FIGURE 2.—Interpretability vs. equivalent resolution for hard targets, roads, and other transportation—all data sets combined.

types (fig. 4), all of which showed similarity in surface configuration. The studies of cultural features by Lewis (1968) also revealed a significant contrast in the like and cross polarized return signal of manmade linear features (fig. 5). In the Gulf Coast (fig. 6), MacDonald and Waite (1971b) noted strong contrasts in the return

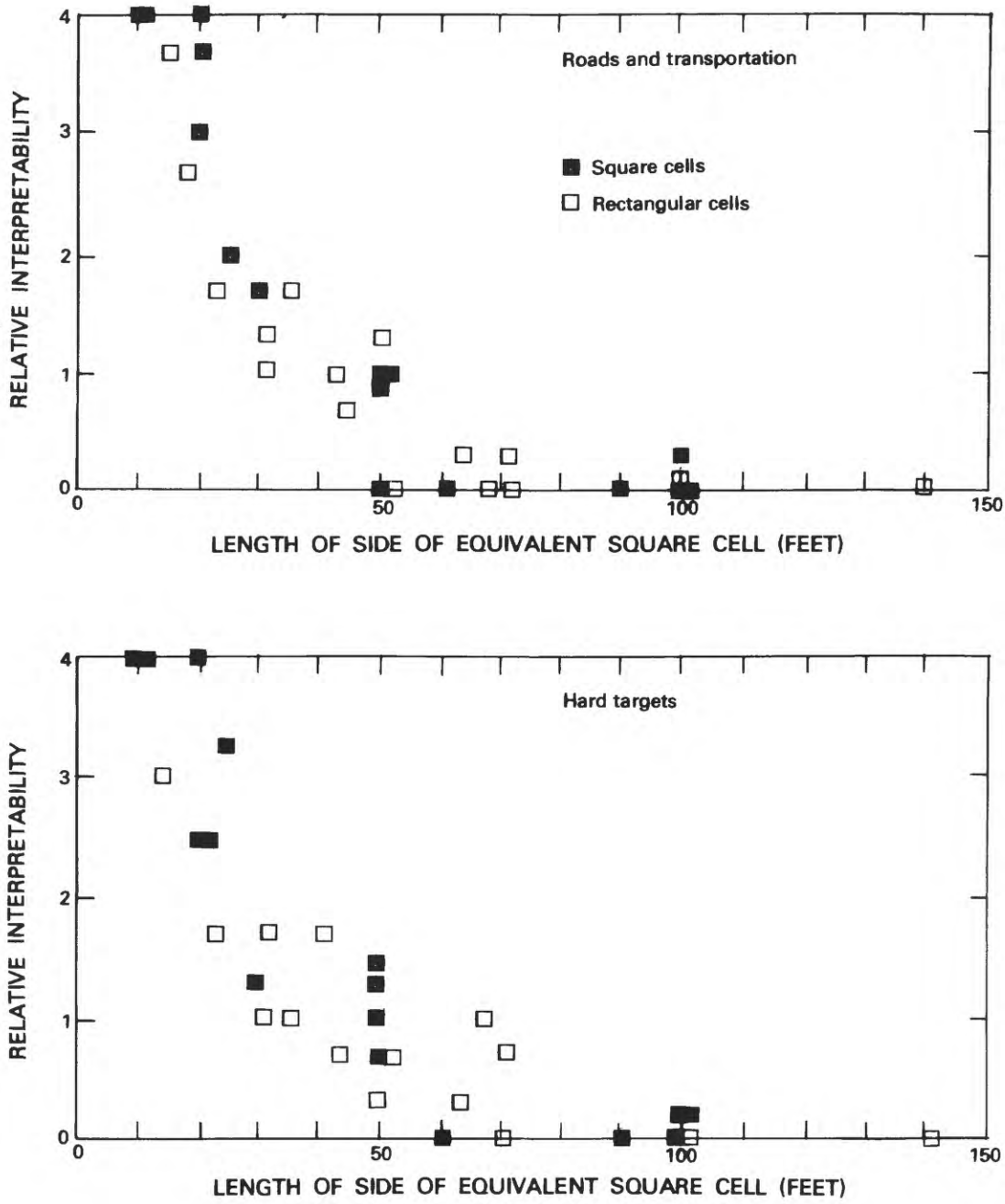

FIGURE 3.—Comparison of square and rectangular cells.

in the near range between the like and cross polarized signal, a contrast which they attributed to a difference between moist and dry terrain surface. Utilizing the MAS system, Ulaby and others (1974) and Batlivala and Ulaby (1975) have recorded such contrasts in return signal.

In order to place a value on dual polarization imaging one must first define the cause for tonal reversals, and secondly must be able to utilize this contrast regardless of the subtlety of expression. For example, on casual examination of the like and cross polarized imagery of Freeport, Texas (fig. 7), some tonal con-

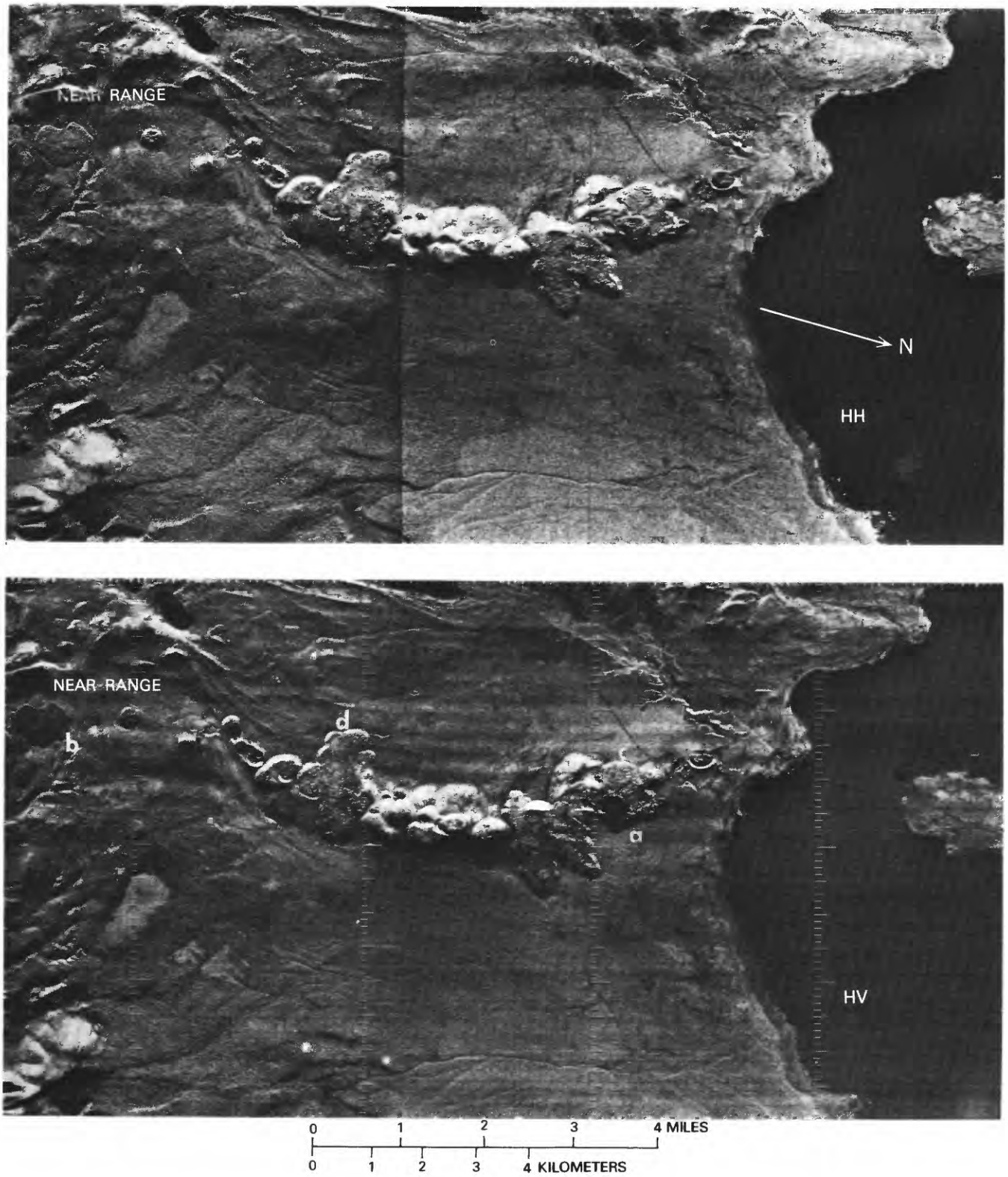

FIGURE 4.—Mono Craters, California, AN/APQ–97 (ka-band) SLAR imagery. Flows a and b are blocky lavas and have lower returns on cross polarized (HV) imagery. Flows c and d are covered by ash and appear the same on both polarizations.

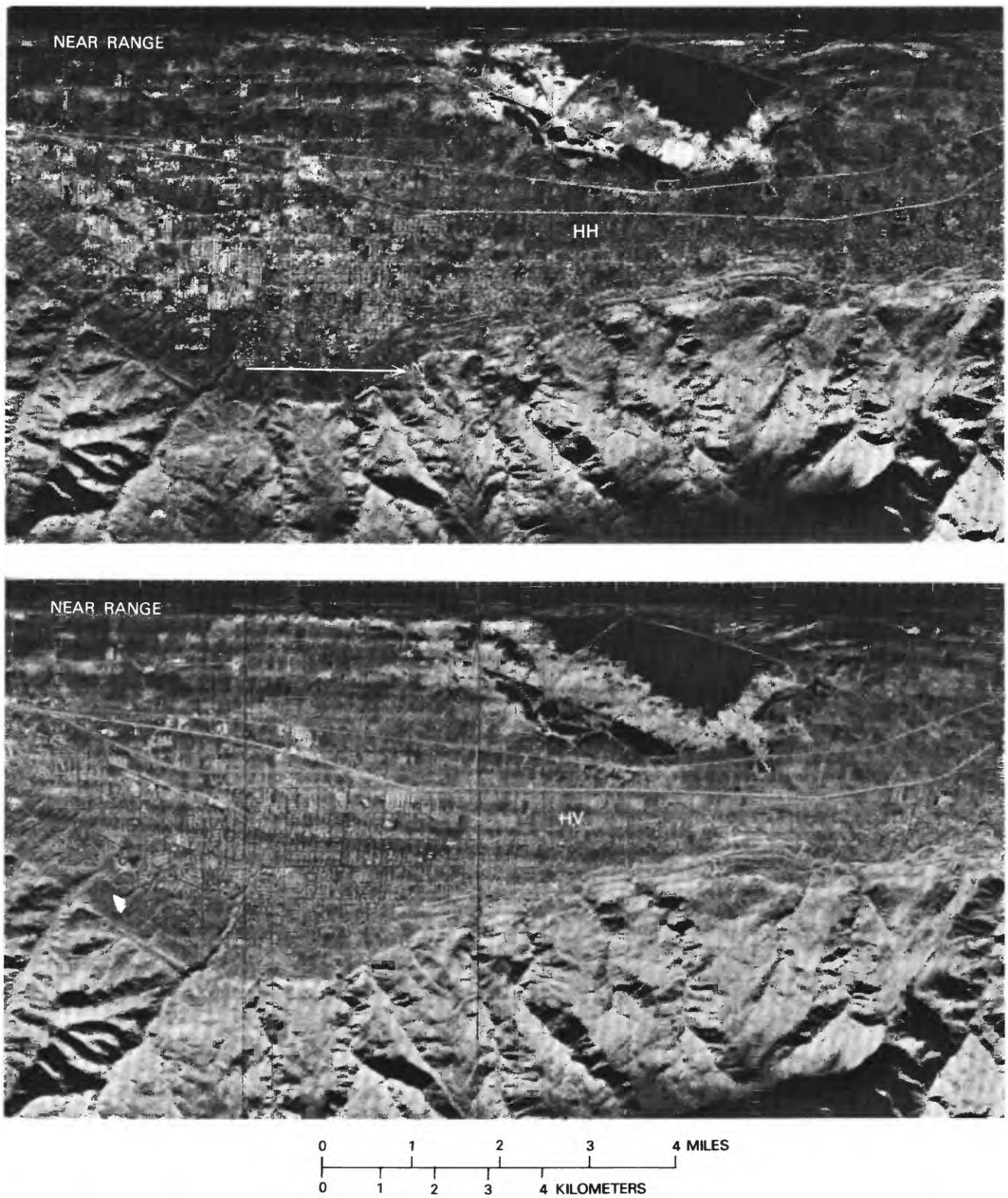

FIGURE 5.—Bountiful, Utah, AN/APQ–97 (Ka-band) SLAR imagery. Urban and industrial areas are more apparent on HH (like) polarization. Communication networks are more accurately mapped on HV (cross) polarization.

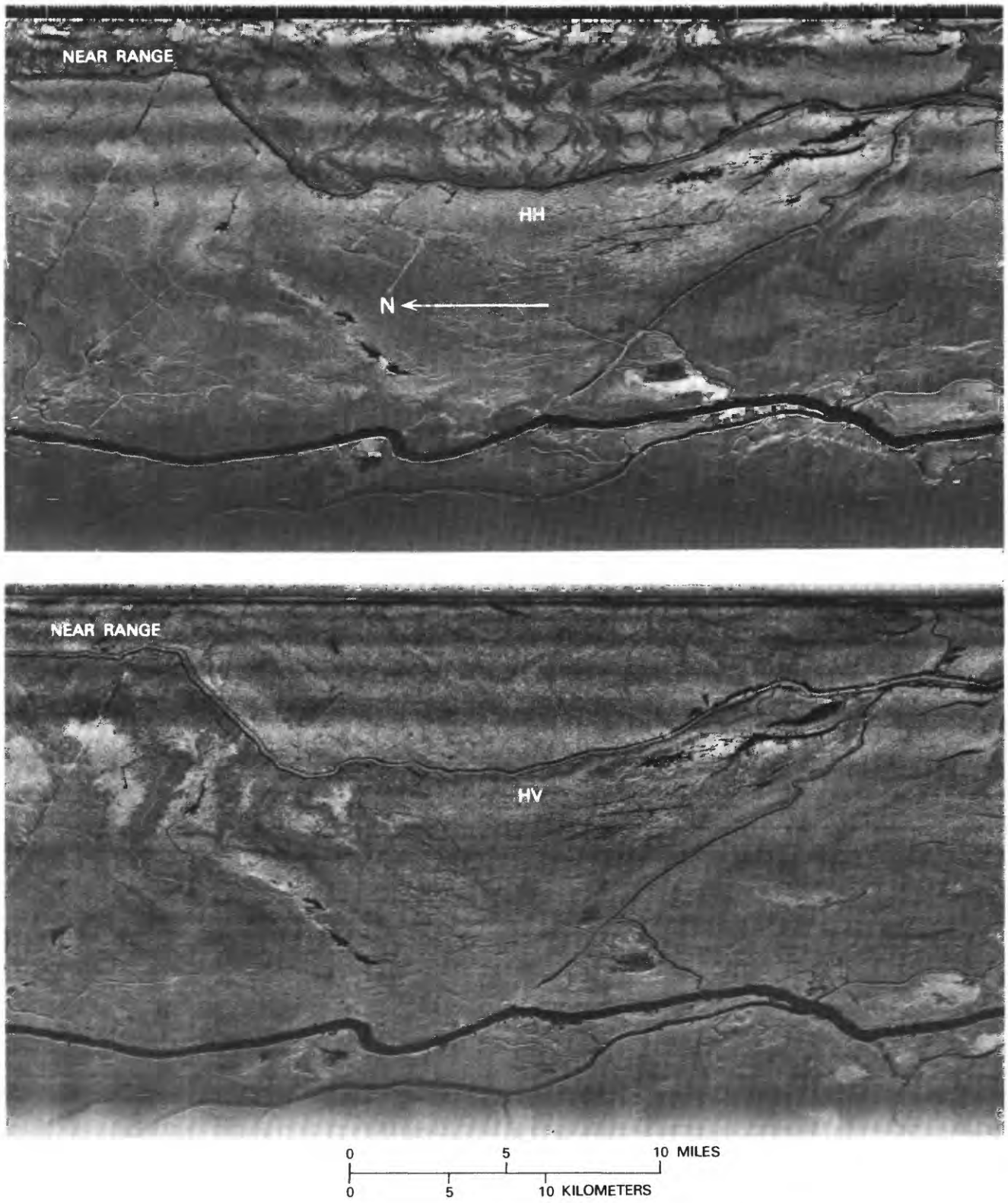

FIGURE 6.—Atchafalaya River Basin, Louisiana, AN/APQ–97 (Ka-band) SLAR imagery. Areas of high soil moisture appear dark in near range HH (like) polarization imagery. Dry areas appear light in tone. Soil moisture differences are not detectable on HV (cross) polarized imagery.

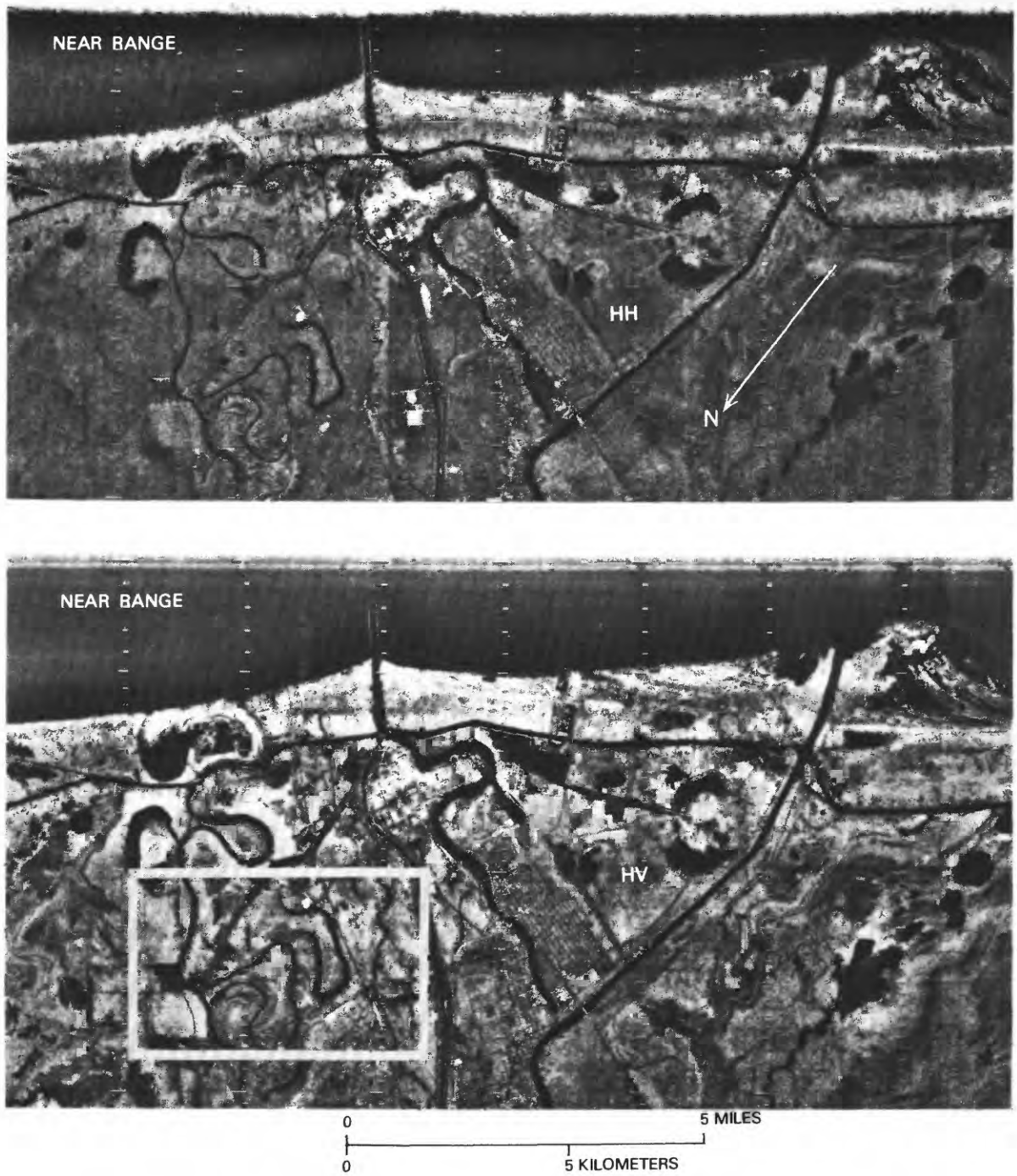

FIGURE 7.—Freeport, Texas, AN/APQ–97 (Ka-band) SLAR imagery. Area of figure 8 outlined in HV image.

trasts may be obvious but others will escape the interpreter's naked eye. However, by adding these two images in contrasting colors, the interpreter can easily define the extent of any unique signature and rapidly effect interpretation (fig. 8, p. XXI).

LOOK DIRECTION AND DEPRESSION ANGLE

The need for control of look direction and depression angle has been well established by numerous

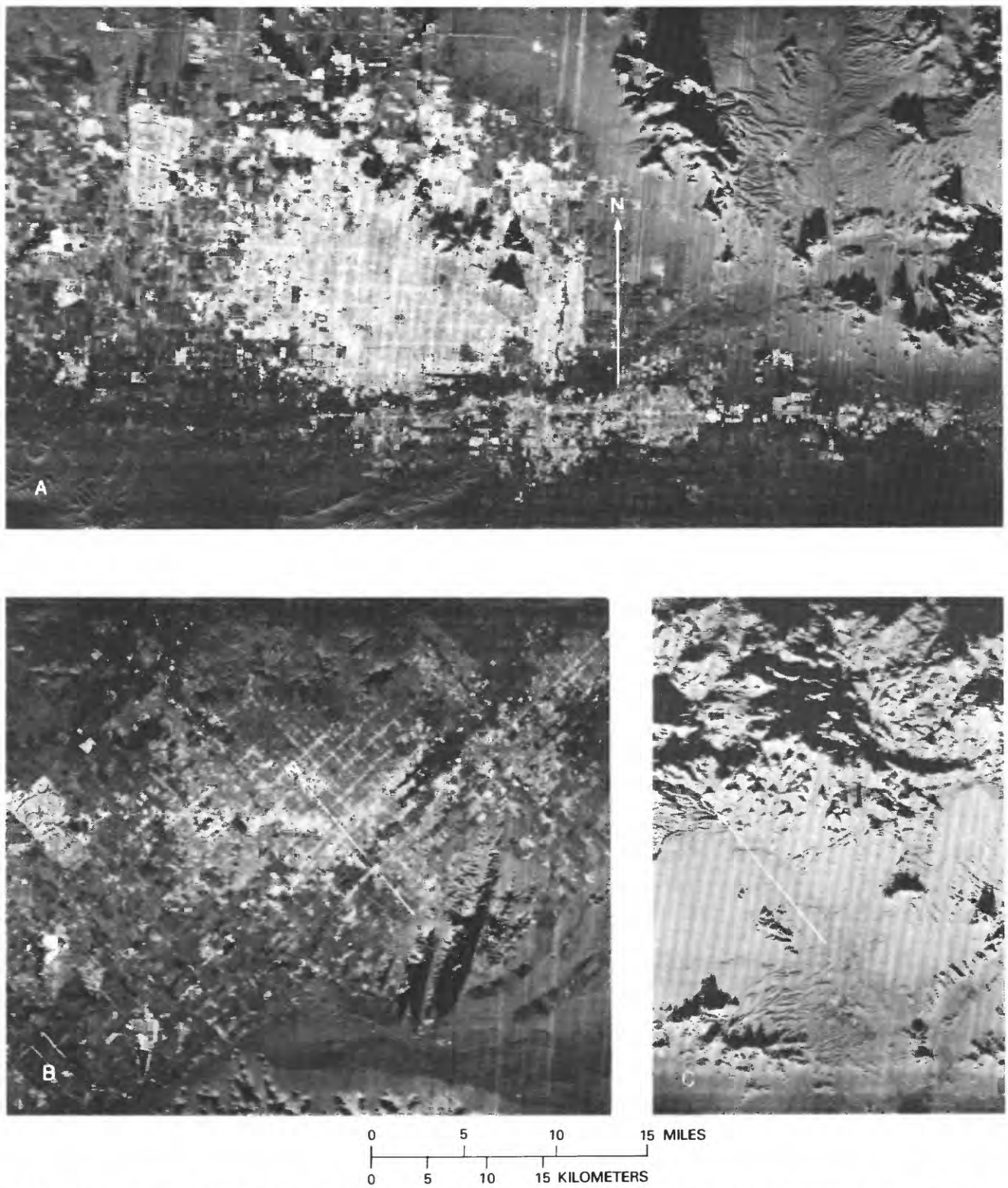

FIGURE 9.—Phoenix, Arizona, AN/APS–94D (X-band) SLAR imagery. A, North look of Phoenix and mountains and alluvial fans (middle to far range) to the northeast. B, Northeast look of Phoenix. C, Northeast look of alluvial fans (near to middle range).

investigators, among them, MacDonald and Waite (1971a) who pointed to the desirability of selecting specific ranges of depression angles for regions of varying relief. However, relief is not always uniform throughout an area and in areas that in general may be of relatively low relief, occasionally local high relief will result in excessive shadowing if low depression angles (deemed best for relatively flat terrain) are

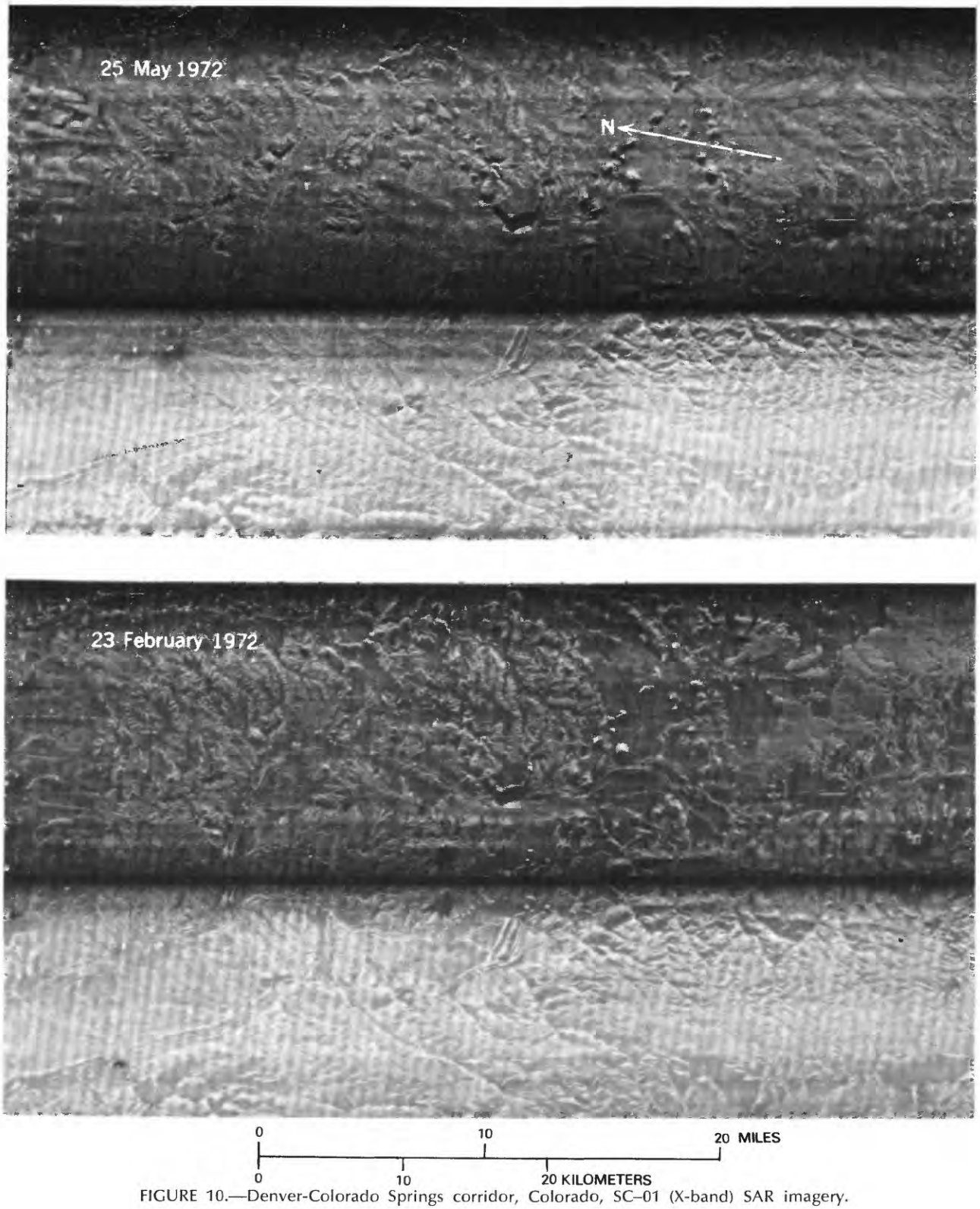

FIGURE 10.—Denver-Colorado Springs corridor, Colorado, SC–01 (X-band) SAR imagery.

used. The significance of control of look direction and depression angle is indicated once again in the Phoenix area over which two looks at the city (fig. 9A,B), one to the north and normal to the overall street plan and the other to the northeast and oblique to the overall north-south, east-west street pattern give strongly contrasting views of the urban area. Similarly, two different looks at natural terrain features as is indicated in

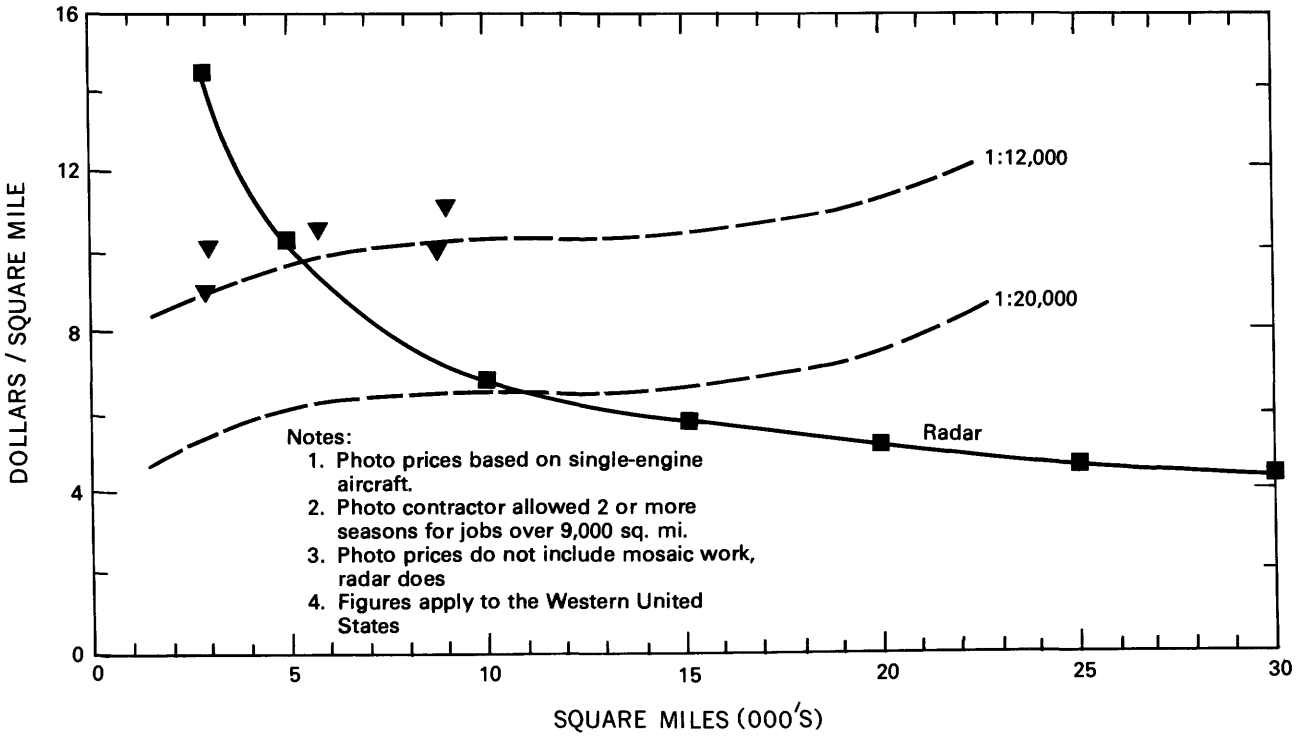

FIGURE 11.—Price comparisons—photos vs. radar, spring 1975.

another pair of Phoenix images (fig. 9A,C) give contrasting indications of the degree of relief that should be expected in the area covered by alluvial fans. In the one image, because of look direction and depression angle, little contrast is seen between the arroyos and the interfluve areas, whereas in the second image, due to a change in look direction and depression angle, the contrast between the arroyos and the interfluve areas is sharp. The extensive shadowing behind isolated mountain peaks and the revelation of terrain data in the shadow area through a look from the opposite direction, further points to the desirability of obtaining two looks of an area in order to obtain the maximum amount of terrain data. Such was first demonstrated by MacDonald (1969) in the Darien Province, Panama, where it was determined that, with each additional look, additional data were revealed.

TIME

Numerous investigators utilizing ERTS imagery have been able to document data increase through second and even third or fourth season imagery evaluation. Such should also be true for radar imagery especially in vegetated terrain due to seasonal variations in dielectric properties and surface configuration of the vegetal cover (fig. 10). Not only is the change in data content of winter and spring imagery documented, but also it emphasized the need for selection of imaging season depending on the nature of the desired data.

COST

Perhaps not a system parameter, but an important factor to be considered in the determination of optimum system parameters for specific types of earth science investigations is cost. Mobilization charges and flight line density control to a large degree the cost of imaging—a cost which is essentially prohibitive for the obtaining of detailed data in relatively small areas. Even assuming that imaging systems of resolutions not presently available would become available in the future, it appears that cost would be prohibitive when compared with aerial photography. Only when real time or near real time (13 seconds between imaging and viewing on a currently operating experimental Dutch imaging radar and instant viewing at the end of a frame on the Kansas University radar [Eichel and others, 1975]) data are absolutely necessary (although certainly to be desired under most conditions) could the utilization of radar for small-scale mapping be justified (fig. 11). Conversely, for mapping large areas,

unless the resolution now only achieved by aerial photography is absolutely necessary, one finds difficulty in justifying the utilization of any system other than radar.

OPTIMUM RADAR-PARAMETERS

You would like 1-ft resolution, wide swath width, multiple polarization, controllable depression angles, opposite looks and a range of frequencies and a real time display? Dream away! Even Uncle will have trouble affording that system.

REFERENCES

Batlivala, P. P., and Ulaby, F. T., 1975, Effects of roughness on the radar response to soil moisture of bare ground: Univ. Kansas Center for Research, Inc., RSL Tech. Rept. 264–5, 50 p.

Dellwig, L. F., 1969, A geoscience evaluation of multifrequency radar imagery of the Pisgah Crater area, California: Modern Geology, v. 1, p. 65–73.

Dellwig, L. F., Kirk, J. N., and Walters, R. L., 1966, The potential of low resolution radar imagery in regional geologic studies: Jour. Geophysical Research, v. 71, p. 4995–4998.

Eichel, L. A., Moore, R. K., Weilert, M., and Schlude, F., 1975, An inexpensive side-looking radar with a novel display, *in* Institute of Electrical and Electronic Engineers Internat. Radar Conf., Arlington, Va., April 21–23, 1975, Proc.

Lewis, A. J., 1968, Evaluation of multiple polarized radar imagery for the detection of selected cultural features: U.S. Geol. Survey Tech. Letter NASA–130, 52 p.

MacDonald, H. C., 1969, Geological evaluation of radar imagery for Darien Province: Modern Geology, v. 1, p. 1–62.

MacDonald, H. C., and Waite, W. P., 1971a, Optimum radar depression angles for geological analysis: Modern Geology, v. 2, p. 179–193.

———1971b, Soil moisture detection with imaging radars: Water Resources Research, v. 7, p. 100–110.

———1972, Terrain roughness and surface materials discrimination with SLAR in arid environments: Univ. Kansas Center for Research, Inc., RSL Tech. Rept. 177–25, 37 p.

McCauley, J. R., 1972, Surface configuration as an explanation for lithology-related cross-polarized radar image anomalies, *in* NASA Manned Spacecraft Center, Annual Earth Resources Program Review, 4th, Houston 1972, Proc., v. 2, p. (36–1)–(36–9).

Moore, R. K., 1975, SLAR image interpretability—Tradeoffs between picture element dimensions and non-coherent averaging: Univ. Kansas Center for Research, Inc., RSL Tech. Rept. 287–2, p. B1–91; p. I1–11.

Moore, R. K., Waite, W. P., and Rouse, J. W., Jr., 1969, Panchromatic and polypanchromatic radar: Inst. Electrical Electronic Eng. Proc., v. 57, no. 4, p. 590–593.

Rydstrom, H. O., 1970, Capabilities of advanced radar systems for monitoring land resources: Goodyear Aerospace Rept. GERA–1604, Arizona Div., 10 p.

Schaber, G. G., Berlin, G. L., and Brown, W. E., Jr., 1975, Variations in surface roughness within Death Valley, California: Geologic evaluation of 25 cm wavelength radar images: U.S. Geol. Survey Interagency Rept., Astrogeology 65, 63 p.

Ulaby, F. T., Cihlar, J., and Moore, R. K., 1974, Active microwave measurement of soil water content: Remote Sensing of Environment, v. 3, p. 185–203.

PROCEEDINGS OF
THE FIRST ANNUAL WILLIAM T. PECORA MEMORIAL SYMPOSIUM,
OCTOBER 1975, SIOUX FALLS, SOUTH DAKOTA

Worldwide Indexing and Retrieval of Landsat Images

By Floyd F. Sabins, Jr.,
Chevron Oil Field Research Company,
La Habra, California 90631

ABSTRACT

More than 100,000 Landsat images have been produced since the first satellite was launched in July 1972. In order to select images on a worldwide basis, index maps are necessary. Manual sorting and plotting lists of images onto base maps are tedious, time-consuming and error-prone tasks. Computers, however, are ideally suited for this work. The Landsat Index Map System described here employs a computer mapping program and the EROS Landsat digital index tape to produce a series of 22 index maps covering the world at a scale of 1:5,000,000.

Only the highest quality images are plotted. One set of maps is plotted for images with zero cloud cover. Other sets are plotted for 10-, 20-, and 30-percent cloud cover, if necessary, to provide complete coverage. The index maps are updated periodically from new index tapes. In addition to locating images, the maps indicate areas that lack coverage and image centers located away from the nominal image center points.

INTRODUCTION

BACKGROUND

Since the launch on July 23, 1972, Landsat–1 has transmitted approximately 100,000 images covering much of the land area of the world. Landsat–2, launched on January 22, 1975, is supplying additional images. The 18-day repetition cycle of each satellite results in many areas being imaged numerous times. For users requiring many images of large regions, especially in foreign areas, the plotting of images onto index maps is a time-consuming, tedious, and error-prone operation. This paper describes an index map system developed by Chevron Oil Field Research Company that greatly simplifies and expedites the location and selection of Landsat images throughout the world. Numerous other papers have described the Landsat vehicles and imagery, which are not discussed here.

CONVENTIONAL INDEXING METHODS

The National Aeronautics and Space Administration provides monthly index listings for domestic and foreign Landsat images. In addition, the EROS Data Center at Sioux Falls can provide, upon request, computer printouts of image coverage for specific geographic areas. For the conterminous United States, EROS also provides an index map based on "nominal image" center points. This map does not show specific images but rather the center points at which the repetitive images are positioned. This system originated at the Canada Centre for Remote Sensing. Microfilm browse files of Landsat images are maintained for public use at various U.S. Geological Survey offices. Useful Landsat indexes are prepared by the U.S. Agricultural Stabilization and Conservation Service aerial photographic laboratory in Salt Lake City. Images for each 18-day cycle are positioned on a U.S. base map to form a photo index mosaic. In addition to ground coverage, image quality and cloud cover can be determined directly. I understand that the laboratory is no longer updating these indexes.

For foreign areas, the index data consist of lists of Landsat identification numbers which must be sorted and plotted on a base map. Sorting is done on the basis of image quality and cloud cover in order that the best image can be selected for each center point. For mosaic preparation, it is desirable to use images

acquired at the same time of year to minimize tonal changes between adjacent images. This involves a separate sorting step. All of these sorting and plotting operations are tedious and error prone when done manually but are ideally suited for computer processing. The balance of this paper describes the system developed at Chevron Oil Field Research Company (COFRC) for producing Landsat index maps on a worldwide basis.

ACKNOWLEDGMENTS

My role in this work was to recognize the need for a worldwide Landsat index map system and suggest the approach described here. The actual programming and plotting was accomplished by the following COFRC colleagues to whom I am deeply indebted: H. L. Haines, E. B. Hill, L. C. Bonham, C. D. Boyd, C. C. Davis, W. T. Miller, and G. S. MacKenzie. Personnel at the EROS Data Center were very helpful in explaining the format of their index tape.

INDEX MAP SYSTEM

One of the truly unique features about the COFRC system is that we have not seen fit to title it with an acronym. The system comprises two essentially separate operations: (1) preparation of a base map showing coastlines, drainages, and political boundaries together with a latitude and longitude grid and (2) plotting of Landsat center points and identification numbers on the base map.

BASE MAP PLOTTING

Figure 1 shows the location of the 23 individual maps which we use to index the world. Most of these maps are plotted to the same scale (1:5,000,000) and projection (Lambert conic conformal) as the Global Navigation Charts (GNC) published by the U.S. Air Force Chart and Information Center and distributed by the Distribution Division, National Ocean Survey, Washington, D.C. 20235. By plotting the index maps on translucent paper, they may be overlain on the GNC to determine coverage of particular mountain ranges, sedimentary basins and other features not noted on the index maps.

As shown on the flow chart, figure 2, two digital files are used in base map plotting: (1) world map file containing land outlines and (2) political boundaries and drainage file. Latitude and longitude coordinates are designated for the specific index map, which on figure 2 happens to be Index Map 11 covering southern

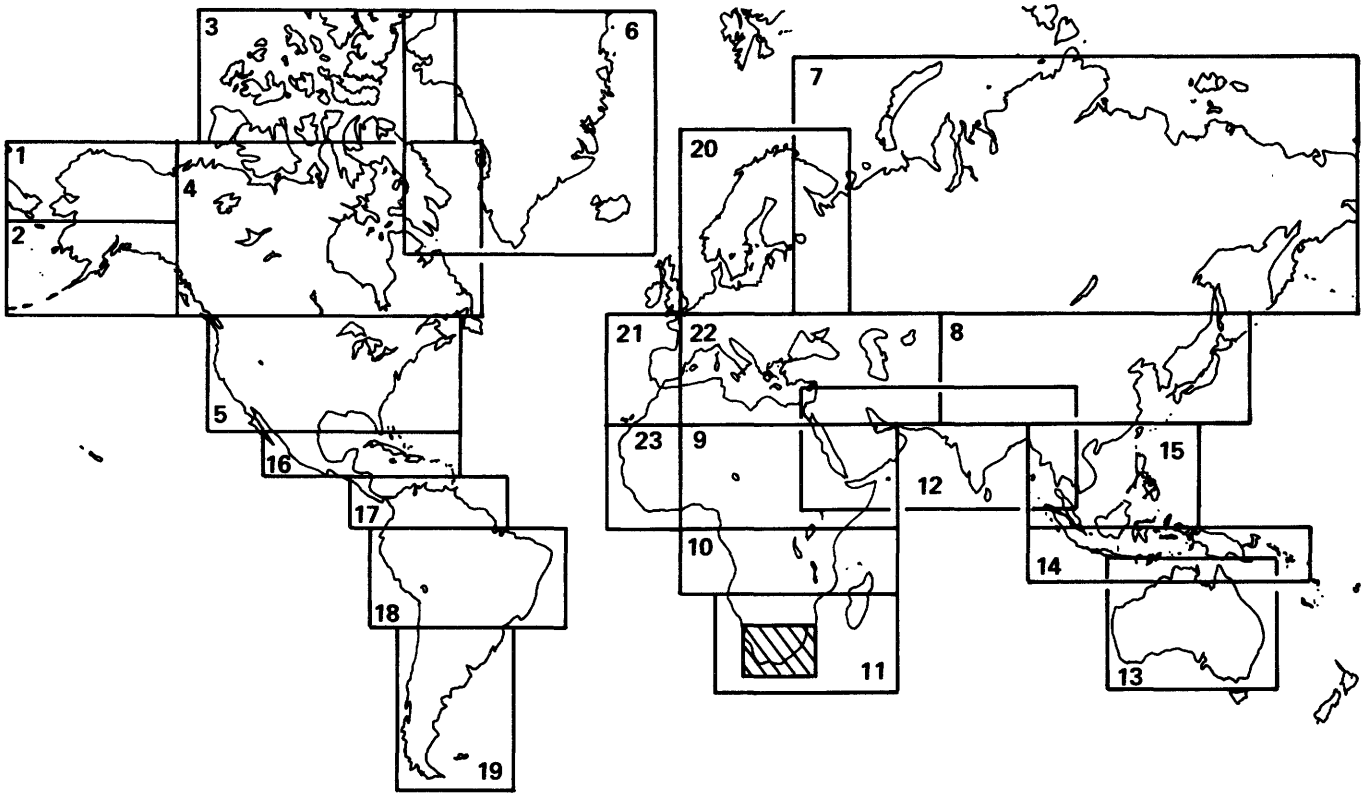

FIGURE 1.—Location of COFRC Landsat index maps. Note portion of Index Map 11 that is shown on figures 4–9.

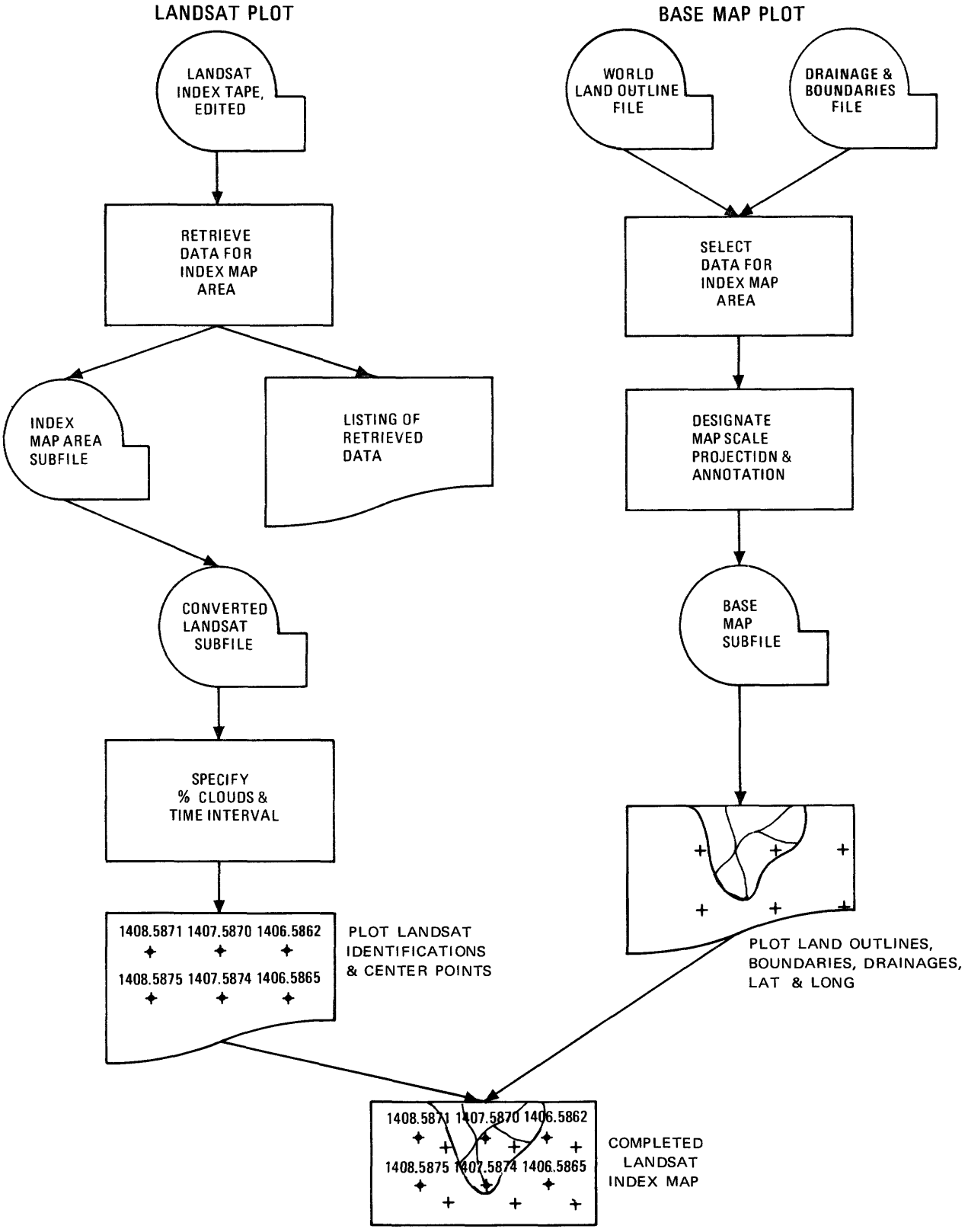

FIGURE 2.—COFRC Landsat index map plotting routine.

Africa. The scale and map projection are designated and the base map is plotted preparatory to adding the Landsat information.

LANDSAT IMAGE PLOTTING

The first step is to acquire from the EROS Data Center a copy of their Landsat index tape which lists all the images on file at the Data Center. The latest Landsat tape we acquired lists 126,005 images covering the period from launch through April 1975 and cost $135. EROS also provides a description of the tape format. The first step is to edit the tape and delete nonstandard and duplicate entries. Using the edited tape as a source, a subfile tape is created listing only the images located within the boundaries of the particular index map (fig. 2). At this stage we eliminate images with poor quality or significant cloud cover.

A listing of all these images in numerical (time) sequence is also produced. This printout eliminates much of the information on the original index tape (such as image corners, scale and altitude) which is not required for retrieval. On the sample printout of figure 3, an explanation is provided for the various entries. The Landsat identification number (ID. No.) which is unique for each image, is employed on all of our index maps and merits a description. The nine-digit number (example, 1055.08041) originates as follows:

1—Landsat–1 (This digit is a 5 for 1000 days and more after launch)
055—Days after launch (July 23, 1972). This day is September 16, 1972.
08—Hour of observation (Greenwich time)
04—Minute of observation
1—tens of seconds

On our index maps, the leading zeros are deleted on the time code. This image is plotted as 1055.8041.

The digital tape subfile for the index map area is then converted to a format compatible with our plotter. Before plotting the Landsat center points on the base maps, we determine from the listing the approximate number of images in the subfile. Owing to the 18-day repetition cycle there would be much overprinting of identification numbers if an entire subfile were printed on one map. By referring to the listing, we designate time intervals, each of which is plotted on a separate map with a minimum of overprinting. For the southern Africa map, the following intervals were plotted and are illustrated:

Figure	Days after launch	Dates
4	0–73	72/07/23–72/10/10
5	74–144	72/10/11–72/12/14
6	145–248	72/12/15–73/03/28

March 28, 1973, was the latest entry on the initial index tape. Updating the maps is described later.

For ease of illustration, these maps are the portion of the entire southern Africa index map indicated on figure 1. This series of maps is restricted to images with 0-percent cloud cover. Successive map series can be plotted for 10, 20, and higher percent cloud cover if needed to provide complete coverage.

On figure 4, note that the center points for paths 1050 and 1068 (18 days apart) nearly coincide. Any additional images plotted along this path would be overprinted and produce an illegible map. Where minor overprinting occurs (fig. 5), the index numbers are readily resolved by referring to the printout list. On figure 6 note that the center points for paths 1177, 1178, and 1179 are located between the normal positions for these paths. This would present a problem on an index map based on nominal image centers and is discussed later.

The 115- by 115-statute-mile outline on figure 4 shows coverage of a Landsat frame. By centering this template over an image point with east and west borders parallel with the orbit path, the ground coverage of each image can be determined.

UPDATING THE INDEX MAPS

To maintain a current set of index maps, we order new Landsat index tapes at intervals. Each tape is cumulative from the day of launch. We observed that later index tapes commonly list images taken within the time span of an earlier tape, but which are not listed on the earlier tapes. Using the southern African maps (figs. 4, 5, and 6) as an example, our initial tape extended through 248 days after launch (March 28, 1973). A later tape extending through 478 days (November 13, 1973) included 33 images acquired during the first 248 days but not listed on the early tape covering that period. For this reason we always search each new index tape for earlier entries which are plotted. Figure 7 is a retroactive plot of the 13 cloud-free images that were missing from the initial index tape, but present on the later tape. The other 21 earlier images have higher cloud cover percentages. One explanation is that the EROS Data Center enters images on the tape as they are received from the processing facility at Goddard Space Flight Center, and the images are not necessarily received and entered into the data base in a strict time sequence. They are listed sequentially by Landsat index number, however. Another explanation is that the retroactive points may have contained nonstandard characters on the initial tape which would have eliminated them during

ID NO	ZONE NO	LAT CTR	LONG CTR	SENSOR TYPE	IMAGE QUAL	CLOUD COVER	DATE TAKEN	MSS 4567 RBV 123
8105007371 5A000	3	-30.235	-25.932	S11	8	0	72/09/11	MSS 1111
8105007373 5A000	3	-31.676	-25.521	S11	8	0	72/09/11	MSS 1111
8105007380 5A000	3	-33.100	-25.093	S11	8	0	72/09/11	MSS 1111
8105207454 5A000	3	-20.193	-25.774	S11	8	0	72/09/13	MSS 1111
8105207461 5A000	3	-21.626	-25.405	S11	8	0	72/09/13	MSS 1111
8105207463 5A000	3	-23.055	-25.029	S11	8	0	72/09/13	MSS 1111
8105207470 5A000	3	-24.496	-24.648	S11	8	0	72/09/13	MSS 1111
8105207472 5A000	3	-25.932	-24.262	S11	8	0	72/09/13	MSS 1111
8105207475 5A000	3	-27.363	-23.873	S11	8	0	72/09/13	MSS 1111
8105207431 5A000	3	-28.795	-23.476	S11	8	0	72/09/13	MSS 1111
8105207434 5A000	3	-30.219	-23.069	S11	8	0	72/09/13	MSS 1111
8105207490 5A000	3	-31.647	-22.651	S11	8	0	72/09/13	MSS 1111
8105307513 5A000	3	-20.258	-24.339	S11	8	0	72/09/14	MSS 1111
8105307515 5A000	3	-21.692	-23.976	S11	8	0	72/09/14	MSS 1111
8105307522 5A000	3	-23.122	-23.600	S11	8	0	72/09/14	MSS 1111
8105307524 5A000	3	-24.552	-23.215	S11	8	2	72/09/14	MSS 1111
8105307540 5A000	3	-28.849	-22.036	S11	8	0	72/09/14	MSS 1111
8105307542 5A000	3	-30.274	-21.630	S11	8	1	72/09/14	MSS 1111
8105307545 5A000	3	-31.701	-21.217	S11	8	1	72/09/14	MSS 1111
8105407571 5G000	3	-20.289	-22.895	S11	8	0	72/09/15	MSS 1111
8105508035 5A000	3	-23.145	-20.719	S11	8	0	72/09/16	MSS 1111
8105508041 5A000	3	-24.581	-20.332	S11	8	0	72/09/16	MSS 1111
8105508041 5A200	3	-24.581	-20.332	S11	8	0	72/09/16	MSS 1101

1 = ERTS 1, 8 = NASA
DAYS SINCE LAUNCH
HOUR OF OBSERVATION
MIN. OF OBSERVATION
TENS OF SECONDS
A = ALASKA, N = GODDARD, G = GOLD STONE
2 = RBV, 5 = MSS
GEOGRAPHIC ZONE: 1 = NE, 2 = NW, 3 = SE, 4 = SW
LATITUDE OF CENTER: + = N, − = S
LONGITUDE OF CENTER: + = W, − = E
SENSOR: S10 = RBV, S11 = MSS
IMAGE QUALITY: 9 = EXCELLENT, 0 = INFERIOR
CLOUD COVER IN 10'S OF PERCENT
YEAR, MONTH, DAY OF OBSERVATION
MSS OR RBV
BAND AVAILABILITY

FIGURE 3.—Portion of COFRC printout of Landsat–1 index tape. The area is southern Africa (Index Map 11), shown on index map, figure 1.

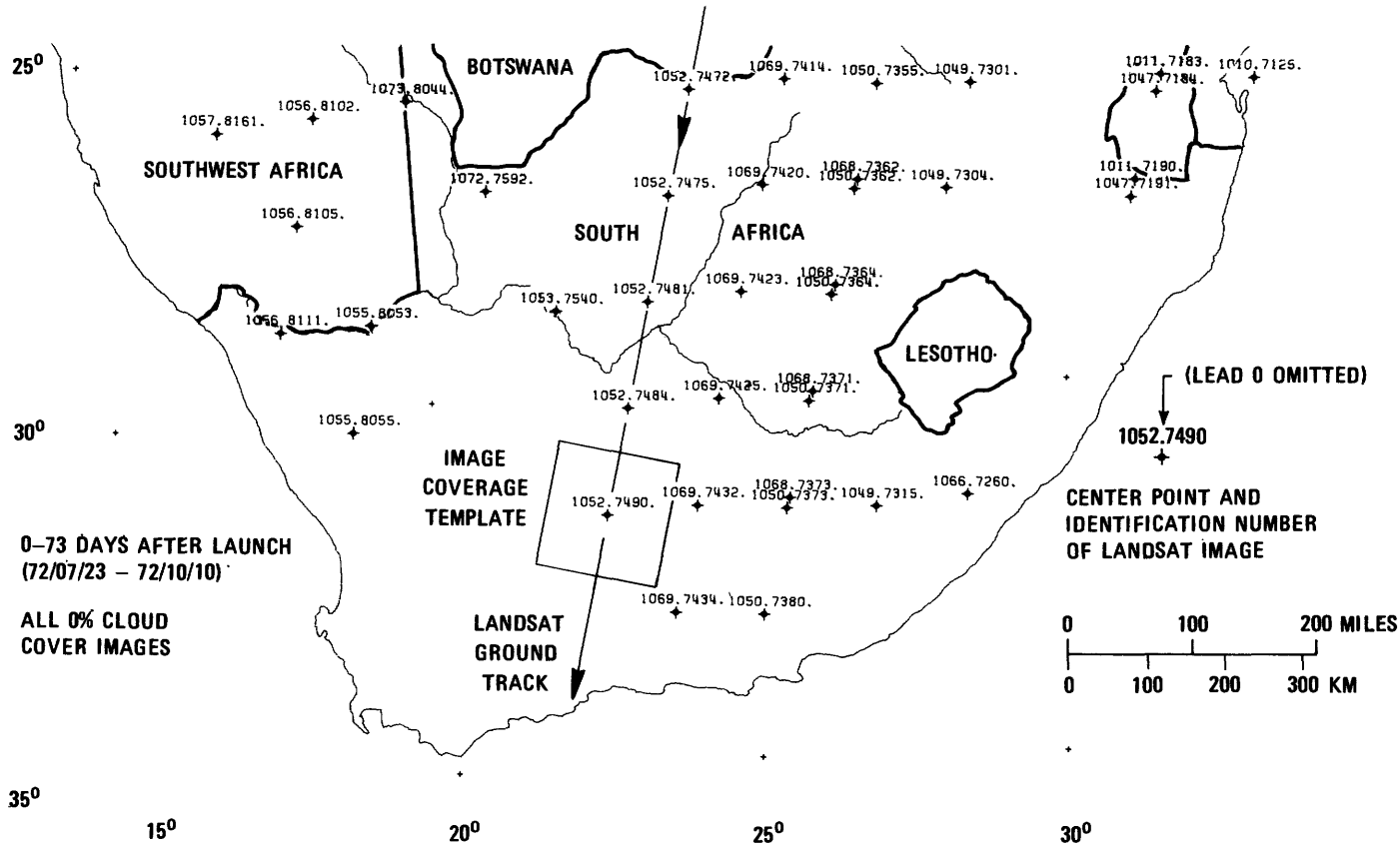

FIGURE 4.—Landsat–1 index map of southern Africa, 0–73 days. This is a portion of Index Map 11 located on figure 3 and was reduced from the original 1:5,000,000-scale computer plot.

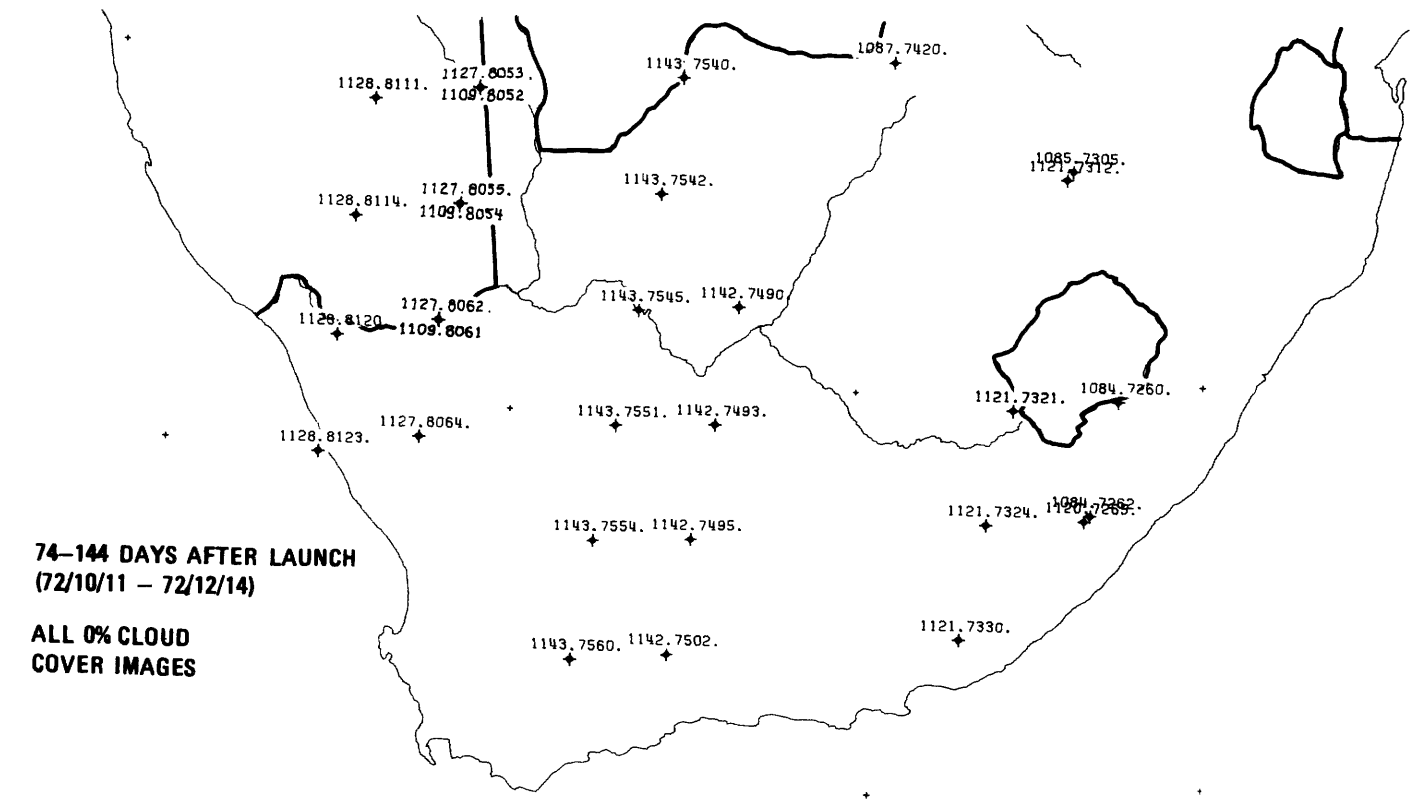

FIGURE 5.—Landsat–1 index map of southern Africa, 74–144 days.

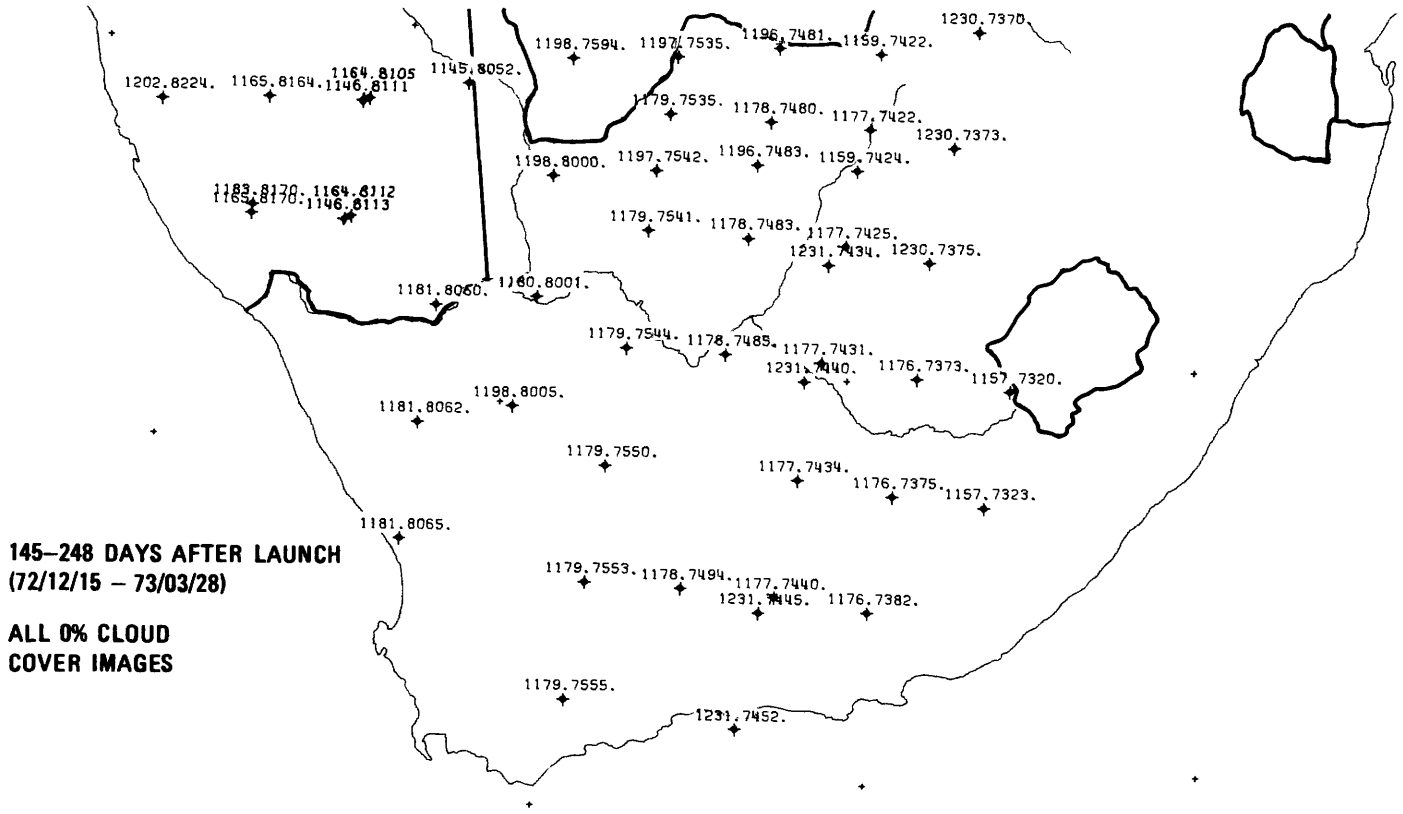

FIGURE 6.—Landsat–1 index of southern Africa, 145–248 days.

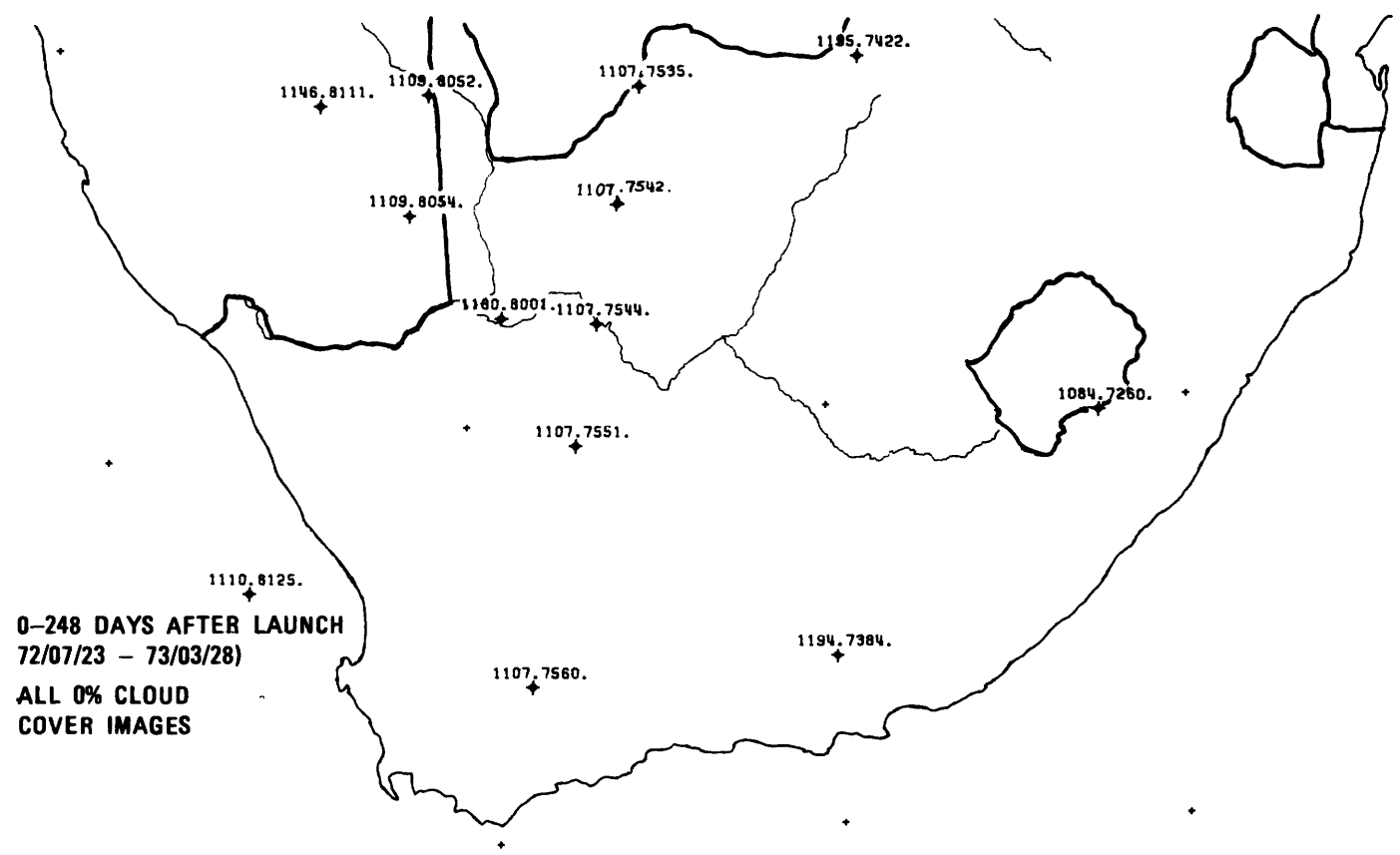

FIGURE 7.—Retroactive index map for first 248 days plotted from second index tape. These 13 cloud-free images were not listed on initial index tape.

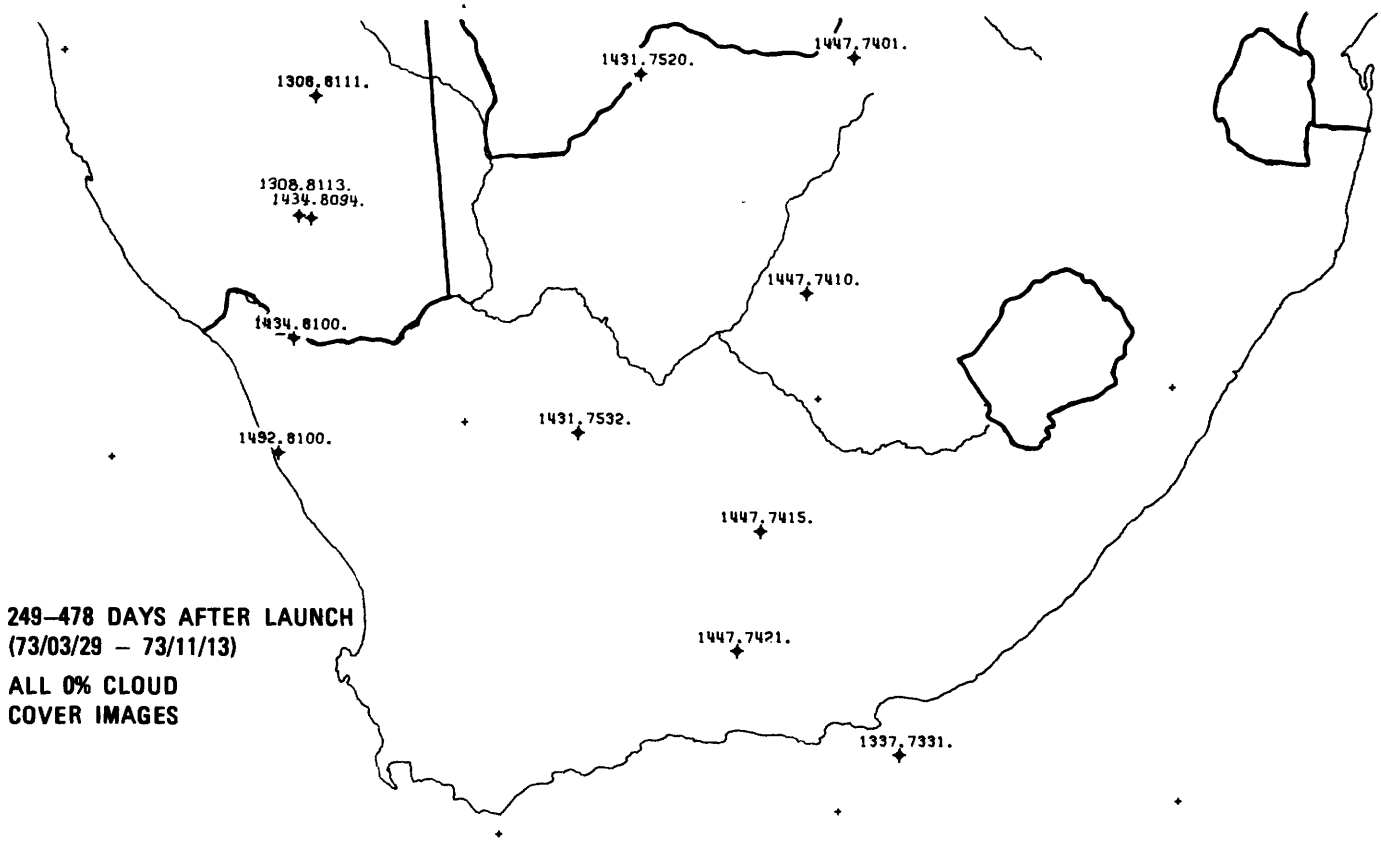

FIGURE 8.—Updated Landsat–1 index map, 249–478 days, plotted from second index tape.

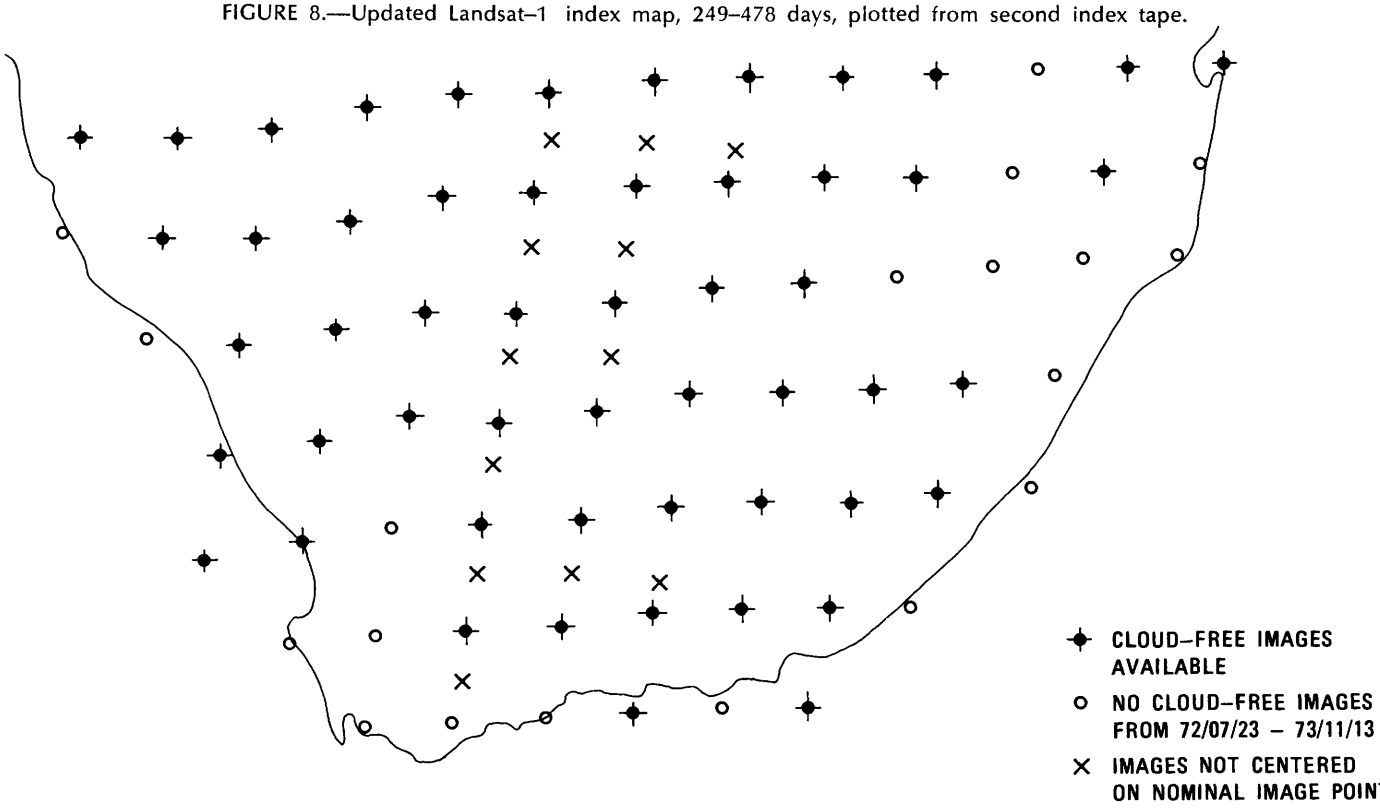

FIGURE 9.—Composite of 0% cloud cover index maps to indicate areas lacking cloud-free images. Also note images positioned between nominal image points.

our editing operation. Subsequent correction at EROS Data Center would make these images available on the later index tape.

Figure 8 is the updated index map for the period following the initial index map (March 29–November 13, 1973). Landsat–1 has acquired little foreign imagery since the later date because of malfunctioning of the onboard image tape recorder which had exceeded its design life.

Figure 9 is a composite index map of cloud-free images showing the nominal center points that have coverage and those that lack coverage. Also indicated are the 11 image center points mentioned earlier that are not positioned at nominal center points. An index map system based on nominal center points would have difficulty locating these images.

WORLD ZONE MAPS

In addition to the 23 individual index maps, we also routinely plot "World Zone Maps" for the four geographic zones or quadrants of the world. The zones are designated as follows:

1. Northeast.
2. Northwest (includes United States).
3. Southeast.
4. Southwest.

The maps are plotted on a smaller scale to display the large area on a single map sheet. Image center points are plotted without index numbers to avoid clutter and enable us to plot long time intervals. The example on figure 10 is a portion of the southeast world quadrant (zone 3) showing Australia. All the cloud-free

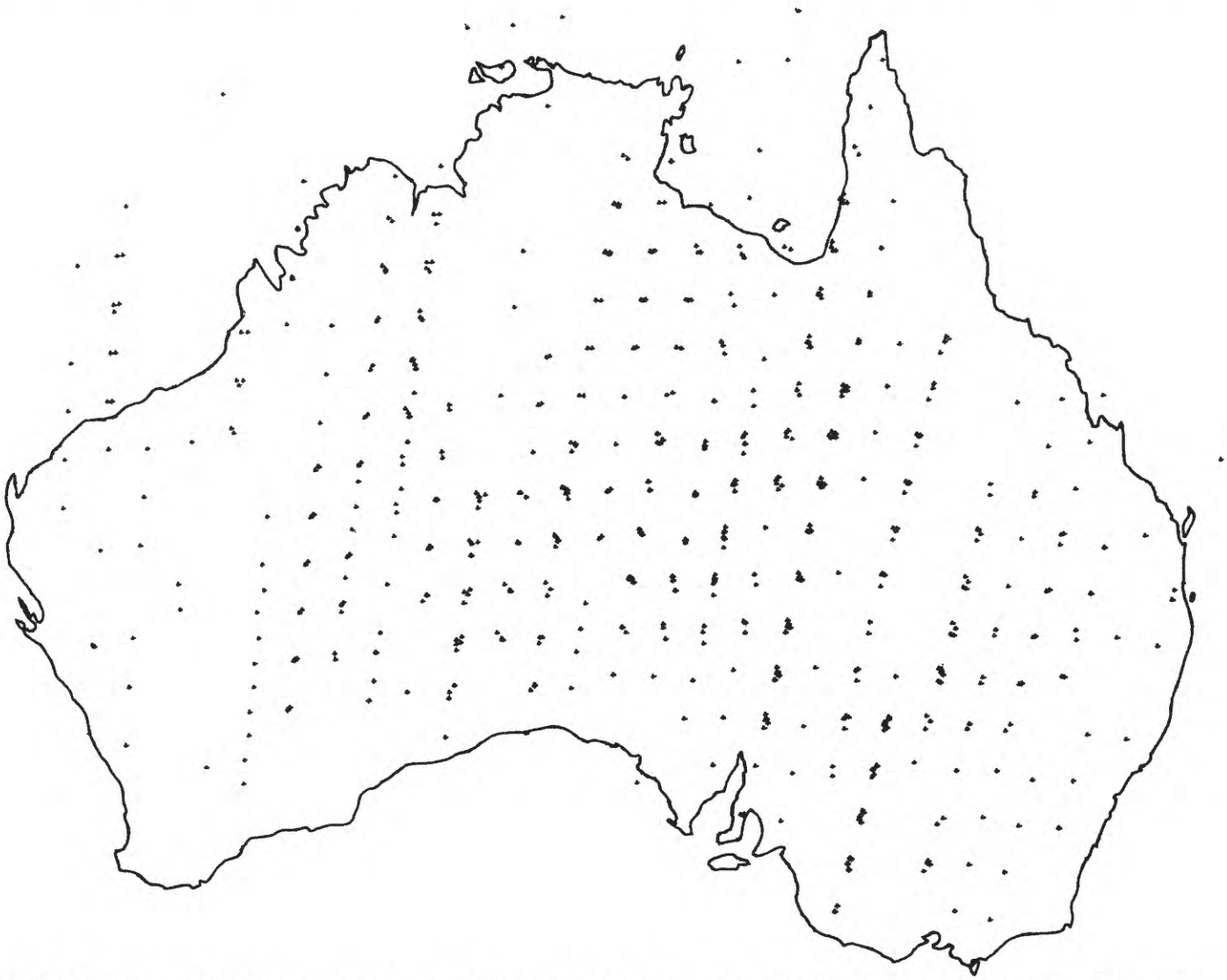

FIGURE 10.—Portion of COFRC world zone map for southeast qu adrant (zone 3). All cloud-free Landsat–1 images of Australia acquired during first 478 days (through 73/11/13) are shown. Index numbers are omitted for clarity. Note scatter of points about nominal centers. Also note areas lacking cloud-free images.

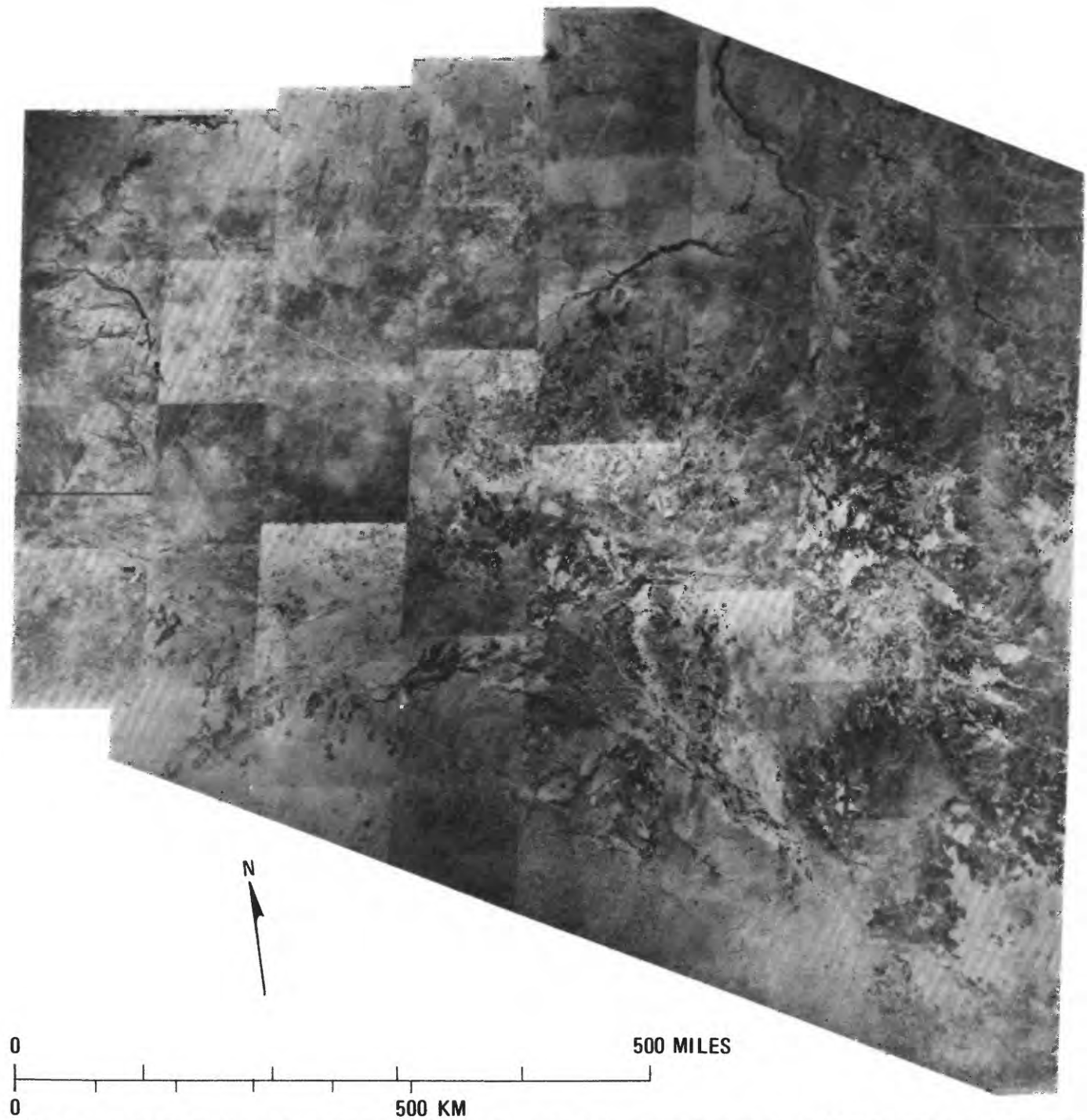

FIGURE 11.—Landsat mosaic of southern part of Sudan, compiled from images selected using COFRC index maps. Courtesy of Chevron Overseas Petroleum, Inc.

images acquired during the first 478 days (through November 13, 1973) by Landsat–1 are shown.

Although Landsat–1 is still in orbit, this time period includes almost all the foreign imagery acquired prior to failure of the onboard tape recorder that stored foreign data until the satellite came within range of an Earth receiving station.

Zone maps such as this are useful for rapidly determining the status of image availability before consulting the individual index maps. Figure 10, for example, shows that parts of Australia, especially in the west, lack cloud-free imagery, and we must resort to higher

degrees of cloud cover, if available, for complete coverage. The clustering of image center points indicate multiple coverage, which is useful information for conducting seasonal analyses of Landsat images. This map also illustrates the typical scatter of image centers from the nominal center points, which was described earlier in the southern Africa example.

APPLICATION

The greatly reduced Landsat–1 mosaic of southern Sudan shown on figure 11 was compiled by Chevron Overseas Petroleum, Inc., from images selected using Index Map 9. The 55 cloud-free images were selected in a short time by this method. The images were also selected to cover the same season of the year to provide optimum uniformity for the mosaic. The Landsat mosaics are especially valuable in areas lacking adequate base maps. Towns, roads, drainage, and other features important to field operations are commonly presented in more detail and accuracy than on existing maps. The major problem is that the latitude and longitude marginal annotations on the images are not accurate.

SUMMARY

The COFRC index map system is a rapid and reliable method for locating Landsat images of any area in the world. It eliminates the time-consuming, tedious, and error-prone manual sorting and plotting of the 100,000-plus Landsat–1 and Landsat–2 images. The maps are readily updated as new imagery becomes available.

Being a private research institution, COFRC does not have the capability to provide index maps or programs. The concepts described here, however, should be sufficient for computer-oriented users to prepare their own index maps.

PROCEEDINGS OF
THE FIRST ANNUAL WILLIAM T. PECORA MEMORIAL SYMPOSIUM,
OCTOBER 1975, SIOUX FALLS, SOUTH DAKOTA

Intercrossing Crustal Structure and the Problem of Manifestation of its Deep-Seated Elements on the Surface [1]

(as exemplified by Tien Shan and the Turan plate)

By V. I. Makarov and L. I. Solov'yeva,
Geological Institute of the USSR Academy of Sciences,
Moscow, U.S.S.R.

ABSTRACT

Recent years have been characterized by an ever increasing inculcation of means of space technology, including those of space imagery (photography and television), into practice of geological studies. One of the achievements of space geology is the identification of certain elements of deep crustal structure on space images of the Earth. These elements range from the features of buried folded foundation of a platform or ancient complexes of folded mountain systems down to those of the Conrad discontinuity and the Mohorovicic discontinuity (Lowman, 1966, 1968; Skaryatin, 1970; Bashilova, 1971; Bashilova et al., 1972; Makarov et al., 1974; a number of papers published in "The study of natural environment by space means" (1973), v. 1 and (1974), v. 2; also papers published in the Soviet journal "Izvestya Vysshikh Uchebnykh Zavedenii, ser. geologiya i razvedka" (1973), no. 7; (1974), no. 12; (1975), no. 2.

At the same time, many investigators still have their doubts regarding the validity of such identification, questioning the very possibility of seeing through the Earth's crust, especially if the ancient buried structures are concerned, which are supposed to have ceased their evolution a long time ago. These doubts are, to a large extent, due to the fact that the meaning of generalization of an image of the Earth's surface with the increasing distance of its observation is yet unknown. The mechanism, by which information about deep crustal structure is conveyed to the surface, is also unclear. Because it is primarily the Earth's surface that is expressed in the visible band of electromagnetic radiation on space images or, for that matter, on any other photographic or television image, regardless of their scale and their degree of generalization.

This surface, or "the face of the Earth," is a result of the entire history of the geologic development of the continents, which has been imprinted in the character of landscapes. A landscape reflects the resulting geological structure, as transformed by the whole variety of exogenetic processes.[2]

In viewing the geological structure of a surface, one should clearly distinguish its ancient elements from those produced by neotectonic movements. The latter elements have, to a greater or lesser degree, used and transformed the ancient structures. Having thus acquired the specific character of their morphology, they have generated the main features of the terrestrial relief, which are, in turn, the basic elements of landscapes and which are expressed in space images. Reflecting primarily the total result of neotectonic deformations of crustal layers, the relief, first of all, conveys the largest amount of information about the youngest structure, including the deep-seated one.

[1] Printed verbatim as received from the authors, except for minor changes in format and spelling.

[2] The role of the exogenetic factors in landscape formation is not considered here, as we are discussing not the differences in manifestation of identical structural forms in different climatic zones, but the principle of their manifestation; for example, under similar climatic conditions.

This fact manifests itself very distinctly in the areas of intensive orogenesis, where it is not uncommon that the total amplitude of the vertical movements exceeds 5 or even 10 kilometres and where separate fragments of once unbroken ancient complexes have been found displaced with respect to one another by hundreds or even thousands of metres. New forms have become distinctly pronounced both in relief and structure, for example, warpings of great radius of curvature combined with and complicated by faults of various orders of magnitude. At the present time, by using diverse methods, among them the geomorphological ones, it has been established that the neotectonic deformations of the Earth's crust and its surface manifest themselves everywhere not only in the mountain areas, but also on the plains, in the platform areas.

We think it necessary to emphasize that the deep-seated structures of contemporary platforms and fold-mountain regions represent chiefly the youngest deformations of deep crustal layers, which reproduce, in near-surface layers, only some individual features of their Hercynian, Caledonian, or more ancient structures, which have been transformed by the processes of subsequent geotectonic cycles.

Another important, though not so prominent, endogenous factor affecting landscape formation is the geochemistry of the Earth's surface, which is decisively predetermined by the chemical composition of more or less ancient substratum, as well as by the fluids that have ascended toward the surface from various depths and that appear to yield some information about both their sources and those layers through which they have passed.

From this standpoint, the study of deep-seated crustal structures by analyzing their surface manifestations, in particular those observed on space images, appears quite realistic and highly promising.

I

Interpretation of space images, obtained for various regions of the Earth's surface and by various investigators, has revealed a dense network of different-trending, intersecting lineaments of various orders of magnitude, which can be found in every area. These lineaments partly correspond to zones of more or less significant crustal fractures, which have been recognized (or are supposed) from various geologic and geophysical data. When placed on the crustal structure pattern depicted on the previously published geologic maps, these lineaments have especially clearly indicated the superimposed character of structure both of fold-mountain and platform regions, thereby revealing new structural relationships between their elements. Such a valuable quality of space images as their great coverage favours the long-attempted explanation of the regional and planetary regularities governing the spatial arrangement of variously scaled forms of tectonic structure and relief. More or less distinctly formulated in their various versions, the concepts of superimposed crustal structure have their roots deep in the history of geology (Elie de Boumont, 1830; Buch, 1867; Karpinsky, 1883; Argand, 1924). Properly speaking, it is a question of the principal deformational trends of the Earth, which in the long run determine the complicated mosaic of the Earth's surface.

The conceptions of spatial and temporal regularities governing the surface manifestations of some or other deformational directions are various. There are two extreme concepts maintaining either that the different-trending dislocations have occurred at different periods of time and that they may be associated with one or another tectonic stage or that they took place during a single period of geologic time and that they are conjugated, differing only in the intensity and form of their manifestation. In the spatial aspect, these tectonic trends are considered by some investigators as either local or regional, while the other classify them as planetary.

In recent years, the concepts of superimposed crustal structure have been developed essentially along two lines. The first of them is concerned with planetary jointing (Shults, 1966, etc., see also in "Planetary Jointing"), the other is dealt with in an ever-increasing number of papers devoted to the so-called transverse structures. Of particular interest is the study of the transverse structures, because they are ore-concentrating and seismically active. Such studies, stressing one or another aspect of the problem, have been carried out in the Caucasus (I. V. Anan'in, M. G. Lomize, M. A. Kashkai, and G. P. Tamrazyan, E. E. Milanovsky, L. M. Rastsvetaev, V. Z. Sakhatov, V. G. Trifonov, V. E. Khain, Yu. K. Shchukin, and others), in Kazakhstan and the Soviet Middle Asia (N. P. Kostenko, V. I. Knauf, N. V. Lukina, V. I. Makarov, R. I. Pavlov, E. I. Patalakha, K. D. Pomazkov, D. P. Rezvoy, Z. A. Svarichevskaya, V. M. Sinitsyn, L. I. Solov'yeva, O. K. Chediya, G. N. Shcherba, Yu. K. Shchukin, and others), in the region east of Baikal and in the Primorski Territory (M. A. Favorskaya, E. P. Izokh, I. K. Volchanskaya, N. T. Kochneva, E. A. Radkevich, I. N. Tomson, and others). Much evidence for the transverse zoning, transverse folding, and local transverse structures has been reported also for other regions, both

fold-mountain and platform. The transverse or cross-cutting [3] structures, the existence of which is still debated by many geologists, have been distinctly delineated on space images and, finally, they have attracted attention of numerous geologists, geophysicists, and geomorphologists.

In what follows, we consider some elements of the youngest superimposed crustal structure, as exemplified by Tien Shan and the adjacent areas. The Paleozoic structure of the Soviet Middle Asia and Kazakhstan very clearly suggests that the structural character of the Paleozoic basement of the epiplatform orogen of Tien Shan and that of the Turan platform are common (Petrushevsky, 1955). The area of Caledonian folding, which is bounded in the south by the Karatau-Turgai deep fault, forms a smooth arc embracing the northeastern margin of the Turan platform and Northern Tien Shan. Parallel to this area, the zones of Hercynian folding also form arcs extending from the north, from the Urals and Turgai through the Turan plate into the region of Tien Shan, where they occupy the central and southern areas.

So far as the general plan of the above-mentioned concentric arcs of different-aged folding of Paleozoic basement is concerned, the Tien Shan orogen occupies the southeastern sector, the northwestern sector being taken up by the Turan plate. The boundary between these sectors is formed by the western Tien Shan geosuture zone, which has first been delineated by A. V. Peive (1947) and which has been characterized subsequently by O. M. Borisov (1962, etc.), D. P. Rezvoy (1962, etc.), B. B. Tal-Virsky (1964–1972), and by a number of other investigators.

TIEN SHAN

The Tien Shan sector belongs to the planetary Sayany-Hindu Kush (or, according to D. V. Nalivkin, 1936, Turkestan-Sayany) belt of epiplatform orogenesis, stretching along the northeastern trend from the Hindu Kush to Baikal and intersecting the area of finished folding of various ages. The first-order elements of the youngest structure of Tien Shan are represented by sublatitudinal and northeast-trending system of uplifts and troughs, which are fractured and faulted crustal upwarpings and downwarpings of large radius of curvature. They are formed by linearly extending zones of young elevations and depressions, that is, by second-order structural elements. The latter, in turn, are represented by en echelon conjugated, individual depressions or elevations, which, in general, are independent megafolds of lesser radius of curvature (according to S. S. Shults, basement folds) or their fragments.

Within the general framework of the neotectonic structure of Tien Shan, any area can be characterized by a simultaneous manifestation of two or more structural trends (Makarov and Solov'yeva, 1975). But to this characteristic one should add that, of several intersecting trends, one or, less frequently, two stand out like the principal ones, determining the strike of a structural form as a whole and its overall configuration in plan, whereas the other trends are subordinate, forming merely details of its structure and morphology. In various districts of Tien Shan this principal trend varies from sublatitudinal to northeastern and northwestern. In previous publications, when analyzing the youngest structure of the Susamyr-Dzhumgol district of Northern Tien Shan, we paid attention to the intensive fragmentation, mosaic arrangement, as well as isometric, often rhombic outlines of individual elevations and depressions. We believe that these features have been predetermined by the presence of two intersecting structural trends of about equal intensity, one of which is sublatitudinal and the other northwestern (Kostenko et al., 1972).

The northeastern trend plays the principal role in Southeastern Ghissar, in the Ugam-Chatkal system of elevations, and also in the eastern part of Central Tien Shan. In other areas, this trend is less pronounced, interrupted, or local. At the same time, it should be mentioned that the northeast-trending deformations, which do not always give rise to independent structures (at least, obvious ones), run through the entire orogenic region and can be traced into the adjacent platforms (fig. 1). Omitting the characteristics of northeast-trending zones, which have been given in our preceding paper (Makarov and Solov'yeva, 1975), we only note that in elevation systems this trend manifests itself as alternating zones of gentle uplift and relative subsidence, which are conjugated with cross-cutting fractures. When going out into depressions covered by Mesozoic and Cenozoic sedimentary rocks, this trend is no longer subsidiary, but becomes principal. It should be borne in mind, however, that not everywhere the northeastern trend is neogenetic. It was distinctly pronounced already in the orientation of Hercynian linear zones of geosynclinal troughs and uplifts (Chatkal, Atbash, Eastern Kokshaal, and other ranges). This trend manifested itself also as zones of cross-cutting faults during the late Hercynian stage of

[3] The latter term we consider to be more exact when we have in mind various discordant structural trends, only some of which are in fact transverse.

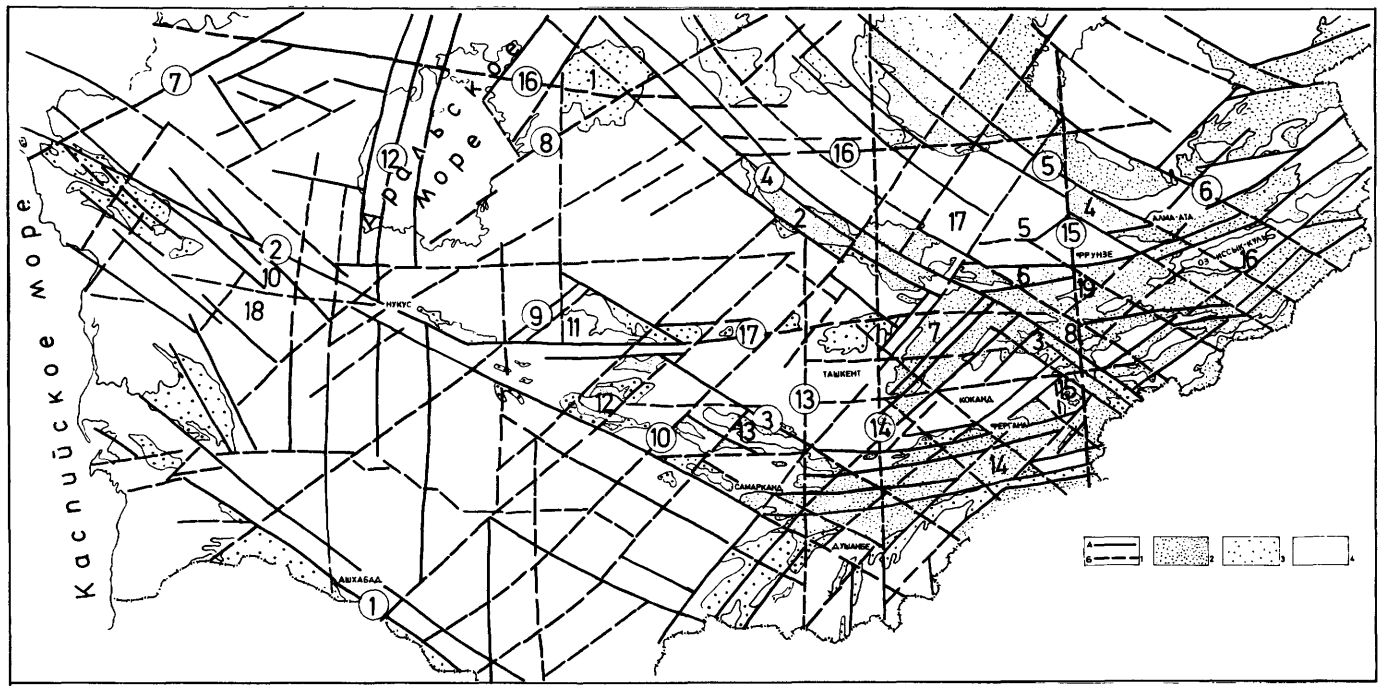

FIGURE 1.—Scheme of intercrossing structure of the Turan platform and Tien Shan based on the results of interpretation of space images, structural analysis of the relief, and geologic data.

1—Crustal fractures and crustal zones of ruptural-flexural dislocations determining the trend and configuration of the neotectonic structural forms (a, leading; b, subordinate); 2—surface exposures of Paleozoic and Pre-Paleozoic rocks; 3—areas of outcropping Mesozoic deposits; 4—areas of outcropping Cenozoic deposits.

The names of structural forms mentioned in the paper. Fractures or zones of ruptural—flexural dislocations (denoted by ciphers in circles): 1—Kopet Dag; 2—Mangyshlak—Central Ustyurt; 3—Nuratau; 4—Karatau—Fergana; 5—Dzhalair—Naiman; 6—Aksu—Ili; 7—Southern Emba; 8—Sarykamysh—Uspensk; 9—Western Bukantau; 10—Western Nuratau; 11—Western Tien Shan; 12—Aral; 13—Turkestan-Akchai; 14—Keles—Oksu; 15—Karakul—Balkhash; 16—Emba—Chu; 17—Taldybulak.

Neotectonic elevations: 1—Dzhusaly; 2—Karatau; 3—Fergana; 4—Chu—Ili; 5—Kuragata; 6—Kirghiz; 7—Ugam—Chatkal; 8—Moldotau; 10—Karabaur; 11—Bukatantau; 12—Zirabulak; 13—Nuratau; 14—Ghissar—Alai; 15—Aldyyar—Namazdek; 16—Orgocher—Dzhetyoguz.

Neotectonic depressions: 17—Chu; 18—Southern Mangyshlak-Ustyurt; 19—Susamyr; 20—Fergana.

orogenesis (Pavlov, 1972; Voronich, 1964; Porshnyakov, 1973). The trend is well-pronounced in the seismicity of the region, too (fig. 2).

The northwest-trending structures, like the northeast-trending ones, are expressed also as zones of elevations, depressions, and cross-cutting fault-and-flexure dislocations. Within Tien Shan, the Karatau-Fergana zone of elevations, which is conjugated with a deep fault zone, is morphologically best pronounced. The manifestation of other zones is less certain; however, these zones can be recognized by structural and geomorphologic analyses as well as from a number of indirect indications (Kostenko et al., 1972). In contrast to the northeastern trend, the northwestern is not recognized as the principal one within the mountain structure of Tien Shan, with the exception of the Fergana Range uplift. But beyond the system of deep marginal faults, forming its northwestern boundary, this trend in places becomes principal.

Such are elevations of the ranges Nuratau, Karatau, and Chu-Ili mountains, which are conjugated with deep fracture zones (Nuratin, Karatau, and Dzhalair-Naiman). These fracture zones appear to be planetary. They are repeated every 300 or 400 km, dividing Tien Shan into several sectors of different strikes, different morphology of the modern structure, and also different regime of tectonic movements. Between these global zones, there occur the transverse zones of regional significance, which are spaced at 50 or 60 km intervals (Makarov and Solov'yeva, fig. 1).

The northwestern trend of the modern structures of Tien Shan, like the northeastern one, inherits more or less completely (and with different intensity in different areas) the Caledonian and Hercynian structures.

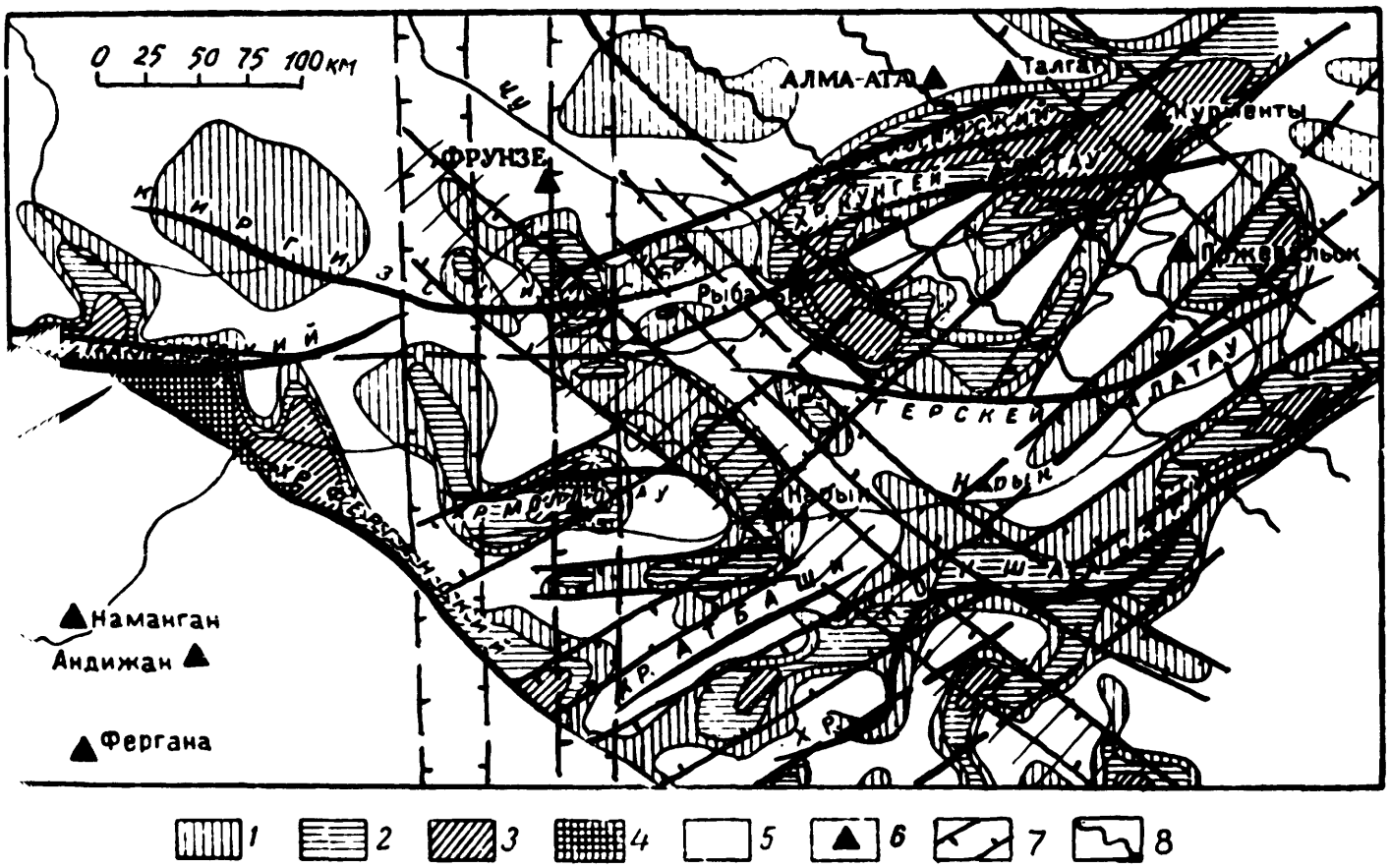

FIGURE 2.—Scheme showing the location of zones of higher seismic activity in Northern and Central Tien Shan. According to V. I. Knauf (1962) and supplemented by data of the present authors.

1 through 5: The number of earthquake epicenters per 625 km² registered between 1929 and 1956 (after Knauf, 1962): 1—from 1 to 2; 2—from 2 to 4; 3—from 4 to 8; 4—from 8 to 16; 5—epicenters undetected; 6—seismic stations; 7—zones of increased seismic activity; 8—Barskaun and Orgocher zones of cross-cutting dislocations recognized using other criteria (Makarov and Solov'yeva, 1975).

The maximum density of earthquake epicenters is observed at the knots of zone intersections.

In the latter, this trend has also manifested itself in various regular "disturbances" of longitudinal (main) structural elements, including zones of higher mobility and permeability of the Earth's crust, which are marked by a regular spatial arrangement of magmatogene formations (Pomazkov, 1962). The other important indications are a considerable narrowing or even (which is not uncommon) wedging out of Paleozoic troughs in elevated zones. On the other hand, relatively lowered transverse zones are characterized by broadened areas of Late Paleozoic troughs, in particular, by red-coloured, residual and superimposed troughs, as well as by fields of development of Paleozoic volcanic rocks. Right-lateral flexural warpings of Paleozoic structure-and-facies zones and marginal faults, concentrations of Late Paleozoic faults, as well as the manifestation of the anomalous northwestern trend of minor folds in the Paleozoic basement, are all confined to zones of recent fault-and-flexure dislocations.

The recent zones of northeast- and northwest-trending fractures, which intersect sublatitudinal Paleozoic zones, are incorporated in the ancient structure in such a manner that they inherit northeastern or northwestern fragments of Paleozoic fractures where the latter are geniculately curved.

Let us discuss at greater length the characteristics of some north-south-trending elements of the recent structure of Tien Shan, because this trend and those close to it have been studied here less than the other ones, despite the fact that they deserve considerable attention.

Within the area under consideration and within the adjacent territories, the north-south trend is practically nowhere the leading one, though it determines many important features of different-trending structures, as

well as the relationships between them. In general, it manifests itself as zones of higher jointing and fragmentation, faults, flexures, and, associated with them, more or less pronounced negative undulations of basement folds, and also as other structural and morphological features, thus enabling us to associate with this trend a preferable tension stress.

As an illustration, let us consider the Karakul-Balkhash submeridional [4] zone of dilatation. On small-scale space images, with the aid of which this zone has been detected (Skaryatin, 1973; Makarov and Solov'yeva, 1975), it appears as a lineament zone [5], which can be traced with some interruptions from the Hindu Kush through the Pamirs and Tien Shan. This zone is especially prominent in the area extending from the Karakul lake in the Northern Pamirs to the western end of the Balkhash lake. It will be noted that the latter trends here correspondingly and also has the maximum width. It seems that the confinement of the lake basin to the lineament zone is not coincidental, since the structures of relative subsidence are its main feature, at least, so far as Cenozoic is concerned. This is a wide submeridional trough [6] between the Kuragata swell of the Muyunkum region and the Kendyktas uplifts (which form a structurally single zone). Here the basement of the Eastern Chu trough occurs at the greatest depth. Also, a wide bench of young piedmont elevations, which are developed to the east, at the foot of the Kirghiz Ridge, falls off abruptly here (incidentally, this repeats the difference in the hypsometric position of Paleozoic basement in the Kendyktas-Kuragata elevation zone). Farther to the south there follow the meridional through-going valleys of the Karabalty and Aksu Rivers, which cut through the situated en echelon and going far behind one another structures of the complicated Kirghiz Ridge. These valleys become aligned, which is accompanied by an abrupt broadening of the Susamyr trough jutting out far to the south as a wide bay. Here the Susamyr trough is superimposed on a series of sublatitudinal and northeast-trending, relatively narrow basement up- and down-warpings of the Susamyr-Dzhumgol system. This superposition (or rather interference) has given rise to an abrupt subsidence of anticlinal structures, as well as to the deepening and geomorphologic merging of synclinal zones.

Still farther to the south, the Karakul-Balkhash zone is marked by a distinctly pronounced negative undulation of the Kokirim-Moldotau anticlinal zone, to which a meridional antecedent gorge is confined (through this gorge the rivers of the entire Naryn basin are drained from the Naryn system of intermontane troughs into the Toktogul and, then, into the Fergana troughs). Still farther to the south, there lies the triangle of the Toguztorau trough, which, in many features, is similar to the Susamyr trough.

Changing its direction apparently in the zone of Talas-Fergana deep fault and in the conjugate diagonal zone of elevations, the Karakul-Balkhash lineament zone goes out into the Pamirs through the Gulcha graben in the Alai system of elevations and through the Kyzylart depression in the structure of the Zaalai elevation. Within the Pamirs, the lineament zone is also marked by negative deformations, in particular, by the basin of Karakul lake. This part of the Karakul-Balkhash zone seems to correspond to a deep division between the Western and Eastern Pamirs, which has been described by B. A. Petrushevsky (1961, 1969), V. N. Krestnikov (1961, 1962), N. P. Kostenko (1964), and L. P. Vinnik and B. A. Lukk (1974). One may suppose that the Karakul-Balkhash submeridional zone is linked directly with the Hindu Pamirs deep fault zone (B. A. Petrushevsky, 1969), which can be traced far to the south in the structure of the Hindustan platform and the Indian Ocean.

When tracing the Karakul-Balkhash zone northward, one may suppose that its continuation is fixed by the major bends of the Irtysh valley near Omsk, going out, through the system of the Great Yugan, into the Surgut area and farther north into the Ob Bay. The complex of data, which is available for this zone and which has partly been outlined above, enables one to describe it with sufficient certainty as a part of the planetary zone of deep-occurring tension.

Another major submeridional zone, characterized by flexures and breaks in continuity, has been interpreted on space images in the area of extreme western spurs of Tien Shan, about 500 km west of the Karakul-Balkhash zone. This is the Turkestan-Akchai lineament zone (after V. D. Skaryatin, 1973). The previously published geologic and geomorphological characteristics of this zone (Makarov, 1973, 1974) permit us to regard it as a tension zone, too. As an interesting detail, which has not been noted before,

[4] It should be mentioned that the submeridional lineaments found in the Pamirs and Tien Shan mostly tend somewhat to the east (clockwise).

[5] By the lineament zone we understand here sufficiently long (on a regional scale) bands of concentration of comparatively short lineaments, which intermittently follow one another (often en echelon) along the strike of the zone.

[6] To this trough a submeridional part of the Chu river valley is confined, which has a clear antecedent behaviour and in which a wide fan of streams flowing from the northern slope of the Kirghiz Ridge converges.

we can mention the probably genetic confinement to the zone of numerous large karst caverns in the massive (massif, ed.) of the western slope of Kugitangtau. Measurements of strikes of the karst caverns made in one of them have revealed their general confinement to and extension along meridionally striking cracks, which can clearly be seen on the cave ceiling. The measurements have also revealed their confinement to the places of intersection of meridionally striking cracks with WNW–ESE ones.

A less prominent submeridional fault-and-flexure zone can be recognized on small-scale phototelevision space images for the area lying somewhat to the east. This is the Keles-Oksui zone, which distinctly bounds the Ugam-Chatkal elevation system and clearly separates benches of relief of different height. The contrast in their elevations somewhat decreases within the Ghissar-Alai elevation system, though it still remains quite perceptible.

This brief outline of the Tien Shan recent structure indicates that it is constituted by the forms of diagonal and orthogonal trends, conjugated and simultaneously manifested practically everywhere, although these manifestations are different, as is their intensity. And the trends of structures of different order do not coincide generally. The study of numerous examples of different orientation of structural forms of different orders has shown that one of the causes of this phenomenon resides in the peculiar transformation and adaptation of Paleozoic structures to the recent process of orogenesis.

THE TURAN PLATE

The superimposed structure of Tien Shan passes directly into (and is continued by) a similar structure of the region of less active neotectonic movements lying to the north and northwest the Turan plate and Central Kazakhstan (fig. 1).

The Turan plate together with the outer troughs setting off the epiplatform orogen of Tien Shan, is characterized by a highly differentiated mosaic structure of its sedimentary cover and basement.

Vast domes and troughs representing here first-order structural forms, have outlines, which can be called isometric only in a general sense. Actually, their outlines are highly complicated, abounding in numerous protrusions and "bays," which are well reflected, for example, on "The map of neotectonics of the South of the USSR" (1972). Analysis of this map, as well as of various geologic, geophysical, and geomorphological data, enables one to conclude that all the above-mentioned complications are caused by the mutual superposition and interference of zones of uplift and depression of several trends. In the order of decreasing activity, these trends are northwestern, northeastern, submeridional, and sublatitudinal.

The northwestern trend corresponds to the strike of the Caucasus-Kopet Dag alpine epigeosynclinal orogen bounding the Turan plate from the southeast. The northeastern trend is parallel to (and, probably, closely linked with) the Sayany-Hindu Kush belt of epiplatform orogenesis. The orthogonal trends are subordinate, manifesting themselves only as fragmentary segments. The intensity of manifestation of all these trends decreases from south to north, or, to put it more exactly, in the direction running from the orogens—Sayany-Hindu Kush in the eastern sector and Caucasus-Kopet Dag in the western one, which are separated by the Urals-Oman meridional planetary zone of troughs and dislocations (Argand, 1924; Furon, 1941; Amursky et al., 1966).

The superimposed character of the platform structure is best pronounced in the Mangyshlak-Ustyurt and Karatau-Kyzylkum regions representing the most active and elevated parts of the plate.

The northwestern trend, which, as has been mentioned above, manifests itself in Tien Shan mostly indirectly, gives rise to independent structures beyond the "official" boundary of Tien Shan. There are, first of all, the Dzhusaly-Karatau and the Mangyshlak-Nurata systems of elevations.

The Dzhusaly-Karatau system, sharply limited in the northeast by the Karatau-Fergana planetary fault zone, is well traced in the sedimentary cover and relief structure from Tien Shan to the southern termination of the Urals. The development of this system of elevations in the relief has led to isolation of the river valleys of Turgai, Sarysu, Chu, and Talas from the Aral Sea basin, which started in Late Pleistocene. This resulted in the formation of a chain of drainless basins in the relief, which distinctly mark, as can be seen also on space images, a synclinal zone cojugated with the elevation system.

About as far as the lower course of Sarysu, the elevation zone under consideration runs along the boundary of the Ulutay-Northern Tien Shan region of occurrence of Caledonian structures, inheriting their trend. But farther it can be traced directly to the northwest and is sharply discordant with the edge of the Caledonian massive (massif, ed.), which deflects here northward forming an arc (the Ulutau Ridge). The Dzhusaly-Karatau elevation system, which generally sinks toward the northwest, in this area is somewhat uplifted and expanded, thus giving rise to

the isolation of the so-called Dzhusaly dome. The dome is situated at the intersection of the elevation zone under consideration with the less distinctly manifested zone of elevations of the northeast trend, to which, in particular, the Sarysu-Teniz divide is confined. It should also be noted that some features of the overall configuration of the Dzhusaly dome have been predetermined by the fact that it was, as it were, inscribed in a grid formed by intersecting fractures belonging to the two above-mentioned elevation systems, as well as by less developed orthogonal trends (fig. 3, example 5). The knots of intersection of some fractures are marked by minor salt-bottom depressions, which set off the dome in a chain.

The Mangyshlak-Nurata linear system of elevations is confined to the Mangyshlak-Central Ustyurt deep fault, representing a link in the Donets-Tien Shan belt of deep crustal dislocations (Karpinsky, 1883). Against the background of general subsidence of the system from the southeast to the northwest, it undergoes, like the Dzhusaly-Karatau system, repetitive undulations of various orders of magnitude. The most significant subsidence occurs in the Urals-Oman submeridional zone and also in the similarly trending Caspian belt.

Transverse troughs of much less order are clearly expressed in the neotectonic structure of the eastern part of the zone in question, which borders on Tien Shan and which represents a direct structural and orographic continuation of the Turkestan-Alai elevations. The transverse troughs may be typified by the Western Nuratau group of troughs (between the Zirabulak-Nuratau and Central Kyzylkum elevations) and the Tadzhikazgan depression, separating the elevations of Central Kyzylkum from those of Sultan-Uizdag. These troughs separate and emphasize in the relief the areas of positive undulations of Zirabulak-Ziaetdin mountains, Gobduntau, Nuratau, Central Kyzylkum, Sultan-Uizdag, Karabaur, and Mangyshlak, which form in the general system of elevations a series of sinistral and dextral en echelon structures (fig. 4).

Analysis of spatial arrangement of cross-cutting deformations has revealed that they are confined mainly to more or less extensive zones of relative uplift and subsidence of northeast trend. In contrast to the similar structures of northwest trend, they, however, do not give rise to sharply distinct independent structural form. An exception to this rule is the outward, marginal area of the Turan plate which borders on the epiplatform orogen of Tien Shan. The zones of cross-cutting lineaments, parallel to the Western Tien Shan

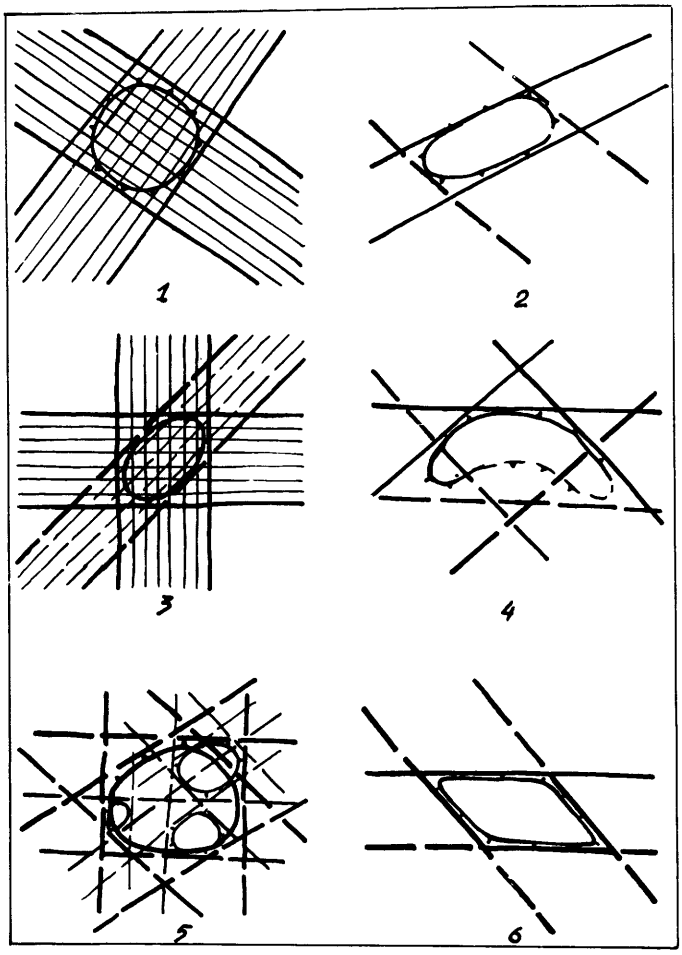

FIGURE 3.—Some examples of interference between the elevation (depression) zones of various trends.

1—Principal structural trends; 2—subordinate structural trends; 3—the same for subsidiary structures; 4—generalized contours of local elevations (depressions); 5—axes of local elevations (depressions); 6—not explained [ed.].

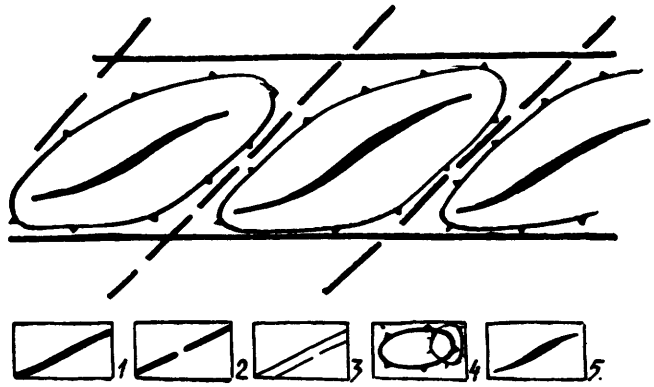

FIGURE 4.—Scheme of echelon-like structure of elevation (depression) zones.

1—Principal structural trends; 2—subordinate structural trends; 3—the same for subsidiary structures; 4—generalized contours of local elevations (depressions); 5—axes of local elevations (depressions).

deep-seated geosuture, confined, as it were, the steps of progressively expanding Tien Shan Uplift, a consistent penetration of its fore-uplifts into the platform, which takes place primarily along the above-mentioned zones of northwest trend. The northeast-trending zones of elevations, representing the direct continuation of Tien Shan elevation zones, have been formed parallel to the zone of the deep geosuture in the structure of sedimentary cover of marginal troughs of the platform (Tashkent, Beshket, etc.).

Within the inner parts of the Turan plate, the significance of the northeast trend is much lower. On space images received from the space ships "Soyuz-8" (cosmonauts V. A. Shatalov and A. S. Eliseyev), "Soyuz-9" (cosmonauts A. G. Nikolaev and V. I. Sevast'yanov), "Soyuz-12" (cosmonauts O. G. Makarov and V. G. Lazarev), and from meteorologic satellites of "Meteor" type, one can clearly trace the highly extensive Western Nuratau and Sarykamysh-Uspensk lineament zones, as well as a series of regional northeast-trending lineaments of Ustyurt and Mangyshlak, which have first been recognized with the help of space images (see also, Beregovoi et al., 1972; Bogorodsky et al., 1973; Florensky, 1973; Abrosimov et al., 1974; Makarov et al., 1974).

The Western Nuratau lineament has been called so provisionally, after the zone of regional transverse dislocations, which is situated at the western termination of the Zirabulak and Nuratau elevations, described and named by R. I. Pavlov (1972). This lineament is a fragment of a lineament zone of the same name, which can be traced to the southwest through the lower course of Zeravshan river and the delta of Murgab river in the direction of the Meshkhed basin in Iran. Toward the northeast, the lineament is traced in the low of the Karatau Ridge, corresponding structurally to an area of conjugation between two echelons. Within the Chu-Sarysu syneclise the lineament limits the Akkum-Talas elevation.

The Sarykamysh-Uspensk lineament zone bounds from the southeast the mountains of Tuarkyr and the Ustyurt Plateau, controls (fixes) the southeastern coast of the Aral sea. It can farther be traced through a sharp bend of the Syr Dar'ya river along the southern flank of the Mynbulak depression, where it is marked in the relief by a straight-line "chink" (border scarp) and by a "thousand springs" (Mynbulak) at its foot. Within the Central Kazakhstan massive (massif, ed.) the lineament runs through the upper part of the Sarysu valley and, apparently, through the Uspensk crush zone (Suvorov, 1968) or the Spassk crustal fracture zone.

Local lineaments of northeast trend of the Ustyurt and Mangyshlak, which have first been recognized on space images, are identified (Bogorodsky et al., 1973; Florensky, 1973; Abrosimov et al., 1974) as regional fractures in the basement. This is evidenced by the configuration of gravity and magnetic anomalies within the area (Artamonov and Isayev, 1971). Moreover, the lineaments are distinctly inscribed in the structures of sedimentary cover, which have been recognized from deformations in reflecting horizons.

The orthogonal trends in the structure of the Turan plate have little been studied so far. *The meridional* trends of fracture and fold structures are especially marked in the structure and relief of the Turan plate in the zone of the Urals - Oman lineament, where they play the part of the principal trend of dislocations. West and east of this zone, these trends gradually grow weaker. For example, within the Ustyurt Plateau these trends already manifest themselves as subordinate (Bogorodsky et al., 1973).

The sublatitudinal trend is expressed within the Turan plate by several extensive lineaments, which have been identified on space images as the Southern Mangyshlak, Erbent-Donguzsyrt, and Karabal crustal fractures belonging to the extensive system of Southern Mangyshlak-Ustyurt troughs.

Let us consider the morphology of superimposed structures of the platform regions by taking the Central Ustyurt Plateau as an example.

The recent elevations of the Mangyshlak-Karabaur system have the west-northwest (sublatitudinal) trend, running along the Mangyshlak-Central Ustyurt deep crustal fracture zone, which has been developed during a long time. However, just as it has been mentioned for the Tien Shan elevation systems, individual elevations of Karatau, Western Chink, and Karabaur, constituting these systems, appear here as dextral echelon-like structures of northwest orientation, making an acute angle (about 30°) with the fracture zone and the elevation system as a whole. Only the core of the Karatau anticlinorium, composed of Permian and Triassic rocks, strictly retains the strike of Paleozoic crustal fracture. But, as the interpretation of space images from "Soyuz-12" has revealed, it is also dissected by a system of recent northwest-trending fractures and, like the structures of the upper stage, forms a system of dextral echelon-like structures.

Zones of highly extensive lineaments of northeast and, more seldom, submeridional trends, which intersect the Central and Southern Ustyurt and which have been recognized on space images (Bogorodsky et al., 1973), fall within the transverse zones of relative sub-

sidence, embracing transverse troughs isolated both in the relief and in structure, while the elevation system as a whole undergoes gentle subsidence at the intersection with these zones. Local structures forming the elevation system are arranged here in echelons.

Thus, the systems of intersecting trends, developing in time and space and represented by flexure-and-fault zones (these zones correspond to relative lows in structure and relief) and by zones of elevation, underlie the highly differentiated mosaic structure of the Turan plate. Where the intersecting zones of different sign (up and down) are superimposed, there occur structures of intermediate amplitude, whereas in places of mutual superposition and interference of different-oriented structures of the same sign there are formed either the lowest (− −) or the highest (+ +) structures of the basement and its mantle. And, as the analysis of superimposed structure has shown, the areas of maximum uplift or subsidence correspond to the triple coincidence of structures of the same signs. For example, the Sarykamysh depression, which is an area of intensive contemporary subsidence (absolute elevation of its surface is minus 38 m), lies at the intersection of regional depressions: the northeast-trending Sarykamysh-Uspensk zone, the sublatitudinal trough system of Southern Mangyshlak and Ustyurt, where the Paleozoic basement occurs predominantly at depths between −3,000 and −5,000 m, and the highly extensive submeridional trough zone of Sarykamysh and Barsakelmes. As a rule, the boundaries of structural forms are predetermined by the framework in the interfering zones. The interference pattern of different-trending zones of elevations and troughs just considered is completely analogous to that observed in the Pamirs and Tien Shan (Kostenko, 1964; Chediya, 1964; Kostenko et al., 1972; Makarov, 1969; Solov'yeva, 1971; Makarov and Solov'yeva, 1975), evidently representing a general regularity.

Thus, it is clear that in the overall superimposed crustal structure of both platforms and orogens, the localization, configurations, boundaries, and orientation of structural elements have been predetermined. The configuration and orientation of structural elements is determined by the most intensively developing trend. Within Tien Shan, under the conditions of intensive vertical movements and horizontal compression there have been formed different-trending linear structures naturally inscribed in warpings of large radius of curvature. The influence of superimposed trends has manifested itself in the echelon-like character of linear structures of all orders: systems, zones, and local forms. It can be noticed that the width of the linear structures is inversely related to the degree of compression, which is maximum in zones of transverse elevations. The length of structural forms is dependent upon the manifestation of cross-cutting trends, too. Generally, it is determined by intervals between the cross-cutting zones and by the degree of their manifestation. For example, the cross-cutting zones, giving rise to negative undulations in anticlines break the extensive linear zones of elevations into separate echelon-like links, the orientation of which, being affected by the cross-cutting trends, usually does not coincide with the general strike of the zone. A similar situation can be observed also on the platform, for example, in the Central Ustyurt and in other linear elevations, where subordinate cross-cutting trends are expressed in the orientation of echelon-like structures, constituting the elevation zones.

When equally manifested trends interfere with one another, there arise isometric structures, for example, arches, domes, basins, and other similar attributes of the so-called intermittent folding. And not only in the conditions of weak recent uplift of the platform can such configurations be produced, but also in areas of intensive folding and orogenesis. For example, in Tien Shan, in the southeastern part of the Fergana intermontane trough, there are known the isometric structures of the Aldayar and Namazdek domes, which have been formed under conditions of intensive recent deformations at the intersection of longitudinal (northeastern) and transverse (northwestern) elevation zones. Such are the elevations of Orgocher and Dzhetyoguz in the Issyk Kul' trough.

Analysis of the neotectonic structure of such vast regions as Tien Shan and the Turan plate has convincingly shown that there are no structural forms determined by a single trend, but that they are generally caused by the more or less active development of two (or more) trends. And, as is evidenced by various structural sections, the cross-cutting trends vary both in intensity and with time.

In various stages of development, the overall (principal) trend (configuration) of troughs and elevations may change significantly.

Taking into consideration the peculiarities of interference between different-trending structures is obviously of great practical value, because it provides a basis for a directed structural forecast in searching for a number of useful minerals, in particular, for oil and gas.

A comparative analysis of structural elements, recognized on variously scaled space images of the Cau-

casus, Tien Shan, and other regions, has shown that, as the distance from the object photographed increases (or as the image resolution decreases), the structural elements of the increasingly deeper crustal layers (down to those of the upper mantle) come into focus of space images. And these deep-seated structural elements do not always coincide in trend with one another or with the main elements of near-surface structures. This fact has enabled the investigators to suppose (and this has been confirmed by a variety of geophysical and seismological data) that definite elements of disharmony between different structural stages and crustal layers manifest themselves on space images (Makarov et al., 1974).

The causes of this disharmony are probably different for different crustal layers. For the structural groups of upper crustal layers composed of Phanerozoic and Late Pre-Cambrian sedimentary and volcanic (to a greater or lesser degree metamorphosed) rock complexes, this disharmony has been predetermined by different-trending deformations that occurred in different tectonic cycles. As for the deeper crustal layers and those of the upper mantle, the causes of the differences in the behaviour of their boundaries still remain obscure and may be essentially different.

It should be emphasized that the above-mentioned disharmony is not absolute. One may only point out that separate structural groups of crustal layers are autonomous, but that, at the same time, they are united by certain, more general, structural relationships, which are predetermined, in particular, by interactions between the continental blocks. This structural unity of deep and near-surface crustal layers is supported, in particular, by the similarity between data on tensions in earthquake focuses located at various depths in deep crustal layers and those on tensions manifested in near-surface structures and imprinted in peculiarities of arrangement and morphology of faults and folds. Furthermore, the comparative analysis of structural trends indicates that practically all these trends are inherent to all structural stages. The differences (sometimes, very significant) lie only in the degree of activity and in the form of manifestation of a particular trend. It may be assumed that all these considerations go also for the deeper crustal layers. In any case, the trends observed in them by some or other means are not exceptional and can be detected more or less clearly in structures of upper crustal layers and on the surface. We should like to mention, for instance, a striking resemblance of the surface structure of Central and Northern Tien Shan (fig. 1) with a generalized arrangement of zones of higher seismic activity, which reflect the structure of much deeper crustal layers (fig. 2).

Therefore, not only in plan does the structure of crustal layers display its superimposed character, but also in section. This characteristic should evidently determine and explain many features of the interrelated and inherited development of crustal structures of different ages and depths of occurrence. The essential similarity between the main structural features of platforms and those of orogens, which have passed through different histories of tectonic development, convincingly bears out the conclusions made by S. S. Shults (1971, 1973) regarding the existence of planetary fractures of various orders forming "the canvas on which tectonics embroiders its pattern." Knowledge of such regularities facilitates a purposeful search for structures with which commercial minerals are associated.

II

When studying a possible mechanism of conveyance of some features of deep-seated structure to the surface of the Earth (for it should once again be emphasized that the observer sees principally and primarily the Earth's surface), we come to the conclusion that this conveyance can be realized through mechanical deformations and geochemical transformations of the surface, which are imparted from various depths of the Earth's interiors. It is evident that the gravity, magnetic, and thermal local fields, created by crustal heterogeneities and by processes operating at great depths, play a definite, though entirely unknown role in forming the surface structure and its landscapes. These fields are obvious surface manifestations of the above-mentioned abyssal factors and thus can be of assistance in expressing the latter on space images.

Turning our attention to the problem of how the deep-seated structures can appear through the Earth's surface, we should emphasize that by the deep-seated structures we understand not so much the structures of ancient buried Pre-Paleozoic and Paleozoic complexes and not only deformations of the surface of buried folded basement, but also the modern structure of deeper crustal layers.

The determining factor of the mechanical mode of transmitting deformations from great depths to the surface of the Earth is the continuity of tectonic movements at all levels of the Earth's crust and upper mantle. In this way, most of the structural sutures of quite different orders of magnitude are kept "alive," thus ensuring the crustal plasticity.

Neotectonic deformations of deep crustal layers, (among them quite recent deformations), have caused some distortions in all overlying horizons, comprising the day surface (surface, ed.). The most intensive mechanical transformation of crustal layers and, consequently, of the surface takes place in the regions of modern orogenesis and within young platforms. Within orogens, the total amplitude of the neotectonic movements is as high as 10 or even 15 km; within young platforms it usually does not exceed 2 km. The evolution of the neotectonic structural forms of orogens and platforms, for example, folds of great radius of curvature complicated by faults, has modified the structure and morphology of formations of previous stages of development. In the process, they have to some extent, used elements of old structures, developing in accordance with their trends and inhomogeneities, thereby renewing, though in a new combination, some features of these. Examples of utilization of elements on the Tien Shan Paleozoic structure by neotectonic deformations have been described elsewhere (Makarov and Solov'yeva, 1975).

The study of the recent structure of Tien Shan has shown that the response of various crustal layers to the submeridional compression, which is characteristic of the recent orogenesis of this region taken as a whole, is different. Deep-lying layers, for example, Pre-Cambrian crystalline basement and even deeper layers, which appear to be more homogeneous than the overlying ones, respond to compression by forming rather simple, elongated, in general, normally to the direction of compression, linear folds of basement (as conceived by E. Argand), systems of elevations and troughs, which directly reflect deformations of the Conrad and Mohorovicic deep-seated discontinuities. The deep crustal fractures, which confine the basement folds or are conjugated with them, directly reflect the canvas of the deep-seated structure. They represent deformations of shear and tension. The former are expressed by thrust and upthrown faults aligned with the strike of basement folds, and also by lateral faults which are diagonal with respect to the folds strike. The tension fractures are expressed on the surface by systems of normal faults, flexures, grabens, zones of higher jointing and permeability elongated in the direction of compression. The dynamic characteristic of fractures is confirmed by various seismological data on stress and deformations in earthquake focuses (Shirokova, 1962, 1963; Panasenko and Meshkova, 1964).

This category of major fold and faults, which, as a rule, are expressed on space images as modified in the structure of near-surface formations, is far from being expressed everywhere sufficiently clearly in the intricate pattern of relatively small deformations of Paleozoic series constituting most of the surface of Tien Shan. Repeatedly changed by the above-mentioned details, the deep crustal fractures often disappear (on aerophotographs and, especially, in field observations) when a close-up of the locality is taken. Therefore, the deformations under consideration (megafolds and deep crustal fault zones) may remain unnoticed on large-scale photographs. Moreover, the immediate manifestations of these deformations may quite be related to structures of different genesis or order and thus will also be lost. The foregoing considerations are especially important in recognizing concealed deep crustal faults which do not come to the day (surface, ed.) (as, for example, the Talas-Fergana and San Andreas faults do) but die out as breaks in continuity at some depth in the crust. Being represented in the overlying layers as diverse deformational derivatives and other structural features, they scatter into more or less wide (up to several tens of kilometres) zones of deformations with indistinct boundaries. Such zones were recognized from a number of indirect indications; for example, in Paleozoic structures of Kazakhstan and the Soviet Middle Asia such zones have been referred to as deep mobile zones (Shcherba, 1955; Pomazkov, 1962). In the neotectonic structure of Tien Shan, this category comprises the zones of cross-cutting regional disturbances, which have also been recognized from indirect data of integrated geologic-geophysical and structural-geomorphological analyses (Kostenko et al., 1972; Makarov and Solov'yeva, 1975). Similar concealed systems of disturbances, the systems of "through-going" deep crustal fractures of a peculiar type have been discovered in structures of the Soviet Far East and the area east of Baikal (Tomson, 1962, 1964; Tomson and Favorskaya, 1968; Favorskaya et al., 1969, 1974).

On the whole, one may conclude that recent deformations of deep crustal layers, being imparted to the overlying strata, are modified by numerous details of old structures and near-surface topography, thus becoming to a greater or less degree masked and concealed from the ground observer. But a generalization of the surface pattern, which is due to photographing from space, makes these deformations visible. Using (and thus reviving to a greater or lesser degree) separate elements of old structures (including the buried ones) the neotectonic movements assist in expressing these elements on the surface, thereby ensuring their appearance on space images.

On the vast platform territories, where the basement (or folded foundation) is overlain by more or less thick sedimentary cover, the deep-seated crustal structures, like those of orogens, also appear as generalized outlines of landforms. And it is not uncommon that in such a case they are recognized even more distinctly, because the weak deformations of sedimentary cover reflect practically directly the modern deformations of the buried folded foundation and deeper crustal layers. In other words, here the masking effect of deformations of the sedimentary cover is minimum, as compared with that observed in folded complexes of fold-mountain regions.

It should be added that with the increasing distance of such concealed deformations in the platform regions from active tectonic regions they become less pronounced. This can clearly be observed in the Turan plate, where it seems to be associated with the corresponding decrease in the intensity of excitation of "inert" tectonic areas by their more active neighbors. Such regularities also suggest that active regions (in the given case, orogen), and platforms are not separated by an impenetrable screen. For example, the boundary between the epi-Hercynian Turan platform and the Tien Shan orogen (the regions of a single pre-Neogene history, but of different activity of manifestation of neotectonic orogenesis) appears as an extensive transitional zone, whose deformational intensity gradually increases toward the orogen. These two regions are closely linked structurally, but at different structural levels and along different trends the activity of their association is different. Thus, notwithstanding all existing differences between these geostructural regions, one may speak about their peculiar "intergrowth," or at least, about the more active region growing into the less active one.

Let us now turn to the geochemical mode of conveying information from deep crustal layers to the surface. The possibility of such conveyance is defined by the following main conditions:

1. Constancy of abyssal geologic processes and related ascending flows of abyssal degassing products and heat fluxes.
2. Difference between various layers and parts of the crust in the chemical composition.
3. Non-uniform permeability of crustal layers.

Among the geologic processes operating throughout the Earth's crust and upper mantle, the most important for the problem in hand are the constant mobility, repeated renewal (reactivation) of mechanical movements, embracing all crustal layers, as well as physico-chemical changes in crustal matter, accompanied by the release, transformation, and vertical migration of various fluid components and the heat flux.

The material, geochemical difference between various crustal layers may be considered in two aspects. This is, first of all, the result of development of crustal layers over the whole period of geologic history, reflecting separate stages of their formation and long-continued transformation. Among such differences are, for example, the well-known structural-formational and geochemical differences between variously aged structural stages and between their various blocks (zones, regions). In this connection, it is appropriate to mention the well-known differences in the mineralization and chemical composition of waters contained in various structural, stratigraphic, and hydrogeological complexes. Such geochemical distinctions may conditionally be classified as static, relatively stable factors.

In addition, there are differences in physico-chemical processes occurring at various structural levels, under various thermodynamic conditions, and in chemically different environments. These processes of transformation of the crustal substance at various lithospheric levels, including the Earth's surface, taking place under the influence of ascending from depth solutions and gases, may be classed as the dynamic factors. The above-mentioned geochemical differences of the two categories may be both qualitative and quantitative.

The permeability of crustal layers is assured by its "live" intercrossing structure, and primarily by the network of mutually intersecting (both in plan and in section) joints and fractures of various genesis, order of magnitude, and depth of occurrence (from the planetary jointing to regional and local fractures). These fractures are of principal importance, because they form the framework of the intercrossing structure. The continuity of tectonic movements (in the given case, amplitudes are unimportant) supports "life" of these fractures, thereby keeping the Earth's interiors open.

The concepts of the significant role played by the ascending flows of heat and products of abyssal degassing have long been advanced within the framework of tectonomagmatic hypotheses, proceeding from the supposition that the evolution of the Earth's crust is associated with magmatic differentiation of the lithospheric substance. The problems of vertical migration of fluids in the crust of the Earth (its "gaseous breath," as V. I. Vernadsky put it) have been discussed by numerous investigators, among them metallogeny studiers and, especially, petroleum geologists. But whereas the latter, along with the search for directions of fluid motion and areas of their

flow, are highly interested in the areas of "closed" interiors, it is of great importance for the problem under consideration to study the places of outflow (points of issue) and the peculiarities of the fluid surface distributions, as well as the fluid composition, which would enable the investigators to relate some or other components of this ascending flow to the deep sources generating them.

The wealth of information about the regularities governing the areal and sectional changes in the chemical composition of fluids (water, oil, gases, especially helium, argon, hydrogen, nitrogen, and so on), which has been accumulated in hydrogeology, petroleum geology, and volcanology, clearly testifies to their intensive vertical migration, taking place primarily in zones of "live" fractures and shaping geochemical and geothermal anomalies on the Earth's surface. Here, we should bear in mind that the vertical migration occurs not only along through-going straight-line ducts whose role may be played by certain fractures. A multitude of facts suggest,—and this we endeavored to demonstrate by examples of Tien Shan and Turan,—that fractures, breaks in continuity, and fissures change their activity of manifestation and their amplitudes both in strike and with depth, as changes the mode of motion along them; the open ones turn into the closed, and so on. But, as has been stressed above, dying out in one direction, their activity shifts to another, in order to return subsequently (perhaps, having changed their trend many times) to the initial one. (This may be a channel that either continues the old one or runs parallel to it.) It is this complicated, repeatedly changed, and practically unlimited way, formed in the above described manner, that assures the vertical migration of fluids reaching the surfaces with some or other losses. This is confirmed, for example, by emanations of inert gases, which, no doubt, have the abyssal origin (Yakutseni, 1968; Eremeyev et al., 1969; Nikonov, 1972; Voitov, 1975; Korobeinik and Yanitsky, 1975).

The way passed by fluids from the deep interior upward to the day surface may be compared to a bed of a stream, which, running down an inclined surface of a structurally and lithologically inhomogeneous substratum, repeatedly changes its direction in conformity with these inhomogeneities in order to take the easiest path.

We may suppose that the fluid flow from the deep interiors toward the surface has a regional diffusive character, i.e., it is practically continuous. Its density and composition, however, vary both in area and time. This non-uniformity has the primary (genetic), as well as the secondary (superimposed) causes. It is known, for example, that the density of regional flow of helium, which of all inert gases of deep origin is the best studied in this respect, varies as a function of the original concentration of radioactive elements in the substratum, above all, in the granitic layer. The secondary non-uniformity is determined by structural features, being associated with the fact that in its way the fluid flow passes through numerous "filters." Even if we assume that initially the flow was uniform and chemically homogeneous, its final heterogeneity, observed on the surface, should reflect, in one way or another, the spatial distribution of these filters, which is largely due to the deep-seated structure. Thus, the peculiarities of landscapes (soils, vegetation, and so on) contain a specific "record," which manifests itself on aerospace images and lends itself to the geologic interpretation. The previous attempts at such interpretation permits us to state that it is both feasible and necessary. This is confirmed by the results of investigations of the chemical composition and peculiarities in the distribution of gases both in area and in section, which have been carried out in various regions. Thus, the study of the presence of helium in the layers making up the Turan plate (Bakirov et al., 1970) has enabled those investigators to assert that a correct and unambiguous geologic interpretation of abnormal values in helium distribution is feasible.

Thus, the fluids, which ascend from various depths of the Earth's crust toward its surface, shape its contemporary geochemistry by interacting with the geochemical structure of the surface that has already been formed in the previous geologic epochs. Therefore, the complex geochemical spectrum of a particular part of the Earth's surface (hence, some features of its landscapes) contain a highly diverse information, including that carried by fluids, telling about their source media and the crustal layers through which they have passed on their way toward the surface.

III

The fundamental possibilities of expressing some features of the deep crustal structure in the character of the Earth's surface that we have just considered, are realized in different ways, depending on the geologic and climatic conditions. And this fact must determine what specific method should be used in every particular case.

In most cases, the mechanical deformations of the Earth's surface are reflected in the features of its relief. Given the conditions of sufficiently active neotectonic (including contemporary) movements, we are

justified in expecting that the deep deformations directly manifest themselves in those of the day surface. Depending on their intensity, the latter may develop as conerosional, condenudational, and, finally, consedimentational forms.

In order to elucidate the character of structures of the first group, one may use the whole diversity of techniques of the structural-geomorphologic analysis, which allows one to recognize the developing structures of the platform mantle, to map them sufficiently reliably, to study their arrangement, conjugative peculiarities, character of development, and so on.

The identification of condenudational and consedimentational structures is somewhat more difficult, especially when the latter are found in the regions of active sedimentation, for example, in the Syr Dar'ya and Chu syneclises, and in the central part of the Fergana intermontane trough. In these cases, the surface deformation is negligibly small. But the facies-lithological peculiarities of sedimentation, which are determined by the developing structural form and which, in turn, characterize it, are expressed in the more or less distinct hydrogeological and lithologic-geochemical features and, through them, in those of the soil and vegetational cover. Thereby, they also determine some features of the landscape and may appear on high-altitude images in some or other spectral band.

The reason for the appearance of consedimentational structures on space images is essentially the same. When the image resolution is sufficient, the pattern of these structures becomes complicated by the old deformations of the folded basement if the latter is exposed in cores of such elevations.

Thus, in the cases of consedimentational and condenudational development of mechanical deformations, they become expressed more or less distinctly in the pattern of the Earth's surface indirectly, through the material composition of deposits making up the surface. The ensuing possibilities of identifying on space images major consedimentational structures, including consedimentational elevations, which are highly promising as possible places of oil and gas accumulation, attract special attention to the development of methods for studying such structures by means of remote sensing.

That the structures of consedimentational type occur widely in the region under consideration is clearly suggested by the following facts. The relative elevation in the relief of the Turan plate is not more than 300 to 500 m. The platform basement topography, however, is characterized by amplitudes of movements, which are higher by an order of magnitude. The total amplitude of movements that took place in the Neogene-Quaternary epoch within the Mangyshlak varies from 200 to 2,000 m. Whereas the total amplitudes of Meso-Cenozoic movements in certain areas of the Turan plate are as high as 6 or even 8 km. Because of more active tectonic movements of the platform during the Neogene-Quaternary time, consedimentational elevations have partly passed into the condenudational and then into the conerosional stage of development in the relief. However, a large number of local structures of the sedimentary cover retain their previous consedimentational regime of development and, therefore, are not reflected directly in the elevations of the relief.

The geochemical relationships between the Earth's surface and its deep interiors manifest themselves in finer peculiarities of landscapes (especially soils, and vegetation), which are far from being always open to the eye. And, since these relationships also have some significance in the relief formation, they are expressed in landscape features as inseparable from the mechanical factor, which is by far predominant in the areas of orogenesis. On the contrary, within the platform regions the geochemical factors begin to play a more significant role in forming the appearance of the Earth's surface, because for them to be active the amplitudes of displacements are of no importance provided the crustal layers are permeable throughout.

The specificity of methods for investigating deep-seated structures within both the platforms and the orogens has already become apparent in ground-based studies and in the interpretation of space imagery data.

An analysis of the network of the main regional fractures, which (as a rule, though not always) are pronounced in the relief sufficiently distinctly, gives us the most general idea of the character of the deep-seated structure of platforms. Mapping based on images showing the network of lower order fractures and jointing, which are inscribed in the framework of deep crustal fractures, enable one to disclose the peculiarities in the composition of individual forms. Of great importance in such studies is the determination of regional slopes which can be restored from the grade of surface and subsurface waters, manifested in the trend of river drainage, as well as in the overall pattern of drainage systems. Areas sloping in one direction are, as a rule, united structurally, too. The boundaries separating areas of different slopes usually coincide with deep crustal fracture zones. This can be exemplified by deep crustal fractures within the Turan plate, for example, those of Amu Dar'ya and Repetek.

Let us dwell in more detail upon the peculiarities of "X-raying" the deep crustal fracture zones through

a thick cover of sediments of the platform. The recent reconstruction of the intercrossing structure of the region with respect to the structures of the preceding geotectonic cycles gives rise to changes in the leading, most active trends. Those of the deep crustal fracture zones which have coincided in the new platform structure with the most active trends become distinctly expressed in the modern structure and, therefore, in the relief. Such are the fracture zones of predominantly northwest trend, which disturb the entire sedimentary cover and which are directly pronounced on the surface as a system of ruptural dislocations and folds.

The orthogonal deep crustal fractures, for example, the submeridional fractures of the Urals-Oman dislocation system, are not expressed so distinctly in the neotectonic structure. They serve as boundaries for consedimentationally developed structures, and these boundaries are of smooth or flexural character. Because of low activity of the modern movements, these zones, being active and highly permeable in the Hercynian structure, have turned out to be sort of sealed under the sedimentary cover. But, although ultimately these zones have not been expressed directly in the overlying layers (even as zones of low-amplitude dislocations of flexural-ruptural type), they, as a rule, are accompanied by a system of conjugated joints developed in the sedimentary cover. It is just these joints, that, being altered under the influence of varied factors of the exogenetic processes, create a picture of lineaments, which can be recognized on photographs from a set of indirect characteristics. In the neotectonic structure of the Turan plate one can observe a large number of flexural zones of this type. Their surface manifestation is extremely veiled, they are barely traceable in a series of indirect features of the landscape, which, at first glance, have little to do with one another and are hardly remarkable.

Being generalized on space images, all these features of the landscape taken as a whole, delineate such structures by distinct changes in the density of photographic tone or become apparent in geometric peculiarities of minor drainage patterns. The change in the photographic tone may, as a rule, be associated either with a change in the composition of sediments, of ground waters, their regime and geochemical composition, which determine different soils and vegetation.

Thus, the information about the deep crustal structure is transmitted either mechanically, by deformations of deep crustal layers being reflected in all overlying strata, including the Earth's surface, or geochemically, by ascending flows of fluid products arising from transformations of matter constituting deep layers of the Earth's crust and upper mantle.

Both mechanical and, especially, geochemical mode of expressing the deep-seated structure in the appearance of the Earth's surface are afforded by the intercrossing character of crustal structure, by its high mobility, and, as a consequence of both these factors, by its permeability in every area.

Such an approach toward the study of the Earth's surface allows one to explain possible mechanisms by which deep crustal layers "appear" on the surface and by which deep crustal structure, or, at least, some of its elements are depicted on space images. This makes space images highly promising not only in comparing maps of the Earth's surface, but, what perhaps is more important, in studying deep crustal layers and associated minerals.

Of particular interest in this respect is the geochemical aspect of the problem at hand. It may be supposed that some time in the future the geologists will be able to recognize quite easily the components of the geochemical field observed on the surface, which are associated with sources of various depths of occurrence. At present, it is required that we should discuss the essential possibility of such a mechanism of formation of the structure of the Earth's surface in order to broaden the aspects of geologic interpretation of space images, and also to put on the agenda the geotectonic aspects of landscape geochemistry, and to attract attention to the underestimated geochemical factor in structural and geomorphological studies.

It seems to us that the possibility of recognizing the genetically different components in the geochemical spectrum of the Earth's surface may have far-reaching practical consequences for the search for minerals. Such a decomposition of the geochemical spectrum will possibly be carried out using multispectral imagery, including space imagery. For the prospecting potentialities of various bands of electromagnetic radiation (their addition, subtraction, and other manipulations with them) have little been studied so far and, of course, are far from being exhausted. In other words, the time has come to raise the question of application of space imagery to the direct purposeful prospecting for zones of various depths of occurrence and metallogenetic significance.

Along with the importance and fundamental possibilities of employing space images in studying the deep crustal structure, the problems raised in the present paper attract attention also to the independent and not yet quite understood significance and possibilities of geomorphological and geochemical studies

of the Earth's surface in order to gain a deeper insight into the structure of the Earth's interiors.

REFERENCES

Amursky, G. I., Geiman, B. M., and Koy, V. G., Concerning the links of the Urals-Oman lineament in the Middle Asia. Izvestiya Vysshikh Uchebnykh Zavedenii, geologhiya i razvedka, 1966, no. 2.

Abrosimov, I. K., Bogorodsky, S. M., and Vostokova, E. A., Landscape relationships and their use in the interpretation of data of aerospace imagery in connection with the study of the deep-seated structure of western Turan plate. In : "The study of natural enviornment by space means. Geology and geomorphology", Moscow, All-Union Institute of Scientific and Technical Information (AISTI) Publishers, 1974, vol. 2.

Agrand, E., La tectonique de l'Asie, Congres géologique International. C. R. de la XIII session en Belgique, 1922. Leige, 1924.

Artamonov, M. A., and Bogorodsky, S. M., The peculiarities in manifestation of local elevations and regional fractures within the Ustyurt Plateau and the Mangyshlak, as seen on aerospace images. Izvestiya Vysshikh Uchebnykh Zavedenii, geologhiya i razvedka, 1974, no. 12.

Artamonov, M. A., and Isayev, E. N., The geophysical informativity of space images for the Mangyshlak Peninsula. Doklady Akad. Nauk SSSR, 1971, vol. 199, no. 1.

Bakirov, A. A., Bykov, R. I., Gavrilov, V. P., Knyazev, V. S., and others, The basement and main fractures of the Turan plate in connection with the presence of oil and gas within its territory. Moscow, 1970, Nedra Publishers.

Beregovoy, G. T., Buznikov, A. A., Vasiliyev, O. B., and others, The study of natural environment from manned orbital stations. Leningrad, 1972, Ghidrometeoizdat (Hydrometeorology Publishers).

Bogorodsky, S. M., Gavrilov, V. P., and others, The structure of the Turan platform from the results of the combined interpretation of the data of geologic, geophysical, and space-geologic studies. Izvestiya, Vyshikh, Uchebnykh, Zavedenii, geologhiya i razvedka, 1973, no. 7.

Voytov, G. I., The Earth's gasesous breath. Priroda, 1975, no. 3.

Vinnik, L. P., and Lukk, A. A., Lateral inhomogeneities in the Earth's upper mantle beneath the Pamirs-Hindu Kush system. Izvestiya Akad. Nauk SSSR, ser. "Physics of the Earth", 1974, no. 1.

Garetsky, R. G., Samodurov, V. I., Shlezinger, A. E., and Yanshin, A. L., Tectonics of the Turan plate cover. In: "The problems of regional tectonics of Eurasia", Transactions of the Institute of Geology, the USSR Academy of Sciences, 1963, vol. 92.

Eremeyev, A. N., et al., The relationship of the helium concentration distribution in upper crustal layers with the deep crustal structure and endogenous metallization. Bulletin of Inventions and Discoveries (Soviet), 1969, no. 35.

Karpinsky, A. P., Comments on the character of rock dislocations in southern European Russia. Gorny zhurnal (Journal of Mining), 1883, no. 3.

The map of neotectonics of the south of the USSR (scale 1:1,000,000). Ed. L. P. Polkanova, Moscow, 1972, All-Union Department of Geodesy and Cartography.

Kashkai, M. A., and Tamrazyan, G. P., The transverse (anticaucasian) dislocations of the Crimea-Caucasus region, their role in magnatism and regularities governing location of minerals. Moscow, 1967, Nedra Publishers.

Korobeinik, V. M., and Yanitsky, I. N., On the transcrustal gas flow. Doklady Akad. Nauk SSSR, vol. 221, no. 2, 1975.

Kostenko, N. P., Concerning neotectonics of the Fergana trough and its mountain setting (the results of geomorphologic analysis of the process of development of structural forms in the relief). In: "Problems of Regional Geology of the USSR", MSU Publishers, 1964.

Kostenko, N. P., Makarov, V. I., and Solov'yeva, L. I., The modern tectonics of the Kirghiz SSR. In: "Geology of the USSR", vol. 25, part 2, Nedra Publishers, Moscow, 1972.

Krestnikov, V. N., and Nersesov, I. L., The relationship of the deep crustal structure of the Pamirs and Tien Shan with tectonics. Abstracts of the Dushanbe Session of the 2nd All-Union Conference on Tectonics, Dushanbe, 1962.

Makarov, V. I., Structural and morphological analysis of the neotectonic deformations in Central Tien Shan. Summary of Candidate Thesis. MSU, Moscow, 1969.

Makarov, V. I., The interpretability of tectonic structures in regions of recent epiplatform orogenesis, as seen on space images of the Earth (example of south-western Tien Shan) Izvestiya Vysshikh Uchebnykh Zavedenii, geologhiya i razvedka, no. 7, 1973.

Makarov, V. I., Trifonov, V. G., and Shchukin, Yu. K., Manifestation of deep crustal structure of folded areas on space images. Gheotektonika, no. 3, 1974.

Makarov, V. I., Skobelev, S. F., Trifonov, V. G., Florensky, P. V., and Shchukin, Yu. K., Deep crustal structure on space images. In: "The study of natural environment by space means", Moscow, 1974, the USSR Academy of Sciences, All-Union Institute of Scientific and Technical Information Publishers, vol. 2.

Makarov, V. I., and Solov'yeva, L. I., Neotectonic transverse structures of Tien Shan and their expression on space images. Izvetiya Vysshikh, Uchebnykh Zavedenii, geologhiya i razvedka, no. 2, 1975.

Nalivkin, D. V., Paleogeography of the Soviet Middle Asia. In: "Scientific results of the Tajik-Pamirs expeditions". Moscow-Leningrad, the USSR Academy of Sciences Publishers, 1936.

Nesmelova, Z. N., and Soldatova, K. S., On the origin of argon found in hydrocarbonic gases. Gheokhimiya, no. 4, 1967.

Nikonov, V. F., Formation of helium-bearing gases and the direction of search for them. "Soviet geology", 1972, no. 7.

Pavlov, R. I., On the system of regional transverse structures in the western part of southern Tien Shan and their geologic manifestation. Soviet geology, no. 10, 1972.

Panasenko, G. D., and Meshkova, Z. S., Concerning the direction of action of the tangential tensions in the Hindu-Kush zone of earthquake foci. Doklady Akad. Nauk SSSR, vol. 155, no. 1, 1964.

Patalakha, E. I., and Slepykh, Yu. F., Intercrossing folding. Moscow, Nedra Publishers, 1974.

Peive, A. V., The asymmetry of deep-seated tectonic structure of the Urals-Tien Shan orogen and the origin of its virgations. Bul. Mosc. Obshchestva Ispytatelei Prirody (MOIP), ser. gheol., vol. XXII, issue 5, 1947.

Petrushevsky, B. A., The Urals-Siberian epihercynian platform and Tien Shan. The USSR Academy of Sciences Publishers, 1955.

Petrushevsky, B. A., The Hindu-Pamirs deep-seated zone and the Western Deccan earthquake. "Gheotektonika," no. 2, 1969.

Planetary jointing, Leningrad. Leningrad State University (LSU) Publishers, 1973.

Pomazkov, K. D., Deep-seated mobile zones of Tien Shan and their ore-controlling significance. Transactions of the Department of Geology and Interiors Protection of the Kirghiz SSR Council of Ministers, vol. 2, Frunze, 1962.

Rezvoi, D. P., The "anti-Tien Shan" structural trend in the tectonics of the Soviet Middle Asia. Transactions of the Geologic Society of Lvov, no. 9, 1965.

Solov'yeva, L. I., The neotectonic transverse structures of the Turkestan-Alai system and the history of their development. "Lomonosov Readings", VI-th Conference of the Faculty of Geology, MSU Publishers, 1971.

Solov'yeva, L. I., On the inherited-superimposed character of the neotectonic structure of the Turkestan-Alai system. Izvestiya Vysshikh Shkoly, gheol. no. 7, 1972.

Skaryatin, V. D., Concerning the study of ruptural tectonics using a set of variously-scaled space images of the Earth. Izvestiya Vysshikh Uchebnykh Zavedenii, gheologhiya i razvedka, no. 7, 1973.

Suvorov, A. I., The regularities governing formation and structure of deep fractures. Nauka Publishers, 1968.

Tomson, I. N., Features of structure of low coherence zones above concealed fractures of basement. In: "Concealed deep crustal ore-controlling fractures". Transactions of the Institute of Geochemistry and Mineralogy, the USSR Academy of Sciences, issue 84, 1962.

Tomson, I. N., and Favorskaya, M. A., Ore-concentrating structures and the principles of local prognostication of endogenous mineralization, Soviet geology, no. 10, 1968.

Trifonov, V. G., Byzova, S. L., Vedeshin, L. A., Derevyanko, O. S., Ivanova, T. P., Kopp, M. L., Kurdin, N. P., Makarov, V. I., Skobelev, S. F., and Florensky, P. V., The methodological problems of interpreting space images of the Earth. In: "The study of natural environment by space means. Geology and geomorphology". The USSR Academy of Sciences, All-Union Institute of Scientific and Technikal Information Publishers, Moscow, 1973.

Favorskaya, M. A., Tomson, I. N., and others, The relationship of magmatism and endogeneous mineragenesis with the block tectonics. Moscow, Nauka Publishers, 1969.

Favorskaya, M. A., Tomson, I. N., Baskina, V. A., Volchanskaya, I. K., and Polyakova, O. P., The global regularities governing localization of ore deposits. Moscow, Nedra Publishers, 1974.

Florensky, P. V., Interpretation of deep-seated structure and local elevations from space images of the Turan plate. Izvestiya Vysshikh Uchebnykh Zavedenii, gheologhiya i razvedka, no. 7, 1973.

Chediya, O. K., The youngest transverse elevations, their types and practical significance (example of the Soviet Middle Asia). Materials on the geology of the Pamirs, issue 2, Dushanbe, 1964.

Shirokova, E. I., Concerning tensions in foci of minor earthquakes in the Soviet Middle Asia. Izvestiya Akad. Nauk SSSR, ser. geophys., no. 6, 1961.

Shirokova, E. I., On tensions in earthquake foci of the northwestern part of the Asian-Mediterranean seismic belt. Bulletin of the Council on Seismology, no. 15, 1963.

Shcherba, G. N., Deep mobile zones of Central Kazakhstan. Izvestiya Kazakh SSR, Academy of Sciences, ser. geol, issue 20, 1955.

Shults, S. S., Concerning various orders of planetary jointing. Gheotektonika, 1966, no. 2.

Shults, S. S., Some problems of planetary jointing and associated phenomena. Vestnik. Leningrad State University (LSU), (geol. and geography) no. 6, issue 1, 1969.

Shults, S. S., Lineaments. Vestnik LSU, no. 24, 1970.

Shults, S. S., Planetary fractures and tectonic dislocations, Gheotektonika, no. 4, 1971.

Shults, S. S., Planetary jointing. In: "Planetary Jointing", LSU Publishers, Leningrad, 1973.

Yanshin, A. L., Methods of studying buried folded structures by elucidating the relationships between the Urals, Tien Shan and the Mangyshlak. Izvestiya Akad. Nauk SSSR, ser. geol., no. 5, 1948.

Yakutseni, V. P., Geology of helium, Moscow, Nedra Publishers, 1968.

Furon, R., La geologie du plateau Iranian (Perse, Afganistan, Beloutchistan). Mem, Mus. Hist., Nouv. ser., VII, f. 2, Paris, 1941.

PROCEEDINGS OF
THE FIRST ANNUAL WILLIAM T. PECORA MEMORIAL SYMPOSIUM,
OCTOBER 1975, SIOUX FALLS, SOUTH DAKOTA

Combined Formalized Processing of Space Image and Geologic-Geophysical Data in Connection with the Study of Deep Structure of Petroliferous Platform Regions [1]

By P. V. Florensky, A. S. Petrenko, and B. P. Shorin-Konstantinov,
Moscow Institute of Petrochemical and Gas Industry

INTRODUCTION

Analysis of space images made with the purpose of recognizing the geologic features of some or other region has become one of the indispensible elements of regional geologic studies. This is an entirely new element, which neither removes the necessity of carrying out all other works nor does it lower the requirements to their comprehensiveness, but permits their more definite coordination, as well as the extraction of new information. For the present, these observations are being performed, as a rule, merely for individual regions. Such specific work, which is sufficiently subjective and in each case unique, is unquestionably justified in developing the required procedures. The amount of the diverse material obtained from space is, however, so large that confining our attention to such processing alone would mean that we leave out of consideration tens, hundreds and sometimes even thousands of TV and photographic images covering vast territories. Therefore, our most immediate task is to bring about a formalized computer processing of space images which would enable us to encompass a significantly greater amount of information.

Of all useful minerals contained in the platform mantle, only oil and gas are extracted from depths exceeding two or even three kilometres. It is natural therefore that the petroleum geologists are to a large extent interested in the character of basement surface and basement internal structure. Accordingly, much credit for the study of the platform basement buried under sedimentary mantle goes just to them.

The importance of such study was emphasized by Academician I. M. Gubkin who illustrated it by considering the petroliferous province between the Volga and the Urals. Subsequently, the behaviour of the basement in question in the course of time has been analyzed (Bakirov, 1957) and its comprehensive geologic and geophysical study carried out (Belyaevsky, 1974; Borisov, 1967; Krats, Nevolin, and others). It is just on this territory that the problem of petrographical study of basement rocks from core samples taken from deep boreholes supplemented by geophysical data has first been stated and, in principle, solved. The problem is being further investigated at the department of petrography of the Moscow Institute of Petrochemical and Gas Industry under the guidance of T. A. Lapinskaya (until 1956 the work was directed by V. P. Florensky). At present, the study of basement is one of the most important elements of the comprehensive study of all petroliferous provinces of the Soviet Union.

As has been demonstrated by considering the Turan platform (Florensky, 1973; Trifonov et al., 1973; Makarov et al., 1974; Bogorodsky et al., 1974), small-scale photographs of the Earth made from space allow one to judge about the deep-seated structure of the platform regions. The present work is devoted to a combined, sufficiently formalized, processing of geologic and geophysical materials in conjunction with space image data in order to clarify the deep-seated structure of the Lower Volga region (fig. 1). The purpose of the work is to evaluate just to what extent is a space image of a part of the Earth's surface illuminating in regard to the study of the deep structure of a platform and to establish criteria for comparing space

[1] Printed verbatim as received from the authors, except for minor changes in format and spelling.

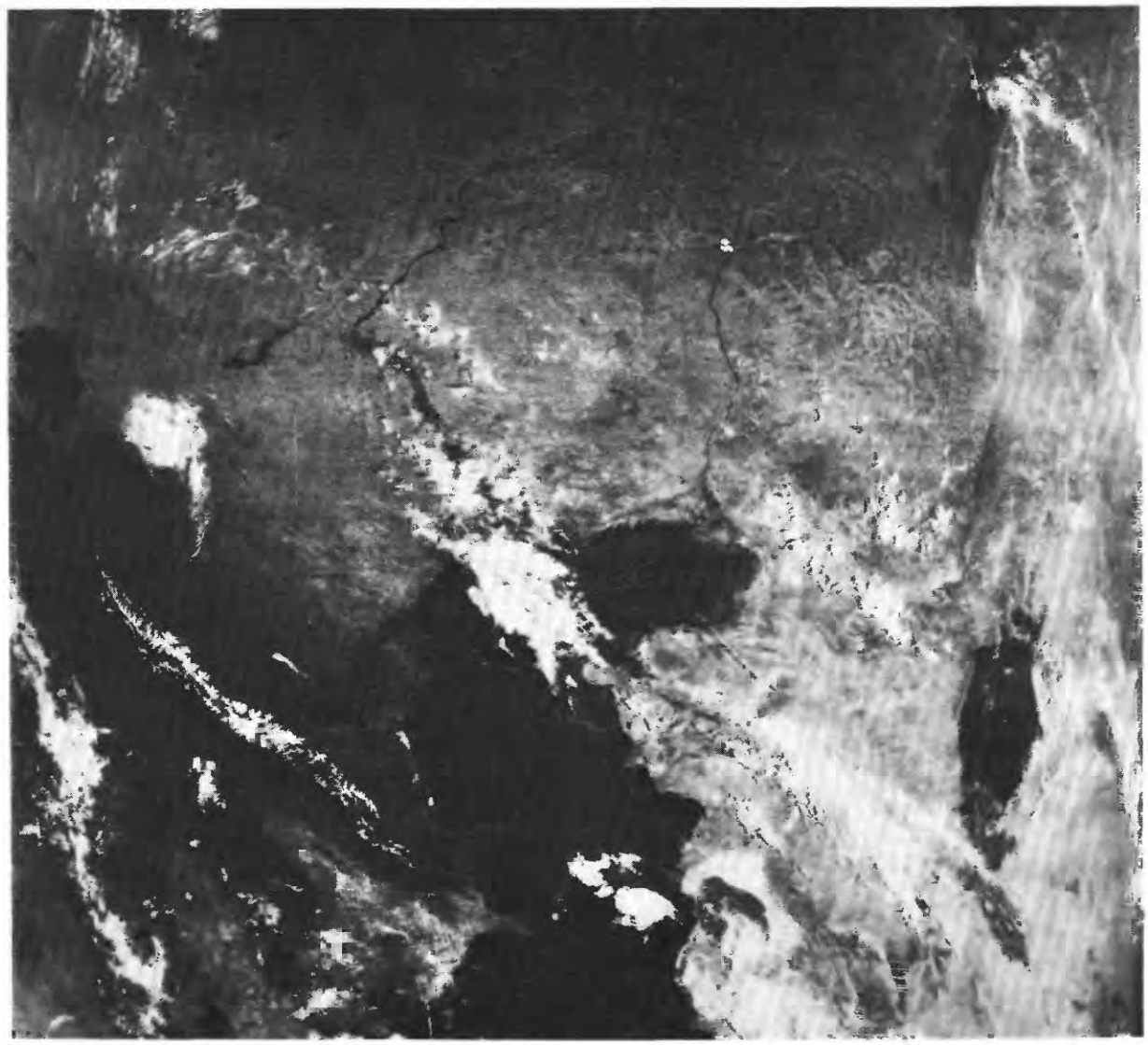

FIGURE 1.—Southern Russian plain. TV image obtained by the Soviet Earth-orbiting satellite "Meteor."

images with geomorphological, geologic, and geophysical information.

In the course of this study, we have used television and scanner images of the region under consideration, which have repeatedly been transmitted from the Soviet automatic satellites "Meteor" (resolution about 1.5 km (fig. 1)), and earlier objects of the "Meteor" series (resolution from 0.8 to 1.0 km), as well as a scanner image (fig. 2), transmitted in July 16, 1973, from the American automatic satellite ERTS–1 (resolution about 0.1 km). The latter images have thoroughly been processed photometrically and the results of the deciphering thus made have been compared with the various geologic and geophysical data for the region. In the final geologic interpretation, the results of deciphering of other space images of the region have been taken into account as well.

The photometric measurements were made by B. P. Shorin-Konstantinov, the geophysical data were reduced by A. S. Petrenko and subsequently analyzed geologically by Petrenko together with P. V. Florensky.

PROCEDURE OF PHOTOGRAPHIC AND PHOTOMETRIC PROCESSING OF SPACE IMAGES

In working with space images there arises the necessity of artificial improvement of deciphering properties of the images with respect to some or other objects. Ways of such a transformation of images are various

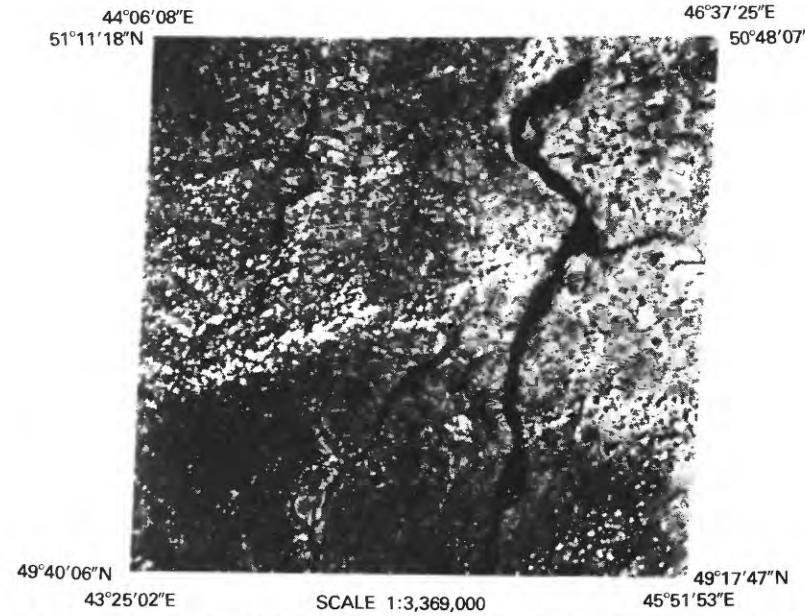

FIGURE 2.—Lower Volga region. TV image transmitted from the American satellite ERTS–1 on 16 July 1973.

(Mikhailov, 1972; Kuchko, 1974). One of the most extensively employed methods is that based on the separation between zones with different photometric densities, which is more distinct than one seen on the original image.

In the present paper, account has been taken of the data on specialized processing and photometry of space images to allow the evaluation of the amount and quality of geologic information contained in the space images. The images of the Lower Volga region we have selected are of interest not only from the standpoint of geology but also from the standpoint of the development of methods for processing and photometry of space images.

On the original image one clearly sees arable land mottled with small fields of various coloration. At the same time, bedrocks here do not come out to the day (surface, ed.), in contrast to those of the mountainous regions. In the course of this work it was necessary to identify regional geologic objects and, with this purpose, to suppress, in particular, the local differences in brightness associated, for example, with the distribution of arable land, i.e., to generalize the image and, simultaneously, to increase the contrast with which elements of larger geologic structures manifest themselves on these images. To achieve both these aims, we have employed a combined method of photographic filtration of photometry and photometric processing of the image.

The photographic positive image of the region in question has been obtained on a sheet phototechnical film of T–41 type at 1:1,500,000 scale (developer—62, cuvette development), which has made it possible to raise the degree of image contrast at a comparatively small value of haze density $D = 0.14$. As a result, the double positive obtained on the sheet film had only five fields of the light wedge, in contrast to the original image (also obtained on the sheet film) that had fifteen fields of the wedge. This artificial increase in image contrast has resulted in filtration and generalization of the initial information contained in the photographic image. However, because of the increase in the general image contrast, the brightness characteristics of the varying elements (such as sown fields, districts) have also become exaggerated.

It has been possible to get rid of unnecessary details by varying integrally the optical densities of images along the profiles. The system of the profiles has been chosen to cover uniformly the whole area of study, with the distance between two profiles about 20 or 25 km. This assured a sufficiently detailed picture and permitted compilation of the scheme of optical densities for the territory (fig. 3). Measurements were made using a registering microphotometer 0–451. The defining slit of the microphotometer was opened as much as possible (18 by 4). From the photometric curves along the profiles, the values of relative maxima of density (D max) were taken, which have subsequently served for constructing the scheme of photographic anomalies. The maximum values of optical density were used to eliminate the influence of cloudiness, whose density on the measured positive corres-

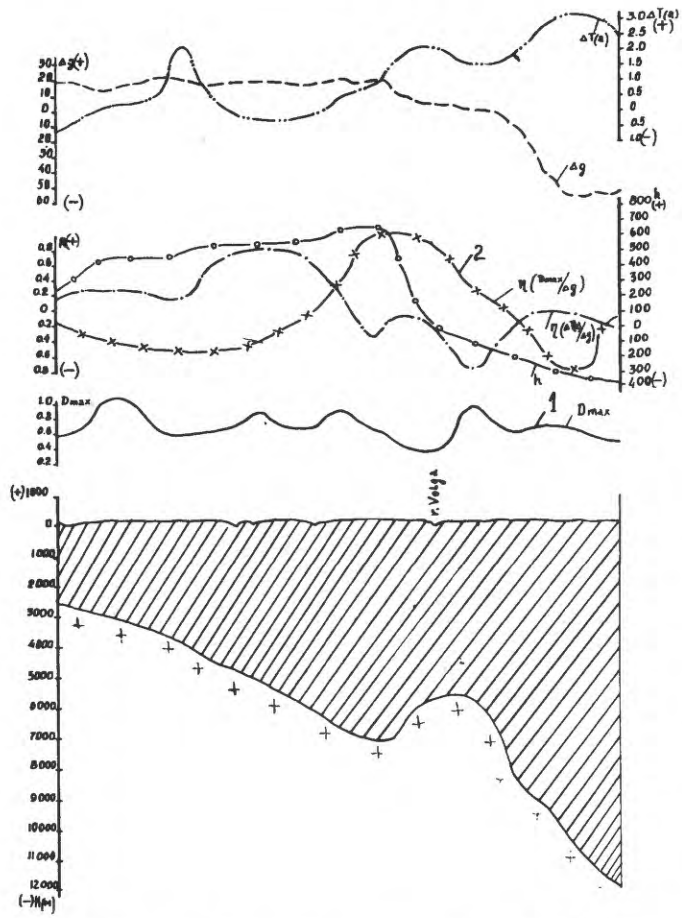

FIGURE 3.—Example of a composite profile of geologic-geophysical and photometric information. 1—Optical density; 2—coefficient of correlation between the gravity field and the optical density.

ponds to that of the haze ($D_{clouds} = D_o = 0.14$). The scheme was compiled using the averaged values of the relative maxima of optical density, which, in turn, has led to artificial filtration. In constructing the scheme, the Volga itself was disregarded. The interpolation step was 0.2 (D=0.2), which is greater than the gradients of random variations of the optical density.

The fully opened defining slit (18 by 4) has ensured generalization of the ciphers obtained, which has weakened the influence of fractional and small-in-area elements of the image on the positive measured. The scheme of photographic anomalies has been constructed by taking into account all the above-mentioned artificial alterations introduced while processing the images along the profiles. Interpolation made in the scheme compilation was controlled all the time directly from the photographs.

On the scheme of photographic anomalies (fig. 4), which has been compiled with considerable generalization, the northern half is lighter than the southern one. The gradients of variation of the optical density are insignificant almost everywhere on the scheme; as spots, they outline various areas, forming an arbitrary photometric "surface." The orientation of trends of the photographic anomalies varies from northwestern in the northwest of the area to north-south in the east to sublatitudinal in the south.

This scheme of photographic anomalies, which is the first interpretation, has been compared with the geologic and geophysical data available.

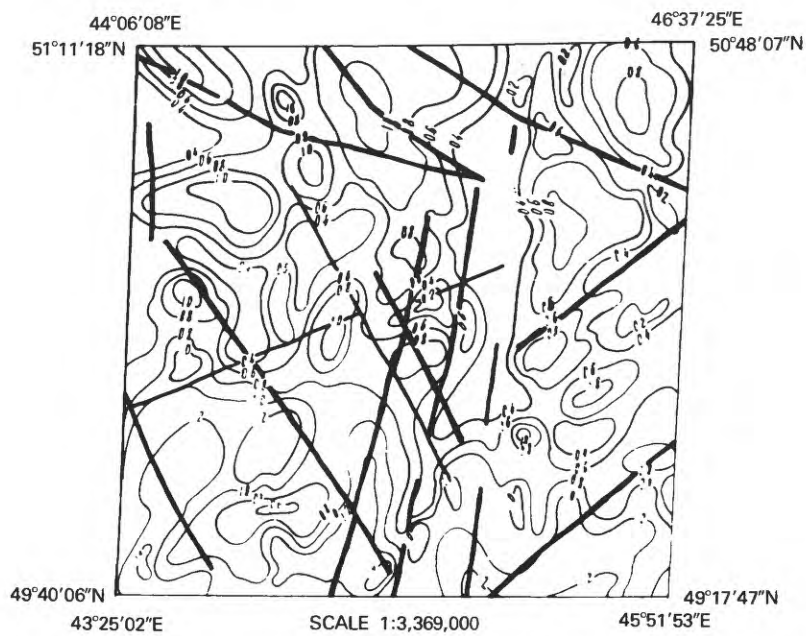

FIGURE 4.—Photometric scheme of the image shown in figure 2 in arbitrary units (clouds removed); isolines and coloration are in arbitrary balls, lineaments are shown by the solid lines.

GEOLOGIC AND GEOPHYSICAL FEATURES

The general description of blocks is presented in table 1.

RELIEF

The area under consideration forms in plan a somewhat elongated toward NNE square 180 by 190 km. Its central part is occupied by the Don-Medveditsa Ridge bordering on the Volga Upland whose absolute elevations range from 250 to 300 m. These uplands separate the basins of the Medveditsa and Ilovlya rivers flowing into the Don from the valley of the Volga whose floor is occupied here by the Volgograd reservoir. The right bank rises above the Volga by 100 to 150 m; on the Volga's left bank there lies a plain elevated by only 50 m above sea level, i.e., only slightly above the water level in the Volga.

GEOLOGIC SURFACE STRUCTURE

Geologically, the area under study is the bordering one between the Voronezh anteclise in the west and the Cis-Caspian depression in the east. Within the area, Carboniferous deposits outcropping in the roof of the Linevsk Elevation are overlain by Jurassic, Cretaceous, Paleogene, and (on the left side of the Volga) Quaternary deposits (fig. 5). These Carboniferous bedrocks, however, are almost everywhere covered by soil (arable land). The section of the platform mantle displays here complicated paleofacial replacements (Bush et al., 1968).

NEOTECTONICS

By analyzing the variations in topography, peculiarities of river beds and of ravines and other geomorphological features, V. P. Bukhartsev (1974) and A. V. Tsigankov (1971) have compiled variously detailed maps showing the amplitudes of neotectonic movements. On the presented scheme, due to Tsigankov (fig. 6), one can recognize a single submeridional band,

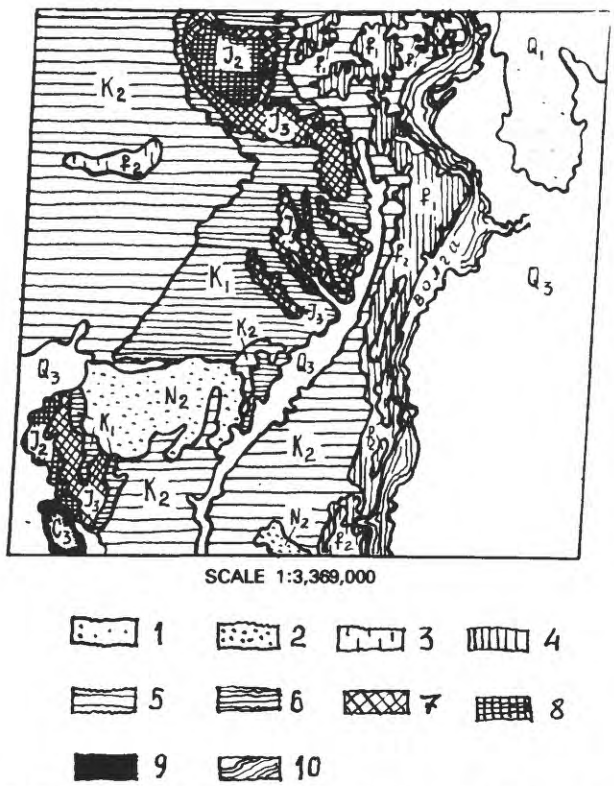

FIGURE 5.—Geologic map for the Lower Volga region (from the Geologic Map of the USSR).
1—Lower Quaternary deposits; 2—neogenic deposits; 3—ecocenic deposits; 4—oligocenic deposits; 5—Upper Cretaceous deposits; 6—Lower Cretaceous deposits; 7—Upper Jurassic deposits; 8—Mid-Jurassic deposits; 9—Carboniferous deposits; and 10—bed of the Volga river. Same area as that shown in figure 2.

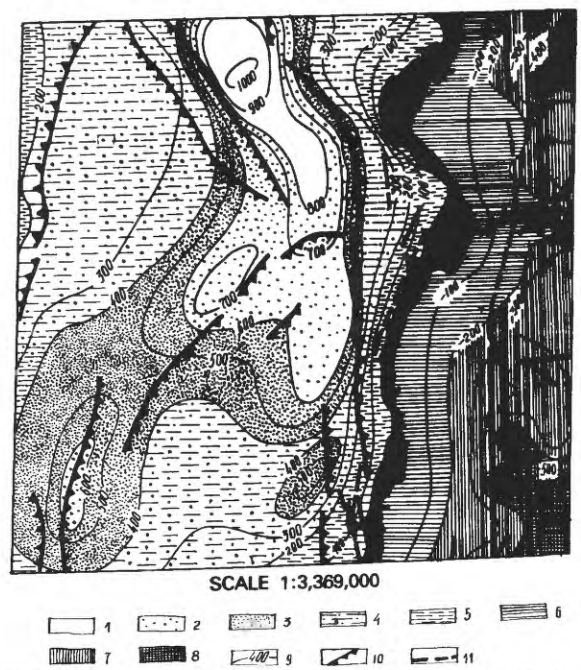

FIGURE 6.—Scheme of neotectonic movements of the Lower Volga region shown in arbitrary isolines (after A. V. Tsigankov, 1971).
Elevations: 1—1,000 to 800 m; 2—800 to 600 m; 3—600 to 400 m; 5—200 to 0 m. Areas of depression: 6—0 to —200 m; 7——200 to —400 m; 8——400 to —600 m; 9—isolines of equal amplitudes of neotectonic movements; 10—flexures; and 11—fractures.
Scale 1:3,369,000.

TABLE 1.—*Quantitative characteristics of the identified blocks*

Zone block		Photometric characteristic (fig. 4)	Age of the rocks exposed (fig. 5)	Relief and neotectonic movements (fig. 6)	Geophysical characteristics			Relationship (correlation) with the optical density			
					Gravity field	Magnetic field	Correlation between the gravity and magnetic fields	With topography and neotectonic movements	With the gravity field	With the magnetic field	With the correlation coefficients for the gravity and magnetic fields
Western	I. Northern	----------	Carboniferous, Jurassic and Cretaceous overlain by Neogenic and Quaternary.	Uplift, especially intensive in the central part.	High-gradient, positive isometric anomalies.	Steep-gradient, positive, nearly isometric anomalies sublatitudinal in the northwest and submeridional in the east.	Positive ----	Alternating sign in the north, high negative in the south.	----------	Positive ----	Alternating sign, but mainly negative.
	II. Southern.	Average (0.4–1.0) dark sublatitudinal anomalies in the west and light southeastern submeridional in the east.	Upper Cretaceous.	Slight uplift, more prominent to the east and south.	Positive, elongated submeridional anomalies.	High positive submeridional elongated anomalies.	Positive, high in the north and negative in the south.	Positive, high.	Positive, low in the central part passing into negative on the periphery.	Negative and slight positive in the west.	Positive, high.

Central	III. _____	Light in the north, dark in the south, anomalies submeridional and subparalleled to the boundaries.	Jurassic in the north and Cretaceous in the south.	Submeridional land of intensive uplift.	Average intensity submeridional positive anomalies subparallel to the strike.	Weak negative anomalies in the north and weak positive in the south.	Negative ___	Positive, high in the northwest.	Positive average negative, weak to the south.	Positive, weak.	Negative in the northwest, high.
Eastern	IV. Northeastern.	The most light.	Cretaceous, Paleogenic.	Slightly rising on the right bank and slightly sinking on the left.	Weak positive mosaic anomalies.	The same as above.	Positive, high.	Negative ____	Negative, weak.	Negative ___	Negative, high.
	V. Eastern.	Light.	Upper Quaternary.	Low plain, intensive sinking.	Highly intensive northeastern anomalies.	The same as above.	Negative, high.	Negative, high.	Negative ___	Negative in the north and positive in the south.	Negative, high.
	VI. Southeastern.	Very dark.	Upper Quaternary.	Low plain, very intensive sinking.	The same as above.	Positive tranquil anomalies.	Positive, weak.	Negative, weak.	Negative, weak.	Positive ____	Positive.

which corresponds tectonically to the zones of the Umerovsky graben and the Kamyshin projection. It is here where the maximum erosion of ancient deposits has taken place during Quaternary time, reaching 1,000 m in the north, in the area of the Linevsk Elevation. The area lying on the left side of the Volga has, on the contrary, been a zone of subsidence and sediment accumulation during a long time.

GRAVITY FIELD

The character of Bouguer anomalies is determined chiefly by the internal structure and chemical composition of basement and by the basement surface topography, i.e., by factors operating at depth, as well as by structural and lithologic inhomogeneities inside the sedimentary cover, which give rise to density differentiation of rocks. So far as the gravity field is concerned, the territory is divided into two parts: northwestern area characterized by a weakly differentiated gravity field and southeastern one—an area of very low, exceedingly separated gravity anomalies. The boundary between these two areas is very distinct and is commonly drawn along a gravitational bench coinciding roughly with the right bank of the Volga, where in a band 10 km wide the gravity intensity decreases by a factor of 3 or 4 in the southeastern direction. This boundary corresponds to the flange of the Cis-Caspian depression. According to some concepts, the boundary corresponds to the zone of a major fracture and abrupt subsidence of the basement, whereas by other concepts it reflects a relatively gentle sinking of basement and the appearance of thick low-density salt-bearing strata in the platform mantle section, which were the cause of the gravity bench formation.

In the right-bank territory there are three areas. The northern area bounded by the line running through the Melovatsk-Ilovlensk oil fields and by the Volga bank is characterized by variously trending anomalies of low amplitudes. Here the character of gravity anomalies is the most mosaic. The central area, which is bounded by the lines Melovatsk-Ilovlensk, Severo-Dorozhensk-Yuzhno-Umetovsk and by the Volga bank, displays predominantly northwestern-trending elevated anomalies. The most intensive are the isometric anomalies observed south of the Ilovlensk oil-and-gas field and southwest of the Melovatsk gas field. Whereas in the north of the central area northwestern-trending anomalies prevail, in the south submeridional anomalies are encountered. According to the results of gravity field recalculation into the upper semi-infinite space (Gilod et al., 1970), a single elevated-density massive was isolated here, in the zone of the southeastern slope of the Voronezh anteclise, which was given by these authors the name of the Lower Volga core.

The southern area has high-amplitude west-northwest-trending elliptical anomalies extended in a chain.

Within the Cis-Caspian depression, east of the gravity bench, there are small-in-area negative anomalies of high amplitude, which are elongated subparallel to the bench trend.

MAGNETIC FIELD

The character of magnetic anomalies is mainly due to the chemical composition and structural features of the folded basement, as well as to the behaviour of its surface. The differences in shape and amplitude between magnetic anomalies found within the neighbouring blocks may be attributed to the different types of rocks, of which these blocks are composed, and to their differing metamorphism. The latter factor may lead, for example, to the secondary enrichment of basement rocks in magnetic minerals, which, in turn, is one of the causes of elevated magnetic anomalies.

CORRELATION BETWEEN THE GRAVITY AND MAGNETIC FIELDS

A simple visual comparison between the gravity field and the magnetic field does not allow one to establish any relationship between the parameters under consideration for each locality. Accordingly, a scheme showing the correlation between the gravity field and the magnetic field has been constructed (fig. 7) using the computer program "Ankor" and employing the procedure suggested by M. S. Zhdanov and V. I. Shraibman (1973) for the Turan platform.

A calculation of correlation between these two geophysical fields reflecting the integrated characteristic of the density and magnetic properties of the upper layers of the Earth's crust, which was carried out by the procedure suggested, has made it possible to establish the direction of change in these fields in various localities. On the scheme, positive and negative areas have a largely mosaic character. But whereas the areas of positive correlation are mainly isometric, those of negative correlation are, as a rule, elongated. Since the character of both the gravity field and the magnetic field in the area under consideration is chiefly determined by the composition and topography of the basement, which, in turn, was formed under the influence of tectonic processes, one may suppose that the same factors are reflected on the presented scheme, too.

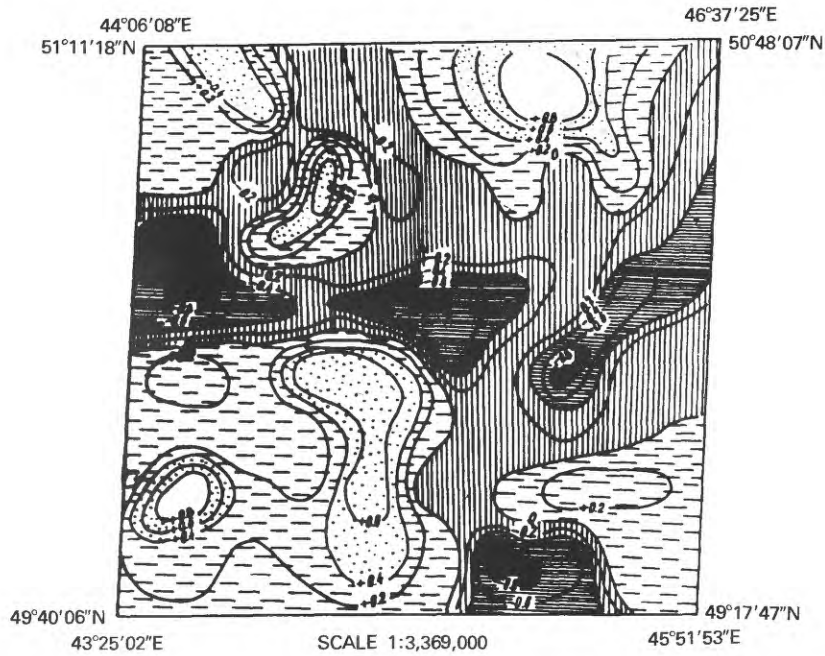

FIGURE 7.—Scheme of isolines showing the correlation coefficients for the gravity and magnetic fields.

A simultaneous analysis of the correlation scheme presented in fig. 7 and of the structural map showing the basement surface has revealed that areas of both positive and negative correlation correspond to positive and negative features of the basement structure. A weak resemblance can be observed between .the patterns of depth isolines and isolines of correlation coefficients. This suggests that the constructed scheme reflects but weakly the basement surface structure. At the same time, when matching the scheme of correlation coefficients with the petrographical scheme of Pre-Riphean basement, due to Bogdanova, Lapinskaya, and Podoba (1971), one can note that the localities of both individual intrusive bodies and fields of occurrence of definite rock complexes coincide. Thus, in particular, over intrusions of gabbonorites in the northwestern part of the photograph under examination one can observe an increase in positive correlation up to 0.79 which suggests rather a close relationship between gravity and magnetic anomalies in the localities indicated. Another extensive area of positive correlation found in the southwestern part of the photograph corresponds to a granulitic block of the basement recognized from drilling data (Bogdanova et al., 1973). In the northeastern part of the photographic sheet, isolines of positive correlation (correlation coefficient here is as high as 0.89 or even 0.97) outline a body of granitoids of the granulite facies of metamorphism (plagiogranites containing garnet and cordierite). In the central part, a submeridional zone of negative correlation can be observed.

BASEMENT STRUCTURE

In regard to structure, the area under study is made up of major elements differing one from another (fig. 8). In the west of the area, there is a periclinal termination of the Voronezh anteclise, where the basement occurs at a depth of 2.5 km; on the southeast, the Cis-Caspian depression slopes down, where the basement has sunk down to 10 or even 11 km. In the boundary zone between these major structural elements, there are several projections and troughs in the basement surface, which are complicated by local structures. Generally, these structures fall within the Saratov offset of the Pachelmsk aulacogen stretching, according to Nevolin (1971), towards Volgograd. On the northwest, a ramification of the other elements borders on the Cis-Caspian depression. The western and northwestern boundaries of the depression are drawn in conformity with a drastic decrease in the amplitudes of gravity anomalies.

The basement has been stripped by deep boreholes only in the relatively elevated western part of the territory (fig. 8). Most of core samples have been studied in detail at the department of petrography of the Moscow Institute of Petrochemical and Gas Industry, where a group headed by V. P. Florensky and T. A. Lapinskaya has systematically processed during many years practically all the core samples taken from the basement of the Volga-Urals region (Florensky, Lapinskaya, Knyazev, and others, 1956). The above-mentioned boreholes have stripped a variety of deeply metamorphosed rocks (Lapinskaya, Bogdanova, and

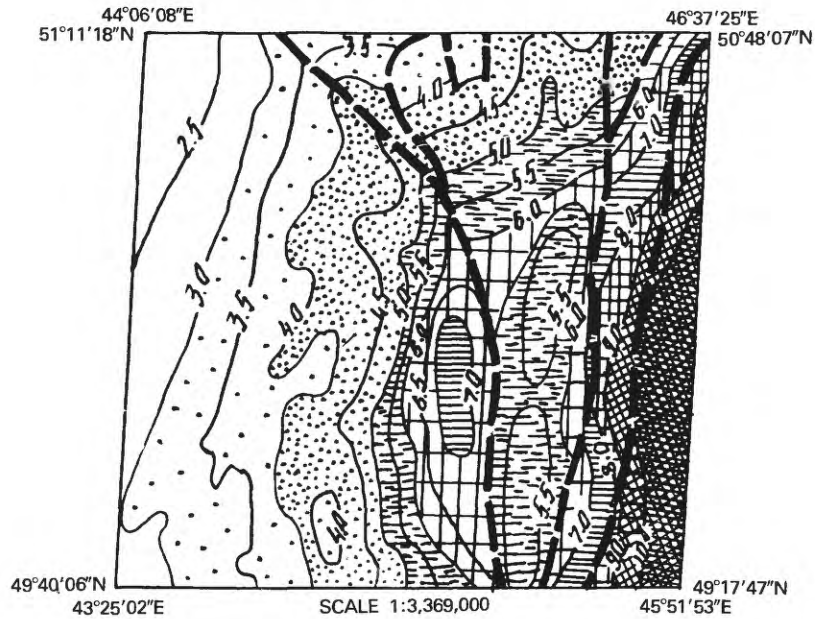

FIGURE 8.—Basement surface topography (after N. N. Nevolin, 1974).

Podoba, 1971). In the southwest of the area, there have been stripped Archean high-alumina gneisses of the granulite facies pierced by granitoids. In the extreme southwest, these rocks are overlain by Proterozoic phyllites, shales, and metasandstones (Bogdanova, Podoba, and Serova, 1973). To the north of this area, there has been stripped a field of rocks of the amphibolite facies (biotite-amphibolic gneisses, microclinic granites, etc.) containing relics of rocks of the granulite facies. This testifies to a deep diaphthoritic reworking of a part of the granulitic block in the presence of amphibolitic facies. A large massive (massif, ed.) of granitoids of Archean age has been stripped in the north of the area. In the central and eastern parts, where the basement occurs at a great depth and has not been stripped by boreholes, the composition and structure of the basement can be judged only indirectly from the geophysical materials available. It has been assumed that in the central part of the area there occur gneisses of decreased density which were reworked by the Svecofennian-Karellian folding (Gafarov, 1973; Nevolin, 1971).

The structure of the Pre-Cambrian basement of southeastern area has only been hypothesized tentatively. Specifically, east of the zone of decreased-density gneisses R. A. Gafarov (1973) recognizes a stable block made up of rocks that have not experienced the secondary reworking.

COMPARISON BETWEEN THE SCHEME OF PHOTOANOMALIES AND A COMPLEX OF GEOLOGIC AND GEOPHYSICAL DATA

A relief of the studied area is very gentle; being shaded by contrasting spots of vegetation, it is reflected very weakly in the distribution of optical densities.

The surface exposures of sedimentary rocks shown in the geologic map are also weakly reflected in the optical density distribution, which may be associated with the fact that the bedrock composition is monotonous, while the bedrocks themselves are covered by soil (mainly plowed).

Neotectonic movements shown in isolines of the erosion section (fig. 6) perhaps are best reflected in the optical density distribution (fig. 4). There emerges a single submeridional zone corresponding to a band of the greatest neotectonic uplifts and erosion. The areas of accumulation situated on the left bank of the Volga are lighter in tone; it would appear that the overlying sediments should have concealed the distinctions in this territory; nevertheless, it is differentiated photometrically, thus allowing its separation.

So far as the pattern of anomalies is concerned, the gravity field has in general a number of features similar to those of the optical density distribution. This similarity, however, manifests itself differently in different parts of the area. In order to compare them more objectively, a scheme of two-dimensional correlation of the gravity field with the optical density has

been constructed (fig. 9) along the direction of the photometric profiles. The values of the gravity field and optical density along the profiles were taken from a sliding interval 45 km long using a step of 30 km. The results of the calculations along the profiles have been extrapolated.

The curve showing the correlation of gravity with optical density is not high, but it is not smooth and usually oscillates by ± 0.7 or even ± 0.9 in some parts. From the sign of correlation, however, it turns out possible to single out only several individual zones. Across the central part of the photograph, there extends a wide submeridional band of positive correlation (its width reaches 70 km), which ramifies in the south of the photographed area into two branches, one of them being sublatitudinal and the other submeridional. In some parts of the above band, within the Kamyshin protrusion and northeast of the Kudinovsk elevation, the correlation increases up to 0.98. A second area of positive correlation occurs in the northwest and roughly corresponds to the eastern slope of the Voronezh anteclise. Zones of negative correlation found in the east are typical of the left-bank area, where in some parts the correlation coefficient reaches -0.95. The aforesaid allows a distinct division of the region discussed into three submeridional zones and, further, into a number of subzones, which is based on the correlation between gravity and optical density.

The magnetic field also exhibits a varying relationship with the optical density, which enables one to isolate in the territory under consideration several zones, which partly coincide with those isolated previously.

When comparing the map of magnetic anomalies with that of photographic anomalies, one cannot help seeing that the two are considerably related. In this case, as in comparing the scheme of optical density with the map of gravity anomalies, one may isolate various zones. The central part of the photograph is taken up by a submeridional zone of negative correlation coinciding with the zone of positive correlation between the optical density and the gravity field. The other parts of the area display, however, a more complicated and differentiated pattern. In particular, the area of positive correlation coincides with the slopes of the Voronezh anticlise, the left-bank region of the Volga is also characterized by the positive correlation between the optical density and the magnetic field.

The scheme showing the correlation between the magnetic and gravity fields (fig. 7) makes it possible to single out a submeridional zone bounding the darkest part in the southwest of the area, as does the scheme for optical densities (fig. 4). The principal trends of correlation anomalies coincide with those of optical density anomalies. The area of positive correlation between geophysical fields is relatively dark in the west ($D = 0.8$ to 1.0), while in the east, the areas of negative correlation between these fields are light ($D = 0.4$). Thus, areas of different correlation of geophysical fields (fig. 7), as well as those between geophysical fields and optical density (fig. 9), yield additional geo-

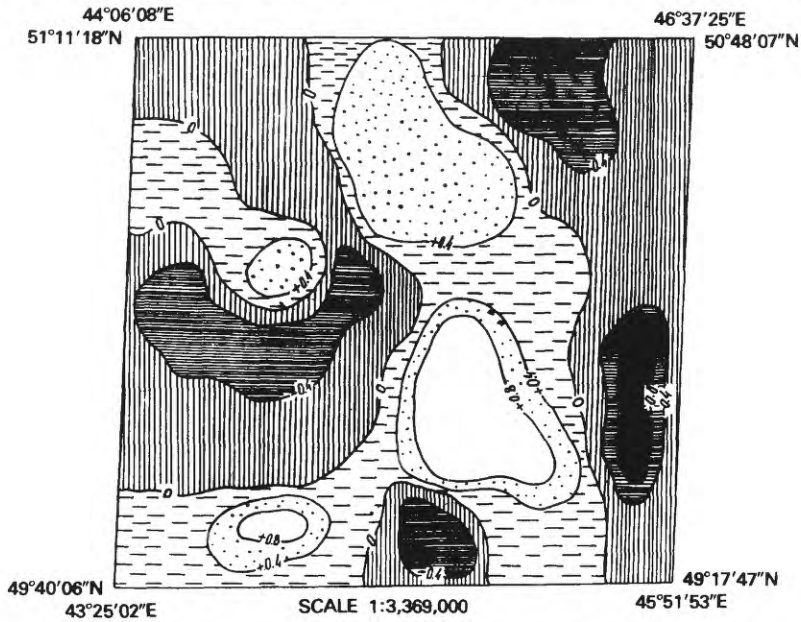

FIGURE 9.—Scheme of isolines showing the coefficient of correlation of the gravity field with the optical density.

logical information, which may be used in territory regioning.

Finally, comparison of the scheme of photographic anomalies with a complex of original geologic and geophysical materials enables one to consider the territory from the standpoint of the character of the relations established. The secondary schemes of correlations we have constructed are significantly different from the original ones. The reality of the new recognized fields is evidenced by the similarity in their patterns as observed in various, almost independent schemes. When analyzing the results obtained, it should be borne in mind that the photometric characteristics of space images of the platform territory reflect not so much surface geological objects, as regional tectonic elements of structure of both the sedimentary strata and the basement.

LINEAMENT IDENTIFICATION

When separating various fields, we have not discussed the character of their boundaries. However, it is just the geological boundaries between areas of contrast in some or other properties that are deciphered with the most certainty on space images.

In small-scale observations of the Earth's surface, the existence of the so-called lineaments has been established, i.e., lines of structural significance recognized from the gradients of photographic tone. These lines are only partly associated with the geologic and geomorphological structures visible on the surface in field observations. This applies primarily to fractures, whose deciphering on space images has been developed especially well for different tectonic regions and images of the different degrees of generalization (Skaryatin, 1973; Trifonov et al., 1973; Makarov et al., 1974). In mountainous and folded areas with abruptly changing topography or with distinct boundaries between the occurrences of different rocks, the recognition of fractures by conventional geological techniques and of lineaments by deciphering space images reduces, in effect, to the identification of one and the same structures and structural trends. In the platform regions, however, the methods of lineament recognition are quite different, as are the recognized structures themselves. Indeed, on the platforms, lineaments are expressed as slight (of several metres) changes in topography elevations, as bends in the river and ravine network, or as merely insignificant changes in the composition of outcropping rocks. Such geologic boundaries, even when confined to fractures, have very often stratigraphic rather than tectonical significance. Thus, the search for the geologic and geomorphological criteria for the identification of lineaments in the platform regions is a highly contradictory task. At the scale used in direct geological observations in field work, most of lineaments are unrecognizable at all. Thanks to space images of the platform regions, it has turned out possible to recognize especially many lineaments heretofore unknown. It appears that a considerable number of lineaments are not accompanied by anywhere near essential one-directional displacements of blocks, which would immediately be reflected on structural maps based on drilling data. One gets the impression that zones of extremely low-amplitude, but, probably, systematically different in direction, displacements, reducing merely to an extended band of increased jointing, are confined just to such lineaments. The latter probably intersect the Usturt Plateau leading to formation of straight parts of its chinks (border scarps) (Florensky, 1973; Bogorodsky et al., 1974).

On small-scale television images transmitted from satellites such as "Meteor" and "Meteor-Priroda" (fig. 1) a submeridional lineament can be seen, which strikes along the general direction of the Volga bed and corresponds geologically to the northwestern flange of the Cis-Caspian depression. There appears also a secondary (with respect to the meridional one) northeastern trend of lineaments.

On ERTS–1 images (fig. 2) lineaments appear quite differently. The meridional lineament is scarcely traceable; only straight parts of it on the Volga's right-bank are present on the images. One succeeds, however, in recognizing a number of other, less significant, lineament systems (fig. 10). The best pronounced is the northeast trending lineament traversing the image. In the western and central parts of the image, a bank of clouds is confined to this lineament; the boundary which is known to mark a change in weather in this district coinciding with northeast trending structures also corresponds to this trend. The remaining lineaments are expressed on the space image as very thin lines of change in photographic tone; only some of them can be identified with straight-line valleys of rivers and streams. Not always can such lineaments coincide with geological boundaries of a locality.

After independent identification of the lineaments on both space images followed by independent identification of them by different geologists (V. P. Bukhartsev, A. S. Petrenko, P. V. Florensky, and others), an attempt has been made to correlate their position with the gradients of geophysical fields, as well as with the basement surface structure and composition.

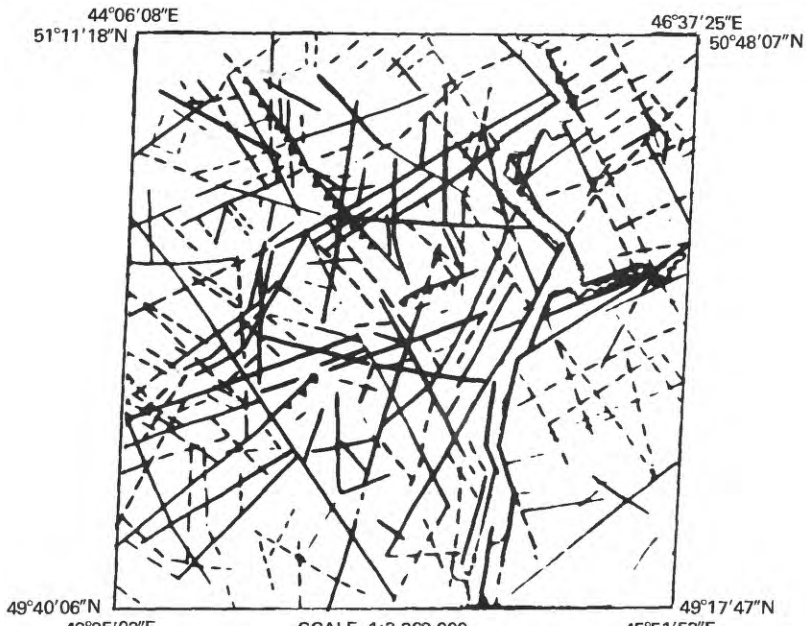

FIGURE 10.—Scheme of lineaments (of various degrees of expression on images).

One can observe a definite relationship between the northwest-trending fractures and the gradients of the gravity and magnetic fields. Two lineaments coinciding in trend with the fractures form the southwestern slope of the Saratov ramification of the Pachelmsk trough. Other lineaments striking parallel to them separate blocks of the basement composed of rocks of different compositions, which have already been described in the paper. Northwest-trending fractures are mainly characteristic of the right-bank region, whereas in the left-bank region northeast-trending fractures are especially prominent, only one of which can be traced from the right-bank area. The zone separating the areas of manifestation of lineaments trending predominantly northwest or northeast corresponds geographically to the Volga bed. Here fractures form something like branches of a fir tree whose trunk is the valley of the Volga, the acute angle of their intersection opening toward the south.

Thus, the lineaments that have been identified on the territory under consideration very weakly control its geomorphological structure. Not all of them affect the structure of the sedimentary cover. Almost all of the most prominent lineaments, however, appear to control the degree of metamorphic reworking of the basement, the structure of its surface and, in places, even the boundaries of variously aged pre-Riphean folding. One gets the impression that the inhomogeneities in the basement composition turn out to be just those weak spots along which there have developed the inherited zones of slight displacements taking place in the course of the entire platform stage, up to the recent time. When these displacements are inherited, singly directed and significant, only then are local structures confined to these lineaments. Where, however, the displacements along fractures have different directions, a zone of higher jointing is formed, which controls the character of reservoir. From this standpoint, the identification of such "fractures without displacements" is advantageous, as it has allowed a more exact determination of the position of jointy zones possessing improved reservoir properties. Wells that have been drilled in such zones are characterized by high yields.

IDENTIFICATION OF BLOCKS AND THEIR GEOLOGIC INTERPRETATION

As a result of the integrated analysis of diverse data, it has turned out possible to recognize on the territory under investigation a number of blocks characterized by different values of optical density, different surfaces, different geologic and geophysical parameters, and their different relationships (fig. 11, table 1). The structural elements identified in this way have different amplitudes of neotectonic movements, different characters of gravity and magnetic anomalies and varying optical densities of images. But they are recognized especially distinctly when the technique of pairwise correlation of the indicated parameters is applied. The method of local correlation of geologic and geophysical, as well as photometric, pa-

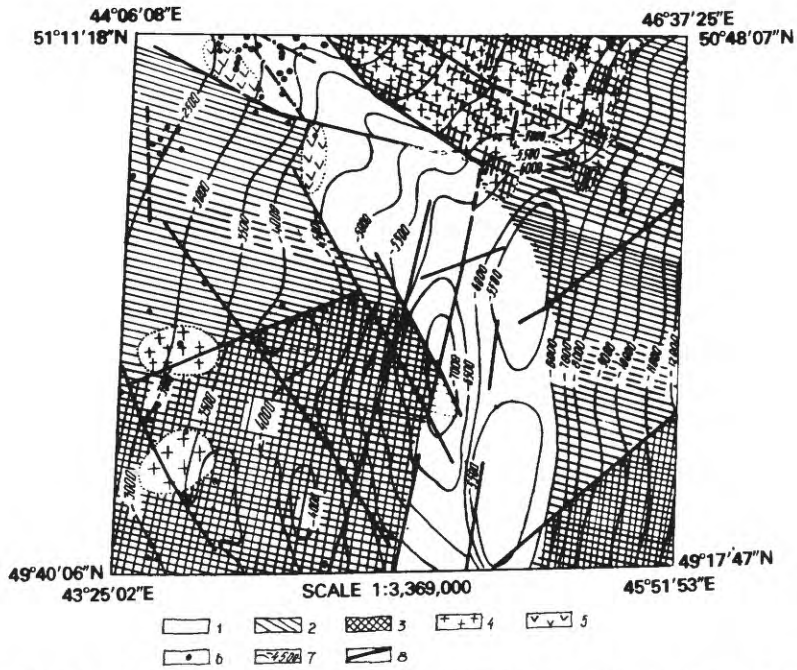

FIGURE 11.—Zoning scheme for the crystalline basement of the Lower Volga region compiled from a complex of geologic and geophysical data and taking into account the results of deciphering and photometry of TV-space images.
1—Zone of Svecofennian-Karellian reworking of the basement; 2—areas of metamorphic amphibolite facies; 3—areas of metamorphic granulite facies; 4—granitoids; 5—basic rocks; 6—boreholes that stripped the basement; 7—structure contours of the basement as shown in fig. 8; and 8—lineaments as shown in fig. 4.

rameters has proved to be the most effective in territory regioning. Generally speaking, the whole area under study is divided into three submeridional bands: Western, corresponding to the periclinal closure of the Voronezh anteclise, central, and eastern, corresponding to the western flange of the Cis-Caspian syneclise. These zones, in turn, are divided, according to the internal structure of the basement, into blocks, which, in places, are outlined by fractures.

The combined geologic-geophysical and photometric characteristics of these blocks are given in the table and, therefore, are not discussed in the text.

In what follows, some considerations concerning the internal, block-type structure of the basement are outlined, which are based on a generalization of the whole material investigated.

The Western zone, which is the periclinal closure of the Voronezh anteclise, is distinguished by the homogeneous character of the gravity and magnetic field. Its eastern boundary coincides with a system of meridional and submeridional fractures, identified as lineaments on space images and coinciding with gradients and local anomalies of the geophysical fields. With respect to the orientation of gravity and magnetic anomalies, the zone is divided into two blocks by a sublatitudinal fracture, to which steep gradients in the gravity and magnetic fields are confined.

The Southern block is characterized by sublatitudinal geophysical anomalies and by an increased optical density. Within the territory of the block, within the Korobkovskoye elevation, wells have stripped deeply metamorphozed rocks of the granulite facies (crystalline shales with granite) weakly changed by diaphthoresis. Here, local anomalies correspond to granitoid bodies. In the southwest of the area (within the Kudinovsk structure and in the Panin wells 74, 152, 154, etc.), younger (Proterozoic) phyllite shales spreading farther to the west have been stripped (Bogdanova et al., 1974).

The Northern block is remarkable for submeridionally trending geophysical anomalies and for its lighter colored surface. Within the territory of the block (within the Zhirnovskaya, Linevskaya, Severo-Dorozhanskaya, and Mishinskaya structures), diaphthorites of the granulite facies have been stripped; for example, bi-amphibolitic plagiogneisses, granodiorites, and amphibolites.

The Central zone is characterized by rather low gravity and magnetic anomalies, as well as by their negative correlation. For this zone, the tendency to uplift and the positive correlation between gravity anomalies and optical density are characteristic. Along its strike, the zone is especially dissected by fractures and is noted for the lowered values of gravity anomalies and for the presence of an extensive negative magnetic anomaly. These features are not at variance with the suppositions that here there occur rocks reworked last by the Svecofennian-Karellian folding (Gafarov, 1973), which resulted in lowered densities of these rocks and in their intrusive injections. If the supposition is correct, the identified zone is a submeridional branch of the Pachelmsk trough, bordering on the southeastern slope of the Voronezh anteclise.

As a result of a comprehensive comparison of the geologic and geophysical data available with those of visual deciphering, and as a result of a formalized processing of space images of the area under consideration, it has turned out possible to establish that the correlative analysis enables one to make the most complete use of the information one possesses to study the deep-seated structure of parts of the ancient platform. Further, the conventional techniques for processing and generalizing the geologic and geophysical information have made it possible to outline, by using the results of direct study of core samples of the basement rocks, some features of the tectonic structure of the basement of the Lower Volga region and to add new details to the existing schemes. Thus, it has been possible to outline one of the sides of the relationship between the character of space images and the features of the internal structure of the region under study realized through neotectonic movements, which have evidently been caused by a compensated uplift of the decreased-density zones in the basement.

The presented complex of data on the deep-seated structure of a part of the Lower Volga region permits one to compare the information capacity of a space television image with that of other sources in regard to understanding of the deep-seated structure of the region.

First, in recognizing lineaments, fractures, and dislocations with a break in continuity and in specifying their positions space images have no equal sources of information. It is likely that the introduction of space images into scientific use signifies an essentially new stage in fracture study. This is especially true of the platform regions, in which displacements along the fractures are insignificant and their traces are concealed by the sedimentary cover.

Second, when taken by itself, the analysis of variations in optical density has shed but little light on the regioning of the studied territory, but when integrated with the analysis of geophysical data, its informative capacity has radically increased. It is likely that, at least for the platform regions, the informativity of space images for our understanding of the deep-seated structure of the area under consideration and its regioning approaches the informativity of regional geophysical investigations. And only in a combination with the results of regional geophysical studies can the space image information be interpreted.

This work has been done at the laboratory for Deciphering Aerospace Images (Institute of Geology, the USSR Academy of Sciences) under the general guidance of V. G. Trifonov, to whom the authors express their deep gratitude.

REFERENCES

Bakirov, A. A., Present-day concepts of the geologic structure of the crystalline basement of the Russian platform. Trudy Akad. neftyanoy promyshlennosti, issue 1, 1957.

Bogdanova, S. V., Lapinskaya, T. A., and Podoba, N. V., Petrographical characteristics of basement. In: "The study of the geologic structure of the East European platform by geophysical methods," Moscow, Nedra Publishers, 1971, pp. 69–84, illus.

Bogdanova, S. V., Poboda, N. V., and Serova, A. D., On the deep-seated structure and composition of the basement of eastern Russian platform. Izvestiya Akad. Nauk SSSR, ser. geol., 1975, no. 12, pp. 19–31, illus.

Belyaevsky, N. A., The earth's crust within the USSR territory. Moscow, Nedra Publishers, 1974, p. 283, illus.

Borisov, A. A., The deep-seated structure of the USSR territory according to geophysical data. Moscow, Nedra Publishers, 1967.

Bukhartsev, V. P., Geological prerequisites for the probabilistic forecast of oil- and gas-bearing zones from local ruggedness of relief of platform territories. In: "Mathematics, Computers, and Automatic Control Systems in petroleum geology." Moscow, Institute of Fuel Mineral Geology and Prospecting, 1973, p. 130, illus.

Bush, E. A., Kuznetsov, V. G., Ryabchenko, F. M., Sokolov, V. L., and Shornikov, B. Ya., Geologic structure and objects of search for gas in the flange zone of the cis-Caspian depression in

southern Volga region. "Geol. nefti i gaza," no. 5, 1968.

Gafarov, R. A., The basement structure of the East European platform and some problems of comparative tectonics of ancient platforms. In: "Tectonics of basement of ancient platforms." Moscow, Nauka Publishers, 1973, pp. 82–94, illus.

Gilod, D. A., Vostokov, E. N., and Dabizha, A. I., On some features of the basement structure of the south-eastern slope of the Voronezh anteclise (according to geophysical data). Vestnik MSU, ser. geol. no. 5, 1970, p. 115–120, illus.

Zhdanov, M. S., and Shraibman, V. I., A correlation method for separating geophysical anomalies. Moscow, Nedra Publishers, 1973, p. 128, illus.

Kuchko, A. S., Aerophotography. Moscow, Nedra Publishers, 1974.

Makarov, V. I., Skobelev, S. F., Trifonov, V. G., Florensky, P. V., and Shchukin, Yu. K., Deep crustal structure as seen on space images. In: "The study of natural environment from space," issue 2. Geology and geomorphology. Moscow All-Union Institute of Scientific and Technical Information, 1974, pp. 9–42, illus.

Mikhailov, V. Ya., Photography and aerophotography. Moscow, Geodezizdat, 1972.

Nevolin, N. V., The main features of the geologic structure of the basement of the East European platform. In: "The study of the geologic structure of the East European platform by geophysical methods." Moscow, Nedra Publishers, 1971, pp. 87–91, illus.

Skaryatin, N. D., On the study of rupture tectonics from a set of variously-scaled space images of the Earth's surface (the multistep generalization technique) Geologiya i razvedka, 1973, no. 7, p. 34–50, illus.

Trifonov, V. G., Byzova, S. D., Vedeshin, L. A., Derevyanko, O. S., Ivanova, T. P., Kopp, M. L., Kurdin, N. N., Makarov, V. I., Skobelev, S. F., and Florensky, P. V., Concerning the procedure of geologic deciphering of space images of the Earth. In: "The study of natural environment from space," issue 2, Geology and geomorphology, Moscow, All-Union Institute of Scientific and Technical Information, 1973, pp. 8–78, illus.

Florensky, P. V., Lapinskaya, T. A., and Knyazev, V. S., Some results of the petrographic study of the crystalline basement of the Volga-Urals petroliferous region. Trudy Moskovskogo Instituta Neftekhimicheskoy i Gazovoy Promyshlennosti (Moscow Institute of Petrochemical and Gas Industry) Gostoptekhizdat, issue 26, 1969.

Florensky, P. V., Deciphering of the deep structure of the Turan platform from space images in connection with the prospecting for oil and gas fields. Izvestiya Vysshikh Uchebnykh Zavedenii, Geologiya i razvedka, 1973, no. 7, pp. 112–117, illus.

PROCEEDINGS OF
THE FIRST ANNUAL WILLIAM T. PECORA MEMORIAL SYMPOSIUM,
OCTOBER 1975, SIOUX FALLS, SOUTH DAKOTA

Geological Studies by Space Means in the U.S.S.R.[1]

By V. G. Trifonov, V. I. Makarov, V. M. Panin, S. F. Scobelev,
P. V. Florensky, and B. P. Shorin-Konstantinov,
Geological Institute of the Academy of Sciences of the U.S.S.R.
Moscow, U.S.S.R.

Wide spectrum of the geological tasks requires the using of various methods of research: from studies of the atomic, molecular, and crystal structure of minerals and rocks to studies of the large structural forms and distribution of them in the planet. In the recent stage of the development of geology the solution of its many problems (first of all tectonic problems) is possible only by studies and correlations of the geological objects and events in the planetary scale and taking into consideration of peculiarities of the Earth as a space body. Such planetological aspect of the geological studies is provided (beside the traditional means and methods) with the new source of information on principle, that is the Earth's pictures from the satellites and orbital stations. These images are in visible and infrared parts of spectrum and are received by photographic, televisional and scannering means.

Geological using of the space visible information that started about 10 years ago, now has achieved large successes in the USSR, USA and number of the other countries. We don't want here to review the common progress in this branch of studies, but limit ourselves by observation of some works carried out in the Geological Institute of the Academy of Sciences of the USSR.

First of all the space images started to be used for compiling and correction of geological, structural, and tectonic maps, for mapping and correlation of the large structural forms and zones. So, the map of the major faults and zones of deformations of southeastern Kazakhstan, Middle and Central Asia was compiled with help of TV images with resolution 1–2 km from meteorological satellites. The geological map of the central part of Tadjik depression (figs. 1 and 2) was compiled by deciphering of space photos from "Sojuz–9" with the higher resolution (100–200 m). The rather good quality of picture and integration of the brightnesses of the individual layers permitted to map objectively the lithological-stratigraphic units, folds and faults. The results of interpretation checked by the field observations. The comparison showed that deciphered map required essentially less of time and means than the earlier geological maps of the area in the same scale; but it didn't yield them in image of details, excelled them in exactness of image of faults and represented more objective generalization of the fold structure.

The further development of the structural-geological trend of the space information using is connected with analysis of images in different spectral bands and its combinations. In the examples of images with resolution about 100 m of Eastern Fergana and the northwestern foreland of Pamir in Middle Asia we can see that in bands 0.5–0.7 mkm the Quaternary deposits and the more old rocks with rather high collector ability are deciphered better than all (figs. 3 and 4). In arid conditions of the Middle Asia the most evaporation occurs from these formations, because of it and peculiarities of vegetation they are seen as the more or less light places independently to the real color of the rocks.

In near infrared part of spectrum the Prequaternary formations are deciphered better. The surface geological structure is reflected with essential detailness in the images in band 0.8–1.1 mkm (mainly because of the reflection of various formations in the relief). In

[1] Printed verbatim as received from the authors, except for minor changes in format and spelling.

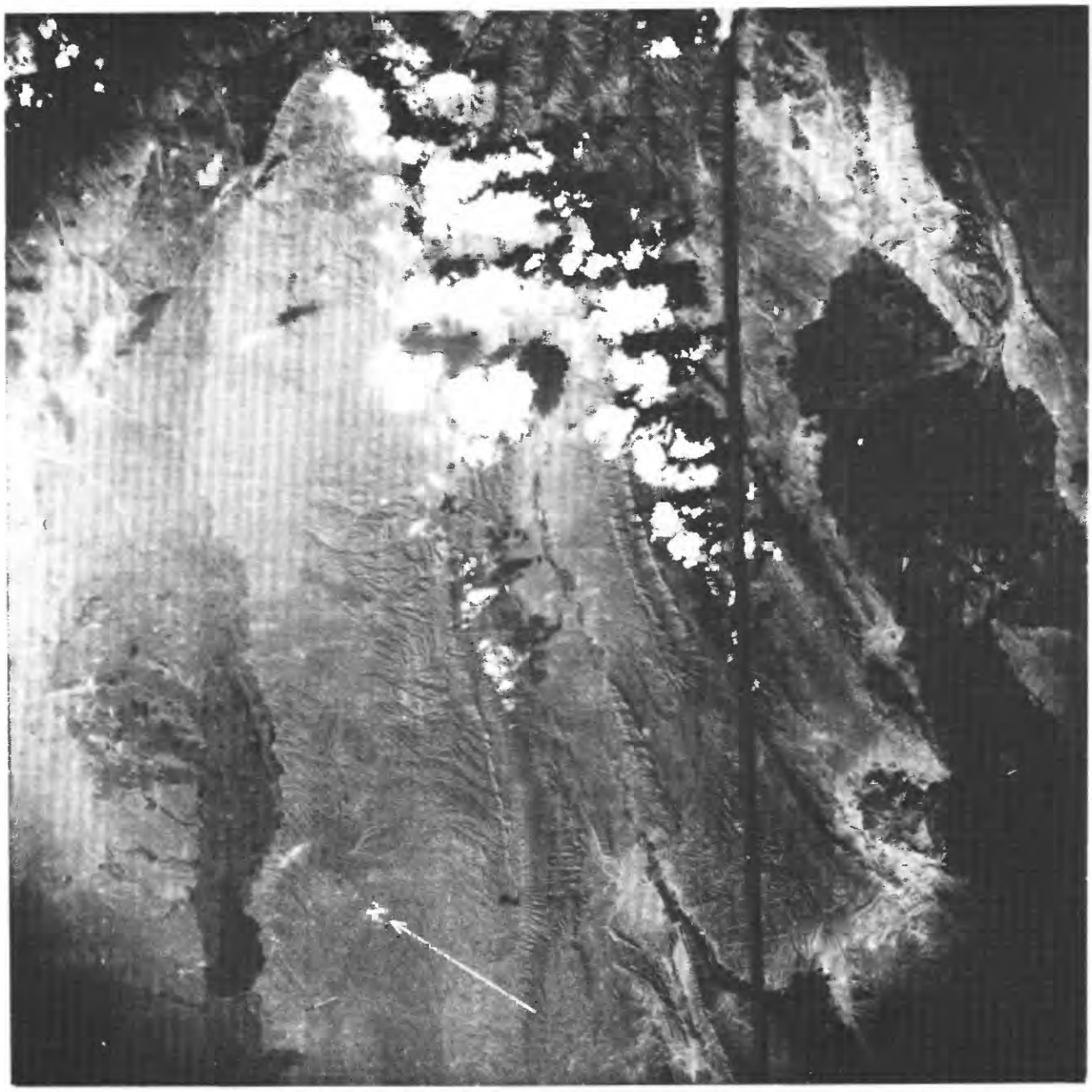

FIGURE 1.—Large-scale space photo of Babadag-Karatau region of the central part of the Tadjik depression (spacecraft "Sojuz–9," cosmonauts A. G. Nikolaev and V. J. Sevastianov)

band 0.7–0.8 mkm both the relief and the color of the rocks have the indicative role. The possibility of deciphering of details is less than in band 0.8–1.1. It permit to find the main structural elements, for example, the large tectonic lineaments (figs. 5 and 6) that are not seen in surface sometimes, but reflect the deep structure that we shall discuss below. Such lineaments are deciphered better in images that are received by combination of various bands, for example by "subtraction" of bands from each other.

It is especially productive to use the space images for studies of the geomorphology, the Neogene-Quaternary deposits and the modern structure of the Earth's surface. In the orogenic areas there can be deciphered the genetic types and sometimes the age of relief; the units of the Quaternary cover (1, figs. 8, 9); and the modern folds and faults (figs. 7 and 8). It is possible to see not only large structural forms, reflected by deformations of the modern deposits and the erosional forms, but very gently sloping uplifts

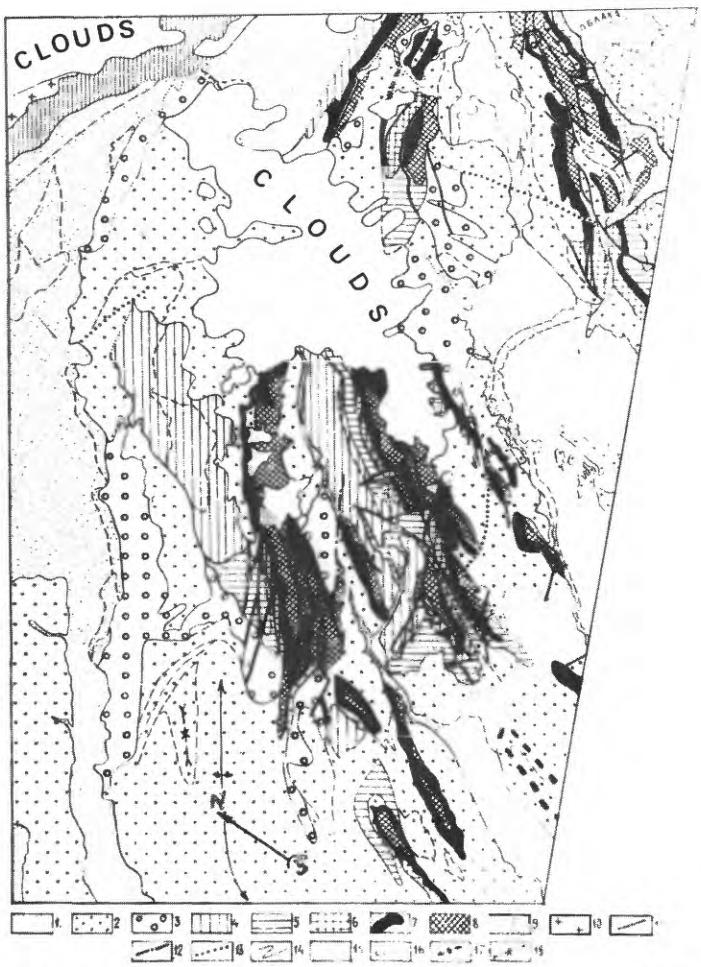

FIGURE 2.—Structural-geologic map of the central part of the Tadjik depression compiled using space photos.
1—Holocene and Upper-Pleistocene alluvium and proluvium; 2—Mid-Pleistocene loesses and loess-like deposits; 3—Lower-Pleistocene conglomerates (dashed lines are the boundaries of the geomorphological levels); 4—Mid-Miocene-Pliocene conglomerates and sandstones; 5—Oligocene-Lower-Miocene sandstones, alevzolites, and conglomerates; 6—Eocene-Oligocene deposits mainly clays; 7—Campan-Bukhara clays, gypsum, and limestones (k-p); 8—Alb-Santon clays with limestones, sandstones, and gypsum (k); 9—Mesozoic and Cenozoic de- and limestones (k-p); 8—Alb-Santon clays with limestones by geological methods; 12—found by geomorphological meth-posits, undivided; 10—Paleozoic deposits. Faults: 11—found by geological methods; 12—found by geomorphological methods; 13—masked by the Quaternary deposits and supposed. Geological boundaries: 14—mapped; 15—masked by the Quaternary deposits and inner boundaries in units; 16—supposed; 17—axes of the anticlines; and 18—axes of the synclines.

among intermountain basins. The same uplifts are found also in space pictures of platform, where they reflected the masked structures of the plate cover that are in prospect for search of oil and gas (figs. 9 and 10).

It is possible to receive the essential information from space pictures on a modern volcanism. In Kamchatka and Caucasus, the faults, the eruptive fractures and various types of the volcanoes are deciphered. In Landsat–1 images of Iceland, it can be seen not only volcanoes, volcanic chains, and faults of rift strike, but some hidden transverse elements of structure, not found before by land observations.

The information from small-scale space images is uniform and independent on approachness of regions. It gives us the possibility to map and correlate the major neotectonic forms and zones and finally to compile the pattern of modern structure of the continents as a whole. It will permit to give answer such significant questions of geotectonics as the planetary regularity in localities and strikes of various modern structural elements, and, at last, sources and mechanism of structural formation.

The good expressiveness of modern structural forms, deposits, and relief, the minimum of the latest complications, and the general distribution made them the best subject for the solution of the tasks of the detail planetary correlation of the tectonic processes. The role of the space information for the solution of such tasks is not so large, but some utilizations can be presented. At first, the mapping of structural forms and fault zones and the determination of age of deformed deposits are the elements of correlation themselves. At second, the studies in Middle Asia showed that forms of relief of different ages have the specific peculiarities and indicative features permitting to map them on the large distance and by this way to correlate the modern structural elements of the distant regions.

New possibilities of the geological application of the space pictures that differ them from airphotos on principle are due to peculiarities of the generalization of image with the decrease of scale of the survey. The correlation of the results of deciphering of the space pictures with the geological, geomorphological, and geophysical data show that structural elements that one can see on them, are not only large, but located in deep horizons of the Earth's crust and its basement.

Geological manifestations of such zones of deep deformations are often masked by the numerous surface deformations, so they can't be found by field researches and on airphotos. They are reflected better in the modern structure, but here the fragmentation of manifestations prevents to compile the common picture that is seen in space images only.

Let us observe that problem on the data of Eastern Caucasus. Space pictures of it were received from spacecrafts "Sojuz–9" and "Meteor" series. The elements of "Caucasus" strike predominate in the geological and modern surface structure of this region.

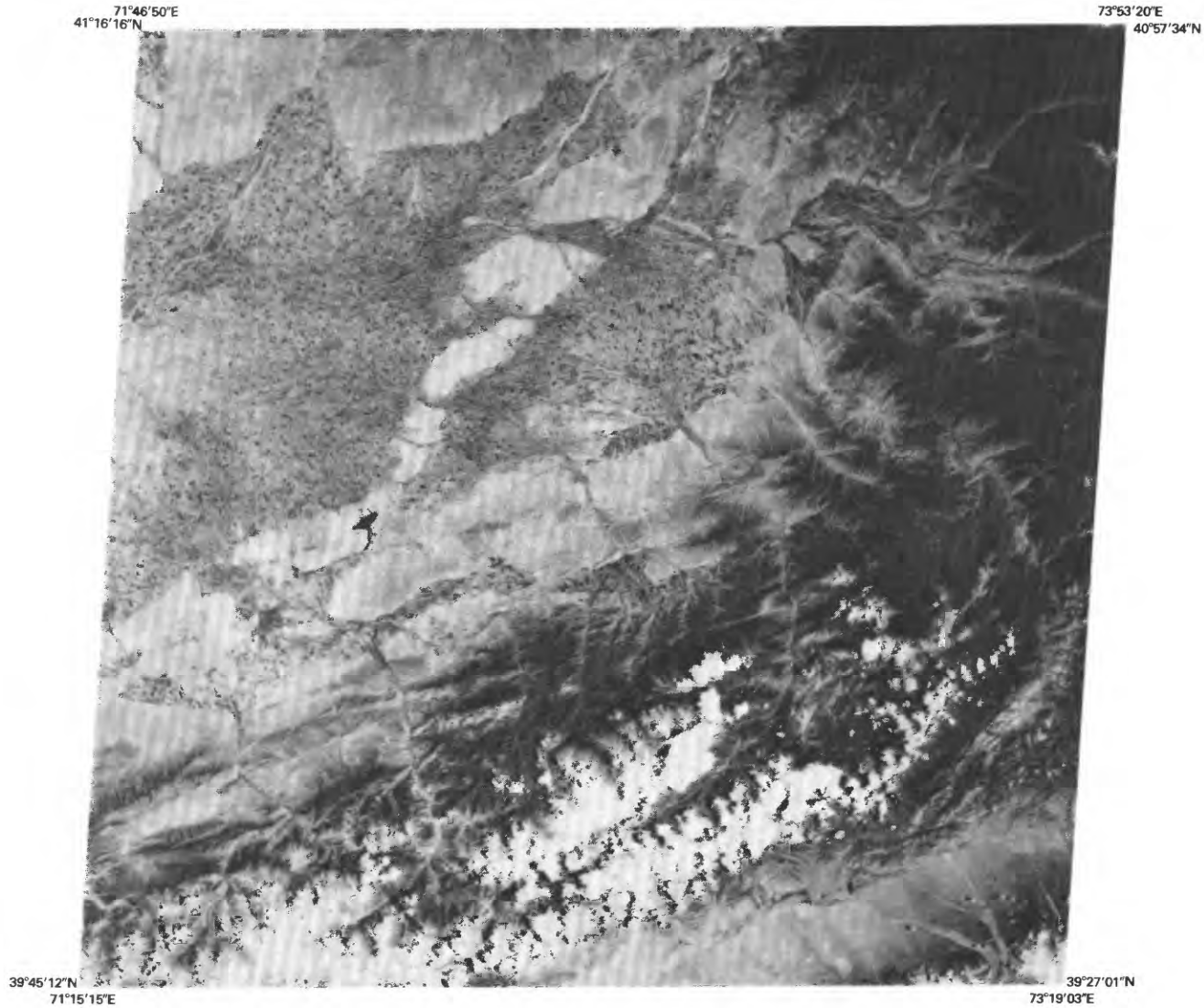

FIGURE 3.—Scanner image of Eastern Fergana, Landsat–1, June 24, 1973, band 5.

They are reflected on space photos with resolution 300–400 m, but the transverse lineaments are seen here beside them (fig. 11). The last correspond to the surface faults only partly, but often represent the boundaries of the different facies and thicknesses of deposits and the areas with different tectonic styles. Increasing of the intensivity of surface deformation, the Late Quaternary displacements and concentration of the air volcanoes occur along some lineaments. They correspond to the zones of high gradients of dipping, boundaries and bends of structural forms of the surface of the crystalline basement (where it is the deepest) and of the Conrad surface. The analysis of instrumental and microseismic data shows that the zones of abnormal going out of the seismic waves (fig. 12) and zones of high density of epicenters (mainly of shallow earthquakes) strike along the lineaments.

The lineaments seem to reflect the zones of deformations on the depths 5–20 km.

On the "Meteor" pictures with resolution about 1 km (fig. 13) the more part of those lineaments are seen badly absent. The lineament of "Caucasus" strike are seen here the best of all. They correspond to the long zone of southern slope of Big Caucasus where the area of strong and relatively deep (10–60 km) earthquakes is located (fig. 14) according to the data of I. V. Ananjin. Along this zone the thickness of the Earth's crust is essentially changed. Two lineamental zones of NE-SW strike are deciphered less clearly. They correspond to the areas of epicenters on depths to 20–30 km.

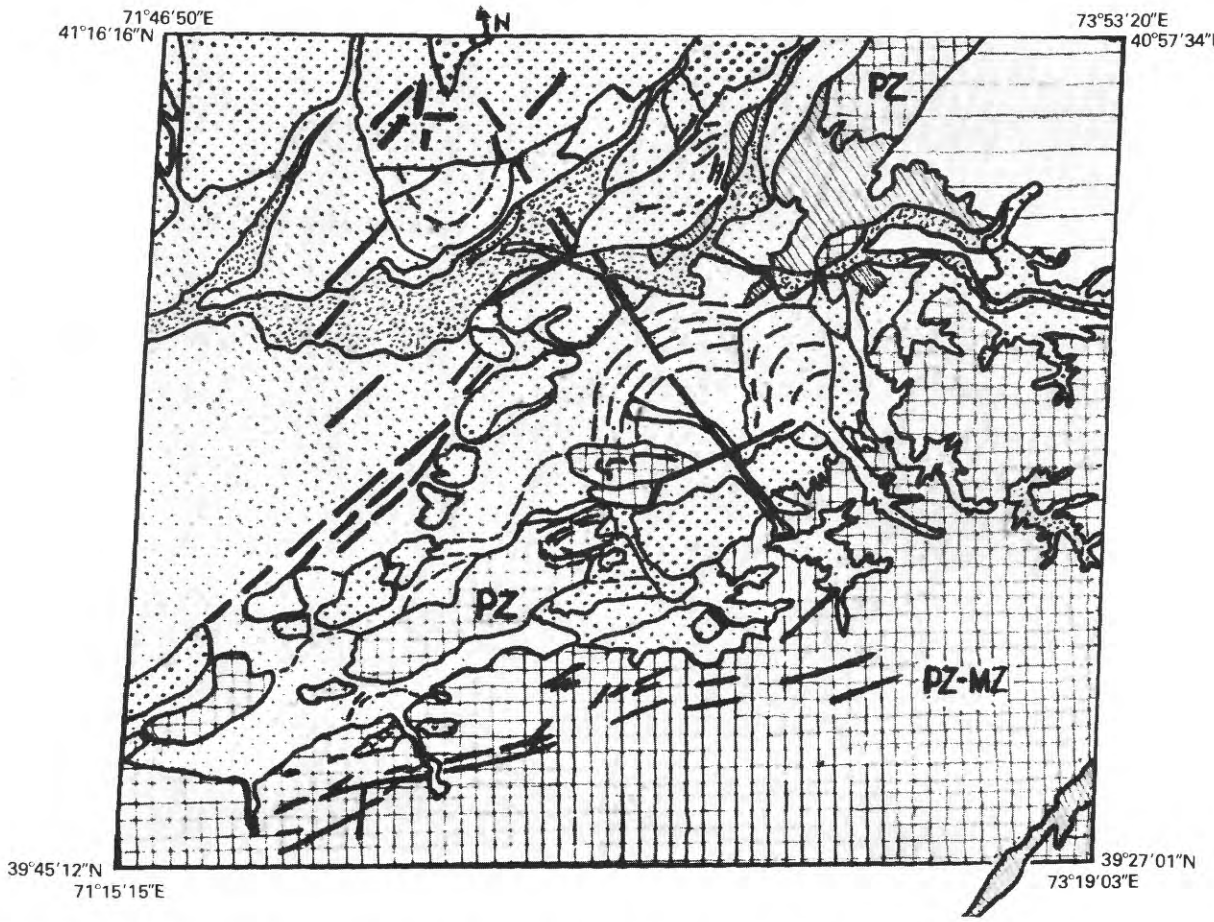

FIGURE 4.—Geological interpretation of the image figure 3. Points are the various Quaternary deposits; lines dipped to right are the Lower-Cretaceous deposits; horizontal lines are Upper-Cretaceous deposits; crossing lines are the Paleozoic formations.

Thus, the structural elements of the various depths are deciphered on the space pictures. The more the degree of generalization of image is, the deeper elements of structure are reflected on it. The differences found in the structures of various depths permit sometimes to assume the structural disharmony between the different depths. At the same time the tectodynamic analysis of the geological structural of surface and its comparison with the results of determination of the earthquake focus mechanisms and the directions of displacements in the Late-Quaternary faults, striked along the lineaments, give the arguments to suppose that the various horizons of the Earth's crust are under the same stresses and differ only by the types of the rock deformations created by them.

The analogous picture takes place in Tjan-Shan. On the space images of this mountain country there are two types of the modern structural forms: (1) various bands that correspond to ridges-uplifts and intermountain basins and (2) the lineaments of the different orders. On space photos with the relatively high resolution the ridges and basins that correspond to the individual foundation folds (anticlines and synclines), are seen. With the generalization of image there are observed the anticline and syncline zones and then only the up-warping and down-warping systems, that are the major elements of the modern structure. According to the geological, geomorphological, and geophysical data, the individual ridges-anticlines and basins-synclines and their zones are the deformations of the folded basement surface and reach only the Conrad surface; while the anticline and syncline systems are fixed by the changes of depth of Mohorovicic surface.

The longitudinal lineament corresponding to the zone of sharp change of basement depth, is deciphered on the space photos with resolution 300–400 m of Southwestern Tjan-Shan. On the TV-pictures with resolution 0.8–1.5 km this lineament is absent, but the long lineament of NE-SW strike is seen. The last cor-

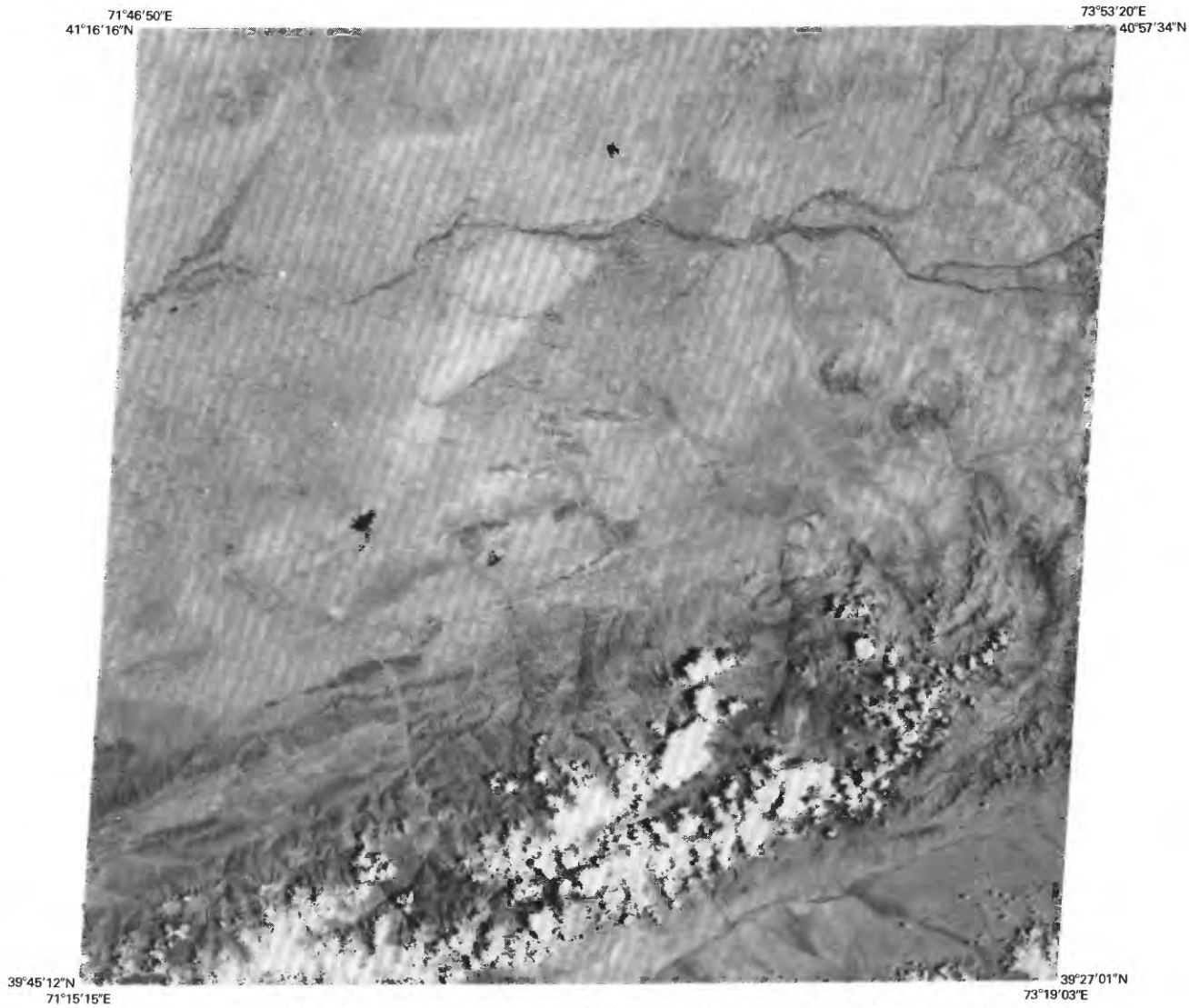

FIGURE 5.—Scanner image of Eastern Fergana, Landsat–1, June 24, 1973, band 6.

respond to the zone of the essential change of the Earth's crust thickness, to the boundary of high seismic activity area, and to zones of abnormal going out of the seismic waves.

On the relatively large-scale space photos of Tadjik depression (resolution 100–150 m; "Sojuz–9" and Landsat–1) the elements of surface geological structure with longitudinal folds are deciphered well. When the degree of generalization of image increases, the transverse lineaments are seen better and better. They reflect the disposition of the geophysical anomalies and correspond to the deformations of the crystalline basement surface and the deeper horizons of the Earth's crust.

The data under consideration show the possibility to advance with help of space pictures the problem of the structural and genetic relations of the different horizons of the lithosphere. Space pictures can't claim to be the only source of information about deep structure, but results of their deciphering permit to interpret the geophysical data more objectively. Of course, we can see on visible and infrared space pictures only the different elements of landscape, but the elements reflecting the structure of various deep horizons, are "in focus" on pictures with various degrees of generalization.

Space pictures permit also a new interpretation of the correlation between the lithosphere and the atmosphere. On the images of Tjan-Shan, Turan plate, Mongolia, and northeastern part of the Russian platform there is observed the coincidence between the elements of the cloud cover and the large disturbed zones

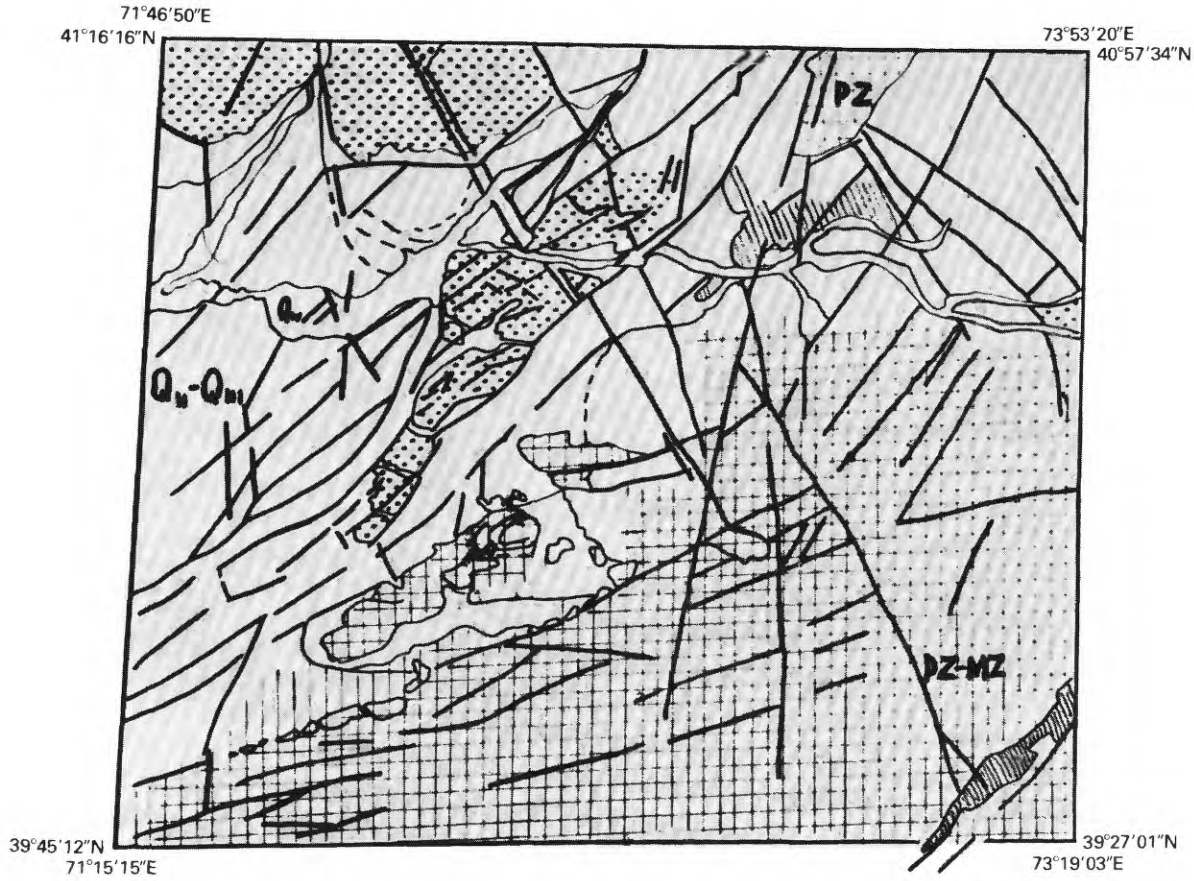

FIGURE 6.—Geological interpretation of the image figure 5. Points are the various Quaternary deposits; lines dipped to right are the Lower-Cretaceous deposits; horizontal lines are Upper-Cretaceous deposits; crossing lines are the Paleozoic formations.

of the Earth's crust, the last reflected on the surface only indirectly sometimes. The relief can't define such localities of the clouds in these cases.

The process of geological deciphering of the space pictures can be conditionally divided into three stages. The task of the preliminary stage is to represent the materials of the space survey in the most informative and convenient forms. The photographic filtering is very useful, for example "addition" or "subtraction" of the pictures in various spectral bands. The specific kind of filtering and of the objective analysis of pictures is its photometry in various scale.

In the stage of deciphering (in basis of brightness and geometry of the images of the geological objects) the essential significance belong to the comparison of the pictures of various spectral bands and their combinations, of the different degrees of generalization, and of the different season. So, the snow on the winter pictures masks many geological details, but emphasizes some large linear elements of the structure.

In the stage of interpretation the comparison of the results of deciphering with the geological, geomorphological, and geophysical data is carried out. The interpretation is found on the studies of the indicative signs of the geological objects of the region under researches and of the similar ones. For studies of the indicative signs is useful the observation of the objects with different degrees of generalization (on land, from helicopters, aircrafts, on air and space pictures) is useful. As usual, the field check of the results of deciphering and interpretation is necessary.

Let us consider the operations of each stage in the example of the studies of space pictures of the Lower Volga region (southeastern part of Russian platform). We have used as a basis the scanner color picture of the area with resolution about 100 m (fig. 15). Almost all the surface is the combination of the agricultural lands with the different brightnesses, so it does not permit to decipher geological elements, the larger, but poorly differed in brightness. It has been necessary to decrease the influence of brightness differences of the agricultural lands and to develop the features of picture that reflect the geological structure. For this the contrast has been developed by the photographic

FIGURE 7.—Middle-scale photo of the Issik-Kul region (spacecraft "Sojuz–9," cosmonauts A. G. Nikolaev and V. I. Sevastianov).

means. The received picture has been photometried along the frequent net of profiles. The using of the most open split of the photometer and big step of interpolation have permitted to exclude the small fluctuations of the density and to develop the differences connected with the geological structure. It is the generalization and the specific photometric filtering of the primary picture.

The received map of the conditional brightness (fig. 16) has been compared with the maps of the geology the neotectonics and the basement surface structure, the gravimetric and magnitometric data. The comparison has been carried out by the calculation of the coefficients of correlation, represented on the special maps. The geological map is not correlated with the photometric one, but the magnitometric and partly gravimetric data are in accordance with the last. It has been shown by the correlation of the data that distribution of the brightnesses reflect the structure of the basement of this part of the plate. The application of the materials of the deep bore holes and the geophysical data permit to compile (with using of the other space images of the area) the hypothetic structural-geological scheme of the basement (fig. 17). The modern movements of the Earth's crust correlate partly with structure of basement.

All the operations under consideration (beside the compiling of the final scheme) are formalized and can be carried out by the computer. Thus, the last can be widely used for the solution of some tasks of deciphering, the signals of TV and scanner systems not been necessary to present in visible form.

So, the geological deciphering and interpretation of space images can be used for the solution of the main matters of recent geology. The practical significance of the geological application is in the possibility to cheapen and to increase the quality of the geological survey, to plan the expensive geophysical researches better and to interpret their results more objective. Space pictures can be used for correction of the maps of seismic danger; for finding of structural forms and zones that are in prospect to search the underground waters, oil, gas, and number of the ore deposits; at last, for solution of the tasks of the engineer geology,

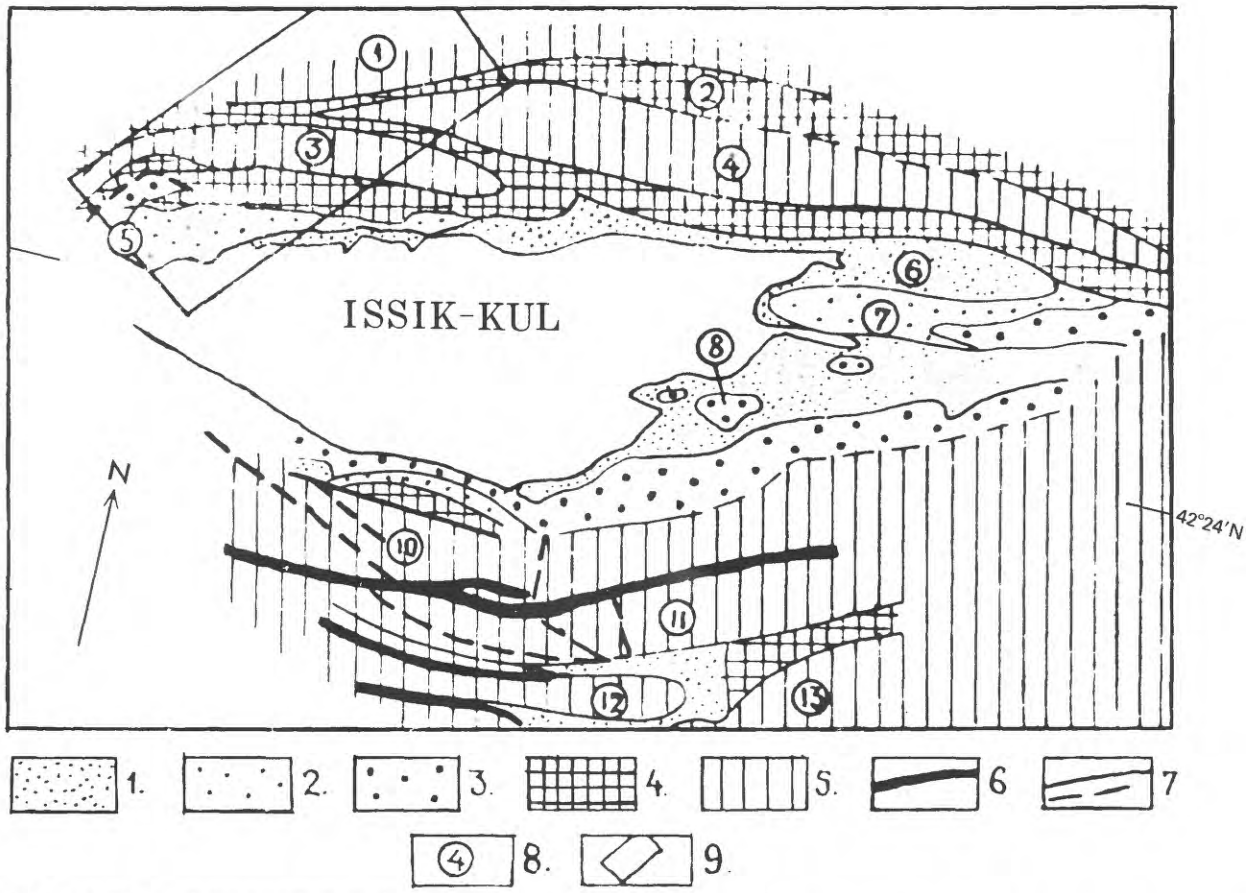

FIGURE 8.—Geological-geomorphological interpretation of the photo figure 7.
1—Limneous and alluvium-proluvium plains of Late Pleistocene and Holocene; 2—fragments of the high accumulated plains of Mid-Pleistocene; 3—marginal and inner uplifts in basin, mainly Neogene deposits; 4–5—systems of modern uplifts built by the Paleozoic formations (4—zone of the young relief, steep deeply eroded slopes of uplifts; 5—zone of the fragments of the old relief of intervalley areas); 6—zones of intermountain narrow fault-basins; 7—faults; 8—figures of structural forms (1, 3, 4, 7–13, anticline forms; 2, 5, 6, syncline forms); and 9—area of detail observations.

that is the election of the routes of communications, the places for reservoirs, dams, et cetera.

BIBLIOGRAPHY

Trifonov, V. G., Bysova, S. L., Vedeshin, L. A., Derevjanko, O. S., Ivanova, T. P., Kopp, M. L., Kurdin, N. N., Makarov, V. I., Scobelev, S. F., Florensky, P. V., Problems of techniques of geological investigation of space images of the Earth. Investigation of the natural environment by space means. Geology and geomorphology. Printing house VINITI, Moscow, 1973 (in Russian).

Makarov, V. I., Scobelev, S. F., Trifonov, V. G., Florensky, P. V., Shchukin, Yu. K., Plutonic structure of the Earth's crust on space images. Proceedings of the Ninth International Symposium on Remote Sensing of Environment, vol. I. pp. 369–438. 15–19 April 1974. Ann Arbor, Michigan.

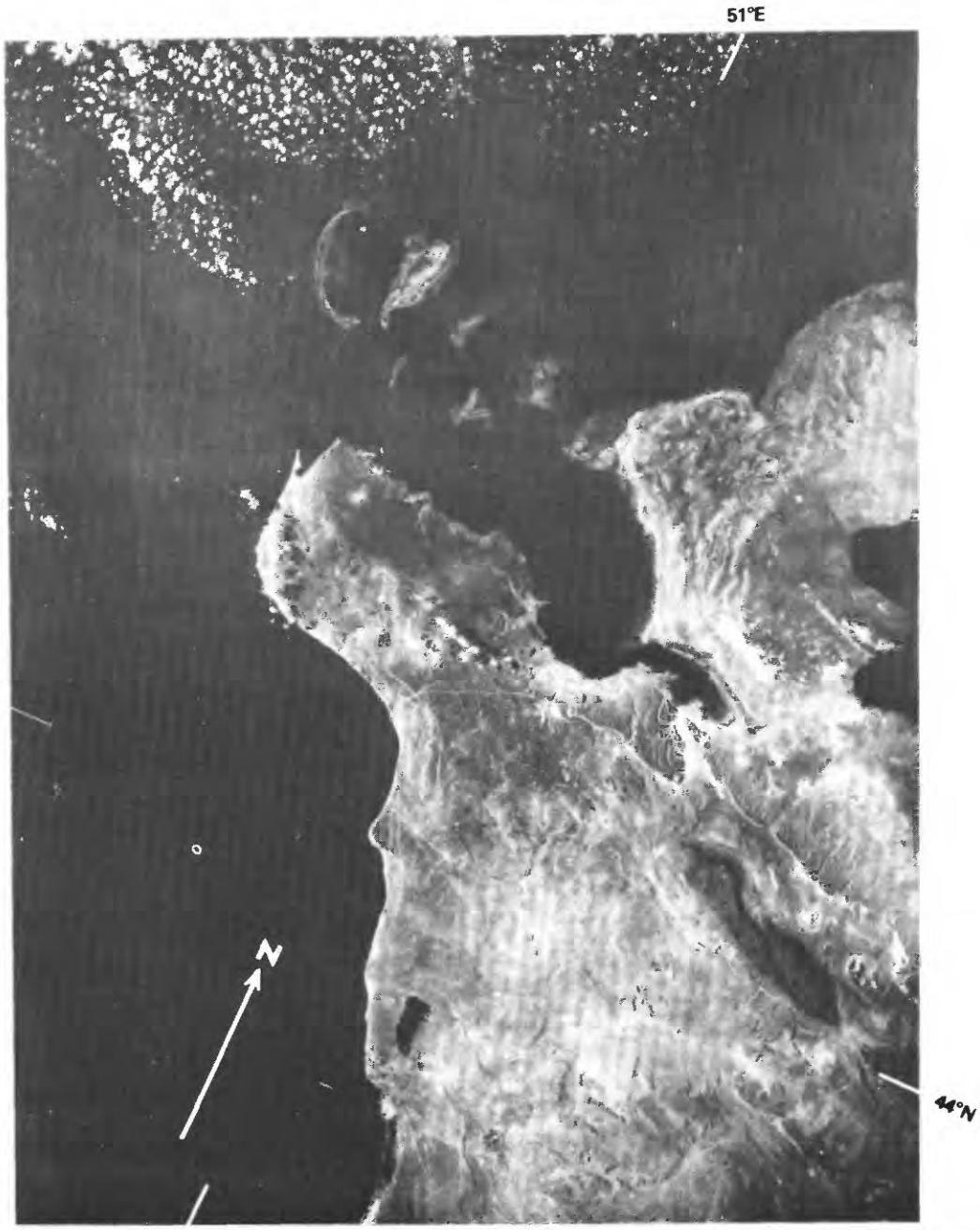

FIGURE 9.—Large-scale photo of the eastern coast of Caspian Sea, Manghyshlak Peninsula, and Ustjurt (spacecraft "Sojuz–12," cosmonauts V. G. Lasarev and O. G. Makarov).

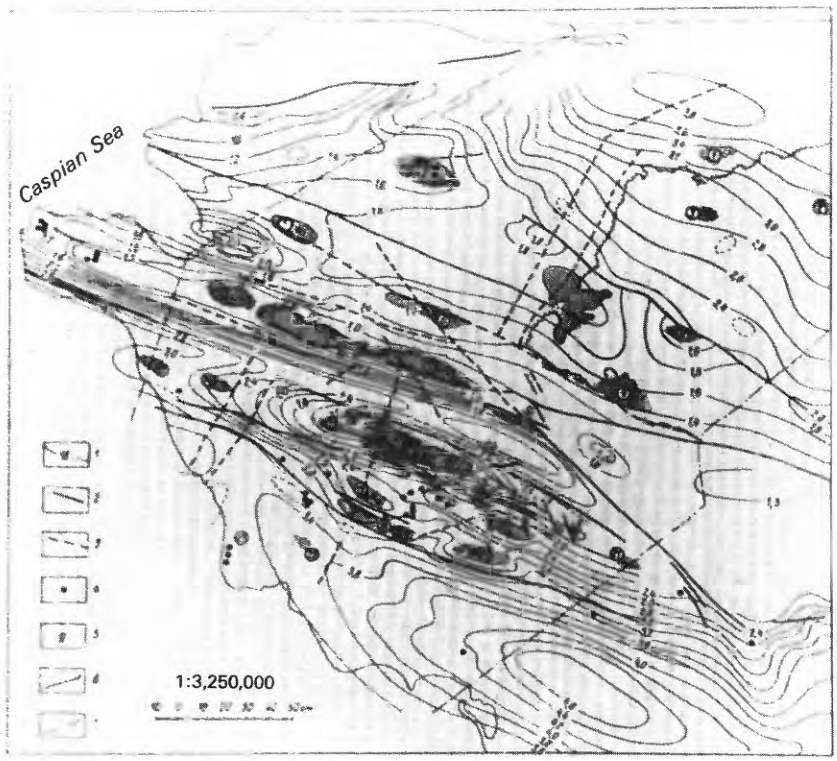

FIGURE 10.—Structural map of Manghyshlak and Ustjurt compiled using photos from "Sojuz–8" and "Sojuz–12." There are shown the anomalies on space photos that correspond to local structures being in prospect for search of oil and gas.
1—Isolines of the surface of the Permian-Triassic deposits; 2—fault found by various methods; 3—faults found on space photos; 4—bore holes reached the Pre-Jurassic deposits; 5—photo-anomalies corresponding to local structures (their figures are on the map); 6—scarps of Ustjurt plateau; 7—boundaries of space photos from "Sojuz–8." Scale 1:3,250,000.

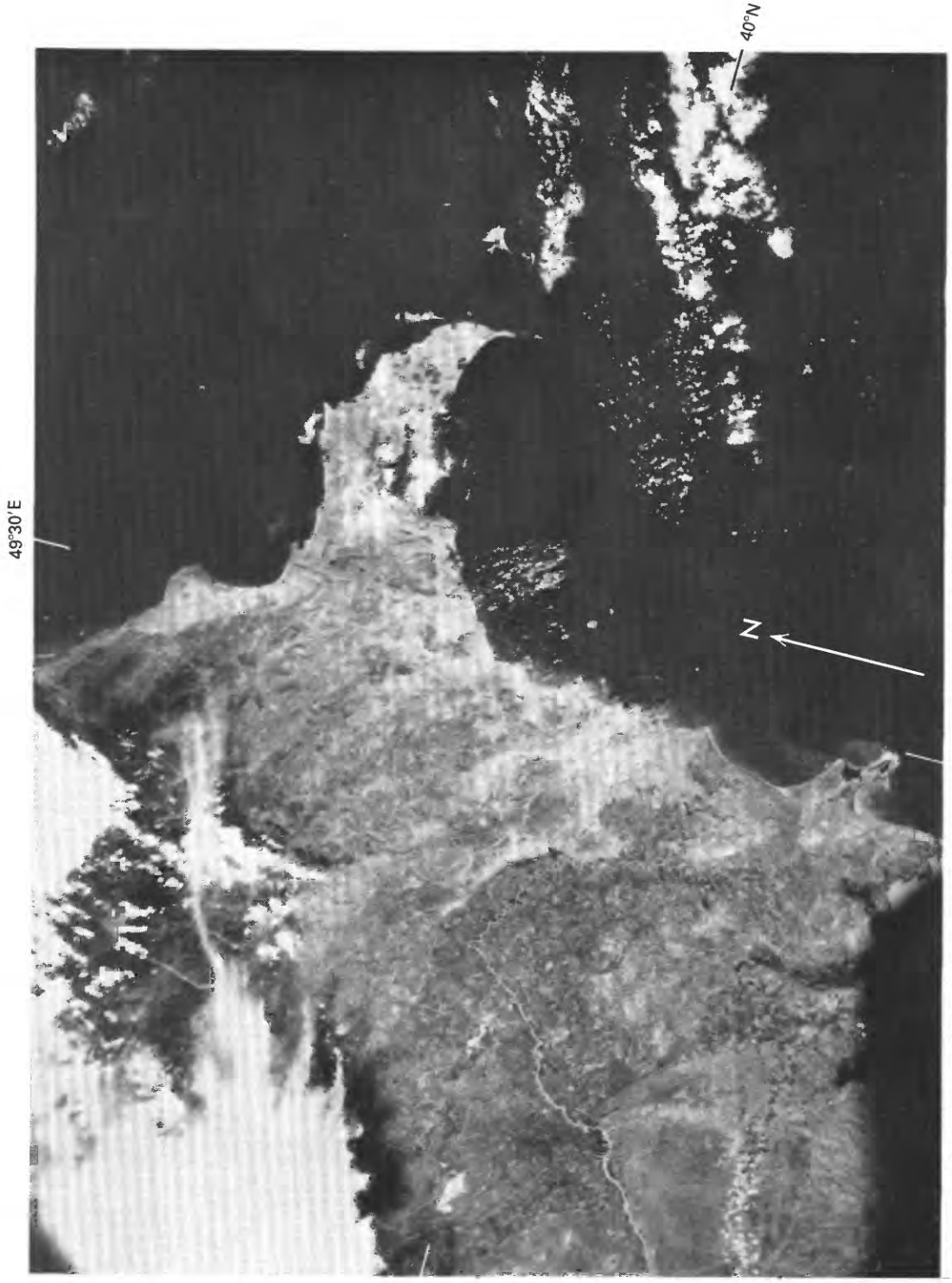

FIGURE 11.—Middle-scale space photo of Eastern Caucasus and Lower Kura lowland (spacecraft "Sojuz–9," cosmonauts A. G. Nikolaev and V. I. Sevastianov, June 1970).

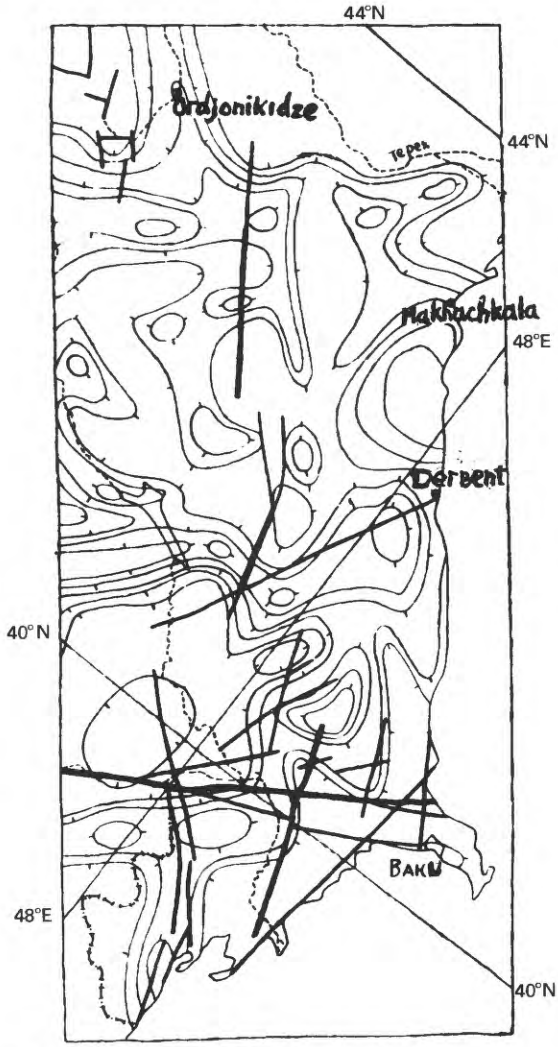

FIGURE 12.—Correlation of lineaments deciphered on "Sojuz–9" photos and zones of deep seismic deformations of Eastern Caucasus (the last are shown according to the data of Gu. K. Shchukin, 1973). Thick lines are the major lineaments, middle lines are the other lineaments, and thin lines are the isolines of the density of deep seismic deformations in conditional figures.

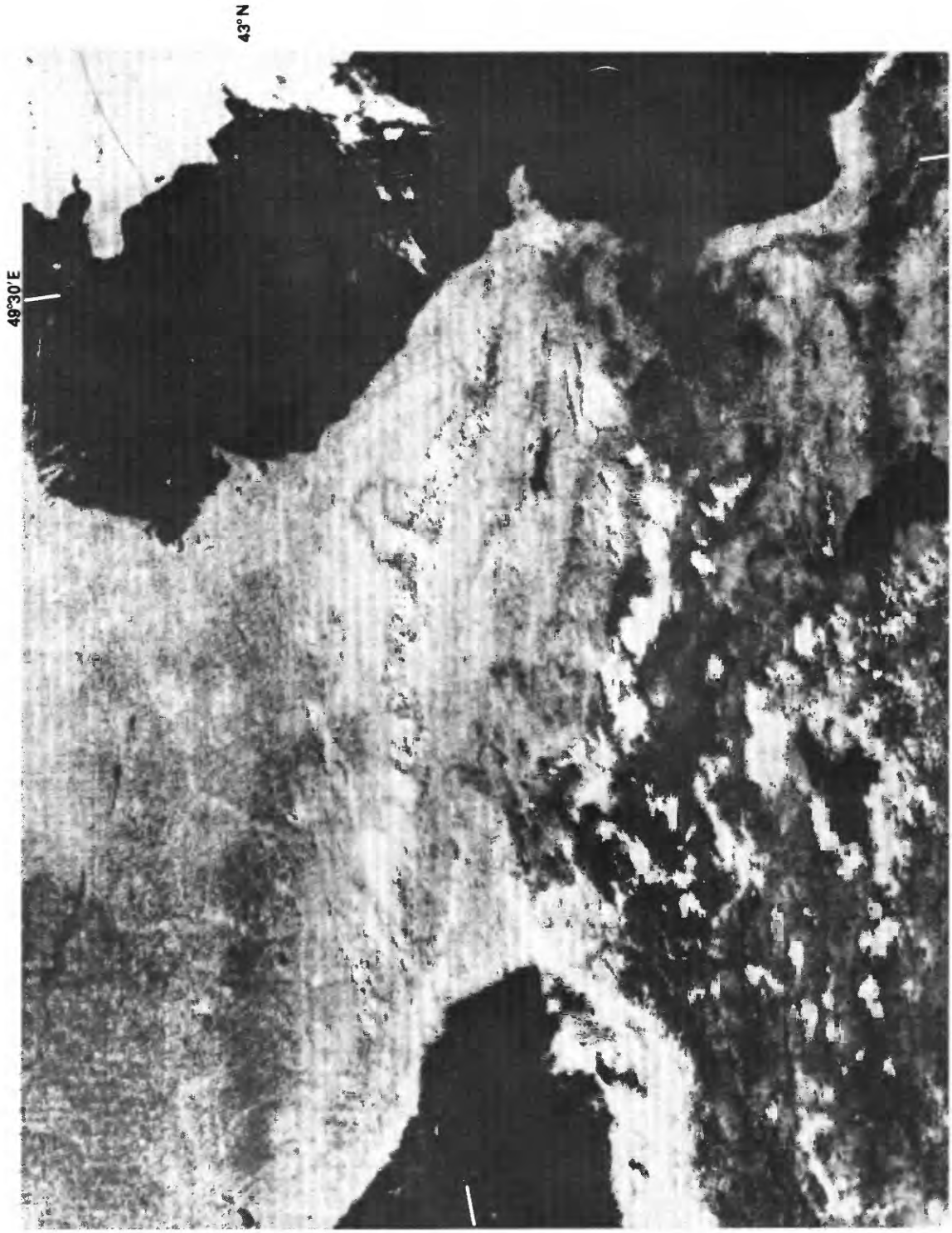

FIGURE 13.—Small-scale scanner image of Caucasus, 18 satellite "Meteor," August 21, 1974, band 0.6–0.7 mkm.

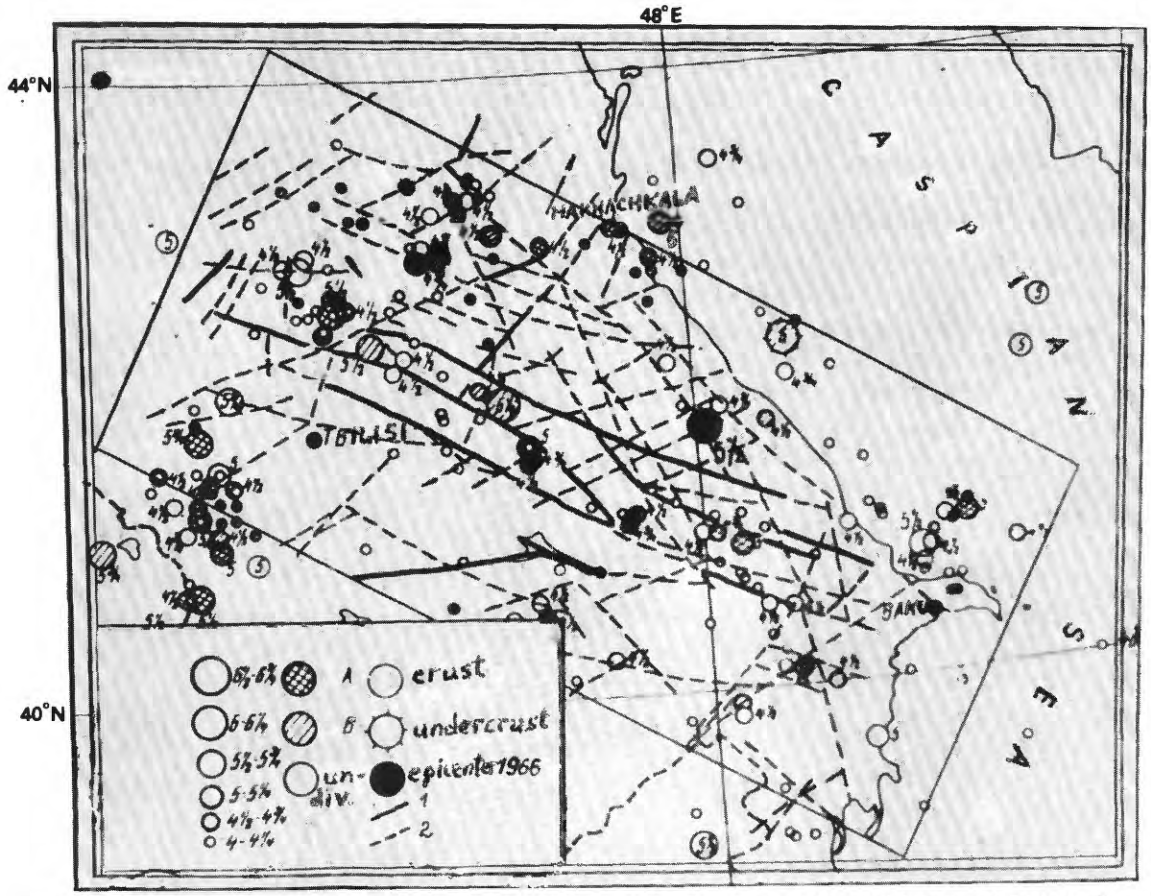

FIGURE 14.—Correlation of lineaments deciphered on TV and scanner "Meteor" images of Eastern Caucasus and epicenters of earthquakes 1911–1966 (the last are shown according to the data of I. V. Ananjin). 1—Lineaments, well seen and repeated on different images and 2—lineaments, seen worse or on some images only. See the other symbols on figure 12. The circles show the location of epicenters.

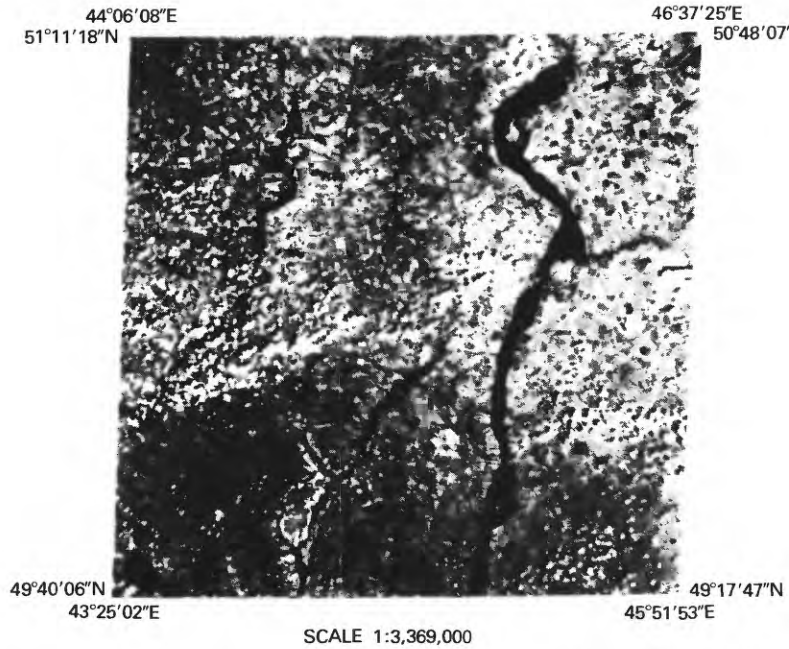

FIGURE 15.—Scanner image of Lower Volga region, Landsat–1, July 16, 1973. Scale 1:3,369,000.

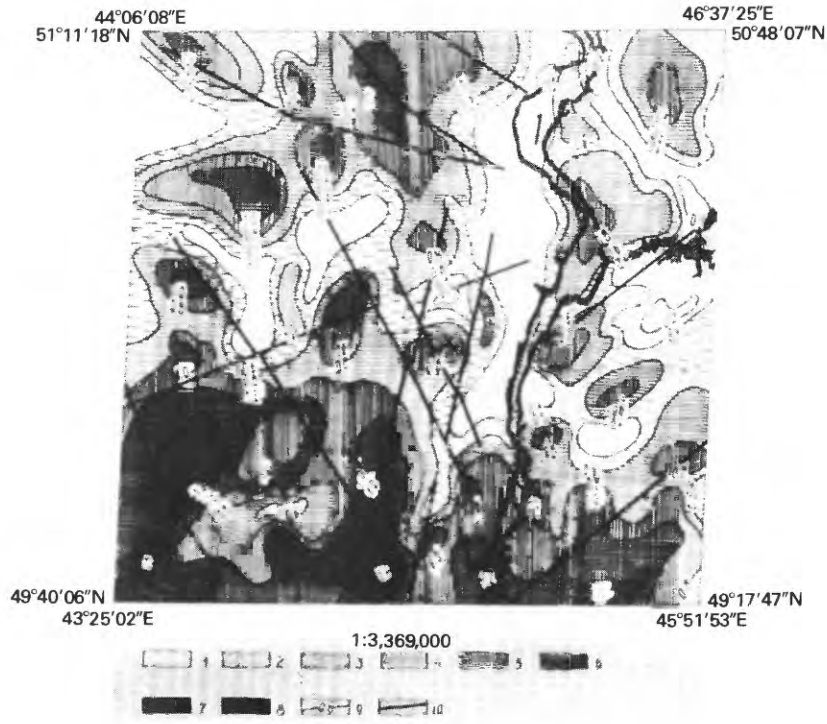

FIGURE 16.—Photometrical map of image figure 15 in conditional figures without clouds. Scale 1:3,369,000.
1–8—Different magnitudes of the optical density of image; 9—isolines of the optical density in conditional figures; 10—lineaments. Volga River is shown.

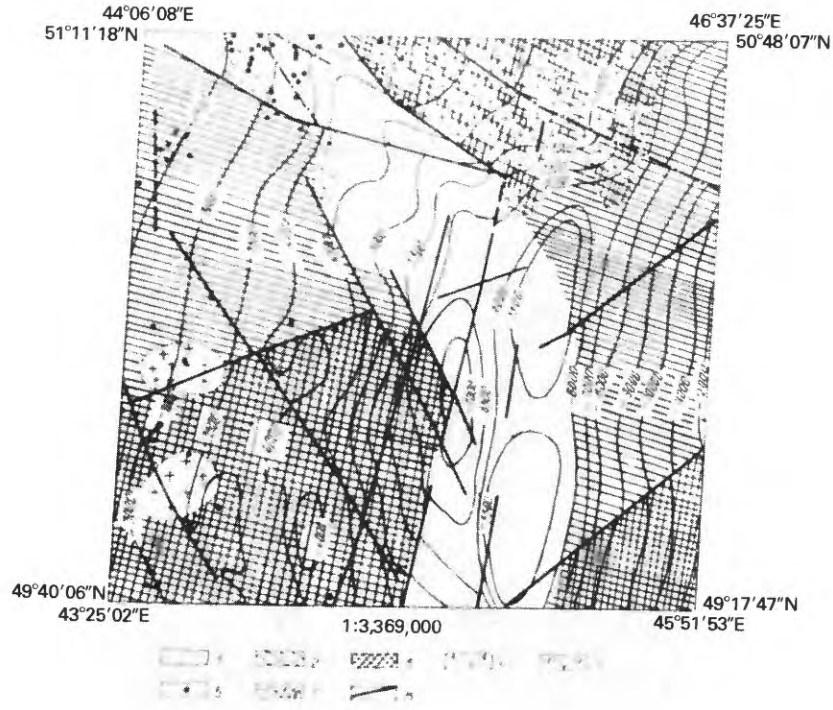

FIGURE 17.—Schematic structural-geologic map of crystalline basement of Lower Volga region using geological and geophysical data and space photo interpretation. Scale 1:3,369,000.
1—Zone of Sfekofen-Karelian rebuilding of basement; 2—areas of amphibolite facea of metamorphism; 3—areas of granulite facea of metamorphism; 4—granitoides; 5—basic rocks; 6—bore holes reached the basement; 7—isolines of basement surface according to the data of N. V. Nevolin, 1974; and 8—lineaments.